MATERIALS CENTRAL TECHNICAL LIBRARY
OFFICIAL FILE COPY

WADD-TR-60-517
Volume I

THERMO-STRUCTURAL ANALYSIS MANUAL

TECHNICAL REPORT NO. WADD-TR-60-517, Vol. I

August 1962

Flight Dynamics Laboratory
Directorate of Materials and Processes
Aeronautical Systems Division
Air Force Systems Command
Wright-Patterson Air Force Base, Ohio

Project No. 1367, Task No. 136710

(Prepared under Contract AF 33(616)-6066 by
the Republic Aviation Corporation, Farmingdale, L. I., New York;
H. Switzky, M. J. Forray, and M. Newman, authors.)

NOTICES

When Government drawings, specifications, or other data are used for any purpose other than in connection with a definitely related Government procurement operation, the United States Government thereby incurs no responsibility nor any obligation whatsoever; and the fact that the Government may have formulated, furnished, or in any way supplied the said drawings, specifications, or other data, is not to be regarded by implication or otherwise as in any manner licensing the holder or any other person or corporation, or conveying any rights or permission to manufacture, use, or sell any patented invention that may in any way be related thereto.

Qualified requesters may obtain copies of this report from the Armed Services Technical Information Agency, (ASTIA), Arlington Hall Station, Arlington 12, Virginia.

This report has been released to the Office of Technical Services, U.S. Department of Commerce, Washington 25, D.C., in stock quantities for sale to the general public.

Copies of this report should not be returned to the Aeronautical Systems Division unless return is required by security considerations, contractual obligations, or notice on a specific document.

MATERIALS CENTRAL TECHNICAL LIBRARY
OFFICIAL FILE COPY

WADD-TR-60-517
Volume I

THERMO-STRUCTURAL ANALYSIS MANUAL

TECHNICAL REPORT NO. WADD-TR-60-517, Vol. I

August 1962

Flight Dynamics Laboratory
Directorate of Materials and Processes
Aeronautical Systems Division
Air Force Systems Command
Wright-Patterson Air Force Base, Ohio

Project No. 1367, Task No. 136710

(Prepared under Contract AF 33(616)-6066 by
the Republic Aviation Corporation, Farmingdale, L. I., New York;
H. Switzky, M. J. Forray, and M. Newman, authors.)

NOTICES

When Government drawings, specifications, or other data are used for any purpose other than in connection with a definitely related Government procurement operation, the United States Government thereby incurs no responsibility nor any obligation whatsoever; and the fact that the Government may have formulated, furnished, or in any way supplied the said drawings, specifications, or other data, is not to be regarded by implication or otherwise as in any manner licensing the holder or any other person or corporation, or conveying any rights or permission to manufacture, use, or sell any patented invention that may in any way be related thereto.

Qualified requesters may obtain copies of this report from the Armed Services Technical Information Agency, (ASTIA), Arlington Hall Station, Arlington 12, Virginia.

This report has been released to the Office of Technical Services, U.S. Department of Commerce, Washington 25, D.C., in stock quantities for sale to the general public.

Copies of this report should not be returned to the Aeronautical Systems Division unless return is required by security considerations, contractual obligations, or notice on a specific document.

FOREWORD

This manual was prepared by the Structural Research and Development Group, the Structures Section, Research and Development Division of the Republic Aviation Corporation. The work was accomplished under Contract AF 33(616)-6066 and the 750A Applied Research Program entitled "Mechanics of Flight", Project No. 1367, Structural Design Criteria in Task No. 13002, Structural Analysis Methods. This work was initiated under the direction of the Structural Analysis Unit, Structures Branch, Aircraft Laboratory, Directorate of Laboratories, Wright Air Development Center.* Mr. I. Winnegrad acted initially as project engineer and was succeeded by Mr. C. Richard. The Manual was completed under the direction of the Structural Analysis Unit, Configuration Research Section, Structures Branch, Flight Dynamics Laboratory, with Mr. G. E. Maddux as Project Engineer.

The work was coordinated and supervised by Dr. R. S. Levy, Head of Structural Research and Development Group. His valuable suggestions and criticisms are gratefully acknowledged as are names of the following personnel of the Applied Research and Development Division of Republic Aviation Corporation. Mr. A. Alberi, Acting Manager of Technical Engineering; Mr. C. Rosenkranz, Acting Chief Structures Engineer; and Mr. C. Meissner, Principal Structures Engineer.

* (Now designated Aeronautical Systems Division)

4-99M, 500, 9-24-62

ABSTRACT

This Manual includes a compilation of methods of solution for thermal stress problems of the types frequently encountered by aircraft designers. Some of the methods represent original work done at Republic Aviation Corporation and others were obtained from the general literature. Where feasible, graphs and formulas are presented from which the user may obtain answers directly. These are presented in non-dimensional form to extend their applicability. In other cases, tables are furnished which describe methods of solution. Liberal use is made of illustrative problems and examples.

Within the limitations of linear elastic theory, the following problems are treated in detail:

(1) Statically determinate beams,
(2) Redundant beams and frames,
(3) Riveted or bolted joints,
(4) Plates,
(5) Axially symmetric shells.

For more complex linear problems, a general method of attack is presented which reduces the thermal stress problem to an equivalent mechanical loading problem. This approach permits utilization of the great variety of analytical methods which have been developed for stress analysis of structures under purely mechanical loads. A brief review of some of these methods is included with pertinent remarks on their applicability to thermal stress problems.

In many cases of practical interest, thermal effects introduce non-linearity by causing large deflections, by affecting the mechanical properties of the material, or by introducing creep. Solutions for these problems are quite limited. However, they are discussed in some detail and a generalized stress-strain-time-temperature relationship is postulated which is applied to buckling of columns and plates.

PUBLICATION REVIEW

This report has been reviewed and is approved.

FOR THE COMMANDER:

William C. Nielsen

WILLIAM C. NIELSEN
Colonel, USAF
Chief, Flight Dynamics Laboratory

PREVIOUS PAGE IS BLANK

TABLE OF CONTENTS*

		Page
Abstract		iii
List of Illustrations		x
Notes on Using the Manual		xviii
Introduction		xix
Paragraph		**Page**
	SECTION 1 - THEORETICAL CONSIDERATIONS	1.0
	Table of Contents	1.1
1	Theoretical Considerations	1.2
1.1	Strain	1.2
1.1.1	Compatibility	1.6
1.2	Traction and Stress	1.7
1.2.1	Stress Equations of Equilibrium in Cartesian Coordinates	1.9
1.3	Boundary Conditions	1.11
1.4	Stress-Strain Relationship	1.12
1.5	Uniqueness	1.15
1.6	Special Orthogonal Coordinate Systems	1.15
1.7	Energy Principles	1.18
1.7.1	Principle of Virtual Work	1.18
1.7.2	Variational Principles	1.19
1.8	References	1.27

* This Table of Contents lists the prefatory material, sections, and sub-sections of the Manual. Paragraphs with numbers of more than three tiers are omitted. However, each section has its own complete table of contents.

TABLE OF CONTENTS (Cont'd)

Paragraph		Page
	SECTION 2 - STRUCTURAL TECHNIQUES	2.0
	Table of Contents	2.1
2	Structural Techniques	2.3
2.1	Linear Structures	2.5
2.1.1	Virtual Work Techniques	2.5
2.1.2	Strain Energy in Terms of Internal Loads and Deformations	2.9
2.1.3	Application of Virtual Force Technique - Flexibility Coefficient	2.11
2.1.4	Applications of Virtual Displacement Techniques	2.16
2.1.5	Properties of Influence Coefficients Matrix	2.19
2.1.6	Equivalent Thermal Load	2.21
2.1.7	Plane Stress and Plane Strain Problem	2.23
2.1.8	St. Venant's Principle	2.25
2.2	Non-Linear Structures	2.26
2.2.1	Incremental Linear Solutions	2.27
2.2.2	Inverse Solution	2.27
2.2.3	Approximate Solutions	2.28
2.3	References	2.29
	SECTION 3 - MATERIAL CONCEPTS	3.0
	Table of Contents	3.1
3	Material Concepts	3.2
3.1	Deformation Mechanism	3.4
3.2	Stress-Temperature-Time-Strain Relationship	3.5
3.2.1	Uniaxial Stress-Strain Relationship	3.6
3.2.2	Experimental Determination of the Material Constants	3.9
3.2.3	Complex Loading	3.14
3.3	References	3.19

TABLE OF CONTENTS (Cont'd)

Paragraph		Page
	SECTION 4 - THERMO-ELASTIC ANALYSIS OF BEAMS	4.0
	Table of Contents	4.1
4	Thermo-Elastic Analysis of Beams	4.4
4.1	Thermo-Elastic Analysis of Statically Determinate (Unrestrained) Beams	4.6
4.1.1	General Solution	4.7
4.1.2	Evaluation of Integrals	4.11
4.2	Statically Indeterminate (Externally Restrained) Beams	4.58
4.2.1	Beam Deflections (with illustrative problem)	4.58
4.2.2	Fixed End Reactions	4.63
4.2.3	General Solution of Statically Indeterminate Beams	4.86
4.2.4	Mechanics of Solution by the Flexibility Method	4.88
4.2.5	Mechanics of Solution by the Stiffness (Slope-Deflection) Method	4.92
4.2.6	Selection of Method of Analysis	4.95
4.2.7	Curved Beams	4.105
4.3	References	4.117
	SECTION 5 - THERMO-ELASTIC ANALYSIS OF JOINTS	5.0
	Table of Contents	5.1
5	Thermo-Elastic Analysis of Joints	5.2
5.1	The One-Dimensional Problem	5.4
5.1.1	The Joint Equations	5.5
5.1.2	The Special Case of Constant Bay Properties	5.8
5.1.3	Constant Bay Properties - Rigid Sheets	5.24
5.1.4	Constant Bay Properties - Rigid Attachments	5.28
5.1.5	The Influence of "Slop" on the Load Distribution	5.30

TABLE OF CONTENTS (Cont'd)

Paragraph		Page
5.2	The Two-Dimensional (Bowing) Problem	5.36
5.2.1	The Joint Equations	5.37
5.3	Determination of the Attachment-Hole Flexibility Factor	5.39
5.4	References	5.40
	SECTION 6 - THERMO-ELASTIC ANALYSIS OF PLATES	6.0
	Table of Contents	6.1
6	Thermo-Elastic Analysis of Plates	6.3
6.1	Theory of Deformation of Plates	6.4
6.1.1	Definition of a Plate	6.4
6.1.2	Assumptions for Linear Plate Theory	6.4
6.1.3	Three Kinds of Plate Problems	6.6
6.1.4	Fundamental Equations of Thermo-Elastic Plate Theory	6.7
6.2	Bending of Plates	6.13
6.2.1	Bending of Rectangular Plates with Linear Gradient Through the Thickness	6.13
6.2.2	Bending of Circular Plates with Linear Temperature Gradient Through the Thickness	6.17
6.2.3	Circular Plates - Temperature Difference as a Function of the Radial Coordinate	6.18
6.2.4	Approximate Solution of Free Plate with Arbitrary Temperature Variation Through the Thickness Only	6.26
6.3	Slab Problems - Plates	6.29
6.3.1	Thermal Stresses in Rings- Asymmetrical Temperature Distribution	6.31
6.3.2	Thermal Stresses in Solid Circular Plates Due to Asymmetrical Temperature Distribution	6.34
6.3.3	Circular Disk with Concentric Hole Subject to a Power Law Temperature Distribution	6.42

TABLE OF CONTENTS (Cont'd)

Paragraph		Page
6.3.4	Circular Plate - Central Hot Spot	6.48
6.4	References	6.57
	SECTION 7 - THERMO-ELASTIC ANALYSIS OF SHELLS	7.0
	Table of Contents	7.1
7	Thermo-Elastic Analysis of Shells	7.2
7.1	Truncated Conical Shells	7.3
7.1.1	Radial Loading Perpendicular to the Cone Axis	7.4
7.1.2	Meridional Loading - Membrane Analysis	7.20
7.1.3	Meridional Temperature Variation	7.26
7.2	Approximate Solution for Non-Conical Axisymmetric Shells	7.28
7.3	Cylindrical Shells	7.30
7.3.1	Cylindrical Shells with Axisymmetric Loading and Meridional Temperature Variation	7.30
7.3.2	Cylindrical Shells with Temperature Gradient Through the Thickness	7.37
7.4	References	7.51
	SECTION 8 - STRUCTURAL ASSEMBLIES	8.0
	Table of Contents	8.1
8	Structural Assemblies	8.2
8.1	Shells of Revolution with Bulkheads	8.3
8.2	Determination of Interaction Forces and Moments	8.6
8.2.1	Solution for the Interior Bulkhead	8.7
8.2.2	Solution for the External Bulkhead	8.8

TABLE OF CONTENTS (Cont'd)

Paragraph		Page
	SECTION 9 - STABILITY OF STRUCTURES	9.0
	Table of Contents	9.1
9	Stability of Structures	9.2
9.1	Stability Criteria	9.4
9.1.1	Stability by Eigenvectors	9.7
9.1.2	Stability by Virtual Work	9.14
9.1.3	Properties of Eigenvectors (Deflection Modes) and Eigenvalues (Critical Loads)	9.15
9.1.4	Approximate Methods of Determining Stability	9.18
9.1.5	Shear Energies	9.26
9.1.6	Plasticity and Eccentricity	9.29
9.1.7	Temperature	9.31
9.2	Non-Dimensional Buckling Curves	9.32
9.2.1	Non-Dimensional Stability	9.32
9.3	Curved Plates and Shells	9.48
9.4	References	9.50

LIST OF ILLUSTRATIONS

Figure		Page
	SECTION 1 - THEORETICAL CONSIDERATIONS	
1.1-1	Displacement of a Structure Under Mechanical and/or Thermal Loads	1.4
1.1-2	Types of Strain	1.6
1.2-1	Tractions at the Point Q Acting on the Plane with Normal $\vec{n}$	1.8
1.2-2	Stress Components	1.9
1.2.1-1	Stress Components on Rectangular Parallelepiped	1.10
1.3-1	Specification of Surface Tractions	1.12
1.7.1-1	Elastic Body with Applied Forces	1.18
1.7.2.2-1	Variation of Extremizing Function	1.22
1.7.2.3-1	Elastically Propped Cantilever Beam	1.24
1.7.2.4-1	Beam with Three Supports	1.27
	SECTION 2 - STRUCTURAL TECHNIQUES	
2.1.1.1-1	Body Under Load	2.6
2.1.1.2-1	Vertically Loaded Beam in Equilibrium	2.8
2.1.2-1	Beam Under Load	2.9
2.1.3.2-1	Superposition of Flexibilities	2.12
2.1.3.2-2	Equivalent Structures in Series	2.13
2.1.4.3-1	Stiffness Coefficients for a Double Beam	2.19
	SECTION 3 - MATERIAL CONCEPTS	
3.1-1	Deformation and Energy Potential Under Shearing Action	3.5
3.2.1-1	Non-Dimensional Stress-Strain Curves	3.7
3.2.1-2	Non-Dimensional Secant Modulus Curves	3.7
3.2.1-3	Non-Dimensional Tangent Modulus Curves	3.7
3.2.1-4	Non-Dimensional Tangent-Secant Modulus Ratio Curves	3.7
3.2.2.1-1	Short Time Stress-Strain Curve	3.9
3.2.2.2-1	Determination of Material Constants from Short Time Stress-Strain Data	3.11
3.2.2.2-2	Determination of Material Constants from Constant Creep Rate Data	3.12
3.2.2.3-1	Creep Curve	3.13
3.2.2.4-1	Variation of Material Parameters with Temperature	3.14

LIST OF ILLUSTRATIONS (Cont'd)

Figure		Page
3.2.3.1-1	Principal Directions and Octahedral Planes	3.16
3.2.3.2-1	Uniaxial Stress-Strain Curve	3.18
3.2.3.2-2	Hydrostatic Stress-Strain Curve	3.18
3.2.3.2-3	Octahedral Stress-Strain Curve	3.18
3.2.3.2-4	Biaxial Stress-Strain Curve	3.18
	SECTION 4 - THERMO-ELASTIC ANALYSIS OF BEAMS	
4.1.1-1	Elastic Area Cross Section	4.8
4.1.2.1-1	Finite Sum Method - Element Breakdown of Cross Section	4.12
4.1.2.1-2	Finite Sum Method	4.15
4.1.2.1-3	Stress Distribution for Problem of Figure 4.1.2.1-2	4.18
4.1.2.2-1	Sandwich Beam Cross Section	4.20
4.1.2.3-1	Typical Configurations of Elastic Cross Section Areas	4.22
4.1.2.3-2	Determination of Average αT Profile for Bending About UU Principal Axis	4.22
4.1.2.3.1-1	αT Profile	4.23
4.1.2.3.1-2	αT Values at Five Equally Spaced Points	4.24
4.1.2.3.1-3	Polynomial αT Profiles of Illustrative Problem	4.27
4.1.2.3.2-1	Continuous Cross Section with Monotonic Elastic Width Variation	4.28
4.1.2.3.2-2	Monotonic Geometric Shapes Defined by Parameters β and K	4.29
4.1.2.3.3-1	Elongation, γ_L, for Continuous Geometry of the Form $Eb = E_o b_o (1 + \beta s^K)$, with K = 1 (Straight Sides)	4.32
4.1.2.3.3-2	Curvature, δ_L, for Continuous Geometry of the Form $Eb = E_o b_o (1 + \beta s^K)$, with K = 1 (Straight Sides)	4.33
4.1.2.3.3-3	Elastic Cross Section	4.34
4.1.2.3.3-4	Thermal Stresses for Polynomial αT Distributions	4.39
4.1.2.3.3-5	Decomposition of Total αT Profile into Symmetrical and Antisymmetrical Components	4.41
4.1.2.3.3-6	Symmetric Elastic Cross Section with Unsymmetric αT Profile	4.43
4.1.2.3.3-7	Thermal Stresses for the Beam of Figure 4.1.2.3.3-6	4.45

LIST OF ILLUSTRATIONS (Cont'd)

Figure		Page
4.1.2.3.4-1	General Multi-Rectangular Section	4.46
4.1.2.3.4-2	Unrestrained Beam Cross Section and Temperature Distribution	4.48
4.1.2.3.4-3	Multi-Rectangular Section with a Bending Axis of Symmetry	4.51
4.1.2.3.4-4	Approximate Representation of a Zee by a Two Rectangle Symmetrical Geometry	4.53
4.1.2.3.4-5(a)	Elongation $(\gamma_L)_s$ Versus Width Parameter (e)	4.54
4.1.2.3.4-5(b)	Curvature $(\delta_L)_a$ Versus Width Parameter (e)	4.55
4.1.2.3.4-6	Bi-Metallic Box Beam with Symmetrical Geometry	4.56
4.2.1-1	Curvature $w_t(x)$ and Elongation $\bar{\epsilon}_t(x)$ Due to Combined Mechanical and Thermal Loading as a Function of Distance Along the Span	4.59
4.2.1-2	Indeterminate Beam Deflections	4.61
4.2.2.1-1	Sign Convention for Combining Fixed End Reactions of Beams to Determine Resultant Fixed End Reactions at a Joint	4.64
4.2.2.2-1	Mechanical and Thermal Loads Acting on Cantilever Beam	4.66
4.2.2.3-1	Fixed End Reaction for Constant EI; Transverse End Load (P_o)	4.70
4.2.2.3-2	Fixed End Reaction for Constant EI; End Moment (M_o)	4.71
4.2.2.3-3	Fixed End Reactions for Linear 1/EI; Transverse End Load (P_o), ($c = 1$, $\nu = 1$)	4.72
4.2.2.3-4	Fixed End Reactions for Linear 1/EI; End Moment (M_o), ($c = 1$, $\nu = 1$)	4.73
4.2.2.3-5	Fixed End Reaction for Parabolic 1/EI; Transvere End Load (P_o), ($c = 2$, $\nu = 1$)	4.74
4.2.2.3-6	Fixed End Reaction for Parabolic 1/EI; End Moment (M_o), ($c = 2$, $\nu = 1$)	4.75
4.2.4-1	Flexibility Method	4.90
4.2.5-1	Stiffness Method	4.93
4.2.6.1-1	Beam with Degrees of Freedom	4.97
4.2.6.1-2	Temperature and Load on Beam	4.98
4.2.6.1-3	Solution	4.101
4.2.7-1	Sign Convention	4.106
4.2.7-2	Determination of Virtual Forces m, f, p	4.107
4.2.7.2-1	Elastic Center Method	4.111

LIST OF ILLUSTRATIONS (Cont'd)

Figure		Page
4.2.7.3-1	Resolution of Force into Symmetrical and Antisymmetrical Components	4.113
4.2.7.3-2	Frame Problem	4.114
	SECTION 5 - THERMO-ELASTIC ANALYSIS OF JOINTS	
5-1	Mechanical Joint	5.2
5.1-1	Splice Strap for a Rigid Beam Flange	5.4
5.1.1-1	One-Dimensional Joint Equilibrium	5.5
5.1.1-2	One-Dimensional Compatibility	5.6
5.1.1-3	Deformation of the Joint Due to Axial Stretching of the Sheets	5.7
5.1.1-4	Deformation of the Joint Due to Local Distortions of the Holes and Attachments	5.8
5.1.2-1(a)	Joint Coefficients for Constant Bay Properties (A_{1N} vs. Z)	5.10
5.1.2-1(b)	Joint Coefficients for Constant Bay Properties (B_{1N} vs. Z)	5.11
5.1.2-1(c)	Joint Coefficients for Constant Bay Properties (A_{2N} vs. Z)	5.12
5.1.2-1(d)	Joint Coefficients for Constant Bay Properties (B_{2N} vs. Z)	5.13
5.1.2-1(e)	Joint Coefficients for Constant Bay Properties (A_{3N} vs. Z)	5.14
5.1.2-1(f)	Joint Coefficients for Constant Bay Properties (B_{3N} vs. Z)	5.15
5.1.2-1(g)	Joint Coefficients for Constant Bay Properties (A_{4N} vs. Z)	5.16
5.1.2-1(h)	Joint Coefficients for Constant Bay Properties (B_{4N} vs. Z)	5.17
5.1.2-1(i)	Joint Coefficients for Constant Bay Properties (A_{5N} vs. Z)	5.18
5.1.2-1(j)	Joint Coefficients for Constant Bay Properties (B_{5N} vs. Z)	5.19
5.1.2-2	Joint with Constant Bay Properties	5.21
5.1.2-3	Alternate Top and Bottom Sheet Designation	5.22
5.1.3-1	Rigid Sheet Solution	5.26
5.1.3-2	Attachment Loads Due to Thermal Loading when the Joint Has Constant Bay Properties	5.27
5.1.5-1	Attachment in an Oversize Hole	5.30
5.1.5-2	Attachment Displacements Due to Slop - Positive Loads	5.31
5.1.5-3	Scarfed Splice	5.34
5.2.1-1(a)	Joint in Unbowed Configuration	5.37
5.2.1-1(b)	Bowing of Joint Due to Combined Effects of Non-Uniform Temperature Distribution and Mechanical Loading	5.37
5.3-1	Attachment-Hole vs. Deflection Curve	5.39

LIST OF ILLUSTRATIONS (Cont'd)

Figure		Page
	SECTION 6 - THERMO-ELASTIC ANALYSIS OF PLATES	
6.1.2-1	Cross Section of Plate Before and After Deformation	6.5
6.1.4-1	Positive Directions of Forces and Moments	6.8
6.1.4-2	Clamped Circular Plate with Linear Gradient Through Thickness	6.11
6.2.1-1	Plate Geometry Showing a Positive Linear Thermal Gradient Through the Thickness	6.13
6.2.1.3-1	Deflection (w) vs. Position (x) for y Parameters	6.15
6.2.1.3-2	Bending Moment (M_y) vs. Position (x) for y Parameters	6.16
6.2.1.3-3	Bending Moment (M_x) vs. Position (x) for y Parameters	6.16
6.2.2-1	Plate Geometry	6.17
6.2.3.1-1	Non-Dimensional Deflection	6.20
6.2.3.1-2	Non-Dimensional Radial Moment	6.21
6.2.3.1-3	Non-Dimensional Tangential Moment	6.22
6.2.4-1	Plate with Arbitrary Planform and Constant Thickness	6.26
6.3.2-1	Radial Stress Distribution in a Disk when a Temperature Distribution $T = T_o (r/b)^K \cos n\Theta$ (n = 0, 1, 2, 3) is Maintained	6.36
6.3.2-2	Hoop-Stress Distribution in Disk when Temperature Distribution $T = T_o (r/b)^K \cos n\Theta$ (n = 0, 1, 2, 3) is Maintained	6.37
6.3.2-3	Shear-Stress Distribution in Disk when Temperature Distribution $T = T_o (r/b)^K \cos n\Theta$ (n = 1, 2, 3) is Maintained	6.38
6.3.2-4	Radial and Hoop-Stress Distribution for the Axisymetric Temperature Case, $T = T_o (r/b)^K$	6.39
6.3.3-1	Temperature Profiles for n = 1/3, 1/2, 1, 2 and 3	6.45
6.3.3-2	Radial Variation of Radial Stress for a Disk with a Hole (a/b = 0, 0.4, 0.8; n = 1/3, 1 and 3	6.45
6.3.3-3	Variation of Maximum Radial Stress with n and a/b for a Disk with a Hole	6.45
6.3.3-4	Variation of Tangential Stress at Inner Boundary with n and a/b for a Disk with a Hole	6.45
6.3.3-5	Variation of Tangential Stress at Outer Boundary with n and a/b for Disk with a Hole	6.46
6.3.3-6	Variation of Radial and Tangential Stress at Center and Boundary with n for a Solid Disk	6.46

LIST OF ILLUSTRATIONS (Cont'd)

Figure		Page
6.3.3-7	Variation of Radial and Tangential Stress at Inner Boundary of Disk with n and a/b for a Disk on a Shaft	6.46
6.3.3-8	Variation of Tangential Stress at Outer Boundary of Disk with n and a/b for a Disk on a Shaft	6.46
6.3.4-1	Plate and Hot Spot	6.49
6.3.4-2(a)	Radial Displacement at Boundary of Hot Spot (ν = 0.3)	6.51
6.3.4-2(b)	Radial Displacement at Outer Boundary of Plate (ν = 0.3)	6.52
6.3.4-3	Stresses in Plate (ν = 0.3)	6.53
6.3.4-4	Variation of Stress Difference with b/a (ν = 0.3)	6.54
6.3.4-5	Variation of Maximum Stress Difference with t for b/a Large. Maximum Occurs at r = a.	6.55
	SECTION 7 - THERMO-ELASTIC OF SHELLS	
7.1-1	Truncated Conical Shell Geometry	7.3
7.1.1-1(a)	Conical Shell with Axisymmetric but Otherwise Arbitrary Loading	7.4
7.1.1-1(b)	Radial and Meridional Load Components P_h and P_x, Respectively	7.4
7.1.1.1-1	Conical Shell - Hooprings and Meridional Beam Strips	7.5
7.1.1.1-2(a)	Non-Dimensional Particular Solution of Eq. (2) for the Radial Deflection of a Conical Shell, K = 0, 1, 2	7.10
7.1.1.1-2(b)	Non-Dimensional Particular Solution of Eq. (2) for the Radial Deflection of a Conical Shell, K = 3, 4	7.11
7.1.1.2-1	Self-Equilibrating Loads and Moments $\mathcal{H}$ and $\mathcal{M}$ at a Conical Shell Edge	7.13
7.1.1.2-2	Edge Loading Functions	7.15
7.1.1.2-3	Conical Shell Under Uniform Radial Loading	7.16
7.1.1.2-4(a)	Edge Forces and Moments Corresponding to the Particular Solution	7.19
7.1.1.2-4(b)	Edge Loading Equal in Magnitude but Opposite in Direction to the Particular Solution Edge Loading	7.19
7.1.1.2-5	Meridional Moment and Radial Load Measured from Base of the Shell Shown in Figure 7.1.1.2-4	7.21
7.1.2-1	Meridional Loading on a Conical Shell	7.22
7.1.2-2	Conical Shell Under Vertical Loading	7.23
7.1.3-1	Reduction of Thermal Problem to Equivalent Mechanical Loading Problem	7.27
7.2-1	Approximation of a Non-Conical Shell by a Series of Conical Sections	7.29

LIST OF ILLUSTRATIONS (Cont'd)

Figure		Page
7.3.1.2-1	Self-Equilibrating Loads and Moments $\mathcal{H}$ and $\mathcal{M}$ at at Cylinder Edge	7.33
7.3.1.2-2	Infinitely Long Cylinder with Discontinuous Axisymmetric Temperature Distribution	7.34
7.3.1.2-3	Horizontal Loads and Moments at Cut Edges	7.36
7.3.1.2-4	Non-Dimensional Stresses and Radial Deflections	7.38
7.3.2.1-1(a)	Shell Geometry	7.39
7.3.2.1-1(b)	Variation of Stresses Through the Cylinder Thickness	7.39
7.3.2.1-2	Maximum Tangential and Longitudinal Stress in Cylinder per °F Temperature Difference Between the Outer and Inner Radii	7.41
7.3.2.1-3	Tangential Stress at Outside Radius per °F Temperature Difference Between the Outer and Inner Radii	7.42
7.3.2.1-4	Maximum Radial Stress per °F Temperature Difference Between the Outer and Inner Radii	7.43
7.3.2.1-5	Location of the Position of Maximum Radial Stress	7.44
7.3.2.2-1	Non-Dimensional Radial Stress as Function of $\frac{Kt}{a^2}$ for the case ah = 5	7.49
7.3.2.2-2	Non-Dimensional Tangential Stress as Function of $\frac{Kt}{a^2}$ for the case ah = 5	7.49
7.3.2.2-3	Non-Dimensional Surfaces Tangential Stress as Function of $\frac{Kt}{a^2}$ with ah as a Parameter	7.50
7.3.2.2-4	Non-Dimensional Surfaces Tangential Stress for a Hollow Cylinder with Outer Surfaces at Temperature T_1 and Inner Surface Insulated	7.50
	SECTION 8 - STRUCTURAL ASSEMBLIES	
8.1-1	Deflections, Loads and Moments at a Shell and Bulkhead Junction	8.4
8.1.2	Edge Rotation of Solid Circular Bulkhead Due to Uniform Pressure Loading	8.5
8.2-1	Long Cylinder with Interior and End Bulkheads	8.7
8.2.1-1	Interior Bulkhead	8.8
8.2.2-1	External Bulkhead	8.9
	SECTION 9 - STABILITY OF STRUCTURES	
9.1-1	Stability of Columns	9.6
9.1.1.1-1	Loads on Plate	9.8
9.1.1.2-1	Pin-Ended Column	9.11

LIST OF ILLUSTRATIONS (Cont'd)

Figure		Page
9.1.1.2-2	Eigenvectors and Eigenvalues of Column	9.13
9.1.4.1.2-1	Virtual Force on Pin-Ended Column	9.19
9.1.4.2-1	Pin-Ended Column with Variable Stiffness	9.23
9.1.4.2-2	Clamped Column	9.24
9.1.5-1	Shear and Torsional Load on a Pin-Ended Column	9.27
9.1.7-1	Deflection and Load in a Restrained Column	9.32
9.2.1-1(a)	Stability of Simple Free Flange, Shear Panel, or Shells	9.35
9.2.1-1(b)	Stability of Simple Free Flange, Shear Panel, or Shells	9.36
9.2.1-2(a)	Stability of Column or Plate Column	9.37
9.2.1-2(b)	Stability of Column or Plate Column	9.38
9.2.1-3(a)	Stability of Simple-Simple Plate	9.39
9.2.1-3(b)	Stability of Simple-Simple Plate	9.40
9.2.1-4	Stability of Clamped-Free Plate	9.41
9.2.1-5	Stability of Clamped-Clamped Plate	9.42
9.2.1-6	Sheet Stringer Cross Section	9.45
9.2.1-7	Sandwich Panel	9.47
9.3-1	Cylinder in Compression	9.50

NOTES ON USING THE MANUAL

This Manual consists of nine basic sections, divided into numbered sub-sections and paragraphs. For simplicity in cross-referencing material in the text, all portions of the Manual designated with a two-tier number (i.e., 1.1) are considered sub-sections, and all portions designated by numbers of three or more tiers (i.e., 1.1.1 or 1.1.1.1) are considered paragraphs.

Throughout the Manual, the numbered paragraphs (or sub-sections) have been used as the basis for numbering figures, tables, and equations, with new sequences beginning with each numbered paragraph. Figure and table numbers consist of an appropriate paragraph number, followed by a sequence number for the particular figure or table. For convenience the paragraph designations have been omitted from the equation numbers. When an equation from another paragraph is cited in the text, the number of the paragraph in which that equation occurs is also cited. When a paragraph number is not given in conjunction with the citation of an equation, it is to be assumed that the equation is included in the paragraph in which the citation occurs.

References are listed at the end of those sections which have more than one reference. In addition,each section contains its own complete table of contents and list of symbols.

INTRODUCTION

Aerodynamic heating of bodies moving at supersonic and hypersonic speeds results in non-uniform temperature rises. High velocity airplanes and missiles are thus subjected to transient and steady state non-uniform temperature distributions which produce thermal stresses. In its broadest sense, the thermal problem encompasses both the fields of mechanics and thermodynamics of non-rigid bodies. This Manual is not concerned with the solution of the thermodynamic problem. The purpose of the Manual is to provide analytical techniques for the determination of deformations and stresses in structures subjected to mechanical loads and prescribed temperature distributions.

In order to render problems amenable to engineering application, simplifying assumptions and idealizations are made. These are enumerated in the appropriate sections of the Manual. The subject matter is oriented toward the engineer rather than the mathematician in that detailed derivations of techniques and formulas are not emphasized. Instead, more space is devoted to application and qualitative discussions. Mathematical derivations can be found in the references listed at the end of each section.

The choice of subject material was primarily dictated by those problems which are tractable analytically and which occur most frequently in practice. However, in many instances, suggestions are made for the extension of techniques to more complex problems. Most of the problems treated are linear elastic, in which the stiffness may vary pointwise over the structure but does not vary with load. Furthermore, in the more difficult problems (e.g., plates and shells), it is assumed that temperature variations do not affect the stiffnesses significantly. Non-linear problems are, for the most part, discussed qualitatively.

Brief summaries of the nine sections of the Manual follow.

Sections 1 and 2 of the Manual briefly discuss the theoretical considerations and fundamental techniques which underlie the structural applications. Section 1 presents the essential ideas of strain and stress, the concepts of equilibrium and compatibility, and discusses the important energy theorems. General techniques (e.g., virtual work, virtual displacements, flexibility and stiffness methods) are covered in Section 2. It is recommended that standard texts and the references listed at the ends of the sections be consulted for a more complete development of these subjects.

Elevated temperature environments generally cause the non-linear behavior of engineering materials to become more pronounced, and the designer is forced to reassess the interacting effects of stress, temperature, and time upon structural materials. Section 3 discusses the deformation mechanism and postulates a stress-strain-temperature-time relationship which takes these non-linear effects into account. Methods of determining the necessary material parameters from simple test data are indicated.

Section 4 presents the thermo-elastic analysis of beams. Since beam analysis is a frequently occuring structural problem, much space is devoted to the presentation of approximate time-saving techniques. The deformations and stresses in unrestrained beam cross

sections are discussed in detail. Temperature distributions are represented by polynomials, cross sectional geometries are expressed parametrically, and non-dimensional solutions are developed. The common form of tabular solutions is also included. General techniques are then presented for the solution of indeterminate beam systems. The concept of equivalent fixed end reactions is employed in reducing the thermal problem to a mechanical loading problem.

Section 5 deals with the thermo-elastic analysis of joints subjected to mechanical loads and temperature. The loads in the attachments are presented in non-dimensional graphical form. The flexibility of the plate material and of the hole-pin combination are considered in the solutions. The effects of rigid pins, rigid sheets and "slop" are evaluated. The problem is initially presented for a joint which does not bend and then is modified to indicate the change in the non-dimensional parameters with bending.

Section 6 is concerned with the determination of thermal stresses and deflections in plates due to temperatures which vary through both the plate plane and the plate thickness. The major problem areas considered are

(1) The bending of ciruclar and rectangular plates.
(2) The axisymmetrical and asymmetrical slab problem (plane stress and plane strain) for circular plates and rings.

Sections 7 and 8 present the thermo-elastic analysis for the stresses and deformations of axisymmetric shells subjected to axisymmetric loads and temperatures. Solutions are given for the conical shells which can approximate the solutions for other structural shapes. Solutions for the compatibility forces which are generated at boundaries of conical segments, edges, or bulkheads are included to complete the analysis.

Section 9 deals with the instability of structures. Approximate methods are emphasized in order to include the effects of temperature on stiffness and plastic behavior. Use is made of non-dimensional buckling curves to reduce the amount of data required by instability problem solutions.

Manuscript released by the authors September 1960 for publication as a WADD Technical Report.

SECTION 1

THEORETICAL CONSIDERATIONS

SECTION 1

THEORETICAL CONSIDERATIONS

TABLE OF CONTENTS

Paragraph	Title	Page
1	Theoretical Considerations	1.2
1.1	Strain	1.3
1.1.1	Compatibility	1.6
1.2	Traction and Stress	1.7
1.2.1	Stress Equations of Equilibrium in Cartesian Coordinates	1.9
1.3	Boundary Conditions	1.11
1.4	Stress-Strain Relationship	1.12
1.5	Uniqueness	1.15
1.6	Special Orthogonal Coordinate Systems	1.15
1.7	Energy Principles	1.18
1.7.1	Principle of Virtual Work	1.18
1.7.2	Variational Principles	1.19
1.7.2.1	Definitions of Terms	1.20
1.7.2.2	Variational Techniques	1.21
1.7.2.3	Minimum Potential Energy	1.23
1.7.2.4	Minimum Complementary Energy	1.25
1.8	References	1.27

SECTION 1 - THEORETICAL CONSIDERATIONS

The general problem considered is the determination of the stresses and deformations in a structure when subjected to a given load-temperature distribution. The problem can be exceedingly complex and it is essential that the engineer have some concept of the structure's behavior. Many difficult problems can be approximated by neglecting parameters which are of small significance. The significance of a parameter can only be estimated if the behavior of the structure is known. The introduction of temperature into the problem may complicate the solution but it does not alter the structural techniques. It is, therefore, mandatory that the engineer become cognizant of the structural principles before he attempts to solve the thermal problen .

When a structure is subjected to mechanical and thermal stimuli, it responds by deforming and storing energy. The deformation is characterized by a "strain distribution" with an accompanying "stress and energy density distribution". The determination of these distributions requires an understanding of the concepts of strain and compatibility, stress and equilibrium, boundary conditions, uniqueness of solutions, and the stationary characteristics of the energy forms. These concepts are briefly discussed in this section.

The following symbols are used throughout this section:

$\underline{\ell}$	Length of beam
$\underline{n}$	Unit vector normal to surface
n_i	Cosine of angle between normal to the surface and i axis
$\underline{r}$	Cylindrical or spherical coordinate
$\underline{t}$	Traction vector
$\underline{u}$	Displacement vector with components u_1, u_2, u_3
x, y, z	Distances along the coordinate axes
B	Body
E	Young's modulus
E_s	Secant modulus
F_i	Body force per unit of volume acting in i direction
G	Shear modulus
K	Spring constant
L	Potential energy
L*	Complementary potential energy
P	Point in a body; Concentrated load
Q	Point in a body
R	Region of body; Reaction
S	Surface
T	Temperature
U	Strain energy
U*	Complementary strain energy
U_V	Strain energy per unit volume
U^*_V	Complementary strain energy per unit volume
V	Volume
W	Loss in potential energy of the surface tractions and body forces
W_t	Loss in potential energy where the tractions are prescribed

W_u	Loss in potential energy where the displacements are precribed
X, Y, Z	Traction in x, y, z directions
α	Coefficient of linear expansion
δ	Operator indicating a small change
Δ	Deflection
ϵ_{ij}	i=j: Extensional strain in the i^{th} direction i≠j: Shearing strain. Half the angle change between two initially perpendicular lines in the i and j directions.
Θ	Cylindrical or spherical coordinate
Θ	$\sigma_{xx} + \sigma_{yy} + \sigma_{zz}$
ν	Poisson's ratio
σ	Stress
σ_{ij}	Stress components acting on plane perpendicular to i direction and in the j direction
ψ	Spherical coordinate
ω	Rotation

Subscripts

i, j	Dummy subscripts
n	Acting on plane perpendicular to n direction
x, y, z	Referring to x, y, z directions
r, Θ, ψ	Referring to r, Θ, ψ directions.
,	Symbol for differentiation; e.g., $u_{i,j} \equiv \frac{\partial u_i}{\partial x_j}$

Superscripts

'	Displaced position

1.1 STRAIN

A body is said to be strained when the relative positions of points in the body are altered. The changes in the relative positions of points are called deformations, and the study of deformations is the province of the analysis of strain.

Although all material bodies are to some extent deformable, it is useful to introduce the ideal case of a rigid body, i.e., one which does not deform. A rigid body is one for which the distance between every pair of points remains the same throughout its history.

Let the non-rigid body B, in the undeformed state, occupy some region R referred to an orthogonal set of Cartesian axes $0\text{-}x_1\ x_2\ x_3$ (Figure 1.1-1) fixed in space. Let $P\ (x_1, x_2, x_3)$ represent a typical point P. In the strained state, the points of B will occupy some region R' and the point $P\ (x_1, x_2, x_3)$ will displace to the point $P'\ (x_1', x_2', x_3')$. The displacement $\bar{u}$ is a vector and is given by

$$\bar{u} = (u_1, u_2, u_3) = (x_1' - x_1, x_2' - x_2, x_3' - x_3) .$$

1.1 (Cont'd)

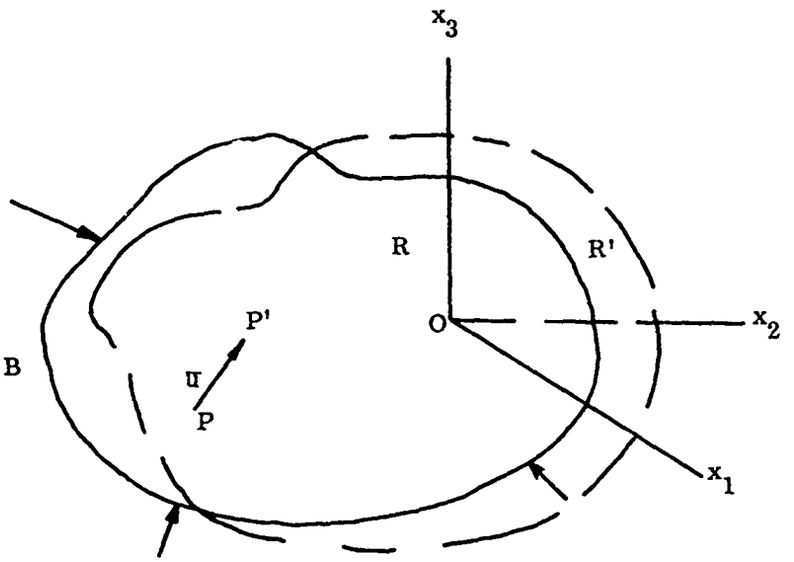


FIGURE 1.1-1 DISPLACEMENT OF A STRUCTURE UNDER MECHANICAL AND/OR THERMAL LOADS

Now consider two neighboring points O (0, 0, 0) and O' (x_1, x_2, x_3) before deformation. Determination of their relative displacements due to some external stimulus is of interest. From the Taylor's Expansion Theorem of the calculus,

$$u_i(x_1, x_2, x_3) = u_i(0,0,0) + \left(\frac{\partial u_i}{\partial x_1}\right)_{(0,0,0)} x_1 + \left(\frac{\partial u_i}{\partial x_2}\right)_{(0,0,0)} x_2 + \left(\frac{\partial u_i}{\partial x_3}\right)_{(0,0,0)} x_3$$

+ terms involving the higher derivatives, (1a)

or, more compactly,

$$u_i(x) = u_i(0) + \sum_{j=1}^{3} \left(\frac{\partial u_i}{\partial x_j}\right)_0 x_j + \ldots \quad . \tag{1b}$$

Let the symbol $u_{i,j}$ be defined by $u_{i,j} = \dfrac{\partial u_i}{\partial x_j}$.

Then the expression (1a) becomes

$$u_i(x) = u_i(0) + \sum_{j=1}^{3} (u_{i,j})_0 x_j + \ldots \quad . \tag{1c}$$

1.1 (Cont'd)

Furthermore,

$$(u_{i,j}) = \frac{1}{2}\,(u_{i,j} + u_{j,i}) + \frac{1}{2}\,(u_{i,j} - u_{j,i}) \quad ,$$

is an algebraic identity.

Introduce the symbols

$$\epsilon_{ij} = \frac{1}{2}\,(u_{i,j} + u_{j,i}) \quad ,$$

and (2)

$$\omega_{i,j} = \frac{1}{2}\,(u_{i,j} - u_{j,i}) \quad ,$$

so that the relative displacement of the neighboring points is

$$u_i(x) - u_i(0) = \sum_{j=1}^{3} \left[\epsilon_{ij} + \omega_{ij}\right]_0 x_j + \ldots \quad .$$

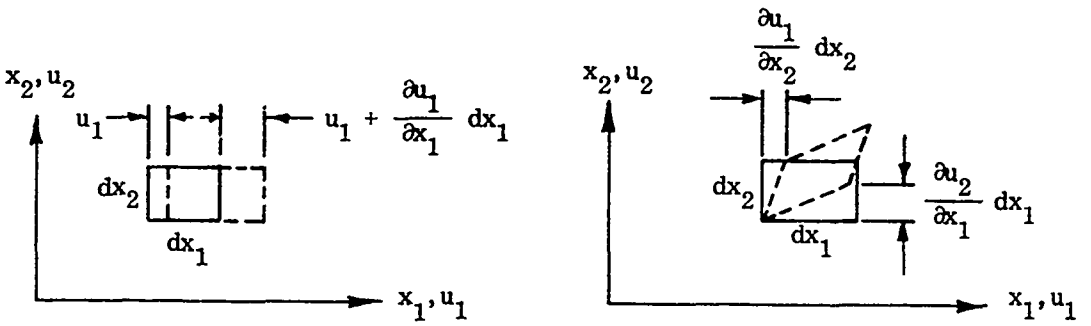
The quantities ϵ_{ij} are symmetrical in the indices, i.e., $\epsilon_{ij} = \epsilon_{ji}$ and are known as the components of strain (Reference 1-1).

Example 1: $\epsilon_{11} = u_{1,1} = \dfrac{\partial u_1}{\partial x_1}$ is the longitudinal component of strain in the x_1 direction, (Figure 1.1-2(a)) $u_{i,i} = \dfrac{\partial u_i}{\partial x_i}$ is the longitudinal or extensional component of strain in the x_i direction.

Example 2: $\epsilon_{12} = \epsilon_{21} = \dfrac{1}{2}\left[\dfrac{\partial u_1}{\partial x_2} + \dfrac{\partial u_2}{\partial x_1}\right]$ is half the change in the angle between two line elements which were originally at right angles to each other and is referred to as the shearing component of strain in the x_1-x_2 plane (Figure 1.1-2(b)).

The quantities ω_{ij} are skew symmetrical, i.e., $\omega_{ij} = -\omega_{ji}$ and are known as the components of rotation because they can be shown to represent components of a rigid body rotation (Reference 1-1).

At each point of the body, there exists a set of three mutually orthogonal directions for which the shearing strains are zero. These directions are called the principal axes of strain and the corresponding extensional strains are the principal strains. The principal axes of strain remain perpendicular to each other after the deformation, and an elemental rectangular parallelepiped with edges parallel to the principal axes remains a rectangular parallelepiped after deformation. In general, it will have also undergone a small rotation (Reference 1-2).



(a) Extensional Strain (b) Shearing Strain

FIGURE 1.1-2 TYPES OF STRAIN

1.1.1 Compatibility

From a physical point of view, the displacement u_i in a simply-connected continuous body must be single valued and continuous. Certain restrictions must be placed on the strains ϵ_{ij} in order that this be so. These restrictions constitute the so-called strain-compatibility equations.

The compatibility equations are obtained by considering the defining formulas for the strain components in rectangular coordinates:

$$\frac{1}{2}\left[u_{i,j} + u_{j,i}\right] = \epsilon_{ij} \quad , \tag{1}$$

as a system of partial differential equations from which the displacements u_i are to be determined when the strain components ϵ_{ij} are prescribed functions of the coordinates. If the body is simply-connected, it can be shown (Reference 1-1) that the conditions on the strains necessary and sufficient to ensure single-valued, continuous solutions for the displacements constitute six independent partial differential equations. Expressed in Cartesian coordinates, they are:

1.1.1 (Cont'd)

$$\frac{\partial^2 \epsilon_{xx}}{\partial y \partial z} = \frac{\partial}{\partial x}\left(-\frac{\partial \epsilon_{yz}}{\partial x} + \frac{\partial \epsilon_{zx}}{\partial y} + \frac{\partial \epsilon_{xy}}{\partial z}\right)$$

$$\frac{\partial^2 \epsilon_{yy}}{\partial z \partial x} = \frac{\partial}{\partial y}\left(-\frac{\partial \epsilon_{zx}}{\partial y} + \frac{\partial \epsilon_{xy}}{\partial z} + \frac{\partial \epsilon_{yz}}{\partial x}\right)$$

$$\frac{\partial^2 \epsilon_{zz}}{\partial x \partial y} = \frac{\partial}{\partial z}\left(-\frac{\partial \epsilon_{xy}}{\partial z} + \frac{\partial \epsilon_{yz}}{\partial x} + \frac{\partial \epsilon_{zx}}{\partial y}\right) \qquad (2)$$

$$2\frac{\partial^2 \epsilon_{xy}}{\partial x \partial y} = \frac{\partial^2 \epsilon_{xx}}{\partial y^2} + \frac{\partial^2 \epsilon_{yy}}{\partial x^2}$$

$$2\frac{\partial^2 \epsilon_{yz}}{\partial y \partial z} = \frac{\partial^2 \epsilon_{yy}}{\partial z^2} + \frac{\partial^2 \epsilon_{zz}}{\partial y^2}$$

$$2\frac{\partial^2 \epsilon_{zx}}{\partial z \partial x} = \frac{\partial^2 \epsilon_{zz}}{\partial x^2} + \frac{\partial^2 \epsilon_{xx}}{\partial z^2} \quad .$$

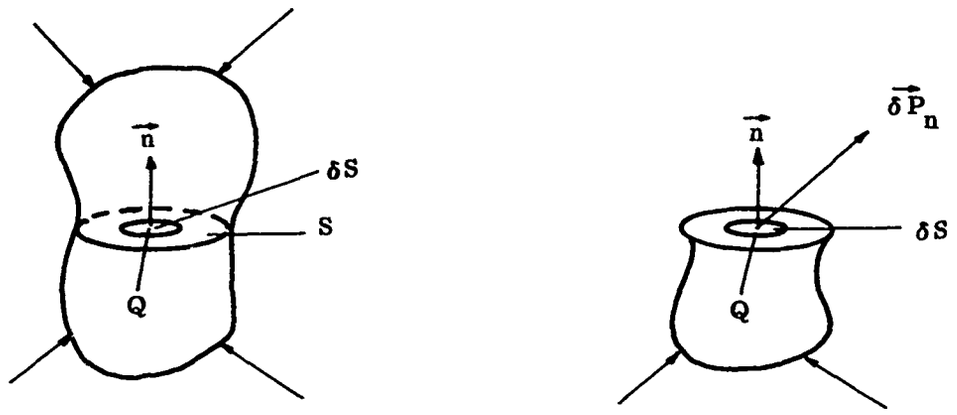
The above compatibility equations (valid for both thermal and mechanical problems) also ensure the determination of the relative displacements from Eq. (1).

If the body is multiply connected (has internal cavities), then additional conditions are necessary to ensure single-valued displacements. These conditions specify that the limiting values of the displacements at imaginary cuts which make the body simply connected, be the same when a cut is approached from either side.

1.2 TRACTION AND STRESS

The internal forces in a body are usually described in terms of the "stress states" throughout the body. Consider some point Q lying on the surface S of the body shown in Figure 1.2-1. Let the unit normal vector to the surface at the point Q be designated by $\vec{n}$, and the force acting on δS, which encompasses the point, by $\delta \vec{P}_n$. Then the traction acting across the surface S at the point Q is defined as

$$\vec{t}_n = \lim_{\delta S \to 0} \frac{\delta \vec{P}_n}{\delta S} \quad . \qquad (1)$$



(a) Uncut Body (b) Free Body

FIGURE 1.2-1 TRACTIONS AT THE POINT Q ACTING ON THE PLANE WITH NORMAL $\vec{n}$

The traction is thus a vector which specifies the force acting per unit of area at a point. The components of the traction vector in a given set of directions are defined as the stress components. The stress components at a given point are dependent upon the orientation of the plane through the point with respect to the chosen coordinate system. Thus, for example, in a rectangular coordinate system (Figure 1.2-2), the stress components in the x, y, and z directions of the traction $\vec{t}_x$, acting on the face normal to the x axis, are σ_{xx}, σ_{xy} and σ_{xz}, respectively. Here, the first subscript indicates the direction normal to the area on which the stress component acts and the second subscript refers to the direction of the component.

All the remarks pertinent to principal strains apply to the stresses. In addition, when the material is isotropic, then the principal directions of stress and strain coincide.

1.2 (Cont'd)

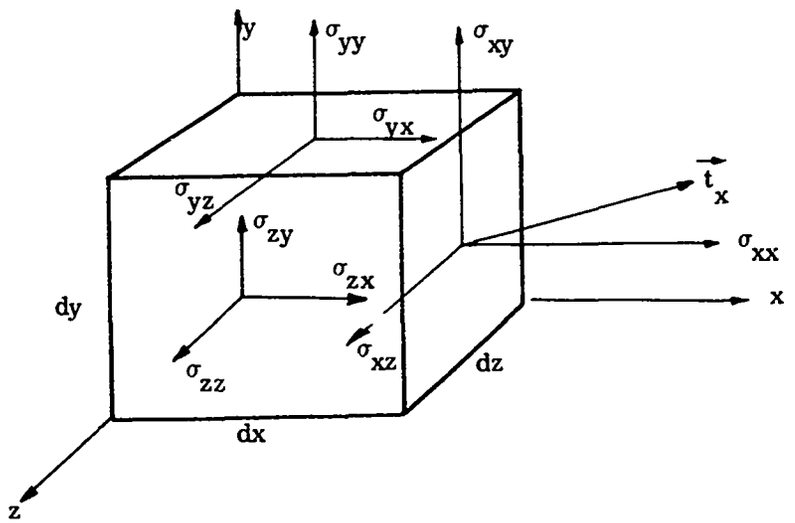


FIGURE 1.2-2 STRESS COMPONENTS

1.2.1 Stress Equations of Equilibrium in Cartesian Coordinates

The equilibrium equations state that the sum of the forces acting on a differential element of material are in static or dynamic equilibrium.

Figure 1.2.1-1 illustrates an elemental rectangular parallelepiped with edges parallel to the x, y and z axes. In addition to the stresses acting on the faces, there may exist body forces $\vec{F}$ dxdydz, where $\vec{F}$ is the body force per unit of volume. In most practical applications, the body forces are due either to the weight of the body in a static problem or D'Alembert inertia forces in a dynamic problem.

Equilibrium of forces in the x direction requires that:

$$\frac{\partial \sigma_{xx}}{\partial x} + \frac{\partial \sigma_{yx}}{\partial y} + \frac{\partial \sigma_{zx}}{\partial z} + F_x = 0$$

Similarly, for the y and z directions,

1.2.1 (Cont'd)

$$\frac{\partial \sigma_{xy}}{\partial x} + \frac{\partial \sigma_{yy}}{\partial y} + \frac{\partial \sigma_{zy}}{\partial z} + F_y = 0$$

$$\frac{\partial \sigma_{xz}}{\partial x} + \frac{\partial \sigma_{yz}}{\partial y} + \frac{\partial \sigma_{zz}}{\partial z} + F_z = 0 \ . \qquad \text{(1a)}$$

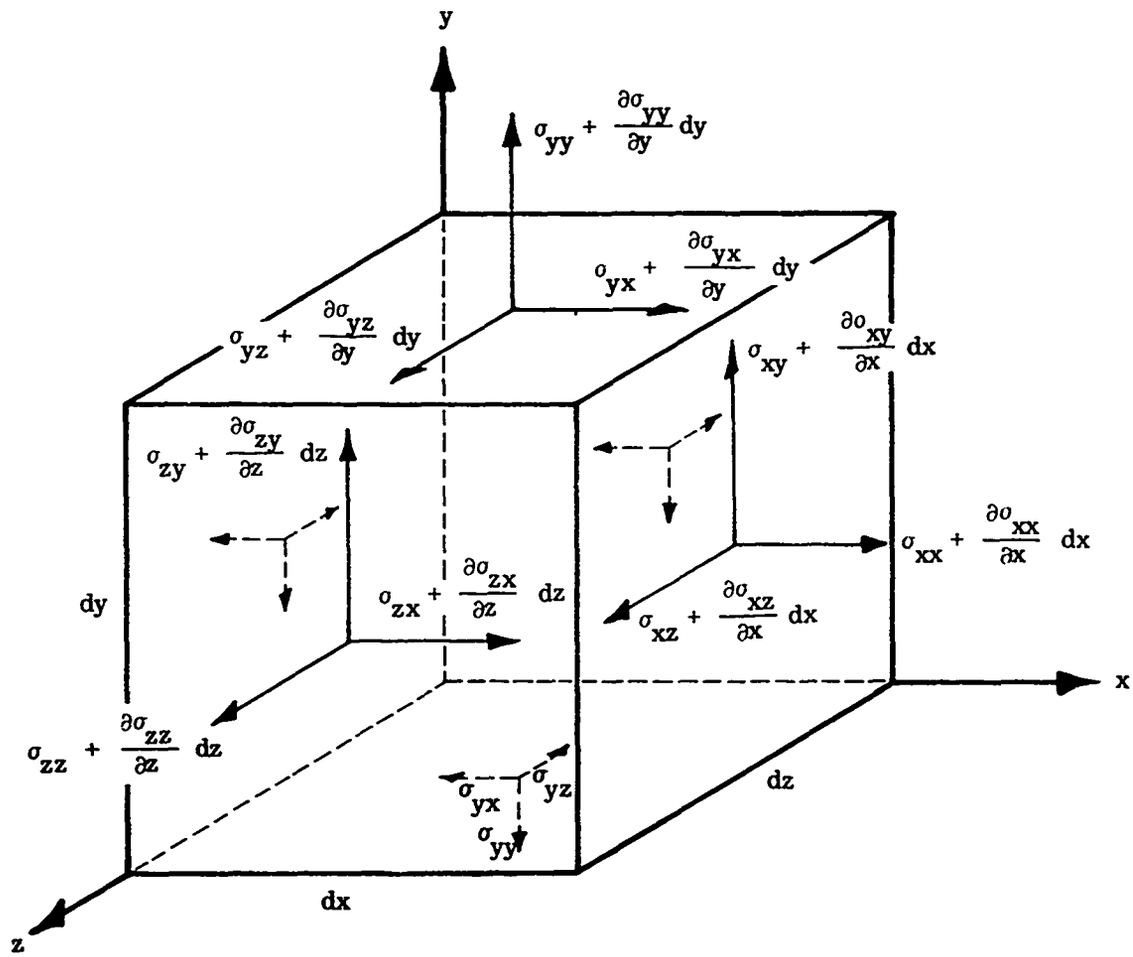


FIGURE 1.2.1-1 STRESS COMPONENTS ON RECTANGULAR PARALLELEPIPED

1.2.1 (Cont'd)

Conservation of angular momentum (equilibrium of moments) leads to equality of cross-shears, or

$$\sigma_{xy} = \sigma_{yx}$$
$$\sigma_{yz} = \sigma_{zy} \qquad (1b)$$
$$\sigma_{zx} = \sigma_{xz} \quad .$$

Consequently, the significant number of stress components is reduced from nine to six. The equations of equilibrium in other than Cartesian coordinates take different forms (Section 1.6).

1.3 BOUNDARY CONDITIONS

In order to have a complete solution, something must be known about each point on the bounding surface of a structure. Either the surface tractions (applied stresses) must be known or the displacements must be specified (e.g., zero displacements at a support) or a known relationship between the tractions and displacements must be prescribed (e.g., flexible support of known stiffness).

The prescribed traction components in the directions of the chosen coordinate axes may be expressed in terms of the surface stresses by means of the equilibrium equations

$$X = \sigma_{xx} n_x + \sigma_{yx} n_y + \sigma_{zx} n_z$$
$$Y = \sigma_{xy} n_x + \sigma_{yy} n_y + \sigma_{zy} n_z \qquad (1)$$
$$Z = \sigma_{xz} n_x + \sigma_{yz} n_y + \sigma_{zz} n_z \quad ,$$

where X = component of traction in the x direction, etc. (Figure 1.3-1), $n_x = \cos(n,x)$ = cosine of the angle between the normal to the surface and the x axis.

1.3 (Cont'd)

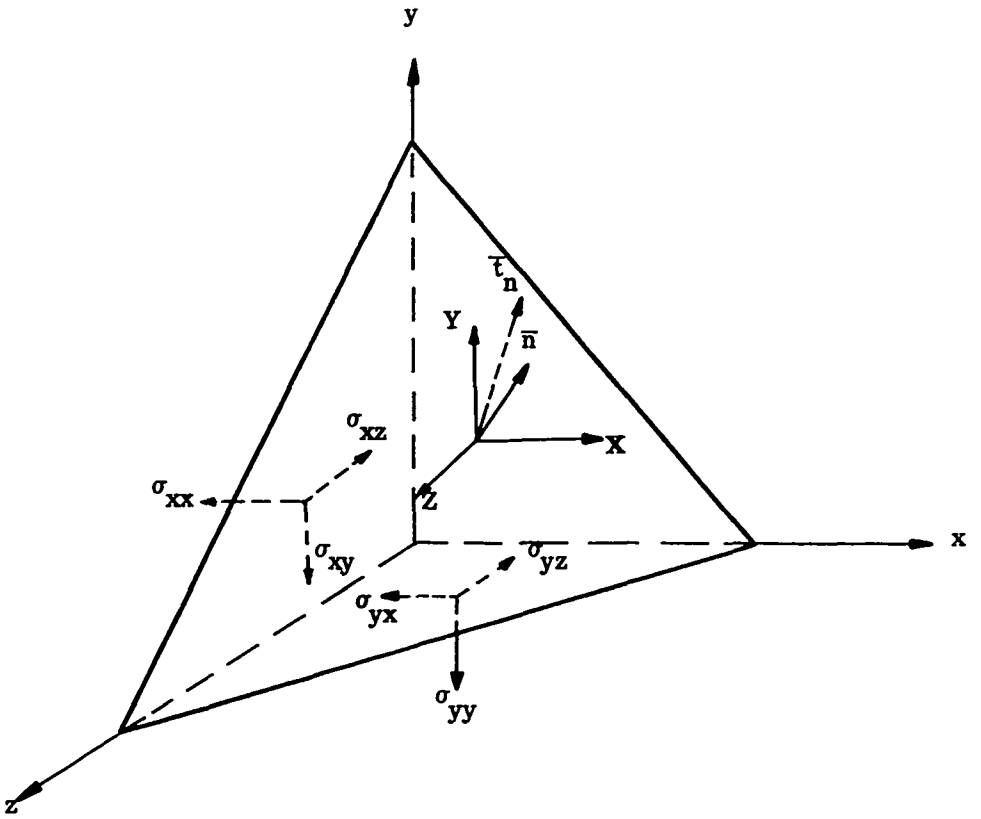


FIGURE 1.3-1 SPECIFICATION OF SURFACE TRACTIONS

1.4 STRESS-STRAIN RELATIONSHIP

The complete solution of a problem in elasticity requires the determination of six stress components, three displacement components and six strain components at each point of a body. Fifteen independent equations are required for the evaluation of these quantities. Nine of these equations have already been presented, namely the six strain displacement relations (Eqs. (2) of Sub-section 1.1, which ensure that the compatibility equations are satisfied when the displacements are single-valued) and the three equilibrium equations (Eqs. (1) of Paragraph 1.2.1). Both of these sets of equations are independent of the material properties of the body.

1.4 (Cont'd)

The remaining six equations are obtained from a stress-strain relationship between the six stresses and six strains. It is through this relationship, which is a property of the material, that the effects of plasticity, temperature, creep, etc., come into play.

If the material is isotropic and linearly elastic, then the stress-strain relationship can be expressed as

$$\epsilon_{ii} = \frac{1}{E}\left[\sigma_{ii} - \nu\,(\sigma_{jj} + \sigma_{kk})\right] + \alpha T$$

$$\epsilon_{ij} = \frac{1+\nu}{E}\,\sigma_{ij} \qquad \left(i,j,k = 1,2,3\right), \tag{1a}$$

where E = elastic modulus,
ν = Poisson's ratio
α = linear coefficient of thermal expansion
T = Temperature above room temperature as a datum.

The shear modulus is defined by

$$G = \frac{E}{2(1+\nu)} \quad . \tag{1b}$$

Because of the isotropy of the material, the expansions due to temperature cause no shearing strains. The linear elastic-stress-strain relations for an isotropic material are of the form of Eq. (1a) for any orthogonal coordinate system (rectangular or curvilinear). For example, in a rectangular coordinate system,

$$i,j,k = 1,2,3 = x,y,z \quad ,$$

while for a cylindrical coordinate system,

$$i,j,k = 1,2,3 = r,\ \Theta,\ z \quad .$$

The linear stress-strain relationships of Eq. (1a) can be modified to provide stress-strain relationships for materials which are not linear elastic by employing an equivalent secant modulus $E_S = \frac{\sigma}{\epsilon - \alpha T}$ in place of E. Unfortunately, E_S will not be constant and direct solution of problems may be extremely difficult. A progressive solution may be possible by solving the problem for small increments of load-time histories where it is assumed that the modulus is constant in each interval, evaluating new constant moduli for the next increment, and continuing the process until the final load-time history is applied. This technique must assume the sense of the incremental stress since a material may have different moduli dependent on the direction of loading.

The strain-compatibility equations can now be converted to stress-compatibility equations through the stress-strain relationships. Thus for a linear-elastic stress-strain relationship with temperature, Eqs. (2) of Paragraph 1.1.1 become

$$(1+\nu)\,\nabla^2\,\sigma_{xx} + \frac{\partial^2 \Theta}{\partial x^2} + \alpha E\left[\frac{1+\nu}{1-\nu}\,\nabla^2 T + \frac{\partial^2 T}{\partial x^2}\right] = 0$$

$$(1+\nu)\,\nabla^2\,\sigma_{yy} + \frac{\partial^2 \Theta}{\partial y^2} + \alpha E\left[\frac{1+\nu}{1-\nu}\,\nabla^2 T + \frac{\partial^2 T}{\partial y^2}\right] = 0 \tag{2}$$

1.4 (Cont'd)

$$(1+\nu)\ \nabla^2 \sigma_{zz} + \frac{\partial^2 \Theta}{\partial z^2} + \alpha E \left[\frac{1+\nu}{1-\nu}\ \nabla^2 T + \frac{\partial^2 T}{\partial z^2} \right] = 0$$

$$(1+\nu)\ \nabla^2 \sigma_{xz} + \frac{\partial^2 \Theta}{\partial x \partial z} + \alpha E\ \frac{\partial^2 T}{\partial x \partial z} = 0$$

$$(1+\nu)\ \nabla^2 \sigma_{xy} + \frac{\partial^2 \Theta}{\partial x \partial y} + \alpha E\ \frac{\partial^2 T}{\partial x \partial y} = 0 \qquad \text{(2) cont'd}$$

$$(1+\nu)\ \nabla^2 \sigma_{yz} + \frac{\partial^2 \Theta}{\partial y \partial z} + \alpha E\ \frac{\partial^2 T}{\partial y \partial z} = 0\ ,$$

where

$$\Theta = \sigma_{xx} + \sigma_{yy} + \sigma_{zz}\ ,$$

or, in shorthand notation,

$$(1+\nu)\ \nabla^2 \sigma_{ij} + \Theta_{,ij} + \alpha E \left[\delta_{ij}\ \frac{1+\nu}{1-\nu}\ \nabla^2 T + T_{,ij} \right] = 0\ ,$$

where

$$\left.\begin{array}{l} \\ \delta_{ij} \end{array}\right\} \begin{array}{l} = 0,\ i \neq j \\ = 1,\ i = j \end{array}\ .$$

The stress compatibility equations can be employed to show that the only time the thermal stresses are identically zero in an unrestrained linear-elastic body is when the temperature is a linear function of the rectangular (x,y,z) coordinates. Assume all stress components $\sigma_{xx}, \ldots, \sigma_{yz}$ are zero. Then certainly the equilibrium equations are satisfied throughout the interior of the body and on the surface. Equations (2) reduce to

$$\frac{1+\nu}{1-\nu}\ \nabla^2 T + \frac{\partial^2 T}{\partial x^2} = 0 \qquad \frac{\partial^2 T}{\partial x\ \partial z} = 0$$

$$\frac{1+\nu}{1-\nu}\ \nabla^2 T + \frac{\partial^2 T}{\partial y^2} = 0 \qquad \frac{\partial^2 T}{\partial x\ \partial y} = 0 \qquad \text{(3)}$$

$$\frac{1+\nu}{1-\nu}\ \nabla^2 T + \frac{\partial^2 T}{\partial z^2} = 0 \qquad \frac{\partial^2 T}{\partial y\ \partial z} = 0\ ,$$

1.4 (Cont'd)

$$(1+\nu)\ \nabla^2 \sigma_{zz} + \frac{\partial^2 \Theta}{\partial z^2} + \alpha E \left[\frac{1+\nu}{1-\nu}\ \nabla^2 T + \frac{\partial^2 T}{\partial z^2} \right] = 0$$

$$(1+\nu)\ \nabla^2 \sigma_{xz} + \frac{\partial^2 \Theta}{\partial x \partial z} + \alpha E\ \frac{\partial^2 T}{\partial x \partial z} = 0$$

$$(1+\nu)\ \nabla^2 \sigma_{xy} + \frac{\partial^2 \Theta}{\partial x \partial y} + \alpha E\ \frac{\partial^2 T}{\partial x \partial y} = 0 \qquad (2)\ \text{cont'd}$$

$$(1+\nu)\ \nabla^2 \sigma_{yz} + \frac{\partial^2 \Theta}{\partial y \partial z} + \alpha E\ \frac{\partial^2 T}{\partial y \partial z} = 0\ ,$$

where

$$\Theta = \sigma_{xx} + \sigma_{yy} + \sigma_{zz}\ ,$$

or, in shorthand notation,

$$(1+\nu)\ \nabla^2 \sigma_{ij} + \Theta_{,ij} + \alpha E \left[\delta_{ij}\ \frac{1+\nu}{1-\nu}\ \nabla^2 T + T_{,ij} \right] = 0\ ,$$

where

$$\left.\begin{array}{l} \\ \delta_{ij} \end{array}\right\} \begin{array}{l} = 0,\ i \neq j \\ = 1,\ i = j \end{array}\ .$$

The stress compatibility equations can be employed to show that the only time the thermal stresses are identically zero in an unrestrained linear-elastic body is when the temperature is a linear function of the rectangular (x,y,z) coordinates. Assume all stress components $\sigma_{xx}, \ldots, \sigma_{yz}$ are zero. Then certainly the equilibrium equations are satisfied throughout the interior of the body and on the surface. Equations (2) reduce to

$$\frac{1+\nu}{1-\nu}\ \nabla^2 T + \frac{\partial^2 T}{\partial x^2} = 0 \qquad \frac{\partial^2 T}{\partial x\ \partial z} = 0$$

$$\frac{1+\nu}{1-\nu}\ \nabla^2 T + \frac{\partial^2 T}{\partial y^2} = 0 \qquad \frac{\partial^2 T}{\partial x\ \partial y} = 0 \qquad (3)$$

$$\frac{1+\nu}{1-\nu}\ \nabla^2 T + \frac{\partial^2 T}{\partial z^2} = 0 \qquad \frac{\partial^2 T}{\partial y\ \partial z} = 0\ ,$$

1.4 (Cont'd)

which yields the condition

$$\frac{\partial^2 T}{\partial x^2} = \frac{\partial^2 T}{\partial y^2} = \frac{\partial^2 T}{\partial z^2} = \frac{\partial^2 T}{\partial x\,\partial y} = \frac{\partial^2 T}{\partial y\,\partial z} = \frac{\partial^2 T}{\partial x\,\partial y} = 0 \quad . \tag{4}$$

Equations (4) have the unique solution that T must be of the form

$$T = Ax + By + Cz + D \quad , \tag{5}$$

where A, B, C, D are constants; i.e., T is at most a linear function of the rectangular coordinates x, y, and z.

NOTE: If T = Ar for an unrestrained circular plate where r is the radial coordinate measured from the center, there will be thermal stresses. This follows because T is linear in r but not in x and y where

$$r = \sqrt{x^2 + y^2} \quad .$$

1.5 UNIQUENESS

The strain displacement relations, equilibrium equations, and linear stress-strain relations provide a set of equations from which the stresses, strains, and displacements are to be determined at each point of a linear elastic body. From this set of equations, together with appropriate boundary conditions, it can be proven not only that there exists a solution to the linear elasticity problem but also that the solution is unique.

In a simple form (see Reference 1-1 for a more complete discussion), Kirchhoff's Uniqueness Theorem can be stated as follows: If the initial displacements, velocities, body forces and temperatures are specified throughout the volume, and if the compatibility conditions discussed in Paragraph 1.1.1 are satisfied and the appropriate boundary conditions (Sub-section 1.3) are specified over the entire surface, there exists only one form of equilibrium in the sense that the distribution of stresses and strains is determined uniquely.

The above theorem applies to elasticity problems with infinitesimal strains and displacements. If the strains and displacements are finite, the solution may not be unique as in problems concerning elastic stability (Section 9), where different equilibrium configurations are possible. The uniqueness of the solution for infinitesimal strains suggests the utilization of the incremental method for closer approximations of the non-linear problem. Consideration should be given to changes in stiffness, geometry, etc., with load-temperature history.

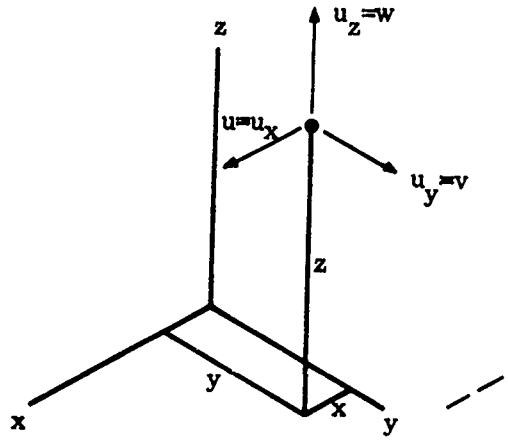
1.6 SPECIAL ORTHOGONAL COORDINATE SYSTEMS

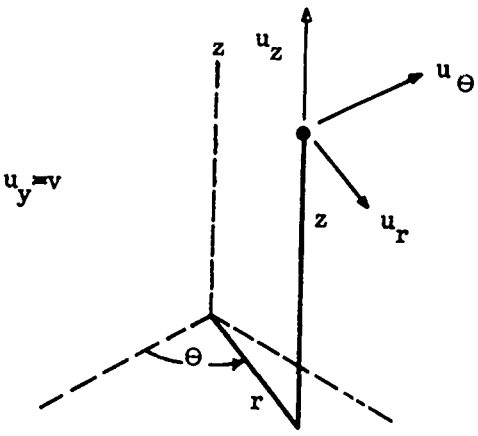
The representation of the stress-strain relationships, strain-displacement equations and the equilibrium equations depends upon the system of reference employed. It is often convenient to select a coordinate system which will simplify the boundary conditions and required solution. The three most useful orthogonal coordinate systems are the rectangular, cylindrical and the spherical. For linear elastic, isotropic bodies, the stress-strain relationships (Eq. (1a) of Sub-section 1.4) are of the same form for all orthogonal coordinate systems. The strain-displacement equations and equilibrium equations have already been presented in rectangular coordinates. The cylindrical and spherical counterparts are shown in Tables 1.6-1 and -2. These expressions are simplified if the three dimensional problem reduces to a two or one dimensional problem.

TABLE 1.6-1

STRAIN-DISPLACEMENT RELATIONSHIP

Rectangular	Cylindrical	Spherical
$\epsilon_{xx} = u_{,x}$	$\epsilon_{rr} = u_{r,r}$	$\epsilon_{rr} = u_{r,r}$
$\epsilon_{yy} = v_{,y}$	$\epsilon_{\theta\theta} = \frac{1}{r}(u_{\theta,\theta} + u_r)$	$\epsilon_{\theta\theta} = \frac{1}{r}(u_{\theta,\theta} + u_r)$
$\epsilon_{zz} = w_{,z}$	$\epsilon_{zz} = u_{z,z}$	$\epsilon_{\psi\psi} = \frac{1}{r \sin\theta} u_{\psi,\psi} + \frac{1}{r} u_r + \frac{\cot\theta}{r} u_\theta$
$\epsilon_{xy} = \frac{1}{2}(u_{,y} + v_{,x})$	$\epsilon_{r\theta} = \frac{1}{2}(\frac{1}{r} u_{r,\theta} + u_{\theta,r} - \frac{1}{r} u_\theta)$	$\epsilon_{r\theta} = \frac{1}{2}(\frac{1}{r} u_{r,\theta} + u_{\theta,r} - \frac{1}{r} u_\theta)$
$\epsilon_{xz} = \frac{1}{2}(u_{,z} + w_{,x})$	$\epsilon_{rz} = \frac{1}{2}(u_{z,r} + u_{r,z})$	$\epsilon_{r\psi} = \frac{1}{2}(\frac{1}{r \sin\theta} u_{r,\psi} + u_{\psi,r} - \frac{1}{r} u_\psi)$
$\epsilon_{yz} = \frac{1}{2}(v_{,z} + w_{,y})$	$\epsilon_{\theta z} = \frac{1}{2}(\frac{1}{r} u_{z,\theta} + u_{\theta,z})$	$\epsilon_{\psi\theta} = \frac{1}{2}(\frac{1}{r} u_{\psi,\theta} + \frac{1}{r \sin\theta} u_{\theta,\psi} - \frac{\cot\theta}{r} u_\psi)$





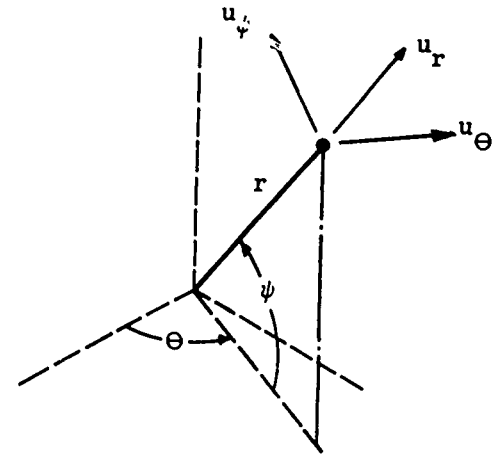


TABLE 1.6-2

EQUATIONS OF EQUILIBRIUM

$$\sigma_{ij,i} + F_j = 0$$

Rectangular

$$\sigma_{xx,x} + \sigma_{yx,y} + \sigma_{zx,z} + F_x = 0$$

$$\sigma_{xy,x} + \sigma_{yy,y} + \sigma_{zy,z} + F_y = 0$$

$$\sigma_{xz,x} + \sigma_{yz,y} + \sigma_{zz,z} + F_z = 0$$

Cylindrical

$$\sigma_{rr,r} + \frac{1}{r}\sigma_{r\theta,\theta} + \sigma_{rz,z} + \frac{\sigma_{rr} - \sigma_{\theta\theta}}{r} + F_r = 0$$

$$\sigma_{r\theta,r} + \frac{1}{r}\sigma_{\theta\theta,\theta} + \sigma_{z\theta,z} + \frac{2}{r}\sigma_{r\theta} + F_\theta = 0$$

$$\sigma_{rz,r} + \frac{1}{r}\sigma_{\theta z,\theta} + \sigma_{zz,z} + \frac{1}{r}\sigma_{rz} + F_z = 0$$

Spherical

$$0 = \sigma_{rr,r} + \frac{1}{r}\sigma_{\theta r,\theta} + \frac{1}{r\sin\theta}\sigma_{\psi r,\psi} + \frac{2\sigma_{rr} - \sigma_{\theta\theta} - \sigma_{\psi\psi} + \sigma_{r\theta}\cot\theta}{r} + F_r$$

$$0 = \sigma_{r\theta,r} + \frac{1}{r}\sigma_{\theta\theta,\theta} + \frac{1}{r\sin\theta}\sigma_{\psi\theta,\psi} + \frac{3\sigma_{r\theta} + (\sigma_{\theta\theta} - \sigma_{\psi\psi})\cot\theta}{r} + F_\theta$$

$$0 = \sigma_{r\psi,r} + \frac{1}{r}\sigma_{\theta\psi,\theta} + \frac{\partial}{r\sin\theta}\frac{1}{\sigma_{\psi\psi,\psi}} + \frac{3\sigma_{r\psi} + 2\cot\theta\,\sigma_{\theta\psi}}{r} + F_\psi$$

1.7 ENERGY PRINCIPLES

The behaviour of a structure can be described by means of energy principles which yield relationships between the stresses, strains, displacements and forces when adequate conditions (boundary, temperature-load-time history, material properties, etc.) are defined. These principles can be derived from the "Principle of Virtual Work" which is a restatement of conservation of energy.

1.7.1 Principle of Virtual Work

"If a body is in equilibrium under the action of prescribed body and surface forces, the work done by these forces in a small additional displacement, the virtual displacement δu, is equal to the change in the internal strain energy, second order terms in the increments of strain being neglected." The strain energy is defined in Paragraph 1.7.2.1.

A qualitative argument supporting this theorem is as follows:

The body "B" with surface S (Figure 1.7.1-1) is in equilibrium under the action of the applied external force, body forces, and internal stress systems, represented

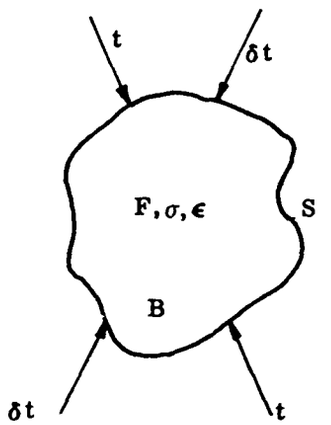


FIGURE 1.7.1-1 ELASTIC BODY WITH APPLIED FORCES

symbolically by "t", "F" and "σ", respectively. If an incremental, self-equilibrating external force system "δt" is imposed, there result corresponding internal stresses $\delta\sigma$, strains $\delta\epsilon$ and continuous displacements δu. From conservation of energy,

$$\int_S t\delta u dS + \int_B F\delta u dV + (\text{terms of order } \delta u\delta t)$$

$$= \int_B \sigma\delta\epsilon \, dV + (\text{terms of order } \delta\sigma\delta\epsilon) \quad .$$

1.7.1 (Cont'd)

Neglecting second order terms,

$$\int_S t\delta u dS + \int_B F\delta u dV = \int_B \sigma\delta\epsilon dV, \tag{1}$$

which is the mathematical statement of the theorem.

A consequence of the theorem of virtual work is the Reciprocal Theorem of Betti and Rayleigh: If an elastic body is subjected to two systems of body and surface forces, then the work that would be done by the first system t_i, F_i (surface tractions and body forces, respectively) in acting through the displacements u_i' due to the second system of forces, is equal to the work that would be done by the second system t_i', F_i' in acting through the displacements u_i due to the first system of forces. In symbols, the theorem becomes:

$$\int_S t_i u_i' dS + \int_B F_i u_i' dV = \int_S t_i' u_i dS + \int_B F_i' u_i dV \quad . \tag{2a}$$

where the repeated subscript i implies summation.

An alternate form of the reciprocal theorem is

$$\int_S t_i u_i' dS + \int_B F_i u_i' dV = \int_B \sigma_{ij} \epsilon'_{ij} dV \quad , \tag{2b}$$

where the unprimed quantities correspond to surface tractions, body forces, and stresses of the first system and the primed quantities to the displacements and strains of the second system. It is important to note that the forces and stresses of the first system can be unrelated to the displacements and strains of the second system, and may include thermal effects. The only requirements are that the force-stress system be in equilibrium and the strain displacement system be compatible. This feature of the reciprocal theorem makes it extremely useful in the solution of statically indeterminate problems (Paragraph 2.1.1).

REMARK: The virtual work and reciprocal theorems are quite general and are not restricted to elastic problems.

1.7.2 Variational Principles

The solution of three dimensional problems in the theory of elasticity represents in many cases an almost impossible task even for the isothermal or mechanical problem. For isotropic and homogeneous bodies, the literature contains only approximate solutions which are based upon simplifying assumptions. One very powerful method of attack which will yield approximate solutions is based upon that branch of mathematics which is known as the calculus of variations. The application of the calculus of variations to the field of elasticity and thermoelasticity depends upon the following variational principles:

(1) The principle of minimum potential energy, and

(2) The principle of minimum complementary energy (sometimes called complementary potential energy).

These in turn follow from the principle of virtual work which was discussed in Paragraph 1.7.1.

1.7.2 (Cont'd)

Before discussing the variational principles, in detail, it will be desirable to first define the energy terms employed and the mathematical operations which are essential to their proper application.

1.7.2.1 Definitions of Terms

Potential Energy of Surface Tractions and Body Forces: The loss in potential energy of the surface tractions t_i and body forces F_i is defined by

$$W = \int_S t_i u_i dS + \int_B F_i u_i dV \quad , \tag{1}$$

where the tractions t_i have the dimensions of force per unit of area and the body forces F_i have the dimensions of force per unit of volume. The displacements u_i, and hence the potential energy, are measured from a datum defined by the undeformed position of the body.

Strain Energy: The strain energy density in a deformable body is defined as the work done per unit of volume by the internal stresses when the stresses and corresponding strains vary from zero to their terminal values. The strain energy density may be expressed in terms of the stresses and strains as

$$U_V = \int_0^{\epsilon} \sigma d\epsilon \quad , \tag{2}$$

where, in Cartesian coordinates,

$$\begin{aligned} \sigma d\epsilon &= \sigma_{xx}\, d\epsilon_{xx} + \sigma_{yy}\, d\epsilon_{yy} + \sigma_{zz}\, d\epsilon_{zz} + 2\sigma_{xy}\, d\epsilon_{xy} \\ &\quad + 2\sigma_{yz}\, d\epsilon_{yz} + 2\sigma_{zx}\, d\epsilon_{zx} = \sigma_{ij}\, d\epsilon_{ij} \quad . \end{aligned} \tag{3}$$

Similarly

$$U_V^* = \int_0^{\sigma} \epsilon d\sigma \quad .$$

The strain energy of the body is then

$$U = \int_B U_V dV \quad . \tag{4}$$

In most problems it is convenient to express the strain energy in terms of internal forces and displacements rather than stresses and strains. Appropriate expressions are given in Section 2.

Potential Energy: The potential energy L of a body is defined as

$$L = U - W_t \quad , \tag{5a}$$

where U is given by Eq. (4) and W_t is the loss in potential energy of the body forces over the

1.7.2.1 (Cont'd)

total volume (assuming the body forces to be prescribed throughout the volume) and of the surface tractions over that portion of the surface where the tractions are prescribed.

That is,

$$W_t = \int_B F_i u_i dV + \int_{S_t} t_i u_i dS \quad , \tag{5b}$$

where S_t denotes that portion of the surface where the traction and not the displacements are prescribed. This statement is amplified in Paragraph 1.7.2.3 where the principle of minimum potential energy is discussed. Note that an elastic support may be considered to be part of the structure so that displacements or tractions may still be prescribed on the boundary.

Complementary Potential Energy: The complementary potential energy L^* is defined as

$$L^* = U^* - W_u \quad ,$$

where U^* is the complementary strain energy of the body and (assuming the body forces to be prescribed throughout the body) W_u is the loss in potential energy of the surface traction over that portion of the surface, S_u where the displacement and not the traction is prescribed.

That is,

$$W_u = \int_{S_u} t_i u_i dS \quad . \tag{5c}$$

1.7.2.2 Variational Techniques

Stationary Values: Application of minimum energy principles involves the definition of stationary values for functions or, more generally, functionals (integrals of functions). A stationary condition is necessary in order that an extremum (maximum or minimum) exist. In the case of a function $f(x_1, x_2, \ldots, x_n)$, the conditions for a stationary value at a point P are

$$\frac{\partial f}{\partial x_1}\Big|_P = \frac{\partial f}{\partial x_2}\Big|_P = \ldots = \frac{\partial f}{\partial x_n}\Big|_P = 0. \tag{1}$$

In the case of functionals, the problem is more complex. For example, given the functional $I(y) = \int_{x_0}^{x_1} F\ (x, y, y')\ dx$, where F is a given explicit function of x, y, y', the question may be asked, what is the function $y(x)$ (if it exists) which makes $I(y)$ stationary where $y(x_0)$ and $y(x_1)$ are prescribed? The aim of the calculus of variation is to solve problems such as this. A typical procedure is shown as follows:

1.7.2.2 (Cont'd)

Consider the integral

$$I = \int_{x_0}^{x_1} F\ (x, y, y', y'')\, dx \quad ,$$

and seek the function $y = y\ (x)$ which makes I stationary where y and y' are prescribed at x_0 and x_1. The existence of such a function is assumed and the effect on I is examined of a variation in y by a small amount δy where $\delta y = \delta y' = 0$ at $x = x_0$ and $x = x_1$ (Figure 1.7.2.2-1).

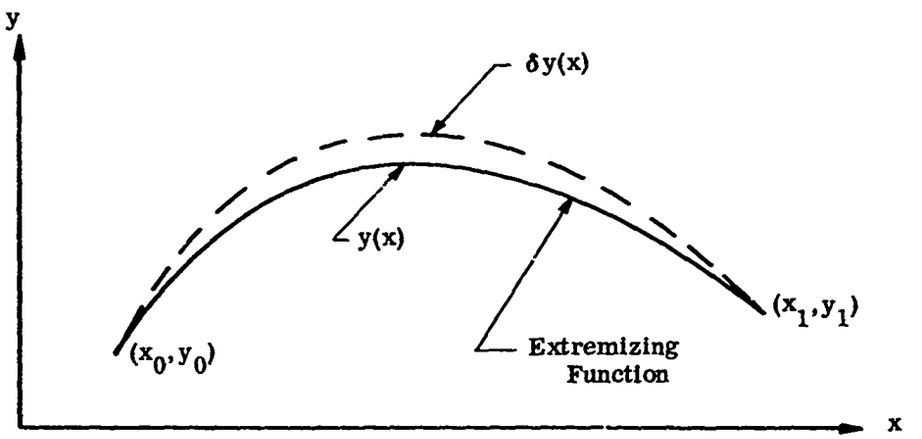


FIGURE 1.7.2.2-1 VARIATION OF EXTREMIZING FUNCTION

If I is an extremizing function, then

$$\delta I = \int_{x_0}^{x_1} \left[\frac{\partial F}{\partial y}\, \delta y + \frac{\partial F}{\partial y'}\, \delta y' + \frac{\partial F}{\partial y''}\, \delta y'' \right] dx = 0 \quad . \tag{2}$$

The left hand side is called the first variation of the integral I.

In order to eliminate the variations $\delta y'$ and $\delta y''$ from Eq. (2), the second and third terms are integrated by parts:

$$\int_{x_0}^{x_1} \frac{\partial F}{\partial y'}\, \delta y'\, dx = \left[\frac{\partial F}{\partial y'}\, \delta y \right]_{x_0}^{x_1} - \int_{x_0}^{x_1} \frac{d}{dx} \left(\frac{\partial F}{\partial y'} \right) \delta y\, dx \tag{3a}$$

1.7.2.2 (Cont'd)

$$\int_{x_0}^{x_1} \frac{\partial F}{\partial y''}\, \delta y''\, dx = \left[\frac{\partial F}{\partial y''}\, \delta y' \right]_{x_0}^{x_1} - \left[\frac{d}{dx} \frac{\partial F}{\partial y''}\, \delta y \right]_{x_0}^{x_1} \tag{3b}$$

$$+ \int_{x_0}^{x_1} \frac{d^2}{dx^2} \left(\frac{\partial F}{\partial y''} \right) \delta y\, dx \quad .$$

Because of the assumed boundary conditions, the bracketed terms in (3a) and (3b) vanish so that

$$\delta I = \int_{x_0}^{x_1} \left[\frac{\partial F}{\partial y} - \frac{d}{dx} \frac{\partial F}{\partial y'} + \frac{d^2}{dx^2} \frac{\partial F}{\partial y''} \right] \delta y\, dx = 0 \quad . \tag{4}$$

The above integral must vanish for all admissible δy, which requires that the expression in the bracket of Eq. (4) be zero, i.e.,

$$\frac{\partial F}{\partial y} - \frac{d}{dx} \left(\frac{\partial F}{\partial y'} \right) + \frac{d^2}{dx^2} \frac{\partial F}{\partial y''} = 0 \quad . \tag{5}$$

This differential equation is known as the Euler differential equation from which the function y can be determined.

1.7.2.3 Minimum Potential Energy

The functional called potential energy was defined in Paragraph 1.7.2.1. We now state the following important theorem for elastic bodies:

Theorem of Minimum Potential Energy: Of all compatible displacements for a stable structure satisfying given displacement boundary conditions, those which satisfy the equilibrium equations make the potential energy, L, a minimum. The converse theorem, which is the one used most often, is as follows:

"Of all the displacements satisfying the boundary conditions, those which make the potential energy a minimum satisfy the equilibrium equations." The proofs of these theorems and the other theorems discussed may be found in Reference 1-1.

Since the potential energy ($L = U - W_t$) is a minimum for the true equilibrium state, it must also be stationary, i.e.,

$$\delta L = \delta (U - W_t) = 0 \quad , \tag{1a}$$

where the quantities U and W_t are defined in Paragraph 1.7.2.1. Equation (1) is stated quite simply; however, a full understanding of its meaning requires further explanation. According to Kirchhoff's Uniqueness Theorem, either the displacements or the tractions (but not both) must be prescribed at each point of the boundary of the body. Variations of the potential energy, Eq. (1a),

1.7.2.3 (Cont'd)

are effected by varying the displacements only over those portions of the body where the tractions are prescribed. The displacement variation must vanish over those portions of the boundary where the displacements are prescribed. As a consequence, if the displacements are given over the entire surface and there are no body forces ($W_t = 0$), then Eq. (1a) becomes

$$\delta U = 0 \ . \tag{1b}$$

This is, in effect, a stationary (minimum) strain energy principle:

If there are no body forces present then, of all the arbitrary sets of continuous displacements which satisfy the compatibility equations and the specified displacement conditions over the entire boundary, those displacements which satisfy equilibrium make the strain energy a local minimum with respect to neighboring displacements.

(Remark: Since variations of the potential energy are expressed in terms of the displacements, the strain energy must be given in terms of displacements.)

Example: The following elementary problem illustrates the application of the principle of minimum potential energy.

A cantilever beam of flexural rigidity EI is propped by an elastic spring with spring constant K (force/unit of deflection). Find the end deflection Δ due to an applied load P.

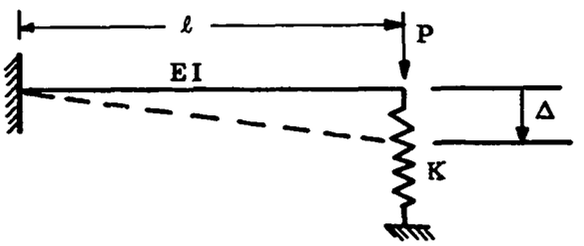


FIGURE 1.7.2.3-1 ELASTICALLY PROPPED CANTILEVER BEAM

The internal (strain) energy for the beam-spring system, expressed in terms of the end displacement is

$$U = \frac{3EI\Delta^2}{2\ell^3} + \frac{K\Delta^2}{2}$$ (see any elementary text on strength of materials).

According to the theorem, the loss in potential energy of the external loads W_t is taken only over those portions of the body where the forces are prescribed. In this problem the only prescribed force is the end load P. Thus,

1.7.2.3 (Cont'd)

$$W_t = P\Delta,$$

so that

$$L = U - W_t$$

$$= \left(\frac{3EI}{\ell^3} + K\right) \frac{\Delta^2}{2} - P\Delta.$$

It follows from Eq. (1a) that

$$\delta L = \frac{dL}{d\Delta}\,\delta\Delta = \left[\left(\frac{3EI}{\ell^3} + K\right)\Delta - P\right]\delta\Delta = 0.$$

The factor $\delta\Delta$ is arbitrary and, therefore, the bracketed term is zero, i.e.,

$$\Delta = \frac{P}{\frac{3EI}{\ell^3} + K} \quad .$$

Note that

$$\frac{d^2L}{d\Delta^2}(\delta\Delta)^2 = \delta^2 L = \left(\frac{3EI}{\ell^3} + K\right)(\delta\Delta)^2 > 0,$$

which establishes a minimum.

1.7.2.4 Minimum Complementary Energy

Another important variational principle relates to the complementary energy functional ($L^* = U^* - W_u$) defined in Paragraph 1.7.2.1.

The Theorem of Minimum Complementary Energy: "Of all states of stress in a stable structure satisfying equilibrium and given traction boundary conditions, that state which satisfies compatibility requirements makes the complementary energy L^* a minimum."

Since the complementary energy is a minimum for the compatible state, it must also be stationary, i.e.,

$$\delta L^* = \delta\,(U^* - W_u) = 0 \quad , \qquad (1a)$$

where the quantities U^* and W_u are as defined in Paragraph 1.7.2.1.

The strain energy, in this case, is expressed in terms of the stresses or forces, and variations of the complementary energy are effected by varying the stresses such that tractions vary only over those portions of the surface where the displacements are prescribed.

1.7.2.4 (Cont'd)

The stress variation must vanish over those portions of the boundary where the tractions are prescribed. Consequently, if the tractions are given over the entire surface ($W_u = 0$) then Eq. (1a) becomes

$$\delta U^* = 0 \quad . \tag{1b}$$

Equation (1b) is known as The Minimum Strain Energy Theorem, which states:

"Of all arbitrary stress states which satisfy equilibrium and the specified tractions over the entire boundary, that state which satisfies compatibility makes the complementary strain energy a minimum." When a problem is linearly elastic $U^* = U$.

Example: The theorem of minimum complementary energy will now be demonstrated for the case of a beam on three supports.

A beam (constant EI) is loaded and supported as shown in Figure 1.7.2.4-1. It is assumed that there is no displacement at the supports. The support reactions are to be determined.

Solution: This is a statically indeterminate beam of 1 degree of indeterminancy. Let 2R represent the center reaction. Because of symmetry, the other two reactions are equal to W-R. External equilibrium of the structure is satisfied for all values of R. However, there is only one value of R which will also satisfy compatibility conditions, i.e., that the slope is continuous, and the displacement is zero at the middle support.

Since the loads are prescribed everywhere except at the supports, force variations, according to the theorem, are permitted only at the supports where displacements are prescribed as zero ($W_u = 0$). Thus the complementary strain energy, expressed in terms of the forces must be a minimum with respect to variations in R, i.e., $\delta U^* = 0$, $\delta^2 U^* > 0$.

Considering only bending energy, the complementary strain energy

$$U^* = \int_0^{2\ell} \frac{M^2}{2EI}\, dx = 2 \int_0^{\ell} \frac{M^2}{2EI}\, dx \quad ,$$

where

$$M = (W - R)\, x \quad ; \quad 0 \le x \le \ell/2$$

$$= \frac{W\ell}{2} - Rx \quad ; \quad \ell/2 \le x \le \ell \quad ,$$

or

$$U^* = 2\left[\int_0^{\frac{\ell}{2}} \frac{(W - R)^2}{2EI}\, x^2\, dx + \int_{\frac{\ell}{2}}^{\ell} \frac{\left(W\,\frac{\ell}{2} - Rx\right)^2 dx}{2EI} \right]$$

1.7.2.4 (Cont'd)

$$\delta U^* = \frac{\ell^3}{EI}\left[-\frac{(W-R)}{12} - \frac{3}{8}W + \frac{7}{12}R\right]\delta R = 0 \quad .$$

FIGURE 1.7.2.4-1 BEAM WITH THREE SUPPORTS

Since δR is arbitrary, the bracketed expression is zero, which yields

$$R = \frac{11}{16}W \quad .$$

The two end reactions are, therefore,

$$W - R = \frac{5}{16}W \quad ,$$

and the center reaction is

$$2R = \frac{11}{8}W \quad .$$

Note also that

$$\delta^2 U^* = \frac{\ell^3}{EI}\left[\frac{1}{12} + \frac{7}{12}\right](\delta R)^2 > 0 \quad .$$

1.8 REFERENCES

1-1 Sokolnikoff, I.S., Mathematical Theory of Elasticity, McGraw-Hill Book Company, Inc., 1956.

1-2 Timoshenko, S. and Goodier, J.N., Theory of Elasticity, McGraw-Hill Book Company, Inc., 1951

SECTION 2

STRUCTURAL TECHNIQUES

SECTION 2

STRUCTURAL TECHNIQUES

TABLE OF CONTENTS

Paragraph	Title	Page
2	Structural Techniques	2.3
2.1	Linear Structures	2.5
2.1.1	Virtual Work Techniques	2.5
2.1.1.1	Virtual Forces	2.5
2.1.1.2	Virtual Displacements	2.7
2.1.2	Strain Energy in Terms of Internal Loads and Deformations	2.9
2.1.3	Application of Virtual Force Technique - Flexibility Coefficient	2.11
2.1.3.1	Flexibility Coefficient for a Beam-Like Structure	2.11
2.1.3.2	Addition of Flexibility Coefficients	2.12
2.1.4	Applications of Virtual Displacement Techniques	2.16
2.1.4.1	Load on a Structure	2.16
2.1.4.2	Stiffness Coefficients	2.16
2.1.4.3	Addition of Stiffness Coefficients	2.17
2.1.5	Properties of Influence Coefficients Matrix	2.19
2.1.5.1	Symmetry	2.20
2.1.5.2	Positive Definiteness	2.20
2.1.6	Equivalent Thermal Load	2.21
2.1.6.1	Three Dimensional Hydrostatic Loading	2.21
2.1.6.2	Fixed End Beam Reactions	2.23
2.1.7	Plane Stress and Plane Strain Problem	2.23
2.1.7.1	Plane Strain	2.23
2.1.7.2	Plane Stress	2.25

TABLE OF CONTENTS (Cont'd)

Paragraph	Title	Page
2.1.8	St. Venant's Principle	2.25
2.2	Non-Linear Structures	2.26
2.2.1	Incremental Linear Solutions	2.27
2.2.2	Inverse Solution	2.27
2.2.3	Approximate Solutions	2.28
2.3	References	2.29

SECTION 2 - STRUCTURAL TECHNIQUES

The solution of the structural equations can be performed in many ways. The technique selected depends upon the type of problem, the type of boundary conditions, the complexity and the required accuracy, etc. The problem is simplified if the structure is linear and permits the addition of simple solutions to obtain the final solution.

The following symbols are used throughout this section:

a, b, i, j, k, r	Degrees of freedom of a structure
f_i	Internal axial load in beam due to a unit load at "i"
$^{r}f_{ij}$	Deflection at "i" due to a unit load at "j" with respect to a datum at "r"
k	Modulus of rupture factor = $M_{ult.}/M_{elastic}$
m_i	Internal moment in beam due to a unit load at "i"
n	Unit normal to bounding surface
n_x, n_y, n_x	Direction cosines of normal with x, y, z axes
q_i	Internal torque in beam due to a unit load at "i"
r	Distance from origin in polar coordinates; distance from shear center
u_i	Generalized displacement
δu	Arbitrary displacement satisfying compatibility
u, v, w	Displacement in x, y, z direction
v_i	Internal transverse shear due to unit load at "i"
x, y, z	Coordinates in x, y, z directions
y	Distance in beam cross section from neutral axis
A	Area
A_V	Effective transverse shear area
E	Linear modulus of material
F_i	Surface or body force acting in x_i direction
δF	Arbitrary force system satisfying equilibrium
G	Linear shear modulus
I	Moment of inertia of cross section
K_{ji}	Load at "j" due to a unit (virtual) displacement at "i"
L	Length of beam
M	Internal moment due to applied loads
P	Internal axial load due to applied loads
Q	Internal torque load due to applied load
T	Temperature
U	Internal strain energy $= \int_V \int_0^{\epsilon_{ij}} \sigma_{ij} \, d\epsilon_{ij} \, dV$
U^*	Complementary strain energy $= \int_V \int_0^{\sigma_{ij}} \epsilon_{ij} \, d\sigma_{ij} \, dV$
V	Transverse shear load; volume; potential for a conservative force system
W	Loss in potential energy of surface tractions and body forces
$\delta W_t \equiv \delta W$	Change in potential due to a virtual displacement
$\delta W_u^t \equiv \delta W^*$	Change in complementary potential due to a virtual force system

$\overline{AE}$	Axial stiffness of cross section = $\int E_S \, dA$
$\overline{A_V G}$	Transverse shear stiffness of cross section = $\int G_S \, dA_V$
$\overline{EI}$	Bending stiffness of cross section = $\int E_S y^2 \, dA$
$\overline{JG}$	Torsional stiffness of cross section = $\int G_S r^2 \, dA$
α	Linear coefficient of thermal expansion
$\bar{\gamma}$	Average shear strain - transverse shear displacement per unit length
δ	Incremental operator
δ_{ij}	Krcnecker delta = 1 if i = j 0 if 1 ≠ j
Δ_i	Deflection at "i"
ϵ	Strain
$\epsilon_{xx}; \epsilon_{yy}; \epsilon_{zz}$	Extensional strains
$\epsilon_{xy}; \epsilon_{yz}; \epsilon_{zx}$	Shear strains
$\bar{\epsilon}_M$ and $\bar{\epsilon}_T$	Axial strain of cross section due to applied loads and temperature, respectively
Θ	Polar coordinate - angle between r and x axis
Θ_i	Rotation at "i"
κ_M and κ_T	Curvature of cross section due to applied loads and temperature, respectively
λ	Transformation matrix converting applied loads to loads on the substructures
ν	Poisson's ratio
σ	Stress
σ_{xy}	Stress on plane perpendicular to x axis and in y direction
τ	Torsion - change in twist of cross section per unit length
φ	Airy function
∇	Gradient operator

Subscripts

a, b, i, j	Pertaining to degrees of freedom a, b, i, j
i, j	Pertaining to x_i, x_j directions
r	Pertaining to datum structure
A	Pertaining to axial energy, stresses or strains; allowable
B	Body
M	Pertaining to bending energy; deformation due to mechanical loads
Q	Pertaining to torsional energy, stresses or strains
S	Surface; secant modulus
T	Deformation due to temperature
V	Pertaining to transverse shear energy, stresses or strains

Superscripts

1, 2	Substructure
'	Pertaining to a rotational degree of freedom (e.g., b')

2.1 LINEAR STRUCTURES

If the structural response to mechanical and thermal loads is directly proportional to these loads and independent of past history, the structure is said to be linear elastic. For a linear elastic structure, it is possible to solve the general structural problem by the solution of a few unit-type problems, and to add these solutions to obtain the final complete solution. The technique is that each unit solution shall satisfy equilibrium and compatibility and, when superposed upon each other, satisfy the given boundary conditions. Thus, it is possible to remove boundary conditions and solve for the new structure and superpose self-equilibrating force systems which will have the net effect of satisfying the boundary conditions (flexibility method). It is also possible to divide the structure into smaller sub-structures, solve each sub-structure and impose compatibility conditions to satisfy the boundary conditions of the over-all structure and the sub-structures (stiffness method). These techniques are illustrated in the flexibility and stiffness coefficient methods of Sub-section 4.3 and are derivable from the "Principle of Virtual Work" discussed in Paragraph 1.7.1.

No structure is truly linear elastic with respect to thermal stimulation since the stiffness of the structure will change with temperature. The structure can be treated as linear elastic, for approximate solutions, where the changes in temperature or stresses are not severe enough to significantly change the stiffness of the material and where the strains are small and geometry changes can be ignored.

2.1.1 Virtual Work Techniques

As a consequence of the reciprocal theorem (Paragraph 1.7.1), the loss in potential energy of the body and surface forces acting on a structure in its true equilibrium state, due to a compatible set of arbitrary virtual displacements (not necessarily satisfying any displacement boundary conditions), is equal to the gain in strain energy. In equation form,

$$\delta U = \delta W \equiv \delta W_t, \tag{1}$$

where $\delta U = \int_B \sigma \delta \epsilon \, dV$

$$\delta W = \int_B F_i \delta u_i \, dV + \int_S t_i \delta u_i dS \quad .$$

In addition, the loss of complementary potential energy of the body and surface forces acting, on a structure in its true equilibrium state, due to a self-equilibrating set of arbitrary virtual forces or stresses (not necessarily satisfying traction boundary conditions) is equal to the gain in complementary strain energy, i.e.,

$$\delta U^* = \delta W^* \equiv \delta W_u, \tag{2}$$

where $\delta U^* = \int_B \epsilon \delta \sigma dV$

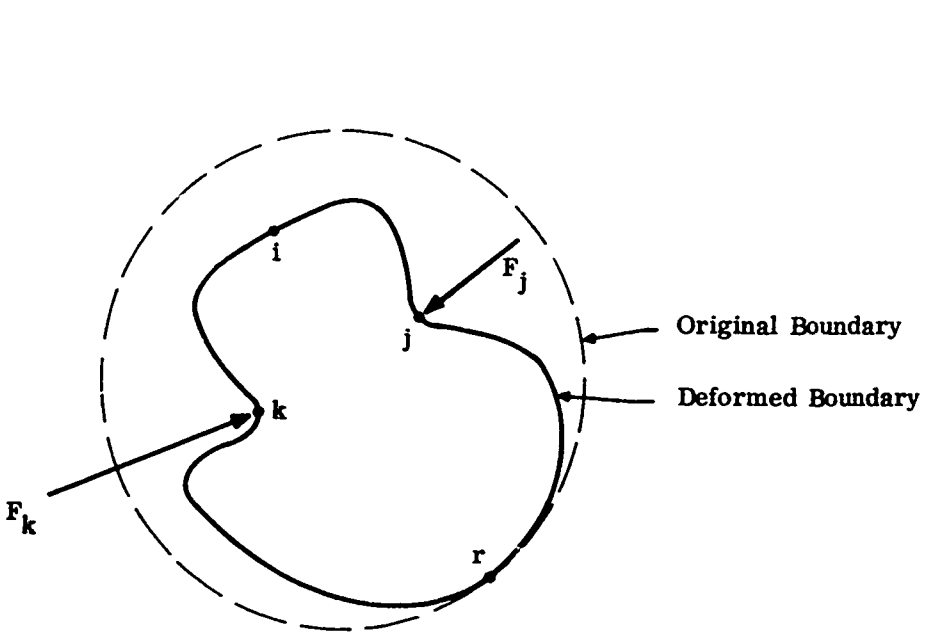
$$\delta W^* = \int_B u_i \delta F_i \, dV + \int_S u_i \delta t_i \, dS \quad .$$

An inequality results if the structure is not in its true equilibrium state.

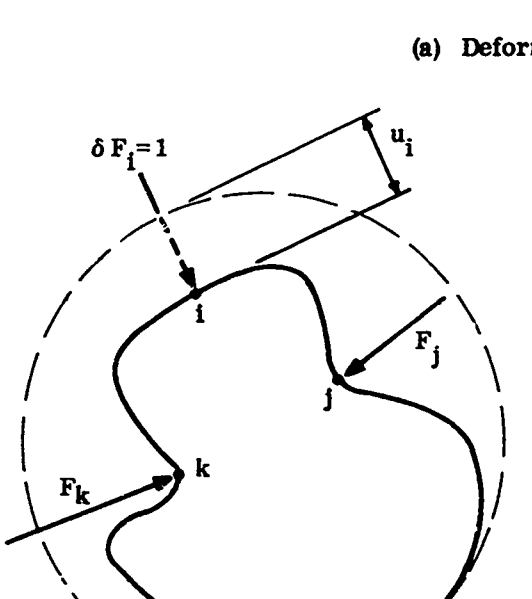
2.1.1.1 Virtual Forces

Figure 2.1.1.1-1(a) shows a body in equilibrium under the force systems F_j and F_k.

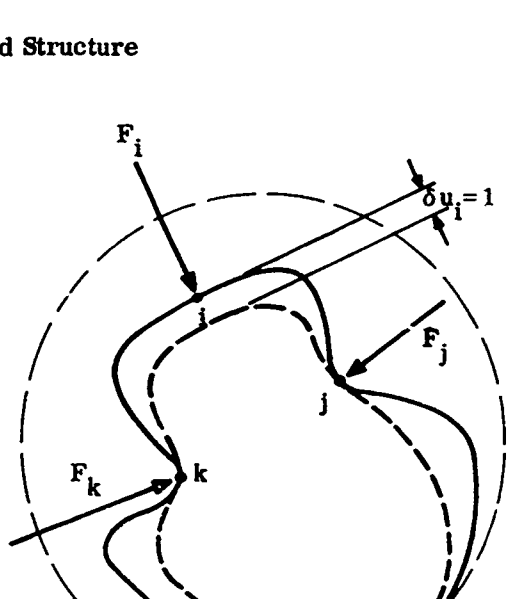
2.1.1.1 (Cont'd)



(a) Deformed Structure



(b) Virtual Force



(c) Virtual Displacement

FIGURE 2.1.1.1-1 BODY UNDER LOAD

2.1.1.1 (Cont'd)

Determine the displacement in some chosen direction of point i. To do this, apply a unit force $\delta F_i = 1$, acting at the point in the chosen direction (Figure 2.1.1.1-1(b), and react this force by δF_r. This force system is in equilibrium and thus satisfies the requirements of a virtual force system. From Eq. (2) of Paragraph 2.1.1,

$$\delta U^* = \delta W^* = 1 \cdot u_i + \delta F_r \cdot u_r \tag{1a}$$

If the reaction points of δF_r are chosen as the datum with respect to which the deflection is to be measured, then $u_r = 0$ and

$$\delta U^* = u_i = \int_B \epsilon \, \delta\sigma \, dV \tag{1b}$$

The deflection can always be measured with respect to a datum defined by the reaction points for the applied virtual load. Statically determinate virtual reactions at points which are reactions for the actual statically indeterminate structure will always yield deflections with respect to the structural datum with a minimum amount of calculation. A rigid body correction must be made to determine the deflection of a point with respect to a structural datum if the chosen datum is not the same as the structural datum. The rigid body correction is the displacement of the chosen datum with respect to the structural datum.

2.1.1.2 Virtual Displacements

To determine a load F_i which is in equilibrium with the force systems F_j and F_k [Figure 2.1.1.1-1(c)], a displacement $\delta u_i = 1$ is imposed in the direction of F_i with corresponding arbitrary but compatible deformations throughout the body. This displacement system satisfies the requirements of a virtual displacement system. From Eq. (1) of Paragraph 2.1.1,

$$\delta U = \delta W = F_i \cdot 1 + F_j \, \delta u_j + F_k \, \delta u_k \tag{1a}$$

If the displacement system is chosen in such a manner that

$$\delta u_j = \delta u_k = 0,$$

then

$$\delta U = F_i = \int_B \sigma \, \delta\epsilon \; dV \; . \tag{1b}$$

The virtual displacement principle can also yield an alternate statement of the equilibrium equations. To illustrate this, consider the beam of Figure 2.1.1.2-1 to be subjected to a rigid body virtual displacement in the vertical direction,

$$\delta u = 1 \; .$$

Since no straining occurs in a rigid body displacement,

$$\delta U = \int_B \sigma \, \delta\epsilon \, dV = 0,$$

and

$$\delta W = \sum_{i=1}^{n} F_i \delta u = \delta u \sum_{i=1}^{n} F_i \; .$$

2.1.1.2 (Cont'd)

However

$$\delta U = \delta W,$$

which results in

$$\sum_{i=1}^{n} F_i = 0.$$

The above is a statement of equilibrium of vertical forces.

Consider next a rigid body virtual rotation $\delta\Theta = 1$ about point O.

Again

$$\delta U = 0 \ ,$$

But

$$\delta W = \sum_{i=1}^{n} F_i \, \delta\Theta \, x_i = \delta\Theta \sum_{i=1}^{n} F_i x_i \ .$$

Therefore,

$$\sum_{i=1}^{n} F_i x_i = 0,$$

which is a statement of equilibrium of moments.

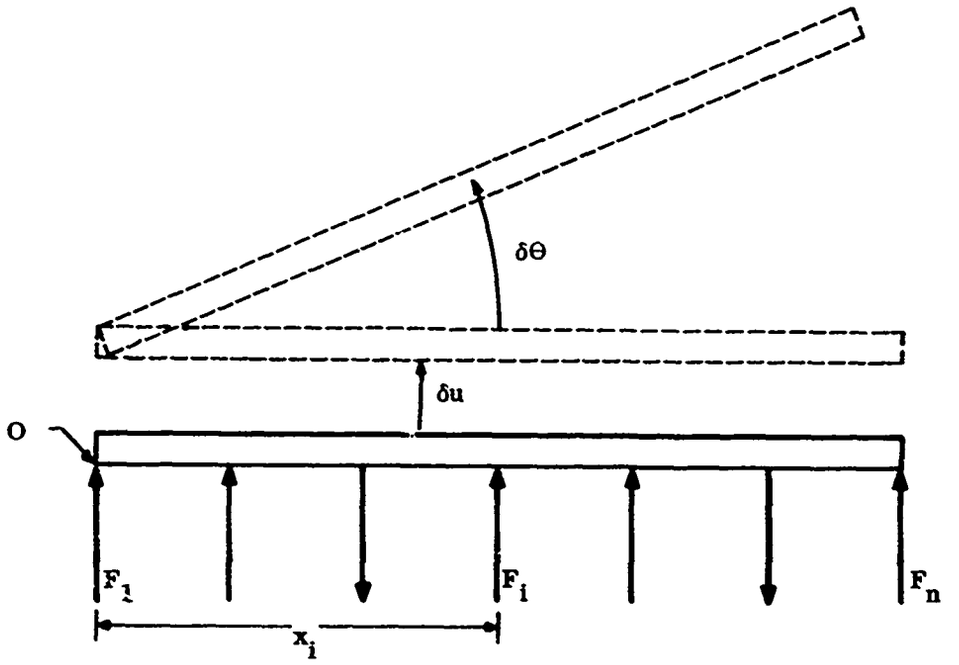


FIGURE 2.1.1.2-1 VERTICALLY LOADED BEAM IN EQUILIBRIUM

2.1.2 Strain Energy in Terms of Internal Loads and Deformations

It is most often convenient to express the strain energy of the body in terms of internal forces and the deformations of these forces rather than as stresses and strains. Consider a body in equilibrium and compatibility under a given set of loads and a temperature distribution. Cut the body into elemental volumes and apply tractions at the cuts which are equal to those stresses which existed in the body before it was cut. These tractions are exactly those necessary to insure a perfect fit between the elemental volumes. It can be shown by the Divergence Theorem that the strain energy expressed by these internal forces acting through the displacement of the cuts is equal to the work done by the body and surface forces acting through their displacement, and that the complementary strain energy is equal to the complementary work of the body and surface forces.

Figure 2.1.2-1 illustrates a beam subjected to temperature and mechanical loads. The equivalent internal loads and the deformation of the cross section are defined by an

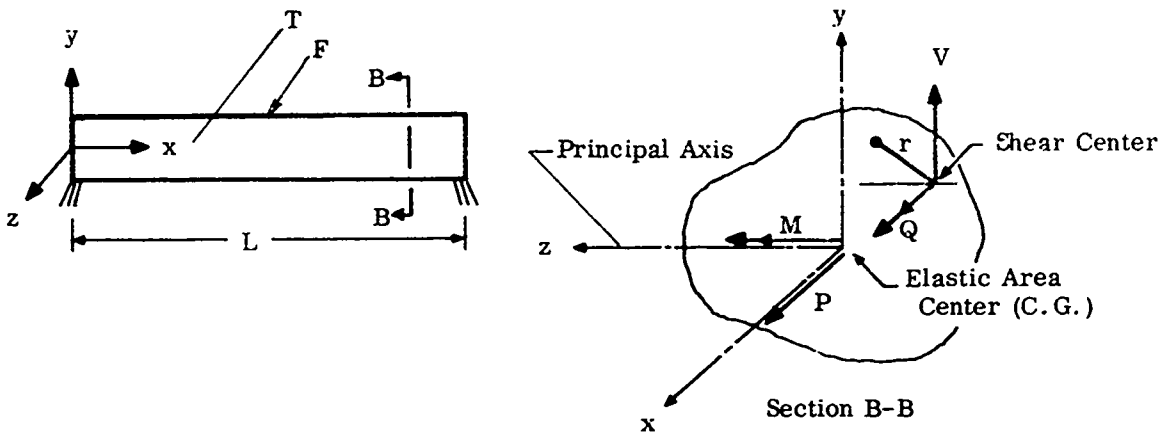


FIGURE 2.1.2-1 BEAM UNDER LOAD

axial load P and an axial deformation per unit length of $\bar{\epsilon}_M + \bar{\epsilon}_T$; a bending moment M and a change in slope per unit length (curvature) of $K_M + K_T$; a twisting moment Q and a change in twist per unit length (torsion) of τ ; a transverse shear load V and a relative shear displacement per unit length (shear strain) of $\bar{\gamma}$. The subscript M implies the deformation associated with the mechanical load and the subscript T implies deformations associated with temperature.

Assuming linear strains over the beam cross section, let

ϵ_A = Axial strain

ϵ_Q = Torsional shearing strain

and

ϵ_V = Transverse shearing strain (may be nonlinear)

2.1.2 (Cont'd)

These strains may be expressed in terms of the internal deformations by the relations

$$\epsilon_A = \bar{\epsilon}_M + \bar{\epsilon}_T + (\kappa_M + \kappa_T)\ y$$

$$\epsilon_Q = \tau \cdot r \qquad (1)$$

$$\int G_S \epsilon_V\ dA = (\overline{A_V G})\ \bar{\gamma}\ .$$

Similarly let

σ_A = Axial stress

σ_Q = Torsional shearing stress

σ_V = Transverse shear stress.

These internal stresses can be expressed in terms of the internal loads by the relations

$$\sigma_A = E_S(\epsilon_A - \alpha T) = E_S\left[\bar{\epsilon}_M + \bar{\epsilon}_T + (\kappa_M + \kappa_T)\ y - \alpha T\right]$$

$$\sigma_Q = G_S\ \epsilon_Q = \frac{G_S Qr}{\overline{JG}} \qquad (2a)$$

$$\int \sigma_V\ dA = \int G_S\ \epsilon_V\ dA = V\ ,$$

where

$$\bar{\epsilon}_M = \frac{P}{\overline{EA}} \qquad , \tau \approx \frac{Q}{JG}\ ,$$

$$\bar{\epsilon}_T = \frac{\int E_S\, \alpha T\, dA}{\overline{EA}} \qquad , \bar{\gamma} = \frac{V}{A_V G}\ , \qquad (2b)$$

$$\kappa_M = -\frac{M}{\overline{EI}}$$

$$\kappa_T = \frac{\int E_S\, y\, \alpha T\, dA}{\overline{EI}}\ ,$$

and

$$\overline{EI} = \int E_S\, y^2\, dA$$

$$\overline{EA} = \int E_S\, dA$$

$$\overline{JG} = \int G_S r^2\ dA \text{ (for circular sections only)} \qquad (2c)$$

$$\overline{A_V G} = \int G_S\, dA_V$$

$$0 = \int E_S\, y\, dA\ .$$

Evaluating the strain energy $\int_V \int_0^{\epsilon} \sigma\, d\epsilon dV$ and the complementary strain energy $\int_V \int_0^{\sigma} \epsilon\, d\sigma dV$ results in

$$U = U_A + U_M + U_Q + U_V$$

$$U^* = U_A^* + U_M^* + U_Q^* + U_V^*\ , \qquad (3a)$$

2.1.2 (Cont'd)

where

$$U_A = \int_0^L \int_0^{\bar{\epsilon}_M + \bar{\epsilon}_T} P\, d(\bar{\epsilon}_M + \bar{\epsilon}_T)\, dx \qquad U_A^* = \int_0^L \int_0^P (\bar{\epsilon}_M + \bar{\epsilon}_T)\, d\, P\, dx$$

$$U_M = \int_0^L \int_0^{\kappa_M + \kappa_T} -M d(\kappa_M + \kappa_T)\, dx \qquad U_M^* = \int_0^L \int_0^M -(\kappa_M + \kappa_T)\ dM\, dx$$

$$U_Q = \int_0^L \int_0^{\tau} Q\, d\, \tau\, dx \qquad U_Q^* = \int_0^L \int_0^Q \tau\, dQ\ \ dx \qquad \text{b)}$$

$$U_V = \int_0^L \int_0^{\bar{\gamma}} V\, d\, \bar{\gamma}\ dx \qquad U_V^* = \int_0^L \int_0^V \bar{\gamma}\ dV\ dx \quad .$$

In addition,

$$\delta U = \int_0^L \left[P \left\{ \delta\ (\epsilon_M + \epsilon_T) \right\} - M \left\{ \delta\ (\kappa_M + \kappa_T) \right\} + Q \left\{ \delta\ \tau \right\} + V \left\{ \delta \bar{\gamma} \right\} \right] dx \qquad (4a)$$

$$\delta U^* = \int_0^L \left[\left\{ \delta P \right\} (\epsilon_M + \epsilon_T) - \left\{ \delta M \right\} (\kappa_M + \kappa_T) + \left\{ \delta Q \right\} \tau + \left\{ \delta V \right\} \bar{\gamma} \right] dx \quad . \qquad (4b)$$

Thus, the change in strain energy is equivalent to the internal loads acting through the change in the internal deformations. The change in complementary strain energy is equivalent to the internal deformations acting through the change in the internal loads.

Using expression (4b) and the virtual force technique, the displacement at some point on the beam (when shear energy is neglected), is given by the expression

$$u_i = -\int_0^L (\kappa_M + \kappa_T)\ m_i\ \ dx + \int_0^L (\bar{\epsilon}_M + \bar{\epsilon}_T)\ f_i\ \ dx \quad . \qquad (5)$$

where $\delta M = m_i$
$\delta P = f_i$

Beam deflections are further discussed in Paragraph 4.2.1.

2.1.3 Application of Virtual Force Technique - Flexibility Coefficient

The flexibility coefficient ${}^{r}f_{ij}$ is defined as the deflection (or rotation) at point i with respect to some datum r, when the structure is subjected to a unit load at point j and reacted at points defining the datum r.

2.1.3.1 Flexibility Coefficient for a Beam-Like Structure

Using the virtual force technique and the equivalent loads and displacements for a

2.1.3.1 (Cont'd)

beam-like structure, results in

$$f_{ij} = \int_0^L \left[\frac{f_j f_i}{\overline{AE}} + \frac{m_j m_i}{\overline{EI}} + \frac{q_j q_i}{\overline{JG}} + \frac{v_j v_i}{\overline{A_V G}} \right] dx . \qquad (1)$$

The deflection of the structure can be obtained by employing Eq. (5) of Paragraph 2.1.2 or by adding the effects of each load times the corresponding flexibility coefficient,

$$\Delta_i = \sum_j f_{ij} P_j = f_{ij} P_j \text{ , where repeated indices indicate summation.} \qquad (2)$$

When the structure is linear elastic, the values of $\overline{AE}$, $\overline{EI}$, $\overline{JG}$, and $\overline{A_V G}$ do not change with load or temperature stimuli and linear simultaneous equations can be set up to solve for the desired quantities (see Paragraph 4.2.4).

2.1.3.2 Addition of Flexibility Coefficients

Equation (1) of Paragraph 2.1.3.1 can be visualized as a group of springs in series. The energy content of a spring is directly proportional to its flexibility and the approximation of ignoring all energies but the bending energy is equivalent to assuming $0 = \frac{1}{AE} = \frac{1}{JG} = \frac{1}{A_V G}$. The flexibility of a structure can be analyzed by superposing the flexibilities of structures where all flexibilities except one are assumed zero as shown in Figure 2.1.3.2-1.

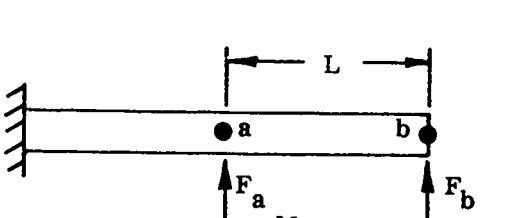


	AXIAL	BENDING	TWIST	SHEAR	
f_{ijP} =	$\int_0^L \frac{f_j f_i}{\overline{AE}} dx$ +	0 +	0 +	0	Axial Energy
f_{ijM} =	0 +	$\int_0^L \frac{m_j m_i}{\overline{EI}} dx$ +	0 +	0	Bending Energy
f_{ijQ} =	0 +	0 +	$\int_0^L \frac{q_j q_i}{\overline{JG}} dx$ +	0	Twisting Energy
f_{ijV} =	0 +	0 +	0 +	$\int_0^L \frac{v_j v_i}{\overline{A_V G}} dx$	Shear Energy
f_{ij} =	f_{ijP} +	f_{ijM} +	f_{ijQ} +	f_{ijV}	Total Energy

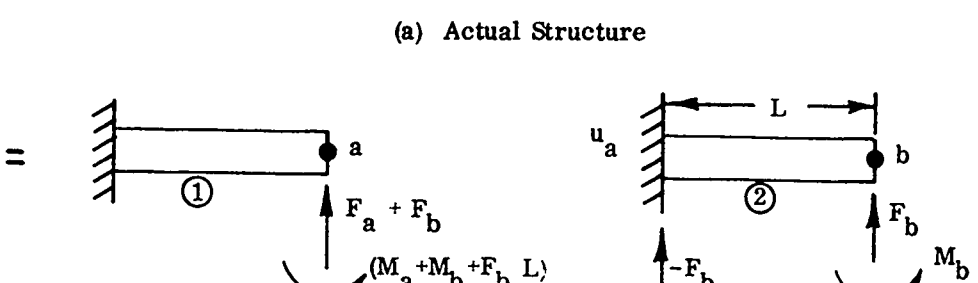
FIGURE 2.1.3.2-1 SUPERPOSITION OF FLEXIBILITIES

A structure (e.g., a cantilever) can be analyzed by the solutions of individual portions (springs) which are then placed together by satisfying compatibility and equilibrium at each of the common contacts. This is also equivalent to analyzing the over-all structure where all flexibilities but one portion are identically zero and adding the solutions as shown in Figure 2.1.3.2-2.

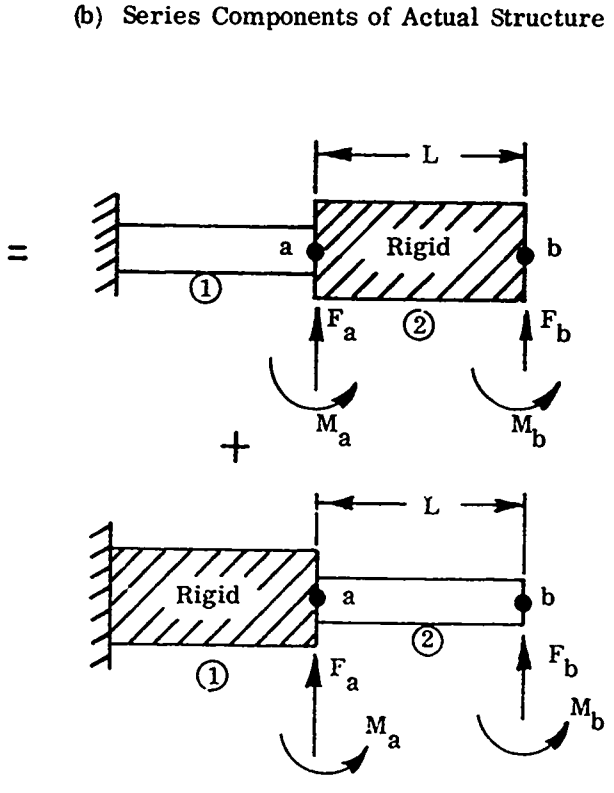
2.1.3.2 (Cont'd)



(a) Actual Structure



(b) Series Components of Actual Structure



(c) Superposable Equivalents

FIGURE 2.1.3.2-2 EQUIVALENT STRUCTURES IN SERIES

2.1.3.2 (Cont'd)

In Figure 2.1.3.2-2(a) and -2 (b) the actual structure is shown to be equivalent to two substructures 1 and 2 connected in series. Substructure 1 has the same displacement datum as the actual structure, with end loads equal and opposite to the reactions of substructure 2. Substructure 2 has the same loads as the actual structure but the displacements are corrected for a rigid body motion corresponding to the translation and rotation (u_a) of the end of substructure 1. The same results and calculations would be obtained by adding the solution of the two rigid flexible beam problems shown in Figure 2.1.3.2-2(c).

The elemental substructures are much easier to analyze than the over-all structure. The loads on the substructures ($\overline{F}$) are expressed in terms of the applied loads on the actual structure (F) by means of the equilibrium equations.

$$\left\{\overline{F}\right\} = \left[\lambda\right]\left\{F\right\} = \begin{bmatrix} 1 & 0 & 1 & 0 \\ 0 & 1 & L & 1 \\ 0 & 0 & 1 & 0 \\ 0 & 0 & 0 & 1 \end{bmatrix} \begin{Bmatrix} F_a \\ M_a \\ F_b \\ M_b \end{Bmatrix} \tag{1}$$

The displacements of the actual structures can be similarly expressed in terms of the loads and flexibility of substructures.

$$\begin{aligned} \Delta_a &= {}^1f_{aa}\ (F_a + F_b) + {}^1f_{aa'}\ (M_a + M_b + F_b L) \\ \Theta_a &= {}^1f_{a'a}\ (F_a + F_b) + {}^1f_{a'a'}\ (M_a + M_b + F_b L) \\ \Delta_b &= \Delta_a + L\Theta_a + {}^2f_{bb}\ F_b + {}^2f_{bb'}\ M_b \\ \Theta_b &= \Theta_a + {}^2f_{b'b}\ F_b + {}^2f_{b'b'}\ M_b \end{aligned} \tag{2}$$

In matrix form:

$$\left\{\Delta_i\right\} = \begin{Bmatrix} \Delta_a \\ \Theta_a \\ \Delta_b \\ \Theta_b \end{Bmatrix} = \left[\begin{array}{c|c|c|c} {}^1f_{aa} & {}^1f_{aa'} & {}^1f_{aa} + L\,{}^1f_{aa'} & {}^1f_{aa'} \\ \hline {}^1f_{a'a} & {}^1f_{a'a'} & {}^1f_{a'a} + L\,{}^1f_{a'a'} & {}^1f_{a'a'} \\ \hline {}^1f_{aa} + L\,f_{a'a} & {}^1f_{aa'} + L\,f_{a'a'} & {}^1f_{aa} + L\,{}^1f_{aa'} + {}^2f_{bb} + L\,f_{a'a} + L^2 f_{a'a'} & {}^1f_{aa'} + {}^2f_{bb'} + L\,f_{a'a'} \\ \hline {}^1f_{a'a} & {}^1f_{a'a'} & {}^1f_{a'a} + L\,{}^1f_{a'a'} + {}^2f_{b'b} & {}^1f_{a'a'} + {}^2f_{b'b'} \end{array}\right] \begin{Bmatrix} F_a \\ M_a \\ F_b \\ M_b \end{Bmatrix}$$

$$= \left[f_{ij}\right]\left\{F_j\right\} \tag{3}$$

2.1.3.2 (Cont'd)

The above influence coefficients of the actual structure can be expressed in terms of the influence matrices of the substructures and the matrix expressing the loads on the substructures in terms of the applied loads, as follows:

$$\left[f_{ij}\right] = \left[\lambda'\right] \begin{bmatrix} {}^{1}f_{aa} & {}^{1}f_{aa'} & 0 & 0 \\ {}^{1}f_{a'a} & {}^{1}f_{a'a'} & 0 & 0 \\ 0 & 0 & {}^{2}f_{bb} & {}^{2}f_{bb'} \\ 0 & 0 & {}^{2}f_{b'b} & {}^{2}f_{b'b'} \end{bmatrix} \left[\lambda\right] \qquad (4a)$$

where $\left[\lambda'\right]$ is the transpose of $\left[\lambda\right]$.

The above transformation of the influence coefficients matrices of the substructures to the influence matrix of the actual structure can be readily verified by utilizing the fact that the total work done on the substructures is equal to the total work done on the actual structure.

Thus

$$\left\{F'_i\right\} \left\{\Delta_i\right\} = \left\{\overline{F}'_K\right\} \left\{\overline{\Delta}_K\right\} \quad .$$

But from (3)

$$\left\{\Delta\right\} = \left[f\right] \left\{F\right\} \quad ;$$

therefore:

$$\left\{F'_i\right\} \left[f_{ij}\right] \left\{F_j\right\} = \left\{\overline{F}'_K\right\} \left[\overline{f}_{Kr}\right] \left\{\overline{F}_r\right\} \quad . \qquad (4b)$$

From Eq. (1),

$$\left\{\overline{F}_r\right\} = \left\{\lambda_{rj}\right\} \left\{F_j\right\} \quad ,$$

so that

$$\left\{\overline{F}'_K\right\} \equiv \left\{F'_i\right\} \left[\lambda'_{Ki}\right] \quad .$$

Substituting the above in Eq. (4b) yields

$$\left\{F'_i\right\} \left[f_{ij}\right] \left\{F_j\right\} = \left\{F'_i\right\} \left[\lambda'_{Ki}\right] \left[\overline{f}_{Kr}\right] \left[\lambda_{rj}\right] \left\{F_j\right\}$$

or

$$\left[f_{ij}\right] = \left[\lambda'_{Ki}\right] \left[\overline{f}_{Kr}\right] \left[\lambda_{rj}\right] \quad .$$

2.1.4 Applications of Virtual Displacement Techniques

The loads on the structure and the stiffness coefficients can be obtained by applying the principle of virtual displacement. The stiffness coefficient K_{ji} is defined as the force (or moment) at a point j when the structure is subjected to a unit displacement at point i.

2.1.4.1 Load on a Structure

Apply a virtual displacement pattern which does not violate compatibility and is unity at F_i and zero at all other points where other forces act (see Figure 2.1.1.1-1(c)).

From Eq. (1b) of Paragraph 2.1.1.2,

$$\delta U = F_i = \int_B \sigma \, \delta \epsilon \, dV.$$

For beam-like structures using the equivalent internal loads and deformation of Eq. (4) of Paragraph 2.1.2,

$$\delta U = F_i = \int_0^L \left[P \, \delta \epsilon - M \, \delta \kappa + Q \, \delta \tau + V \, (\delta \bar{\gamma}) \right] dx , \qquad (1)$$

where the changes in the deformation are due to the virtual displacement and the loads acting on the cross section constitute the self-equilibrating thermal stress system.

For beam-like structures the bending energy predominates and the following is obtained as an approximation

$$F_j \sim - \int_0^L M \, \delta \kappa \, dx . \qquad (2)$$

Thus, to obtain the force at a point in the structure, evaluation of the virtual work due to the virtual displacement is required. This is equal to the internal forces in the structure acting through the virtual internal deformation. This procedure is employed in Section 9, "Stability of Structures."

2.1.4.2 Stiffness Coefficients

Applying a displacement at point j causes loads to be generated at j and points where displacements are kept zero. These forces are the counterpart of the flexibility coefficients which give the deflection at points of interest due to a unit load at a given point and zero load everywhere else. The stiffness coefficients are the loads at points of interest due to the unit displacement at the given point and zero displacement at the other points of interest. The elements of the stiffness coefficients matrix are the loads which result in the unit deflection matrix and can be obtained by inverting the flexibility coefficient matrix. The forces at the datum can be obtained from the equilibrium equation. Similarly, the influence coefficient matrix can be obtained by inverting the non-singular stiffness matrix. The non-singular matrix is obtained by removing the elements associated with the datum of the structure.

$$f_{ij} \, K_{ji} = I \qquad (1a)$$

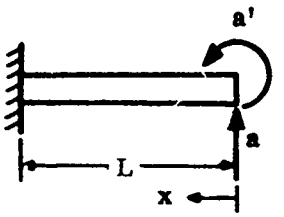
$$K_{ji} = f_{ij}^{-1} \qquad (1b)$$

$$f_{ij} = K_{ji}^{-1} \qquad (1c)$$

The stiffness coefficients for an elemental beam can be obtained by inverting the flexibility coefficients as shown in the following example.

2.1.4.2 (Cont'd)

Example - Cantilever Beam of Constant EI (Bending Energy Only):



$m_a = x$

$m_{a'} = 1$

$$f_{aa} = \int_0^L \frac{m_a m_a}{EI}\,dx = \int_0^L \frac{x^2 dx}{EI} = \frac{L^3}{3EI}$$

$$f_{aa'} = \int_0^L \frac{m_{a'} m_a}{EI}\,dx = f_{a'a} = \int_0^L \frac{x\,dx}{EI} = \frac{L^2}{2EI} \qquad (2)$$

$$f_{a'a'} = \int_0^L \frac{m_{a'} m_{a'}}{EI}\,dx = \int_0^L \frac{dx}{EI} = \frac{L}{EI}$$

where prime (a') refers to rotational loads or displacements at point a.

$$\begin{bmatrix} K_{aa} & K_{aa'} \\ K_{a'a} & K_{a'a'} \end{bmatrix} = \left(\frac{1}{EI}\right)^{-1} \begin{bmatrix} \frac{L^3}{3} & \frac{L^2}{2} \\ \frac{L^2}{2} & L \end{bmatrix}^{-1} = EI \begin{bmatrix} \frac{12}{L^3} & -\frac{6}{L^2} \\ -\frac{6}{L^2} & \frac{4}{L} \end{bmatrix} \qquad (3)'$$

From equilibrium and symmetry the entire stiffness matrix can be obtained for the loads which are required when a joint is moved a unit displacment and all other joints are fixed. This is shown in Table 2.1.4.2-1

TABLE 2.1.4.2-1 STIFFNESS COEFFICIENTS OF BEAM-LIKE STRUCTURE

		Displacement at Joint			
		①	①'	②	②'
Load at Joint	①	$\frac{12EI}{L^3}$	$-\frac{6EI}{L^2}$	$-\frac{12EI}{L^3}$	$-\frac{6EI}{L^2}$
	①'	$-\frac{6EI}{L^2}$	$\frac{4EI}{L}$	$\frac{6EI}{L^2}$	$\frac{2EI}{L}$
	②	$-\frac{12EI}{L^3}$	$\frac{6EI}{L^2}$	$\frac{12EI}{L^3}$	$\frac{6EI}{L^2}$
	②'	$-\frac{6EI}{L^2}$	$\frac{2EI}{L}$	$\frac{6EI}{L^2}$	$\frac{4EI}{L}$

2.1.4.3 Addition of Stiffness Coefficients

If two or more elements of a structure have a common point (joint) of interest, then the load necessary to obtain the displacement at that point is the sum of the forces necessary to apply the displacement to each element. This is analogous to a set of springs in parallel.

2.1.4.3 (Cont'd)

It is important to maintain a sign convention which is invariant in space for the stiffness coefficients since the forces of elements with a common point may be so oriented that the load in the adjacent elements may be of opposite sign (References 2-1 and 2-2).

Coupled stiffness coefficients can be obtained by repeating basic stiffness coefficients and adding those terms which are in common. Thus the stiffness at a joint is additive (the springs are in parallel) and the total stiffness at a joint is the sum of the stiffnesses of all members coming into the joint. This is shown in Table 2.1.4.3-1 and Figure 2.1.4.3-1.

TABLE 2.1.4-3-1. COUPLED STIFFNESS COEFFICIENTS

Displacement at Joint

Load at Joint	①	①'	②	②'	③	③'
①	$\frac{12E_1I_1}{L_1^3}$	$-\frac{6E_1I_1}{L_1^2}$	$-\frac{12E_1I_1}{L_1^3}$	$-\frac{6E_1I_1}{L_1^2}$	0	0
①'	$-\frac{6E_1I_1}{L_1^2}$	$\frac{4E_1I_1}{L_1^2}$	$\frac{6E_1I_1}{L_1^2}$	$\frac{2E_1I_1}{L_1}$	0	0
②	$-\frac{12E_1I_1}{L_1^3}$	$\frac{6E_1I_1}{L_1^2}$	$\frac{12E_1I_1}{L_1^3}+\frac{12E_2I_2}{L_2^2}$	$\frac{6E_1I_1}{L_1^2}-\frac{6E_2I_2}{L_2^2}$	$-\frac{12E_2I_2}{L_2^3}$	$-\frac{6E_2I_2}{L_2^2}$
②'	$-\frac{6E_1I_1}{L_1^2}$	$\frac{2E_1I_1}{L_1}$	$\frac{6E_1I_1}{L_1^2}-\frac{6E_2I_2}{L_2^2}$	$\frac{4E_1I_1}{L_1}+\frac{4E_2I_2}{L_2}$	$\frac{6E_2I_2}{L_2^2}$	$\frac{2E_2I_2}{L_2}$
③	0	0	$-\frac{12E_2I_2}{L_2^3}$	$\frac{6E_2I_2}{L_2^2}$	$\frac{12E_2I_2}{L_2^3}$	$\frac{6E_2I_2}{L_2^2}$
③'	0	0	$-\frac{6E_2I_2}{L_2^2}$	$\frac{2E_2I_2}{L_2}$	$\frac{6E_2I_2}{L_2^2}$	$\frac{4E_2I_2}{L_2}$

2.1.4.3 (Cont'd)

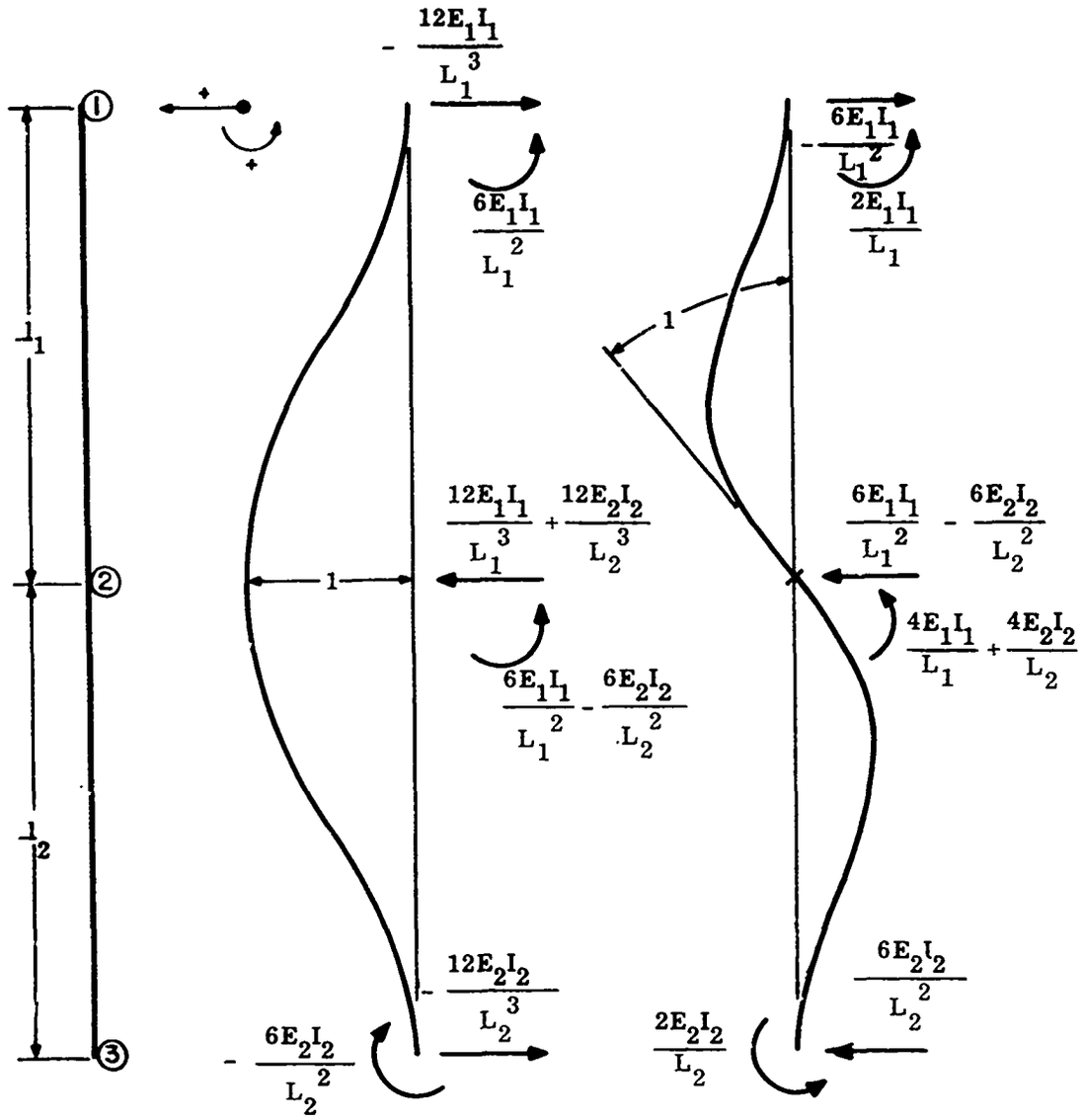


FIGURE 2.1.4.3-1 STIFFNESS COEFFICIENTS FOR A DOUBLE BEAM

2.1.5 Properties of Influence Coefficients Matrix

The influence (flexibility and stiffness) coefficients are utilized in the solution of indeterminate structures (e.g., Sub-section 4.3). The coefficients can be obtained by calculation (References 2-1 and 2-3) or by experimental techniques. It is possible to employ available structural relationships to simplify or check the calculation or experimental determination of these coefficients. The results are presented for flexibility coefficients but apply equally well to stiffness coefficients.

2.1.5.1 Symmetry

The deformation of a point i due to a unit load at a second point j is equal to the deformation of the second point j due to a unit load at the original point i. The deformation (linear or rotational) at a point corresponds to the type of load (force or moment) at the other point.

$$f_{ij} = f_{ji} \tag{1a}$$

$$\Delta_{ij} = \Delta_{ji} \; ; \quad \Theta_{ij'} = \Theta_{ji'} \tag{1b}$$

$$\Delta_{ij'} = \Theta_{ji} \; ; \quad \Theta_{ij} = \Delta_{ji'} \; , \tag{1c}$$

where Δ_{ij} = linear displacemement at i due to unit linear load at j

Θ_{ij} = rotational displacement at i due to unit load at j

$\Delta_{ij'}$ = linear displacement at i due to a unit moment at j

$\Theta_{ij'}$ = rotational displacement at i due to unit moment at j

The symmetry of the matrix is evident by noting the equivalence of the energy terms similar to

$$\int_0^L \frac{(m_i)(m_j)}{EI}\, dx \quad = \quad \int_0^L \frac{(m_j)(m_i)}{EI}\, dx \; .$$

This symmetry can be utilized to reduce the number of calculations or to average the experimental results.

2.1.5.2 Positive Definiteness

The fact that each structure absorbs energy in deforming requires that the displacement of a point on a structure cannot have a component which is opposite to the direction of the applied load. This is demonstrated by the positiveness of the energy terms similar to $\int_0^L \frac{(m_i)^2 dx}{EI}$. Thus the influence coefficient defining the deflection of a point due to a load at that point must never be negative (always positive except for the reaction for which it is zero). Thus the main diagonal of the influence coefficient matrix must be non-negative,

$$f_{ii} \geq 0. \tag{1}$$

Another relationship derivable from the positive definiteness of the structural matrix is that the product of two main diagonal elements must never be less than the square of the corresponding off-diagonal element.

$$\therefore \quad f_{ii}\, f_{jj} \geq (f_{ij})^2 \tag{2}$$

This is evident from the Schwartz inequality,

$$\left(\int \frac{m_i^2\, dx}{EI}\right)\left(\int \frac{m_j^2\, dx}{EI}\right) \geq \left(\int \frac{m_i\, m_j}{EI}\, dx\right)^2 \; . \tag{3}$$

2.1.5.2 (Cont'd)

The positive definiteness property can be employed to check on the accuracy of the experimentally determined values.

2.1.6 Equivalent Thermal Load

The linear elastic structure permits a solution by the superposition of various loading conditions as long as the total effects add up to the original problem. This approach is particularly adaptable to structures subjected to temperature. The effect of a temperature is to cause an axial expansion of each elemental volume of the structure. The stresses which arise due to temperature are the self-equilibrating stresses necessary to make each elemental volume compatible with the adjacent elemental volumes and the boundary conditions.

There are basically two methods of solving the equivalent mechanical loading problem for the linear-elastic structure subjected to both temperature and mechanical loading. In each method, the structure is first decomposed into elemental units. The behavior of each elemental unit for temperature and mechanical loading is readily determinable. In the first method, the elemental units are permitted to deform independently of each other and the displacement of the boundaries of adjacent elemental units are observed. Attempt is then made to put the decomposed structure together again. This requires that the elemental boundaries be compatible with each other. Self-equilibrating force systems (internal forces) are applied, wherever necessary, at adjacent boundaries to guarantee compatibility. For beam-like structures, this is called the flexibility method. In the second method, the elements are restrained from deforming when subjected to the temperature and load by infinitely rigid restraints. The mechanical loads generated at the restraints are supplied by the structure if this restraint actually exists. If the restraint does not exist then the boundaries of the elemental units are permitted to deform (always maintaining compatability) until the load in the artificial restraint vanishes. For beam-like structures, this is called the stiffness method. These techniques are described for beam-like structures in Sub-section 4-3.

The solution for beam-like structural units is usually expressed as influence coefficients, that is, in terms of the deformation due to unit type loading, or the loading due to a unit type deformation. It is advantageous, therefore, to convert a thermal loading to an equivalent mechanical loading so as to treat a temperature problem as an equivalent mechanical problem and simplify the amount and type of calculations. All the structural techniques available for mechanical loads could then be employed to solve the structure subjected to mechanical loads and temperature.

2.1.6.1 Three Dimensional Hydrostatic Loading

Assume that the body is cut into elemental volumes which are then supported with infinitely rigid restraints so that compatibility between the elemental volumes is maintained. Application of temperature distribution to the structure will now try to expand these elemental volumes which will be counteracted by hydrostatic stresses equal to $-\frac{E\alpha T}{1-2\nu}$ at the artificial restraints. The artificial restraints must supply the difference $\frac{-E\alpha\nabla T}{1-2\nu}$ of the restraining hydrostatic stress loads applied to adjacent elemental volumes. Since the restraints are artificial, the structure must be allowed to deform so as to balance out these "equivalent body forces." By this means the original problem has been changed into two problems. The stresses in the first problem of the artificially restrained body are simply:

2.1.6.1 (Cont'd)

$$
\begin{aligned}
{}^1\sigma_{xx} &= {}^1\sigma_{yy} = {}^1\sigma_{zz} = -\frac{E\alpha T}{1-2\nu} \\
{}^1\sigma_{xy} &= {}^1\sigma_{yz} = {}^1\sigma_{zx} = 0
\end{aligned}
\tag{1}
$$

The second problem is the classical linear elastic problem with body forces which are proportional to the thermal gradient.

$$
\begin{aligned}
F_x &= -\frac{E\alpha}{1-2\nu}\ \frac{\partial T}{\partial x} \\
F_y &= -\frac{E\alpha}{1-2\nu}\ \frac{\partial T}{\partial y} \\
F_z &= -\frac{E\alpha}{1-2\nu}\ \frac{\partial T}{\partial z}\ ,
\end{aligned}
\tag{2}
$$

and the boundary conditions,

$$
\begin{aligned}
{}^2\sigma_{xx}n_x + {}^2\sigma_{xy}n_y + {}^2\sigma_{xz}n_z &= \frac{E\alpha T}{1-2\nu}\, n_x \\
{}^2\sigma_{yx}n_x + {}^2\sigma_{yy}n_y + {}^2\sigma_{yz}n_z &= \frac{E\alpha T}{1-2\nu}\, n_y \\
{}^2\sigma_{zx}n_x + {}^2\sigma_{zy}n_y + {}^2\sigma_{zz}n_z &= \frac{E\alpha T}{1-2\nu}\, n_z\ .
\end{aligned}
\tag{3}
$$

The equilibrium equations,

$$
\begin{aligned}
\frac{\partial\left({}^2\sigma_{xx}\right)}{\partial x} + \frac{\partial\left({}^2\sigma_{xy}\right)}{\partial y} + \frac{\partial\left({}^2\sigma_{xz}\right)}{\partial z} - \frac{E\alpha}{1-2\nu}\ \frac{\partial T}{\partial x} &= 0 \\
\frac{\partial\left({}^2\sigma_{yx}\right)}{\partial x} + \frac{\partial\left({}^2\sigma_{yy}\right)}{\partial y} + \frac{\partial\left({}^2\sigma_{yz}\right)}{\partial z} - \frac{E\alpha}{1-2\nu}\ \frac{\partial T}{\partial y} &= 0 \\
\frac{\partial\left({}^2\sigma_{zx}\right)}{\partial x} + \frac{\partial\left({}^2\sigma_{zy}\right)}{\partial y} + \frac{\partial\left({}^2\sigma_{zz}\right)}{\partial z} - \frac{E\alpha}{1-2\nu}\ \frac{\partial T}{\partial z} &= 0\ ,
\end{aligned}
\tag{4}
$$

and the strain displacement (or compatibility) equations (Paragraph 1.1), together with the stress-strain relations (Paragraph 1.4), provide the necessary and sufficient equations for a solution.

The final solution is the sum of the individual solutions,

$$
\sigma_{ij} = {}^1\sigma_{ij} + {}^2\sigma_{ij}\ . \tag{5}
$$

Thus the temperature problem is the mechanical equivalent of applying a hydrostatic loading, proportional to the temperature, to all the elements and the boundary of the structure and then apply body forces to the structure, equivalent to the gradient of the hydrostatic loading, along with boundary forces which negate the $-\frac{E\alpha T}{1-2\nu}$ boundary forces.

2.1.6.2 Fixed End Beam Reactions

If the behavior of the elemental structures when subjected to mechanical and thermal loads is known (e.g., determinate beams of Section 4) within acceptable engineering accuracy, the artificial restraints (jacks) need not be constructed at each elemental volume but only at the common boundaries (joints) of these larger elemental structures. First the thermal stimulation is applied to the structure. Each joint of the elemental beams will tend to deform but will be restrained by the artificial jacks. The loads introduced in the artificial jacks are commonly termed fixed end reactions. The artificial jacks must supply the unbalance of the fixed end reactions coming into the common joint from the various structural elements. The original structural problem is thereby reduced to two simpler problems. The first problem is the solution of the elemental (fixed end) beams which are restrained from any motion at the ends. The solution of this type of problem is indicated in Sub-section 4.2. The second problem is the deformation necessary to eliminate the artificial restraints and internal loads in a structure with mechanical loads equal to the negative of the unbalanced fixed end reactions acting at each joint. The solution of this type problem is indicated in Sub-section 4.3. The solution of the original problem is thus the sum of the solutions of the two simpler problems. Reference 2-2 indicates that the deformation at the joints of the structure, due to the applied temperatures and loads, is identical to those calculated by the equivalent fixed end reactions. The relative deformations of the elemental beams between the joints must be added to the joint deformations to obtain the total deformations.

2.1.7 Plane Stress and Plane Strain Problem

The three dimensional problem, in general, requires the determination of 15 quantities (6 stress, 6 strain, and 3 displacements), given the body forces and the boundary conditions. This problem can be greatly simplified if the given geometry or loading makes some of the unknown quantities zero (or insignificant). This is the case in the plane strain and plane stress problems.

The state of plane strain is defined as one in which the displacement component in a given direction is zero (e.g., z direction, $w = 0$) and the other displacement components are independent of this direction ($u_{,z} = v_{,z} = 0$). This condition arises in a long (axial dimension large with respect to cross sectional dimensions) prismatic body under loads and temperatures which are independent of the axial coordinates.

The state of plane stress is defined as one in which the stresses acting on faces parallel to a given plane are zero. This condition arises in a short (axial dimension small with respect to cross sectional dimensions) prismatic body, e.g., a flat plate, whose face are unrestrained and unloaded. The axial dimension is sufficiently small so that the axial stress cannot change significantly.

Solutions can be obtained by an "Airy" function which satisfies the equation of equilibrium identically and is made to satisfy the compatibility equations. A general solution can be obtained by the sum of such functions (which also satisfies compatibility and equilibrium) and whose total boundary condition duplicates the actual boundary condition. The St. Venant's principle (Paragraph 2.1.8) can be employed to obtain approximate solutions which are satisifactory at distances away from the area where the boundary conditions are not satisfied identically.

2.1.7.1 Plane Strain

The technique is demonstrated for a rectangular coordinate system but is equally applicable to other orthogonal systems.

2.1.7.1 (Cont'd)

Plane strain is defined by the condition $w = 0$; $u = u(x,y)$; $v = v(x,y)$.

From Table 1.6-1 the following strain conditions are obtained:

$$\epsilon_{xx} = \epsilon_{xx}(x,y) \; ; \; \epsilon_{yy} = \epsilon_{yy}(x,y); \; \epsilon_{xy} = \epsilon_{xy}(x,y)$$
$$\epsilon_{zz} = \epsilon_{xz} = \epsilon_{yz} = 0. \tag{1}$$

Assume that the body forces are derivable from a potential function (-V), (e.g., gravity, temperature, etc.). Thus $-V_{,x} = F_x$.

From Table 1.6-2, since $\sigma_{yz} = \sigma_{xz} = 0$, the equilibrium equations are obtained,

$$(\sigma_{xx} - V)_{,x} + \sigma_{yx,y} = 0 \tag{2a}$$
$$\sigma_{xy,x} + (\sigma_{yy} - V)_{,y} = 0. \tag{2b}$$

From Eq. (1) of Paragraph 1.1.1 the compatibility equations reduce to

$$\epsilon_{xx,yy} + \epsilon_{yy,xx} - 2\epsilon_{xy,xy} = 0 \; , \tag{3}$$

and from a linear stress-strain relationship this becomes

$$\frac{1+\nu}{E}\left\{\left[(1-\nu)\sigma_{xx} - \nu\sigma_{yy}\right]_{,yy} + \left[(1-\nu)\sigma_{yy} - \nu\sigma_{xx}\right]_{,xx} - 2\sigma_{xy,xy}\right\} = 0 \tag{4}$$

The Airy function φ is defined as

$$\sigma_{xx} - V = \varphi_{,yy}; \; \sigma_{yy} - V = \varphi_{,xx}; \; -\sigma_{xy} = \varphi_{,xy} \; , \tag{5}$$

which satisifies the equilibrium equations identically and substituting (5) in (4) results in

$$0 = \varphi_{,xxxx} + 2\varphi_{,xxyy} + \varphi_{,yyyy} + \left(1 - \frac{\nu}{1-\nu}\right)\left[V_{,xx} + V_{,yy}\right], \tag{6a}$$

or

$$\nabla^4 \varphi + \left(\frac{1-2\nu}{1-\nu}\right)\nabla^2 V = 0 \tag{6b}$$

which satisfies the elastic compatibility condition.

An Airy function satisfies the equations of equilibrium and linear compatibility and each one will determine characteristic boundary conditions.

The potential (-V) can be viewed as the restraint forces generated by the artificial restraints to maintain compatibility by restraining the elemental volumes when stimulated by load or temperature. In a gravity field it is simply the density and in a temperature field it is the hydrostatic stress $\left(-\frac{E\alpha T}{1-2\nu}\right)$.

The temperature problem reduces to

$$\nabla^4 \varphi + \frac{E\alpha}{1-\nu}\nabla^2 T = 0 \; , \tag{7}$$

2.1.7.1 (Cont'd)

and for zero mechanical boundary tractions,

$$\varphi = \varphi_{,n} = 0. \tag{8}$$

In polar coordinates, $\nabla^2 T = T_{,rr} + \frac{1}{r} T_{,r} + \frac{1}{r^2} T_{,\Theta\Theta}$, (9a)

and

$$\nabla^4 \varphi = \left(\frac{\partial^2}{\partial r^2} + \frac{1}{r} \frac{\partial}{\partial r} + \frac{1}{r^2} \frac{\partial^2}{\partial \Theta^2} \right)^2 \varphi. \tag{9b}$$

The total solution is the sum of the stresses obtained from the above formulation with the stresses from the restrained conditions $\sigma_{xx} = \sigma_{yy} = \sigma_{zz} = - \frac{E\alpha T}{1 - 2\nu}$.

2.1.7.2 Plane Stress

In the case of plane stress, the technique is similar. Utilizing $\sigma_{zz} = \sigma_{zx} = \sigma_{zy} = 0$ and the equilibrium, compatibility, and stress-strain relationship, the following is obtained:

$$\nabla^4 \varphi + (1 - \nu) \nabla^2 V = 0. \tag{1}$$

For thermal stimulation it is no longer necessary to restrain the thermal expansion in the axial (z) direction since the structure is free to expand in this direction. The necessary artificial restraints are just the xz and yz planes without the xy plane. The potential or equivalent hydrostatic pressure becomes $(-V) = \left(- \frac{E\alpha T}{1 - \nu} \right)$. The thermal plane stress problem then becomes

$$\nabla^4 \varphi + \alpha E \nabla^2 T = 0, \tag{2}$$

and for zero mechanical boundary tractions,

$$\varphi = \varphi_{,n} = 0. \tag{3}$$

The total solution is the sum of the stresses obtained from the above formulation with the stresses from the restrained conditions $\sigma_{xx} = \sigma_{yy} = - \frac{E\alpha T}{1 - \nu}$.

2.1.8 St. Venant's Principle

In many instances the solution to the problem can be simplified by obtaining an approximate solution in which the surface tractions (which may be impossible to prescribe) are not satisfied identically. In general, the engineer only knows the resultant force and not the traction distribution. "If the local applied tractions are replaced by a statically equivalent load system, then the solution will be satisfactory at points sufficiently removed from the region of application of the local tractions." This is known as the "St. Venant's Principle" and is extremely useful when the exact solution is too complex (or may not be solvable with available mathematical tools). This principle is employed in Section 4 where the zero tractions on the free end of the thermoelastic beam were replaced by a self-equilibrating thermal stress system. The solutions are satisfactory at a cross section away (approximately 2 to 3 depths) from the free end and a local approximation is employed in the vicinity of the free end rather than attempting an exact solution.

2.2 NON-LINEAR STRUCTURES

The necessary conditions that a structure will be linear-elastic in going from its original state to its final state is seldom fully realized in an actual airframe design where minimum weight is required.

The advent of high speed venicles has forced the designer of airframe structures to re-assess the non-linear effects of stress, temperature and time upon the structural material. Formerly the design was based on a linear elastic analysis of the structure because of the simplicity and wealth of analyses in the literature employing classical "elasticity" (linear) theories.

An examination of experimental data, however, revealed some discrepancies between the linear analyses and the actual results. In some cases the analysis underestimated the maximum load while in other instances it overestimated the load.

The problem of a beam in bending is a well known example of underestimating the maximum load. The classical linear theory results in a stress distribution which is proportional to the distance from the neutral axis ($\sigma = -\frac{My}{I}$) and the maximum allowable moment (M_A) would occur when the maximum allowable stress (σ_A) is attained $M_A = -\frac{\sigma_A I}{y_{max}}$. This value, obtained by assuming a stress distribution, is significantly lower than the experimental value of $M_A = -k\frac{\sigma_A I}{y_{max}}$ (modulus of rupture) by a factor of $k \geq 1$ which depends upon the geometry and the stress-strain curve of the material. The discrepancy is primarily due to the fact that the linear analysis results in a significant stress gradient which will be reduced as the stresses approach the maximum allowable stress due to the actual stress-strain curve of the material. Additional examples are stress-concentrations, thermal stresses, interaction stresses of shells, etc. The problem of the buckling of a structure is a well known example of overestimating the maximum load. The classical linear theory assumes a stress distribution with a constant upper bound on the modulus. The calculated value can be significantly above the actual value which depends upon the stress level and the stress gradient. This is qualitatively discussed in Section 9 on the effect of plasticity and eccentricity upon stability. Additional examples of overestimating maximum load is the ignoring of stress concentrations, fatigue damage, etc.

The designer was forced, therefore, to modify the linear analysis by introducing a plasticity factor to account for the non-linearity of the stress-strain relationship. This procedure is fairly successful when the effects of time and thermal gradients are negligible and the non-linear behavior of the structure can be estimated from the experimentally determined uniaxial (short-time) stress-strain relationship at the design temperature.

The problem of the effects of a general stress-temperature-time history upon a structure is quite complex and available analyses are usually lacking in reliability and ease of application. Attempts to employ modified linear procedures are fraught with danger and may lead to excessive errors in estimating the life of a structure. The errors can occur in either direction; either in underestimating the structural life and resulting in an excessively heavy structure, or in overestimating the structural life which would cause a premature failure. Any attempt to experimentally determine adequate empirical analysis procedures would be defeated by the tremendous amount of test time and the high costs necessary to determine the effect of all possible stress-temperature-time histories upon various geometric configurations. The time available to do this experimental work before a design must be selected would be far from adequate in the rapidly advancing technology of materials, structures, etc. It is imperative, therefore, that all analysis methods be based on fundamental concepts and simple procedures which best approximate the available experimental data. The empirical design factors should be obtainable with as little

2.2 (Cont'd)

experimental data as possible and the analysis procedures should be presented in as simple a manner as possible to minimize the amount of labor required to analyze the structure. A non-dimensional approach should be investigated in order to reduce the amount of experimental data and analysis curves required.

An incremental time technique as described in Section 1 can be employed in special cases. In general, however, the amount of necessary computations will be prohibitive. Approximations based on deformation theory could be attempted to make the problem solvable and the approximations would give a clue as to whether the solution overestimates or underestimates the true behavior of the structure. The effect of approximations (neglecting energies, approximating variables by constants, additional assumptions, etc.) can be more readily evaluated by simplifying the non-linear general equations than by trying to modify the solutions of over-simplified linear equations.

The equations of equilibrium and of compatibility, it was shown, do not depend upon a stress-strain relationship. They can be obtained from energy principles alone (virtual work). The equations of equilibrium are basically a relationship of the stresses, and the equations of compatibility are a relationship of strains. The stress-strain relationships are the additional conditions necessary to combine the equations of equilibrium and compatibility in terms of the stresses or strains alone. The material behavior is discussed in Section 3 to obtain reasonable and non-dimensional stress-strain relationships.

Methods of analyzing non-linear structures are briefly discussed in the following paragraphs. Most non-linear problems are considered beyond the present scope of this Manual. The non-linear problem of stability is presented in more detail in Section 9 because of the great need, the utility, and availability of approximate methods.

2.2.1 Incremental Linear Solutions

Incremental linear solutions were briefly discussed in Section 1. The technique will give the correct results provided the incremental history is sufficiently small and the structure is elastic. An elastic structure may be linear or non-linear and is defined by a stress-strain relationship which is uniquely defined so that a reversal of stress remains on the initial loading curves. The incremental technique is equivalent to approximating the stress-strain relationship by a series of straight lines and solving a set of linear elastic structures with different geometries and stiffnesses. The necessity for recalculating the geometry or including higher derivatives depends upon the effect of these parameters and the required accuracy. The amount of calculation and accuracy are inversely related and good judgement is necessary to obtain a sufficiently accurate solution without prohibitively large numbers of calculations. This technique can be readily adapted to a digital or analog type of calculation machine.

2.2.2 Inverse Solution

The inverse technique can be employed to solve for the loading conditions which result from an assumed displacement and corresponding compatible strain distribution. This technique can be applied to linear or non-linear problems. The stress distribution and the loading can be obtained by utilizing the known stress-strain (linear or non-linear) relationship with the assumed strain distribution. The St. Venant principle (Paragraph 2.1.8) can be employed to extend the solution to structures in which the boundary loadings are not identical but statically equivalent.

2.2.2 (Cont'd)

In many cases it is possible to determine the correct displacement or strain distribution pattern by employing the principle of minimum complementary potential (Paragraph 1.7.2.4). This procedure was utilized in Reference 2-4 to prove the existence of a linear axial strain distribution in a prismatic beam subjected to terminal loads. General solutions can be obtained for beams subjected to axial loads, transverse loads and moments by assuming linear axial strain distributions and employing non-dimensional stress-strain relationships (Section 3). The applied load can then be plotted versus a suitable strain parameter for various material parameters.

Assuming Airy functions (Paragraphs 2.1.7.1 and 2.1.7.2) results in inverse solutions of the linear plane strain and plane stress problems for the boundary conditions satisfied by the Airy functions. A combination of several Airy functions can sometimes be employed to obtain boundary conditions sufficiently close to the actual boundary conditions.

The inverse technique is the upper bound approximation technique described in Paragraph 2.2.3. When the correct strain distribution pattern is assumed, the approximation solution is the correct solution.

2.2.3 Approximate Solutions

The principles of minimum potential and complementary potential energy as described in Paragraphs 1.7.2.3 and 1.7.2.4 do not depend upon the stress-strain relationship. They can be employed to obtain upper and lower bounds to the solution of linear or non-linear problems. For example, assuming an incorrect displacement or strain distribution which satisfies compatibility and the boundary displacement conditions will underestimate the stiffness of the structure, i.e., will overestimate the strain energy (expressed in terms of the displacements) as well as the work done by the surface and body forces. If a virtual displacement is now applied to the incorrectly assumed displacement pattern, the calculated change in strain energy is greater than the work done by the true forces in acting through this virtual displacement. If only one force is acting (.e.g., axial load on column), the calculations will result in an upper bound of the applied force if the change of strain energy is expressed in terms of the displacements. If the change of strain energy can be expressed in terms of the forces, a lower bound of the applied force can be calculated.

Assuming an incorrect force or stress distribution, which satisfies equilibrium and the boundary force conditions, will overestimate the stiffness of the structure, i.e., will overestimate the complementary strain energy (expressed in terms of the stresses) as well as the complementary work done by the surface and body forces. Applying a virtual force system to the incorrectly assumed force system can result in a lower or upper bound on the displacement by expressing the change of complementary strain energy in terms of the forces or displacements, respectively.

The above techniques are employed in obtaining the stability of structures (Section 9). They can also be employed to analyze plastic beams subjected to axial and bending loads (in which linear strain distributions are assumed across the beam cross section). Another application is the determination of an upper bound to the ultimate load of an axial tension member subjected to a stress concentration such as a hole. The strain distribution which corresponds to the linear elastic solution to the problem satisfies compatibility even when multiplied by an arbitrary constant. Employing this strain distribution with a non-linear stress-strain relationship, such as presented in Section 3, will result in stresses and an integrated axial load. Assuming a maximum strain criterion of failure will result in an upper bound on the axial load when the maximum strain is attained at the "stress" concentration.

2.3 REFERENCES

2-1 Meissner, C., Stress Analysis of Aerodynamic Surfaces Using Method of Elastic Coefficients, Republic Aviation Corporation Report ESAM-21, July 1958.

2-2 Switzky, H., Solution of Indeterminate Beam-Like Structures, Republic Aviation Corporation, RDSR-2, to be issued.

2-3 Switzky, H., Influence Coefficients, Republic Aviation Corporation Report ESAM-22, August 1956.

2-4 Switzky, H., Determination of Mechanical Loads and Thermal Stresses from Experimental Data, Republic Aviation Corporation Report RDSR-5, to be issued.

SECTION 3

MATERIAL CONCEPTS

SECTION 3

MATERIAL CONCEPTS

TABLE OF CONTENTS

Paragraph	Title	Page
3	Material Concepts	3.2
3.1	Deformation Mechanism	3.4
3.2	Stress-Temperature-Time-Strain Relationship	3.5
3.2.1	Uniaxial Stress-Strain Relationship	3.6
3.2.2	Experimental Determination of the Material Constants	3.9
3.2.2.1	Apparent Modulus (E_A)	3.9
3.2.2.2	Slip Stress (σ_o)	3.10
3.2.2.3	Work Hardenability Factor ($K = K_t K_T$)	3.13
3.2.2.4	Interpolation of Material Parameters	3.13
3.2.3	Complex Loading	3.14
3.2.3.1	Invariants	3.15
3.2.3.2	Transformation of Stress-Strain Relationship	3.17
3.3	References	3.19

SECTION 3 - MATERIAL CONCEPTS

The ability of a structure to withstand the applied loads is dependent upon the material properties as well as the structure geometry. The material properties are sensitive to the type and magnitude of loading, the temperature, and the chronological history (time) of these factors. The problem would not be so complex if the principle of superposition could be applied. Unfortunately, this is only approximately true and then for only small stresses, temperatures and times.

In general, the structural stiffness will be different from point to point in the structure and will change with load (stress), temperature, and time. The structure becomes an exceedingly difficult non-linear problem. Recourse is made to deformation theory and approximate methods to solve the problem as if a series of incremental changes occur, each of which is a linear problem with a unique solution until the total loading history is applied.

The exceedingly large number of materials and load-temperature-time histories that are possible makes it absolutely imperative to try to represent the behaviour of structural materials as functions of a few material parameters. From a practical design analysis point of view, it is desirable to limit the number of parameters while still retaining an acceptable engineering approximation to the strain relationship. This would permit a relatively simple mathematical expression to interrelate the equilibrium and compatibility equations of Section 1 (which are independent of the stress-strain relationship) to obtain structural solutions. It is also desirable to present the strain relationship in a non-dimensional form to minimize the computational work and to permit non-dimensional graphical solutions of the structural problem. This technique can be utilized in the design of a structure with minimum guaranteed properties.

The stress-strain relationship suggested in this manual is predicated upon empirical relationships which approximate experimental data. A deformation mechanism is assumed which does not contradict experimental evidence and which leads to three (temperature dependent) parameters for the short time stress-strain relationship and in addition, two additional parameters to include the effects of time. Methods of determining these parameters from simple test data are indicated.

The following symbols are used throughout this section:

t	Time, seconds
C_1	Short time (instantaneous) measure of slip ($C_1 K_T \sinh \sigma/\sigma_o$) in which no primary or secondary creep occurs, non-dimensional
C_2	Measure of primary creep ($C_2(1-e^{-t}) K_T \sinh \sigma/\sigma_o$) due to "relaxation," etc., non dimensional
C_3	Measure of secondary creep ($C_3 t K_T \sinh \sigma/\sigma_o$) as the rate of "strain hardening" is balanced by the rate of "softening by recrystallization," 1/sec
C_4	Material constant representing the number of particles per unit time exceeding the thermal potential barrier
E	Elastic modulus (material-temperature parameter) associated with hydrostatic stress and dilation, psi
E_A	Apparent elastic modulus of material (obtained from short time stress-strain curve), psi
E_S	Secant modulus = σ/ϵ (psi)

E_T	Tangent modulus = $d\sigma/d\epsilon$ (psi)
K	Time-temperature work hardenability material parameter directly proportional to slip = $(K_t)(K_T)$, non-dimensional
K_t	Time component of K, non-dimensional
K_T	Temperature component of K, non-dimensional
K_T	$C_4 e^{-Q/T}$ (Suggested by Maxwell-Boltzmann Energy Distribution, Reference 3-2)
L.M.	Larson-Miller parameter = T (C + log t)
Q	Material constant - activation energy per gram atom divided by the universal gas constant, °K
β	KE_A/σ_o = temperature, time, material parameter ($\beta = 0$ elastic material; $\beta = 1$ viscous material)
δ	Deviation = $\epsilon - \sigma/E_A$
$\Delta\sigma$	Stress increment
ϵ	Strain, in/in
$\dot{\epsilon}$	Strain rate, in/in/sec (dot over symbol indicates derivative with respect to time, e.g., $\dot{K}_t$, $\dot{\sigma}$)
ϵ_σ	Instantaneous strain due to stress = $\sigma/E + C_1 K_T \sinh \sigma/\sigma_o$, in/in
σ	Applied stress, psi
σ_o	Stress associated with slip. This is a material-temperature parameter which is a function of the past history of the material, i.e., stress-temperature-time, etc., psi

Subscripts

1, 2, 3,	Principal directions
I, II, III	Invariant values of stress and strain
i	Dummy index

Superscripts

Prime	Deviations, e.g.; σ'_i and ϵ'_i

3.1 DEFORMATION MECHANISM

Deformation is viewed as the movement of atoms from one equilibrium position to another. The energy potential necessary to overcome the potential barrier, i.e., to initiate and continue the motion, is absorbed from the environment; stress potential, temperature, etc. (See Figure 3.1-1). This movement, or slip, occurs initially along planes in crystals where the stress and temperature potential first attains the value of the potential barrier. The external potential (temperature and external loading) necessary to initiate this slip is reduced by dislocations along the shear plane which locally increases the stress potential. The dislocation then migrates to the boundary of the crystal at which time the deformation along the "favored" planes ceases. No more deformation can occur until the energy potential is increased. This phenomenon is known as "strain hardening". If the thermal and residual stress potential is quite small, a reapplication of the applied load would indicate no significant slip would occur until the applied load exceeds the previously applied load.

Continuing to increase the applied load causes planes in other crystals to attain the necessary potential to slip. Simultaneously, the movement of dislocations to the crystal boundaries increases the internal stress potential at the boundaries which, when coupled with the external potential (thermal and stress), causes the deformed crystal to grow at the expense of its neighbors. This phenomenon is known as "softening" or recrystallization". The growth is in the orientation of the "favored" crystal so that the initial slip can now be permitted to continue by moving the dislocation to the new boundary of the crystal (which continues to expand). Thus the total slip is a function of the previous slip and implies an exponential type of stress function (Reference 3-1). The amount of slip is extremely sensitive to temperature (thermal energy). Statistical thermodynamic considerations indicate that an exponential expression which expresses the probability that the atoms will have the required thermal energy would define the effect of temperature on slip (Reference 3-2).

Another factor should be considered. As the deformation proceeds, it induces residual stresses in the surrounding crystals which then seek a state of equilibrium corresponding to a lower energy state. This phenomenon is known as "relaxation" if it occurs under load and "retarded memory" if it occurs under no load after being stressed beyond the "elastic limit" of the material. Both are evidenced by an increase in strain which is exponential in form since its value depends on the instantaneous value of the residual stress. This residual stress, in turn, depends upon the amount of alleviating strains. The residual stress and strain hardening process can account for the "Bauschinger effect" wherein the yield stress is increased in the direction of original loading to a greater extent than in the reverse direction, as well as for the heat treating and annealing phenomena.

The phenomenon of creep can be viewed as a continuation of slip under constant load. The first stage of creep is a relaxation which proceeds exponentially with time $\left[C_2 (1-e^{-t}) \right]$ while the second stage occurs when the strain hardening rate equals the recrystallization rate resulting in a constant slip rate $\left[C_3 t \right]$. The third stage of creep is considered to be a manifestation of material failure and is not included in the strain relationship.

3.1 (Cont'd)

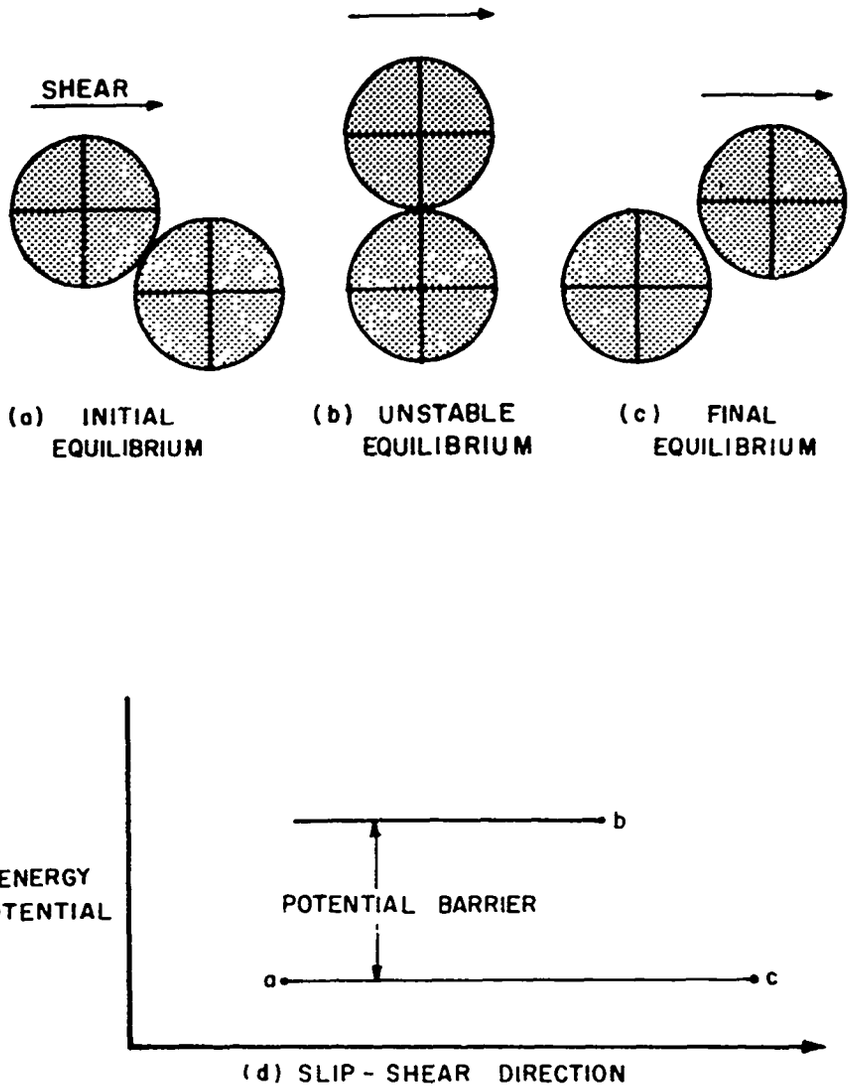


FIGURE 3.1-1 DEFORMATION AND ENERGY POTENTIAL UNDER SHEARING ACTION

3.2 STRESS-TEMPERATURE-TIME-STRAIN RELATIONSHIP

This relationship, presented in Paragraph 3.2.1,is predicated on experimental data obtained from short and long time uniaxial load tests. The mathematical formulation is in terms of material constants which are selected so that the calculated strain curve closely approximates the experimental curve in the regions of interest. Methods of obtaining the material constants from simple uniaxial tests are indicated in Paragraph 3.2.2. Methods of extrapolating the relationship for complex loading conditions (biaxial, etc.) are shown in Paragraph 3.2.3.

3.2.1 Uniaxial Stress-Strain Relationship

Strain can be viewed as composed of two components. One component is elastic (assumed linear) and is associated with the volumetric change (dilation) without distortion due to hydrostatic load. The constant ratio of stress to strain (E) is a material temperature parameter. The other component is inelastic and is associated with distortion (slip) without volumetric change due to shearing load. The slip is assumed proportional to the hyperbolic sine of the stress ratio (as suggested by Reference 3-1) and proportional to a time-temperature constant which varies exponentially with temperature and time. The initial slip for small stresses is almost linear, thus the apparent (initial) modulus (E_A) of the stress-strain curve is slightly less than the true modulus E. This would suggest that the (E_A) modulus determined by dynamic methods would be more consistent and higher than that determined by stress-strain curves at high temperatures (which will contain some inelastic effects, e.g., creep, relaxation, etc.).

The following stress-strain curve is assumed:

$$\epsilon = \sigma/E + K \sinh \sigma/\sigma_o \tag{1a}$$

where

ϵ = strain (in/in)

E = elastic modulus (material-temperature parameter) associated with hydrostatic stress and dilation, psi

σ = applied stress, psi

σ_o = stress associated with slip. This is a material-temperature parameter which is a function of the past history of the material, i.e., stress-temperature-time, psi

K = time-temperature work hardenability material parameter directly proportional to slip = $(K_t)(K_T)$, non-dimensional

K_t = time component of $K = C_1 + C_2 (1 - e^{-t}) + C_3 t$, non-dimensional (1b)

C_1 = short time (instantaneous) measure of slip ($C_1 K_T \sinh \sigma/\sigma_o$) in which no primary or secondary creep occurs, non-dimensional

C_2 = measure of primary creep $\left(C_2 (1 - e^{-t}) K_T \sinh \sigma/\sigma_o\right)$ due to "relaxation", etc., non-dimensional

C_3 = measure of secondary creep (C_3 t $K_T \sinh \sigma/\sigma_o$) as the rate of "strain hardening" is balanced by the rate of "softening by recrystallization", 1/sec

K_T = temperature component of K, non-dimensional

$= C_4 e^{-Q/T}$ (Suggested by Maxwell-Boltzmann Energy Distribution, Reference 3-2)

Q = material constant - activation energy per gram atom divided by the universal gas constant, °K

C_4 = material constant representing the number of particles per unit time exceeding the thermal potential barrier.

The generalized strain relationship, which includes the effects of temperature and time as well as stress, can be employed to obtain short time or isochronous (constant time) stress-strain and stress modulus curves (See Figures 3.2.1-1 through 4). The temperature effect is contained in the dependency of the material parameters upon the temperature and the time

3.2.1 (Cont'd)

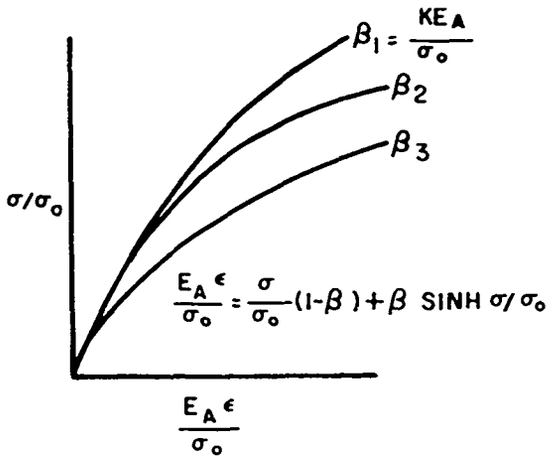


FIGURE 3.2.1-1
NON-DIMENSIONAL
STRESS-STRAIN CURVES

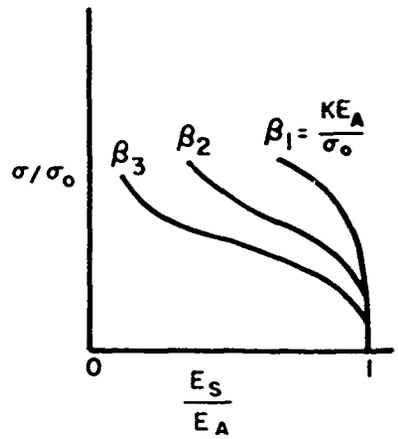


FIGURE 3.2.1-2
NON-DIMENSIONAL
SECANT MODULUS CURVES

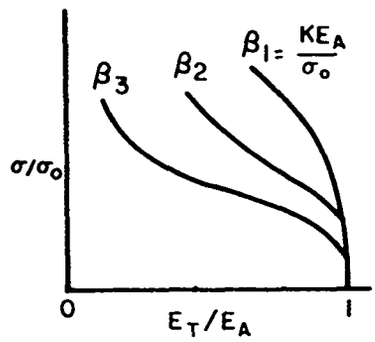


FIGURE 3.2.1-3
NON-DIMENSIONAL
TANGENT MODULUS CURVES

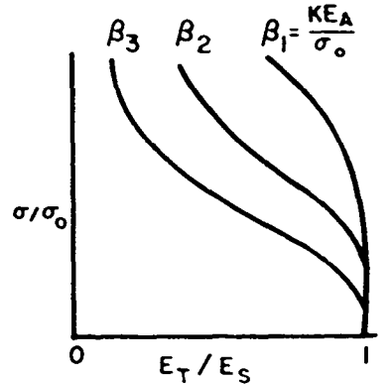


FIGURE 3.2.1-4
NON-DIMENSIONAL
TANGENT-SECANT MODULUS
RATIO CURVES

3.2.1 (Cont'd)

effect is incorporated in the β item described below. The variation of the material parameters with temperature must be determined from experimental data. Initial investigation in this direction has indicated that the functional relationship is smooth and that interpolation should give satisfactory accuracy.

Another justification of the assumed strain relationship is the similarity in formulation to the various diffusion rate processes found in the literature (e.g., Reference 3-3 and 3-4). These formulations agree satisfactorily with the experimental evidence and are employed with available strength and creep data to obtain interpolated or extrapolated strength data. As an example, the Larson-Miller parameter, employed as a correlation parameter (Reference 3-3 and 3-4), is equivalent to the energy of activation Q for an unstressed material, and should be modified by a stress factor if it soaks under load, e.g., $L.M. = T(\ln C_4 + \ln t + \sigma/\sigma_o)$.

The generalized relationship, Eq. (1a) can be manipulated to obtain equivalent stress-strain, secant modulus, tangent modulus, etc., curves and to devise methods to determine material parameters used in design from simple uniaxial short time and long time data. The generalized relationship can be utilized in the same way that a room-temperature stress-strain curve is employed to get allowables. The results are presented in a non-dimensional form in terms of the material design parameters.

Let

E_A = apparent elastic modulus of material (obtained from short time stress-strain curve)

E_T = tangent modulus = $d\sigma/d\epsilon$ (psi)

E_S = secant modulus = σ/ϵ (psi)

$\beta = K E_A/\sigma_o$ = temperature, time, material parameter ($\beta = 0$ elastic material; $\beta = 1$ viscous material)

Then

$$E = E_A / 1 - \beta$$

$$\frac{E_A \epsilon}{\sigma_o} = \frac{\sigma}{\sigma_o} \quad (1-\beta) + \beta \sinh \sigma/\sigma_o \tag{2a}$$

$$\frac{E_A}{E_S} = \left(\frac{E_A \epsilon}{\sigma_o}\right) \Big/ \left(\sigma/\sigma_o\right) \tag{2b}$$

$$\frac{E_A}{E_T} = (1-\beta) + \beta \cosh \sigma/\sigma_o \tag{2c}$$

Figures 3.2.1-1 through 4 illustrate the non-dimensional form of the stress-strain, secant modulus, and tangent modulus curves resulting from Eqs. (1a), (2a), (2b) and (2c). This data is utilized in Section 9 on the stability of structures in which the effective modulus is some combination of E_A, E_T and E_S, and also for use in obtaining approximate solutions of non-linear problems (Reference 3-5).

3.2.2 Experimental Determination of the Material Constants

The material constants are selected so that the mathematical formulation of the strain relationship satisfactorily approximates the experimental data.

3.2.2.1 Apparent Modulus (E_A)

The apparent modulus E_A is obtained as the initial slope of the short time stress-strain curve as shown in Figure 3.2.2.1-1. It may be obtained from the natural frequency of an axial bar or torsional rod if inelastic effects cannot be eliminated from the short time test. The time at stress and the magnitude of the stresses should be small so that the non-linear components are insignificant.

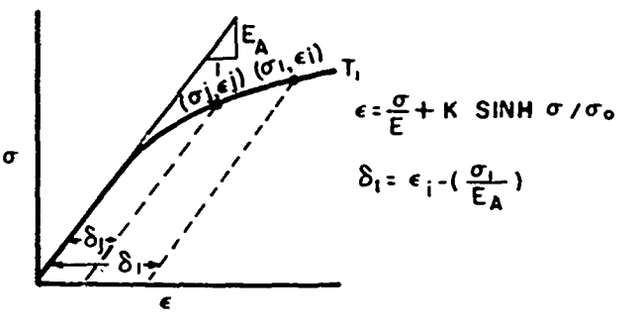


FIGURE 3.2.2.1-1 SHORT TIME STRESS-STRAIN CURVE

3.2.2.2 Slip Stress (σ_o)

The stress (σ_o) which is associated with slip can be determined from a short time stress-strain curve if the creep effect is negligible. The technique is shown in Figure 3.2.2.2-1 in which the deviation $\delta = \epsilon - \sigma/E_A$ is plotted logarithmically versus σ. If the creep effect cannot be ignored, then σ_o can be determined from constant creep rate data shown in Figure 3.2.2.2-2 in which the constant creep is plotted logarithmically versus σ. Justification of this technique follows and is based on the property that the sinh x is approximately $e^x/2$ for large x. From Eq. (1a) of Paragraph 3.2.1

$$\epsilon = \sigma/E + K_t K_T \sinh \sigma/\sigma_o$$

$$\delta = \epsilon - \sigma/E = K_t K_T \sinh \sigma/\sigma_o \sim \frac{C_1 K_T}{2} e^{\sigma/\sigma_o} \qquad (1a)$$

where $t \rightarrow 0$ and $\sigma/\sigma_o > 1$

$$\ln \delta = \ln \frac{C_1 K_T}{2} + \sigma/\sigma_o \qquad (1b)$$

$$\log \delta = \log \frac{C_1 K_T}{2} + \frac{1}{2.3} \left(\sigma/\sigma_o\right) \qquad (1c)$$

On a semi-log plot, (1c) is an equation of a straight line of the form

$$y = b + m x ,$$

where $y = \log \delta$, $b = \log \frac{C_1 K_T}{2}$, $x = \sigma$

and $m = \frac{1}{2.3} \left(1/\sigma_o\right) = \tan \alpha = \frac{\Delta y}{\Delta x} = \frac{\Delta (\log \delta)}{\Delta \sigma}$.

$$\therefore \quad \sigma_o = \frac{1}{2.3} \frac{\Delta \sigma}{\Delta(\log \delta)} = \frac{1}{2.3} \frac{\sigma_2 - \sigma_1}{\log (\delta_{12}/\delta_{11})} \quad \text{(See Figure 3.2.2.2-1)} \qquad (2)$$

Similarly,

$$\dot{\epsilon} = \dot{\sigma}/E + K_t K_T \sinh \dot{\sigma}/\sigma_o + \dot{K}_t K_T \sinh \sigma/\sigma_o \qquad (3a)$$

$$= \dot{K}_t K_T \sinh \sigma/\sigma_o \quad \text{(for constant stress creep test)} \qquad (3b)$$

$$\dot{\epsilon} = \frac{C_3 K_T}{2} e^{\sigma/\sigma_o} \qquad (\text{for } t \rightarrow \infty,\ \sigma/\sigma_o > 1) \qquad (3c)$$

$$\ln \dot{\epsilon} = \ln \frac{C_3 K_T}{2} + \sigma/\sigma_o \qquad (3d)$$

3.2.2.2 (Cont'd)

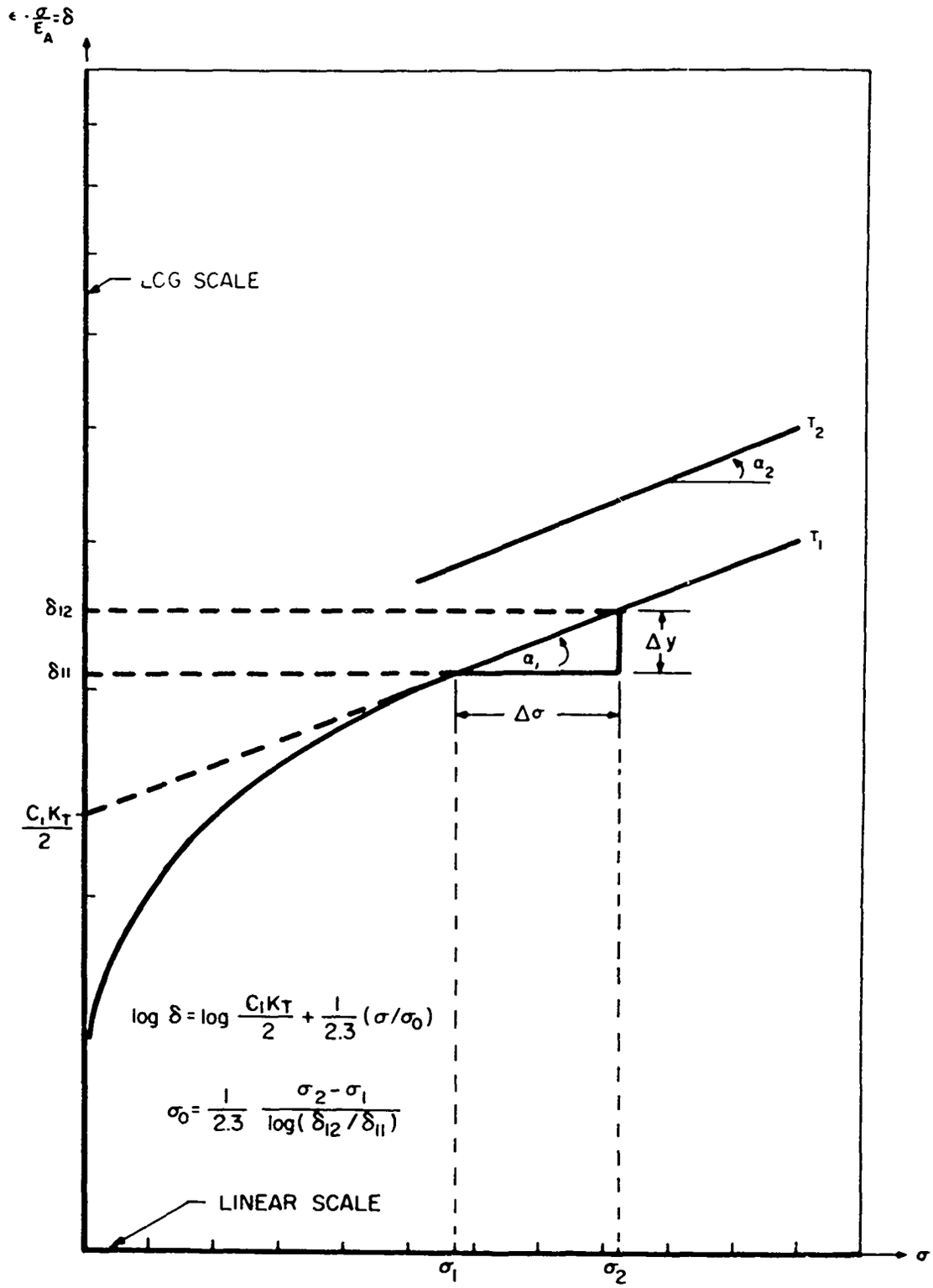


FIGURE 3.2.2.2-1 DETERMINATION OF MATERIAL CONSTANTS FROM SHORT TIME STRESS-STRAIN DATA

3.2.2.2 (Cont'd)

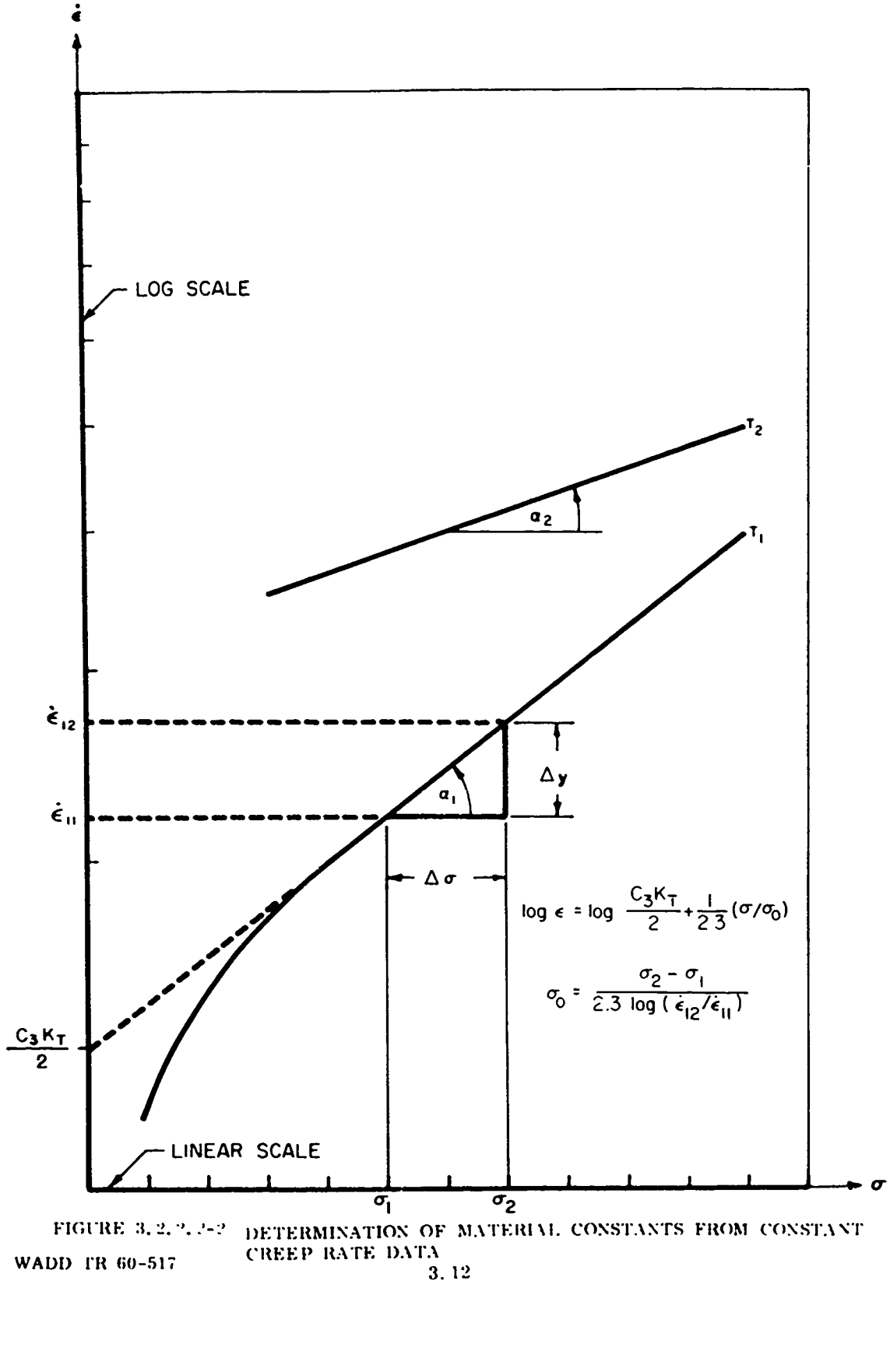


FIGURE 3.2.2.2-2 DETERMINATION OF MATERIAL CONSTANTS FROM CONSTANT CREEP RATE DATA

3.2.2.2 (Cont'd)

$$\log \dot{\epsilon} = \log \frac{C_3 K_T}{2} + \frac{1}{2.3} (\sigma/\sigma_o)$$

$$\sigma_o = \frac{1}{2.3} \frac{\Delta\sigma}{\Delta(\log \dot{\epsilon})} \quad \text{(Reference Figure 3.2.2.2-2)} \tag{4}$$

$$\sigma_o = \left(\frac{1}{2.3}\right) \frac{\sigma_2 - \sigma_1}{\log (\dot{\epsilon}_{12}/\dot{\epsilon}_{11})}$$

3.2.2.3 Work Hardenability Factor ($K = K_t K_T$)

The value of K can be obtained from data shown in Figures 3.2.2.2-1 and -2 and Figure 3.2.2.3-1. $C_1 K_T$ is obtained from the intercept of the straight line in the deviation versus stress curve (Figure 3.2.2.2-1). $C_2 K_T$ is obtained from the intercept of the straight line in the strain versus time curve (Figure 3.2.2.3-1). $C_3 K_T$ is obtained from the intercept of the straight line in the creep rate versus stress curve (Figure 3.2.2.2-2).

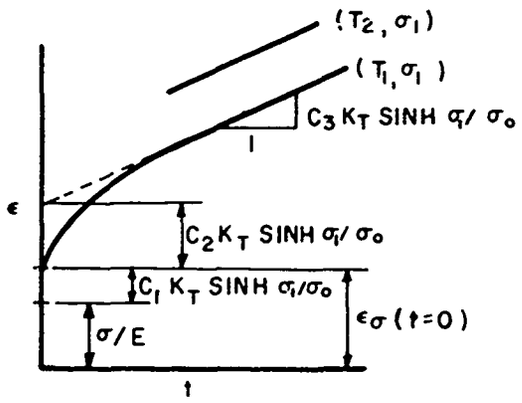


FIGURE 3.2.2.3-1 CREEP CURVE

3.2.2.4 Interpolation of Material Parameters

An increase in temperature or a soaking at temperature will decrease the magnitudes of the material parameters. The temperature potential reduces the magnitude of the stress potential necessary to induce slip. The temperature also increases the rate of recrystallization and relaxation which reduces the strain hardening. Preliminary plots of the material parameters versus either a temperature or an equivalent soaking parameter (e.g., Larson-Miller Parameter) have indicated that the results should be relatively smooth curves as exemplified in Figure 3.2.2.4-1. In order to employ the non-dimensional techniques proposed in this section, it would be expedient to compile data (E_A, σ_o, $C_1 K_T$, $C_2 K_T$, $C_3 K_T$) on the various structural materials in the manner shown in Figure 3.2.2.4-1.

3.2.2.4 (Cont'd)

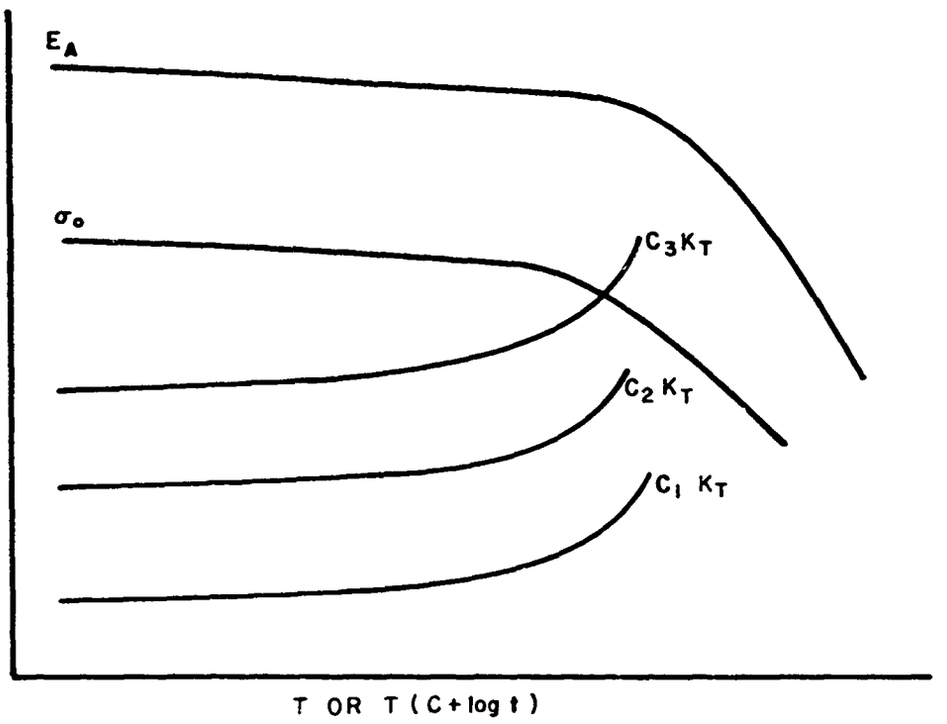


FIGURE 3.2.2.4-1 VARIATION OF MATERIAL PARAMETERS WITH TEMPERATURE

3.2.3 Complex Loading

It is possible to describe the stresses and strains in a material by functions (tensors) which are capable of expressing the state of the stresses and strains at a point. They can always be expressed by the direction and magnitude of their principal components (stresses or strains). For an isotropic material, the principal directions of stress and strain coincide. Associated with the stress or strain are three invariant magnitudes which are independent of the direction of reference. These three invariant magnitudes, or any three combinations of all three quantities, define the tensor. It is assumed that a relationship exists between the invariants of the stress and strain tensors. The uniaxial stress-strain curve would then be an expression of this relationship which is quite simple to obtain experimentally and could be employed to obtain the stress-strain relationship for more complex loadings.

3.2.3.1 Invariants

The three quantities which are characteristic of the stress and strain tensor can be expressed as follows:

Let

$\sigma_1, \sigma_2, \sigma_3$ = principal stresses

$\epsilon_1, \epsilon_2, \epsilon_3$ = principal strains

Then

σ_I = first stress invariant - hydrostatic pressure (1a)

$= 1/3\,(\sigma_1 + \sigma_2 + \sigma_3)$

σ_{II} = second stress invariant - octahedral shear stress

$$= 1/3\sqrt{(\sigma_1 - \sigma_2)^2 + (\sigma_2 - \sigma_3)^2 + (\sigma_3 - \sigma_1)^2} \quad (1b)$$

σ_{III} = third stress invariant

$$= 1/3 \quad \sqrt[3]{(\sigma_1)(\sigma_2)(\sigma_3)} \quad (1c)$$

σ_i' = principal deviatoric stress = $\sigma_i - \sigma_I$ (1d)

ϵ_I = first strain invariant - dilation

$= 1/3\,(\epsilon_1 + \epsilon_2 + \epsilon_3)$ (2a)

ϵ_{II} = second strain invariant - octahedral shear strain

$$= 1/3\sqrt{(\epsilon_1 - \epsilon_2)^2 + (\epsilon_2 - \epsilon_3)^2 + (\epsilon_3 - \epsilon_1)^2} \quad (2b)$$

ϵ_{III} = third strain invariant

$$= 1/3 \quad \sqrt[3]{(\epsilon_1)(\epsilon_2)(\epsilon_3)} \quad (2c)$$

ϵ_i' = principal deviatoric strain = $\epsilon_i - \epsilon_I$ (2d)

Associated with the principal directions (1, 2, 3) are 8 (octahedral) planes which make equal angles (arc cos $1/\sqrt{3}$) with the principal axes. On these planes, the normal stress and strain are σ_I and ϵ_I, respectively, and the tangential (shear) stress and strain are σ_{II} and ϵ_{II} (See Figure 3.2.3.1-1). If it is assumed that the relationship between the normal stress and strains and the tangential stresses and strains are independent (orthogonal) of each other and are uniquely defined for any material, then the invariant stresses and strains for a complex loading can be related to those obtained for a simple one, such as uniaxial tension. Thus, the physical model corresponding to Figure 3.2.3.1-1 suggests that those crystal planes which are oriented so that the applied loads produce higher octahedral shear stresses will slip first (assuming dislocations are uniformly distributed) and that these crystals "strain-harden" requiring higher stresses to cause further slip in these and less favored crystal planes.

3.2.3.1 (Cont'd)

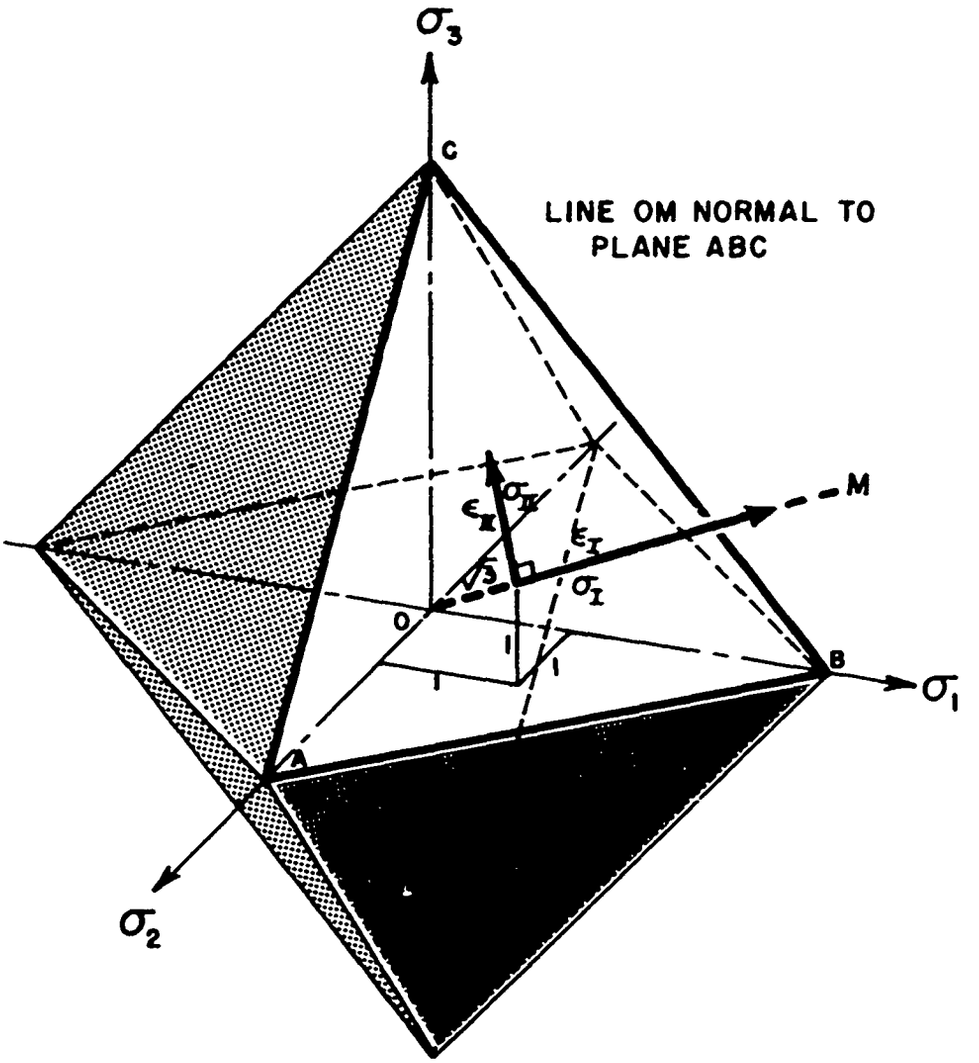


FIGURE 3.2.3.1-1 PRINCIPAL DIRECTIONS AND OCTAHEDRAL PLANES

3.2.3.2 Transformation of Stress-Strain Relationship

The hydrostatic components, stress (σ_I) and strain (ϵ_I) are assumed to vary linearly with volumetric deformation but without any permanent deformation. Experimental evidence indicates that the assumption is quite satisfactory for the ranges of stress-temperature experienced. The relationship between the octahedral components of stress (σ_{II}) and strain (ϵ_{II}) is assumed to be non-linear, with no volumetric deformation, and to constitute the inelastic portion of the stress-strain relationship (Eq. (1a) of Paragraph 3.2.1). The relationship assumes $\epsilon_{II} = \frac{\sigma_{II}}{(1+\nu)E_A} + \frac{(1+\nu)\sqrt{2}C_1K_T}{3} \sinh \frac{3\sigma_{II}}{\sqrt{2}\sigma_o}$.

Figures 3.2.3.2-1 through -4 illustrate how a uniaxial stress-strain curve can be employed to derive a complex stress-strain curve. The uniaxial stress-strain law is obtained experimentally as shown in Figure 3.2.3.2-1. The hydrostatic stress and strain and the octahedral stress and strain are computed in Figures 3.2.3.2-2 and -3. The complex loading is employed to obtain strains from stresses (as shown in Figure 3.2.3.2-4) or stresses from strains, by assuming that the deviatoric to octahedral stress and strain ratios are equal. This is implied by the von Mises yield criteria and the Mises-Levy stress-strain rate relationship (see References 3-6 and 3-7), i.e.,

$$\frac{\sigma_i'}{\epsilon_i'} = \frac{\sigma_i - \sigma_I}{\epsilon_i - \epsilon_I} = \frac{\sigma_{II}}{\epsilon_{II}} \qquad (3)$$

The invariant stress-strain relationships can be employed to postulate allowables of combined loading conditions from allowable invariants of simple (uniaxial) loading conditions wherever applicable, and to obtain approximate solutions to complex problems (assuming a compatible strain distribution results in an upper limit of the applied load, whereas assuming an equilibrium stress distribution results in an upper limit on the displacement of the structure).

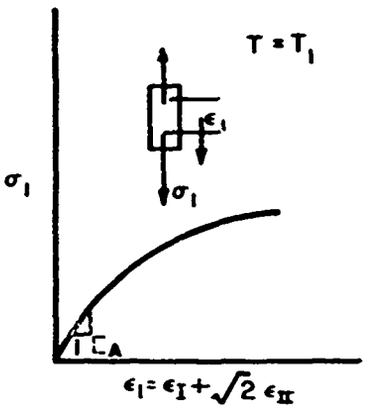


FIGURE 3.2.3.2-1
UNIAXIAL STRESS-STRAIN CURVE

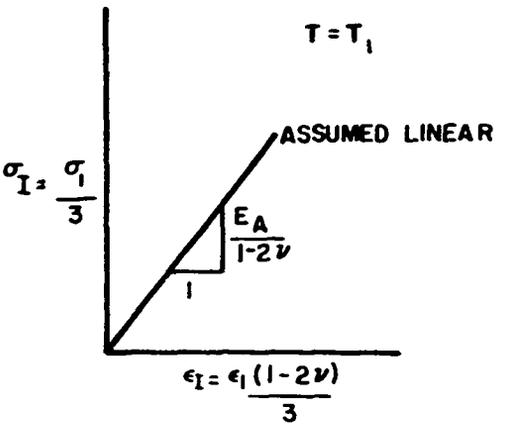


FIGURE 3.2.3.2-2
HYDROSTATIC STRESS-STRAIN CURVE

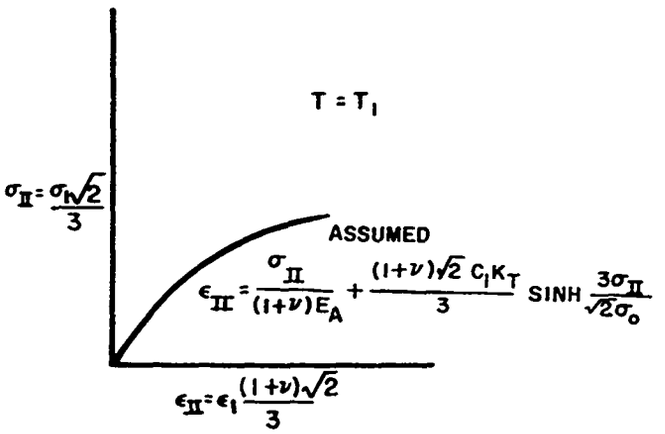


FIGURE 3.2.3.2-3
OCTOHEDRAL STRESS-STRAIN CURVE

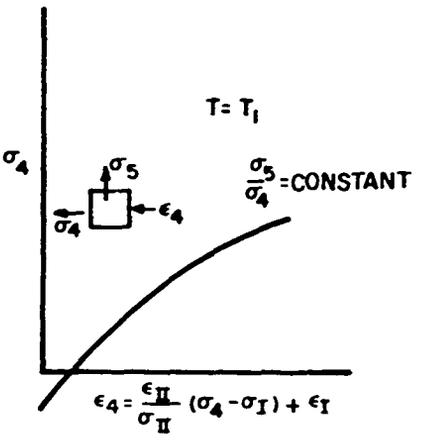


FIGURE 3.2.3.2-4
BIAXIAL STRESS-STRAIN CURVE

3.3 REFERENCES

3-1 Nadai, A., The Influence of Time Upon Creep; The Hyperbolic Sine Creep Law, S. Timoshenko, Anniversary Volume, MacMillan Co., p 155, New York, 1938.

3-2 Tolman, R. C., Principles of Statistical Mechanics, Oxford University Press, p 71, 1938.

3-3 Conrad, H., Correlation of High Temperature Creep and Rupture Data, ASME Preprint Paper No. 58-A 96.

3-4 Heimerl, G. J., Time-Temperature Parameters for Rupture and Creep of Aluminum Alloys, NACA TN-3135.

3-5 Mendelson, A., Hirschberg, M. H., Manson, S.S., A General Approach to the Practical Solution of Creep Problems, ASME Preprint 58-A 98.

3-6 Von Mises, R., Göttinger Nachr., Math.-phys. Kl. p 582, (1913).

3-7 Le'vy, M., C.R. Acad. Sci., Paris, 70,-1323 (1870).

SECTION 4

THERMO-ELASTIC ANALYSIS OF BEAMS

SECTION 4

THERMO-ELASTIC ANALYSIS OF BEAMS

TABLE OF CONTENTS

Paragraph	Title	Page
4	Thermo-Elastic Analysis of Beams	4.4
4.1	Thermo-Elastic Analysis of Statically Determinate (Unrestrained) Beams	4.6
4.1.1	General Solution	4.7
4.1.1.1	Elastic Section Properties of Cross Section	4.9
4.1.1.2	Stresses and Deformations of the Cross Section Due to Temperature	4.9
4.1.1.3	Stresses and Deformations of the Cross Section Due to Combined Mechanical and Thermal Loading	4.10
4.1.2	Evaluation of Integrals	4.11
4.1.2.1	Solution by Finite Sum (with illustrative problem)	4.11
4.1.2.2	Geometry of Concentrated Elastic Areas - Sandwich Beam	4.20
4.1.2.3	Power Series Solution - Bending About One Principal Axis	4.21
4.1.2.3.1	Polynomial Approximation of a Given αT Distribution (with illustrative problem)	4.23
4.1.2.3.2	Binomial Representation of Continuous Elastic Cross Sections	4.28
4.1.2.3.3	Solution for Continuous Elastic Cross Sections (with illustrative problem)	4.30
4.1.2.3.4	Solutions for Discontinuous (Multi-Rectangular) Elastic Cross Sections (with illustrative problem)	4.46
4.1.2.4	Power Series Solution - Corrections for Bending About Both Axes	4.58

TABLE OF CONTENTS (Cont'd)

Paragraph	Title	Page
4.2	Statically Indeterminate (Externally Restrained) Beams	4.58
4.2.1	Beam Deflections (with illustrative problem)	4.58
4.2.2	Fixed End Reactions	4.63
4.2.2.1	Sign Convention	4.63
4.2.2.2	Applied Beam Loads	4.65
4.2.2.3	Determination of Fixed End Reactions	4.67
4.2.2.4	Determination of Fixed End Reaction for Special Cases	4.76
4.2.2.5	Use of Equations and Graphs	4.81
4.2.3	General Solution of Statically Indeterminate Beams	4.86
4.2.3.1	Degrees of Freedom	4.86
4.2.3.2	Equivalent Loading	4.87
4.2.4	Mechanics of Solution by the Flexibility Method	4.88
4.2.5	Mechanics of Solution by the Stiffness (Slope-Deflection) Method	4.92
4.2.6	Selection of Method of Analysis	4.95
4.2.6.1	Problem IA - Statically Indeterminate Beam by the Flexibility Method	4.96
4.2.6.2	Problem IB - Statically Indeterminate Beam by the Stiffness Method	4.101
4.2.6.3	Problem II - Sandwich Beam by the Flexibility Method	4.103
4.2.7	Curved Beams	4.105
4.2.7.1	Values of $\bar{\epsilon}'$, w' and M	4.108

TABLE OF CONTENTS (Cont'd)

Paragraph	Title	Page
4.2.7.2	Special Cases	4.109
4.2.7.3	Sample Problem - Frame Subjected to Thermal and Mechanical Loads	4.112
4.3	References	4.117

SECTION 4 - THERMO-ELASTIC ANALYSIS OF BEAMS

The thermal loading on a beam reduces the stiffness (increasing deformations due to mechanical load), and in general induces thermal stresses and deflections. If the beam is unrestrained externally (statically determinate), then thermal stresses can only occur due to the internal requirements that plane cross sections before bending remain plane after bending, provided that the undeformed beam does not exhibit sharp curvature ($R/d \leq 5$). Experimental evidence does not violate this assumption. If the beam is restrained externally (statically indeterminate), additional thermal stresses will be caused by the redundant restraining forces.

The thermo-elastic analysis of beams, with all of the above factors contributing to the problem, is presented. General solutions are given and methods are presented for the numerical solution of specific problems.

The following symbols are used throughout this section:

a	Non-dimensional thermal strain ratio; Distance from fixed end to initiation of load
a, a'	Coefficients of polynomials
b	Width of cross section
c	Exponent defining variation of $1/(\bar{E}I)$
d	Distance from reference axis to an extreme fiber
e	Non-dimensional width parameter
f	Virtual axial force caused by unit virtual loads
$f_{j,c}$	Influence coefficient for fixed end axial reaction (see text, Paragraph 4.2.2.3)
h	Height
j	Exponent defining variation of curvature
k	Exponent defining variation of axial load; Integer indicating rectangle location
m	Virtual moments caused by unit virtual loads
$m_{j,c}$	Influence coefficient for fixed end moment reaction (See text, Paragraph 4.2.2.3)
m, n	Integers
p	Virtual shear loads caused by unit virtual loads
$p_{j,c}$	Influence coefficient for fixed end transverse reaction
q	Variable transverse load
r	Exponent defining variation of transverse loading
s	Non-dimensional distance u/d
u, v	Distance from reference axes which are oriented parallel to elastic principle axes
$\bar{u}$	Distance from v reference axis to elastic centroid
w	Change in rotation of cross section per unit distance (curvature) due to mechanical loading
w'	Change in rotation of cross section per unit distance (curvature) due to thermal loading
w_t	Total change in rotation of cross section per unit distance, $w_t = w + w'$
x	Distance along length of beam
(x)	Function of x
y, z	Distances from arbitrary but perpendicular reference axes

$\bar{y}, \bar{z}$	Distances $\frac{\int EydA}{\int EdA}$, $\frac{\int EzdA}{\int EdA}$ from Y, Z reference axes to elastic centroid
$\tilde{y}, \tilde{z}$	Distances $\frac{\int Ey\alpha TdA}{\int E\alpha TdA}$, $\frac{\int Ez\alpha TdA}{\int E\alpha TdA}$ from Y, Z reference axes to location of resultant force on the cross section
A	Area = $\int dA$
ΔA, dA	Small element of area
B_j	Level of αT at point "j" above the reference axis value of αT, $B_j = \alpha_j T_j - \alpha_o T_o$
E	Modulus of elasticity = E(T)
Eb	Elastic width = $E_{(avg)}b$
$\overline{EA}$	Effective axial stiffness or force required for unit axial deformation, $\int EdA$
$\overline{EI}$	Effective bending stiffness or moment required for unit rotation, $\overline{EI}_{zz} = \int E\,(y-\bar{y})^2\,dA$
F	Axial force due to mechanical loading
F'	Restoring axial force due to temperature, $F' = \int E\alpha TdA$
$\mathcal{F}_L$	Total cantilever axial load at L due to mechanical loads
I	Moment of inertia of cross section, $I_{zz} = \int (y-\bar{y})^2\,dA$
I_o	Moment of inertia of an element of area about its centroidal axis
K	Non-dimensional shape parameter
L	Length of beam; Power of general term of the αT polynomial
M	Bending moment due to mechanical loading
M'	Restoring bending moment due to temperature, $M'_{zz} = -(\tilde{y}-\bar{y}) \int E\alpha TdA$
$\mathcal{M}_L$	Total cantilever moment at L due to applied mechanical load
P	Transverse load due to mechanical loading
$\mathcal{P}_L$	Total transverse cantilever load at L due to applied mechanical loads
T	Temperature change from a datum value
UU, VV	Elastic principle axes
Y, Z	Arbitrary reference axes
α	Mean coefficient of expansion
αT	Strain due to free thermal expansion
β	Non-dimensional taper parameter
γ	Axial strain parameter
δ	Non-dimensional rotation parameter
ϵ	Strain
$\bar{\epsilon}'$	Axial strain at elastic centroid due to thermal loading
$\bar{\epsilon}$	Axial strain at elastic centroid due to mechanical loading
$\bar{\epsilon}_t$	Total axial strain at elastic centroid, $\bar{\epsilon}_t = \bar{\epsilon} + \bar{\epsilon}'$
ζ	Non-dimensional length parameter defining distance from initiation of load on beam
η	Non-dimensional step parameter
λ	Non-dimensional axial stiffness, $\lambda = \overline{EA}/dE_o b_o$
τ	Variable axial load (shear flow)
μ	Non-dimensional elastic centroid location, $\mu = \bar{u}/d$
ν	Non-dimensional length parameter = a/L; Non-dimensional bending stiffness $\nu = \overline{EI}/d^3 E_o b_o$
σ	Stress
Δ	Deflection

Subscripts

a	Anti-symmetrical
c	Combined
k	At location of k^{th} rectangle
m	Due to mechanical loading
n	At extreme fiber location
o	At reference axis location
s	Symmetrical
t	Due to temperature
u, v, uu, vv	About principal axes
y, z, yy, zz	About arbitrary but perpendicular reference axes
$\bar{y}\bar{y}, \bar{z}\bar{z}$	About y, z centroidal axes
O	Free end of cantilever beam
L	Fixed end of cantilever beam, left side; Due to L^{th} term of αT polynomial
R	Fixed end of cantilever beam, right side

4.1 THERMO-ELASTIC ANALYSIS OF STATICALLY DETERMINATE (UNRESTRAINED) BEAMS

This Sub-section 4.1 presents methods for determining the deformation and stresses of an unrestrained beam subjected to temperature variations through the beam cross section. The section properties for the general case of variable modulus (due to temperature and construction) are given in integral form for the purpose of determining the response of the cross section to both temperature and load. The general solution is then presented in integral form and is evaluated by the methods of finite sum and power series.

The finite sum solution is the most general of those discussed and requires a minimum amount of engineering ingenuity to set up and evaluate tables. It should be used in cases where the directions of the principal axes are not obvious. The power series method, though not as accurate as the finite sum solution, gives a more rapid means of obtaining analytical solutions through the use of approximating analytical functions. The use of approximating functions is further justified by the fact that the functions are to be integrated, thus improving the accuracy of the approximation.

If the beam is unrestrained externally (statically determinate), then the solution presented in this sub-section defines the deformations (axial strain and change of curvature) and the cross sectional stresses. If, however, the beam is restrained externally (statically indeterminate), additional thermal stresses will arise due to compatibility forces (redundants) at the boundary. The deformations of the cross section, obtained in this Sub-section, allow the determination of beam deflections and are thus essential to the thermal solution of indeterminate beams as outlined in Sub-section 4.2.

4.1.1 General Solution

The following paragraphs present the general thermo-elastic solution for an unrestrained beam in integral form, as derived in Reference 4-1. Evaluation of these integrals, which causes most of the difficulty in obtaining numerical solutions to specific problems, is discussed in Paragraph 4.1.2.

The following assumptions and limitations apply to the thermo-elastic solution of the unrestrained beam:

(a) Plane cross sections before bending remain plane after bending. This is the basic assumption in all bending problems. Experimental data indicate that this requirement for the deformations of the cross section is sufficiently accurate for engineering analysis.

(b) Material is linear elastic at any temperature. Thus a single relationship of stress to strain ($\sigma = E\epsilon$) can be utilized to connect the equations of deformation and equilibrium and the principle of superposition can be employed. Any plasticity, buckling, or creep would modify the results, usually by reducing the peak stress but increasing the deflections.

(c) The variation of the cross section and temperature along the length of the beam is both continuous and smooth, and does not produce any significant shear forces. Significant shear forces occur in the vicinity of these abrupt changes (heat sinks, free and clamped ends, and abrupt changes in cross section) and the solution must be modified to account for these effects. These effects should be insignificant at distances greater than the order of the dimensions of the cross section (St. Venant Principle). For example, Reference 4-2 shows that at distances of approximately three beam depths away from free ends, solutions obtained under the assumptions of plane cross sections remaining plane are valid.

The unrestrained beam subjected to temperature (see Figure 4.1.1-1) is analyzed by subjecting the beam to a set of force systems which satisfy equilibrium and produce deformations which are compatible with the requirement of plane cross sections remaining plane after bending.

Consider a unit length of beam. Initially, each fiber of the beam is liberated from the influence of its neighbors. The temperature distribution is then applied to the beam which causes each fiber to expand by an amount αT. In general, the thermal expansion of the fibers will cause the cross sectional plane formed by the ends of the fibers to warp. To satisfy the requirement of plane cross sections remaining plane, a pressure loading of $-E\alpha T$ is applied to eliminate the thermal expansion and return the cross section to its original position and condition (plane). This pressure loading upsets the equilibrium of the cross section. An axial load ($F' = \int E\alpha T da$, equal in magnitude but opposite in direction to the force on the cross section due to the pressure) is applied at the elastic centroid of the cross section. This balancing axial force causes pure translation without rotation of the cross section plane so that the requirement of plane cross sections remaining plane is not violated. Rotational equilibrium still remains to be satisfied since the location of the resultant restoring force $\tilde{y}$, in general, will not coincide with the centroid of elastic area $\bar{y}$. Equilibrium is achieved by applying a balancing moment to the cross section of sufficient magnitude ($M' = \left[\bar{y}-\tilde{y}\right]F'$) to cause pure rotation of the cross sectional plane.

4.1.1 (Cont'd)

The superposed force systems now satisfy equilibrium and produce deformations which are compatible with the requirement of plane cross sections remaining plane. Thus, the procedure outlined above must result in a stress-deformation distribution for an unrestrained beam which is consistent and unique under the assumptions.

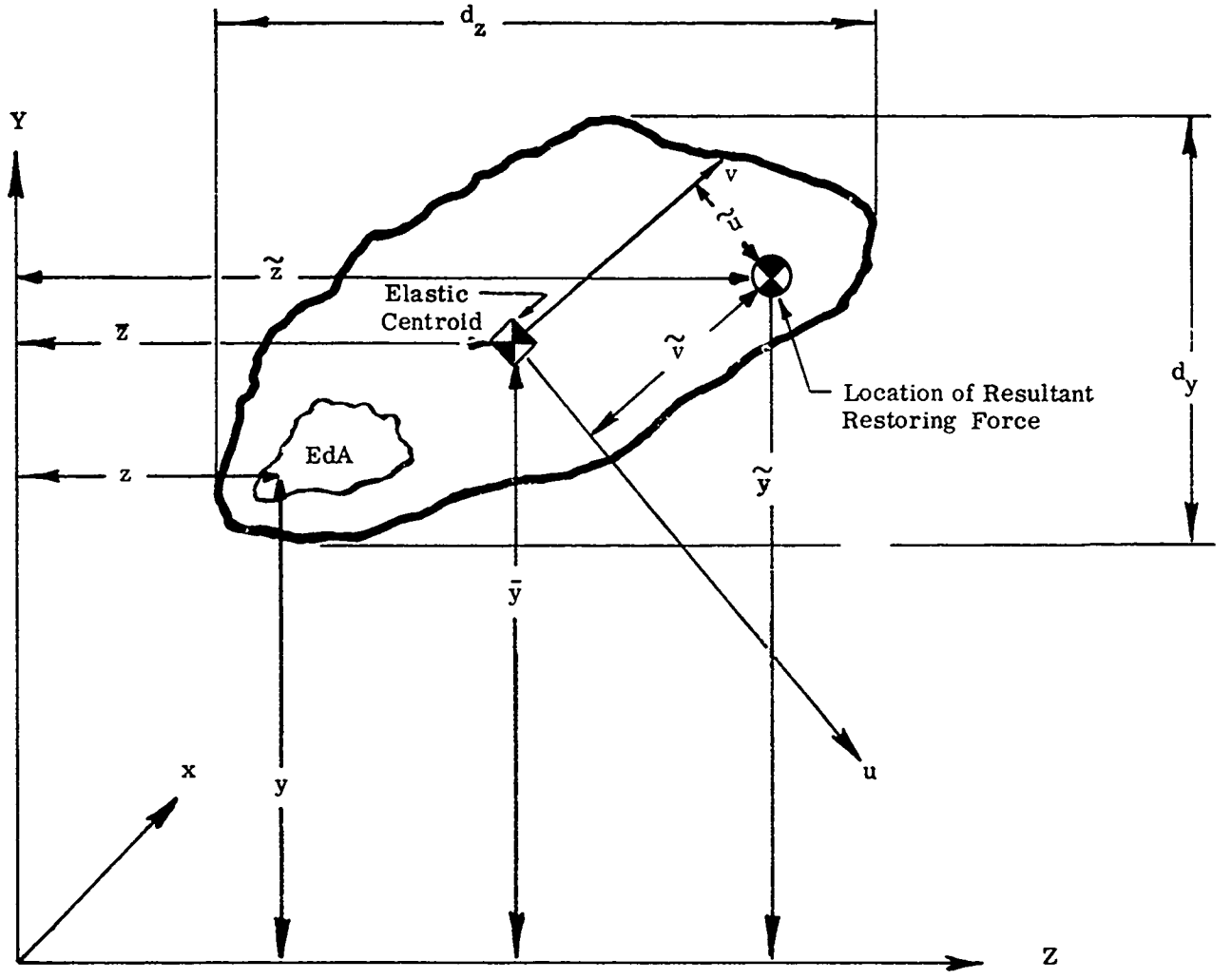


FIGURE 4.1.1-1 ELASTIC AREA CROSS SECTION

4.1.1.1 Elastic Section Properties of Cross Section

The structural response to both mechanical loads and thermal stimulae is governed by both the effective bending ($\overline{EI}$) and axial ($\overline{EA}$) stiffness of the cross section. The equations for these properties, which are stated below, are identical to those for cross sections having constant E except that E is retained within the integral sign since it is permitted to vary over the cross section.

$$\overline{EA} = \int E\,dA \tag{1}$$

$$\bar{y} = \int E\,y\,dA \,/ \int E\,dA \tag{2a}$$

$$\bar{z} = \int E\,z\,dA \,/ \int E\,dA \tag{2b}$$

$$\overline{EI}_{yy}^{--} = \int E\,z^2 dA - \bar{z}^2 \int E\,dA \tag{3a}$$

$$\overline{EI}_{zz}^{--} = \int E\,y^2 dA - \bar{y}^2 \int E\,dA \tag{3b}$$

$$\overline{EI}_{yz}^{--} = \int E\,yz\,dA - \bar{y}\,\bar{z} \int E\,dA \tag{3c}$$

$$(\overline{EI}_{uu}, \overline{EI}_{vv}) = \frac{\overline{EI}_{yy}^{--} + \overline{EI}_{zz}^{--}}{2} \pm \sqrt{\left(\frac{\overline{EI}_{yy}^{--} - \overline{EI}_{zz}^{--}}{2}\right)^2 + (\overline{EI}_{yz}^{--})^2} \tag{4}$$

The distances $\bar{y}$ and $\bar{z}$ (Figure 4.1.1-1) to the elastic centroid are given by Eqs. (2). Thus, the elastic centroid, Eq. (1), is the centroid of the effective elastic area $\overline{EA}$, not of the geometric area. Similarly, the geometric moments of inertia are of no significance when E varies over the cross section. The effective bending stiffnesses, Eq. (3), must be employed.

Equation (4), expresses the bending stiffnesses about the elastic centroid principal axes in terms of the bending stiffnesses about arbitrary centroidal axes. The elastic principal axes are defined as those orthogonal axes for which

$$\overline{EI}_{uv} = \int Euv\,dA = 0.$$

4.1.1.2 Stresses and Deformations of the Cross Section Due to Temperature

No thermal stresses are caused in an unrestrained isotropic, homogeneous, linearly elastic body by an αT distribution which varies linearly in a rectangular coordinate system. Clearly, in the particular case of an unrestrained beam, a linear αT distribution over the cross section produces free thermal expansions which cause plane cross sections to remain plane after deformation. No stresses are required to maintain the plane cross section

In general, a non-linear temperature distribution over the cross section would cause free thermal expansions of the beam fibers which would warp a plane cross section out of plane. Thermal stresses are produced which restore the plane cross section. In this respect, a temperature distribution can be considered as a "thermal load" which, when applied in the absence of mechanical load, still produces stresses and deformations.

Given below are the equations, derived in Reference 4-1, for the stresses and deformations in an unrestrained beam due to thermal load.

4.1.1.2 (Cont d)

$$\bar{\epsilon}' = \frac{F'}{\overline{EA}} \tag{1}$$

$$w'_z = \frac{\left(-\overline{EI}_{yy}\, M'_{zz}\right)+\left(\overline{EI}_{yz}\, M'_{yy}\right)}{\left(\overline{EI}_{yy}\,\overline{EI}_{zz}\right)-\left(\overline{EI}_{yz}\right)^2} \tag{2}$$

$$w'_y = \frac{\left(-\overline{EI}_{zz} M'_{yy}\right)+\left(\overline{EI}_{yz}\, M'_{zz}\right)}{\left(\overline{EI}_{yy}\,\overline{EI}_{zz}\right)-\left(\overline{EI}_{yz}\right)^2} \tag{2b}$$

$$\sigma = E\left[-\alpha T + \bar{\epsilon}' + w'_z\,(y-\bar{y}) + w'_y\,(z-\bar{z})\right] \tag{3}$$

where

$$F' = \int E\alpha T\, dA \tag{4}$$

$$\tilde{y} = \int E\alpha T y\, dA \Big/ \int E\alpha T\, dA \tag{5a}$$

$$\tilde{z} = \int E\alpha T z\, dA \Big/ \int E\alpha T\, dA \tag{5b}$$

$$M'_{zz} = (\bar{y} - \tilde{y})\, F' \tag{6a}$$

$$M'_{yy} = (\bar{z} - \tilde{z})\, F' \tag{6b}$$

4.1.1.3 Stresses and Deformations of the Cross Section Due to Combined Mechanical and Thermal Loading

For a linearly elastic beam, mechanical loads can be combined with thermal loads simply by superposition. Thus

$$\bar{\epsilon}_t = \frac{(F' + F)}{\overline{EA}} \tag{1}$$

$$(w_z)_t = \frac{\left[-\overline{EI}_{yy}\,(M'_{zz} + M_{zz})\right]+\left[\overline{EI}_{yz}\,(M'_{yy} + M_{yy})\right]}{\left(\overline{EI}_{yy}\,\overline{EI}_{zz}\right)-\left(\overline{EI}_{yz}\right)^2} \tag{2a}$$

$$(w_y)_t = \frac{\left[-\overline{EI}_{zz}\,(M'_{yy} + M_{yy})\right]+\left[\overline{EI}_{yz}\,(M'_{zz} + M_{zz})\right]}{\left(\overline{EI}_{yy}\,\overline{EI}_{zz}\right)-\left(\overline{EI}_{yz}\right)^2} \tag{2b}$$

and, as in Paragraph 4.1.1.2

$$\sigma = E\left[-\alpha T + \bar{\epsilon}_t + (w_z)_t\,(y - \bar{y}) + (w_y)_t\,(z - \bar{z})\right] \tag{3}$$

Moments about the $\overline{yy}$ and $\overline{zz}$ centroidal axes are positive when their sense is such that they tend to cause compressive stresses in the positive quadrant (quadrant where both $y - \bar{y}$ and $z - \bar{z}$ have positive values). "F" is positive when tensile, and "T" is positive when above a datum value.

4.1.2 Evaluation of Integrals

The solution of the thermo-elastic beam problem requires the evaluation of the integrals given in Paragraph 4.1.1. Two methods of sufficient engineering accuracy are presented. In the first, integrals are approximated by finite sums; in the second, the goemetry and temperature distributions are approximated by simple integrable functions (polynomials or power series). Approximate methods are justifiable since the functions must be integrated thereby improving the accuracy of approximation.

4.1.2.1 Solution By Finite Sum

The cross section is broken up into a finite number of elemental areas, selected so that the variation of αT and E in each element is small. The procedure is adaptable to all cross sections and the degree of accuracy increases with the decrease in the size of the elements. Digital computing machines can be employed (see Reference 4-3) to solve the problem.

The general solution is outlined in tabular form in Table 4.1.2.1-1 and illustrated by the example which follows, with numerical results given in Table 4.1.2.1-2. The number of tabular columns and labor involved in solving the problem are considerably less when the following simplifying conditions are realized:

(a) y and z axes coincide with principal centroidal axes u and v (example: axis of symmetry)
(b) αT is symmetrical about a principal axis of symmetry of the elastic geometry ($M'_{yy} = 0$ or $M'_{zz} = 0$)

Additional tabular columns are eliminated if E and α are constant over the cross section. Table 4.1.2.1-3 outlines the solution for the case in which all of the above simplifications pertain.

The finite sum solution for the deformations of the cross section is based on an approximating geometry consisting of a finite number of points of concentrated elastic area located at the centroids of elements. Once the deformations ($\bar{\epsilon}$, w_y, w_z) have been calculated from the tabular solution, stresses can be obtained at any points on the cross section as, for example, extreme fiber points (see illustrative problem).

TABLE 4.1 2.1-1

GENERAL TABULAR SOLUTION BY FINITE SUM-UNRESTRAINED THERMO-ELASTIC BEAM

For Rectangular Elements

1	2	3	4	5	6	7	8	9	10	11	12	13	14	15	16	17	18	19	20
Element No. "j"	h	b	ΔA	y	z	T	E	$E\Delta A$	$(E\Delta A)y$	$(E\Delta A)y^2$	I_{ozz}	EI_{ozz}	$(E\Delta A)z$	$(E\Delta A)z^2$	I_{oyy}	EI_{oyy}	$(E\Delta A)yz$	I_{oyz}	EI_{oyz}
	Geometry (See Fig. 4.1.2.1-1)	Geometry (See Fig. 4.1.2.1-1)	② x ③ For Rectangles	Geometry (See Fig. 4.1.2.1-1)	Geometry (See Fig. 4.1.2.1-1)	See Data	See Data	④ x ⑧	⑤ x ⑨	⑤ x ⑩	•	⑧ x ⑫	⑥ x ⑨	⑥ x ⑭	•	⑧ x ⑯	⑥ x ⑩	•	⑧ x ⑲

TABLE 4.1.2.1-1 (Cont'd)

GENERAL TABULAR SOLUTION BY FINITE SUM-UNRESTRAINED THERMO-ELASTIC BEAM

SOLUTION FOR THERMAL LOADS

1	21	22	23	24	25	26	27	28	29	30	31
Element No	α	αT	$(E\Delta A)\,\alpha T$	$(E\Delta Ay)\alpha T$	$(E\Delta Az)\alpha T$	$y - \bar{y}$	$w_z'(y-\bar{y})$	$z - \bar{z}$	$w_y'(z-\bar{z})$	ϵ	$\sigma \quad E\epsilon$
	See Data	(7) × (21)	(9) × (22)	(10) × (22)	(11) × (22)	(5) ×	w_z' (26)	(6) − $\bar{z}$	w_y' (28)	(27) − (29) − (22) · $\bar{\epsilon}$	(8) × (30)
			Σ (23)	Σ (24)	Σ (25)						

SOLUTION FOR MECHANICAL LOADS

32	33	34	35
$w_z'(y-\bar{y})$	$w_y'(z-\bar{z})$	ϵ	$\sigma = E\epsilon$
w_z' (26)	w_y' (28)	(32) − (33) − $\bar{\epsilon}$	(5) × (31)

36
Combined Stress σ_c
(31) + (35)

4.1.2.1 (Cont'd)

The solution of an unrestrained beam by the finite sum method is illustrated below for an unsymmetrical section with an unsymmetrical temperature distribution, $T = T(y,z)$, on the cross section of the Halcomb 218 "zee" spar shown in Figure 4.1.2.1-2. Determination of the following is required:

(1) Thermal stresses and deformations

(2) Stresses and deformations when subjected to a moment about the vertical axis of 10,000 inch-pounds and an axial force of 10,000 pounds, i.e.:

$$M_{yy} = 10,000 \text{ inch-pounds}$$

$$M_{zz} = 0$$

$$F = 10,000 \text{ pounds}$$

The solution is worked out in Table 4.1.2.1-2 by the finite sum method. Stresses are plotted in Figure 4.1.2.1-3.

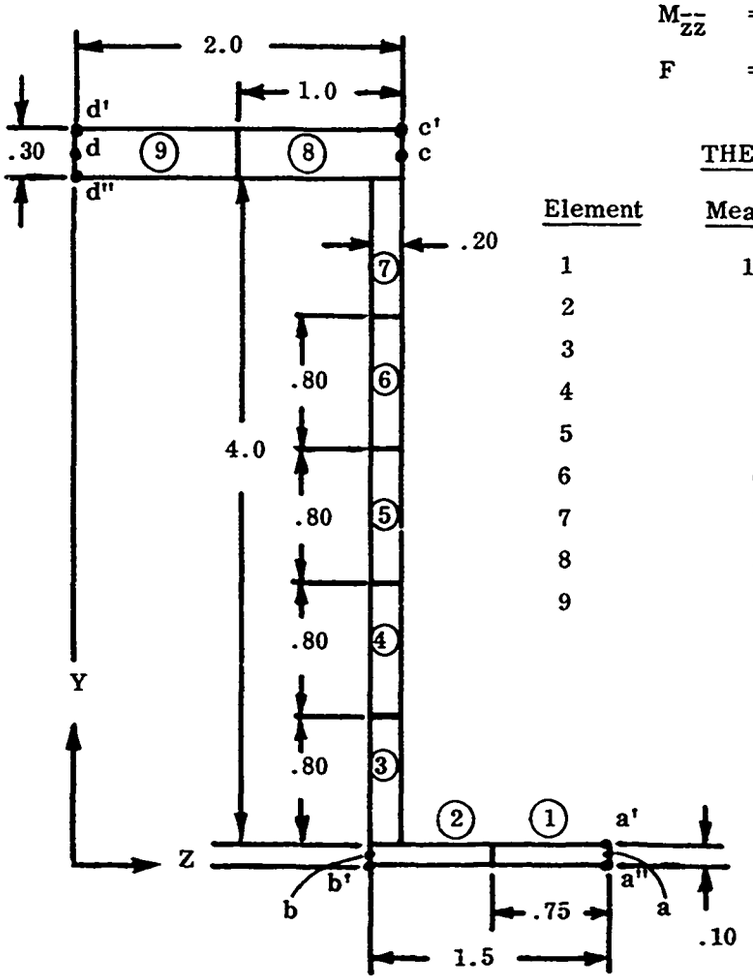
4.1.2.1 (Cont'd)

MECHANICAL LOADS

M_{yy} = 10,000 inch pounds

M_{zz} = 0

F = 10,000 pounds



THERMAL LOADS

Element	Mean Temp.	$E/10^6$	$\alpha(10^6)$
1	1000°F	20.0	6.60
2	950	21.1	6.53
3	850	23.3	6.35
4	770	24.7	6.23
5	700	25.8	6.03
6	650	26.5	5.88
7	700	25.8	6.03
8	800	24.2	6.25
9	900	22.2	6.44

FIGURE 4.1.2.1-2 FINITE SUM METHOD

TABLE 4.1.2.1-2

ILLUSTRATIVE PROBLEM

HALCOMB 218 ZEE WITH AN UNSYMMETRICAL TEMPERATURE DISTRIBUTION, $T = T(y, z)$

1	2	3	4	5	6	7	8	9	10	11	12	13	14	15	16	17	18	19	20
Element No.	h	b	ΔA	y	z	T	E	$E\Delta A$	$E\Delta Ay$	$E\Delta Ay^2$	I_{ozz}	EI_{ozz}	$E\Delta Az$	$E\Delta Az^2$	I_{oyy}	EI_{oyy}	$E\Delta Ayz$	I_{oyz}	EI_{oyz}
Figure 4.1.2.1-1 and -2	Figure 4.1.2.1-1 and -2	Figure 4.1.2.1-1 and -2	② × ③	Figure 4.1.2.1-2	Figure 4.1.2.1-2	Figure 4.1.2.1-2	See Data	④ ⑧	⑤ ⑨	⑤ ⑩	$\frac{③ ②^3}{12}$	⑧ ⑫	⑥ ⑨	⑥ ⑭	$\frac{② ③^3}{12}$	⑧ ⑯	⑥ ⑩	---	⑧ ⑲
	in.	in.	$in.^2$	in.	in.	°F	$\times 10^6$ lb/in^2	$\times 10^6$ lb	$\times 10^6$ in-lb	$\times 10^6$ in^2-lb	$in.^4$	$\times 10^6$ in^2-lb	$\times 10^6$ in-lb	$\times 10^6$ in^2-lb	in^4	$\times 10^6$ in^2-lb	$\times 10^6$ in^2-lb	in^4	$\times 10^6$ in^2-lb
1	.10	.75	.075	.05	2.925	1000	20.0	1.500	.075	.00375	.000063	.00126	4.3875	12.8334	.003516	.07032	.21937	0	0
2	.10	.75	.075	.05	2.175	950	21.1	1.5825	.07913	.00396	.000063	.001329	3.4419	7.4861	.003516	.074188	.17211	0	0
3	.80	.20	.160	.50	1.90	850	23.3	3.728	1.864	932	.008533	.19882	7.0832	13.4581	.000533	.012419	3.5416	0	0
4	.80	.20	.160	1.30	1.90	770	24.7	3.952	5.1376	6.67888	.008533	.21077	7.5088	14.2667	.000533	.013165	9.76114	0	0
5	.80	.20	.160	2.10	1.90	700	25.8	4.128	8.6688	18.20448	.008533	.22015	7.8432	14.9021	.000533	.013751	16.47072	0	0
6	.80	.20	.160	2.90	1.90	650	26.5	4.240	12.296	35.6584	.008533	.22612	8.056	15.3064	.000533	.014125	23.3624	0	0
7	.80	20	.160	3.70	1.90	700	25.8	4.128	15.2736	56.51232	.008533	.22015	7.8432	14.9021	.000533	.013751	29.01981	0	0
8	30	1.00	300	4.20	1.50	800	24.2	7.260	30.492	128.0664	.00225	.05445	10.89	16.335	.025	.605	45.738	0	0
9	30	1.00	.300	4.20	.50	900	22.2	6.66	27.972	117.4824	.00225	.04995	3.33	1.665	.025	.555	13.986	0	0
Σ								37.1785	101.85813	363.54259		1.182999	60.3828	111.1549		1.371719	112.27148		0
Additional Points																			
a'				10	3.30	1000	20.0												
a				.05	3.30	1000	20.0												
a''				0	3.30	1000	20.0												
b				.05	1.80	950	21.1												
b'				0	1.80	950	21.1												
c				4.25	2.00	800	24.2												
c'				4.40	2.00	800	24.2												
d				4.25	0	900	22.2												
d'				4.40	0	900	22.2												
d''				4.10	0	900	22.2												

Extreme Fibers

$$\bar{y} = \frac{\Sigma_j(E\Delta Ay)}{\Sigma_j(E\Delta A)} = \frac{\Sigma ⑩}{\Sigma ⑨} = 2.73971$$

$$\bar{z} = \frac{\Sigma_j(E\Delta Az)}{\Sigma_j(E\Delta A)} = \frac{\Sigma ⑭}{\Sigma ⑨} = 1.62416$$

$$EI_{\bar{z}\bar{z}} = \Sigma_j(E\Delta Ay^2) + \Sigma_j(EI_{ozz}) - \bar{y}\,\Sigma_j(E\Delta Ay) = \Sigma ⑪ + \Sigma ⑬ - \bar{y}\,\Sigma ⑩ = 85.66385 \times 10^6 \text{ in}^2\text{-lb}$$

$$EI_{\bar{y}\bar{y}} = \Sigma_j(E\Delta Az^2) + \Sigma_j(EI_{oyy}) - \bar{z}\,\Sigma_j(E\Delta Az) = \Sigma ⑮ + \Sigma ⑰ - \bar{z}\,\Sigma ⑭ = 14.45367 \times 10^6 \text{ in}^2\text{-lb}$$

$$EI_{\bar{y}\bar{z}} = \Sigma_j(E\Delta Ayz) + \Sigma_j(EI_{oyz}) - \bar{y}\,\Sigma_j(E\Delta Az) = \Sigma ⑱ + \Sigma ⑳ - \bar{y}\,\Sigma ⑭ = -23.16262 \times 10^6 \text{ in}^2\text{-lb}$$

TABLE 4.1.2 1-2 (Cont'd)

ILLUSTRATIVE PROBLEM

HALCOMB 218 ZEE WITH AN UNSYMMETRICAL TEMPERATURE DISTRIBUTION, T = T(y,z)

Solution for Thermal Loads

Solution for Mechanical Loads: M_{yy} = 10 000 in lb; M_{zz} = 0; P = 10,000 lb

1	21	22	23	24	25	26	27	28	29	30	31
Element No "i"	α	αT	$E\Delta A \alpha T$	$E\Delta A y \alpha T$	$E\Delta A z \alpha T$	$y - \bar{y}$	$w'_z (y-\bar{y})$	$z - \bar{z}$	$w'_y (z-\bar{z})$	ϵ	$\sigma = E\epsilon$
	See Data	(7)(21)	(9)(22)	(10)(22)	(14)(22)	(5) - $\bar{y}$	w'_z (26)	(6) - $\bar{z}$	w'_y (28)	(27)·(29)/(22)·$\bar{\epsilon}'$	(8)(30)
	x10^{-6}in/in/°F	x10^{-6}in/in	in-lb/in	in^2-lb/in	in^2-lb/in	in	x10^{-6}in/in	in	x10^{-6}in/in	x10^{-6}in/in	lb/in^2
1	6.60	6600	9900	495	28,957	-2.6897	858	1.3008	-1096	-1868	-37360
2	6.53	6200	9811	491	21,340	-2.6897	858	.5408	-456	-828	-17471
3	6.35	5400	20131	10066	38,219	-2.2397	715	.2758	-232	53	1230
4	6.23	4800	18970	24660	36,042	-1.4397	459	.2758	-232	397	9810
5	6.03	4220	17420	36582	33,098	- .6397	204	.2758	-232	722	18630
6	5.88	3820	16197	46971	30,774	.1603	- 51	.2758	-232	867	22976
7	6.03	4220	17420	64455	33,098	.9603	-306	.2758	-232	212	5470
8	6.25	5000	36300	152460	54,450	1.4603	-466	- .1242	105	-381	-9220
9	6.44	5800	38628	162238	19,314	1.4603	-466	-1.1242	947	-349	-7748
Σ			184777	498418	295,322						
Additional Points											
a'	6.60	6600				-2.6397	841	1.6758	-1412	-2201	-44020
a	6.60	6600				-2.6897	858	1.6758	-1412	-2184	-43680
a''	6.60	6600				-2.7397	874	1.6758	-1412	-2168	-43360
b	6.53	6200				-2.6897	858	.1758	-148	-520	-10972
b'	6.53	6200				-2.7397	874	.1758	-148	-504	-10650
c	6.25	5000				1.5103	-482	.3758	-317	-829	-20000
c'	6.25	5000				1.6603	-530	.3758	-317	-877	-21200
d	6.44	5800				1.5103	-482	-1.6242	1368	56	1240
d'	6.44	5800				1.6603	-530	-1.6242	1368	+8	170
d''	6.44	5800				1.3603	-434	-1.6242	1368	104	2310

Extreme Fibers

$\bar{y} = \frac{\Sigma (E\Delta A)(\alpha T)}{\Sigma (E\Delta A)(\alpha T)} = \frac{(24)}{(22)} = 2.69740$ in

$\bar{z} = \frac{\Sigma (E\Delta A)(\alpha T)}{\Sigma (E\Delta A)(\alpha T)} = \frac{(25)}{(22)} = 1.59836$ in

$M_{yy} = (4)\bar{y}_{iP} = (4)\bar{z}_{iP} = (23) = 6765.72$ in-lb

$M'_{zz} = (5)\bar{y}_{iP} = (5)\bar{z}_{iP} = (23) = 7937.93$ in-lb

$\epsilon'_i = \frac{\cdot EI_{yy} M'_{zz} \cdot EI_{yz} M'_{yy}}{EI_{yy} EI_{zz} \cdot (EI_{yz})^2} = 310.02943 \times 10^{-6}$/in

$\epsilon'_y = \frac{\cdot EI_{zz} M'_{yy} \cdot EI_{yz} M'_{zz}}{EI_{yy} EI_{zz} \cdot (EI_{yz})^2} = 842.36585 \times 10^{-6}$ in

$\bar{\epsilon}' = \frac{P'}{EA} \cdot \frac{(E\Delta A \alpha T)}{\Sigma (E\Delta A)} = \frac{(23)}{(V)} = 4070 \times 10^{-6}$ in/in

32	33	34	35
$w_z (y-\bar{y})$	$w_y (z-\bar{z})$	ϵ	$\sigma = E\epsilon$
w_z (26)	w_y (28)	(32)·(33)/$\bar{\epsilon}'$	(8)x(34)
x10^{-6}in/in	x10^{-6}in/in	x10^{-6}in/in	lb/in^2
-888	+1587	968	+19360
-888	+660	41	+870
-738	+336	-134	-3120
-475	+336	+130	+3210
-211	+336	+394	+10170
+ 53	+336	+658	+17440
+317	+336	+922	+23790
+482	-152	+599	+14500
+482	-1372	-621	-13790
-871	2044	1442	+28840
-888	+2044	1425	+28500
-905	2044	1408	+28160
-888	+214	-405	-8540
-905	+214	-422	-8890
+498	+458	1225	+29700
+548	+458	1275	+30800
+498	-1981	-1214	-26900
+548	-1981	-1164	-25800
+449	-1981	-1263	-28100

$\epsilon_i = \frac{\cdot EI_{yy} M_{zz} \cdot EI_{yz} M_{yy}}{EI_{yy} EI_{zz} \cdot (EI_{yz})^2} = +330 \times 10^{-6}$/in

$\epsilon_y = \frac{\cdot EI_{zz} M_{yy} \cdot EI_{yz} M_{zz}}{EI_{yy} EI_{zz} \cdot (EI_{yz})^2} = +1220 \times 10^{-6}$/in

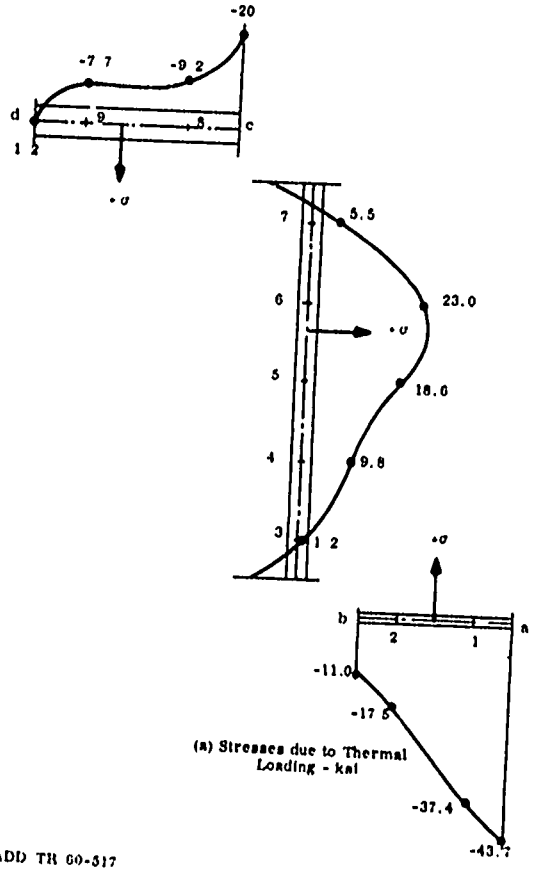
$\bar{\epsilon} = \frac{P}{EA} = \frac{P}{(V)} = 369 \times 10^{-6}$ in/in

36
Combined Stress σ_c
(31)·(35)
lb/in^2
-18000
-16601
-1890
+13020
+28800
+40416
+29200
+5280
-21538
-15180
-15180
-15200
-18512
-18540
+9700
+9600
-25660
-25630
-25790

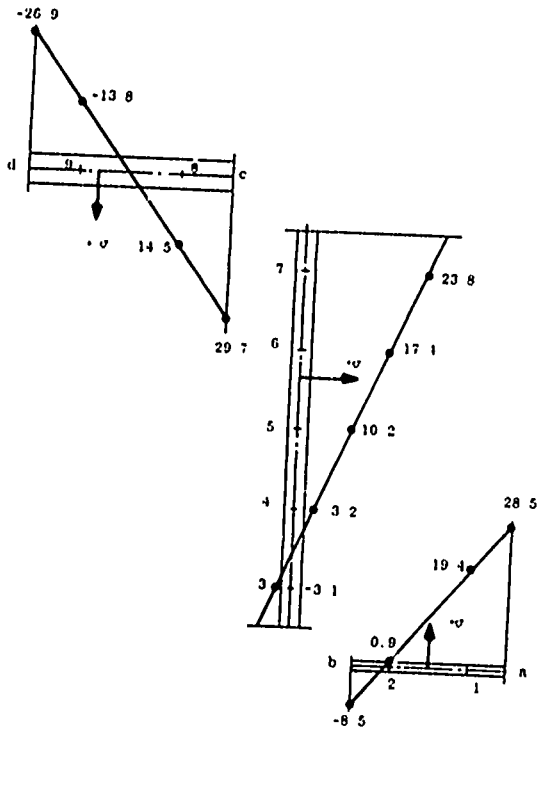
4.1.2.1 (Cont'd)

- Smooth Curves Through Points Calculated in Table 4.1.2.1-2

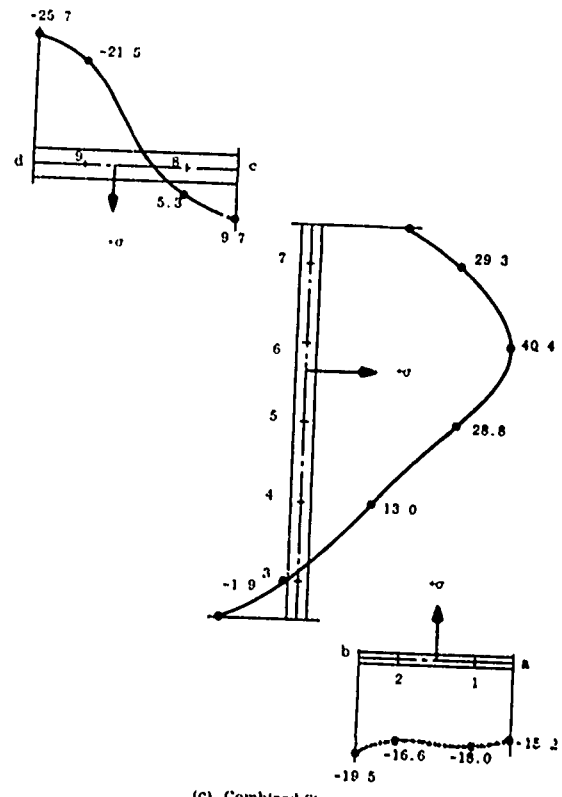
Scale 20 ksi per in.



(a) Stresses due to Thermal Loading - ksi



(b) Stresses due to Mechanical Loading - ksi



(c) Combined Stresses - ksi

FIGURE 4.1.2.1-3 STRESS DISTRIBUTION FOR PROBLEM OF FIGURE 4.1.2.1-2

TABLE 4.1.2.1-3

SIMPLIFIED TABULAR SOLUTION FOR THERMAL STRESSES IN AN UNRESTRAINED BEAM WHEN.

(1) α and E are constant.
(2) y and z axes coincide with principal centroidal axes.
(3) T is symmetrical about y axes.

For Rectangular Elements

1	2	3	4	5	6	7	8	9	10	11	12	13	14	15	16	17	18	19	20
Element No.	h	b	ΔA	y	T	ΔAT	ΔAyT	ΔAy^2	I_{ozz}	αT	yw'_z	σ							
	Geometry (See Fig. 4.1.2.1-1)	Geometry (See Fig. 4.1.2.1-1)	②③ For Rectangles	Geometry (See Fig. 4.1.2.1-1)	See Data	④⑥	⑤⑦	④⑤^2	$\frac{③②^3}{12}$	α⑥	⑤w'_z	$\left[\frac{⑫}{⑪}\cdot\frac{⑤}{d'}\right]$							
			$\Sigma_j(\Delta A)$			$\Sigma_j(\Delta AT)$	$\Sigma_j(\Delta AyT)$	$\Sigma_j(\Delta Ay^2)$	$\Sigma_j(I_{ozz})$										

4.1.2.2 Geometry of Concentrated Elastic Areas - Sandwich Beam

The finite sum method (described in paragraph 4.1.2.1) reduces the continuous cross section into a number of discrete elements, such that each element is considered to be a concentrated point of elastic area (EA), and free thermal strain (αT). This approximation is especially applicable to beam cross sections made up of localized, high area flanges (or caps) and thin shear webs. In beams of this type, the deformations of the cross section and thermal stresses in the caps can usually be determined with sufficient accuracy (especially if peak temperatures occur in the caps) by neglecting the web material, thus considerably reducing the amount of calculation.

As an example, consider the sandwich beam cross section shown in Fig. 4.1.2.2-1. It is assumed that E, α, and T are constant in each face, the face thickness is small compared to the depth of the cross section, and the core carries only shear. Thus the cross section is symmetrical about the y axis and the faces can be considered as concentrations of elastic area (EA) and free thermal strain (αT).

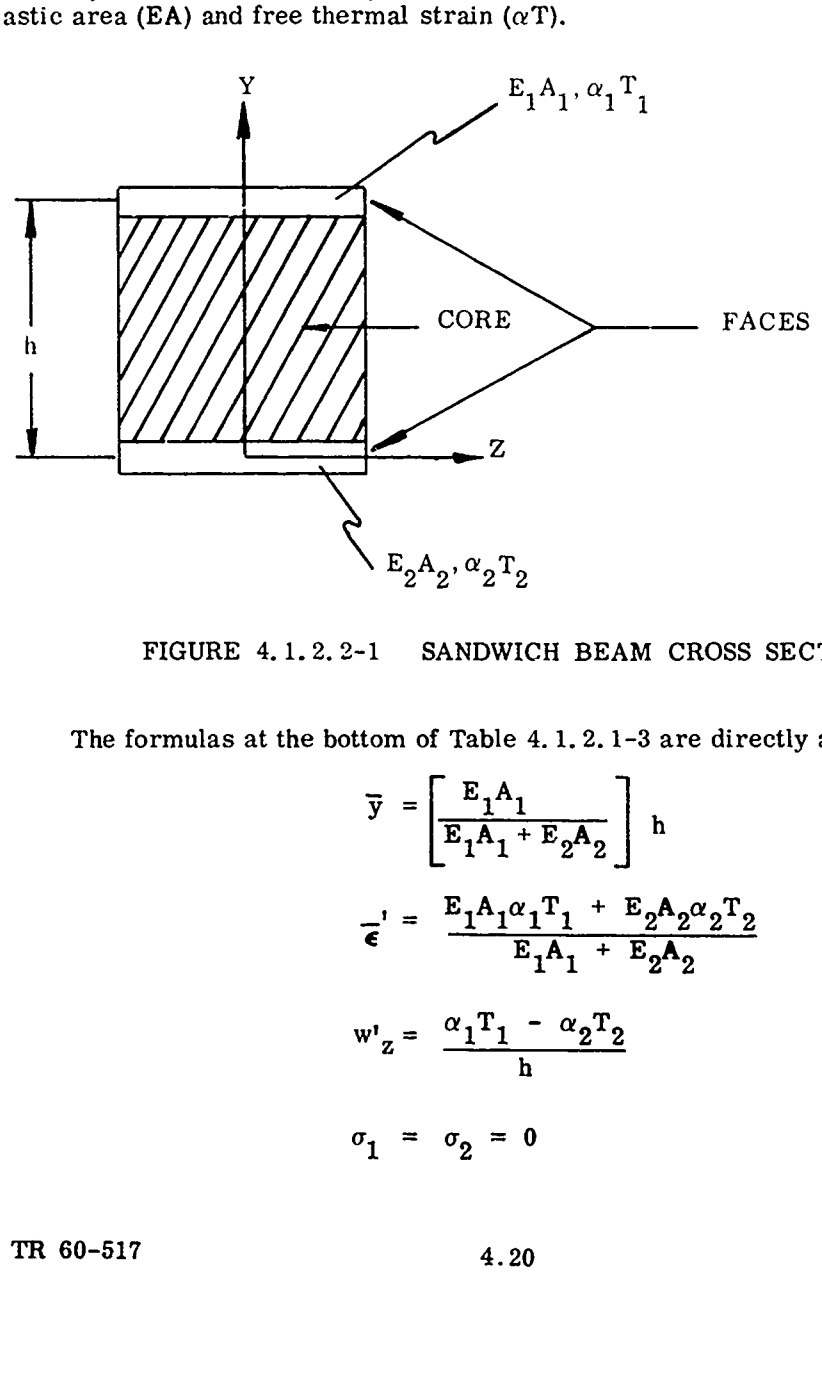


FIGURE 4.1.2.2-1 SANDWICH BEAM CROSS SECTION

The formulas at the bottom of Table 4.1.2.1-3 are directly applicable. They yield

$$\bar{y} = \left[\frac{E_1A_1}{E_1A_1 + E_2A_2}\right] h \qquad (1)$$

$$\bar{\epsilon}' = \frac{E_1A_1\alpha_1T_1 + E_2A_2\alpha_2T_2}{E_1A_1 + E_2A_2} \qquad (2)$$

$$w'_z = \frac{\alpha_1T_1 - \alpha_2T_2}{h} \qquad (3)$$

$$\sigma_1 = \sigma_2 = 0 \qquad (4)$$

4.1.2.2 (Cont'd)

Note that no thermal stresses occur in the faces, Eq. (4). In fact, no thermal stresses can occur in an unrestrained beam when the cross section consists of less than four concentrated areas because, for two or three such areas, a plane can always be passed through the thermally deformed section.

4.1.2 3 Power Series Solution - Bending About One Principal Axis

The power series method gives a non-dimensional solution to the unrestrained thermo-elastic beam problem in terms of non-dimensional parameters which define the thermal loads and section properties.

This paragraph discusses the application of the power series method to problems in which the directions of the principal axes are known and bending occurs about only one of these axes (as, for example, when one of the principal axes is an axis of symmetry for both the elastic area of the cross section and the αT distribution). Under such conditions, the power series method usually has a distinct advantage over the finite sum method.

The method can be extended easily to the general case of bending about both principal axes (Paragraph 4.1 2.4). However, because of the additional numerical computation required, expecially when the directions of the principal axes must first be determined, the method of finite sum should be used in problems involving bending about both axes so as to obtain solutions with the least amount of labor.

Paragraph 4 1.1 1 shows that, in general, the modulus of elasticity, E, varies over the cross section and thus appears under the integral sign in the formulas for the section properties. Accordingly, the structural behavior is governed by the elastic properties of the cross section ($\overline{EA}$, $\overline{EI}$), rather than by the geometric properties of the cross section (A, I).

The power series method will be applied to beams having the following types of elastic cross section configurations:

(a) Cross sections where the elastic width (Eb) is monotonically continuous through the depth or on each side of a bending axis of symmetry. (Figure 4.1.2.3-1(a) and -1(b)).

(b) Cross sections with discontinuous elastic width variation of the multi-rectangular type as exemplified by tees, channels, I-beams, etc. (Figure 4.1.3-1(c)). Cross sections that do not have the above configurations can usually be approximated by them with a reasonable degree of accuracy.

The following steps are taken in arriving at the solution:

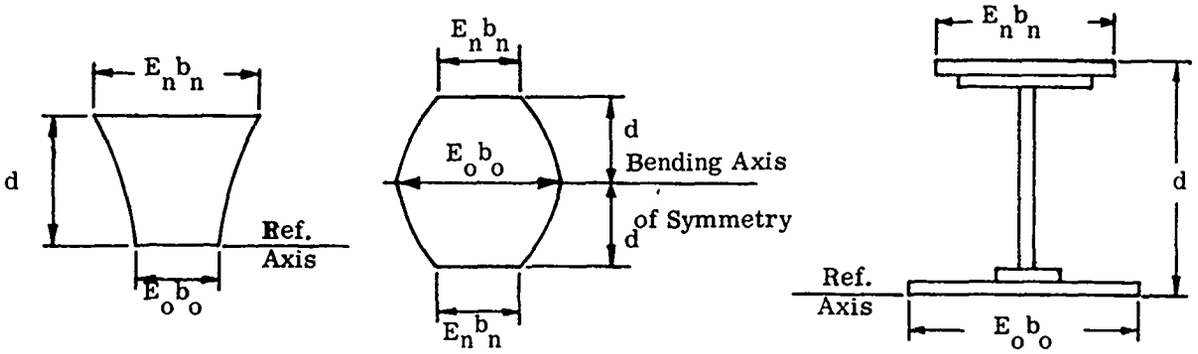
(a) The average αT profile (Figure 4.1.2.3-2 and Paragraph 4.1.2.4) in a direction normal to the principal bending axis is approximated by a power series (polynomial) of the form

$$\alpha T = \sum_{L=o}^{n} a_L s^L = a_n s^n + a_{n-1} s^{n-1} + \ldots + a_o \qquad (1)$$

(b) Continuous cross sectional configurations of the types discussed above are represented by binomials of the form

$$Eb = E_o b_o (1 + \beta s^K) \qquad (2)$$

where β and K are non-dimensional parameters defining the elastic width variation.



(a) Monotonically Continuous Elastic Width Variation

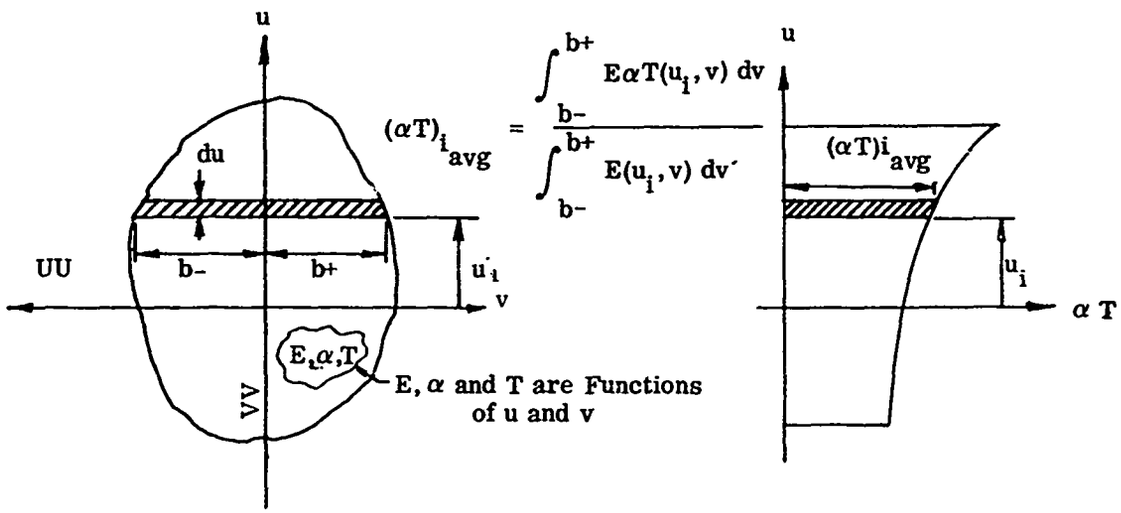
(b) Elastic Widths Monotonically Continuous and Symmetrical About the Bending Axis

(c) Multi-rectangular Discontinuous Elastic Width Variation

FIGURE 4.1.2.3-1 TYPICAL CONFIGURATIONS OF ELASTIC CROSS SECTION AREAS

Discontinuous multi-rectangular configurations are expressed by means of step parameters η_m defined in Eq. (1) of Paragraph 4.1.2.3.4.

(c) The parameters which define the αT distribution and elastic cross section in the above manner are substituted into non-dimensional expressions for the stresses and deformations.



(a) Cross Section With Two Dimensional Distribution of E, α , T

(b) One Dimensional Average αT Profile in u Principal Direction.

FIGURE 4.1.2.3-2 DETERMINATION OF AVERAGE αT PROFILE FOR BENDING ABOUT UU PRINCIPAL AXIS

4.1.2.3.1 Polynomial Approximation of a Given αT Distribution

Consider the temperature (αT) profile shown in Figure 4.1.2.3.1-1, which represents the average variation in the direction of one of the principal axes.

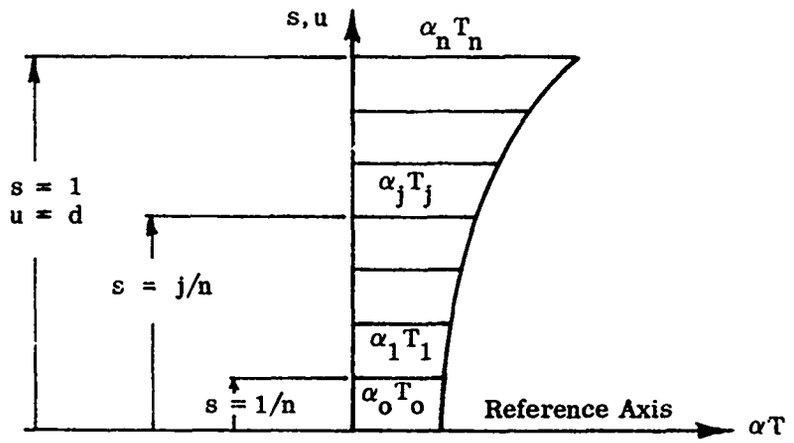


FIGURE 4.1.2.3.1-1 αT PROFILE

It is desired to determine a polynomial expression of the form

$$\alpha T = a_n s^n + a_{n-1} s^{n-1} \ldots\ldots + a_1 s + \alpha_o T_o = \sum_{L=o}^{n} a_L s^L \qquad (1)$$

where s = u/d, which will match the profile values of αT at discrete points equally spaced through the depth. The solution consists of solving n linear algebraic equations for the n unknown coefficients a_n, $a_{n-1} \ldots a_1$, where n is numerically equal to the number of equal subdivisions of the profile. In matrix form, the coefficients are determined from the equation:

$$\begin{Bmatrix} a_1 \\ a_2 \\ \vdots \\ a_j \\ \vdots \\ a_{n-1} \\ a_n \end{Bmatrix} = \begin{bmatrix} \left(\frac{1}{n}\right) & \left(\frac{1}{n}\right)^2 & \ldots & \left(\frac{1}{n}\right)^j & \ldots & \left(\frac{1}{n}\right)^n \\ \left(\frac{2}{n}\right) & \left(\frac{2}{n}\right)^2 & \ldots & \left(\frac{2}{n}\right)^j & \ldots & \left(\frac{2}{n}\right)^n \\ \vdots & \vdots & & \vdots & & \vdots \\ \left(\frac{j}{n}\right) & \left(\frac{j}{n}\right)^2 & \ldots & \left(\frac{j}{n}\right)^j & \ldots & \left(\frac{j}{n}\right)^n \\ \vdots & \vdots & & \vdots & & \vdots \\ \left(\frac{n-1}{n}\right) & \left(\frac{n-1}{n}\right)^2 & \ldots & \left(\frac{n-1}{n}\right)^j & \ldots & \left(\frac{n-1}{n}\right)^n \\ (1) & (1) & \ldots & (1) & \ldots & (1) \end{bmatrix}^{-1} \begin{Bmatrix} B_1 \\ B_2 \\ \vdots \\ B_j \\ \vdots \\ B_{n-1} \\ B_n \end{Bmatrix} \qquad (2)$$

where $B_j = (\alpha_j T_j - \alpha_o T_o)$. (3)

4.1.2.3.1 (Cont'd)

Obviously, as more and more subdivisions are taken, higher order polynomials are obtained which more accurately match the correct temperature profile. However, the additional work and time expended in obtaining high order, extremely accurate, polynomial representations is seldom justified. Since the temperature distribution is to be integrated in the process of obtaining the solution, the accuracy of the approximation using a low order polynomial is improved. Also, an exact representation of the temperature profile may become meaningless if the available data from which the profile is constructed is scant and inaccurate (as is often the case). In most cases, solutions of engineering accuracy can be obtained with polynomials no higher than the 4th order (which matches αT at the extreme fiber, at the reference axis and 3 intermediate equally spaced points). The matrix solutions for the coefficients, presented in Eq. (2) in general form, are given in Table 4.1.2.3.1-1 for polynomials up to the 4th order.

The order of polynomial to be used in any given problem should be determined on the basis of factors such as the completeness of available data, the shape of the temperature profile, and the desired degree of accuracy. The coefficients of polynomials higher than the 4th order can be determined from Eq. (2).

The method of polynominal approximation of the αT profile is illustrated below for the case where the values of αT are given at five equally spaced points, as shown in Figure 4.1.2.3.1-2. The following will be determined:

(1) The polynomial which fits the 3 points ⓪, ② and ④

(2) The polynomial which fits all 5 points

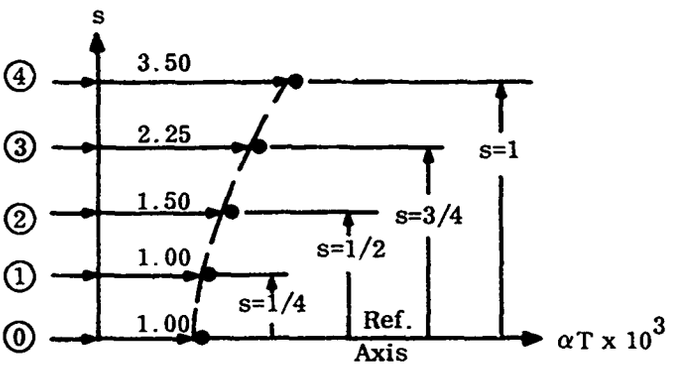


FIGURE 4.1.2.3.1-2 αT VALUES AT 5 EQUALLY SPACED POINTS

For a 3 point fit, Table 4.1.2.3.1-1 gives

$$\alpha T = \sum_{L=o}^{2} a_L s^L = a_2 s^2 + a_1 s + \alpha_o T_o$$

where

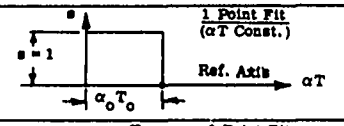
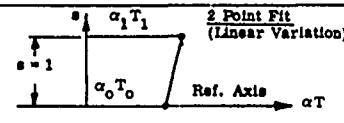
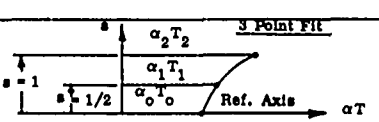
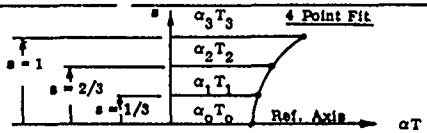
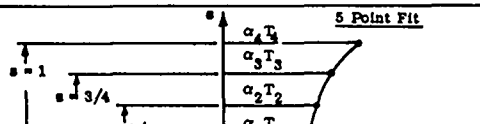
$$\alpha_o T_o = 1.0 \times 10^{-3}$$

and

$$\begin{Bmatrix} a_1 \\ a_2 \end{Bmatrix} \times 10^3 = \begin{bmatrix} 4 & -1 \\ -4 & 2 \end{bmatrix} \begin{Bmatrix} 1.5 - 1.0 \\ 3.5 - 1.0 \end{Bmatrix} = \begin{bmatrix} 4 & -1 \\ -4 & 2 \end{bmatrix} \begin{Bmatrix} 0.5 \\ 2.5 \end{Bmatrix}$$

TABLE 4.1.2.3.1-1

COEFFICIENTS OF THERMAL STRAIN (αT) DISTRIBUTION

ORDER OF POLYNOMIAL	EQUATION FOR αT ($\alpha T = \sum_{L=0}^{n} a_L s^L$)	MATRIX EQUATION FOR COEFFICIENTS	TYPE OF FIT
0	$\alpha T = \alpha_o T_o$ = CONSTANT	---	
1	$\alpha T = a_1 s + \alpha_o T_o$	$a_1 = (\alpha_1 T_1 - \alpha_o T_o) = B_1$ where $B_i = \alpha_i T_i - \alpha_o T_o$	
2	$\alpha T = a_2 s^2 + a_1 s + \alpha_o T_o$	$\begin{Bmatrix} a_1 \\ a_2 \end{Bmatrix} = \begin{bmatrix} 4 & -1 \\ -4 & 2 \end{bmatrix} \begin{Bmatrix} B_1 \\ B_2 \end{Bmatrix}$	
3	$\alpha T = a_3 s^3 + a_2 s^2 + a_1 s + \alpha_o T_o$	$\begin{Bmatrix} a_1 \\ a_2 \\ a_3 \end{Bmatrix} = \begin{bmatrix} (+9) & (-4\frac{1}{2}) & (+1) \\ (-22\frac{1}{2}) & (18) & (-4\frac{1}{2}) \\ (13\frac{1}{2}) & (-13\frac{1}{2}) & (4\frac{1}{2}) \end{bmatrix} \begin{Bmatrix} B_1 \\ B_2 \\ B_3 \end{Bmatrix}$	
4	$\alpha T = a_4 s^4 + a_3 s^3 + a_2 s^2 + a_1 s + \alpha_o T_o$	$\begin{Bmatrix} a_1 \\ a_2 \\ a_3 \\ a_4 \end{Bmatrix} = \begin{bmatrix} (16) & (-12) & (5\frac{1}{3}) & (-1) \\ (-69\frac{1}{3}) & (+76) & (-37\frac{1}{3}) & (7\frac{1}{3}) \\ (96) & (-128) & (74\frac{2}{5}) & (-16) \\ (-42\frac{2}{3}) & (64) & (-42\frac{2}{3}) & (10\frac{2}{3}) \end{bmatrix} \begin{Bmatrix} B_1 \\ B_2 \\ B_3 \\ B_4 \end{Bmatrix}$	

* See illustrative problem for method of matrix multiplication.

The matrix multiplication indicated above yields the desired column matrix $\{a\}$, or

$$\{a\} = [s]\{B\}$$

In general the value of each element, a_i of $\{a\}$ is obtained by selecting the i th row of [s] and summing the products of its elements with the corresponding elements of the column $\{B\}$.

Thus:

$$a_1 \times 10^3 = (4)(0.5) + (-1)(2.5) = -0.5$$

$$a_2 \times 10^3 = (-4)(0.5) + (2)(2.5) = 3.0$$

and therefore

$$\alpha T \times 10^3 = 3.0s^2 - 0.5s + 1.0$$

For a <u>5 point fit,</u> Table 4.1.2.3.1-1 gives

$$\alpha T = a_4 s^4 + a_3 s^3 + a_2 s^2 + a_1 s + \alpha_o T_o$$

where $\alpha_o T_o = 1.0 \times 10^{-3}$

and

$$\begin{Bmatrix} a_1 \\ a_2 \\ a_3 \\ a_4 \end{Bmatrix} \times 10^3 = \begin{bmatrix} (16) & (-12) & (5\frac{1}{3}) & (-1) \\ (-69\frac{1}{3}) & (76) & (-37\frac{1}{3}) & (7\frac{1}{3}) \\ (96) & (-128) & (74\frac{2}{3}) & (-16) \\ (-42\frac{2}{3}) & (64) & (-42\frac{2}{3}) & (10\frac{2}{3}) \end{bmatrix} \begin{Bmatrix} .0 \\ .50 \\ 1.25 \\ 2.50 \end{Bmatrix}$$

or

$$a_1 \times 10^3 = (16)(0) + (-12)(.50) + (5\tfrac{1}{3})(1.25) + (-1)(2.50) = -1.833$$

$$a_2 \times 10^3 = (-69\tfrac{1}{3})(0) + (76)(.50) + (-37\tfrac{1}{3})(1.25) + (7\tfrac{1}{3})(2.50) = +9.667$$

$$a_3 \times 10^3 = (96)(0) + (-128)(.50) + (74\tfrac{2}{3})(1.25) + (-16)(2.50) = -10.667$$

$$a_4 \times 10^3 = (-42\tfrac{2}{3})(0) + (64)(.50) + (-42\tfrac{2}{3})(1.25) + (10\tfrac{2}{3})(2.50) = +5.333$$

Thus

$$\alpha T \times 10^3 = +5.333s^4 - 10.667s^3 + 9.667s^2 - 1.833s + 1.000$$

Plots of the αT profiles resulting from the above polynomial representations are shown in Figure 4.1.2.3.1-3.

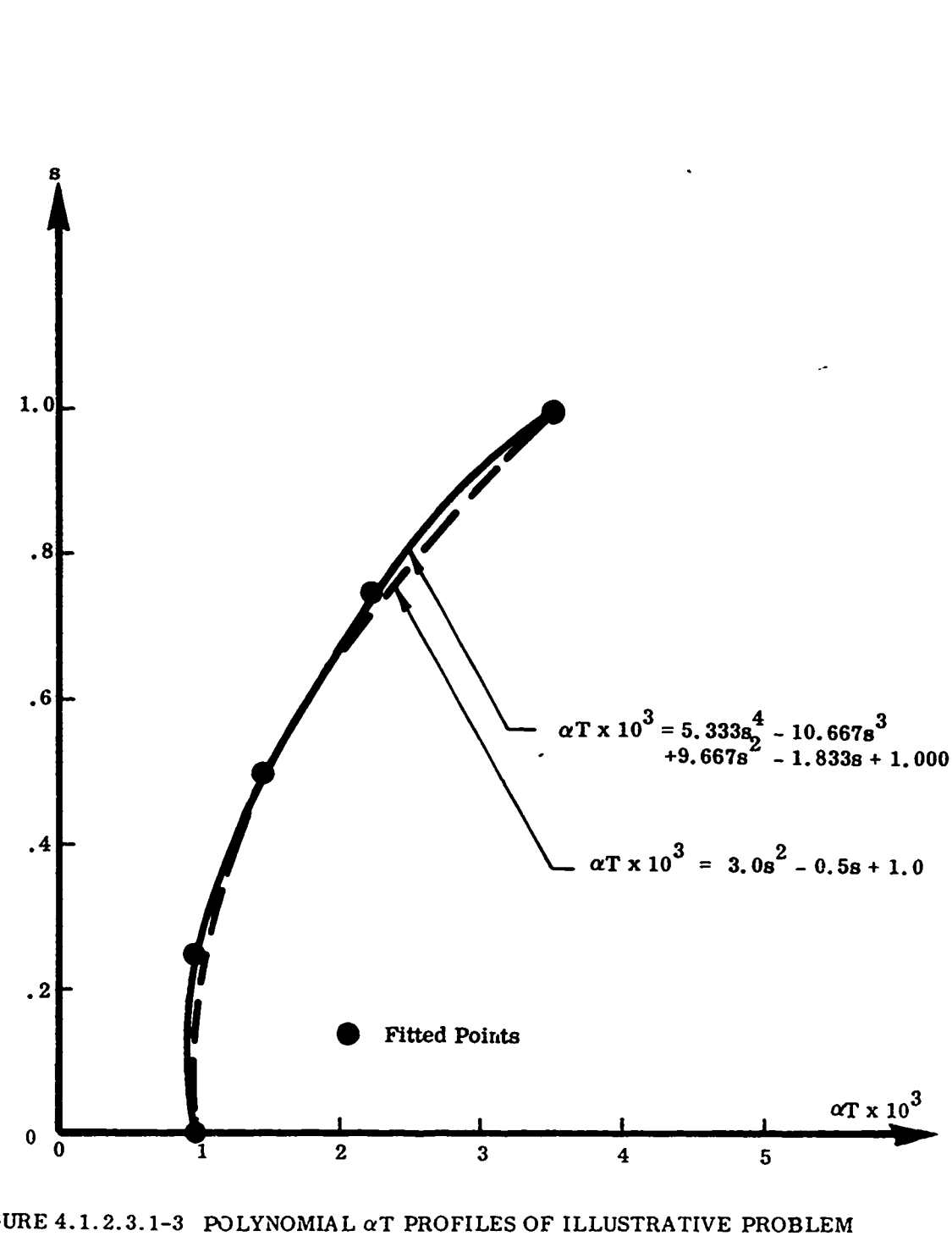


FIGURE 4.1.2.3.1-3 POLYNOMIAL αT PROFILES OF ILLUSTRATIVE PROBLEM

4.1.2.3.2 Binomial Representation of Continuous Elastic Cross Sections

Approximate representations of continuous cross sectional geometries having monotonic elastic width variation (Figure 4.1.2.3.2-1) are given by the following basic expression:

$$Eb = E_o b_o \left[1 + \beta s^K \right] ; \begin{matrix} \beta \geq -1^* \\ K \geq 0 \end{matrix} \qquad (1a)$$

where $s = \frac{u}{d}$

and

$$\beta = \frac{E_n b_n}{E_o b_o} - 1 \qquad \text{(Taper Parameter)} \qquad (1b)$$

The value of K (shape parameter) is determined from the equation

$$K = 3.32 \, \text{Log}_{10} \left[\frac{E_n b_n - E_o b_o}{E_{.5} b_{.5} - E_o b_o} \right] . \qquad (2)$$

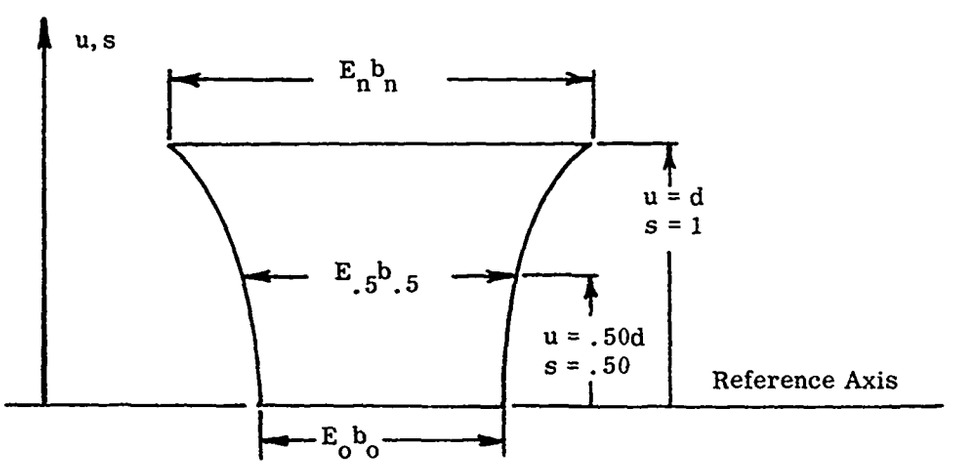


FIGURE 4.1.2.3.2-1 CONTINUOUS CROSS SECTION WITH MONOTONIC ELASTIC WIDTH VARIATION

The taper parameter, β , defines the ratio of the elastic width at the extreme fiber to the elastic width at the reference axis; the shape parameter, K , defines the shape of the sides (elastic width variation). Figure 4.1.2.3.2-2 presents a summary of the geometric shapes represented through the complete range of the parameters β and K.

---

* $\beta < -1$ gives negative width and is thus meaningless. $K < 0$ occurs for non-monotonic width variation and results in infinite width at the reference axis.

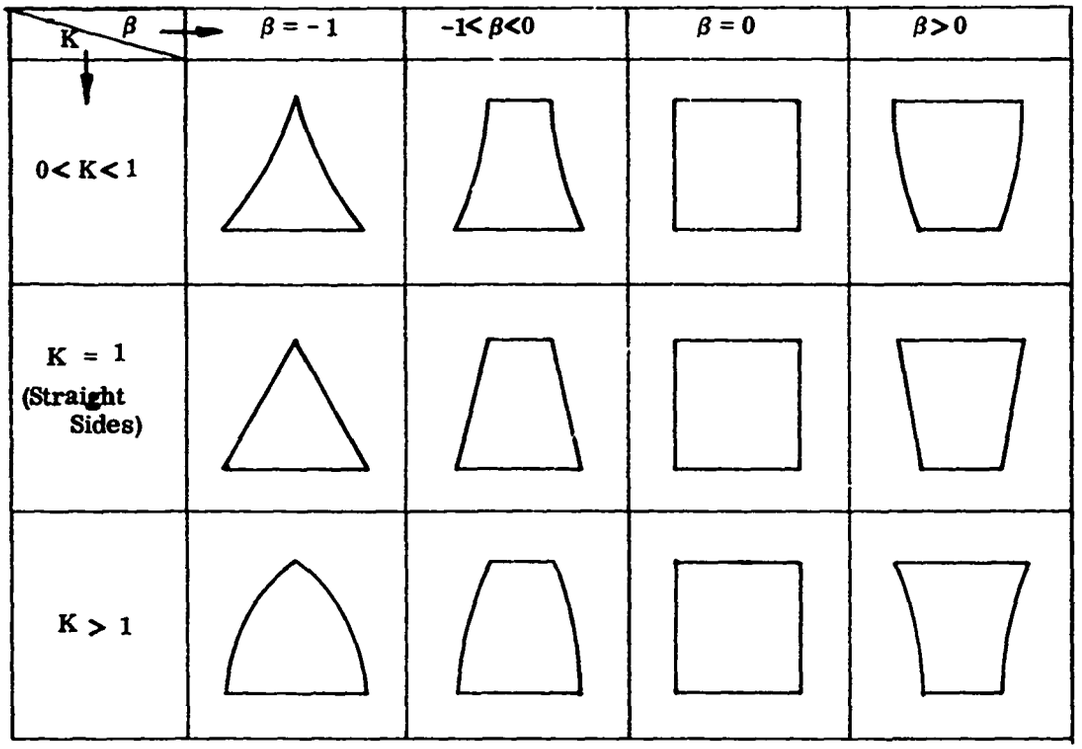


FIGURE 4.1.2.3.2-2 MONOTONIC GEOMETRIC SHAPES DEFINED BY PARAMETERS β AND K

In many cases, the temperature range is such that the variation of modulus of elasticity is insignificant. The actual cross sectional geometry then has the same shape as the elastic geometry, and geometric shapes such as circles, ellipses, etc., can be closely approximated by Eq.(1a). Note that the actual shape of the elastic cross section need not be symmetrical (see Paragraph 4.1.2.4). Figure 4.1.2.3.2-2 is presented in this manner only to emphasize the shape of the sides.

4.1.2.3.3 Solution for Continuous Elastic Cross Sections

For continuous cross sections having monotonic elastic width variation (Figure 4.1.2.3.2-1), the elastic section properties for bending about a principal axis are obtained by substituting Eq. (1a) of Paragraph 4.1.2.3.2 into the general integral equations for elastic section properties which are presented in Paragraph 4.1.1.1. The results, derived in Reference 4-1, are given below in non-dimensional form.

$$\lambda = \frac{\overline{EA}}{d\,E_o b_o} = 1 + \frac{\beta}{K+1} \tag{1}$$

$$\mu = \frac{\bar{u}}{d} = \frac{1}{\lambda}\left(\frac{1}{2} + \frac{\beta}{K+2}\right) \tag{2}$$

$$\nu = \frac{\overline{EI}}{d^3 E_o b_o} = \left(\frac{1}{3} + \frac{\beta}{K+3}\right) - \lambda\mu^2 \tag{3}$$

where β and K are determined from Eqs. (1b) and (2) of Paragraph 4.1.2.3.2. These "elastic" section properties should be employed in the solution of the deformation and stresses of beams subjected to mechanical and thermal loads.

The total thermal deformation of the cross section can be considered as the superposition of the deformations due to the thermal loads represented by each term of the αT polynomial (Eq. (1), Paragraph 4.1.2.3.1). The contribution of the Lth term of the αT polynomial to the total deformation is obtained by substituting $\alpha T = a_L s^L$, and the expressions for the section properties given above, into the general integral equations for the deformations (Paragraph 4.1.1.2).

Thus, in non-dimensional form, the deformations due to an αT profile of the form $\alpha T = a_L s^L$ are

$$\gamma_L = \bar{\epsilon}'_L / a_L = \frac{1}{\lambda}\left(\frac{1}{L+1} + \frac{\beta}{K+L+1}\right) \tag{4}$$

$$\delta_L = dw'_L / a_L = \frac{1}{\nu}\left[\left(\frac{1}{L+2} + \frac{\beta}{K+L+2}\right) - \mu\left(\frac{1}{L+1} + \frac{\beta}{K+L+1}\right)\right] \tag{5}$$

Equations (4) and (5), taken from Reference 4.1, are shown graphically in Figures 4.1.2.3.3-1 and -2 for the case K=1 (elastic cross section with straight sides). Referring to these graphs, note that for the case L=0, corresponding to αT constant through the depth, the non-dimensional elongation γ_o and rotation δ_o have the numerical values one and zero, respectively, for all values of taper parameter β. The case L=1 corresponds to an αT distribution which varies linearly through the depth and thus $\delta_1 = 1$ for all β. Note also that the deformations are relatively insensitive to changes in the taper ratio for large values of β.

The total thermal deformations for an αT profile represented by a polynomial of order "n" are, by superposition:

$$\bar{\epsilon}' = \sum_{L=o}^{n} \bar{\epsilon}'_L = \sum_{L=o}^{n} a_L \gamma_L \tag{6}$$

4.1.2.3.3 (Cont'd)

$$w' = \sum_{L=o}^{n} w'_L = \frac{1}{d} \sum_{L=o}^{n} a_L \delta_L \quad . \tag{7}$$

The stresses due to thermal loading are determined from the total thermal deformations by the relationship

$$\sigma = E \left[-\alpha T + \bar{\epsilon}' + w' (u - \bar{u}) \right] \tag{8a}$$

or alternatively by

$$\sigma = E \sum_{L=o}^{n} a_L \left[-s^L + \gamma_L + \delta_L (s - \mu) \right] \quad . \tag{8b}$$

The stresses due to mechanical loading are, from Eqs. (1) and (3) for the section properties,

$$\sigma = E \left[\frac{F}{\overline{EA}} - \frac{M}{\overline{EI}} (u - \bar{u}) \right]$$

$$= \frac{E}{d E_o b_o} \left[\frac{F}{\lambda} - \frac{M}{\nu d^2} (u - \bar{u}) \right] \quad , \tag{8c}$$

where in the above equations, s, u, E and αT are prescribed for the point at which the stress is to be determined.

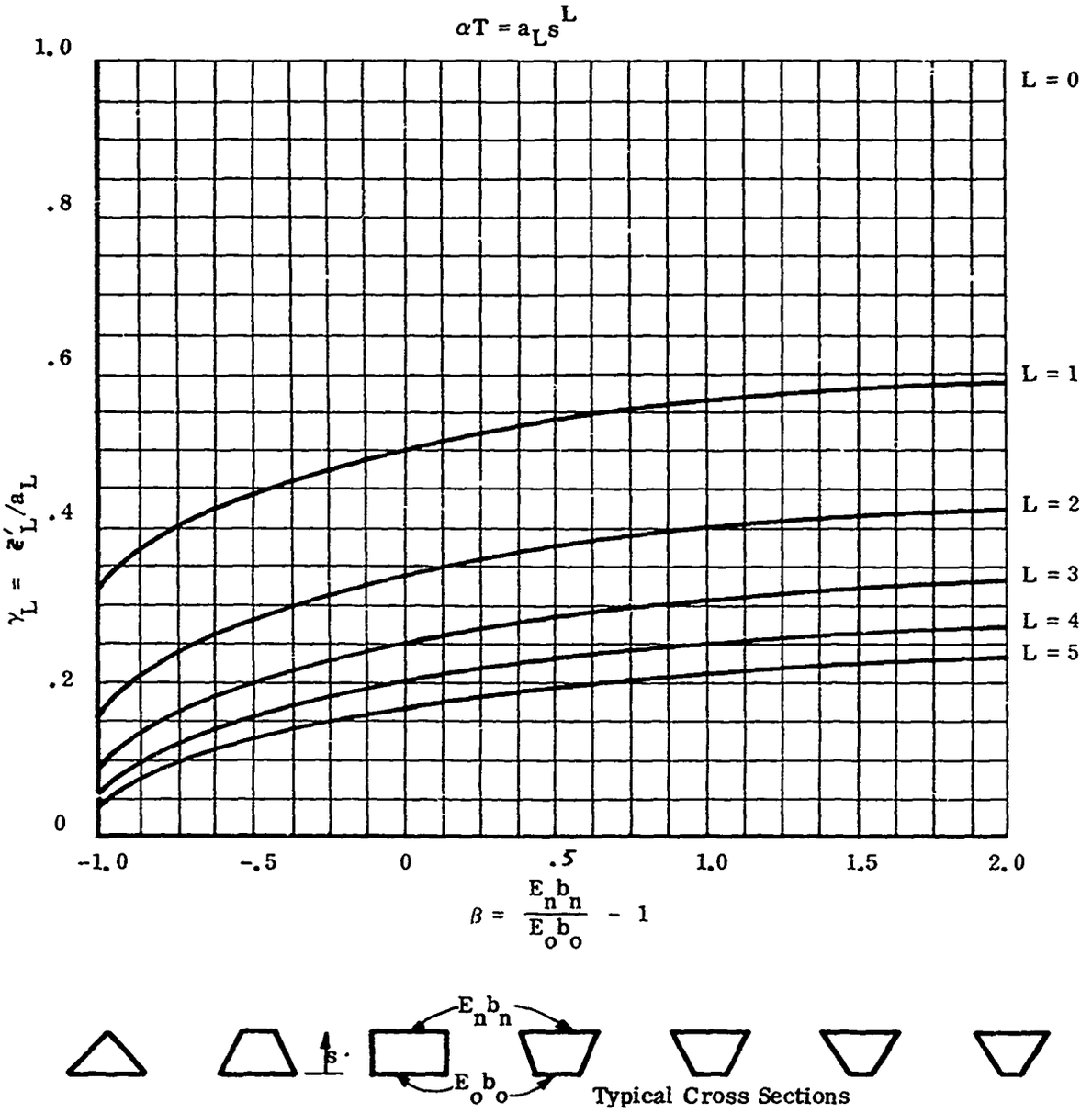


FIGURE 4.1.2.3.3-1 ELONGATION, γ_L, FOR CONTINUOUS GEOMETRY OF THE FORM $Eb = E_o b_o (1 + \beta s^K)$, WITH K = 1 (STRAIGHT SIDES).

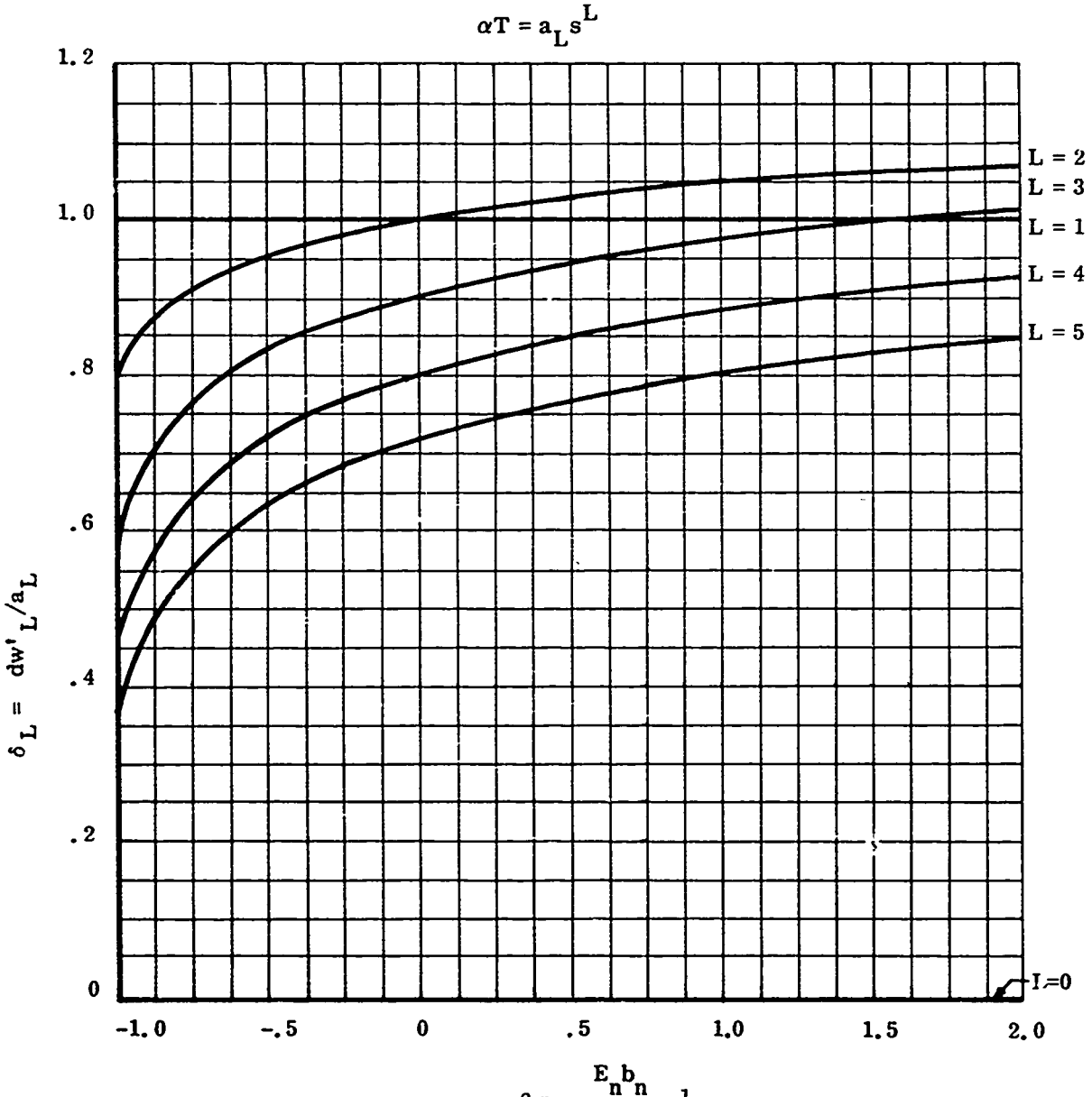


FIGURE 4.1.2.3.3-2 CURVATURE, δ_L, FOR CONTINUOUS GEOMETRY OF THE FORM $Eb = E_o b_o (1 + \beta s^K)$, WITH K = 1 (STRAIGHT SIDES).

The solution of the stress and deformation for an unrestrained beam, with the cross section * shown in Figure 4.1.2.3.3-3, is illustrated below.

It is desired to calculate and compare the deformations and stresses produced by each of the following polynomial approximations to the αT profile:

(a) $\alpha T \times 10^3 = 3.0s^2 - 0.5s + 1.0$

(b) $\alpha T \times 10^3 = 5.333s^4 - 10.667s^3 + 9.667s^2 - 1.833s + 1.000$ (Refer to Figure 4.1.2.3-5)

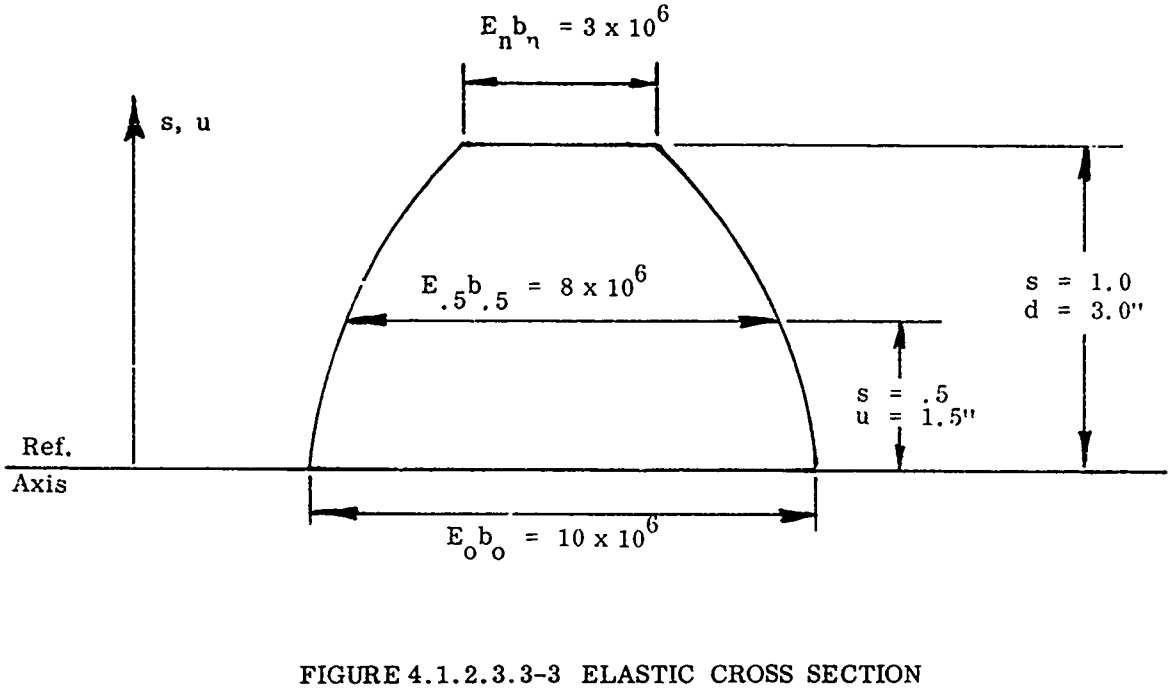


FIGURE 4.1.2.3.3-3 ELASTIC CROSS SECTION

---

* The elastic cross section shown in Figure 4.1.2.3.3-3 makes physical sense in that a cross section which has a physical geometry of constant width b_o has an elastic width Eb which decreases with increasing temperature.

4.1.2.3.3 (Cont'd)

Solution:

(1) The parameters β and K are determined from Eqs. (1b) and (2) of Paragraph 4.1.2.3.2. Thus

$$\beta = \frac{E_n b_n}{E_o b_o} - 1 = \frac{3}{10} - 1 = -.7000$$

$$K = 3.32 \text{ Log}_{10}\left[\frac{E_n b_n - E_o b_o}{E_{.5} b_{.5} - E_o b_o}\right] = 3.32 \text{ Log}_{10}\left[\frac{(3-10)}{(8-10)}\right]$$

$$= 3.32 \text{ Log}_{10}(3.5) = 1.8063 .$$

(2) Substituting the above values of β and K in Eqs. (1), (2) and (3) gives the non-dimensional section properties:

$$\lambda = 1 + \frac{\beta}{K+1} = 1 + \frac{-.7000}{2.8063} = .7506$$

$$\mu = \frac{1}{\lambda}\left(\frac{1}{2} + \frac{\beta}{K+2}\right) = \frac{1}{.7506}\left(\frac{1}{2} + \frac{-.7000}{3.8063}\right) = .4211$$

$$\nu = \left(\frac{1}{3} + \frac{\beta}{K+3}\right) - \lambda \mu^2 = \left(\frac{1}{3} + \frac{-.7000}{4.8063}\right) - .7506\,(.4211)^2 = .0546$$

(3) The solutions of Eqs. (4) through (7) for the deformations caused by each of the polynomial αT distributions, are given below in Tables 4.1.2.3.3-1(a) and -1(b).

(4) The stresses are obtained by substituting the deformations into Eq. (8).

Thus:

For 2nd order αT polynomial

$$\sigma = E\left[-\alpha T + \bar{\epsilon}' + w'(u-\bar{u})\right]$$

$$= E\left[-\alpha T \times 10^3 + 1.5398 + .7563\,(u-\bar{u})\right] \times 10^{-3}$$

For 4th order αT polynomial

$$\sigma = E\left[-\alpha T \times 10^3 + 1.4974 + .7580\,(u-\bar{u})\right] \times 10^{-3}$$

where $\bar{u} = \mu d = (.4211)(3.0) = 1.2633$.

The above stresses are plotted in Figure 4.1.2.3.3-4.

4.1.2.3.3 (Cont'd)

If it is desired to determine the points of maximum tensile and compressive strains without resorting to a plot through the depth, use of the alternate expression for the stress, Eq. 8(b) is advantageous. Thus, by substituting into Eq. 8(b), the 2nd order polynomial approximation

$$\alpha T = \sum_{L=o}^{2} a_L s^L = (3.000s^2 - 0.500s + 1.000) \times 10^{-3}$$

$$\mu = .4211$$

and the values of δ_L and γ_L obtained from Table 4.1.2.3.3-1(a), the following analytic expression is obtained:

$$\frac{\sigma}{E} \times 10^3 = -3.000s^2 + 2.769s - .4157 \ .$$

To obtain the extremum points of strain, set the derivative of σ/E equal to zero, i.e.,

$$\frac{d}{ds}\left(\frac{\sigma}{E}\right) = (-6.000s + 2.769) \times 10^{-3} = 0 \quad ,$$

which gives an extremum point at

$$s = \frac{2.769}{6.000} = .4615 \ .$$

This corresponds to a point of maximum strain since the second derivative $\frac{d^2\left(\frac{\sigma}{E}\right)}{ds^2}$ is negative. Since only one extreme point exists, the minimum (maximum compressive) strain for the cross section must occur at one of the extreme fibers, as verified by Figure 4.1.2.3.3-4.

Evidently, if E is constant over the cross section, then the points of maximum and minimum strain correspond to points of maximum and minimum stress.

A comparision of the deformations obtained from the two polynomial approximations of the αT distribution (Tables 4.1.2.3.3-1(a) and -2(b) shows good agreement. This was to be expected since the αT distributions are integrated in the process of obtaining the deformations, thus improving the accuracy of lower order polynomial approximations. The stresses, on the other hand (Figure 4.1.2.3.3-4), do not show as good an agreement. This is due mainly to the fact that the unrestrained beam thermal stresses are obtained from Eq. (8) as small differences between large numbers, and are therefore sensitive to small changes in the deformations. Thus a very accurate determination of the thermal stresses requires an even more accurate calculation of the deformations, which in turn requires the use of higher order, more accurate, polynomial approximations of the αT profile, or the use of the finite sum method. It becomes apparent that the temperature distribution must be known to a high degree of accuracy (which is usually unobtainable in actual structures) to obtain accurate thermal stresses. The high degree of accuracy of temperature distributions is not required for the determination of thermal deformations.

TABLE 4.1.2.3.3-1(a)

CROSS SECTIONAL DEFORMATIONS CAUSED BY THE 2ND ORDER POLYNOMIAL $\alpha T \times 10^3 = 3.0s^2 - 0.5s + 1.0$ (Ref. Fig. 4.1.2.3.1-3)

①	②	③	④	⑤
L	$\frac{1}{L+1} + \frac{\beta}{K+L+1}$	$\frac{1}{L+2} + \frac{\beta}{K+L+2}$	$\gamma_L = \frac{1}{\lambda}\left(\frac{1}{L+1} + \frac{\beta}{K+L+1}\right)$	$\delta_L = \frac{1}{\nu}\left[\left(\frac{1}{L+2} + \frac{\beta}{K+L+2}\right) - \mu\left(\frac{1}{L+1} + \frac{\beta}{K+L+1}\right)\right]$
	$\frac{1}{① + 1} + \frac{-.7000}{1.8063 + ① + 1}$	$\frac{1}{① + 2} + \frac{-.7000}{1.8063 + ① + 2}$	$\frac{1}{.7506}$ ②	$\frac{1}{.0846}$ [③ - .4211 ②]
0	.7506	.3161	1.0000	0
1	.3161	.1877	.4211	1.0000
2	.1877	.1294	.2501	.9230

①	⑥	⑦	⑧
L	$a_L \times 10^3$	$\bar{\varepsilon}'_L \times 10^3 = a_L \gamma_L \times 10^3$	$w'_L \times 10^3 = (a_L \delta_L / d) \times 10^3$
	Coeff. of Polynomial	④ x ⑥	$\frac{⑥ \times ⑤}{3^{II}}$
0	1.000	1.0000	0
1	-.500	-.2105	- 1667
2	3.000	.7503	.9230
Σ =		1.5398	.7563

Thus, from the summations of columns ⑦ and ⑧ , $\bar{\varepsilon}' = 1.5398 \times 10^{-3}$ and $w' = .7563 \times 10^{-3}$.

TABLE 4.1.2.3.3-1(b)

CROSS SECTIONAL DEFORMATIONS CAUSED BY THE 4TH ORDER POLYNOMIAL $\alpha T \times 10^3 = 5\ 333s^4 - 10.667s^3 + 9.667s^2 - 1\ 833s + 1.000$ (Ref. Fig. 4.1.2.3.1-3)

①	②	③	④	⑤
L	$\frac{1}{L+1} + \frac{\beta}{K+L+1}$	$\frac{1}{L+2} + \frac{\beta}{K+L+2}$	$\gamma_L = \frac{1}{\lambda}\left(\frac{1}{L+1} + \frac{\beta}{K+L+1}\right)$	$\delta_L = \frac{1}{\nu}\left[\left(\frac{1}{L+2} + \frac{\beta}{K+L+2}\right) - \mu\left(\frac{1}{L+1} + \frac{\beta}{K+L+1}\right)\right]$
	$\frac{1}{① + 1} + \frac{-.7000}{1.8063 + ① + 1}$	$\frac{1}{① + 2} + \frac{-.7000}{1.8063 + ① + 2}$	$\frac{1}{.7506}$ ②	$\frac{1}{.0546}\left[③ - .4211②\right]$
0	.7506	.3161	1.0000	0
1	.3161	.1877	.4211	1.0000
2	.1877	.1294	.2501	.9230
3	.1294	.0972	.1724	.7820
4	.0972	.0770	.1295	.6612

①	⑥	⑦	⑧
L	$a_L \times 10^3$	$\bar{\varepsilon}'_L \times 10^3 = a_L \gamma_L \times 10^3$	$w'_L \times 10^3 = (a_L \delta_L/d) \times 10^3$
	Coeff. of Polynomial	④ x ⑥	$\frac{⑤ \times ⑥}{3"}$
0	1.000	1.0000	0
1	-1.833	-.7719	-.6110
2	9.667	2.4177	2.9742
3	-10.667	-1.8390	-2.7806
4	5.333	.6906	1.1754
Σ =		1.4974	.7580

Thus, from the summations of columns ⑦ and ⑧ , $\bar{\varepsilon}' = 1.4974 \times 10^{-3}$ and $w' = .7580 \times 10^{-3}$

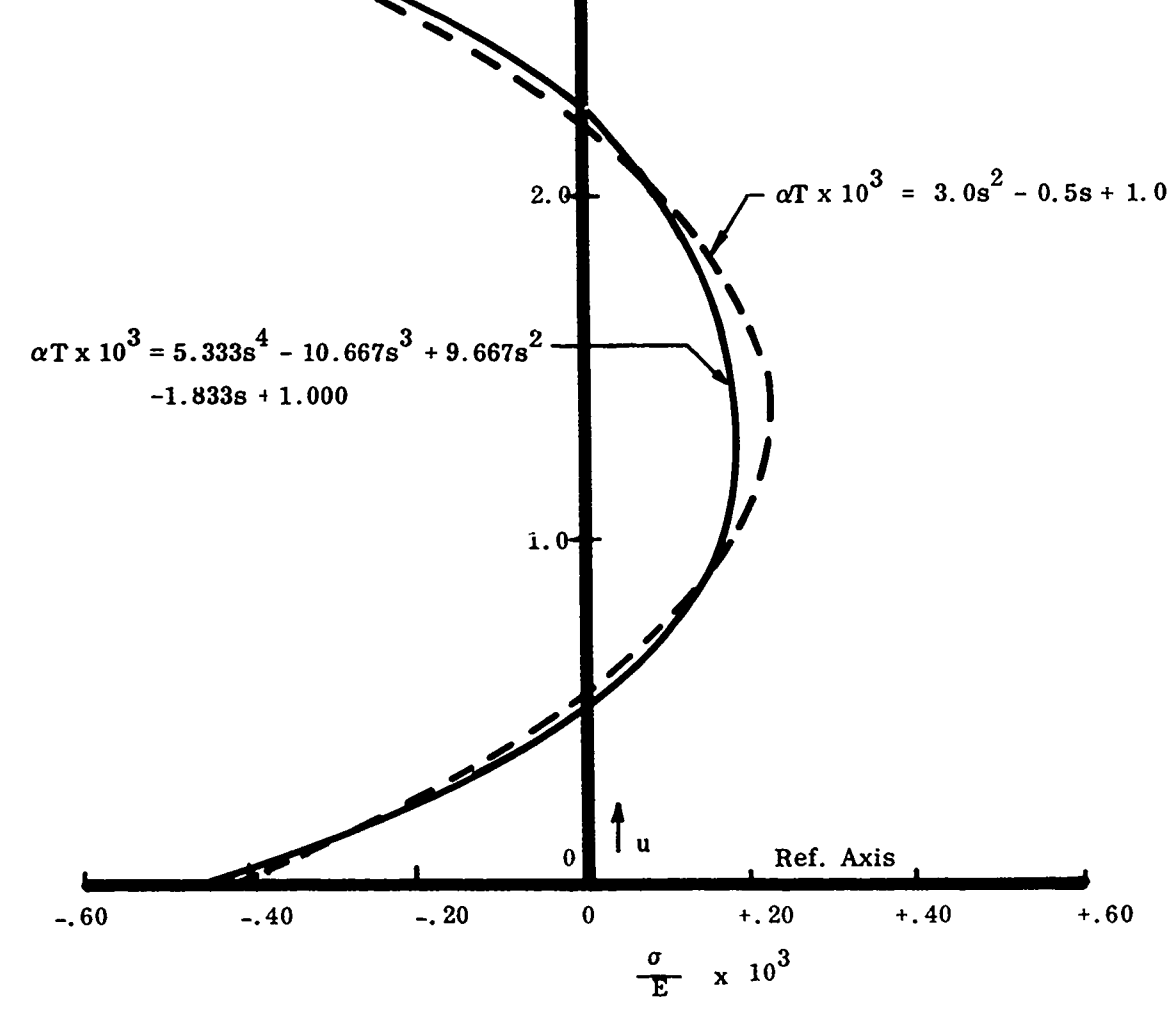


FIGURE 4.1.2.3.3-4 THERMAL STRESSES FOR POLYNOMIAL αT DISTRIBUTIONS

The relationships for the section properties and deformations given in Eqs. (1) through (5) can be simplified if the elastic geometry is symmetric about the bending axis, Figure 4.1.2.3.3-5(a). For this case, the non-dimensional section properties reduce to

$$\lambda_s = \frac{\overline{EA}}{dE_o b_o} = 2\left(1 + \frac{\beta}{K+1}\right) \tag{9}$$

$$\mu_s = \frac{\bar{u}}{d} = 0 \tag{10}$$

and

$$\nu_s = \frac{\overline{EI}}{d^3 E_o b_o} = 2\left(\frac{1}{3} + \frac{\beta}{K+3}\right) \tag{11}$$

where d is the distance from the reference axis to an extreme fiber and β and K are determined from Eqs. (1b) and (2) of Paragraph 4.1.2.3.2 using the elastic width variation on either side of the reference axis (bending axis of symmetry).

The solution for the deformations is obtained by first decomposing the total αT distribution, Figure 4.1.2.3.3-5(b), into components which are symmetrical and anti-symmetrical about the bending axis (Figure 4.1.2.3.3-5(c) and -5(d)).

Thus if, as shown in Figure 4.1.2.3.3-5(b), the αT profile above the bending axis is represented by the polynomial

$$\alpha T = \sum_{L=o}^{n} a_L s^L = a_o + a_1 s + \ldots\ldots\ldots + a_n s^n \tag{12a}$$

and the αT profile below the bending axis by

$$\alpha T = \sum_{L=o}^{n} a'_L (-s)^L = a'_o + a'_1 (-s) + \ldots\ldots\ldots + a'_n (-s)^n , \tag{12b}$$

then the symmetrical component of the total αT profile is

$$(\alpha T)_s = \sum_{L=o}^{n} \left(\frac{a_L + a'_L}{2}\right)(\pm s)^L = \left[\left(\frac{a_o + a'_o}{2}\right) + \left(\frac{a_1 + a'_1}{2}\right)(\pm s) + \ldots + \left(\frac{a_n + a'_n}{2}\right)(\pm s)^n\right] \tag{13a}$$

and the anti-symmetric component is

$$(\alpha T)_a = \pm \sum_{L=o}^{n} \left(\frac{a_L - a'_L}{2}\right)(\pm s)^L = \pm\left[\left(\frac{a_o - a'_o}{2}\right) + \left(\frac{a_1 - a'_1}{2}\right)(\pm s) + \ldots + \left(\frac{a_n - a'_n}{2}\right)(\pm s)^n\right] \tag{13b}$$

where the upper (positive) signs in the above formulas are to be used for points located above the reference axis and the lower (negative) signs for points below the reference axis.

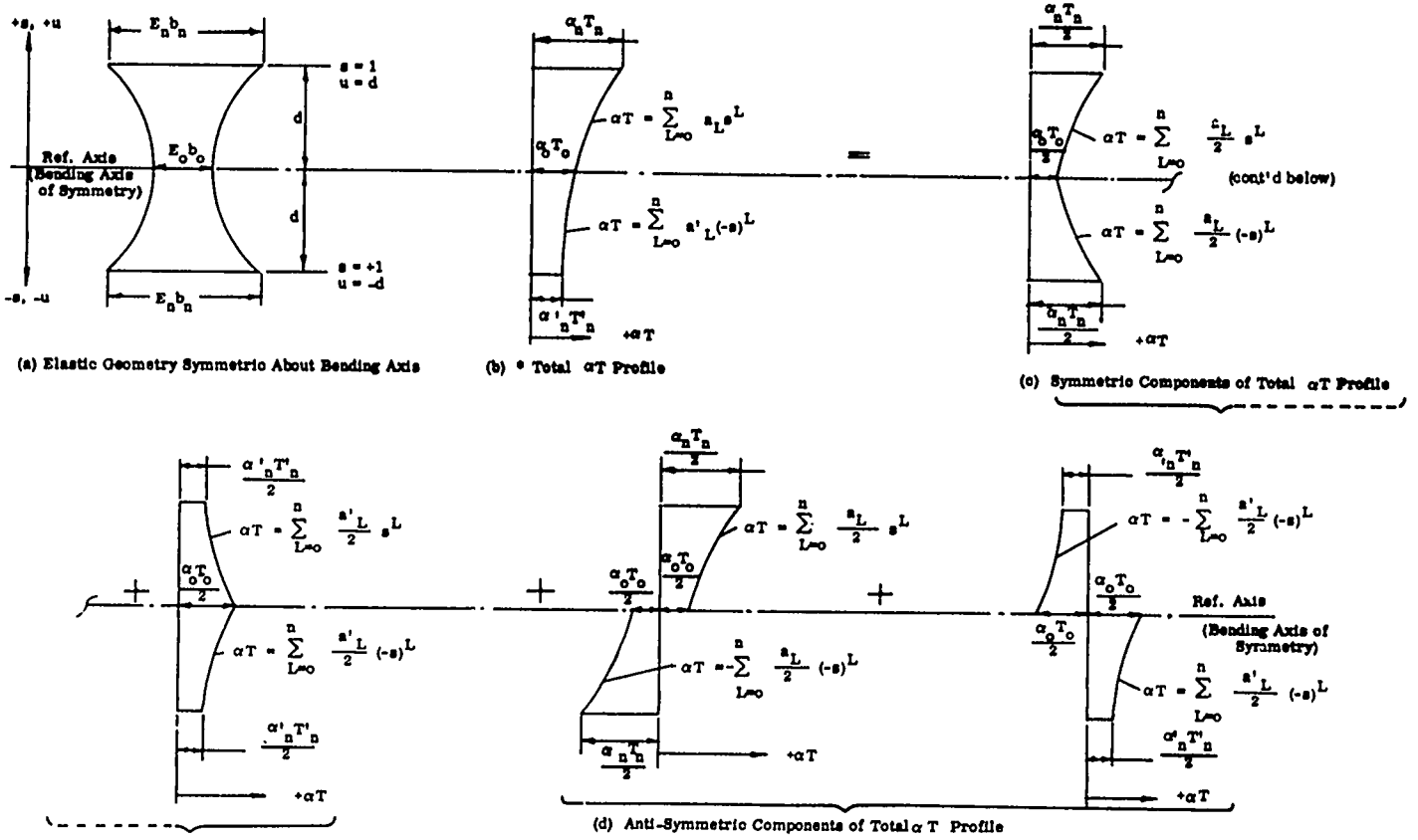


FIGURE 4.1.2.3.3-5 DECOMPOSITION OF TOTAL αT PROFILE INTO SYMMETRICAL AND ANTI-SYMMETRICAL COMPONENTS

For the symmetrical component of the αT profile, Eqs. (4) and (5) reduce to

$$(\gamma_L)_s = \frac{\bar{\epsilon}'_{L,s}}{\left(\frac{a_L + a'_L}{2}\right)} = \frac{2}{\lambda_s}\left(\frac{1}{L+1} + \frac{\beta}{K+L+1}\right) \tag{14}$$

$$(\delta_L)_s = \frac{dw'_{L,s}}{\left(\frac{a_L + a'_L}{2}\right)} = 0 \tag{15}$$

and for the anti-symmetrical component of the αT profile

$$(\gamma_L)_a = \frac{\bar{\epsilon}'_{L,a}}{\left(\frac{a_L + a'_L}{2}\right)} = 0 \tag{14a}$$

$$(\delta_L)_a = \frac{dw'_{L,a}}{\left(\frac{a_L - a'_L}{2}\right)} = \frac{2}{\nu_s}\left(\frac{1}{L+2} + \frac{\beta}{K+L+2}\right) \tag{15a}$$

The total deformations are obtained by superposition of the symmetrical and anti-symmetrical components as

$$\bar{\epsilon}' = \sum_{L=o}^{n} \bar{\epsilon}'_{L,s} = \sum_{L=o}^{n} \left[\left(\frac{a_L + a'_L}{2}\right)(\gamma_L)_s\right] \tag{16}$$

$$w' = \sum_{L=o}^{n} w'_{L,a} = \frac{1}{d} \sum_{L=o}^{n} \left[\left(\frac{a_L - a'_L}{2}\right)(\delta_L)_a\right] \tag{17}$$

Note that the elongation, $\bar{\epsilon}'$ is caused solely by the symmetrical component of the αT profile, while the rotation, w' is caused solely by the anti-symmetric component of the profile.

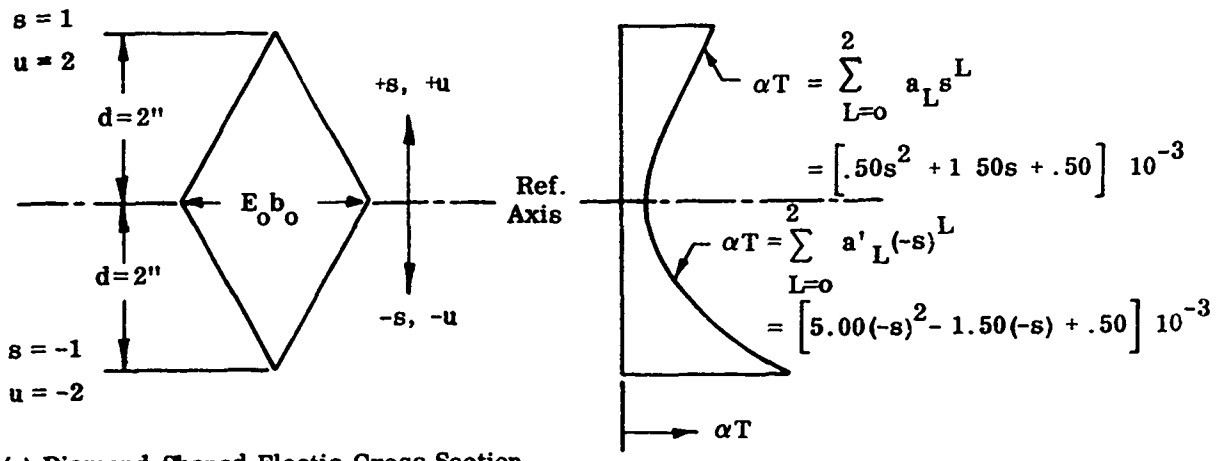
Once the deformations have been determined as above, the stresses can be obtained from the relationship

$$\sigma = E\ (-\alpha T + \bar{\epsilon}' + w' u) \tag{18}$$

where u and αT are prescribed for the point at which the stress is to determined.

The method of solution is illustrated for an unrestrained beam having the geometry and αT profile shown in Figure 4.1.2.3.3-6. Stresses and deformations are determined as follows:

4.1.2.3.3 (Cont'd)



(a) Diamond-Shaped Elastic Cross Section (Straight Sides)

(b) αT Profile

FIGURE 4.1.2.3.3-6 SYMMETRIC ELASTIC CROSS SECTION WITH UNSYMMETRIC αT PROFILE

(1) From Eqs. (1b) and (2) of Paragraph 4.1.2.3.2 or Figure 4.1.2.3.2-2,

$$\beta = -1$$

$$K = +1$$

(2) Substituting the above values of β and K in Eqs. (9) and (11) gives the non-dimensional section properties

$$\lambda_s = 2\left(1 + \frac{\beta}{K+1}\right) = 2\left(1 - \frac{1}{2}\right) = 1$$

$$\nu_s = 2\left(\frac{1}{3} + \frac{\beta}{K+3}\right) = 2\left(\frac{1}{3} - \frac{1}{4}\right) = \frac{1}{6} .$$

(3) The solutions of Eqs. (14), (15a), (16) and (17) for the deformations are worked out in Table 4.1.2.3.3-2.

(4) The stresses are obtained by substituting the deformations in Eq. (18), thus

$$\sigma = E\ (-\alpha T + \bar{\epsilon}' + w'\ u)$$

$$= E\ (-\alpha T \times 10^3 + .9583 + .0750\ u) \times 10^{-3}$$

These stresses are plotted in Figure 4.1.2.3.3-7.

TABLE 4.1.2.3.3-2

DEFORMATIONS OF THE CROSS SECTION

①	②	③	④	⑤	⑥ *
L	$a_L \times 10^3$	$a'_L \times 10^3$	$\frac{(a_L + a'_L)}{2} \times 10^3$	$\frac{(a_L - a'_L)}{2} \times 10^3$	$(\gamma_L)_s = \frac{2}{\lambda_s}\left(\frac{1}{L+1} + \frac{\beta}{K+L+1}\right)$
	Ref. Fig. 4.1.2.3.3-6	Ref. Fig. 4.1.2.3.3-6	$\frac{② + ③}{2}$	$\frac{② - ③}{2}$	$\left(\frac{2}{1}\right)\left(\frac{1}{① + 1} - \frac{1}{1 + ① + 1}\right)$
0	.50	.50	.50	0	1.000
1	1.50	-1.50	0	1.50	.333
2	.50	5.00	2.75	-2.25	.167

①	⑦	⑧	⑨
L	$(\delta_L)_a = \frac{2}{\nu_s}\left(\frac{1}{L+2} + \frac{\beta}{K+L+2}\right)$	$\bar{\epsilon}'_L \times 10^3 = \left(\frac{a_L + a'_L}{2}\right)(\gamma_L)_s \times 10^3$	$w'_L \times 10^3 = \frac{1}{d}\left(\frac{a_L - a'_L}{2}\right)(\delta_L)_a \times 10^3$
	$\frac{2}{(1/6)}\left(\frac{1}{① + 2} - \frac{1}{1 + ① + 2}\right)$	④ x ⑥	⑤ x ⑦ /2
0	2.000	.5000	0
1	1.000	0	.7500
2	.600	.4583	-.6750
Σ =		.9583	+.0750

Thus, from the summations of columns ⑧ and ⑨, $\bar{\epsilon}' = .9583 \times 10^{-3}$ and $w' = .0750 \times 10^{-3}$

* Column 6 can also be obtained from Figure 4.1.2.3.3-1.

4.1.2.3.3 (Cont'd)

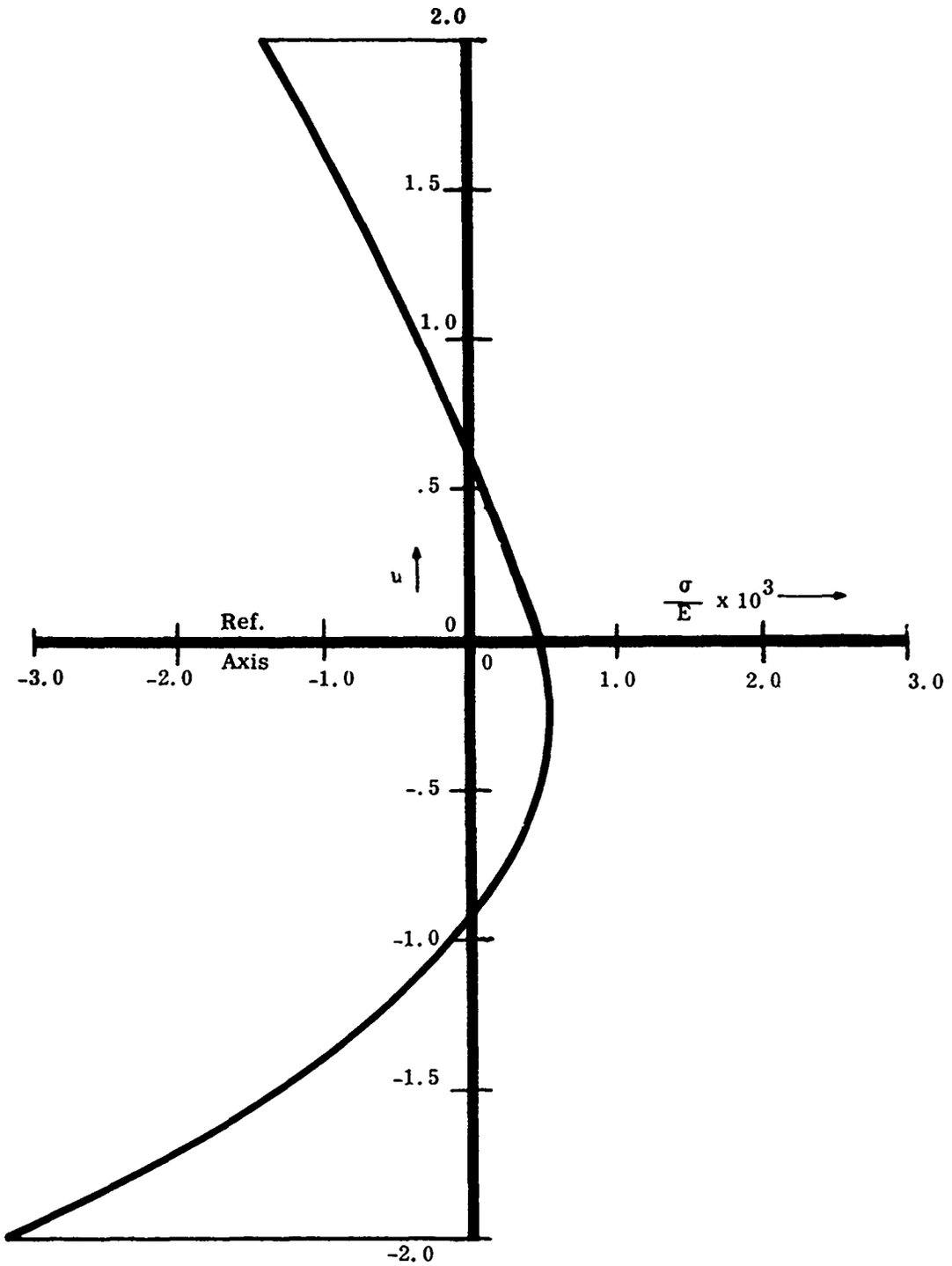


FIGURE 4.1.2.3.3-7 THERMAL STRESSES FOR THE BEAM OF FIGURE 4.1.2.3.3-6

4.1.2.3.4 Solutions For Discontinuous (Multi-Rectangular) Elastic Cross Sections

A wide variety of beams are of the composite or built-up type, fabricated from extruded shapes, bent-up sheet, flat plates, etc. In most such cases, the elastic cross section can be considered to consist of a finite number of rectangles as shown in Figure 4.1.2.3-1(c) where the elastic width Eb varies discontinuously through the depth.

The solution for the deformations and thermal stresses in an unrestrained beam of this type, for bending about a principal axis, as derived in Reference 4-1, is presented below. In order to systematize the solution, a step parameter η_m is introduced, defined as

$$\eta_m = \frac{1}{m} \left[1 + \sum_{k=1}^{n} \left(e_k - e_{k-1} \right) \left(1 - s_k^{\,m} \right) \right] , \qquad (1)$$

where, from Figure 4.1.2.3.4-1,

$$e_k = \frac{E_k b_k}{E_o b_o} \text{ (width parameter)}$$

$$k = 1, 2, \ldots n$$

$$s_k = \frac{u_k}{d}$$

n = number of rectangles less one

m = an integer.

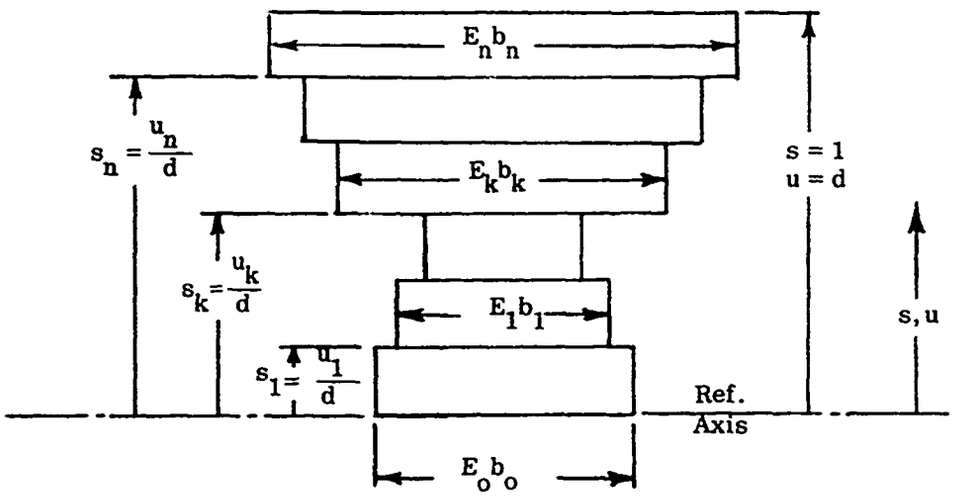


FIGURE 4.1.2.3.4-1 GENERAL MULTI-RECTANGULAR SECTION

4.1.2.3.4 (Cont'd)

Non-dimensional <u>elastic section properties</u> are expressible in terms of the step parameters as

$$\lambda = \frac{\overline{EA}}{dE_o b_o} = \eta_1 \tag{2}$$

$$\mu = \frac{\bar{u}}{d} = \frac{\eta_2}{\lambda} \tag{3}$$

$$\nu = \frac{\overline{EI}}{d^3 E_o b_o} = \eta_3 - \lambda\mu^2 \tag{4}$$

Note that the above expressions correspond to Eqs. (1), (2), and (3) of Paragraph 4.1.2.3.3 for continuous section properties, where

$$(1 + \frac{\beta}{K+1}) \ , \ (\frac{1}{2} + \frac{\beta}{K+2}) \ , \ (\frac{1}{3} + \frac{\beta}{K+3})$$

have been replaced by η_1, η_2, and η_3, respectively.

The deformation modes, for an αT profile expressed as a power series $\alpha T = \sum_{L=o}^{n} a_L s^L$, are

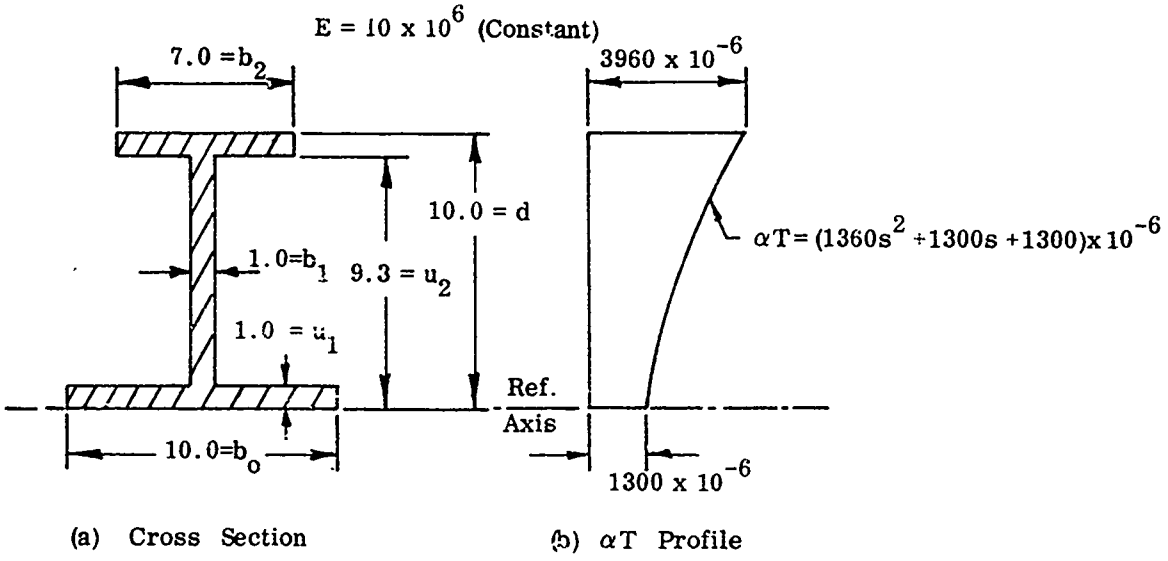
$$\gamma_L = \frac{\bar{\epsilon}'_L}{a_L} = \frac{\eta_{L+1}}{\lambda} \tag{5}$$

$$\delta_L = \frac{dw'_L}{a_L} = \frac{1}{\nu} \left(\eta_{L+2} - \mu \eta_{L+1} \right) \tag{6}$$

The total stresses and deformations are obtained, as in the case of continuous geometry, from Eqs. (6), (7) and (8) of Paragraph 4.1.2.3.3. If the αT polynomial is higher than the first order, then to obtain the stresses and deformations, one must evaluate, in addition to η_1, η_2 and η_3, values of η up to η_{n+2} where n is the order of the αT polynomial.

4.1.2.3.4 (Cont'd)

The solution for the deformations and stresses of the unrestrained beam shown in Figure 4.1.2.3.4-2 is illustrated below.



(a) Cross Section (b) αT Profile

FIGURE 4.1.2.3.4-2 UNRESTRAINED BEAM CROSS SECTION AND TEMPERATURE DISTRUBITION

(1) The numerical calculation for the necessary step parameters, Eq. (1), is carried out in Table 4.1.2.3.4-1(a)

(2) Non-dimensional section properties are calculated by substituting the above step parameters in Eqs. (2), (3) and (4). Thus

$$\lambda = \eta_1 = .2320$$

$$\mu = \frac{\eta_2}{\lambda} = \frac{.0950}{.2320} = .4095$$

$$\nu = \eta_3 - \lambda \mu^2 = .0728 - .2320\ (.4095)^2 = .0339$$

(3) The solution of Eqs. (6) and (7) of Paragraph 4.1.2.3.3 and of (5) and (6) above for the deformations is carried out in Table 4.1.2.3.4-1(b).

(4) The stresses are determined ' Eq. (8) of Paragraph 4.1.2.3.3 by

$$\sigma = E\left[-\alpha T + \bar{\epsilon}' + w'\ (u -\right.$$

$$= E\left[-\alpha T + (2259 \times 10^{-6}) + (26\text{z}\ \ 10^{-6})\ (u - 4.095)\right]$$

where $\bar{u} = \mu d = (.4095)\ (10.0) = 4.095$

TABLE 4.1.2.3.4-1(a)

CALCULATION OF STEP PARAMETERS

① k	② e_k	③ e_{k-1}	④ $e_k - e_{k-1}$	⑤ s_k	⑥ $(1 - s_k)$	⑦ $(1-s^2_k)$	⑧ $(1-s^3_k)$
	Reference Figures 4.1.2.3.4-1 and -2		② - ③	Ref. Fig. 4.1.2.3.4-2(a)	1 - ⑤	$1 - ⑤^2$	$1 - ⑤^3$
1	.10	1.00	-.90	.1000	.9000	.9900	.9990
2	.70	.10	+.60	.9300	.0700	.1351	.1957

①	⑨	⑩	⑪	⑫	⑬
k	$(1-s^4_k)$	$(e_k-e_{k-1})(1-s)$	$(e_k-e_{k-1})(1-s^2)$	$(e_k-e_{k-1})(1-s^3)$	$(e_k-e_{k-1})(1-s^4)$
	$1-⑤^4$	④ ⑥	④ ⑦	④ ⑧	④ ⑨
1	.9999	-.8100	-.8910	-.8991	-.8999
2	.2520	.0420	.0811	.1174	.1512
Σ		-.7680	-.8099	-.7817	-.7487

$$\eta_1 = (1)\left[1 + \sum_{k=1}^{2} (e_k - e_{k-1})(1 - s_k)\right] = (1)\left[1 + \Sigma ⑩\right] = .2320$$

$$\eta_2 = (\tfrac{1}{2})\left[1 + \sum_{k=1}^{2} (e_k - e_{k-1})(1 - s_k^2)\right] = (\tfrac{1}{2})\left[1 + \Sigma ⑪\right] = .0950$$

$$\eta_3 = (\tfrac{1}{3}\left[1 + \sum_{k=1}^{2} (e_k - e_{k-1})(1 - s_k^3)\right] = \cdot\bar{3})\left[1 + \Sigma ⑫\right] = .0728$$

$$\eta_4 = (\tfrac{1}{4})\left[1 + \sum_{k=1}^{2} (e_k - e_{k-1})(1 - s_k^4)\right] = (\tfrac{1}{4})\left[1 + \Sigma ⑬\right] = .0628$$

TABLE 4.1.2.3.4-1(b)

CALCULATIONS OF DEFORMATIONS

①	②	③	④	⑤	⑥	⑦	⑧
L	η_{L+1}	η_{L+2}	$\gamma_L = \frac{\eta_{L+1}}{\lambda}$	$\delta_L = \frac{1}{\nu}\left[\eta_{L+2} - \mu\,\eta_{L+1}\right]$	$a_L \times 10^6$	$a_L\,\gamma_L \times 10^6$	$\frac{a_L\,\delta_L}{d} \times 10^6$
	See Table 4.1.2.3.4-1(a)		$\frac{2}{.2320}$	$\left(\frac{1}{.0339}\right)\left[③ - .4095\ ②\right]$	Coeff. of αT profile* ④ ⑥		$\frac{⑤\ ⑥}{10.0}$
0	.2320	.0950	1.0000	0	1300	1300	0
1	.0950	.0728	.4095	1.0000	1300	532	130
2	.0728	.0628	.3138	.9734	1360	427	132
Σ =						2259	262

$$\epsilon' = \sum_{L=0}^{2} a_L \gamma_L = \Sigma\ ⑦ \times 10^{-6} = 2259 \times 10^{-6}$$

$$w' = \frac{1}{d} \sum_{L=0}^{2} a_L \delta_L = \Sigma\ ⑧ \times 10^{-6} = 262 \times 10^{-6}$$

* See Figure 4.1 2.3.4-2(b)

4.1.2.3.4 (Cont'd)

As in the case of continuous elastic geometry, the equations for the section properties and deformations are simplified if the elastic geometry is symmetric about the bending axis (see Figure 4.1.2.3.4-3).

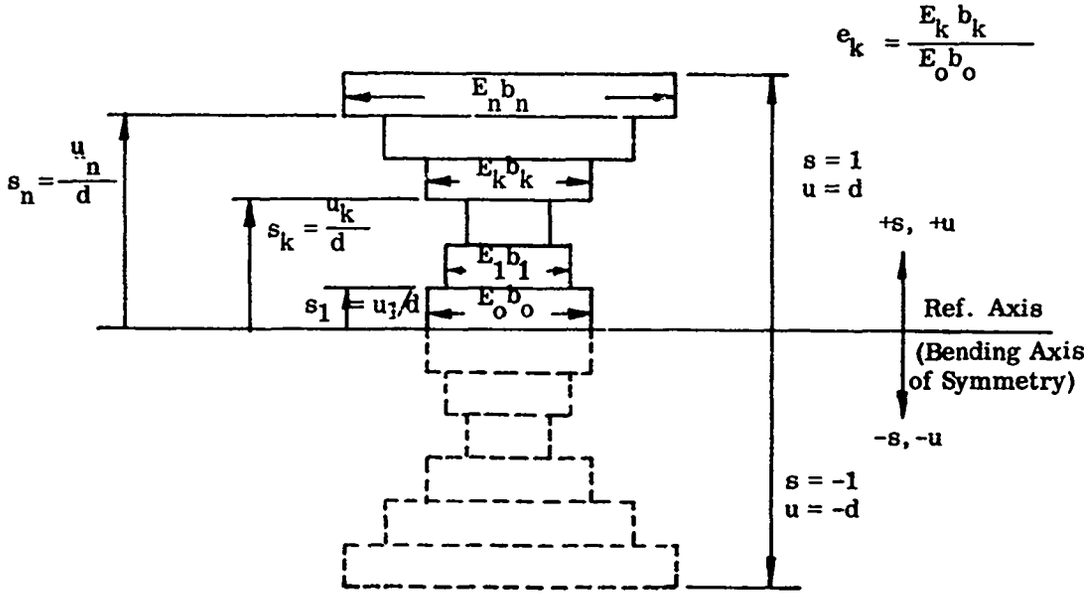


FIGURE 4.1.2.3.4-3 MULTI-RECTANGULAR SECTION WITH A BENDING AXIS OF SYMMETRY

In this case, the non-dimensional section properties of Eqs. (2), (3), and (4) reduce to

$$\lambda_s = \frac{\overline{EA}}{dE_o b_o} = 2\eta_1 \quad , \tag{7}$$

$$\mu_s = \frac{\bar{u}}{d} = 0 \tag{8}$$

and

$$\nu_s = \frac{\overline{EI}}{d^3 E_o b_o} = 2\eta_3 \quad , \tag{9}$$

where the step parameters are determined from Eq. (1) using the geometry on either side of the reference axis and d is the distance from the reference axis to an extreme fiber.

The solution for the deformations is obtained, as in the case of continuous elastic geometry, by decomposing the total αT distribution into components which are symmetrical and anti-symmetrical about the bending axis (see Eqs. (12) and (13) of Paragraph 4.1.2.3.3 and Figure 4.1.2.3.3-5).

4.1.2.3.4 (Cont'd)

For the symmetrical component of the αT profile, Eqs. (5) and (6) reduce to

$$(\gamma_L)_s = \frac{\bar{\epsilon}'_{L,s}}{(a_L + a'_L)/2} = \frac{2}{\lambda_s} \eta_{L+1} \tag{10}$$

$$(\delta_L)_s = \frac{dw'_{L,s}}{(a_L + a'_L)/2} = 0 \tag{11}$$

and for the anti-symmetrical component of the αT profile

$$(\gamma_L)_a = \frac{\bar{\epsilon}'_{L,a}}{(a_L - a'_L)/2} = 0 \tag{12}$$

$$(\delta_L)_a = \frac{dw'_{L,a}}{(a_L - a'_L)/2} = \frac{2}{\nu_s} \eta_{L+2} \tag{13}$$

Once the deformation modes have been determined, the total deformations and stresses are obtained by superposition from Eqs. (16), (17) and (18) of Paragraph 4.1.2.3.3.

Solutions of Eqs. (10) and (13) are plotted in Figures 4.1.2.3.4-5(a) for the special case of two rectangles* (sections such as channels, "I" beams, tees and cruciforms conform to this configuration) with $s_n = .97$.

---

* Practically all aircraft structural sections can be approximated by multi-rectangular configurations with respect to the principal axes. See, for example Figure 4.1.2.3.4-4 in which a zee section is approximated by a symmetrical two rectangle geometry.

4.1.2.3.4 (Cont'd)

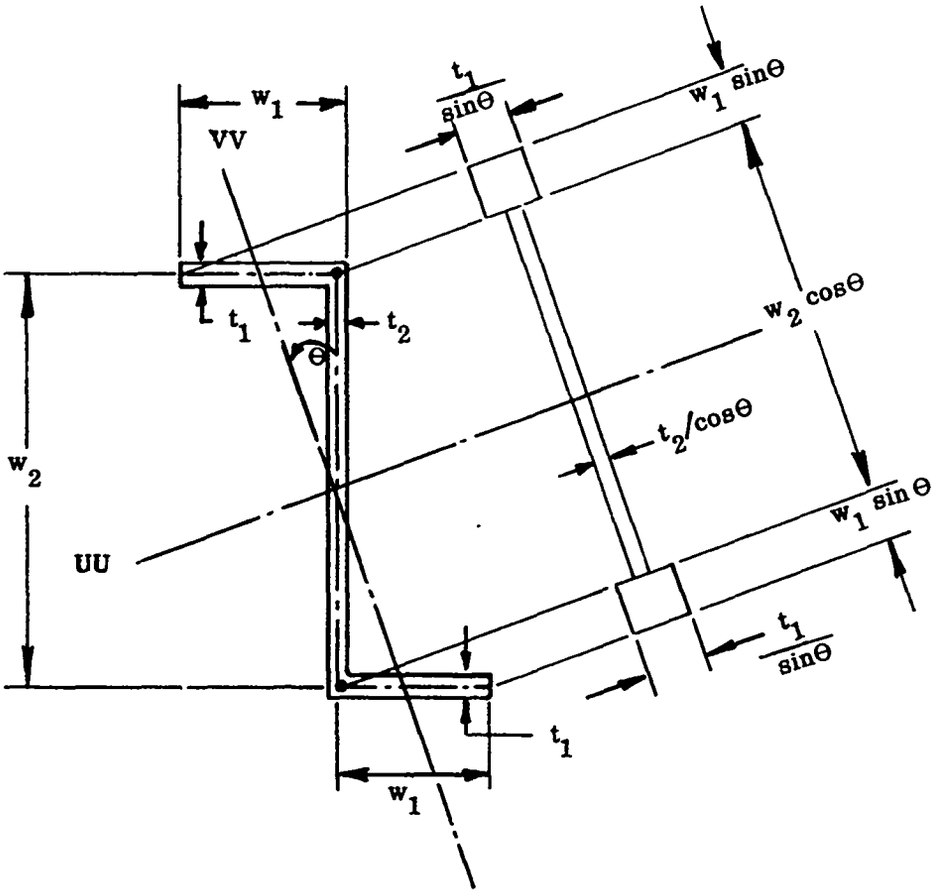
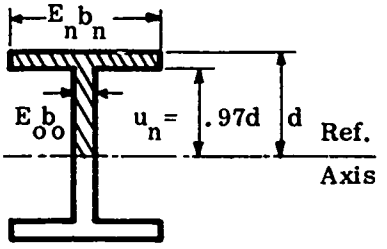


FIGURE 4.1.2.3.4-4 APPROXIMATE REPRESENTATION OF A ZEE BY A TWO RECTANGLE SYMMETRICAL GEOMETRY

Symmetric Temperature Distribution
(NOTE: $(\delta_L)_S = 0$)



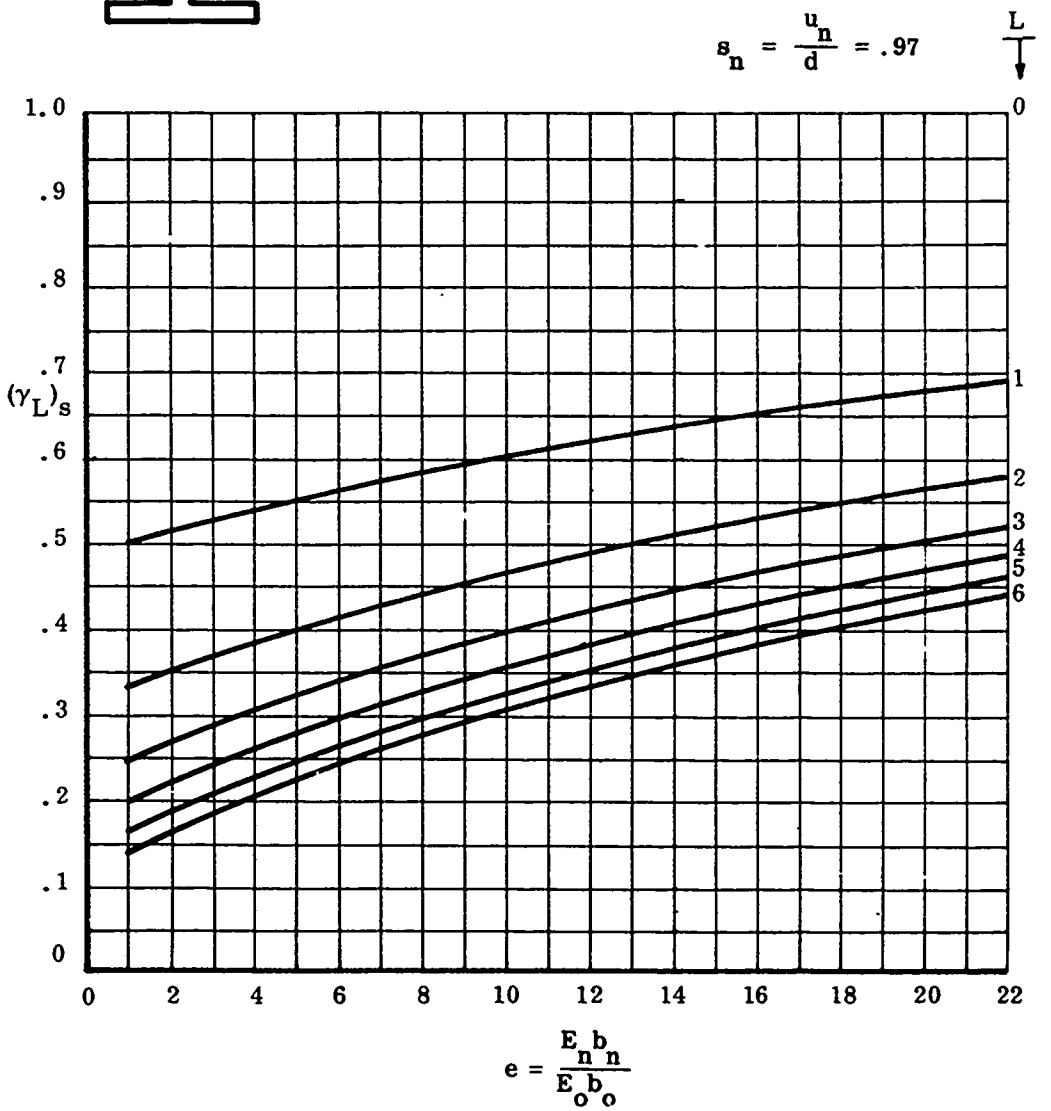
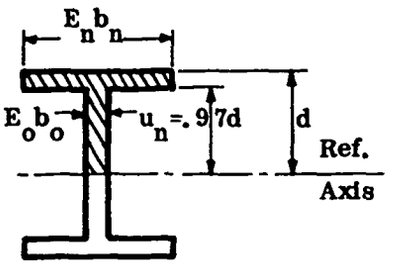


FIGURE 4.1.2.3.4-5(a) ELONGATION $(\gamma_L)_s$ VERSUS WIDTH PARAMETER (e)

Anti-Symmetric Temperature Distribution
(NOTE: $(\gamma_L)_a = 0$)



$$s_n = \frac{u_n}{d} = .97$$

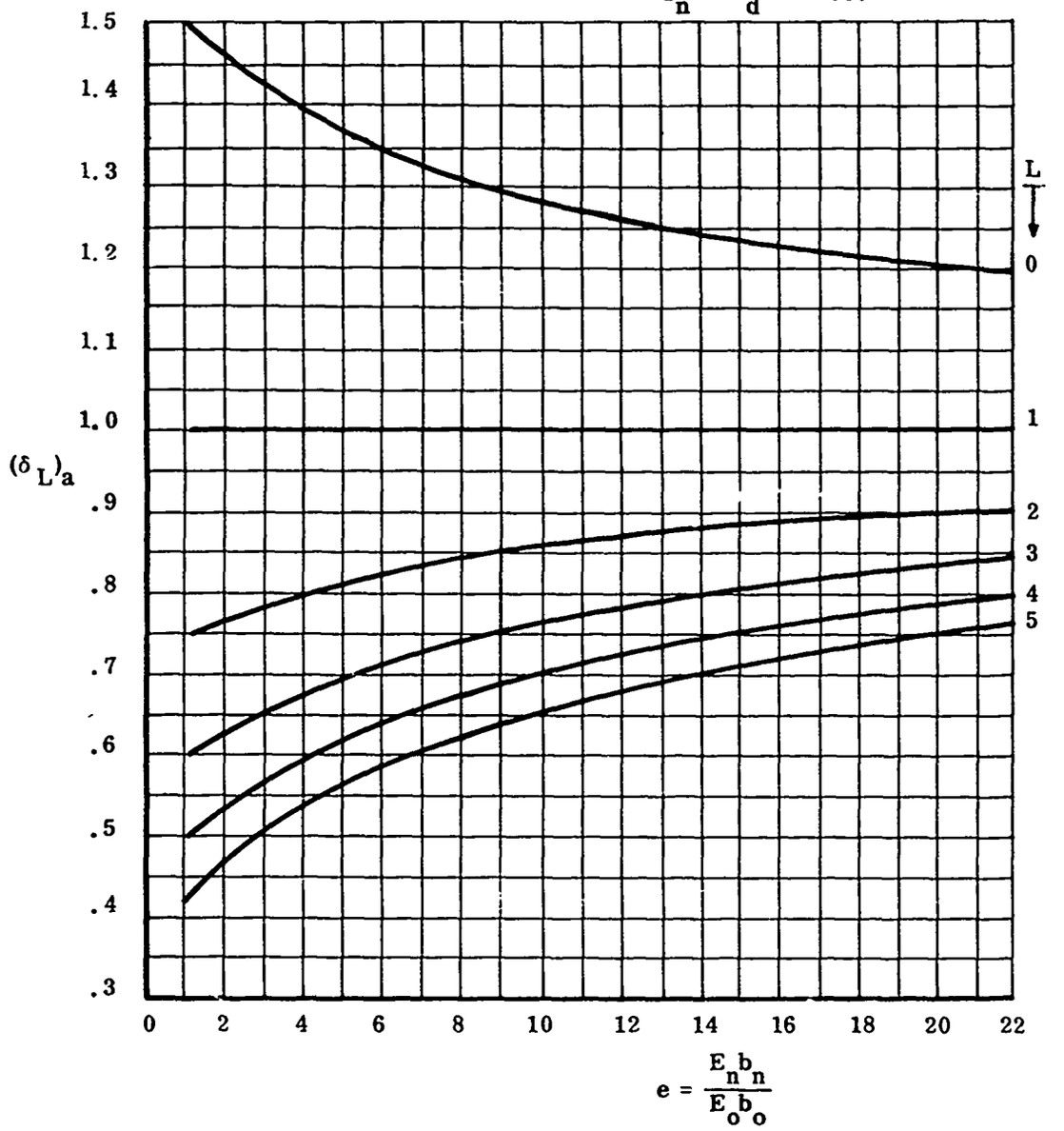


FIGURE 4.1.2.3.4-5(b) CURVATURE $(\delta_L)_a$ VERSUS WIDTH PARAMETER (e)

The solution for a symmetrical elastic geometry is illustrated below.

The box beam shown in Figure 4.1.2.3.4-6 is subjected to an αT distribution which varies through the depth as shown on the right. It is assumed that the αT distribution is constant across the width. To find the deformations $\bar{\epsilon}'$, w' and the thermal stresses, it is necessary that the step parameters be calculated from Eq. (1) in Table 4.1.2.3.4-2(a); the deformation modes as given by Eqs. (10) and (13) are calculated in Table 4.1.2.3.4-2(b).

Thus, from Eqs. (16) and (17) of Paragraph 4.1.2.3.3,

$$\bar{\epsilon}' = \sum_{L=0}^{n} (\bar{\epsilon}')_{L,s} = \Sigma \text{ (10) col.} \times 10^{-6} = 1518 \times 10^{-6}$$

$$w' = \sum_{L=0}^{n} (w')_{L,a} = \Sigma \text{ (11) col.} \times 10^{-6} = 73 \times 10^{-6}$$

and from Eq. (18) of Paragraph 4.1.2.3.3.

$$\sigma = E \left[-\alpha T + (1518 \times 10^{-6}) + (73 \times 10^{-6})\, u \right] .$$

Covers: Titanium, $E = 15 \times 10^6$; Webs: Aluminum, $E = 10 \times 10^6$

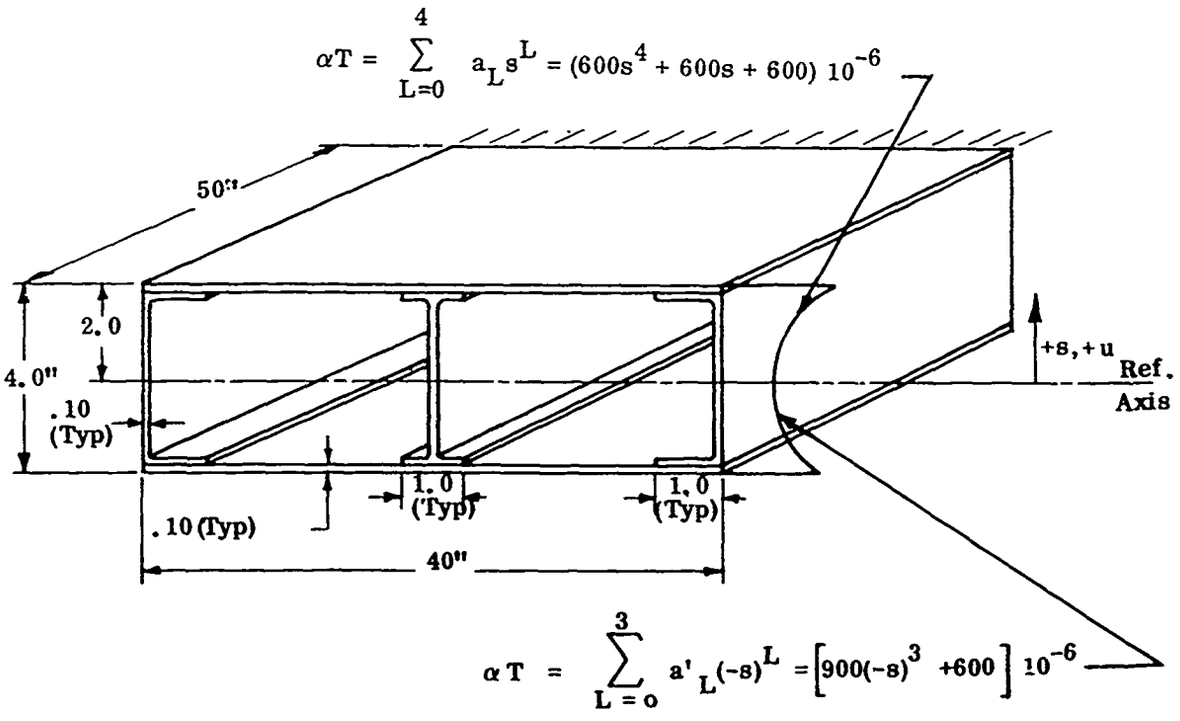


FIGURE 4.1.2.3.4-6 BI-METALLIC BOX BEAM WITH SYMMETRICAL GEOMETRY

TABLE 4.1.2.3.4-2(a)
CALCULATION OF STEP PARAMETERS

1	2	3	4	5	6	7	8	9	10	11	12	13	14	15	16	17	18	19	20
k	$\frac{b_k}{b_o}$	$\frac{E_k}{E_o}$	c_k	c_{k-1}	$c_k - c_{k-1}$	s_k	$(1 - s_k)$	$(1 - s_k^2)$	$(1 - s_k^3)$	$(1 - s_k^4)$	$(1 - s_k^5)$	$(1 - s_k^6)$	$\frac{(c_k - c_{k-1})}{(1 - s_k)}$	$\frac{(c_k - c_{k-1})}{(1 - s_k^2)}$	$\frac{(c_k - c_{k-1})}{(1 - s_k^3)}$	$\frac{(c_k - c_{k-1})}{(1 - s_k^4)}$	$\frac{(c_k - c_{k-1})}{(1 - s_k^5)}$	$\frac{(c_k - c_{k-1})}{(1 - s_k^6)}$	
	Ref. Fig's 4.1.2.3.4-3 and -6		②③	④$_{k-1}$	④ - ⑤	Ref.Fig's 4.1.2.3.4 -3 and -6	1 - ⑦	1 - ⑦^2	1 - ⑦^3	1 - ⑦^4	1 - ⑦^5	1 - ⑦^6	⑥⑧	⑥⑨	⑥⑩	⑥⑪	⑥⑫	⑥⑬	
1	10.00	1.0	10.00	1.00*	9.00	.90	.1000	.1900	.2710	.3439	.4095	.4686	.9000	1.7100	2.4390	3.0879	3.6855	4.2174	
2	133.33	1.5	200.00	10.00	190.00	.95	.0500	.0975	.1426	.1855	.2262	.2649	9.5000	18.5250	27.0940	35.2450	42.9780	50.3310	
Σ													10.4000	20.2350	29.5330	38.3329	46.6635	54.5484	

* $e_o = 1.00$ $\eta_1 = (1)\{1 + \Sigma(14)\} = 11.4000$
$\eta_2 = (1/2)\{1 + \Sigma(15)\} = 10.6175$
$\eta_3 = (1/3)\{1 + \Sigma(16)\} = 10.1777$
$\eta_4 = (1/4)\{1 + \Sigma(17)\} = 9.8332$
$\eta_5 = (1/5)\{1 + \Sigma(18)\} = 9.5327$
$\eta_6 = (1/6)\{1 + \Sigma(19)\} = 9.0914$
$\lambda_s = 2\eta_1 = 22.8000$
$\nu_s = 2\eta_3 = 20.3554$

TABLE 4.1.2.3.4-2(b)
CALCULATION OF DEFORMATIONS

1	2	3	4	5	6	7	8	9	10	11	12	13	14	15	16	17	18	19	20
L	$a_L \times 10^6$	$a'_L \times 10^6$	$\frac{a_L + a'_L}{2} \times 10^6$	$\frac{a_L - a'_L}{2} \times 10^6$	η_{L+1}	η_{L+2}	$(\gamma_L)_s = \frac{2}{\lambda_s}\eta_{L+1}$	$(\delta_L)_s = \frac{2}{\nu_s}\eta_{L+2}$	See (1) Below	See (2) Below									
	Ref. Fig. 4.1.2.3.4-6		② · ③ / 2	② - ③ / 2	See Step Parameters Above		2 ⑥ / 22.8000	2 ⑦ / 20.3554	④ ⑧	5 ⑨ / 2.0									
0	600	600	600	0	11.4000	10.6175	1.0000	1.0432	600	0									
1	600	0	300	300	10.6175	10.1777	.9314	1.0000	279	150									
2	0	0			10.1777	9.8332													
3	0	900	450	-450	9.8332	9.5327	.8626	.9366	388	-211									
4	600	0	300	300	9.5327	9.0914	.8362	.8933	251	134									
Σ									1518	73									

(1) $a'_{L,s} \times 10^6 = \left(\frac{a_L + a'_L}{2}\right)(\gamma_L)_s \times 10^6$

(2) $w'_{L,s} \times 10^6 = \left(\frac{a_L - a'_L}{2}\right)\left(\frac{1}{d}\right)(\delta_L)_s \times 10^6$

4.1.2.4 Power Series Solution - Corrections for Bending About Both Axes

The power series solution discussed in Paragraph 4.1.2.3 assumes that bending takes place about only one principal axis UU . This is the case when the VV principal axis is an axis of symmetry for both the elastic geometry and the αT distribution. Bending about the VV axis ($w'_v \neq 0$) is caused by unsymmetrical geometry and αT distribution about the VV principal axis. The correction requires the addition to the solution of the bending about this principal axis VV. The final deformations are the axial elongation and curvature w'_u about the UU axis solved previously plus the curvature w'_v about the VV axis.

The final thermal stress is

$$\sigma = E \left[-\alpha T + \bar{\epsilon}' + w'_v (u - \bar{u}) + w'_u (v - \bar{v}) \right] \quad (1)$$

Note that any distribution of αT can be solved by superposing the solution into two parts, each being the solution for the average distribution (Figure 4.1.2.3-2) about that principal axis. The solution about any axis can be accomplished by the power series or finite sum method, whichever is most readily solvable.

4.2 STATICALLY INDETERMINATE (EXTERNALLY RESTRAINED) BEAMS

In Sub-section 4.1 it is shown that in externally unrestrained (statically determinate) beams, thermal loads produce deformations and self-equilibrating internal stresses which are compatible with the internal requirement of the plane cross sections remaining plane. In externally restrained (statically indeterminate) beams, compatibility forces are generated at the restraints in order to make the beam deflections satisfy the external (boundary) conditions. These compatibility forces (redundants) and applied mechanical loads produce stresses and deformations within the beam which are superimposed on the unrestrained thermal stresses and deformations.

Paragraph 4.2.1 discusses beam deflections which must be known in order to satisfy compatibility conditions. A knowledge of the deflected shape of a structure is also important from a design point of view.

Fixed end reactions due to distributed thermal and mechanical loadings are presented in Paragraph 4.2.2. It is subsequently shown in Paragraph 4.2.3 how distributed thermal and mechanical loads can be replaced by their equivalent fixed-end reactions at discrete structural load points, thereby facilitating the application of the methods of influence and stiffness coefficients to the solution of indeterminate beam problems.

4.2.1 Beam Deflections

Under the assumption of plane cross sections remaining plane after deformations have occurred (internal shear strain energy neglected), the deflections of a beam subjected to combined thermal and mechanical loading can be determined from a spanwise integration of the total unit deformations of the cross sections.

The total deformations, which are a function of the distance x along the span (see Figure 4.2.1-1), are obtained by superimposing the deformations due to thermal and mechanical loading, i.e.;

4.2.1 (Cont'd)

$$w_t(x) = w'(x) + w(x) = -\left(\frac{M'}{\overline{EI}} + \frac{M}{\overline{EI}}\right) \quad (1)$$

$$\bar{\epsilon}_t(x) = \bar{\epsilon}'(x) + \bar{\epsilon}(x) = \frac{F'}{\overline{AE}} + \frac{F}{\overline{AE}} \quad (2)$$

where

$w_t(x)$ = Total rotation (curvature) of cross section per unit of length.

$w'(x)$ = Rotation of cross section of unrestrained beam, per unit of length due to thermal loading $= -\frac{M'}{\overline{EI}}$

$w(x)$ = Rotation of cross section per unit of length due to applied and redundant (mechanical) loading $= -\frac{M}{\overline{EI}}$

$\bar{\epsilon}_t(x)$ = Total axial strain at elastic centroid

$\bar{\epsilon}'(x)$ = Axial strain of unrestrained beam at elastic centroid due to thermal loading $= \frac{F'}{\overline{AE}}$

$\bar{\epsilon}(x)$ = Axial strain at elastic centroid due to applied and redundant (mechanical) loading $= \frac{F}{\overline{AE}}$

The total curvature $w_t(x)$ and axial strain $\bar{\epsilon}_t(x)$ have the same significance in the calculation of thermo-mechanical deflections that the familiar $\frac{M}{EI}$ and $\frac{F}{AE}$ for purely mechanical loading problems. Thus, once the quantities $\frac{M'}{\overline{EI}}$, $\frac{F'}{\overline{AE}}$, $\frac{M}{\overline{EI}}$ and $\frac{F}{\overline{AE}}$ have been determined by the methods of Sub-section 4.1, the beam deflections can be calculated, as usual, by energy methods.

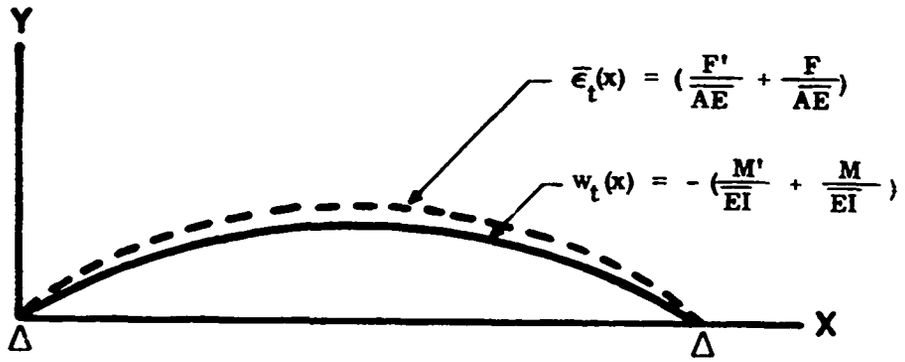


FIGURE 4.2.1-1 CURVATURE $w_t(x)$ AND ELONGATION $\bar{\epsilon}_t(x)$ DUE TO COMBINED MECHANICAL AND THERMAL LOADING AS A FUNCTION OF DISTANCE ALONG THE SPAN

By the principle of virtual work, derivable from energy considerations (Paragraph 2.1.2), the deflection and slope at any point on a line structure subjected to combined mechanical and thermal loading (neglecting shear strain energy) are

$$\Delta = -\int w_t \cdot m\,dx + \int \bar{\epsilon}_t \cdot f\,dx \tag{3a}$$

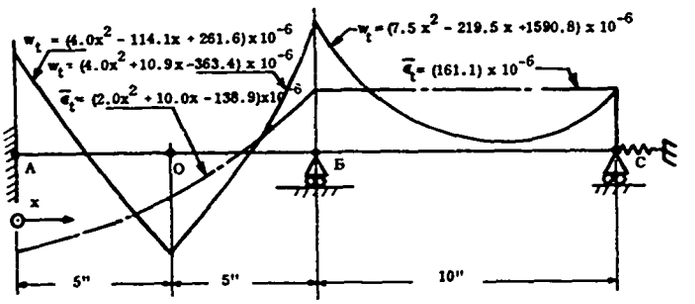
$$\Theta = -\int w_t \cdot m'\,dx + \int \bar{\epsilon}_t \cdot f'\,dx \tag{3b}$$

where m and f are the virtual moments and axial forces, respectively, caused by applying a unit virtual load at the point in the direction of the desired deflection component; m' and f' are the virtual moments and axial forces caused by the application of a unit virtual moment at the point at which the slope is to be determined.

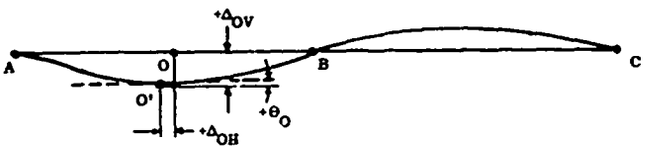
The principle of virtual work equates the external work done by the virtual force system acting through the actual external displacements to the corresponding internal energy due to the internal virtual stresses acting through the actual internal strains. Because of this, the deflection or slope at the point of applied virtual force is determined relative to the datum defined by the reactions to the virtual force. The inherent advantage in this concept lies in the fact that once the actual stresses are determined for a statically indeterminate structure, the deflection or slope of any point on the structure can be determined relative to a datum located in the vicinity of the point by dealing with the portion of the structure lying in that vicinity, since the virtual stresses outside the region affected by the virtual force system are identically zero. The virtual force system can be taken as a simple determinate one, thereby avoiding the solution of an additional indeterminate problem involving the virtual forces and considerably minimizing the work involved.

The preceding concepts are illustrated by the following problem in which Figure 4.2.1-2(a) shows the distribution of curvature and axial elongation in an indeterminate beam; this information has been obtained from the solution of the indeterminate beam problem given in Paragraph 4.2.3.

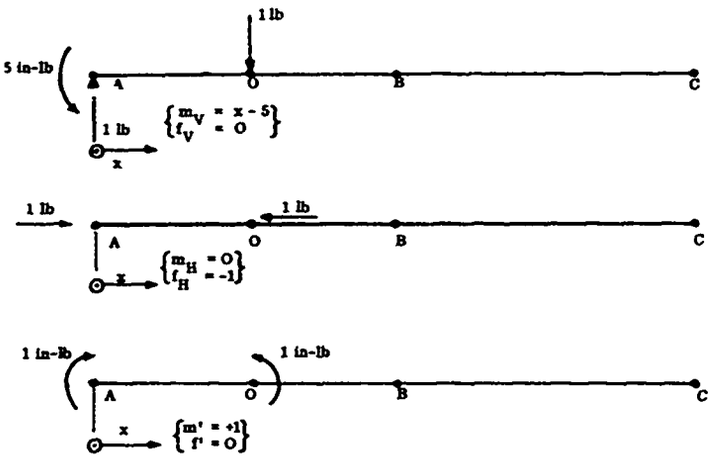
Under the action of thermal and mechanical loads, a point initially located at O moves to the deflected position O'. In order to determine the absolute deflection and rotation of this point (Figure 4.2.1-2(b)), the virtual loads must be reacted at points which define a fixed datum. Point A, located at the fixed wall, provides one such datum since this point has zero vertical and horizontal deflection and zero slope. Thus, as shown in Figure 4.2.1-2(c), the virtual force systems are obtained by reacting unit virtual loads and moments applied at point O by determinate shears, axial loads, and moments at point A.



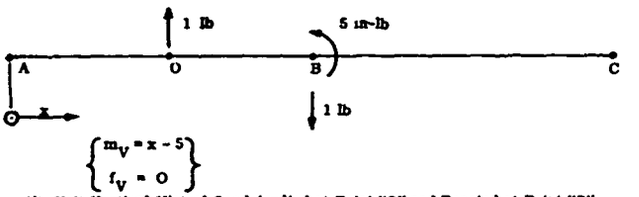
(a) Distribution of Curvature and Axial Elongation in an Indeterminate Beam



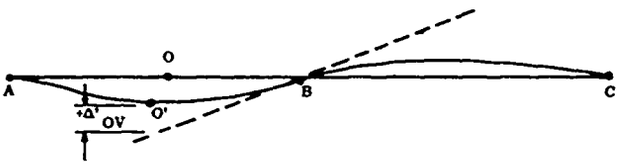
(b) Deflection and Rotation at Point "O" Measured From a Fixed Datum



(c) Unit Virtual Loads Applied at Point "O" and Reacted at Point "A" (3 cases)



(d) Unit Vertical Virtual Load Applied at Point "O" and Reacted at Point "B".



(e) Vertical Deflection at Point "O" Measured From the Deflected Tangent at Point "B"

FIGURE 4.2.1-2 INDETERMINATE BEAM DEFLECTIONS

Substituting in Eqs. (3a) and (3b), the absolute values of the deflections and slope obtained are

$$\Delta_{ov} = -\int_o^5 w_t \cdot m_v \, dx + \int_o^5 \bar{\epsilon}_t \cdot f_v \, dx$$

$$= \left[-\int_o^5 (4.0 x^2 - 114.1 x + 261.6)(x - 5)\, dx + 0 \right] \times 10^{-6}$$

$$= 1100 \times 10^{-6} \text{ inch.}$$

$$\Delta_{oh} = -\int_o^5 w_t \cdot m_h \, dx + \int_o^5 \bar{\epsilon}_t \cdot f_h \, dx$$

$$= \left[0 + \int_o^5 (2.0 x^2 + 10.0 x - 138.9)(-1)\, dx \right] \times 10^{-6} = 486 \times 10^{-6} \text{ inch.}$$

$$\Theta_o = -\int_o^5 w_t \cdot m' \, dx + \int_o^5 \bar{\epsilon}_t \cdot f' \, dx$$

$$= \left[-\int_o^5 (4.0 x^2 - 114.1 x + 261.6)(1)\, dx + 0 \right] \times 10^{-6} = -49 \times 10^{-6} \text{ radians.}$$

Figure 4.2.1-2(d) shows the vertical unit virtual load reacted at point B. Point B does not deflect vertically. However, a rotation does occur at this point. Thus, the vertical deflection of point O obtained by reacting the virtual load in this manner is equal to the vertical distance from the tangent drawn at B to the curve at O' (Figure 4.2.1-2(e)), or

$$\Delta'_{ov} = \left[-\int_5^{10} (4.0 x^2 + 10.9 x - 363.4)(x - 5) \right] \times 10^{-6} = -138 \times 10^{-6} \text{ inch.}$$

The deflections of a beam-like structure can always be obtained by integrating the curvatures and elongations as shown above. However, as shown in Paragraph 4.2.3, a more efficient procedure for obtaining deflections, which lends itself conveniently to digital computing techniques, consists of using flexibility coefficients (Paragraph 2.1.1.1). Ignoring shear and axial energy due to mechanical loads, the flexibility coefficients are

$$\delta_{ij} = \int \frac{m_i \, m_j \, dx}{EI} \tag{4}$$

through which it is possible to determine the deflection at a degree of freedom by superposition, i.e.,

$$\Delta_i = \sum_j \delta_{ij} \, P_j, \tag{5}$$

where the P_j's are the negative of the fixed end reactions due to mechanical and thermal loads, at the locations of the predetermined j degrees of freedom. One of the advantages of using this procedure lies in the fact that the flexibility coefficients are approximately constant structural properties which do not depend on the mechanical and only slightly on the thermal loading. Once calculated, they can be used to obtain the deflections for any set of applied loads.

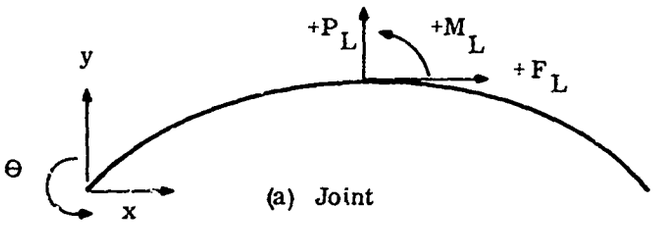
4.2.2 Fixed End Reactions

The fixed end reactions are those mechanical loads applied at the ends of a beam-like structure which do not allow the ends to move when the beam is subjected to mechanical and thermal stimuli. The negative of the fixed end reactions to the applied loads and temperatures can be shown to be equivalent mechanical loads acting at the joints which will produce the same deformations at the joint. This is discussed in Paragraph 2.1.6 and Reference 4-4. The transformation of mechanical and thermal loads acting all along the structure to equivalent loads at the joints assist in permitting the reduction of the structural problem to a finite number of unknowns. This assists in a systematic procedure for solving statically indeterminate structures (also referred to as indeterminate structures) subjected to mechanical and thermal loads as shown in Paragraph 4.2.3.

4.2.2.1 Sign Convention

The sign convention for individual elemental beams is in accordance with standard engineering practices which state that loads which cause tension in a member or compression in upper (positive) fibers are positive. However, care must be taken in determining the resultant fixed end reactions at a joint. This is shown by Eqs. (1) through (3) and Figure 4.2.2.1-1 which indicate that the resultant fixed end reactions at a joint in the structure are obtained by first reversing the signs of the axial and moment reactions of the beam to the right of the joint (the sign of the shear reaction of the beam to the right of the joint is not changed) and then adding algebraically with the corresponding axial, moment and shear reactions of the beam to the left of the joint. The fixed end reaction on each beam is determined from Eqs. (1b), (2b) and (3b) of Paragraph 4.2.2.2 and (1), (2) and (3) of Paragraph 4.2.2.3. The analyst need not bother to combine fixed end reactions on the left and right hand side of a joint until the final loads at a joint are required. This last step is simple to do with Eqs. (1), (2) and (3) or Figure 4.2.2.1-1, and is demonstrated in Illustrative Problem IA of Paragraph 4.2.6.1 and in Figure 4.2.4-1.

4.2.2.1 (Cont'd)



(a) Joint

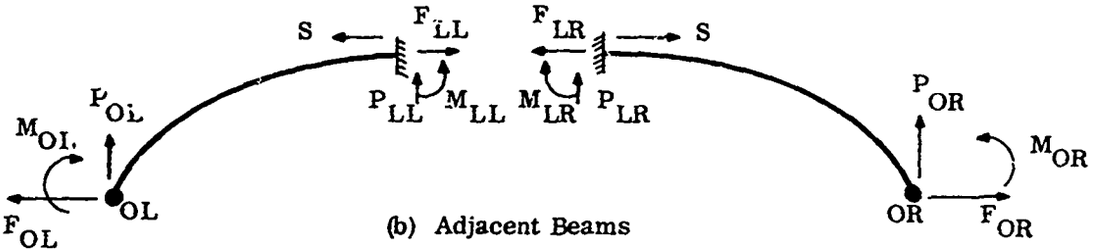
For Joint:

Positive P Loads are up ($P_L = P_{LL} + P_{LR}$) (1)

Positive F Loads are to the right ($F_L = F_{LL} - F_{LR}$) (2)

Positive M Loads are counterclockwise ($M_L = M_{LL} - M_{LR}$) (3)

Positive direction and displacements and rotations are in the same direction as positive loads and moments.



(b) Adjacent Beams

For Adjacent Beams:

Positive curvature w when curve is concave downward
(Inside of curve to right when going to right
Tensile strains for upper fibers)

Positive moment causes compression in upper fibers
(Opposite in sense to positive curvature
Positive moment on right side of beam is counterclockwise
Positive moment on left side of beam is clockwise)

Positive transverse loads are in positive y direction

Positive axial load causes tension in member
(Positive axial load on right side of beam is to the right
Positive axial load on left side of beam is to the left)

FIGURE 4.2.2.1-1 SIGN CONVENTION FOR COMBINING FIXED END REACTIONS OF BEAMS TO DETERMINE RESULTANT FIXED END REACTIONS AT A JOINT

4.2.2.2 Applied Beam Loads

Various types of loading conditions are considered to act on the beam. The location of the load is arbitrary (Figure 4.2.2.2-1) but its distribution is assumed to be expressible as a power function. Any loading can be approximated by the superposition of such loads at different initiation points (see illustrative problems in Paragraph 4.2.2.5) The type of loading (Figure 4.2.2.2-1) is as follows:

(1) Concentrated Moment, M
(2) Concentrated Transverse Load, P
(3) Varying Transverse Load, $q = q_L \zeta^r$
(4) Concentrated Axial Force, F, with eccentricity, y
(5) Varying Eccentric Axial Force (Shear Flow), $\tau = \tau_L \zeta^k$
(6) Varying Thermal Curvature, $w' = w'_L \zeta^j$
(7) Varying Thermal Axial Elongation, $\bar{\epsilon}' = \epsilon'_L \zeta^i$

With reference to Figure 4.2.2.2-1(e), let

$\mathcal{P}_L$ = Total transverse cantilever load at L due to applied mechanical loads

$\mathcal{M}_L$ = Total cantilever moment at L due to applied mechanical load

$\mathcal{F}_L$ = Total cantilever axial load at L due to applied mechanical load

Then

$$\mathcal{P}_L = a\int_0^1 q\,d\zeta + P = \frac{a\,q_L}{r+1} + P \tag{1a}$$

$$\mathcal{M}_L = a^2\int_0^1 q\,(1-\zeta)\,d\zeta + Pa + M - a\int_0^1 \tau y\,d\zeta - Fy$$

$$\mathcal{M}_L = \frac{a^2 q_L}{(r+1)(r+2)} + Pa + M - \frac{a\,\tau_L y}{k+1} - Fy \tag{2a}$$

$$\mathcal{F}_L = a\int_0^1 \tau\,d\zeta + F = \frac{a\,\tau_L}{k+1} + F \tag{3a}$$

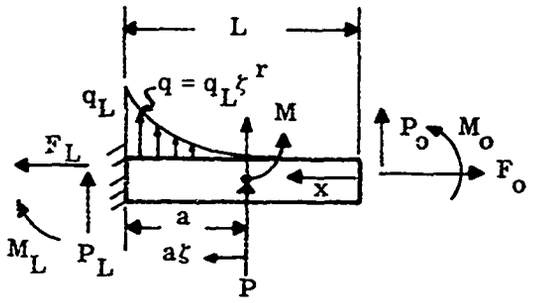
$$-P_L = P_o + \mathcal{P}_L = P_o + \frac{aq_L}{r+1} + P \tag{1b}$$

$$M_L = M_o + P_o L + \mathcal{M}_L = M_o + P_o L + \frac{a^2 q_L}{(r+1)(r+2)} + Pa + M - \frac{a\,\tau_L y}{k+1} - Fy \tag{2b}$$

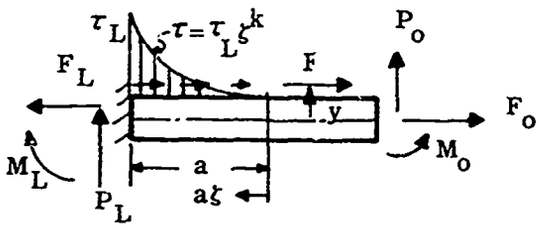
$$F_L = F_o + \mathcal{F}_L = F_o + \frac{a\,\tau_L}{k+1} + F \tag{3b}$$

where P_o, M_o, F_o are to be determined in order to find the fixed end reactions (P_o, P_L, M_o, M_L, F_o and F_L).

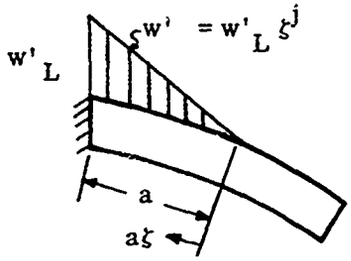
4.2.2.2 (Cont'd)



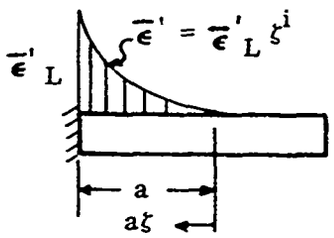
(a) Transverse Mechanical Loads (M, P and q)



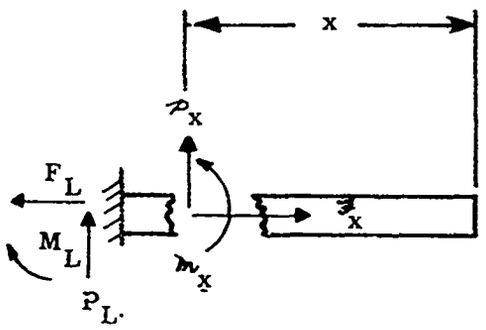
(b) Axial Mechanical Loads (F and τ)



(c) Unrestrained Thermal Curvature



(d) Unrestrained Thermal Axial Elongation



(e) Internal Cantilever Load

FIGURE 4.2.2.2-1 MECHANICAL AND THERMAL LOADS ACTING ON CANTILEVER BEAM

4.2.2.3 Determination of Fixed End Reactions

The mechanical loads (fixed end reactions) that are required at the end of the beam (P_o, M_o, F_o) to negate the deflections due to the applied loads and thermal stimuli are presented below in a general form (as derived in Reference 4-4) and are then reduced for particular types of problems. The reactions at the other end (P_L, M_L, F_L) are obtained by employing the equilibrium Eqs. (1b), (2b), and (3b) of Paragraph 4.2.2.2.

The general solution for the fixed end reactions at the end of the beam (see Figure 4.2.2.2-1) is as follows:

$$\begin{aligned} P_o L = {} & E_o I_o w'_L p_{j,c} + (Fy-M)\left[p_{o,c} + e \sum_{n=o}^{c} ({}_cC_n) \nu^n (1-\nu)^{c-n} p_{n,c} \right] \\ & + \frac{\nu Ly \tau_L}{k+1}\left[p_{k+1,c} + e \sum_{n=o}^{c} ({}_cC_n) \nu^n (1-\nu)^{c-n} p_{k+1+n,c} \right] \\ & - \nu L P\left[p_{1,c} + e \sum_{n=o}^{c} ({}_cC_n) \nu^n (1-\nu)^{c-n} p_{1+n,c} \right] \\ & - \frac{(\nu L)^2 q_L}{(r+1)(r+2)}\left[p_{r+2,c} + e \sum_{n=o}^{c} ({}_cC_n) \nu^n (1-\nu)^{c-n} p_{r+2+n,c} \right] \end{aligned} \tag{1a}$$

$$\begin{aligned} M_o = {} & E_o I_o w'_L m_{j,c} + (Fy-M)\left[m_{oc} + e \sum_{n=o}^{c} ({}_cC_n) \nu^n (1-\nu)^{c-n} m_{n,c} \right] \\ & + \frac{\nu Ly \tau_L}{k+1}\left[m_{k+1,c} + e \sum_{n=o}^{c} ({}_cC_n) \nu^n (1-\nu)^{c-n} m_{k+1+n,c} \right] \\ & - \nu L P\left[m_{1,c} + e \sum_{n=o}^{c} ({}_cC_n) \nu^n (1-\nu)^{c-n} m_{1+n,c} \right] \\ & - \frac{(\nu L)^2 q_L}{(r+1)(r+2)}\left[m_{r+2,c} + e \sum_{n=o}^{c} ({}_cC_n) \nu^n (1-\nu)^{c-n} m_{r+2+n,c} \right] \end{aligned} \tag{2a}$$

$$\begin{aligned} F_o = {} & E_o A_o \bar{\epsilon}'_L f_{j,c} + F\left[f_{o,c} + e' \sum_{n=o}^{c'} ({}_{c'}C_n) \nu^n (1-\nu)^{c'-n} f_{n,c'} \right] \\ & + \frac{(\nu L)}{(k+1)} \tau_L \left[f_{k+1,c} + e' \sum_{n=o}^{c'} ({}_{c'}C_n) \nu^n (1-\nu)^{c'-n} f_{k+1+n,c'} \right] \end{aligned} \tag{3a}$$

where

$$-\frac{P_o L}{\mathcal{M}'_L} = p_{j,c} = \frac{\nu}{(j+1)D}\left[\frac{1}{2} + e\left(\frac{1}{c+1} - \frac{1}{c+2} \right) - \frac{\nu}{j+2}\left(1 + \frac{e}{c+1} \right) \right] \tag{1b}$$

$$-\frac{M_o}{\mathcal{M}'_L} = m_{j,c} = \frac{\nu}{(j+1)D}\left[-\frac{1}{6} - e\left(\frac{1}{c+2} - \frac{1}{c+3} \right) + \frac{\nu}{j+2}\left(\frac{1}{2} + \frac{e}{c+2} \right) \right] \tag{2b}$$

4.2.2.3 (Cont'd)

$$-\frac{F_o}{\mathcal{F}_L'} = f_{j,c} = -\frac{\nu}{(j+1)\left(1+\frac{e'}{c'+1}\right)} \tag{3b}$$

where

$$D = \frac{1}{12} + e\left[\frac{\frac{1}{3}(c+3)(c+2) + (c+1)(c+2)^2 - (c+1)(c+3)}{(c+1)(c+2)(c+3)}\right] + e^2\left[\frac{(c+2)^2 - (c+1)(c+3)}{(c+1)(c+2)^2(c+3)}\right] \tag{4}$$

and

j = exponent describing curvature variation due to temperature or the moment variation due to mechanical loading, e.g.,

when
- $j = o$, pure moment or eccentric axial load
- $j = 1$, concentrated transverse load
- $j = r+2$, for a varying transverse load, $q = q_L \zeta^r$
- $j = k+1$, for a varying eccentric axial load, $\tau = \tau_L \zeta^k$

and also

$$e = \frac{E_o I_o}{E_L I_L} - 1 = \text{bending stiffness ratio parameter} \tag{5a}$$

$$e' = \frac{E_o A_o}{E_L A_L} - 1 = \text{axial stiffness ratio parameter} \tag{5b}$$

$$\nu = a/L = \text{ratio of loaded length of beam to length of beam} \tag{5c}$$

$$c = \text{power variation of } 1/EI = \frac{1}{E_o I_o}\left[1 + e\left(\frac{x}{L}\right)^c\right] \tag{5d}$$

$$c' = \text{power variation of } 1/EA = \frac{1}{E_o A_o}\left[1 + e'\left(\frac{x}{L}\right)^{c'}\right] \tag{5e}$$

$E_o I_o$, $E_L I_L$ = Bending stiffness at x = O and L, respectively

$E_o A_o$, $E_L A_L$ = Axial stiffness at x = O and L, respectively

$c\,C_n$ = (n+1) term of binomial expansion, i.e., the number of combinations of c items taken n at a time = c!/n! (c-n)!

$c\,C_o$ = First term of binomial expansion = 1

The above equations are obtained by applying the mechanical and thermal loads to the statically determinate cantilever fixed at L and determining the deflections at the free end O. The loads necessary to negate these deflections are P_o, M_o, and F_o. The solution is given in terms of each type of load and includes the effect of varying bending and axial stiffness. Solutions are presented in terms of influence parameter ($p_{j,c}$, $m_{j,c}$, $f_{j,c}$) which are the fixed end reactions (P_o, M_o, F_o) to a unit type of mechanical or thermal load. For example, $m_{j,c} = -\frac{M_o}{\mathcal{M}_L'}$ is the negative of the ratio of the fixed end moment, M_o, to the

4.2.2.3 (Cont'd)

cantilever moment, $\mathcal{M}'_L$, which would cause a j^{th} power variation of curvature on a beam whose 1/EI varies as a power of c. Similiarly, $p_{j,c} = \frac{-P_o L}{\mathcal{M}'_L}$ and $f_{j,c} = \frac{-F_o}{\mathcal{F}_L}$. The formulations and graphical aids can be employed to obtain the fixed end reactions due to most types of mechanical or thermal loadings. The mechanical and thermal loads are first allowed to act upon the cantilever beam. Then the loadings and thermal deformation are decomposed into a sum of loadings as described in Paragraph 4.2.2.2 and illustrated in Figure 4.2.2.2-1. Each component is then analyzed for the fixed end reactions (P_o, M_o, and F_o) it causes. This analysis is done in accordance with Eqs. (1) through (5) or with the graphical aids, Figures 4.2.2.3-1 through -6. The total fixed end reactions are the sum of all such effects.

Illustrative examples follow to illustrate the computation technique. Graphical solutions of the equations are shown for special conditions which simplify the general equations by eliminating terms inside the summation sign (i.e., $c = 0$ or $\nu = 1$). These cases are of practical utility and are shown in Figures 4.2.2.3-1 through -6. The special conditions are:

(1) EI constant and any distribution of applied load ($\mathcal{M}'_L = \mathcal{M}_L$)
(2) 1/EI varying linearly and moment expressible as a sum of power functions initiating at point O ($\nu = 1$)
(3) 1/EI varying parabolically and moment expressible as a sum of power functions initiating at point O ($\nu = 1$).

Equations (1b), (2b) and (3b) of Paragraph 4.2.2.3 are simpler to apply then (1a), (2a) and (3a) thereof, but care must be taken that the correct value of j is employed for each type of load.

4.2.2.3 (Cont'd)

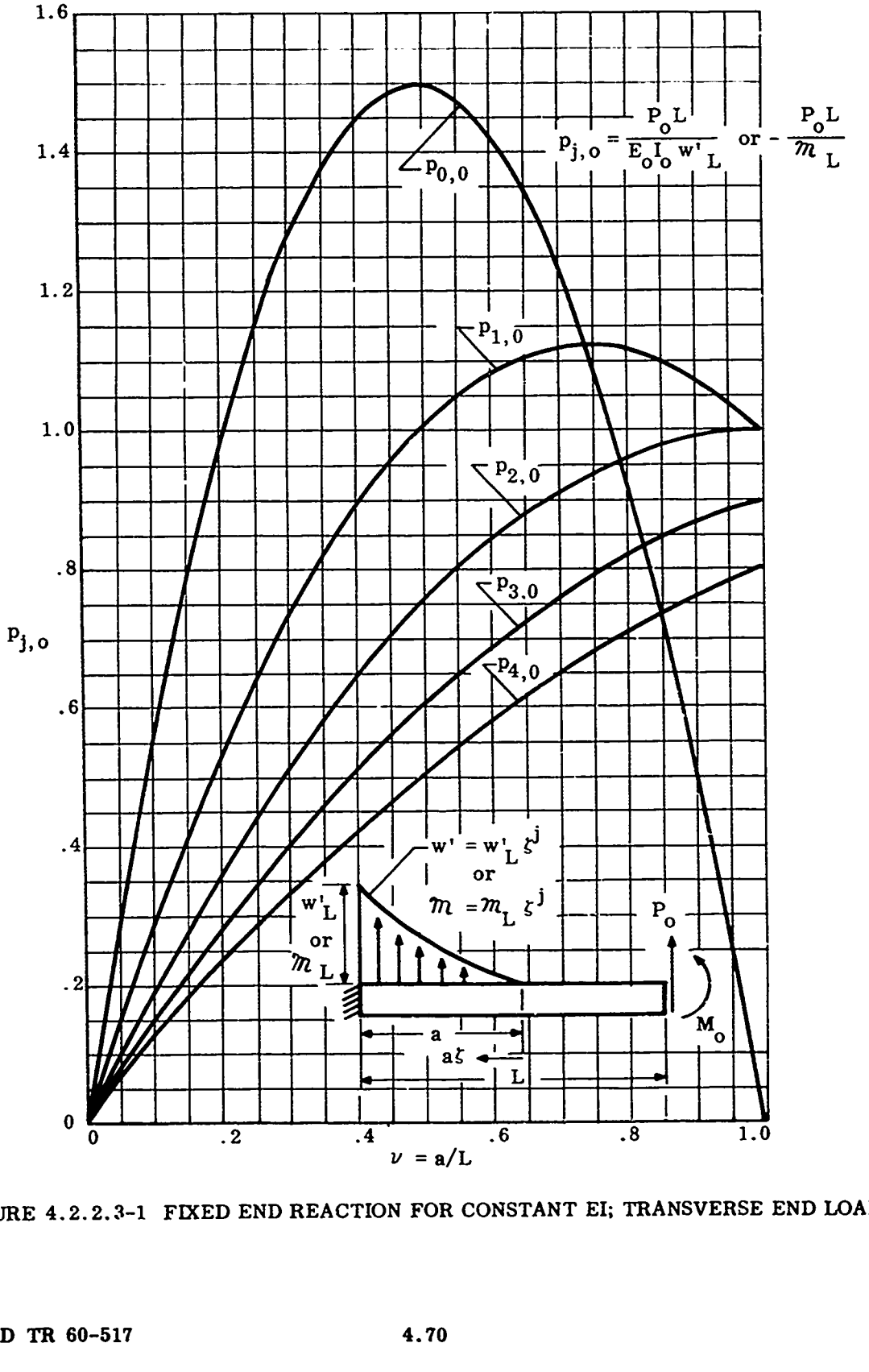


FIGURE 4.2.2.3-1 FIXED END REACTION FOR CONSTANT EI; TRANSVERSE END LOAD (P_o)

4.2.2.3 (Cont'd)

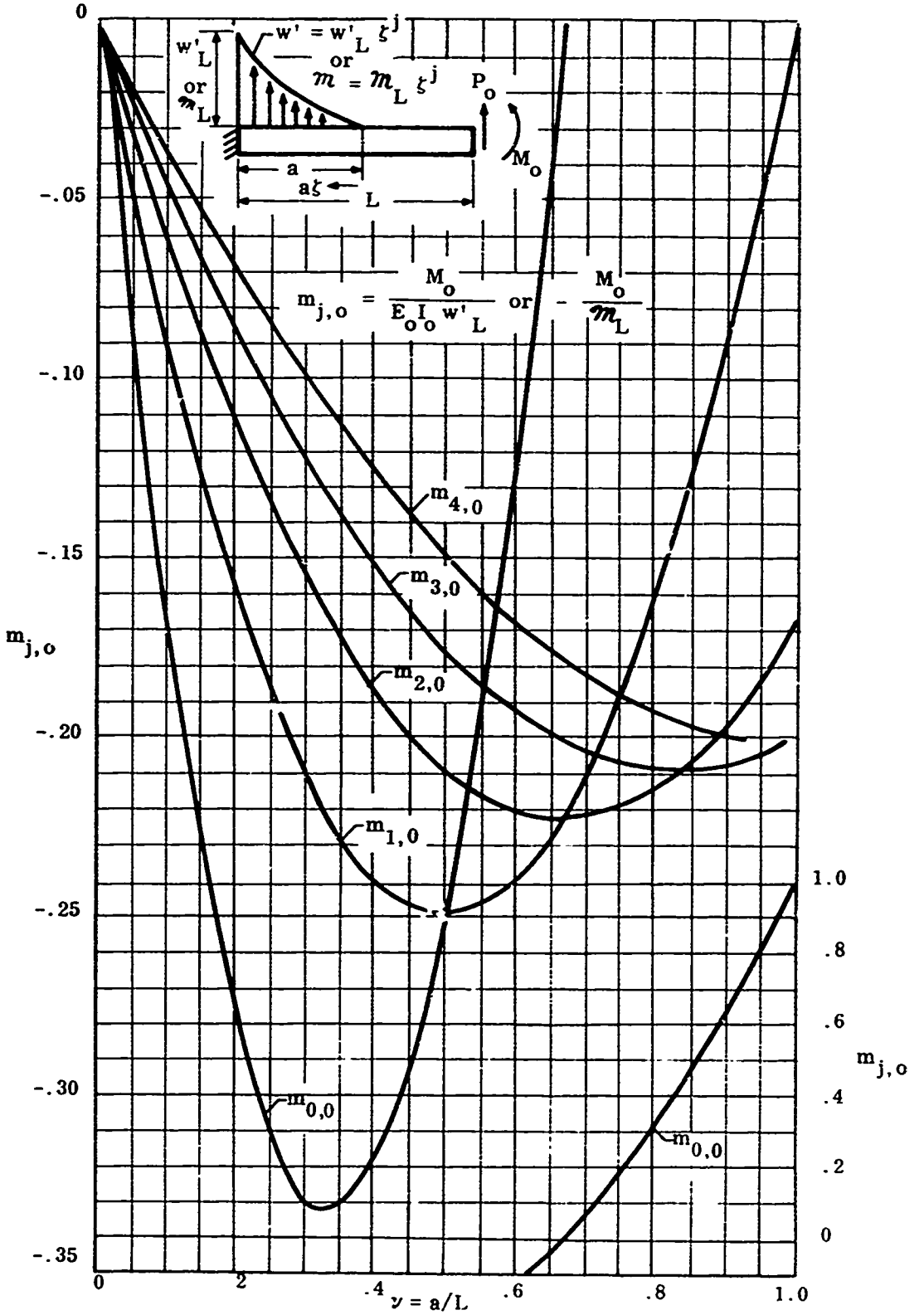


FIGURE 4.2.2.3-2 FIXED END REACTION FOR CONSTANT EI; END MOMENT (M_o)

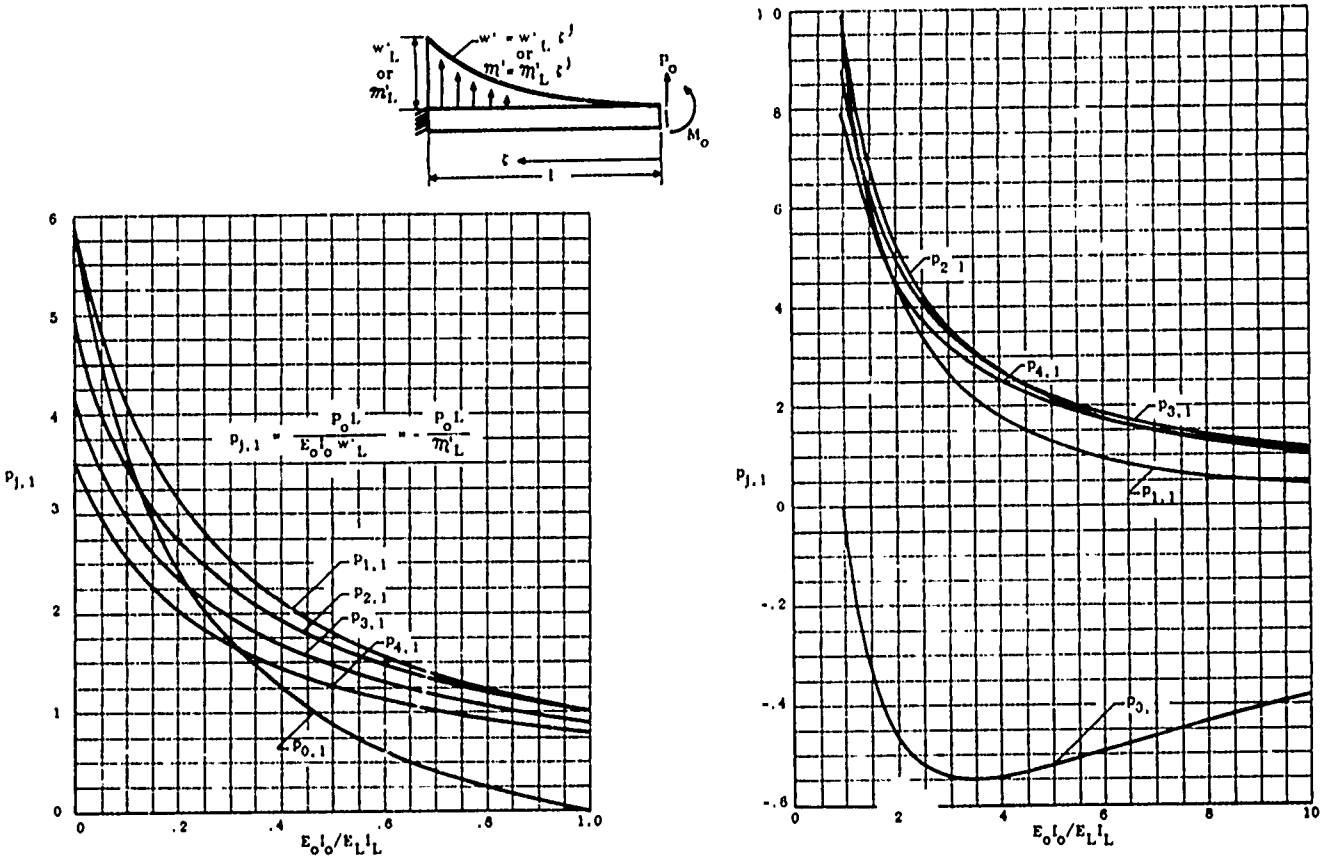


FIGURE 4.2.2.3-3 FIXED END REACTIONS FOR LINEAR $\frac{1}{EI}$; TRANSVERSE END LOAD (P_o), (c=1, ν =1)

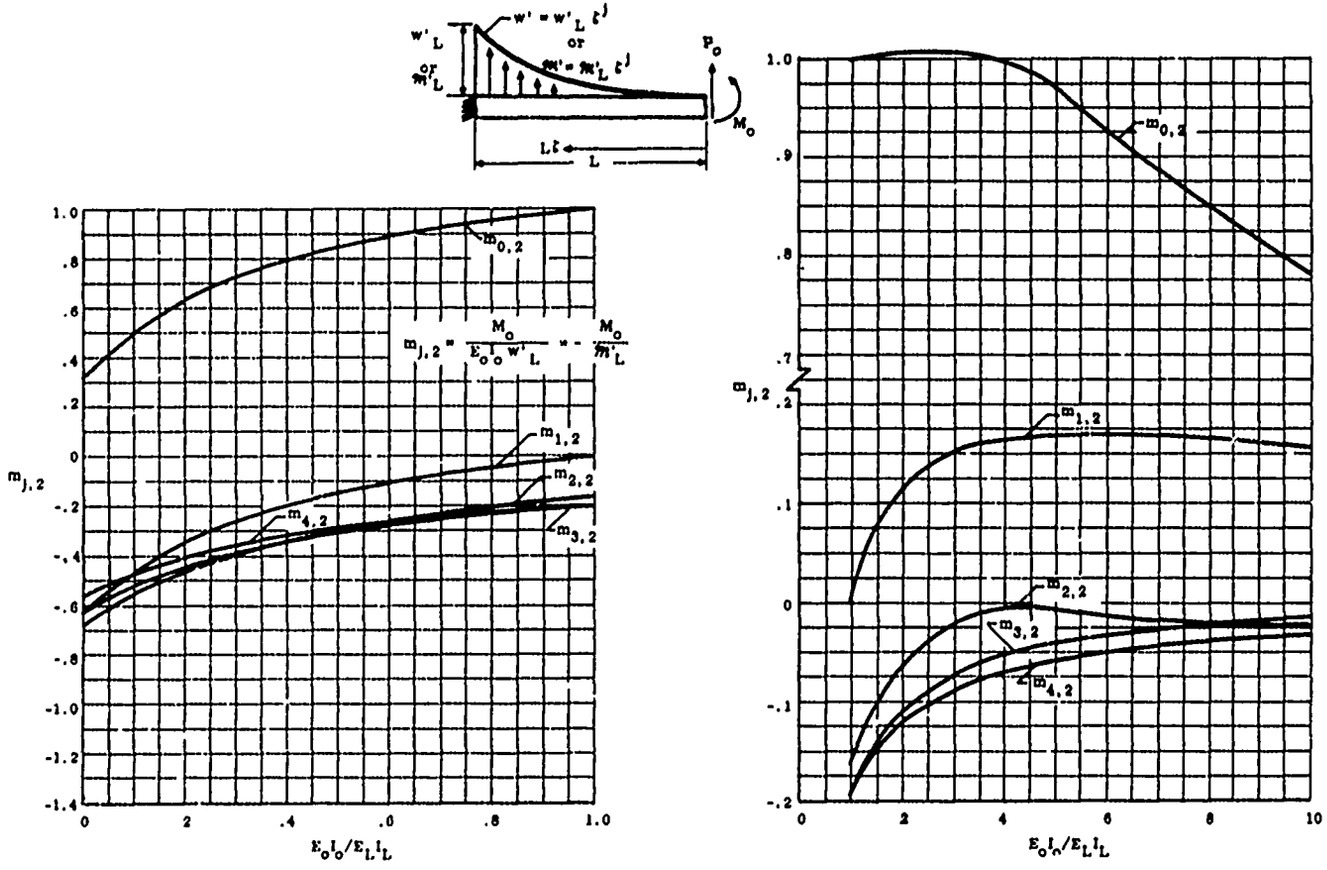


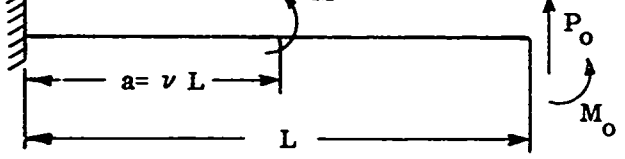
FIGURE 4.2.2.3-6 FIXED END REACTION FOR PARABOLIC $\frac{1}{EI}$; END MOMENT (M_o), (c=2, ν=1)

4.2.2.4 Determination of Fixed End Reaction For Special Cases

CASE A: Constant EI (c=0, e=0, $\therefore$ D=1/12)

The beam of constant bending stiffness (EI) simplifies the general solution by making the term $\sum_{0}^{c}$ in Eqs. (1a), (2a) and (3a) of Paragraph 4.2.2.3 identically zero. Solutions for P_o and M_o are obtained by elemental types of loads and the solutions are the curves plotted in Figures 4.2.2.3-1 and -2. The values of P_L and M_L are obtained from the equilibrium Eqs. (1b), (2b) and (3b) of Paragraph 4.2.2.2.

(1) Pure Moment M (j=0)



From Eq. (2a) of Paragraph 4.2.2.2 and (1b) of Paragraph 4.2.2.3

$$\mathcal{M}_L = M$$

$$p_{o,o} = \frac{-P_o L}{\mathcal{M}_L} = \frac{\nu}{(0+1)(1/12)} \left[\frac{1}{2} + 0 + \frac{\nu}{2} \left(\frac{1}{2} + 0 \right) \right]$$

$$p_{o,o} = 6\nu(1-\nu) \quad \text{(Plotted in Figure 4.2.2.3-1)} \qquad \text{(1a)}$$

$$P_o = \frac{-\mathcal{M}_L}{L} p_{o,o} = \frac{-M}{L} 6\nu(1-\nu).$$

From Eq. (2b) of Paragraph 4.2.2.3,

$$M_{o,o} = \frac{-M_o}{\mathcal{M}_L} = \frac{\nu}{(0+1)(1/12)} \left[-\frac{1}{6} - 0 + \frac{\nu}{2} \left(\frac{1}{2} + 0 \right) \right]$$

$$M_{o,o} = \nu(3\nu - 2) \quad \text{(Plotted in Figure 4.2.2.3-2)} \qquad \text{(1b)}$$

$$M_o = -M\nu(3\nu - 2).$$

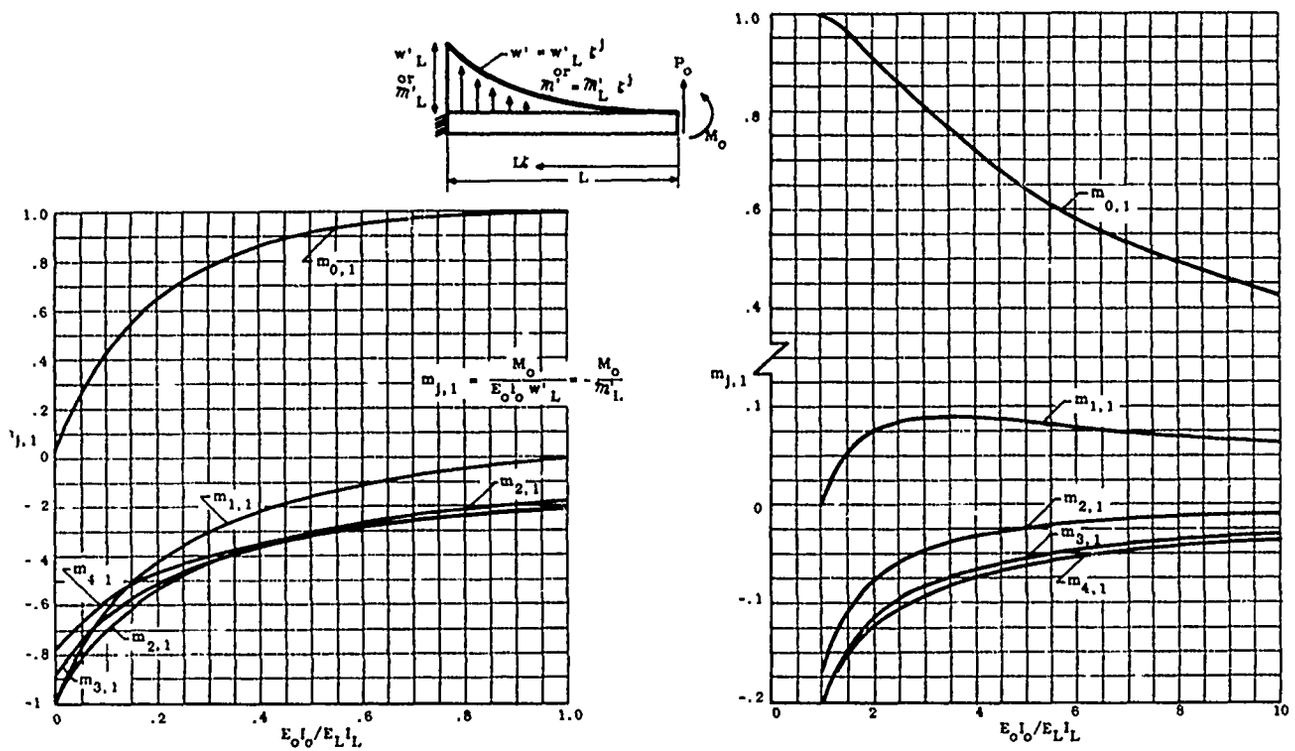
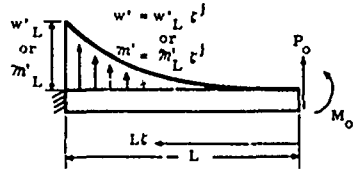
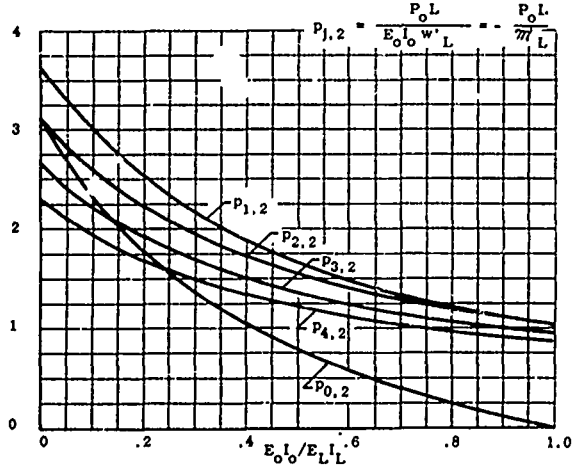


FIGURE 4.2.2.3-4 FIXED END REACTIONS FOR LINEAR $\frac{1}{EI}$; End Moment (M_o), (c=1, ν=1)





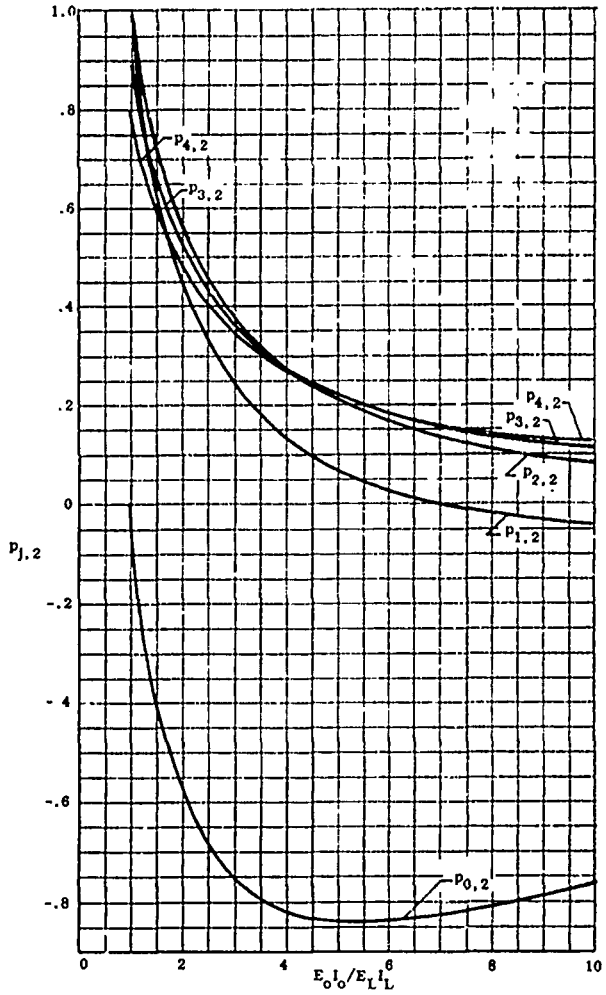
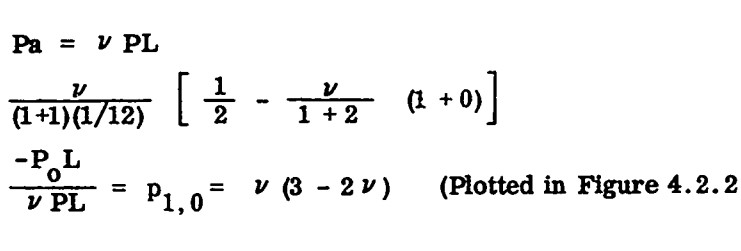


FIGURE 4 2 2.3-5 FIXED END REACTION FOR PARABOLIC $\frac{1}{EI}$; TRANSVERSE END LOAD (P_o), (c=2, ν =1)

4.2.2.4 (Cont'd)

(2) Concentrated Transverse Load P, (j=1)



Employing the same equations as (1) above gives

$$\mathcal{M}_L = Pa = \nu PL$$

$$p_{1,0} = \frac{\nu}{(1+1)(1/12)} \left[\frac{1}{2} - \frac{\nu}{1+2} (1+0) \right]$$

$$\frac{-P_o L}{\mathcal{M}_L} = \frac{-P_o L}{\nu PL} = p_{1,0} = \nu (3 - 2\nu) \quad \text{(Plotted in Figure 4.2.2.3-1)} \qquad (2a)$$

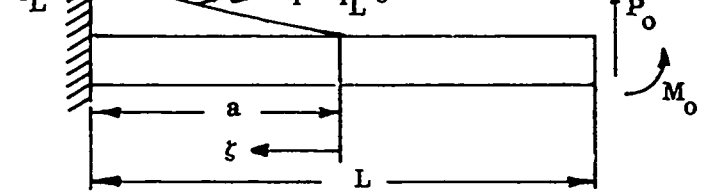
$$\boxed{\frac{P_o}{P} = -\nu^2 (3 - 2\nu)} \qquad (2b)$$

$$\frac{-M_o}{\mathcal{M}_L} = m_{1,0} = \frac{\nu}{2(1/12)} \left[-\frac{1}{6} + \frac{\nu}{3} \left(\frac{1}{2} + 0 \right) \right]$$

$$\frac{-M_o}{\nu PL} = m_{1,0} = -\nu (1 - \nu) \quad \text{(Plotted in Figure 4.2.2.3-2)} \qquad (2c)$$

$$\boxed{\frac{M_o}{PL} = \nu^2 (1 - \nu)} \qquad (2d)$$

(3) Distributed Transverse Load $q = q_L \zeta^r$ (j=r+2)



Employing the same equations gives

$$\mathcal{M}_L = \frac{\nu^2 L^2 q_L}{(r+1)(r+2)}$$

$$p_{r+2,0} = \frac{-P_o L}{\mathcal{M}_L} = \frac{\nu}{r+3} \left[6 - \frac{12\nu}{r+4} \right] \quad \text{(Plotted in Figure 4.2.2.3-1)} \qquad (3a)$$

4.2.2.4 (Cont'd)

$$\boxed{\frac{P_o}{q_L L} = -\frac{\nu^3}{(r+1)(r+2)(r+3)}\left[6 - \frac{12\nu}{r+4}\right]} \tag{3b}$$

$$m_{r+2,0} = -\frac{M_o}{m_L} = \frac{\nu}{r+3}\left[-2 + \frac{6\nu}{r+4}\right] \quad \text{(Plotted in Figure 4.2.2.3-2)} \tag{3c}$$

$$\boxed{\frac{M_o}{q_L L^2} = -\frac{\nu^3}{(r+1)(r+2)(r+3)}\left[-2 + \frac{6\nu}{r+4}\right]} \tag{3d}$$

If r = 0 (uniform load),

$$\frac{P_o}{q_L L} = -\nu^3\left(1 - \frac{\nu}{2}\right) \tag{3e}$$

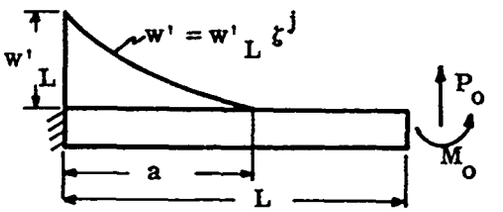
$$\frac{M_o}{q_L L^2} = \nu^3\left(\frac{1}{3} - \frac{\nu}{4}\right) \tag{3f}$$

If r = 1 (linearly varying load),

$$\frac{P_o}{q_L L} = -\nu^3\left(\frac{1}{4} - \frac{\nu}{10}\right) \tag{3g}$$

$$\frac{M_o}{q_L L^2} = \nu^3\left(\frac{1}{12} - \frac{\nu}{20}\right) \tag{3h}$$

(4) <u>Thermal Loading $w' = w'_L \zeta^j$</u>



From Eqs. (1a) and (1b) of Paragraph 4.2.2.3,

$$p_{j,o} = \frac{P_o L}{E_o I_o w'_L} = \frac{\nu}{j+1}\left[6 - \frac{12\nu}{j+2}\right] \tag{4a}$$

$$\boxed{P_o = \left(\frac{E_o I_o w'_L}{L}\right)\frac{\nu}{j+1}\left[6 - \frac{12\nu}{j+2}\right]} \tag{4b}$$

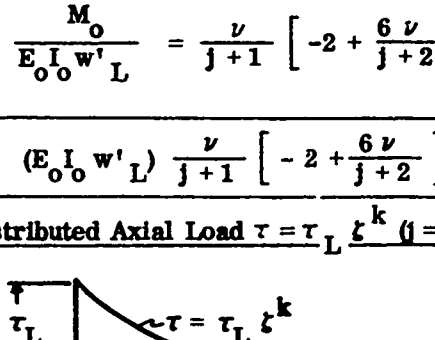
4.2.2.4 (Cont'd)

From Eqs. (2a) and (2b) of Paragraph 4.2.2.3,

$$m_{j,o} = \frac{M_o}{E_o I_o w'_L} = \frac{\nu}{j+1}\left[-2 + \frac{6\nu}{j+2}\right] \tag{4c}$$

$$\boxed{M_o = (E_o I_o w'_L)\,\frac{\nu}{j+1}\left[-2 + \frac{6\nu}{j+2}\right]} \tag{4d}$$

(5) Distributed Axial Load $\tau = \tau_L \zeta^k$ $(j = k+1)$



From Eqs. (2a) and (3a) of Paragraph 4.2.2.2 and (1b), (2b) and (3b) of Paragraph 4.2.2.3,

$$\mathcal{M}_L = \frac{-a\tau_L y}{k+1} = \frac{-\nu L \tau_L y}{k+1}$$

$$\mathcal{F}_L = \frac{a\tau_L}{k+1} = \frac{\nu L \tau_L}{k+1}$$

$$p_{k+1,0} = \frac{P_o L}{(-\nu L y \tau_L)/k+1} = \left(\frac{12\nu}{k+2}\right)\left(\frac{1}{2} - \frac{\nu}{k+3}\right)$$

$$\boxed{\frac{P_o}{y\tau_L} = \frac{12\nu^2}{(k+1)(k+2)}\left[\frac{1}{2} - \frac{\nu}{k+3}\right]} \tag{5a}$$

$$m_{k+1,0} = \frac{M_o}{(-\nu y \tau_L L)/k+1} = \left(\frac{12\nu}{k+2}\right)\left(-\frac{1}{6} + \frac{\nu}{2(k+3)}\right)$$

$$\boxed{\frac{M_o}{y\tau_L L} = \frac{6\nu^2}{(k+1)(k+2)}\left[-\frac{1}{3} + \frac{\nu}{k+3}\right]} \tag{5b}$$

$$f_{k+1,0} = \frac{F_o (k+1)}{\nu L \tau_L} = \frac{\nu}{k+2}$$

$$\boxed{\frac{F_o}{\tau_L L} = \frac{\nu^2}{(k+1)(k+2)}} \tag{5c}$$

4.2.2.4 (Cont'd)

Equations (1) through (5) define the fixed end moments for all types of mechanical and thermal loads on a beam of constant cross section. The solution can be obtained by direct solution in the equations or from the graphical solutions presented in Figures 4.2.2.3-1 and -2 for unit solutions which must be multiplied by $-\mathcal{M}_L$, $-\mathcal{P}_L$ and $-\mathcal{F}_L$ to obtain M_c, P_o and F_o.

CASE B: Variable EI ($c \neq 0$) and Load Distributed Over Complete Span ($\nu = 1$)

Another condition of structural interest and simplicity is a beam of variable EI where the loads are continuously distributed over the entire span ($\nu = 1$).

From substitution of $\nu = 1$ in Eqs. (1), (2) and (3) of Paragraph 4.2.2.3 the general solution becomes:

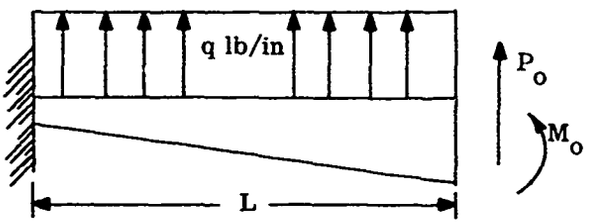
$$P_o L = E_o I_o w'_L p_{j,c} + \frac{L y \tau_L}{k+1}\left(p_{k+1,c} + ep_{k+1+c,\,c}\right) - \frac{L^2 q_L}{(r+1)(r+2)}\left(p_{r+2,c} + ep_{r+2+c,c}\right) \quad (6a)$$

$$M_o = E_o I_o w'_L m_{j,c} + \frac{L y \tau_L}{k+1}\left(m_{k+1,c} + em_{k+1+c,c}\right) - \frac{L^2 q_L}{(r+1)(r+2)}\left(m_{r+2,c} + em_{r+2+c,c}\right) \quad (6b)$$

$$F_o = E_o A_o \bar{\epsilon}'_L f_{j,c'} + \frac{L \bar{\tau}_L}{k+1}\left(f_{k+1,c'} + e' f_{k+1+c',c'}\right) \quad (6c)$$

where the values of $p_{j,c}$ and $m_{j,c}$ are given in Figures 4.2.2.3-3 through -6. Terms such as F, M and P are ignored since they are reacted directly at the support. (Note that recourse must be taken to Eqs. (1), (2) and (3) of Paragraph 4.2.2.3 if $c \neq 0$ or $\nu \neq 1$).

Example: The equations are illustrated for a uniform load on a beam of linear $\frac{1}{EI}$ and $\frac{F_o I_o}{E_L E_L} = 10$.



From the data,

$$c = 1,\ \frac{E_o I_o}{E_L E_L} = 10,\ r = 0,\ q_L = q$$

and from Figures 4.2.2.3-3 and -4,

$$p_{r+2,c} = p_{2,1} = .110 \qquad p_{r+2+c,c} = p_{3,1} = .115$$

$$m_{r+2,c} = m_{2,1} = -.010 \qquad m_{r+2+c,c} = m_{3,1} = -.028$$

Substituting in Eqs. (6a) and (6b) results in

4.2.2.4 (Cont'd)

$$P_o L = -\frac{L^2 q\,[.110 + 9\,(.115)]}{(0+1)(0+2)}$$

$$\therefore\ P_o = -.573\ q\ L$$

and

$$M_o = -\frac{L^2 q\,[-.010 - 9\,(.028)]}{(0+1)(0+2)} = .131\ q\ L^2$$

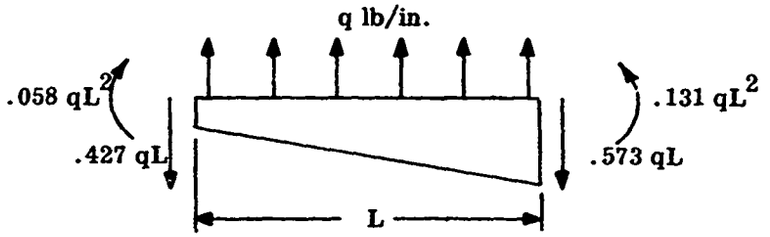
Substituting in Eqs. (1b) and (2b) of Paragraph 4.2.2.2,

$$-P_L = -.573\ q\ L + \frac{L\,q}{0+1}$$

$$P_L = -.427\ q\ L$$

$$M_L = .131\ q\ L^2 + (-.573\ qL)L + \frac{L^2 q}{(0+1)(0+2)} = .058\ q\ L^2$$

The above solution to the problem is illustrated by the following sketch:

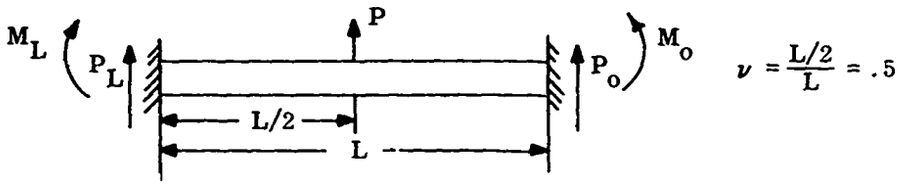


Note how the fixed end reactions increase on the stiffer end.

4.2.2.5 Use of Equations and Graphs

The technique of using the equations or graphs of the previous paragraph is illustrated in a few simple problems which are purposely made simple to compare with known solutions and to show the effect of variable stiffness.

PROBLEM A: Concentrated Load at Center of Span L



$$\nu = \frac{L/2}{L} = .5$$

(1) Constant EI c = e = o (Note: Eq. (2b) and (2d) of Paragraph 4.2.2.4 could be applied directly)

Using the graphical solutions,

$$-\frac{P_o L}{\mathcal{M}_L} = \frac{P_o L}{P\nu L} = p_{1,0} = 1.0 \qquad \text{(Figure 4.2.2.3-1, j = 1)}$$

4.2.2.5 (Cont'd)

$$P_o = -p_{1,0}\left(\frac{\mathcal{M}_L}{L}\right) = -1.0\left(\frac{.5\,PL}{L}\right)$$

$$P_o = -.5\,P$$

From Eq. (1b) of Paragraph 4.2.2.2,

$$P_L = -(P_o + P) = -(-.5P + P) = -.5\,P$$

$$\frac{-M_o}{\mathcal{M}_L} = \frac{-M_o}{P\,\nu\,L} = m_{1,0} = -.25 \qquad \text{(Figure 4.2.2.3-2, j = 1)}$$

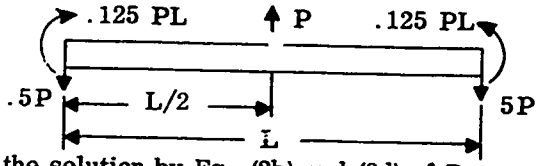
$$M_o = -m_{1,0}\,M_L = .25\,(.5PL)$$

$$M_o = .125\,PL$$

From Eq. (2b) of Paragraph 4.2.2.2,

$$M_L = M_o + P_o L + \mathcal{M}_L = PL\,(.125 - .5 + .5) = .125\,PL$$

The solution (using sign convention) follows:



Checking the solution by Eq. (2b) and (2d) of Paragraph 4.2.2.4,

$$\frac{P_o}{P} = -(.5)^2\left[3-2(.5)\right] = -.5$$

$$\frac{M_o}{PL} = (.5)^2\,(1 - .5) = .125$$

(2) Linear EI and $E_o I_o / E_L I_L = 10$, $(c = 1,\ e = 9,\ \nu = .5)$

From Eq. (4) of Paragraph 4.2.2.3,

$$\frac{1}{D} = \frac{12}{1 + e + \left(e^2/6\right)} = \frac{12}{23.5}$$

From Eq. (1a) of Paragraph 4.2.2.3 for Transverse Load P_o,

$$P_o I_{\cdot} = -\nu\,LP\left\{p_{1,c} + e \sum_{n=o}^{c}\left[\left(cC_n\right)\nu^n\,(1-\nu)^{c-n}\,p_{1+n,c}\right]\right\}$$

$$P_o L = -\nu\,LP\left\{p_{1,1} + e\left[(1-\nu)\,p_{1,1} + \nu\,p_{2,1}\right]\right\}$$

$$P_o L = -\nu\,LP\left\{p_{1,1}\left[1 + e\,(1-\nu)\right] + p_{2,1}\,\nu\,e\right\}$$

4.2.2.5 (Cont'd)

The influence parameters $p_{1,1}$ and $p_{2,1}$ are obtained from Eq. (1b) of Paragraph 4.2.2.3.

$$p_{1,1} = \left(\frac{12}{23.5}\right)\left(\frac{.5}{1+1}\right)\left\{\frac{1}{2} + \frac{9}{6} - \frac{.5}{1+2}\left[1+.5\,(9)\right]\right\} = .1383$$

$$p_{2,1} = \left(\frac{12}{23.5}\right)\left(\frac{.5}{2+1}\right)\left\{\frac{1}{2} + \frac{9}{6} - \frac{.5}{2+2}\left[1+.5\,(9)\right]\right\} = .1115$$

$$P_o = -.5P\left[5.5\,(.1383) + 4.5\,(.1115)\right] = -.631P$$

$$P_L = -(P_o + P_L) = P(.6312 - 1.00) = -.369P$$

Similarly, from Eqs. (2a) and (2b) of Paragraph 4.2.2.3 for Moment M_o:

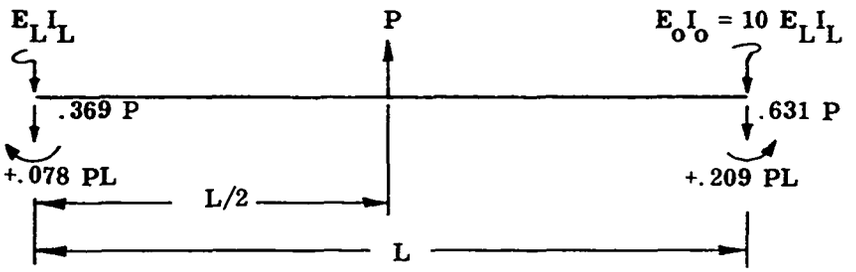
$$m_{1,1} = \left(\frac{12}{23.5}\right)\left(\frac{.5}{2}\right)\left[-\frac{1}{6} - \frac{9}{12} + \frac{3.5}{6}\right] = -.0426$$

$$m_{2,1} = \left(\frac{12}{23.5}\right)\left(\frac{.5}{3}\right)\left[-\frac{1}{6} - \frac{9}{12} + \frac{3.5}{8}\right] = -.0408$$

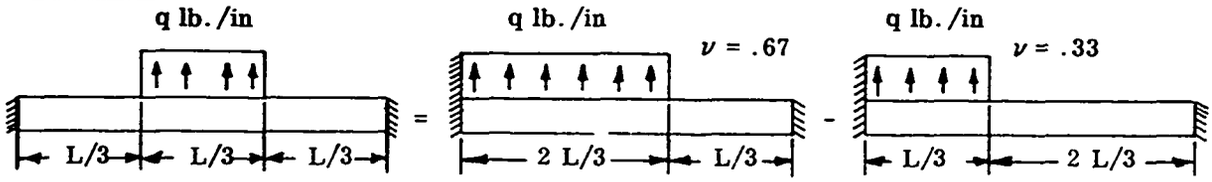
$$M_o = -\nu LP\left\{m_{1,1}\left[1+e\,(1-\nu)\right] + m_{2,1}\,\nu e\right\}$$

$$M_o = -.5LP\left[5.5\,(-.0426) + 4.5\,(-.0408)\right] = .209PL$$

$$M_L = M_o + P_oL + \mathcal{M}_L = PL\left[.209 + (-.6312) + .5\right] = .078PL$$



PROBLEM B: Uniform Load in Center Third of Span and Constant EI



From Eqs. (3e) and (3f) of Paragraph 4.2.2.2 (r=0),

$$\frac{P_o}{q_L L} = \frac{-(.67)^3\left[6 - \frac{12(.67)}{4}\right]}{(1)(2)(3)} - \frac{-(.33)^3}{6}\left[6 - \frac{12(.33)}{4}\right]$$

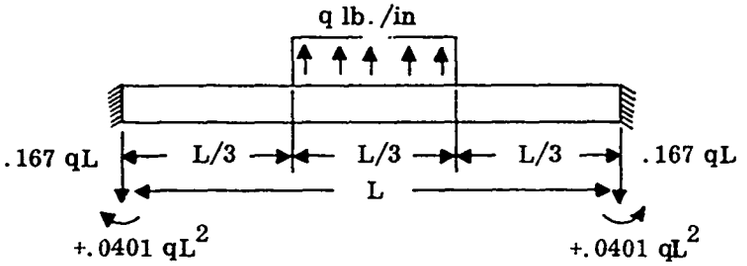
$$\frac{P_o}{q_L L} = \frac{-\frac{8}{27}(4)}{6} - \frac{\frac{-1}{27}(5)}{6} = \frac{\frac{-32+5}{27}}{6} = -1/6$$

4.2.2.5 (Cont'd)

$$\frac{P_L}{q_L L} = -\left(-\frac{1}{6} + \frac{1}{3}\right) = -1/6$$

$$\frac{M_o}{q_L L^2} = \frac{-\frac{8}{27}(-2+1)}{6} - \frac{-\frac{1}{27}(-2+1/2)}{6} = \frac{8-3/2}{(27)(6)} = \frac{13}{12(27)} = .0401$$

$$\frac{M_L}{q_L L^2} = .0401 - .1667 + .1667 = .0401$$



Using Figures 4.2.2.3-1 and -2,

$\nu = .67$, $p_{20} = .89$, $m_{20} = -.225$

$\nu = .33$, $p_{20} = .56$, $m_{20} = -.167$

$$P_o L = \frac{-(.67\,L)^2 q}{2}(.89) - \frac{(.33\,L)^2 q}{2}(.56) = -.167\,q\,L^2$$

$$M_o = \frac{-(.67\,L)^2 q}{2}(1.225) - \frac{(.33)^2}{2}(-.167) = .0407\,q\,L^2$$

} Graphical solution checks analytical equations.

PROBLEM C: Thermal Loading ($\nu = 1$)

A description of the thermal deformation is approximated by a power series.

$$w' = w_{Lo} + w_{L1}\left(\frac{x}{L}\right)^1 + w_{L2}\left(\frac{x}{L}\right)^2 \cdots w_{Lj}\left(\frac{x}{L}\right)^j = \sum_{j=1}^{n} w_{Lj}\left(\frac{x}{L}\right)^j$$

$$\epsilon' = \epsilon_{Lo} + \epsilon_{L1}\left(\frac{x}{L}\right)^1 \cdots + \epsilon_{Lj}\left(\frac{x}{L}\right)^j = \sum_{j=1}^{n} \epsilon_{Lj}\left(\frac{x}{L}\right)^j$$

where x is the distance from the O end.

(1) Constant EI and EA

From Eq. (4b) of Paragraph 4.2.2.4, and $\nu = 1$,

4.2.2.5 (Cont'd)

$$P_o = \frac{E_o I_o}{L}\left[\frac{w_{Lo}}{0+1}\left(6-\frac{12}{0+2}\right) + \frac{w_{L1}}{1+1}\left(6-\frac{12}{1+2}\right) + \frac{w_{Lj}}{j+1}\left(6-\frac{12}{j+2}\right)\right]$$

$$-P_L = P_o = \frac{E_o I_o}{L}\left[w_{L1} + w_{L2} \cdots \frac{w_{Lj}}{j+1}\left(6-\frac{12}{j+2}\right)\right] = 6\,\frac{E_o I_o}{L}\sum\frac{j w_{Lj}}{(j+1)(j+2)} \qquad (7)$$

From Eq. (4d) of Paragraph 4.2.2.4 and $\nu = 1$,

$$M_o = E_o I_o\left[\frac{w_{Lo}}{0+1}\left(-2+\frac{6}{0+2}\right) + \frac{w_{L1}}{1+1}\left(-2+\frac{6}{1+2}\right) + \cdots \frac{w_{Lj}}{j+1}\left(-2+\frac{6}{j+2}\right)\right]$$

$$M_o = E_o I_o\left[w_{Lo} - \frac{1}{6}\,w_{L2} + \cdots + \frac{w_{Lj}}{j+1}\left(-2+\frac{6}{j+2}\right)\right.$$

$$M_o = 2\,E_o I_o \sum\frac{(1-j)\,w_{Lj}}{(j+1)(j+2)} \qquad (8)$$

From Eq. (2b) of Paragraph 4.2.2.2,

$$M_L = M_o + P_o L$$

$$M_L = E_o I_o\left[w_{Lo} + w_{L1} + \frac{5}{6}\,w_{L2} \cdots + \frac{w_{Lj}}{j+1}\left(4-\frac{6}{j+2}\right)\right] = 2\,E_o I_o \sum\frac{(2j+1)w_{Lj}}{(j+1)(j+2)} \qquad (9)$$

From Eqs. (3a) and (3b) of Paragraph 4.2.2.3 and $\nu = 1$,

$$F_L = F_o = -E_o A_o\left(\epsilon_{Lo} + \frac{\epsilon_{L1}}{2} \cdots + \frac{\epsilon_{Lj}}{j+1}\right) = -E_o A_o \sum\frac{\epsilon_{Lj}}{j+1} \qquad (10)$$

(2) Variable (Linear) EI and EA $\left(c=1;\ \frac{E_o I_o}{E_L I_L} = 10;\ e = 9\right)$

From Eqs. (6a) and (6b) of Paragraph 4.2.2.4,

$$-P_L = P_o = \frac{E_o I_o}{L}\left(w_{Lo}\,p_{o,1} + w_{L1}\,p_{1,1} + w_{L2}\,p_{2,1} + \cdots\right)$$

$$M_L = M_o = E_o I_o\left(w_{Lo}\,m_{0,1} + w_{L1}\,m_{1,1} + w_{L2}\,m_{2,2} + \cdots\right)$$

$p_{j,1}$ and $m_{j,1}$ are obtained from Figures 4.2.2.3-3 and -4.

$$\therefore\ -P_L = P_o = \frac{E_o I_o}{L}\left[w_{Lo}\ (-.41) + w_{L1}\ (.05) + w_{L2}\ (.115) + \cdots\right]$$

$$M_L = M_o = E_o I_o\left[w_{Lo}\ (+.46) + w_{L1}\ (+.067) + w_{L2}\ (.007) + \cdots\right]$$

If $c'=1$ and $\frac{E_o A_o}{E_L A_L} = 10$ and $e'=9$, then from Eqs. (3b) of Paragraph 4.2.2.3 and (6c) of Paragraph 4.2.2.4,

4.2.2.5 (Cont'd)

$$F_L = F_o = E_o A_o \quad \bar{\epsilon}_L \, f_{j,c'} = E_o A_o \; \Sigma \; \epsilon_{Lj} \, f_{j,c'}$$

$$= E_o A_o \; \Sigma \; \epsilon_{Lj} \left(\frac{-1}{(j+1)\left(1 + \frac{9}{1+1}\right)} \right) = \frac{-2}{11} \; E_o A_o \; \Sigma \; \frac{\epsilon_{Lj}}{j+1} \quad .$$

4.2.3 General Solution of Statically Indeterminate Beams

The solution of a structural problem requires the simultaneous solution of the equations of compatibility and equilibrium. For linear stable structures it is possible to arrive at the final solution by a series of intermediate steps, cuts, (releases) and restraints, each of which is an artifice to simplify the solution and whose total effect is zero. This is analogous to the addition of a chemical catalyst which aids in the chemical combination of various elements but does not enter into the final form of the chemical solution. Compatibility and equilibrium are maintained (for each degree of freedom) at each intermediate step in the solution so that the final solution simultaneously satisfies equilibrium and compatibility but removes any cuts or restraints that do not exist on the actual structure.

The statically indeterminate problem is simplified with the introduction of generalized coordinates (degrees of freedom). The relationships between these coordinates, and the corresponding loads are sufficient to determine the stresses, and deformations in the structure. The relationships are either the equilibrium and flexibility matrices or the stiffness matrix (which incorporates equilibrium in its derivation). The loads are the negative of the fixed end reactions determined in Paragraph 4.2.2. The solution is accomplished by solving the linear simultaneous equations obtained from the above relationships.

4.2.3.1 Degrees of Freedom

The solution to a stable structural problem is complete when all the loads and displacements (stresses and strains) at each point of the structure are known to an acceptable degree of accuracy. A beam-like structure can be visualized as a network of small beams between points of structural interest, i.e., joints, sudden changes in geometry, changes in direction, etc. The linear solution is also considered complete if the loads and deformations of all such points are known. The relative deformation between the ends of the small beams, together with the loads acting on these beams, could then be employed to determine the internal loads (stresses) acting on the beams. Thus the solution of a structure resolves itself into the determination of loads and deformations at the ends of the elemental beams (all the degrees of freedom).

The possible deformations and loads which each end (point) of the elemental beams could undergo are defined as degrees of freedom of the structure and are the "generalized coordinates" of the structural problem. In a generalized spatial problem of three dimensions there are a maximum of six possible degrees of freedom for a point. These are the displacements in the directions of the three orthogonal axes and the rotations about these axes. In a planar problem of two dimensions there is a maximum of three possible degrees of freedom for a point. These are the displacements in the direction of the two orthogonal axes in the plane of the structure and the rotation about the third axis which is perpendicular to the plane of the structure. In many problems the structure will be such that some of the degrees of freedom can be ignored. In some cases, the loads and deformations coresponding to a degree of freedom are independent of other degrees of freedom (uncoupled) and the structural problem can be solved as separate problems. In any case, all possible degrees of freedom should be investigated and simplified (omitted, uncoupled, etc.) before attempting to continue the solution.

4.2.3.1 (Cont'd)

In a given linear problem of n degrees of freedom, either the applied load or deformation corresponding to each degree of freedom is known, or a known linear relationship exists between the load and displacement. Thus there are essentially n quantities to be determined before the structural problem is solved. The necessary n simultaneous equations are supplied by the equations of equilibrium and/or compatibility at each generalized coordinate.

The solutions will be presented in matrix form to simplify the manipulation and meaning of the equations.

4.2.3.2 Equivalent Loading

In order to minimize the amount of computations necessary to solve the structural problem it is convenient to convert any arbitrary loading on a linear structure to a series of equivalent loadings acting at the points of interest of the structure, which will cause the same deformations as the actual loads and temperatures, at the points of interest. The interrelationship between the generalized displacements and loads can be expressed by a stiffness (K) or flexibility (f) matrix for a given geometry and material prior to applying the loads. There are various methods of obtaining K and f, some of which are demonstrated in Paragraph 2.1.4.2 and 2.1.3 and in References 4-5 and 4-6. The solution would then require obtaining equivalent loads from any arbitrary loading and employing the stiffness and/or flexibility matrix and the requirements of compatibility and equilibrium at each point of interest to obtain n (n degrees of freedom) simultaneous equations for the n unknowns. It is possible to solve the problem for unit loadings. This considerably reduces the work involved in analyzing a structure for more than one set of loads, which can be obtained from linear combinations of the unit loads.

The equivalent loadings at the points of interest are the negatives of the fixed end reactions (see Paragraph 4.2.2). The fixed end reactions are exactly those mechanical loads which, when applied to the elemental beams, will negate the end displacements caused by the applied mechanical and thermal stimulation. Applying the negative of these fixed end reactions to the elemental beams would cause the same deformations as the applied mechanical and thermal loads. If more than one beam has the same degree of freedom (adjacent beams, etc.) then the equivalent mechanical load associated with that degree of freedom would be the negative of the sum of the fixed end reactions of all such beams.

The beam-like structure can be analyzed as follows:

(1) Impose rigid restraints (imaginary jacks) at all the n degrees of freedom of the structure. The jacks are applied at all the joints. This includes the reactions.

(2) Apply the mechanical and thermal loads on the structure and determine the forces in the jacks. These are the fixed end reactions whose solution is shown in Paragraph 4.2.2.

(3) Remove the jacks and applied loads from the structure and apply the equivalent loading (negative of fixed end reactions) to the actual structure.

(4) Employing the flexibility or stiffness method to solve the generalized forces and displacements at the n degrees of freedom.

(5) Employ the forces and displacements at each end of the elemental beams, together with the applied loads and temperatures, to determine the stresses and strains anywhere in the structure.

4.2.4 Mechanics of Solution by the Flexibility Method (Figure 4.2.4-1)

(1) Make sufficient cuts to the indeterminate structure to make it statically determinate. That is, the internal forces acting at any cross section due to an arbitrary mechanical load can be computed from the equations of equilibrium alone.

(2) Every degree of freedom can be characterized by the following subscripts (Figure 4.2.4-1 and Table 4.2.4-1):

(a, b) = subscripts for cases in which the applied ($P_a = - R_a$) is known but the deformation Δ_b is unknown.

(x,y) = subscripts for cases in which the applied load is the unknown cut (redundant = P_x) load but the deformation ($\Delta_y = 0$) is known and equal to zero.

(r, s) = subscripts for cases in which the load is unknown ($P_r = ?$) but the deformation ($\Delta_s = 0$) is known and equal to zero. The s subscripts refer to degrees of freedom which establish the datum of the cut (statically determinate) structure. The datum defines the position in space from which the displacements are measured. The number of subscripts of the cut structures are limited to the number of equilibrium equations of the cut structure (e.g., two subscripts for a straight beam with no axial load, $\Sigma V = \Sigma M = 0$). These coordinates are a sub-group of group (x,y). The selection of this group is arbitrary. However, a wise selection will reduce the computations in determining the flexibility matrix and/or the accuracy and ease of the solution.

(c, d) = subscripts for cases in which the cut load (P_c) is unknown as well as the deformation (Δ_d). There exists, however, a linear relationship between the deformation and loads. The forces of the c type can be visualized as redundants which are on elastic supports rather than on fixed supports such as x type forces. The deformation Δ_d can be computed, once all the loads acting on the structure are know, by the linear relationship which exists between the loads and deformations.

All degrees of freedom described above can exist at a point in a beam, e.g., a rigid transverse support (y or s) with a flexible axial support (d) and with no rotational support (b). Each degree of freedom is associated with two consecutive symbols. One symbol denotes a load and the other symbol denotes a deformation. When a matrix is described by two consecutive subscript symbols it expresses a relationship between degrees of freedom of the same type. When the subscripts are not consecutive the matrix expresses relationships between two different types of degrees of freedom.

(3) The properties of the sub-structure are computed. The equilibrium matrix g_{ij} relates the loads to the reactions. The flexibility matrix f_{ij}, the elements of which express the deflection at i due to a unit load at j, is computed by various method available in the literature, e.g., Paragraph 2.1.1.1 and 2.1.1.2 and References 4-5 and 4-6.

4.2.4 (Cont'd)

(4) The equivalent loads (loads in imaginary jacks) due to mechanical and thermal stimuli are applied at all the degrees of freedom. Each point in a planar structure may have three degrees of freedom and each degree of freedom can be a different type (see (2) above).

(5) Equal and opposite unknown internal loads (P_{x+} - P_{x-} and $P_{c+} = - P_{c-}$) and applied at each side of the cuts. P_x and P_c act on sub-structure and P_{x-} and P_{c-} act on supporting structure (Figure 4.2.4-1). These unknown (redundant) loads are exactly those required to maintain equilibrium and compatibility at each cut.

(6) In essence there are n unknown quantities to find in order to be able to completely solve the problem. They are the b deformations (Δ_b), the x loads (P_x), the r loads (P_r), and the c loads (P_c). Thus $n = b + x + r + c$.

There are r equations of equilibrium, b equations of deformation and x + c equations of compatibility. These are sufficient, in total, to solve for the n unknowns. The following equations are in matrix notation:

"r" Equations of Equilibrium ($\Sigma M = 0$, $\Sigma V = 0$, $\Sigma F = 0$, "r" ≤ 3) for each sub-structure)

$$-P_r = g_{ra} P_a + g_{rc} (P_c + P_{ca}) + g_{rx} (P_x + P_{xa})$$

$$-P_r = (g_{ra} P_a + g_{rc} P_{ca} + g_{rx} P_{xa}) + g_{rc} P_c + g_{rx} P_x \quad (1a)$$

$$-P_r = \bar{g}_{ra} \overline{P}_a + g_{rc} P_c + g_{rx} P_x \quad (1b)$$

"b" Equations of Deformation

$$\Delta_b = f_{ba} P_a + f_{bc} (P_c + P_{ca}) + f_{bx} (P_x + P_{xa})$$

$$\Delta_b = (f_{ba} P_a + f_{bc} P_{ca} + f_{bx} P_{xa}) + f_{bc} P_c + f_{bx} P_x \quad (2a)$$

$$\Delta_b = \bar{f}_{ba} \overline{P}_a + f_{bc} P_c + f_{bx} P_x \quad (2b)$$

"x" Equations of Compatibility of Cut Supports

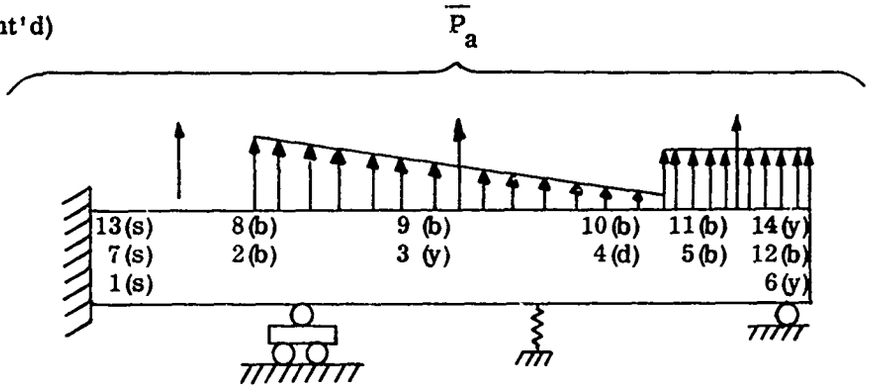
$$0 = \Delta_y = f_{ya} P_a + f_{yc} (P_c + P_{ca}) + f_{yx} (P_x + P_{xa}) \quad (3a)$$

$$0 = \bar{f}_{ya} \overline{P}_a + f_{bc} P_c + f_{bx} P_x \quad (3b)$$

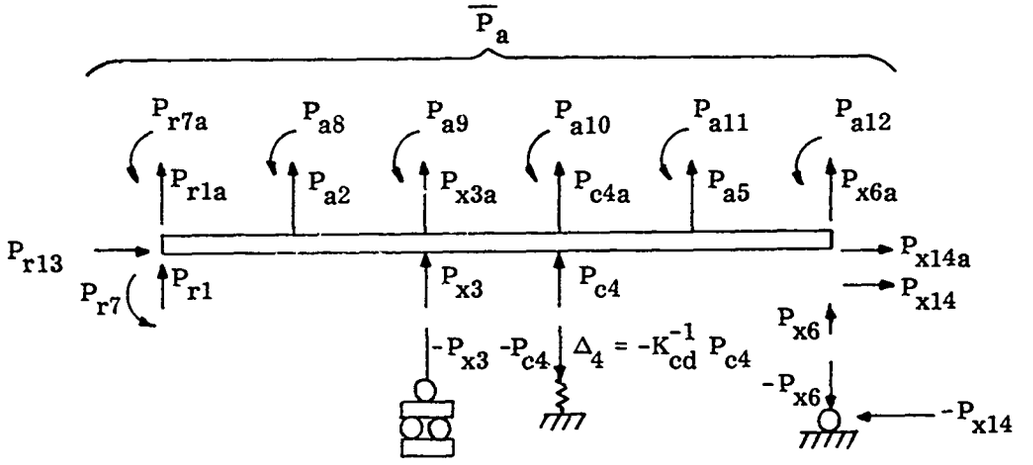
"c" Equations of Compatibility of Cut Flexible Supports

$$\Delta_d = (K_{cd}^{-1}) P_{c-} = (K_{cd}^{-1}) (-P_{c+}) = f_{da} P_a + f_{dc} (P_c + P_{ca}) + f_{dx} (P_x + P_{xa}) \quad (4a)$$

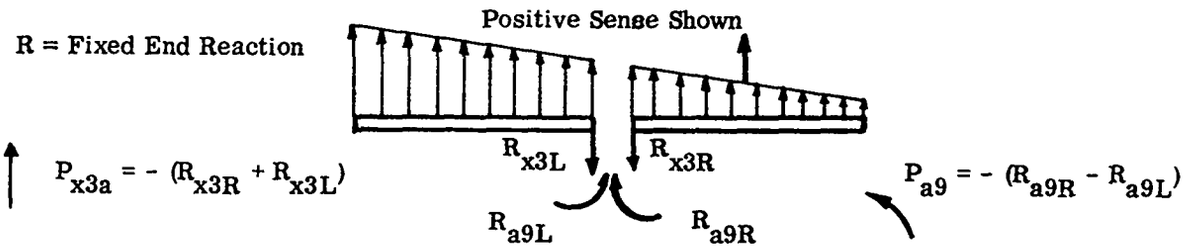
$$-K_{cd}^{-1} P_c = \bar{f}_{da} \overline{P}_a + f_{dc} P_c + f_{dx} P_x \quad (4b)$$



(a) Structure Under Load



(b) Load on Substructures



(c) Addition of Equivalent Load

FIGURE 4.2.4-1 FLEXIBILITY METHOD

TABLE 4.2.4-1 DEGREES OF FREEDOM

Type	Total External Load On the Beam	Deformation	Degrees of Freedom
(a,b)	known	unknown	2,5,8,9,10,11,12
(c,d)	unknown	unknown	4
(x,y)	unknown (compatibility)	known	3,6,14
(r,s)	unknown (equilibrium)	known	1,7,13

4.2.4 (Cont'd)

$$0 = \bar{f}_{da}\,\bar{P}_a + (f_{dc} + K_{cd}^{-1})\,P_c + f_{dx}\,P_x \qquad (4c)$$

where

g_{ij} = geometry of structure employed in equilibrium equations (either 1 or moment arm ratios l_{ij})

f_{ij} = flexibility matrix of statically determinate sub-structure = deflection at i due to unit load at j. (First subscript denotes the row and second denotes the column of matrix. Second subscript of pre-multiplier must be same as first subscript of post-multiplier.)

K_{cd}^{-1} = flexibility of elastic supports of "c-d" coordinates = deflection of d due to a unit load at c (note inversion reverses subscripts)

$\bar{f}_{ja}$ = grouping of flexibility sub-matrices = $(f_{ja} \quad f_{jc} \quad f_{jx})$

$\bar{P}_a$ = grouping of load vectors = which represents the equivalent applied loads. $\begin{Bmatrix} P_a \\ - - - \\ P_{ca} \\ - - - \\ P_{xa} \end{Bmatrix}$

Δ_j = deflection at "j"

P_a = load at "a" (due to applied loads = negative of fixed end reactions)

P_{ia} = equivalent load at coordinate "i" due to applied loads (neg. of fixed end reactions)

P_c, P_x = redundant (cut) loads.

The solution of the simultaneous equation results in unit type solutions in terms of (g_{ij}, f_{ij}, K_{cd}^{-1}) and the applied loads $(\bar{P}_a) = \begin{Bmatrix} P_a \\ - - - \\ P_{ca} \\ - - - \\ P_{xa} \end{Bmatrix}$ (Reference 4-5).

The loads and displacements at each point of interest are as follows:

$$P_c = H_{ca}\,\bar{P}_a \qquad (5a)$$

$$P_x = L_{xa}\,\bar{P}_a \qquad (5b)$$

$$-P_r = Q_{ra}\,\bar{P}_a \qquad (5c)$$

$$\Delta_b = m_{ba}\,\bar{P}_a \qquad (6a)$$

$$\Delta_d = -K_{cd}^{-1}\,H_{ca}\,\bar{P}_a = -K_{cd}^{-1}\,P_c \qquad (6b)$$

4.2.4 (Cont'd)

$$\Delta_y = \Delta_s = 0 \tag{6c}$$

where

$$H_{ca} = -\left\{f_{dc} + K_{cd}^{-1} - \left[f_{dx}\left(f_{yx}^{-1}\right) f_{yc}\right]\right\}^{-1}\left[f_{da} - f_{dx}\left(f_{yx}^{-1}\right) f_{ya}\right] \tag{7}$$

$$L_{xa} = -(f_{yx})^{-1}\left(\bar{f}_{ya} + f_{yc} H_{ca}\right) = \text{influence coefficients of the uncut structure (similiar to influence line)} \tag{8}$$

$$Q_{ra} = \left(\bar{g}_{ra} \mid g_{rc} \mid g_{rx}\right)\begin{Bmatrix} - & I & - \\ & H_{ca} & \\ - & - & - \\ & L_{xa} & \end{Bmatrix} = \text{influence coefficients of the uncut structure} \tag{9}$$

$$m_{ba} = \left(\bar{f}_{ba} \mid f_{bc} \mid f_{bx}\right)\begin{Bmatrix} - & I & - \\ & H_{ca} & \\ - & - & - \\ & L_{xa} & \end{Bmatrix} = \text{flexibility of the uncut structure.} \tag{10}$$

Equation (10) represents the flexibility of the statically indeterminate structure whereas f_{ij} represents the flexibility of the cut structure.

The problem is simplified to a great extent if no flexible supports (c, d degrees of freedom) exist. In that case,

$$P_x = -f_{yx}^{-1}\,\bar{f}_{ya}\,\overline{P_a} \tag{11a}$$

$$P_r = \left(\bar{g}_{ra} \mid g_{rx}\right)\begin{Bmatrix} - & I & - \\ & -f_{yx}^{-1} f_{ya} & \end{Bmatrix}\left\{\overline{P_a}\right\} \tag{11b}$$

$$\Delta_b = \left(\bar{f}_{ba} \mid f_{bx}\right)\begin{Bmatrix} - & I & - \\ & -f_{yx}^{-1} f_{ya} & \end{Bmatrix}\left\{\overline{P_a}\right\} \tag{12a}$$

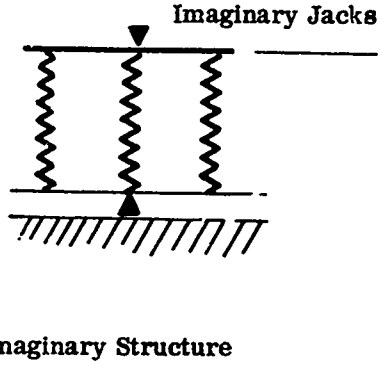
$$\Delta_y = \Delta_s = 0. \tag{12b}$$

4.2.5 Mechanics of Solution by the Stiffness (Slope - Deflection) Method (Figure 4.2.5-1)

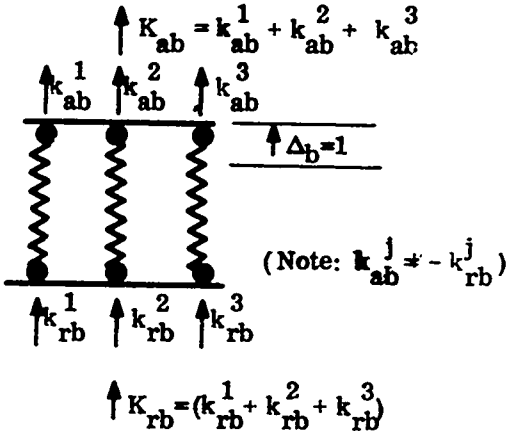
(1) Place imaginary jacks (restraints) at each degree of freedom which fixes all degrees of freedom in space and will not allow them to move no matter what loads are applied.

(2) The stiffness matrix K_{ij} is obtained by forcing one of the imaginary jacks to move a unit deformation while all the others remain fixed in space. The loads imposed on the imaginary jacks are noted as K_{ij} (load at i due to a unit movement at j). Note that element $K_{ij} = 0$ for all points i which are not

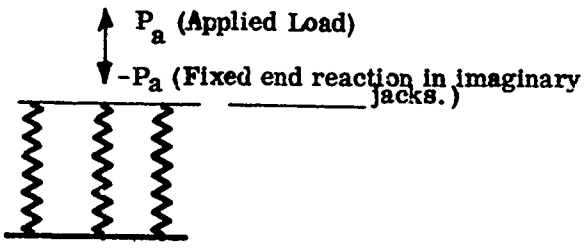
4.2.5 (Cont'd)



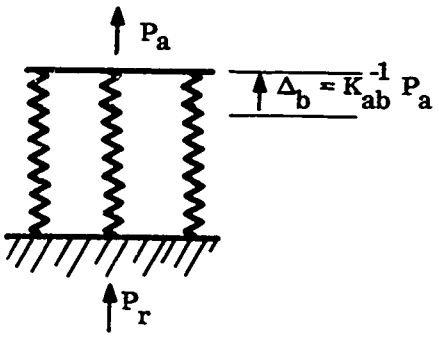
a) Imaginary Structure



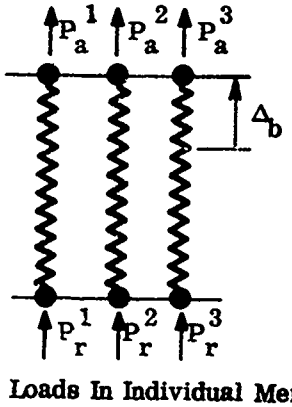
b) Determination of K_{ij}



c) Applied Stimulation To Imaginary Structure



d) Structure With Imaginary Jacks Removed



e) Loads In Individual Members

where $P_a^j = k_{ab}^j \Delta_b = k_{ab}^j K_{ab}^{-1} P_a$

$P_r^j = k_{rb}^j \Delta_b = k_{rb}^j K_{ab}^{-1} P_a$

$P_a^1 = k_{ab}^1 \Delta_b$, $P_r^1 = k_{rb}^1 \Delta_b$

$P_a^2 = k_{ab}^2 \Delta_b$, $P_r^2 = k_{rb}^2 \Delta_b$

$P_a^3 = k_{ab}^3 \Delta_b$, $P_r^3 = k_{rb}^3 \Delta_b$

FIGURE 4.2.5-1 STIFFNESS METHOD

in the immediate vicinity of j since there is relative motion of the jack only at j. It should also be noted that all elemental beams meeting at a common degree of freedom are springs in parallel since they all have the same motion and the $K_{ij} = \Sigma\ k_{ij}^{j}$ where k_{ij}^{j} is a force at i due to a unit deformation at j of elemental beam bounded at j. The values of the elemental k_{ij}^{j}'s are given in Paragraph 2.1.4.

(3) The mechanical and thermal stimuli are now applied to the restrained structure and the equivalent fixed end loads are resisted by the imaginary jacks.

(4) Since the displacements at the degrees of freedom resisted by the imaginary jacks, it is assured that compatibility at each point of interest is satisfied. Equilibrium at each joint is maintained by loads in the imaginary jacks which exactly balance the equivalent applied loads resulting from loads acting on the elemental beams between the joints.

(5) The degrees of freedom can be characterized by the following subscripts:

(a,b) = subscripts for cases in which the deformation is unknown (Δ_b) but the applied loads are known (P_a).

(e,f) = subscripts for cases in which the deformation (Δ_f is unknown but the applied load is zero ($P_e = 0$). This coordinate does not require an imaginary jack except for the determination of K_{ej}.

(r,s) = subscripts for cases in which the deformation is known to be zero ($\Delta_s = 0$, an actual support) but the redundant load (P_r) is unknown. This coordinate does not require an imaginary jack since the structure supplies an actual jack (restraint).

Note that elastic supports (c,d) need not be specified by generalized coordinates but are separated into two components. The elastic member is incorporated into the overall structure and coordinates (c,d) which described where the elastic member supported the sub-structure becomes (a,b); the other end of the elastic member which represented the actual datum becomes (r,s). The (x,y) coordinates are in the general (r,s) group.

(6) Remove all imaginary jacks. The structure will now deform. The load in the imaginary jack produces deformations. The final deformation will be one in which the equivalent applied forces are exactly balanced by the forces produced by the relative deformation of the elemental beams whose common ends all deform the same amount ($K\Delta = P$). The jacks could have been released one at a time and then reapplied; such a procedure would be a trail and error method (e.g., Hardy-Cross Moment Distribution Method).

(7) The requirement of equilibrium at each degree of freedom results in the simultaneous equations

$$k_{ab}\,\Delta_b + K_{af}\,\Delta_f + K_{as}\,\Delta_s - P_a = 0 \qquad (1)$$

4.2.5 (Cont'd)

$$K_{eb}\,\Delta_b + K_{ef}\,\Delta_f + K_{es}\,\Delta_s - P_e = 0 \qquad (2)$$

$$K_{rb}\,\Delta_b + K_{rf}\,\Delta_f + K_{rs}\,\Delta_s - P_r = 0 \qquad (3)$$

The boundary conditions are:

$$P_e = 0 \qquad (4)$$

$$\Delta_s = 0 \qquad (5)$$

whose solution is

$$\Delta_b = +\overline{K}_{ab}^{-1}\,P_a \qquad (6a)$$

$$\Delta_f = -K_{ef}^{-1}\,K_{eb}\,\overline{K}_{ab}^{-1}\,P_a \qquad (6b)$$

$$P_r = \overline{K}_{rb}\,\overline{K}_{ab}^{-1}\,P_a \qquad (7a)$$

$$P_r + P_{ra} = \left(\overline{K}_{rb}\,\overline{K}_{ab}^{-1} \;\vdots\; I\right)\left\{\begin{array}{c} P_a \\ \hdashline P_{ra} \end{array}\right\} = \text{total reaction (including loads directly applied to reactions)} \qquad (7b)$$

where

$$\overline{K}_{ab}^{-1} = \left(K_{ab} - K_{af}\,K_{ef}^{-1}\,K_{eb}\right)^{-1} = \text{flexibility of actual structure} = m_{ba} \text{ of flexibility method,} \qquad (8a)$$

$$\overline{K}_{rb} = \left(K_{rb} - K_{rf}\,K_{ef}^{-1}\,K_{eb}\right) = \text{reactions due to a unit de-deformation at b} \qquad (8b)$$

P_a = equivalent loads acting at points other than the supports

P_{ra} = equivalent loads acting at the supports

k_{ab}^{j} = load in j^{th} member at "a" due to unit displacement at "b"

The end loads on each elemental beam are

$$P_a^j = k_{ab}^j\,\overline{K}_{ab}^{-1}\,P_a \qquad (9a)$$

$$P_r^j = k_{rb}^j\,\overline{K}_{ab}^{-1}\,P_a \qquad (9b)$$

which are combined with the loads and temperatures applied to the beam to obtain the stresses and strains.

4.2.6 Selection of Method of Analysis

The best method to employ cannot be decided arbitrarily but must be evaluated after due consideration is given to the structural problem as regards the computing tools and time available, supplementary structural information (e.g., available solution of sub-

structures larger than the elemental beam), past experience (ease of visualizing problem), etc. Generally, if the structure is primarily a set of elemental beams (e.g., cantilevers) in series, i.e., the number of d + y degrees of freedom is less than the number of b degrees of freedom (d + y < b), then the flexibility method is better*. If however, the structure is primarily a set of elemental beams in parallel (bents, etc.) in which d + y > b, then the stiffness (slope deflection) method is better. When the number of redundant degrees of freedom is relatively small it is usually simpler to visualize the flexibility method. As the number of redundant degrees of freedom increases, however, the selection of the simplest datum becomes more and more complex and the stiffness method which does not require selecting a datum (the datum of the actual structure is employed) becomes less involved. Because of the lack of engineering intuition required in the stiffness method it is more easily adaptable to computing machine techniques. The flexibility method becomes more and more involved as the generalized coordinates (c, d) increase in number, especially when loads can be applied on these elastic supports.

The flexibility and stiffness methods of solving beam-like structures are illustrated below. The problems are treated in great detail to familiarize the analyst with the methods of analysis. The following problems are considered:

PROBLEM IA - Statically indeterminate beam by the flexibility method

PROBLEM IB - Statically indeterminate beam by the stiffness method

PROBLEM II - Sandwich beam by the flexibility method.

4.2.6.1 Problem IA - Statically Indeterminate Beam by the Flexibility Method

The beam shown in Figure 4.2.6.1-1 is loaded with mechanical loads and temperatures as described in Figure 4.2.6.1-2. It is required to determine the redundant loads on the structure. The problem is solved in the following steps:

(1) Determine and classify the degrees of freedom of the beam from the geometry (Figure 4.2.6.1-1).

(2) Establish the static equilibrium equations.

(3) Establish the flexibility matrix by methods described in Section 2 of this Manual.

(4) Invert the flexibility matrix associated with the cut redundant loads and express the cut redundants in terms of the applied loads.

(5) Obtain unit solutions of the redundant loads in terms of the applied loads by combining (2) and (4).

(6) Apply the mechanical loads and temperature and determine the fixed end reaction by employing Paragraph 4.2.2.

(7) Substitute the negative of the fixed end reactions into the relationship established in step (5) to obtain the solution shown in Figure 4.2.6.1-3.

---

* The number of s degrees of freedom is not too significant since the geometry matrix (g_{ij}) need not be inverted.

4.2.6.1 (Cont'd)

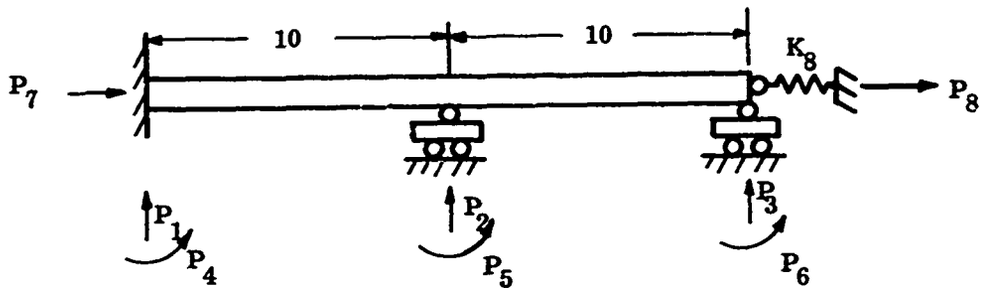


FIGURE 4.2.6.1-1 BEAM WITH DEGREES OF FREEDOM

(1) Classification of Degrees of Freedom

Subscripts	Bending	(Uncoupled Since Beam Is Straight)	Axial
(r, s)	1 ($\Sigma V=0$)	4 ($\Sigma M=0$)	7 ($\Sigma H=0$)
(x, y)	2, 3		---
(a, b)	5, 6		---
(c, d)	---		8

(2) Equilibrium Equations (Ref. Eq. (1b) of Paragraph 4.2.4)

$$-P_r = \bar{g}_{ra}\,\overline{P}_a + g_{rc}\,P_c + g_{rx}\,P_x$$

$$-\begin{Bmatrix} P_1 \\ P_4 \end{Bmatrix} = \begin{bmatrix} 1 & 1 & 1 & 0 & 0 & 0 & 1 & 1 \\ 0 & 10 & 20 & 1 & 1 & 1 & 10 & 20 \end{bmatrix} \begin{bmatrix} P_{1a} \\ P_{2a} \\ P_{3a} \\ P_{4a} \\ P_{5a} \\ P_{6a} \\ P_2 \\ P_3 \end{bmatrix}$$

$\overline{P}_a$

$-P_7 = (1)\,P_8$

(3) Flexibility Matrices (Constant EI and EA)

$$EI\,f_{yx} = \begin{matrix} \\ 2 \\ 3 \end{matrix} \begin{matrix} \begin{matrix} 2 & 3 \end{matrix} \\ \begin{bmatrix} 333 & 833 \\ 833 & 2667 \end{bmatrix} \end{matrix}$$

(Reference 4-6)

$$AE\,f_{88} = 20$$

$$EI\,f_{ya} = \begin{matrix} \\ 2 \\ 3 \end{matrix} \begin{matrix} \begin{matrix} 2 & 3 & 5 & 6 \end{matrix} \\ \begin{bmatrix} 333 & 833 & 50 & 50 \\ 833 & 2667 & 150 & 200 \end{bmatrix} \end{matrix}$$

4.2.6.1 (Cont'd)

(4) Inverse (Stiffness)

$$\frac{1}{EI} f_{yx}^{-1} = \begin{pmatrix} .01373 & -.00429 \\ -.00429 & +.00171 \end{pmatrix} \qquad \frac{1}{AE} f_{88}^{-1} = .05$$

From Eq. (4a) of Paragraph 4.2.2.4, the cut redundant loads can be solved in terms of the applied loads.

$$-P_x = + f_{yx}^{-1} \bar{f}_{ya} \bar{P}_a$$

$$\begin{pmatrix} P_2 \\ P_3 \end{pmatrix} = \begin{pmatrix} 0 & 1 & 0 & 0 & .043 & -.172 \\ 0 & 0 & 1 & 0 & .043 & .129 \end{pmatrix} \begin{pmatrix} P_{1a} \\ P_{2a} \\ P_{3a} \\ P_{4a} \\ P_{5a} \\ P_{6a} \end{pmatrix}$$

$$-\frac{P_8}{K_8} = P_{8a} f_{88} + P_8 f_{88}$$

$$-P_8 = \frac{P_{8a} f_{88}}{f_{88} + 1/K_8}$$

$$-P_8 = \frac{P_{8a}}{1 + AE/K_8 L}$$

$$-P_8 = \frac{\frac{AE}{L}\int_o^L \bar{\epsilon}' dx}{1 + AE/K_8 L}$$

(5) Unit Solutions

$$-P_2 = P_{2a} + .043\, P_{5a} - .171\, P_{6a}$$

$$-P_3 = P_{3a} + .043\, P_{5a} + .129\, P_{6a}$$

$$-P_1 = P_{1a} - .086\, P_{5a} + .043\, P_{6a}$$

$$-P_4 = P_{4a} - .29\, P_{5a} + .14\, P_{6a}$$

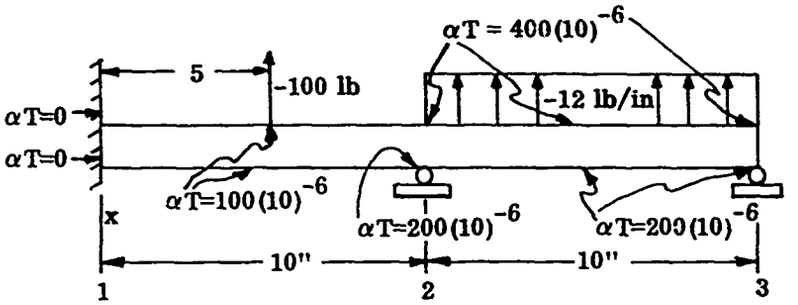
$$\Delta_b = \bar{f}_{ba} \bar{P}_a + f_{bx} P_x$$

$$EI\Delta_5 = 1.40\, P_{5a} - .75\, P_{6a}$$

$$EI\Delta_6 = -.75\, P_{5a} + 2.80\, P_{6a}$$

$$\Delta_8 = \frac{-P_8}{K_8}$$

(6) Applied Loads



$K_8 = 10^6$ lb/in.
$E = 10^7$ lb/in.^{2}
$A = 1$ sq in.
$I = .08$ in.^{4}
$d = 1$ in.
αT Linear Through Depth c.g. at ℄ of Cross Section

FIGURE 4.2.6.1-2 TEMPERATURE AND LOAD ON BEAM

4.2.6.1 (Cont'd)

Thermal Distortion of Cross Section:

$$w' = \frac{\alpha T_{TOP} - \alpha T_{BOT}}{d}$$ (Linear Distribution Through Depth)

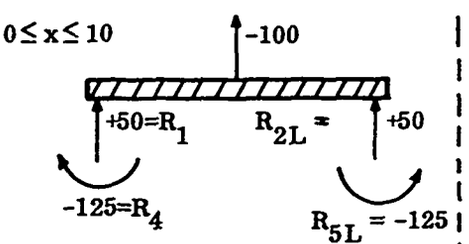
$$\bar{\epsilon}' = \frac{\alpha T_{TOP} + \alpha T_{BOT}}{2}$$ (e.g. at $\mathbb{C}_L$ of Cross Section)

The αT values are given at discrete points of the structure and are assumed to vary continuously. Since there are values at three station (end stations and mid-station), the best parabolic curve passing through these three values is selected. This results in

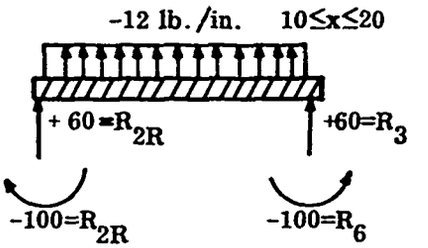
$0 \le x \le 10$	$10^6 w' = 4x^2 - 20x$	$10^6 \bar{\epsilon}' = 2x^2 + 10x$
$10 \le x \le 20$	$10^6 w' = 200$	$10^6 \bar{\epsilon}' = 300$

Fixed End Reactions:

Mechanical Loads (see illustrative problems given in Paragraph 4.2.2.5)

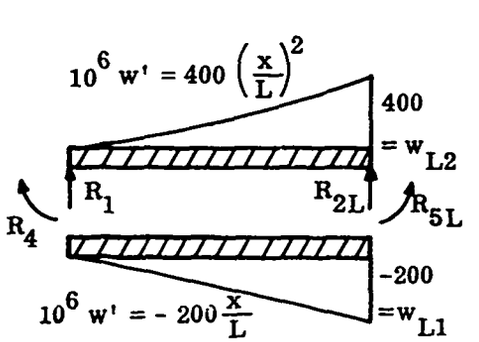


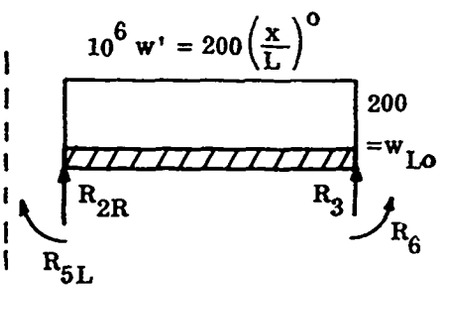
P = - 100, ν = .5



q = - 12, ν = 1.0

Thermal Loads (see Eqs. (7) of Paragraph 4.2.2.5)





$$-P_L = P_o = \frac{E_o I_o}{L}\left[w'_{L1} + w'_{L2} + \cdots \frac{w'_{Lj}}{j+1}\left(6 - \frac{12}{j+2}\right)\right]$$

$$-R_{2L} = R_1 = \frac{10^7(.08)(10)^{-6}}{10}(-200 + 400)$$

$$\frac{(10)^7(.08)(10)^{-6}}{10}(0) = 0 = R_{2R} = -R_3$$

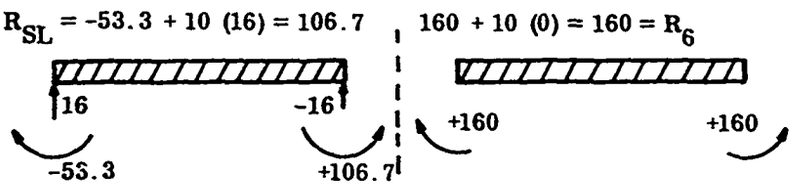
4.2.6.1 (Cont'd)

$$-R_{2L} = R_1 = -16 + 32 = +16$$

$$M_o = E_o I_o \left[w_{L0} - \frac{1}{6} w_{L2} + \cdots \frac{w_{Lj}}{j+1} \left(-2 + \frac{6}{j+2} \right) \right]$$

$$R_4 = (10)^7 (.08)(10)^{-6} \left(0 - \frac{1}{6} 400 \right) = -53.3 \quad | \quad (10)^7 (.08)(10)^{-6} (200) = +160 = R_{5R}$$

$$M_L = M_o + P_o L$$



The total equivalent loads are obtained with the aid of Eqs. (1) and (3) of Paragraph 4.2.2.1

$$R_L = R_{LL} + R_{LR}$$

$$+R_{1a} = 50 + 16 = 66 = -P_{1a}$$

$$+R_{2a} = 50 + 60 - 16 = 94 = -P_{2a}$$

$$+R_{3a} = 60 = -P_{3a}$$

$$M_L = M_{LL} - M_{LR}$$

$$+R_{4a} = \left[0 - (-125) \right] + \left[0 - (-53.5) \right] = 178.2 = -P_{4a}$$

$$+R_{5a} = \left[-125 - (-100) \right] + \left[+106.7 - 160 \right] = -78.3 = -P_{5a}$$

$$+R_{6a} = (-100 - 0) + (160 - 0) = 60 = -P_{6a}$$

(7) <u>The Reaction Loads are Obtained From the Unit Solutions.</u>

$$-P_2 = -94 + .043\ (+78.3) - .172\ (-60) = -80.31 \text{ lb}$$
$$-P_3 = -60 + .043\ (+78.3) + .129\ (-60) = -64.37 \text{ lb}$$
$$-P_1 = -66 - .086\ (+78.3) + .043\ (-60) = -75.31 \text{ lb}$$
$$-P_4 = -178.2 - .29\ (+78.3) + .14\ (-60) = -209.31 \text{ in-lb}$$

4.2.6.1 (Cont'd)

Since the beam is straight, it is easier to determine P_8 by direct solution of the compatibility equation.

$$P_{8a} = \frac{\int_o^L \bar{\epsilon}\, dx}{\int_o^L \frac{1}{AE}\, dx} = \frac{10^{-6}\left[\int_o^{10} (2x^2 + 10x)\, dx + \int_o^{10} 300\, dx'\right]}{\frac{20}{(1)\,10^7}}$$

$$= \frac{1}{2}\left[2\,\frac{(10)^3}{3} + 10\,\frac{(10)^2}{2} + 300\,(10)\right] = 2083 \text{ lb}$$

$$-P_8 = \frac{P_{8a}}{1 + \frac{AE}{KL}} = \frac{2083}{1 + \frac{1\,(10)^7}{10^6(20)}} = 1389 \text{ lb}$$

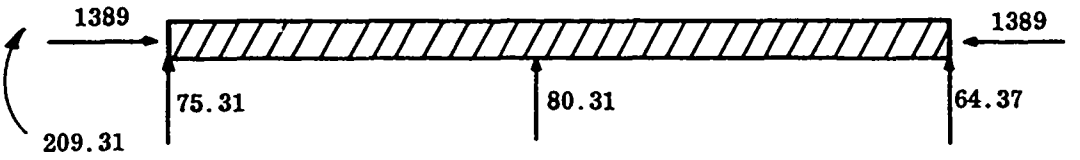


FIGURE 4.2.6.1-3 SOLUTION

4.2.6.2 Problem IB - Statically Indeterminate Beam by the Stiffness Method

The bending portion of the above problem is solved in the following steps:

(1) The degrees of freedom are classified.

(2) The stiffness matrix is determined by methods described in Section 2 of this Manual.

(3) The displacements are determined from the equilibrium equations at each degree of freedom. This requires inverting the stiffness matrix.

(4) The redundant loads are expressed in terms of the displacements to obtain a solution in terms of the applied loads.

(5) Repeat steps (6) and (7) of Problem IA.

Classification of Degrees of Freedom

$(r,s) = (1, 2, 3, 4)$

$(a,b) = (5, 6)$

4.2.6.2 (Cont'd)

Stiffness Matrix - The stiffness matrix is determined as shown in Figure 2.1.4.3-1.

$$\frac{K_{ij}}{EI} =$$

Load at \ Unit Displacement at	3	6	2	5	1	4
3	.012	-.06	-.012	-.06	0	0
6	-.06	.4	.06	.2	0	0
2	-.012	.06	+.024 = (.012 + .012)	0 = (-.60 + .06)	-.012	-.06
5	-.06	2	0 = (.06 - .06)	.8 = (.4 + .4)	+.06	.2
1	0	0	-.012	.06	+.012	.06
4	0	0	-.06	.2	+.06	.4

Equilibrium Equations and Displacements

$$P_{5a} + K_{55}\,\Delta_5 + \Delta_{56}\,\Delta_6 = 0 = P_{5a} + .8\ EI\Delta_5 + .2\ EI\,\Delta_6$$

$$P_{6a} + K_{65}\,\Delta_5 + K_{66}\,\Delta_6 = 0 = P_{6a} + .2\ EI\Delta_5 + .4\ EI\,\Delta_6$$

$$EI\,\Delta_5 = 1.43\ P_{5a} - 72\ P_{6a}$$

$$EI\,\Delta_6 = -.72\ P_{5a} + 2.85\ P_{6a}$$

(Check flexibility equations of Problem 1A)

Reactions

$$-\begin{bmatrix} P_1 \\ P_2 \\ P_3 \\ P_4 \end{bmatrix} = \begin{bmatrix} K_{15} & K_{16} \\ K_{25} & K_{26} \\ K_{35} & K_{36} \\ K_{45} & K_{56} \end{bmatrix} \begin{bmatrix} \Delta_5 \\ \Delta_6 \end{bmatrix} = \begin{bmatrix} .06 & 0 \\ 0 & .06 \\ -.06 & -.06 \\ .2 & 0 \end{bmatrix} \begin{bmatrix} 1.43 & -.72 \\ -.72 & 2.85 \end{bmatrix} \begin{bmatrix} P_{5a} \\ P_{6a} \end{bmatrix}$$

$$-\begin{bmatrix} P_1 \\ P_2 \\ P_3 \\ P_4 \end{bmatrix} = \begin{bmatrix} .086 & -.043 \\ .043 & .172 \\ -.043 & -.129 \\ +.286 & -.144 \end{bmatrix} \begin{bmatrix} P_{5a} \\ P_{6a} \end{bmatrix}$$

(Checks Flexibility Equations of Problem 1A)

4.2.6.3 Problem II - Sandwich Beam by the Flexibility Method

The sandwich beam of this problem is subjected to temperatures of T_1 and T_2 above the datum on the top and bottom faces, respectively. A general solution is presented for the stresses and redundant forces in the sandwich beam in terms of geometry and end fixity. The problem is solved by utilizing the geometric relations for a sandwich beam established in Paragraph 4.1.2.2, solving for the unrestrained deformations, determining the fixed end reactions, and solving for the reactions and stresses.

Geometry (see Figure 4.1.2.2-1)

$$\bar{y} = \left[\frac{E_1A_1}{E_1A_1 + E_2A_2}\right] h = \frac{h}{1 + \frac{E_2A_2}{E_1A_1}} = \frac{h}{1+e}$$ (See Eq. (1) of Paragraph 4.1.2.2)

Unrestrained Deformations

$$w' = \frac{\alpha_1T_1 - \alpha_LT_L}{h} = \frac{\alpha_1T_1}{h}\left(1 - \frac{\alpha_2T_2}{\alpha_1T_1}\right) = \frac{\alpha_1T_1}{h}(1-a)$$ (See Eq. (3) of Paragraph 4.1.2.2)

$$\bar{\epsilon}' = \frac{E_1A_1\alpha_1T_1 + E_2A_2\alpha_2T_2}{E_1A_1 + E_2A_2} = \alpha_1T_1\left(\frac{1+ae}{1+e}\right)$$ (See Eq. (2) of Paragraph 4.1.2.2)

$$\sigma_1 = \sigma_2 = 0$$ (See Eq. (4) of Paragraph 4.1.2.2)

where

$$e = \frac{E_2A_2}{E_1A_1} \quad \text{and} \quad a = \frac{\alpha_2T_2}{\alpha_1T_1} .$$

Fixed End Reactions

$$P_o = 0 \quad M_o = \overline{EI}\, w' \quad F_o = -\overline{EA}\,\bar{\epsilon}$$ (See Eqs. (1) through (3), Paragraph 4.2.2.3; $p_{o,o} = 0$ $m_{o,o} = 1$ $f_{o,o} = 1$)

where

$$\overline{EA} = E_1A_1 + E_2A_2 = E_1A_1(1+e)$$

$$\overline{EI} = E_1A_1h^2 - \bar{y}^2(E_1A_1 + E_2A_2)$$

$$= E_1A_1h^2\left(1 - \frac{1+e}{(1+e)^2}\right) = E_1A_1h^2\left(\frac{e}{1+e}\right)$$

$$M_o = E_1A_1h^2\left(\frac{e}{1+e}\right)\frac{\alpha_1T_1}{h}(1-a) = E_1A_1\alpha_1T_1h\,\frac{e(1-a)}{1+e}$$

$$F_o = -E_1A_1\alpha_1T_1(1+ae)$$

4.2.6.3 (Cont'd)

General Solution

$$f_{dc}\, P_{ca} + f_{dc}\, P_c = - K_{cd}^{-1}\, P_c$$

$$P_c = - \left(f_{dc} + K_{cd}^{-1} \right)^{-1} f_{dc}\, P_{ca}$$

Let K_F = Axial stiffness of support and K_M = Rotational stiffness of support.

$$\therefore \quad F = - \left(\frac{1}{E_1 A_1 (1+e)} + \frac{1}{K_F} \right)^{-1} \left(\frac{(-F_o)}{E_1 A_1 (1+e)} \right)$$

$$F = - \frac{E_1 A_1 \alpha_1 T (1+ae)}{\frac{E_1 A_1 (1+e)}{K_F} + 1} \tag{1a}$$

$$M = - \left[\frac{1}{E_1 A_1 h^2 \left(\frac{e}{1+e} \right)} + \frac{1}{K_M} \right]^{-1} \left[\frac{(-M_o)}{E_1 A_1 h^2 \left(\frac{e}{1+e} \right)} \right]$$

$$M = + \frac{E_1 A_1 \alpha_1 T_1 h \frac{e(1-a)}{1+e}}{\frac{E_1 A_1 h^2 \left(\frac{e}{1+e} \right)}{K_M} + 1} \tag{2a}$$

$$\sigma_j = E_j \left[\frac{F}{AE} - \frac{M}{EI} (y_j - \bar{y}) \right] \tag{3a}$$

$$\frac{F}{AE} = - \frac{\alpha_1 T_1 \left(\frac{1+ae}{1+e} \right)}{\frac{E_1 A_1 (1+e)}{K_F} + 1} = \text{Axial Shortening Caused by Flexible Restraint } (K_F) \tag{1b}$$

$$\frac{M}{EI} = + \frac{\alpha_1 T_1 \left(\frac{1-a}{h} \right)}{\frac{E_1 A_1 h^2 \left(\frac{e}{1+e} \right)}{K_M} + 1} = \text{Curvature Caused by Flexible Restraint } (K_M) \tag{2b}$$

$$\sigma_1 = - \frac{E_1 \alpha_1 T_1}{1+e} \left[\frac{1+ae}{\frac{E_1 A_1 (1+e)}{K_F} + 1} + \frac{(1-a)e}{\frac{E_1 A_1 h^2 \left(\frac{e}{1+e} \right)}{K_M} + 1} \right] \tag{3b}$$

4.2.6.3 (Cont'd)

$$\sigma_2 = - \frac{E_2 \alpha_1 T_1}{1+e} \left[\frac{1+ae}{\frac{E_1 A_1 (1+e)}{K_F} + 1} - \frac{1-a}{\frac{E_1 A_1 h^2 \left(\frac{e}{1+e}\right)}{K_M} + 1} \right] \quad (3c)$$

If $K_F = K_M = 0$ (unrestrained), then $\sigma_1 = \sigma_2 = 0$. (3d)

If $K_F = K_M = \infty$ (completely restrained), then

$$\sigma_1 = \frac{-E_1 \alpha_1 T_1}{1+e} (1+e) = - E_1 \alpha_1 T_1 \quad (3e)$$

$$\sigma_2 = \frac{-E_2 \alpha_1 T_1}{1+e} p (1+e) = - E_2 \alpha_2 T_2 \quad . \quad (3f)$$

4.2.7 Curved Beams

If the beam is straight, the axial problem can be separated from the bending problem. This cannot be done in a curved beam, and the problem must be solved with all the degrees of freedom at a point coupled. Most curved beams in aircraft structures are frames of relatively few load redundants, and the flexibility method is utilized since the frame is essentially a restrained cantilever beam. The utilization of equivalent loads requires determination of fixed end reactions which are quite complex (except for special geometries and loads) and which do not reduce the computation work except in problems involving many redundants.

The flexibility of the frame which results from mechanical loads is primarily determined by the bending flexibility. This is because of the bending energy of the frame, due to mechanical loads, is usually much greater than the axial aid shear energies. This can be seen by comparing the values of $\int \frac{\mathcal{M}^2}{EI} ds$, $\int \frac{\mathcal{J}^2}{AE} ds$, and $\int \frac{\mathcal{P}^2}{A_v G} ds$. The axial energy due to temperature ($\int \bar{\epsilon} \mathcal{J} ds$), however, may be a significant portion of the thermal bending energy ($\int -w' \mathcal{M} ds$) and should be included in the calculations. The change in axial and bending stiffnesses due to temperature can be quite significant and can be calculated with the aid of equations in Paragraph 4.1.1.1.

The frame problem is solved by the flexibility procedure. The structure is made statically determinate by cutting the frame, fixing one end, and applying redundant loads (X_M, X_F and X_P - Figure 4.2.7-1) at the cut to enforce compatibility. The deflection at the cut is computed by virtual work in terms of the mechanical and thermal deformations times the virtual forces and by the redundant loads times the flexibility coefficients.

Let f_{FP} (etc.) = Element of flexibility matrix; deflection at cut in F (axial) direction due to a unit load in P (radial) direction

X_M (etc.) = Redundant load at cut in M (rotational) direction

m_F (etc.) = Internal virtual force of m (rotational) type due to a unit load at cut in F (axial) direction

Δ_P (etc.) = Deflection at cut in P (transverse) direction due to applied loads, temperature, and redundants.



1. Tension is positive (increasing axial strain $\bar{\epsilon}$)
2. Compression on inner (upper) fiber is positive (increasing curvature w)
3. Inward shear is positive
4. Θ = Angle from negative Y axis to normal through section measured counterclockwise
5. Applied clockwise moments are positive
6. Applied horizontal loads are positive to the left
7. Applied vertical loads are positive in the up direction.

FIGURE 4.2.7-1 SIGN CONVENTION

The flexibility coefficients, neglecting axial and shear energy, are evaluated from the virtual moments shown in Figure 4.2.7-2. The results in matrix form are shown as follows:

$$\begin{bmatrix} f_{MM} & f_{MF} & f_{MP} \\ f_{FM} & f_{FF} & f_{FP} \\ f_{PM} & f_{PF} & f_{PP} \end{bmatrix} = \begin{bmatrix} \int \frac{m_M m_M}{EI} ds & \int \frac{m_M m_F}{EI} ds & \int \frac{m_M m_P}{EI} ds \\ \int \frac{m_F m_M}{EI} ds & \int \frac{m_F m_F}{EI} ds & \int \frac{m_F m_P}{EI} ds \\ \int \frac{m_P m_M}{EI} ds & \int \frac{m_P m_F}{EI} ds & \int \frac{m_P m_P}{EI} ds \end{bmatrix} = \begin{bmatrix} \int \frac{ds}{EI} & \int \frac{yds}{EI} & \int \frac{xds}{EI} \\ \int \frac{yds}{EI} & \int \frac{y^2 ds}{EI} & \int \frac{yxds}{EI} \\ \int \frac{xds}{EI} & \int \frac{xyds}{EI} & \int \frac{x^2 ds}{EI} \end{bmatrix} \quad (1)$$

The following compatibility equations express the requirement that the relative motions at the cuts are zero. The virtual force system is the unit load at the counterclockwise side of the cut with reactions on the other side of the cut.

$$\Delta_M = \int \left[\left(-w \quad -w' \right) m_M + \left(\bar{\epsilon} + \bar{\epsilon}' \right) f_M \right] ds + f_{MM} X_M + f_{MF} X_F + f_{MP} X_P = 0$$

$$\Delta_F = \int \left[\left(-w \quad -w' \right) m_F + \left(\bar{\epsilon} + \bar{\epsilon} \right) f_F \right] ds + f_{FM} X_M + f_{FF} X_F + f_{FP} X_P = 0 \quad (2a)$$

$$\Delta_P = \int \left[\left(-w \quad -w' \right) m_P + \left(\bar{\epsilon} + \bar{\epsilon} \right) f_P \right] ds + f_{PM} X_M + f_{PF} X_F + f_{PP} X_P = 0$$

4.2.7 (Cont'd)

or

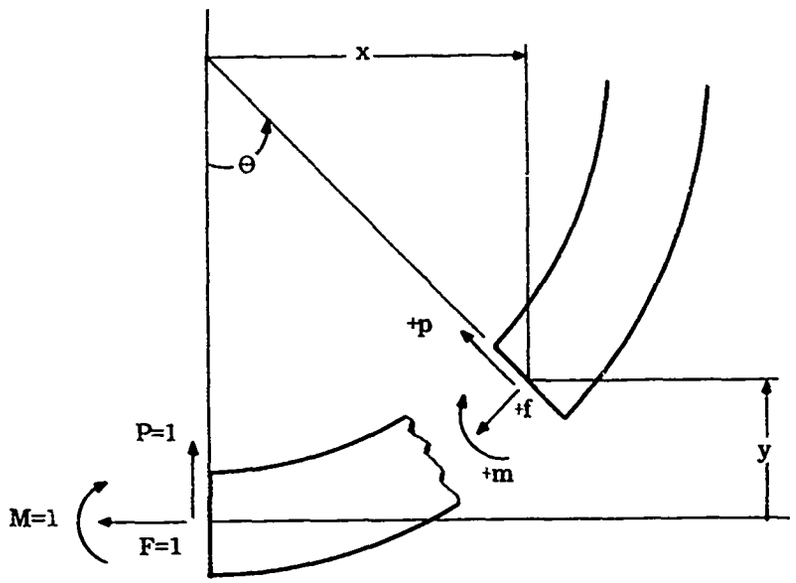
$$\int \frac{M}{EI}\,ds - \int w'\,ds + X_M \int \frac{ds}{EI} + X_F \int \frac{yds}{EI} + X_P \int \frac{xds}{EI} = 0$$

$$\int \frac{My}{EI}\,ds - \int w'\,yds + \int \bar{\epsilon}' \cos\Theta\,ds + X_M \int \frac{yds}{EI} + X_F \int \frac{y^2 ds}{EI} + X_P \int \frac{yxds}{EI} = 0 \quad (2b)$$

$$\int \frac{Mxds}{EI} - \int w'\,xds - \int \bar{\epsilon}' \sin\Theta\,dx + X_M \int \frac{xds}{EI} + X_F \int \frac{xyds}{EI} + X_P \int \frac{x^2 ds}{EI} = 0$$

where $f_M = 0$ and $\int \bar{\epsilon} \cos\Theta\,ds$ and $\int \bar{\epsilon} \sin\Theta\,dx$ are usually small and assumed equal to zero.

The redundants X_M, X_F, X_P are obtained by solving the simultaneous Eqs. (2b).



$m_M = 1$	$m_F = y$	$m_P = x$
$f_M = 0$	$f_F = \cos\Theta$	$f_P = -\sin\Theta$
$p_M = 0$	$p_F = +\sin\Theta$	$p_P = +\cos\Theta$

FIGURE 4.2.7-2 DETERMINATION OF VIRTUAL FORCES m, f, p

4.2.7.1 Values of $\bar{\epsilon}'$, w' and M

The values of $\bar{\epsilon}'$ and w' can be obtained by an analysis of the cross sections as shown in Sub-section 4.1.

A simple approximation of the αT distribution in a cross section is to assume a linear variation through the depth. In the case of a linear distribution, the values of $\bar{\epsilon}'$ would be αT at the centroid of the cross section and the value of w' would be the difference of the (αT)'s divided by the depth $\left(w' = \frac{(\alpha T)_{inside} - (\alpha T)_{outside}}{h}\right)$. The linear variation of αT usually results in a good approximation of the distortions of a cross section ($\bar{\epsilon}'$ and w') due to temperature. These are the parameters that determine the redundant loads.

The moments on the cantilever (cut frame) beam can be determined by statics of the applied loads,

$$M_n = \sum_{i=1}^{n} \left[H_i (y_n - y_i) + V_i (x_n - x_i) + \Delta M_i \right] ,$$

or can be obtained in a table based on incremental moments, as follows:

$$M_{n+1} = M_n + \Delta M_{Mn} + \Delta M_{Vn} + \Delta M_{Hn} \qquad (1)$$

where

$V_{n+1} = V_n + \Delta V_n$; $\Delta M_{Vn} = V_n (x_{n+1} - x_n)$

$H_{n+1} = H_n + \Delta H_n$; $\Delta M_{Hn} = H_n (y_{n+1} - y_n)$

ΔM_{Mn} = Moment about (x_{n+1}, y_{n+1}) of all loads between (x_n, y_n) and (x_{n+1}, y_{n+1})

ΔV_n = Vertical load (positive up) between (x_n, y_n) and (x_{n+1}, y_{n+1})

ΔH_n = Horizontal load (positive to left) between (x_n, y_n) and (x_{n+1}, y_{n+1})

(x_n, y_n) = Coordinates of centroid of n^{th} element

Δs_n = Length of the n^{th} element.

Notes: (a) Frame length between (x_n, y_n) and (x_{n+1}, y_{n+1}) is equal to $.5 (\Delta s_n + \Delta s_{n+1})$.

(b) The loads on the frame must be self-equilibrating. This should be checked before the deformations due to the applied loads are calculated. (See last row of columns 32, 34, and 42 of Table 4.2.7.3-1).

It is advantageous for the purpose of analysis to:

(1) Keep the lengths of Δs small so that section properties are fairly constant in each ΔS
(2) Start new segments when sections change radically
(3) Locate a station (centroid of segment of length Δs) where load changes slightly
(4) Make Δs zero where maximum stresses are expected (concentrated loads, etc.)

4.2.7.1 (Cont'd)

The total loads acting on any section are

$$\mathcal{M}_n = M_n + X_M + y_n X_F + x_n X_P$$

$$\mathcal{F}_n = (H_n + X_F)(\cos\Theta) + (V_n + X_P)(-\sin\Theta) \qquad (2)$$

$$\mathcal{P}_n = (H_n + X_F)(+\sin\Theta) + (V_n + X_P)(+\cos\Theta)$$

4.2.7.2 Special Cases

The solution of the curved beam problem can be modified in special cases to reduce the amount of computations. The following cases are considered:

Case I - Symmetrical Structure
Case II - Elastic Center Method
Case III - Relaxation of Boundary Conditions

Case I: Symmetrical Structure

In many structural problems the geometry s, AE, EI on one side of an axis is a mirror image of the geometry on the other side, e.g., EI $(y_n, +x_n)$ = EI $(y_n, -x_n)$. This is usually the case in aircraft structures (except for some slight variation due to temperature effects) because of the probability of the load being applied from either side of the frame. When the structure is symmetrical, some of the influence coefficients $\left(\int\frac{xds}{EI} = f_{MP} = f_{PM} = \frac{xyds}{EI} = f_{FP} = f_{PF} = 0\right)$ are identially zero and the others need only be evaluated for half the frame and then doubled, e.g.,

$$\int_0^{s(2\pi)} \frac{y^2 ds}{EI} = 2 \cdot \int_0^{s(\pi)} \frac{y^2 ds}{EI}$$

where $s(\pi)$ = length of frame between $\Theta = 0$ and π)

The solution is simplified as follows:

$$X_P = -\left(\int\frac{Mxds}{EI} - \int w' x ds - \int \bar{\epsilon}' \sin\Theta\, ds\right) \Big/ \int \frac{x^2 ds}{EI}$$

$$\begin{pmatrix} X_M \\ X_F \end{pmatrix} = \frac{-\begin{bmatrix} \int\frac{y^2 ds}{EI} & -\int\frac{yds}{EI} \\ \int\frac{yds}{EI} & +\int\frac{ds}{EI} \end{bmatrix} \begin{Bmatrix} \left(\int\frac{Mds}{EI} - \int w' ds\right) \\ \left(\int\frac{Myds}{EI} - \int w' yds + \int \bar{\epsilon}' \cos\Theta\, ds\right) \end{Bmatrix}}{\left(\int\frac{ds}{EI}\right)\left(\int\frac{y^2 ds}{EI}\right) - \left(\int\frac{yds}{EI}\right)^2} \qquad (1a)$$

If the applied loads (thermal and mechanical) are also symmetrical, e.g., $M(y_n, x_n) = M(y_n, -x_n)$, then the radial deflection of the cantilever (in P direction) due to applied loads is zero and the other deflections need only be evaluated for half the frame and then doubled. If the applied loads are antisymmetrical, e.g., $M(y_n, x_n) = -M(y_n, -x_n)$, then the horizontal deflection and rotation of the cantilever is zero and the radial deflection is evaluated for half the frame and then doubled. The following equations summarize the solution of symmetrical frames since any loading can be separated into symmetrical (S) or antisymmetrical (A) components.

For symmetric loads:

$$X_{PS} = 0 \tag{1b}$$

$$\begin{bmatrix} X_{MS} \\ X_{FS} \end{bmatrix} = \frac{-\begin{bmatrix} \int_0^{s(\pi)} \frac{y^2\,ds}{EI} & -\int_0^{s(\pi)} \frac{y\,ds}{EI} \\ \int_0^{s(\pi)} \frac{y\,ds}{EI} & \int_0^{s(\pi)} \frac{ds}{EI} \end{bmatrix} \begin{Bmatrix} \left(\int_0^{s(\pi)} \frac{M\,ds}{EI} - \int_0^{s(\pi)} w'\,ds\right) \\ \left(\int_0^{s(\pi)} \frac{My\,ds}{EI} - \int_0^{s(\pi)} w'y\,ds + \int_0^{s(\pi)} \bar{\epsilon}'\cos\Theta\,ds\right) \end{Bmatrix}}{\left(\int_0^{s(\pi)} \frac{ds}{EI}\right)\left(\int_0^{s(\pi)} \frac{y^2 ds}{EI}\right) - \left(\int_0^{s(\pi)} \frac{y\,ds}{EI}\right)^2} \tag{1b}$$

For antisymmetric loads:

$$X_{MA} = 0\ ;\quad X_{FA} = 0 \tag{1c}$$

$$X_{PA} = \frac{-\left[\int_0^{s(\pi)} \frac{Mx\,ds}{EI} - \int_0^{s(\pi)} w'(x)\,ds - \int_0^{s(\pi)} \bar{\epsilon}'\sin\Theta\,ds\right]}{\int_0^{s(\pi)} \frac{x^2\,ds}{EI}} \tag{1c}$$

Case II: Elastic Center Method

By transforming the reference axes to the "Principal Elastic Axes", it is possible to diagonalize the flexibility matrix. This reduces the three simultaneous equations to three single equations which can be solved quite readily. The solutions can then be expressed as

$$X'_M = \frac{-\left(\int \frac{M\,ds}{EI} - \int w'\,ds\right)}{\int \frac{ds}{EI}}$$

$$X'_F = \frac{-\left(\int \frac{My'\,ds}{EI} - \int w'y\,ds + \int \bar{\epsilon}'\cos\Theta'\,ds\right)}{\int \frac{(y')^2\,ds}{EI}} \tag{2}$$

4.2.7.2 (Cont'd)

$$X'_P = \frac{-\left(\int \frac{Mx'\,ds}{EI} - \int w'\,x'\,ds - \int \bar{\epsilon}'\sin\Theta'\,ds\right)}{\int \frac{(x')^2\,ds}{EI}} \qquad \text{(2) cont'd}$$

where all the above terms are described in Figure 4.2.7.2-1.

It is seldom advantageous to employ the elastic center method unless the location $(\bar{x}, \bar{y})$ and direction (φ) is readily discernible. In the case of symmetry about the "Y" axis the value of $\varphi = 0$ and $\bar{x} = 0$ so that $y' = y - \bar{y}$ and $x' = x$. If symmetry exists about both axes it would be advantageous to establish the origin at the center of symmetry.

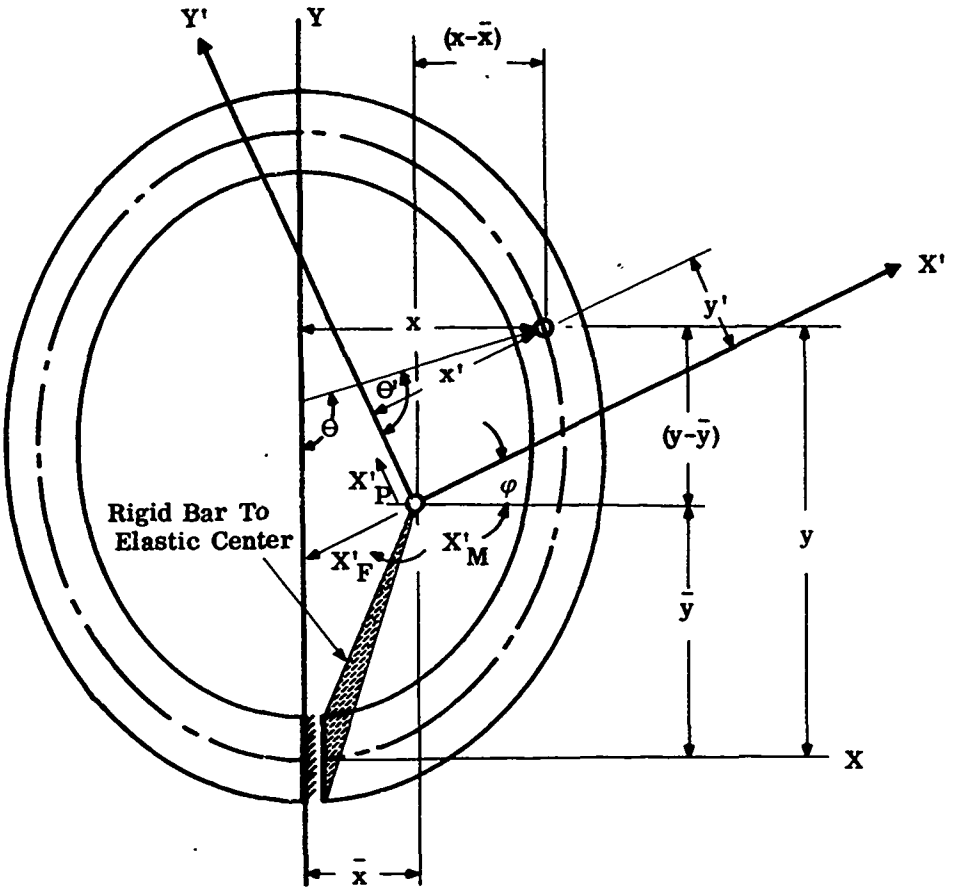


FIGURE 4.2.7.2-1 ELASTIC CENTER METHOD

The transformation equations are:

$$\begin{aligned} y' &= (y-\bar{y})\cos\varphi - (x-\bar{x})\sin\varphi \\ x' &= (y-\bar{y})\sin\varphi + (x-\bar{x})\cos\varphi \\ \Theta' &= \Theta - \varphi \end{aligned} \qquad (3)$$

4.2.7.2 (Cont'd)

$$\tan 2\varphi = \frac{2\int \frac{xy\,ds}{EI}}{\int \frac{y^2 ds}{EI} - \int x^2 \frac{ds}{EI}}$$

$$\bar{y} = \int \frac{y\,ds}{EI} \Big/ \int \frac{ds}{EI}$$

$$\bar{x} = \int \frac{x\,ds}{EI} \Big/ \int \frac{ds}{EI}$$

Case III: Relaxation of Boundary Conditions

It is often convenient to determine the effect of changing the frame by inserting hinges, etc. It is also convenient for computational techniques (digital, etc.) to maintain a standard form to solve all frame problems. Employing the same virtual force system permits to use of standard tabular forms or digital procedures without modification for each special structural problem.

Equations (2a) of Paragraph 4.2.7 can be viewed as the relative deformations at each side of the cut. If a hinge existed, then Δ_M would not equal zero but the redundant load X_M would equal zero.

For the case with a hinge, the compatibility equations become

$$\int \frac{My}{EI}\,ds - \int w'\,y\,ds + \int \bar{\epsilon}'\cos\Theta\,ds + X_F \int \frac{y^2 ds}{EI} + X_P \int \frac{xy\,ds}{EI} = 0 \qquad (4a)$$

$$\int \frac{Mx\,ds}{EI} - \int w'\,x\,ds - \int \bar{\epsilon}'\sin\Theta\,ds + X_F \int \frac{xy\,ds}{EI} + X_P \int \frac{x^2 ds}{EI} = 0 \qquad (4b)$$

Solution of these equations results in the redundant loads X_F and X_P. Note that the tabular form shown in Table 4.2.7.3-1 can be employed to obtain the desired quantities.

4.2.7.3 Sample Problem - Frame Subjected to Thermal and Mechanical Loads

Table 4.2.7.3-1 is designed to solve a general frame problem with a maximum of three redundants. The problem selected was a special one wherein the structure and loads were symmetrical. It was chosen in order to indicate the simplification of work and calculations which result when symmetry of loads and structure exists. Only half the rows in the table need be calculated and many of the columns can be eliminated as indicated below.

(1) Column 8 (denoted by (A)) need not be computed if the structure is symmetrical since Σ (8) would equal zero.
(2) Columns 15, 19, 22, 24 and 27 (denoted by (B)) need not be computed if the loads are symmetrical since Σ of these columns would equal zero
(3) Columns 13, 14, 17, 18, 23 and 26 (denoted by (C)) need not be computed if the loads are assymmetrical since the $\sum$ would be zero.

The summation (value of integral) of the column is therefore either twice the first half ($\Sigma = 2\Sigma'$) or zero since the value of the symmetrically located station in the second half is either the same or opposite to that of the first half. The first half of columns 21 and 22 is usually computed for the purpose of employing Eqs. (2) of Paragraph 4.2.7.1 in obtaining the total loads acting on a cross section.

4.2.7.3 (Cont'd)

Any load distribution can be decomposed into symmetrical and antisymmetrical components by dividing the load vector into two equal parts and applying one of the halves to the structure with its symmetrical equivalent and applying the other half with its antisymmetrical equivalent as shown in Figure 4.2.7.3-1. Using the sign convention for applied loads, a symmetrical load would be defined as

$$M_i = -M_{i'}$$

$$H_i = -H_{i'}$$

$$V_i = +V_{i'}$$

where i' is the station symmetrical to i and an antisymmetrical load would be defined with opposite sign.

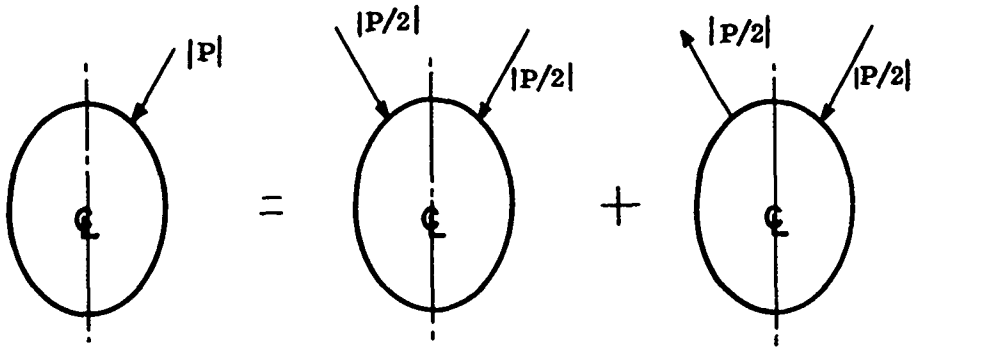


FIGURE 4.2.7.3-1 RESOLUTION OF FORCE INTO SYMMETRICAL AND ANTISYMMETRICAL COMPONENTS

The mechanical and thermal load, together with the geometry of the frame, is shown in Figure 4.2.7.3-2. The solution of the frame problem is obtained by employing Eqs. (1b) and (1c) of Paragraph 4.2.7.2 with the values obtained in Table 4.2.7.3-1.

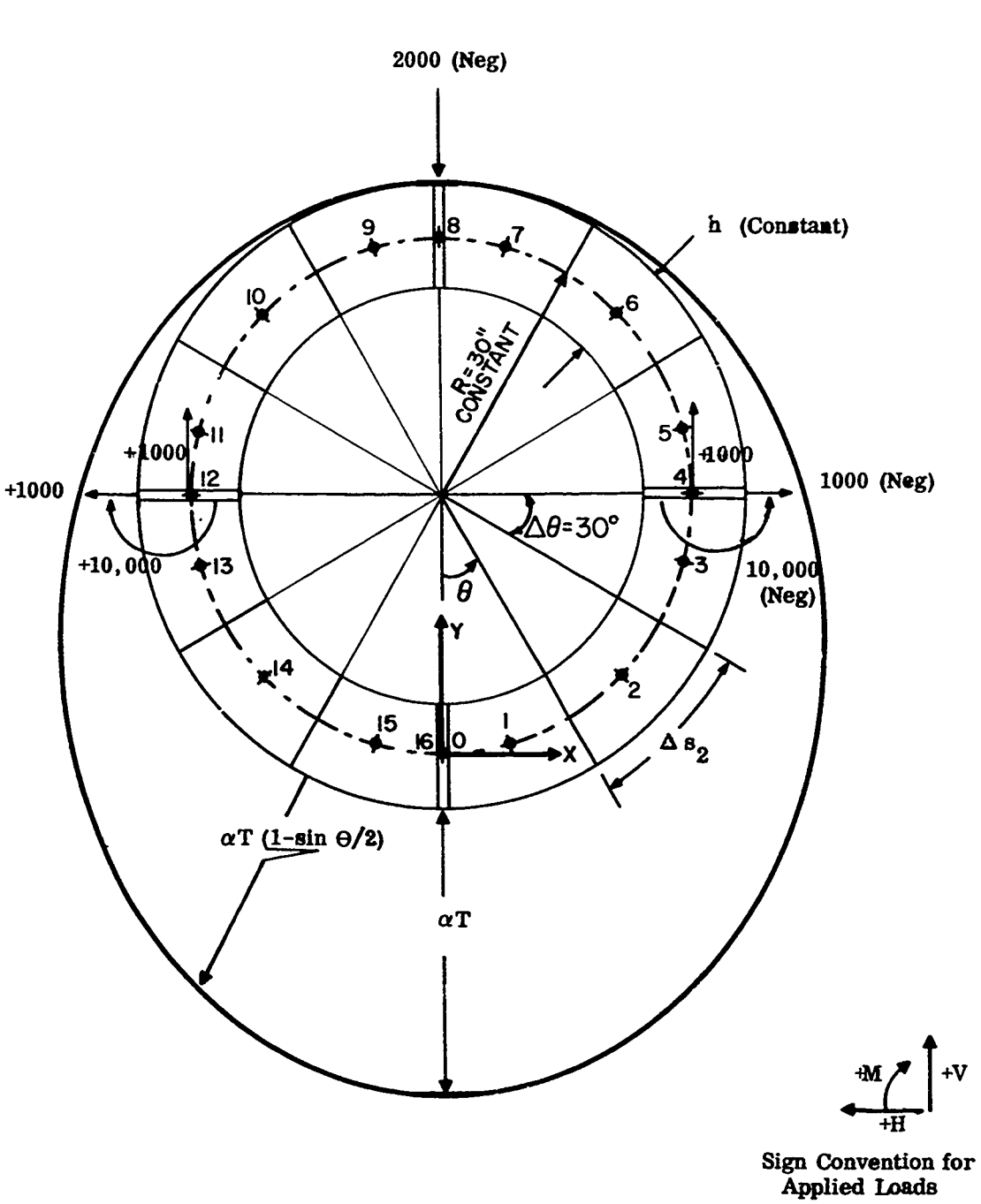


FIGURE 4.2.7.3-2 FRAME PROBLEM

TABLE 4 2 7 3-1 SAMPLE FRAME PROBLEM

(Figure 4 2 7 3-2)

1	2	3	4	5	6	7	8Ⓐ	9	10	11	12	13Ⓒ	14Ⓒ	15Ⓒ	16	17Ⓒ	18Ⓒ	19Ⓑ	20	21
Element Number	y Geom	x Geom	$\frac{\Delta s}{EI}$ Geom	EI Data	$\frac{\Delta s}{EI}$	$y\frac{\Delta s}{EI}$	$x\frac{\Delta s}{EI}$	$y^2\frac{\Delta s}{EI}$	$xy\frac{\Delta s}{EI}$	$x^2\frac{\Delta s}{EI}$	M Data	$M\frac{\Delta s}{EI}$	$My\frac{\Delta s}{EI}$	$Mx\frac{\Delta s}{EI}$	w	$w'\Delta s$	$wy\Delta s$	$wx\Delta s$	θ	$\cos\theta$
	R(1-cosθ)	R sin θ	$R\frac{10}{360}2\pi$	$EI\times10^7$	① $\times10^{-7}$	② × ⑥ $\times10^{-7}$	③ × ⑥ $\times10^{-7}$	② × ⑦ $\times10$	③ × ⑦ $\times10^7$	① × ⑧ $\times10^4$	or ㊷	⑫ × ⑥ $\times10^{-7}$	⑫ × ⑦	⑫ × ④	Data or ⑪	⑯ × ④	⑰ × ②	⑰ × ③	Data in Degrees	Trig. Tables
0	0	0	0	10	0	0		0	0	0	0	0	0		$-1\frac{\partial T}{b}$	0	0		0	1.000
1	1.021	7.764	15.708	10	1.5708	1.6034		1.6439	12.476	94.690	0	0	0		-.8695	-13.658	-13.972		15	.9659
2	3.787	21.21	15.708	10	1.5708	13.303	Ⓐ	121.29	292.76	706.65	0	0	0	Ⓑ	-.6173	- 9.6965	-25.203	Ⓗ	45	.7071
3	22.24	29.95	15.708	5	3.1416	99.309	Need Not Be	1553.9	2024.8	2638.5	0	0 Ⓒ	0 Ⓒ	Need Not Be	-.3912	-6.1450	-136.66	Need Not Be	90	0
4	30	30	0	3	0	0		0	0	0	-10,000	0 Ⓒ	0 Ⓒ		-.2929	0 Ⓒ	0		90	0
5	37.76	29.95	15.708	5	3.1416	118.63	Computed For Sym Structures	4479.5	3437.9	2638.5	-18,787	-59,021	-2.3229	Computed or sym Load	-.2066	-32453	-122.54	Computed For Sym Struct & Load	105	-.2588
6	51.21	21.21	15.708	10	1.5708	80.441		4119.4	1706.2	706.65	-40,000	62,832	-.3218		-.0761	-1.1954	-61.210		135	-.7071
7	59.98	7.764	15.708	10	1.5708	92.646		5464.3	719.30	94.690	-61,213	-96,152	-.5671		-.0086	-.1351	-7.9682		165	-.9659
8	60	0	0	10	0	0		0	0	0	-70,000	0	0		0	0	0		180	-1
9																			195	
10																			225	
11	Ⓕ	Ⓖ	Ⓕ	Ⓕ	Ⓕ	Ⓕ	Ⓖ	Ⓕ	Ⓖ	Ⓕ	Ⓓ	Ⓓ	Ⓓ	Ⓔ	Ⓓ	Ⓓ	Ⓓ	Ⓔ	255	Ⓕ
12	Same as	Neg. of	Same as	Same as	Same as	Same as	Neg. of	Same as	Neg. of	Same as	Same as	Same as	Same as	Neg. of	Same as	Same as	Same as	Neg. of	270	Same as
13	7 to 0	7 to 0	7 to 0	7 to 0	7 to 0	7 to 0	7 to 0	7 to 0	7 to 0	7 to 0	7 to 0	7 to 0	7 to 0	7 to 0	7 to 0	7 to 0	7 to 0	7 to 0	285	7 to 0
14	For Sym Struc	For Sym Struc	For Sym Struc	For Sym Struc	For Sym Struc	For Sym Struc	For Sym Struc	For Sym Struc	For Sym Struc	For Sym Struc	For Sym Struc	For Sym Str. & load	For Sym Str. & load	For Sym Str. & load	For Sym Str & load	For Sym Str & load	For Sym Str & load	For Sym Str & load	315	For Sym Struc
15																			345	
16																			360	
Σ 1-8 =	1/2 Σ 1-	16 = Σ'			12.5665	376.995	---	15.740	---	6879.5		-218.006	-1.1118	-----		-34.0755 $\frac{\partial T}{b}$	-427.56 $\frac{\partial T}{b}$	----		
Σ 1-16					25.133	753.99	0	31.480	0	13.759		-416.112	-2.2236	0		-68.151	-855.12	0		
					f_{MM}	$f_{MF}=f_{FM}$	$f_{MO}=f_{OM}$	f_{FF}	$f_{FP}=f_{PF}$	f_{PP}										

GENERAL

$X_M \Sigma ⑥ + X_F \Sigma ⑦ + X_P \Sigma ⑤ = - \Sigma ⑬ + \Sigma ⑰$

$X_M \Sigma ⑦ + X_F \Sigma ⑨ + X_P \Sigma ⑩ = - \Sigma ⑭ + \Sigma ⑱ - \Sigma ㉘$

$X_M \Sigma ⑧ + X_F \Sigma ⑩ + X_P \Sigma ⑪ = - \Sigma ⑮ + \Sigma ⑲ + \Sigma ㉗$

SYMMETRICAL GEOMETRY AND LOAD

$X_M = - [\Sigma' ⑨ (\Sigma' ⑬ - \Sigma' ⑰) - \Sigma' ⑦ (\Sigma' ⑭ - \Sigma' ⑱ + \Sigma' ㉖)] / \Sigma' ⑥ \Sigma' ⑨ - (\Sigma' ⑦)^2$

$X_F = - [\Sigma' ⑧ (\Sigma' ⑭ - \Sigma' ⑱ + \Sigma' ㉖) - \Sigma' ⑦ (\Sigma' ⑬ - \Sigma' ⑰)] / \Sigma' ⑥ \Sigma' ⑨ - (\Sigma' ⑦)^2$

SYMMETRICAL GEOMETRY AND ANTISYMMETRICAL LOAL

$X_P = - [\Sigma' ⑮ - \Sigma' ⑲ - \Sigma' ㉗] / \Sigma' ⑪$

TABLE 4.2 7.3-1 SAMPLE FRAME PROBLEM (Cont'd) (Figures 4.2.7.3-2)

For Linear αT

22Ⓑ	23Ⓒ	24Ⓑ	25	26Ⓒ	27Ⓑ	28	29	30	31	32	33	34	35	36	37	38	39	40	41	42
sin θ	cos θΔs	sin θΔs	F'	F'cosθΔs	F'sinθΔs	$(\alpha T)_1$	$(\alpha T)_o$	F' = αT c. g.	$\frac{w'=(\alpha T)-(\alpha T)_o}{h}$	ΔH_n	H_n	ΔV_n	V_n	Δy $(y_{n+1}-y_n)$	Δx $(x_{n+1}-x_n)$	ΔM_V $V_n(x_{n+1}-x_n)$	ΔM_H $H_n(y_{n+1}-y_n)$	ΔM_M	ΔM	M
	(21)x(4) Δs=15.708	(22) x (4) Δs=15.708	Data or (30)	(23) x (25)	(24) x (25)	Ref. Figure -.2 $(\alpha T)_1$	$(\alpha T)_o$*	For Sym Sect.**	(29) - (30) x $\frac{1}{h}$	Data Fig.-2	$\sum_o^n$ (32)	Data Fig. -2	$\sum_o^n$ (34)	(2)$_{n+1}$-(2)$_n$	(3)$_{n+1}$-(3)$_n$	(35) x (37)	(33) x (36)	Data Fig. -2	(38)$_n$ + (39)$_n$ +(40)$_n$	(41)$_{n-1}$ +(42)$_{n-1}$
	0		.50αT	$0^{\alpha T}$	$^{\alpha T}$	0	1.0xαT	.5000	-1	0	0	0	0	1.023	7.764	0	0	0	0	0
	15.172		.4348	6.4451		0	.8695	.4348	-.8695	0	0	0	0	7.764	15.449	0	0	0	0	0
Ⓑ	11.107	Ⓑ	.3087	3.4287	Ⓑ	0	.6173	.3087	-.6173	0	0	0	0	13.449	7.764	0	0	0	0	0
Need Not	4.065	Need Not	.1956	.7951	Need Not	0	.3912	.1956	-.3912	0	0	0	0	7.764	1.023	0	0	-10^4	-10^4	0
Be	0 Ⓒ	Be	.1465	0 Ⓒ	Be	0	.2929	.1466	-.2929	-10^3	-10^3	10^3	10^3	7.764	-1.023	-1023	-7764	0	-8787	-10^4
Computed	-4.065	Computed	.1033	-.4199	Computed	0	.2066	.1033	-.2066	0	-10^3	0	10^3	13.449	-7.764	-7764	-13449	0	-21213	-18.787
For Sym Str&load	-11,107	For Sym Str & load	.03805	-.4226	For Sym Str & Ld	0	.0761	.03805	-.0761	0	-10^3	0	10^3	7.764	13.449	-13449	-7764	0	-21213	-40.000
	-15.172		.0043	-.06524		0	.0086	.0043	-.0086	0	-10^3	0	10^3	1.023	-7.764	-7764	-1023	0	-8787	-61.213
	0		0	0		0	0	0	0	0	-10^3	-2000	-10^3			7764	1023	0	8787	-70.000
										(E)	(D)	(D)	(E)		(F)	(E)	(E)	(E)	(E)	(D)
(G)	(F)	(G)	(D)	(D)	(E)	(D)	(D)	(D)	(D)	Neg. Of	Same as	Same as	Neg. Of			Neg. of	Neg. of	Neg. of	Neg. of	Same as
Neg. of	Same as	Neg. of	Same as	Same as	Neg. of	Same as	Same as	Same as	Same as	7 to 0	7 to 0	7 to 0	7 to 0	Neg. of	Same as	7 to 0	7 to 0	7 to 0	7 to 0	7 to 0
7 to 0	7 to 0	7 to 0	7 to 0	7 to 0	7 to 0	7 to 0	7 to 0	7 to 0	7 to 0	For Sym Str & ld	For Sym Str & ld	For Sym Str & ld	For Sym Str & ld	7 to 0	7 to 0	For Sym Str. &ld.	For Sym Str. &'d.	For Sym Str. &ld	For Sym Str. &ld	For Sym Str.& ld.
For Sym. Str.	For Sym. Str.	For Sym. Str.	For Sym Str. & ld	For Sym Str & load	For Sym Str & ld	For Sym Str & ld	For Sym Str. &ld.	For Sym Str & ld	For Sym Str. & ld					For Sym. Str.	For Sym. Str.					
											= 0		= 0	—	—	—	—			= 0
											For Equil		For Equil							For Equil.
				9.761	—															
				αT																
				19.522	0															

Ⓐ Need Not Be Computed For Symmetrical Structure

Ⓑ Need Not Be computed For Symmetrical Structure and Load

Ⓒ Need Not Be Computed For Symmetrical Structure and Assymmetrical Load

Ⓓ Same For Symmetrical Structure and Load, Negative For Symmetrical Structure and Antisymmetrical Load

Ⓔ Negative For Symmetrical Structure and Load, Same For Symmetrical Structure and /Antisymmetrical Load

Ⓕ Same For Symmetrical Structure

Ⓖ Negative For Symmetrical Structure

* $(\alpha T)_o = \alpha T\ (1-\sin\frac{\theta}{2})$

** For Sym. Sect. $\frac{(41)+(38)}{2}$

TABLE 4 2 7 3-1 SAMPLE FRAME PROBLEM

(Figure 4 2 7 3-2)

1	2	3	4	5	6	7	8 (A)	9	10	11	12	13 (C)	14 (C)	15 (C)	16	17 (C)	18 (C)	19 (B)	20	21
Element Number	y Geom	x Geom	Δs Geom	EI Data	$\frac{\Delta s}{EI}$	y $\frac{\Delta s}{EI}$	x $\frac{\Delta s}{EI}$	$y^2 \frac{\Delta s}{EI}$	x $\frac{\Delta s}{EI}$	$x^2 \frac{\Delta s}{EI}$	M Data	M $\frac{\Delta s}{EI}$	My $\frac{\Delta s}{EI}$	Mx $\frac{\Delta s}{EI}$	w	w' Δs	w y Δs	w x Δs	θ	cos θ
	R(1-cosθ)	R sin θ	$R\frac{30}{360}\pi$	EI x 10^7	(1) / (2) x 10^{-7}	(2) x (6) x 10^{-7}	(3) x (6) x 10^{-7}	(2) x (7) $_7$	(3) x (7) x 10^{-7}	(3) x (8) x 10^{-7}	or (42)	(12) x (6) x 10^{-7}	(12) x (7)	(12) x (4)	Data or (31)	(16) x (4)	(17) x (2)	(17) x (3)	Data in Degrees	Trig. Tables
0	0	0	0	10	0	0		0	0	0	0	0	0		$-1\frac{ql^4}{h}$	0	0		0	1.000
1	1.023	7.764	15.708	10	1.5708	1.6069		1.6439	12.476	94.690	0	0	0		- .8695	-13.653	-13.972		15	.9659
2	5.787	21.21	15.708	10	1.5708	13.803	(4)	121.29	292.76	706.65	0	0	0	(B)	- .6173	- 9.6965	-85.203	(H)	45	.7071
3	22.24	29.98	15.708	5	3.1416	69.759	Need Not	1553.9	2024.8	2638.5	0	0	0	Need Not	- .3912	-6.1450	-136.86	Need Not	75	.2588
4	30	30	0	3	0	0	Be	0	0	0	-10,000	0 (C)	0 (C)	Be	- .2929	0 (C)	0	Be	90	0
5	37.76	29.98	15.708	5	3.1416	118.63	Computed	4479.5	3437.9	2638.5	-18,787	-59,021	- .2229	Computed	- .2066	-32453	-122.54	Computed	105	-.2588
6	51.21	21.21	15.708	10	1.5708	80.441	For Sym Structure	4119.4	1706.2	706.65	-40,000	62,832	- .3218	or sym structure & 1 load	- .0761	-1.1954	-61.216	For Sym Struct & 1 load	135	- .7071
7	58.98	7.764	15.708	10	1.5708	92.646		5464.3	719.30	94.690	-61,213	-96,153	- .5671		- .0085	- .1351	-7.9682		165	-.9659
8	60	0	0	10	0	0		0	0	0	-70,000	0	0		0	0	0		180	-1
9																			195	
10																			225	
11	(F)	(G)	(F)	(F)	(F)	(F)	(G)	(F)	(G)	(F)	(D)	(D)	(D)	(E)	(D)	(D)	(D)	(E)	255	(F)
12	Same as	Neg. of	Same as	Same as	Same as	Same as	Neg. of	Same as	Neg. of	Same as	Same as	Same as	Same as	Neg. of	Same as	Same as	Same as	Neg. of	270	Same as
13	7 to 0	7 to 0	7 to 0	7 to 0	7 to 0	7 to 0	7 to 0	7 to 0	7 to 0	7 to 0	7 to 0	7 to 0	7 to 0	7 to 0	7 to 0	7 to 0	7 to 0	7 to 0	285	7 to 0
14	For Sym Struc	For Sym Struc	For Sym Struc	For Sym Struc	For Sym Struc	For Sym Struc	For Sym Struc	For Sym Struc	For Sym Struc	For Sym Struc	For Sym Struc	For Sym Struc & load	For Sym Str. & load	For Sym Str & load	For Sym Str & load	For Sym Str & load	For Sym Str & load	For Sym Str & load	315	For Sym Struc
15																			345	
16																			360	
Σ 1-8 =	1/2 Σ 1-	16 = Σ'			12.5665	376.995	---	15.740	---	6879.5		-218.006	-1.1118	-----		-34.0755 $\frac{ql^3}{h}$	-427.56 $\frac{ql^2}{h}$	----		
Σ 1-16					25.133	753.99	0	31.480	0	13.759		-416.112	-2.2236	0		-68.151	-855.12	0		
					f_{MM}	$f_{MF}=f_{FM}$	$f_{MO}=f_{OM}$	f_{FF}	$f_{FP}=f_{PF}$	f_{PP}										

GENERAL

$X_M \Sigma (6) + X_F \Sigma (7) + X_p \Sigma (9) = - \Sigma (13) + \Sigma (17)$

$X_M \Sigma (7) + X_F \Sigma (9) + X_p \Sigma (10) = - \Sigma (14) + \Sigma (18) - \Sigma (26)$

$X_M \Sigma (8) + X_F \Sigma (10) + X_p \Sigma (11) = - \Sigma (15) + \Sigma (19) + \Sigma (27)$

SYMMETRICAL GEOMETRY AND LOAD

$X_M = - \left[\Sigma' (3)(\Sigma' (13) - \Sigma' (17)) - \Sigma' (7)(\Sigma' (14) - \Sigma' (18) + \Sigma' (26) \right] / \Sigma' (6) \Sigma' (9) - (\Sigma' (7))^2$

$X_F = - \left[\Sigma' (6)(\Sigma' (14) - \Sigma' (18) + \Sigma' (26)) - \Sigma' (7)(\Sigma' (13) - \Sigma' (17)) \right] / \Sigma' (6) \Sigma' (9) - (\Sigma' (7))^2$

SYMMETRICAL GEOMETRY AND ANTISYMMETRICAL LOAD

$X_p = - \left[\Sigma' (16) - \Sigma' (19) - \Sigma' (27) \right] / \Sigma' (11)$

4.2.7.3 (Cont'd)

For symmetrical geometry and load, Eqs.(1b) of Paragraph 4.2.7.2 are utilized.

$$X_M = \frac{-\left[\Sigma' (9) (\Sigma' (13) - \Sigma' (17)) - \Sigma' (7)(\Sigma' (14) - \Sigma' (18) + \Sigma' (26))\right]}{\Sigma' (6)\, \Sigma' (9) - (\Sigma' (7))^2}$$

$$X_M = -\left\{15{,}740\ (10)^{-7}\left[-218{,}006\ (10)^{-7} - (-34.0755\ \frac{\alpha T}{h})\right]\right\}$$

$$\frac{-376.995\ (10)^{-7}\ -11{,}118{,}000\ (10)^{-7} - (-427.56\ \frac{\alpha T}{h}) + 9.761\ \alpha T}{(12.5665)\ (10)^{-7}\ (15{,}740)\ (10)^{-7} - (376{,}995\ (10)^{-7})^2}$$

$$\boxed{X_M = -13652 \text{ in lb} - 67.388\ (10)^6\ \frac{\alpha T}{h} + .361\ (10)^6\ \alpha T}$$

$$X_F = \frac{-\left[\Sigma' (6) (\Sigma' (14) - \Sigma' (18) + \Sigma' (26)) - \Sigma' (7) (\Sigma' (13) - \Sigma' (17))\right]}{\Sigma' (6)\, \Sigma' (9) - (\Sigma' (7))^2}$$

$$\boxed{X_F = 10333 \text{ lb} + 1.3424\ (10)^6\ \frac{\alpha T}{h} - .022\ (10)^6\ \alpha T}$$

$$\boxed{X_P = 0}$$

4.3 REFERENCES

4-1 Switzky, H., Thermal Stresses and Deformations in Unrestrained Beams, Report No. E-SAM 24, Republic Aviation Corporation, December 1957. Appendix, January 1960.

4-2 Klosner, J. M., Thermal Stresses at the End of a Spar, Report No E-SAM-14, Republic Aviation Corporation, October 1955.

4-3 Engineering Structures Data Sheets Manual - IBM Procedures, ESM-IV, Republic Aviation Corporation, January 1958.

4-4 Switzky, H., Solution of Statically Indeterminate Beam-like Structures, RDSR-2, Republic Aviation Corporation (to be issued).

4-5 Meissner, C., Stress Analysis of Aerodynamic Surfaces Using the Method of Elastic Coefficients, Report No. ESAM-21, Republic Aviation Corporation, July 1958.

4-6 Switzky, H., Influence Coefficients, Report No. ESAM-22, Republic Aviation Corporation, August 1956.

SECTION 5

THERMO-ELASTIC ANALYSIS OF JOINTS

SECTION 5

THERMO-ELASTIC ANALYSIS OF JOINTS

TABLE OF CONTENTS

Paragraph	Title	Page
5	Thermo-Elastic Analysis of Joints	5.2
5.1	The One-Dimensional Problem	5.4
5.1.1	The Joint Equations	5.5
5.1.2	The Special Case of Constant Bay Properties (with illustrative problem)	5.8
5.1.3	Constant Bay Properties - Rigid Sheets (with illustrative problem)	5.24
5.1.4	Constant Bay Properties - Rigid Attachments (with illustrative problem)	5.28
5.1.5	The Influence of "Slop" on the Load Distribution (with illustrative problem)	5.30
5.2	The Two-Dimensional (Bowing) Problem	5.36
5.2.1	The Joint Equations	5.37
5.3	Determination of the Attachment-Hole Flexibility Factor	5.39
5.4	References	5.40

SECTION 5 - THERMO-ELASTIC ANALYSIS OF JOINTS

This section considers the thermo-elastic analysis of mechanical joints. The analysis presented is directly applicable to problems where the stress levels lie in the elastic range (low ductility materials such as the ceramics, refractory materials, beryllium, etc., generally remain in the elastic range almost to failure). In addition, certain aspects of the analysis are shown to be of value in the solution of problems with stress levels in the inelastic and plastic ranges.

As shown in Figure 5-1, a mechanical joint is one that is composed of plate-like materials joined by fasteners (such as rivets, pins or bolts) for the purpose of load transfer.

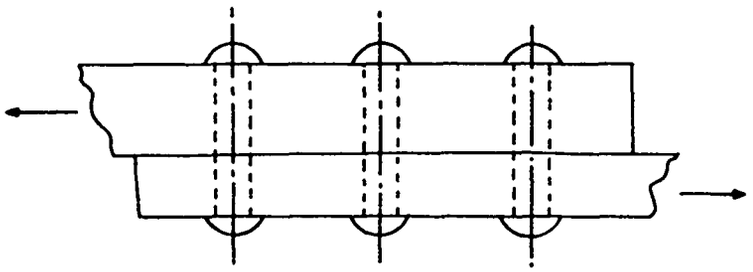


FIGURE 5-1 MECHANICAL JOINT

It is assumed that the heat conduction problem has been solved for the temperature distribution in the joint. To find the loads in the attachments and the stresses in the cross sections for the known temperature distribution and a given applied mechanical load, two classes of problems will be considered. The first is the one-dimensional case, wherein each plate is restrained from deflecting out of its own plane. The second case to be considered is the two-dimensional problem wherein the plates bow or deflect out of plane.

General solutions are presented and it is shown how these degenerate to the more familiar elementary joint equations when the applicable simplifying assumptions are made.

The following symbols are used throughout this section:

e	Difference between attachment and attachment hole diameter (slop), inches
f	Attachment-hole flexibility factor, in/lb
h	Plate thickness, inches
i	Running subscript
j	The j^{th} attachment, or bay
w	Rotation of a plate per unit distance due to thermal loading (thermal curvature, see Paragraph 4.1.1.2)

x	Longitudinal distance along splice, inches
y_T, y_B	Distances from elastic axes of top and bottom plates, respectively, to the contact surface, inches
y	Distance in the thickness direction, inches
A	Cross section area, square inches
$\overline{AE}$	Effective axial stiffness of a plate; $\int EdA$ (see Paragraph 4.1.1.1), lbs.
A_{jN}, B_{jN}	Non-dimensional coefficients for the determination of attachment loads (Figure 5.1.2-1).
D	Diameter, inches
E	Young's Modulus, psi
$\overline{EI}$	Effective bending stiffness of a cross section, (see Paragraph 4.1.1.1), lbs-in^2
I	Cross sectional moment of inertia, in^4
K	Stiffness, lbs/in
L	Longitudinal spacing between adjacent attachments, inches
M	Externally applied bending moment, in-lbs
N	Total number of joint attachments
P	Attachment shear oad, lbs
T	Temperature, degrees F
X	Mechanical load, lbs
Z	Non-dimensional ratio of axial flexibility to attachment-hole flexibility
α	Coefficient of thermal expansion, in/in-°F
Δ	Linear displacement, inches; an increment
δ	Slop displacement between adjacent loaded attachments, inches
$\bar{\epsilon}$	Axial strain of a plate due to thermal loading; $\int E\alpha TdA / \int EdA$
ϕ	Free axial thermal expansion in the plane of the plate; $\int \bar{\epsilon}\, dx$, inches

Subscripts

B	Refers to bottom plate
j	Refers to the j^{th} attachment, or bay
jN	Refers to the j^{th} attachment of a splice having N total attachments
T	Refers to top plate

5.1 THE ONE-DIMENSIONAL PROBLEM

The general problem is simplified if the overall geometry of the joint does not allow the joint to bend out of plane. Such conditions are realized when, for example, the joint consists of a splice strap in a flexurally rigid beam flange as shown in Figure 5.1-1. In such a case, the problem is one-dimensional in that the joint displacements and attachment loads are essentially dependent on the axial flexibility of the joint components in the direction of the applied external loading.

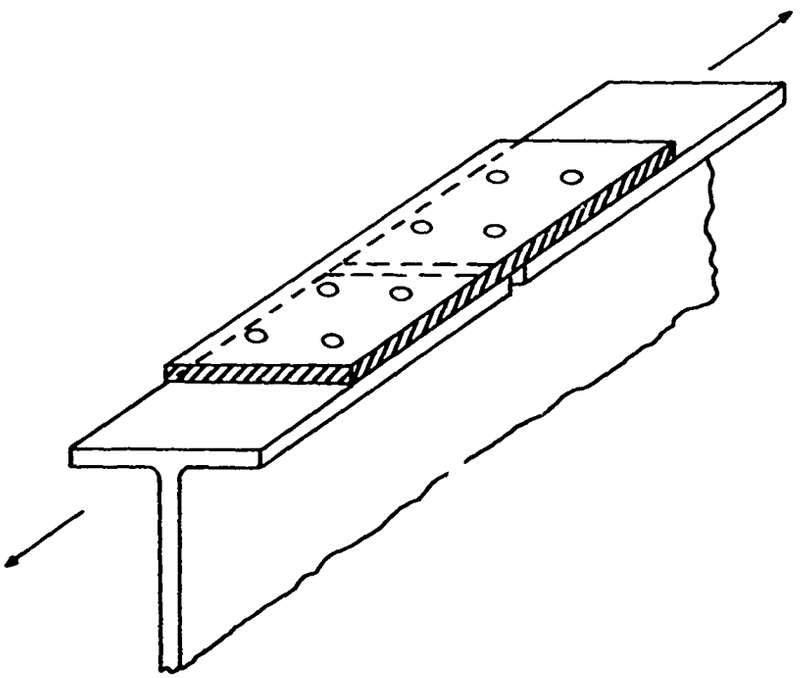


FIGURE 5.1-1 SPLICE STRAP FOR A RIGID BEAM FLANGE

The solution for the load distribution to the joint attachments is obtained by satisfying compatibility conditions for the joint displacements and the equilibrium equation.

The following analysis is applicable to a mechanical joint composed of two arbitrarily dissimilar elastic materials. It is assumed that the attachments initially fill the holes and that each attachment-hole combination deforms elastically under load.

The presence of "slop" (which results from a combination of manufacturing tolerances and differential thermal expansions between the plate holes and attachments) and its influence upon the load distribution, is then considered. A detailed derivation of all solutions is presented in Reference 5-1.

5.1.1 The Joint Equations

Equilibrium

Figure 5.1.1-1 shows a longitudinal section through a typical joint under consideration. Denoting the shear load acting at the j^{th} attachment by P_j, equilibrium of forces requires that

$$X = \sum_{j=1}^{N} P_j \quad , \tag{1}$$

where a tensile applied load X and attachment loads acting to the right on the upper sheet are considered positive.

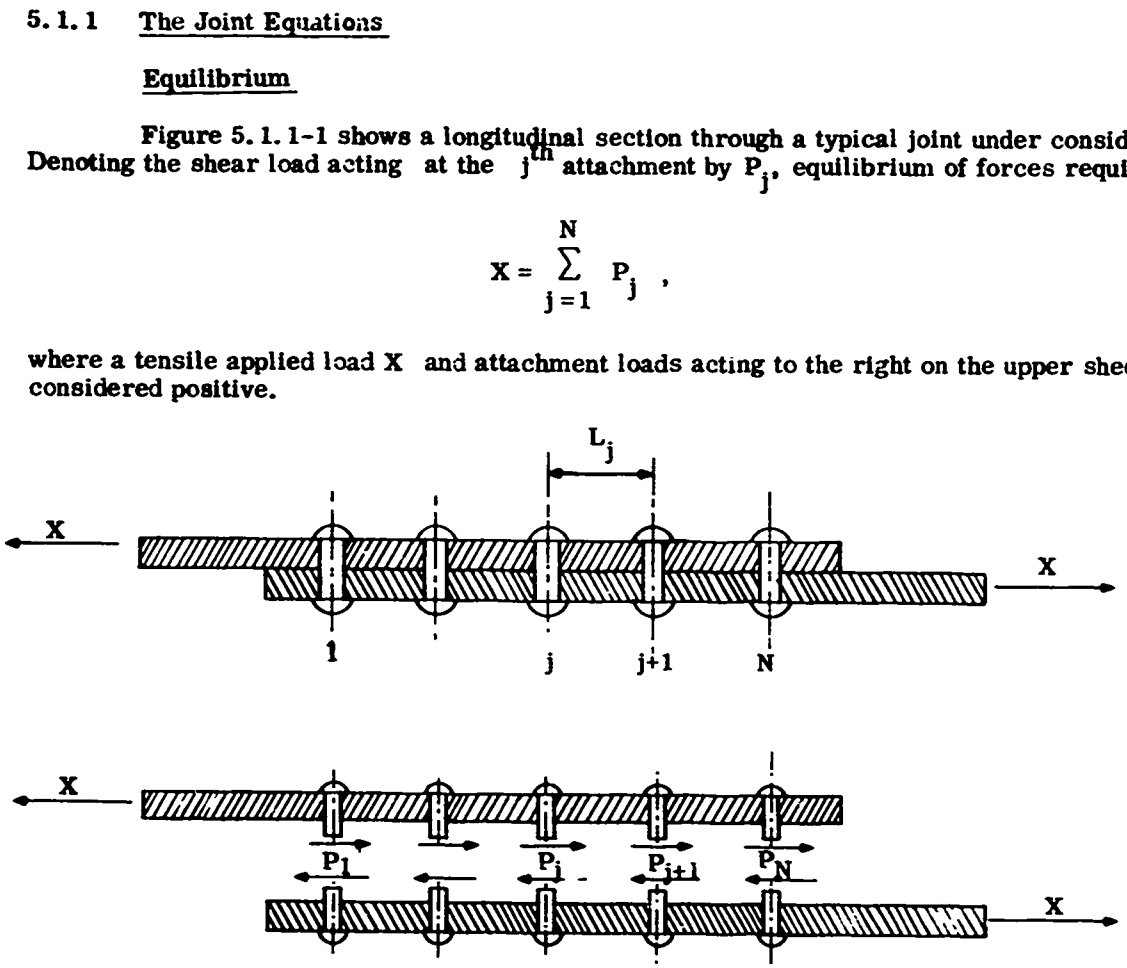


FIGURE 5.1.1-1 ONE-DIMENSIONAL JOINT EQUILIBRIUM

Compatibility Conditions

As shown in Figure 5.1.1-2, compatibility of displacements requires that the axial contraction or expansion of the plate material at the common surface, measured from a datum (defined by the unloaded, unheated spacing between the centerlines of adjacent pins) must be identical for the upper and lower plates.

5.1.1 (Cont'd)

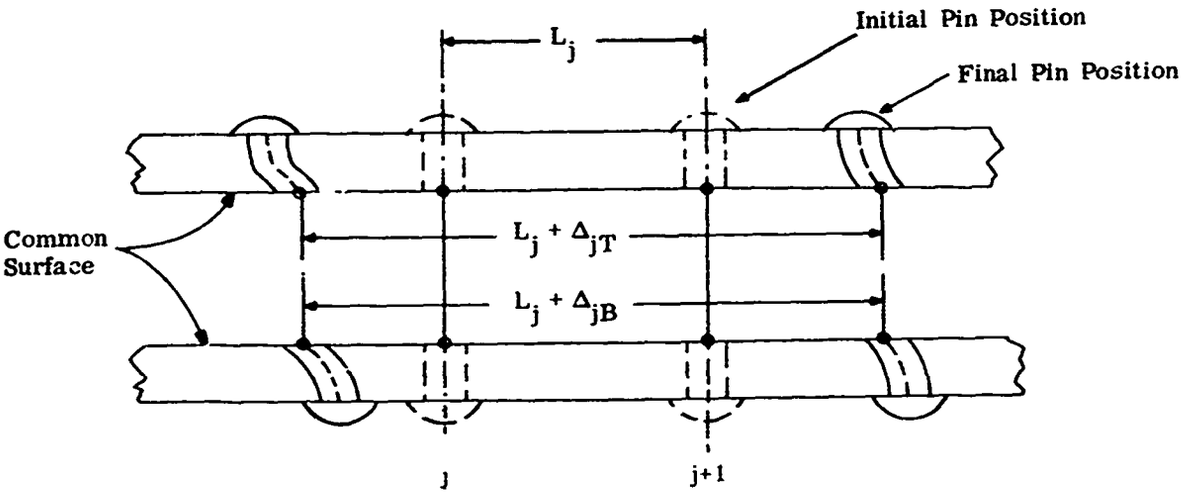


FIGURE 5.1.1-2 ONE-DIMENSIONAL COMPATIBILITY

For the j^{th} general bay the compatibility equation is

$$\Delta_{jT} = \Delta_{jB} \cdot \tag{2}$$

where the subscripts T and B refer to the top and bottom plates, respectively. For the one-dimensional case with no "slop" present, there are basically two types of deformation which contribute to the Δ_j's of the joint.

The first type of deformation is the uniaxial stretching or contraction of the sheets due to the combined effects of temperature and mechanical loading. Referring to Figure 5.1.1-3, the uniaxial stretching for the j^{th} bay is

$$\Delta'_{jT} = \left(X - \sum_{i=1}^{j} P_i\right)\left(\frac{L}{AE}\right)_{jT} + \int_0^{L_j} \bar{\epsilon}_{jT}\, dx \tag{3a}$$

$$\Delta'_{jB} = \left(\sum_{i=1}^{j} P_i\right)\left(\frac{L}{AE}\right)_{jB} + \int_0^{L_j} \bar{\epsilon}_{jB}\, dx \cdot \tag{3b}$$

where a positive Δ increases the spacing between adjacent attachments and

$$\bar{\epsilon} = \frac{\int_o^h E\alpha T dy}{\int_o^h E dy} \cdot$$

If the thermal gradient is linear through the thickness, then $\bar{\epsilon}$ is approximately equal to the value of αT at the plate midplane.

5.1.1 (Cont'd)

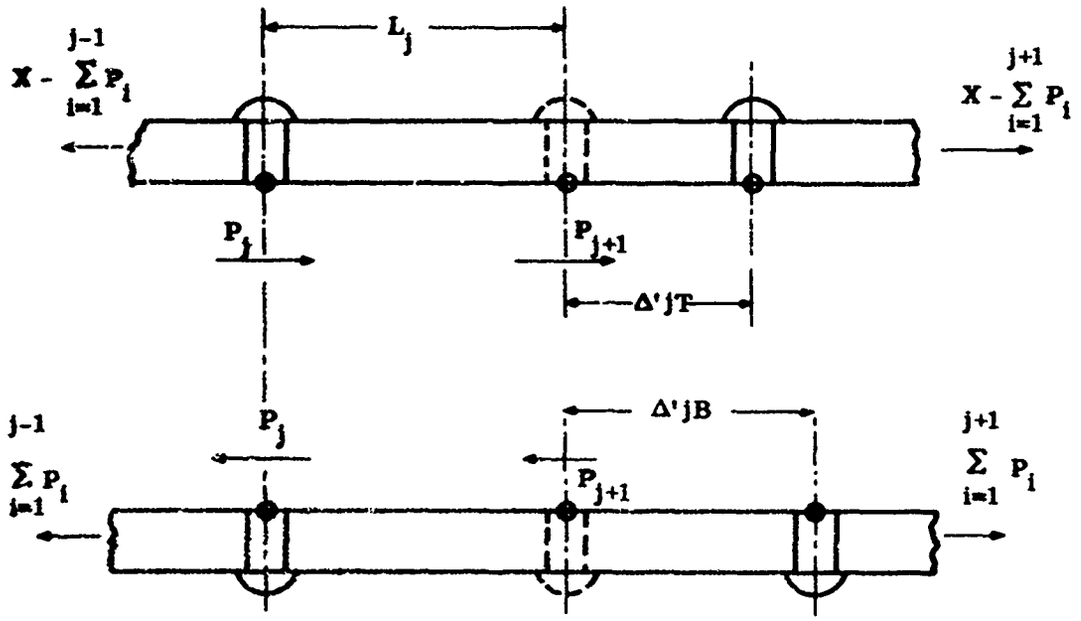


FIGURE 5.1.1-3 DEFORMATION OF THE JOINT DUE TO AXIAL STRETCHING OF THE SHEETS

The second basic type of joint deformation occurs because the internal joint loads create local distortions of the holes and attachments as shown in Figure 5.1.1-4. The deformation is expressed in terms of an experimentally determined attachment hole flexibility factor f for the given attachment-sheet combination (Sub-section 5.3). Thus, for the top sheet,

$$\Delta''_{jT} = P_{j+1} f_{(j+1)T} - P_j f_{jT} \tag{4a}$$

and for the bottom sheet,

$$\Delta''_{jB} = -P_{j+1} f_{(j+1)B} + P_j f_{jB} \quad . \tag{4b}$$

Substituting $\Delta_{jT} = \Delta'_{jT} + \Delta''_{jT}$ and $\Delta_{jB} = \Delta'_{jB} + \Delta''_{jB}$ from Eqs. (3) and (4) into Eq. (2) yields, after rearranging terms,

$$\boxed{\left[\left(\frac{L}{AE}\right)_{jT} + \left(\frac{L}{AE}\right)_{jB}\right]\left[\sum_{i=1}^{j} P_i\right] = \Delta\phi_j - P_j f_j + P_{j+1} f_{(j+1)} + X\left(\frac{L}{AE}\right)_{jT}} \tag{5}$$

where

$$\Delta\phi_j = \int_0^{L_j} (\bar{\epsilon}_{jT} - \bar{\epsilon}_{jB})\, dx \,,$$

and

$$f_j = f_{jT} + f_{jB} \quad .$$

5.1.1 (Cont'd)

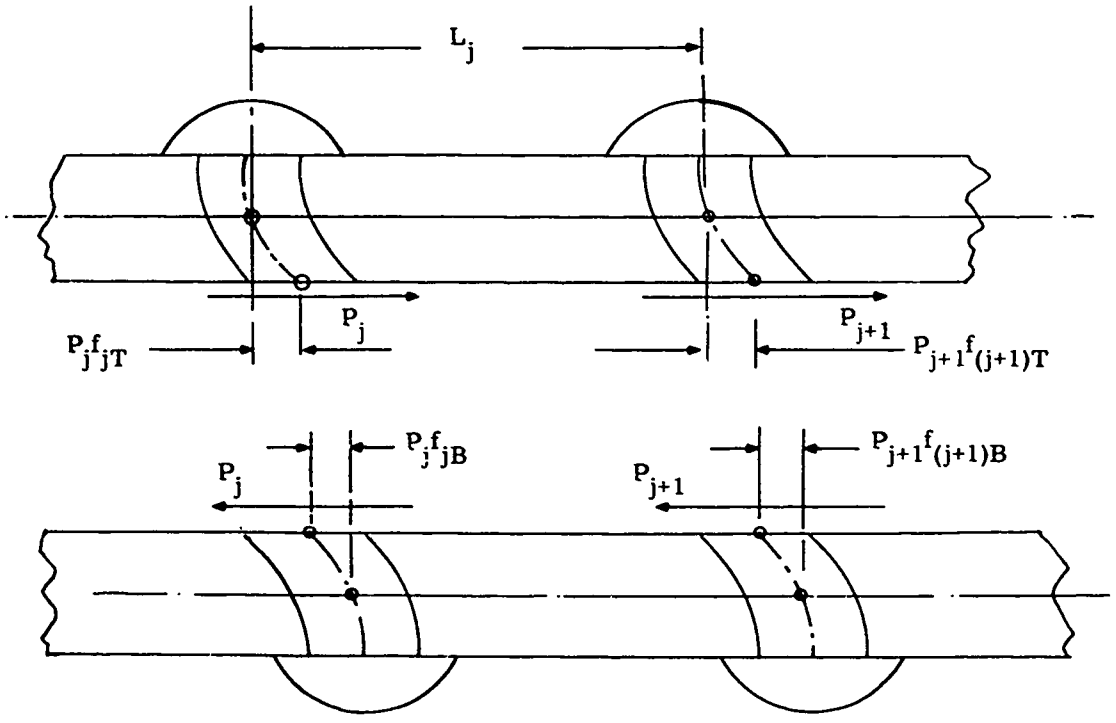


FIGURE 5.1.1-4 DEFORMATION OF THE JOINT DUE TO LOCAL DISTORTIONS OF THE HOLES AND ATTACHMENTS

The compatibility Eq. (5), which constitues N-1 equations, together with the equilibrium Eq. (1) provides N linear algebraic simultaneous equations for N unknown attachment loads, P_j. Since Eq. (5) is in the form of a recurrence equation, it can be used to express all the attachment loads in terms of P_1, the load in the first attachment, that can then be evaluated from the equilibrium equation. Solutions can also be obtained by solving the simultaneous equations directly or by iteration and relaxation techniques. In general, no simple relationships exist between successive P_j's. This difficulty arises from the fact that the recurrence equation coefficients are variable since they are functions of flexibilities and temperature distributions which may vary from bay to bay.

5.1.2 The Special Case of Constant Bay Properties

Consider the case where the flexibilities of the sheets and attachments, as well as the temperature distribution, are the same in each bay (constant bay properties). From a practical point of view this situation is attained when the sheet thicknesses are constant, the attachments are all of the same type, size and spacing, and when the temperature variation through the splice thickness does not vary appreciably in the direction of mechanical loading. The coefficients of the P_j's in the compatibility-recurrence Eq. (5) then become constant and a general solution can be obtained with simple relationships between successive P_j's. Thus, Eq. (5) becomes

5.1.2 (Cont'd)

$$\left[\left(\frac{L}{\overline{AE}}\right)_T + \left(\frac{L}{\overline{AE}}\right)_B\right]\left[\sum_{i=1}^{j} P_i\right] = \Delta\phi - P_j f + P_{j+1} f + X\left(\frac{L}{\overline{AE}}\right)_T , \qquad (1)$$

$$(j=1,\ 2,\ \ldots,\ N-1)$$

where

$$\Delta\phi = \int_0^L (\bar{\epsilon}_T - \bar{\epsilon}_B)\, dx$$

and

$$f = f_T + f_B .$$

Eq. (1), together with the equilibrium Eq. (1) of Paragraph 5.1.1 yields the following solution for the joint loads:

$$\boxed{P_{jN} = \left[A_{jN} + B_{jN}\left(\frac{L}{\overline{AE}}\right)_T \cdot \left(\frac{1}{f}\right)\right] X + B_{jN}\ \frac{\Delta\phi}{f}} \qquad (2)$$

where the subscript jN refers to the j^{th} attachment in a joint of N attachments. Values of the coefficients A_{jN} and B_{jN} vs. Z, where

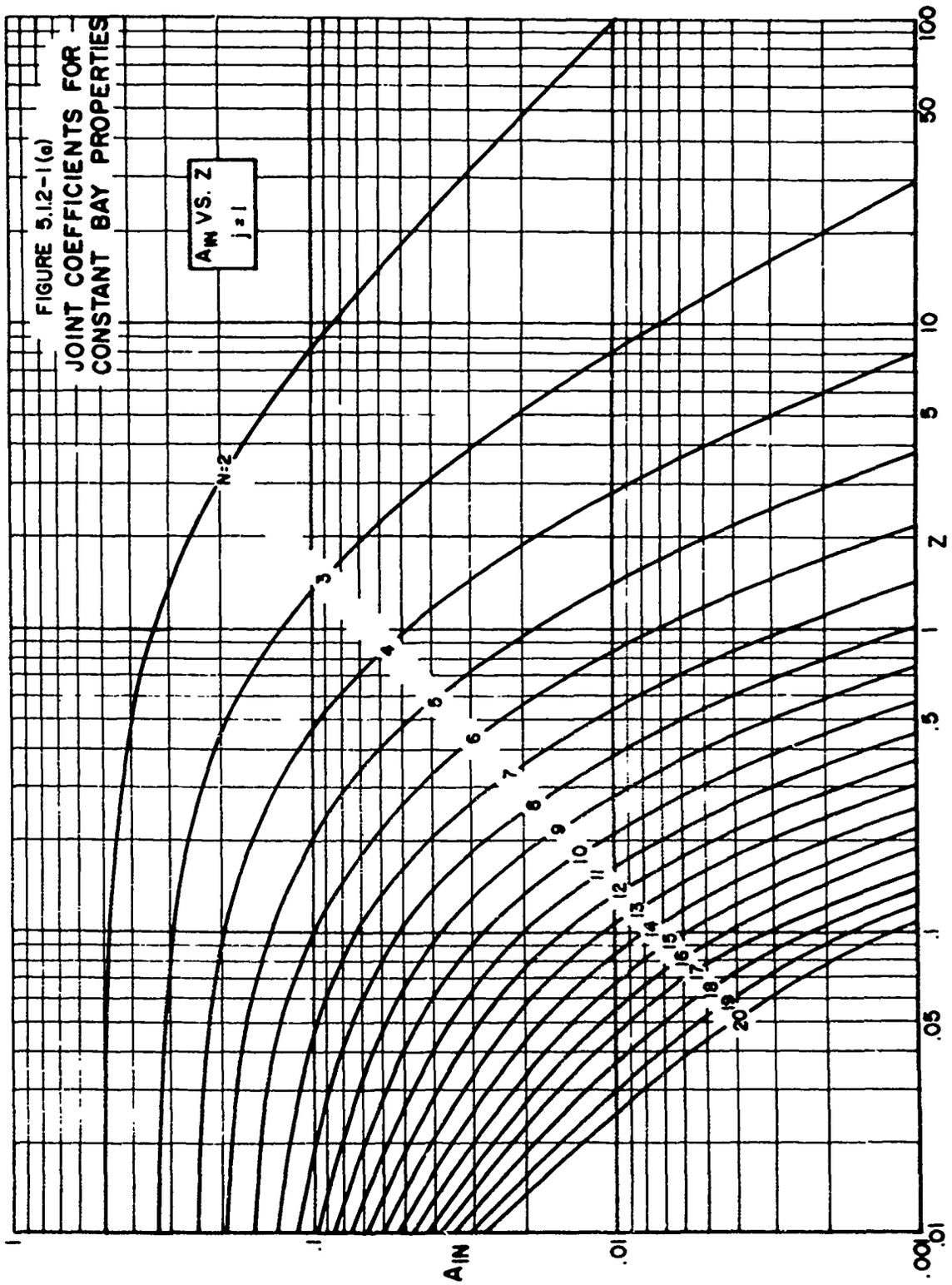
$$Z = \left[\left(\frac{L}{\overline{AE}}\right)_T + \left(\frac{L}{\overline{AE}}\right)_B\right]\left(\frac{1}{f}\right) ,$$

are plotted in Figures 5.1.2-1(a) through -1 (j) for $j = 1 \rightarrow 5$ and $N = 2 \rightarrow 20$. Equations for the numerical calculation of these coefficients are derived in Reference 5-1.

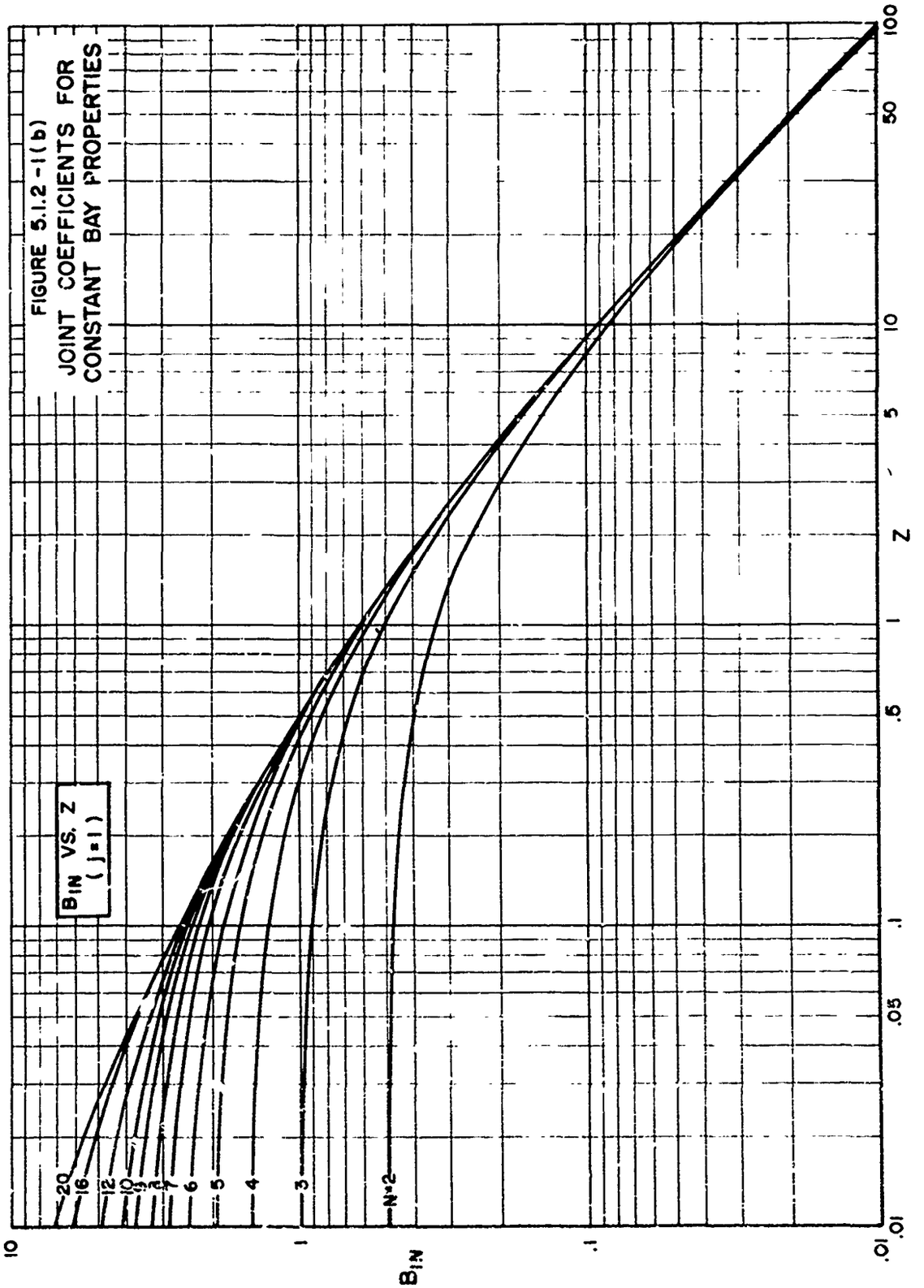
By interchanging the designation of the top and bottom covers, the curves presented can be used to obtain all of the loads in joints having as many as ten attachments. When the total number of attachments exceeds ten, the curves give the loads in the first five attachments from either end of the splice.

The first term on the right hand side of Eq. (2) represents the contribution of mechanical loading to the attachment load. The second term represents the contribution of thermal loading. Thus, Eq. (2) conveniently separates the thermo-mechanical problem into its superimposable components. Note that for constant bay properties the thermal component of load at the center of the joint must be zero from a symmetry argument. Therefore, the center bolt of an odd number of bolts has no load due to thermal effects (Figure 5.1.3-2). Because of this, $B_{23} = B_{35} = B_{47} \ldots = 0$, as indicated in Figures 5.1.2-1. In addition, it is significant that when the joint has constant bay properties, the attachment loads due to thermal loading alone are symmetrical about the center of the splice which yields $B_{1N} = -B_{NN}$, $B_{2N} = -B_{(N-1)N}$, etc.

5. 1. 2 (Cont'd)


FIGURE 5.1.2-1(a)
JOINT COEFFICIENTS FOR
CONSTANT BAY PROPERTIES
A_{MN} VS. Z
j = 1
N=2
3
4
5
6
7
8
9
10
11
12
13
14
15
16
17
18
19
20
100
50
10
5
Z
1
.5
.1
.05
.01
.001
1
.1
.01
AIN

5.1.2 (Cont'd)


FIGURE 5.1.2-1(b)
JOINT COEFFICIENTS FOR
CONSTANT BAY PROPERTIES
BIN VS. Z
(J=1)
20
16
12
10
9
8
7
6
5
4
3
N=2
10
1
.1
.01
BIN
100
50
10
5
1
.5
.1
.05
.01
Z

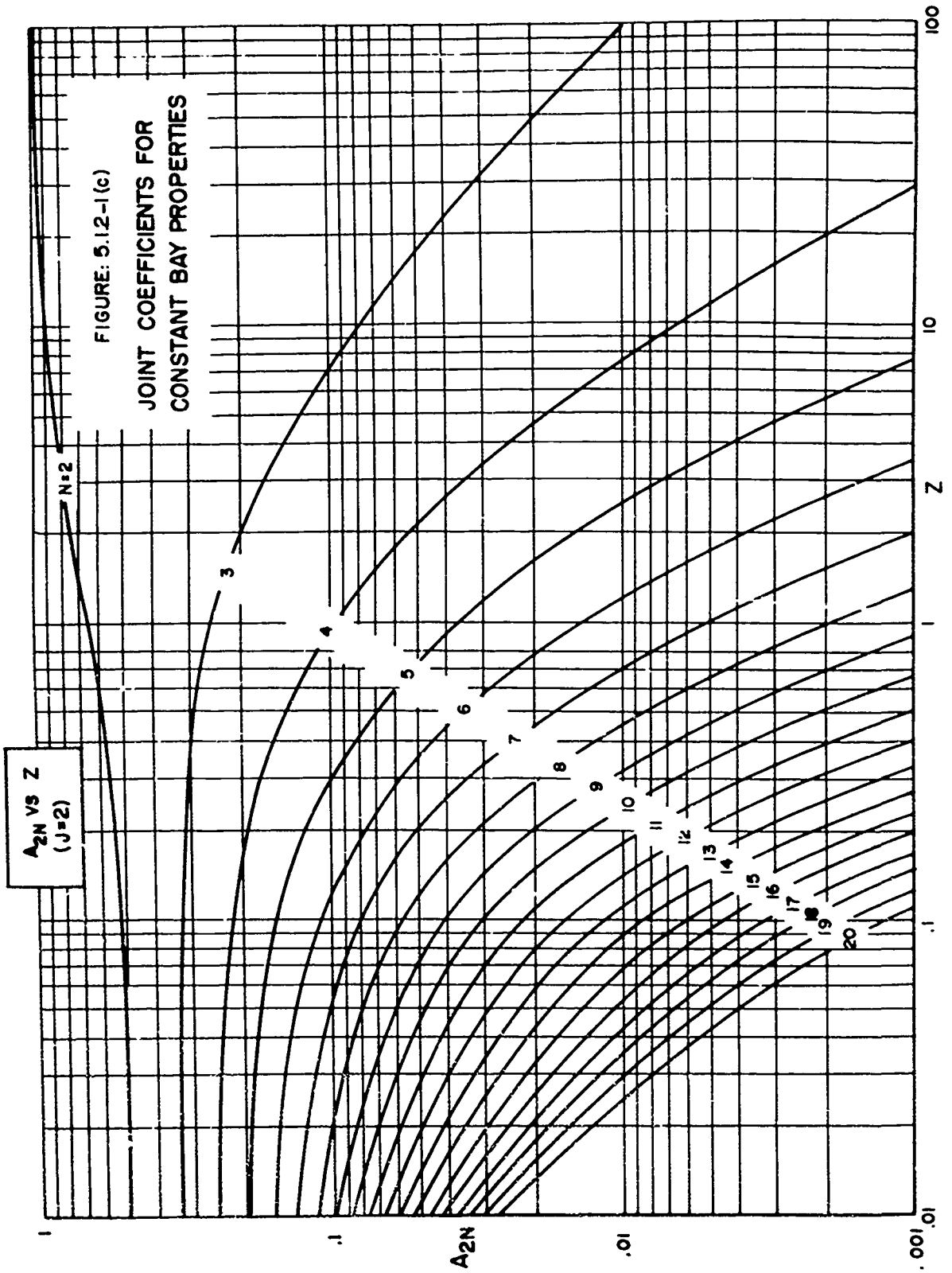
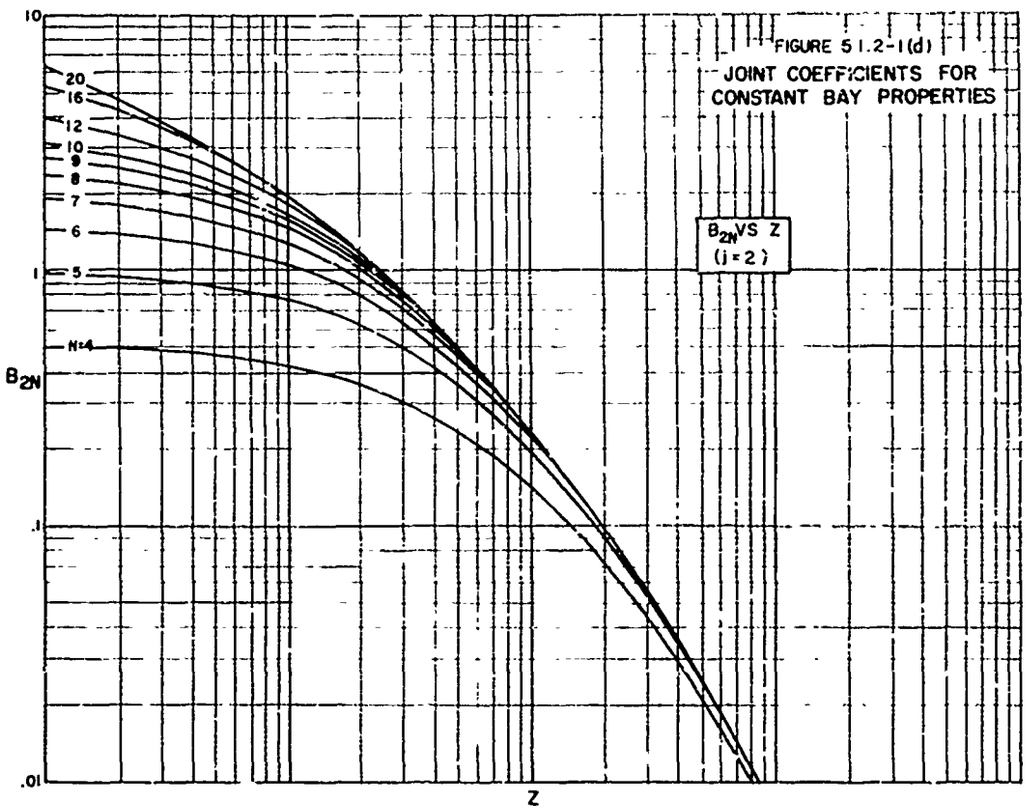
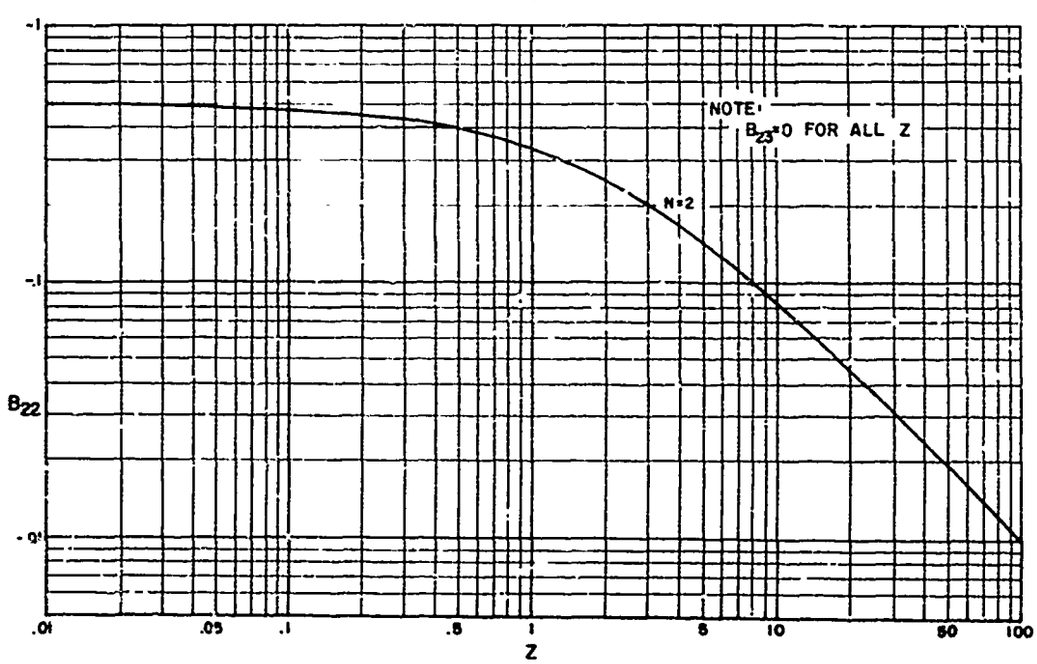
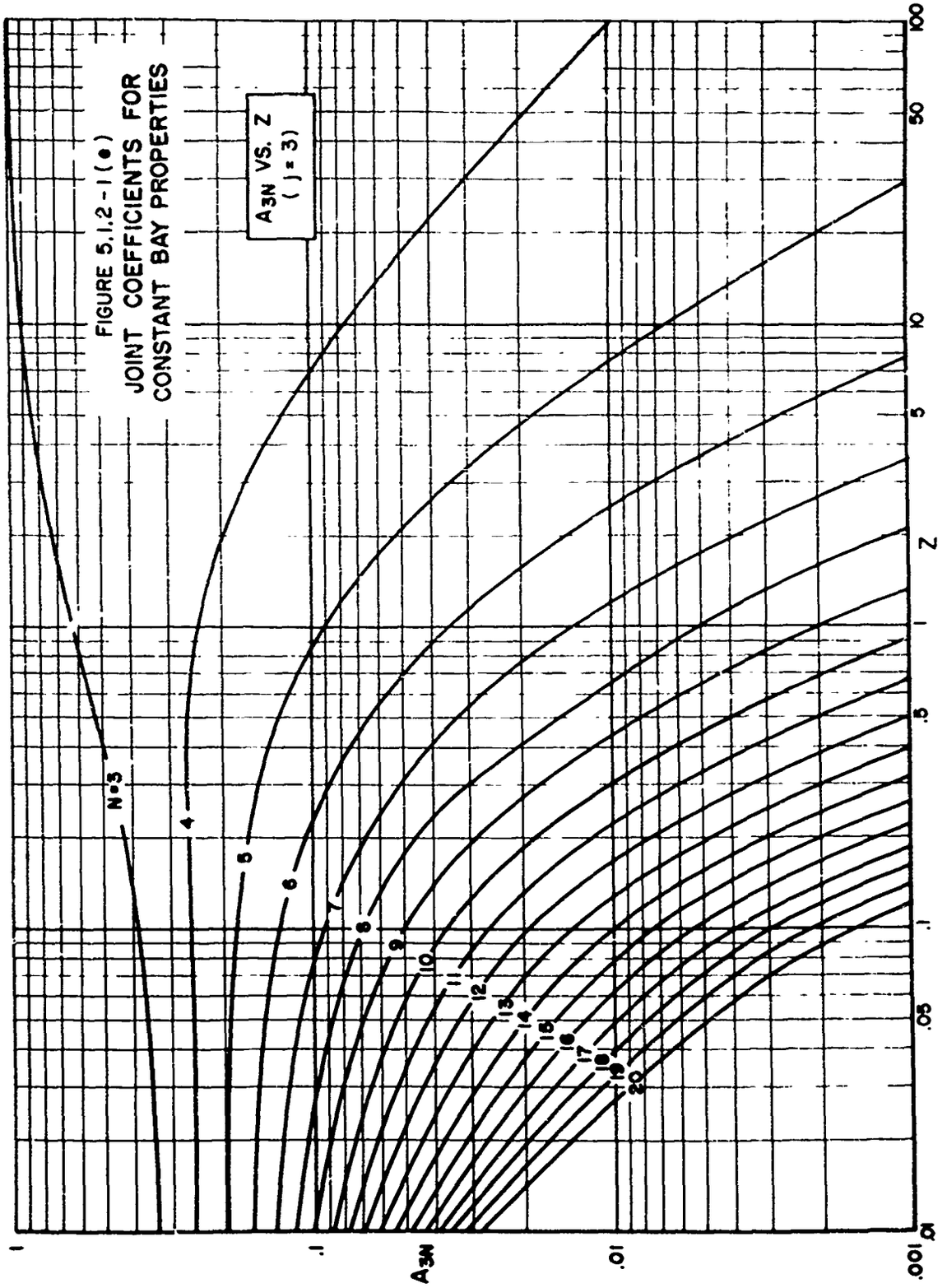

FIGURE: 5.12-1(c)
JOINT COEFFICIENTS FOR
CONSTANT BAY PROPERTIES
A_{2N} VS Z
(J=2)
N=2
3
4
5
6
7
8
9
10
11
12
13
14
15
16
17
18
19
20
1
.1
.01
.001
A_{2N}
100
10
1
.1
.01
Z

FIGURE 5.1.2-1(d)
JOINT COEFFICIENTS FOR
CONSTANT BAY PROPERTIES





5. 1. 2 (Cont'd)


FIGURE 5.1.2-1(●)
JOINT COEFFICIENTS FOR
CONSTANT BAY PROPERTIES
A3N VS. Z
(J = 3)
N=3
4
5
6
7
8
9
10
11
12
13
14
15
16
17
18
19
20
100
50
10
5
1
.5
.1
.05
.01
.001
Z
1
.1
.01
A3N

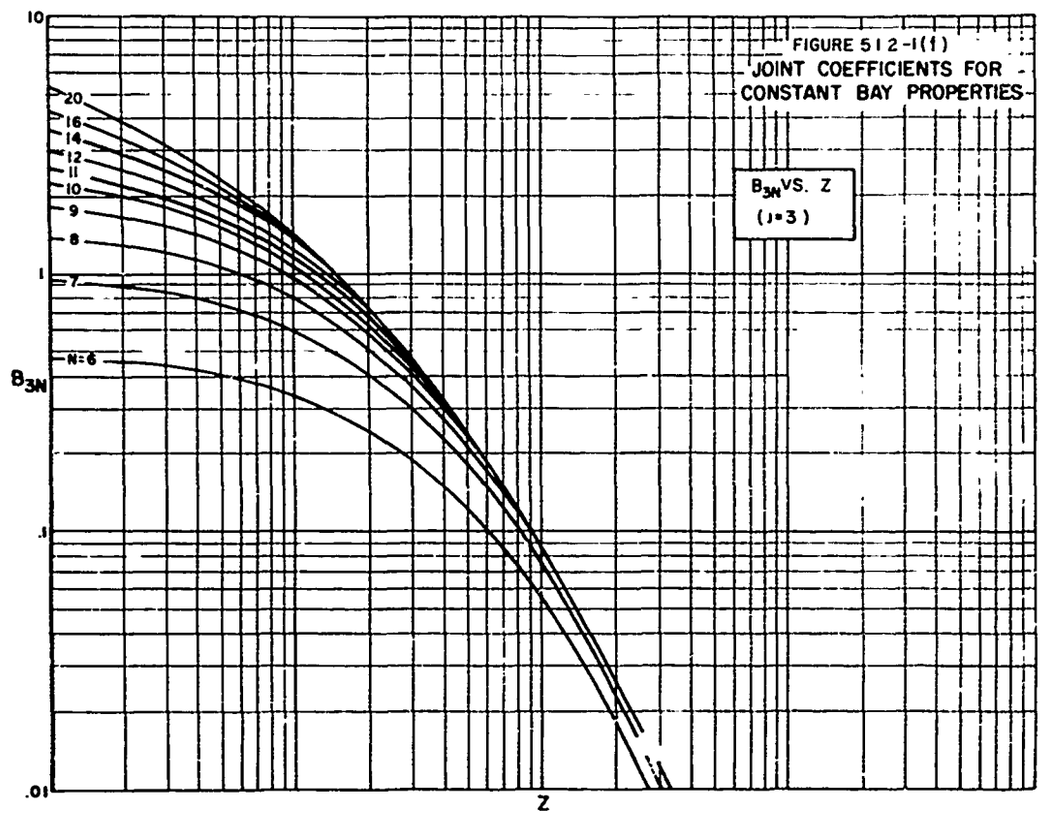
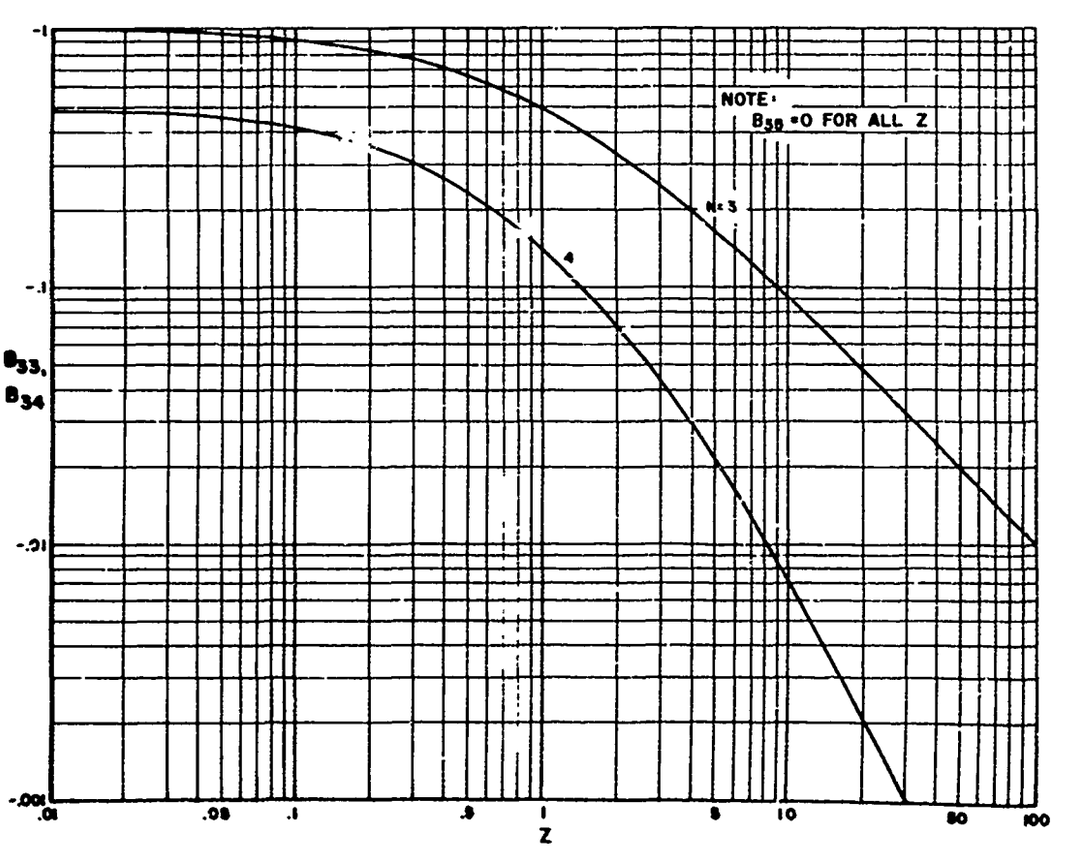
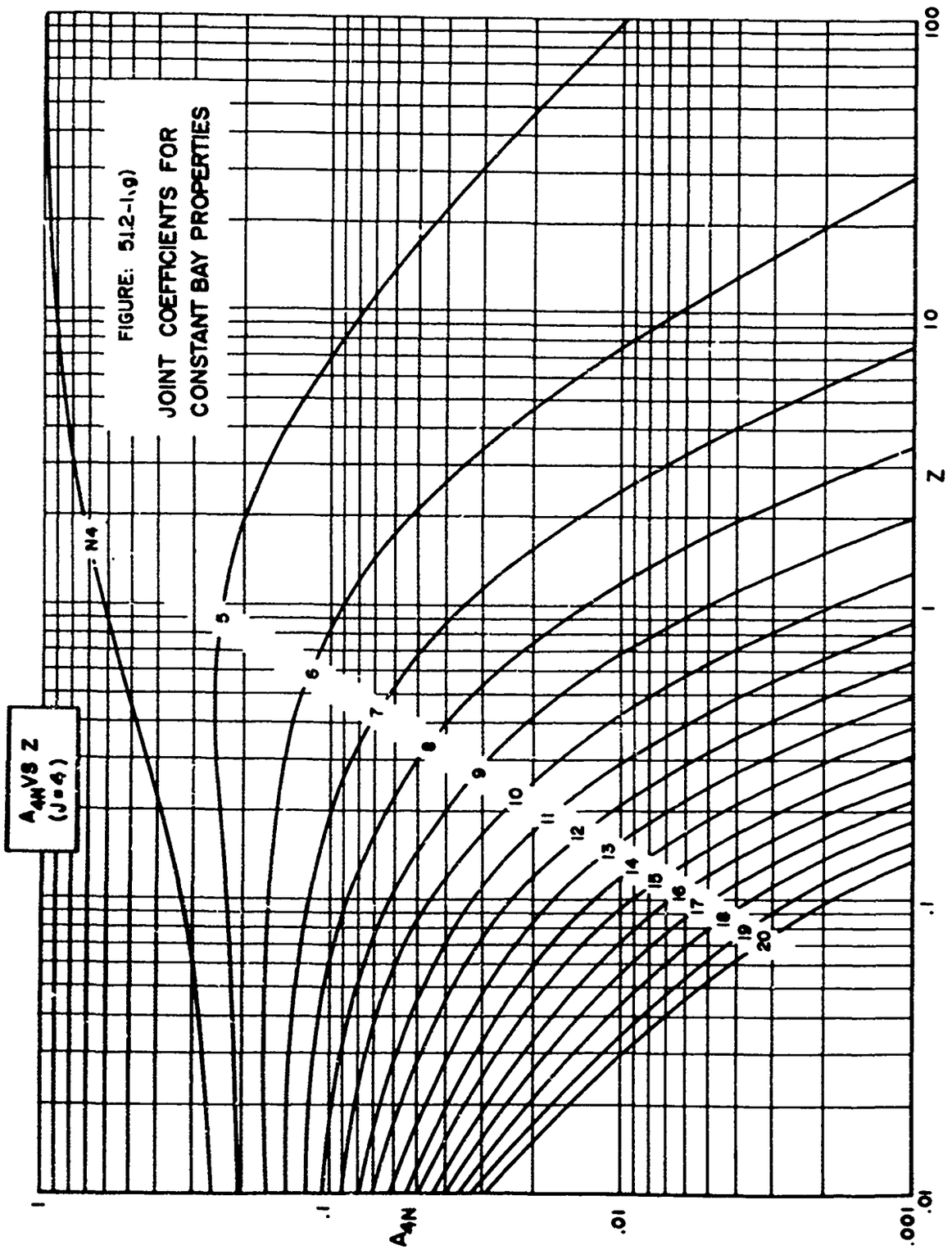


FIGURE 5.1.2-1(1)
JOINT COEFFICIENTS FOR CONSTANT BAY PROPERTIES

B_{3N} VS. Z
(J=3)



5. 1. 2 (Cont'd)


FIGURE: 5.1.2-1(g)
JOINT COEFFICIENTS FOR CONSTANT BAY PROPERTIES
A_{4N} VS Z (J=4)
N4
5
6
7
8
9
10
11
12
13
14
15
16
17
18
19
20
100
10
1
.1
.01
.001
1
.1
.01
.001
A_{4N}
Z

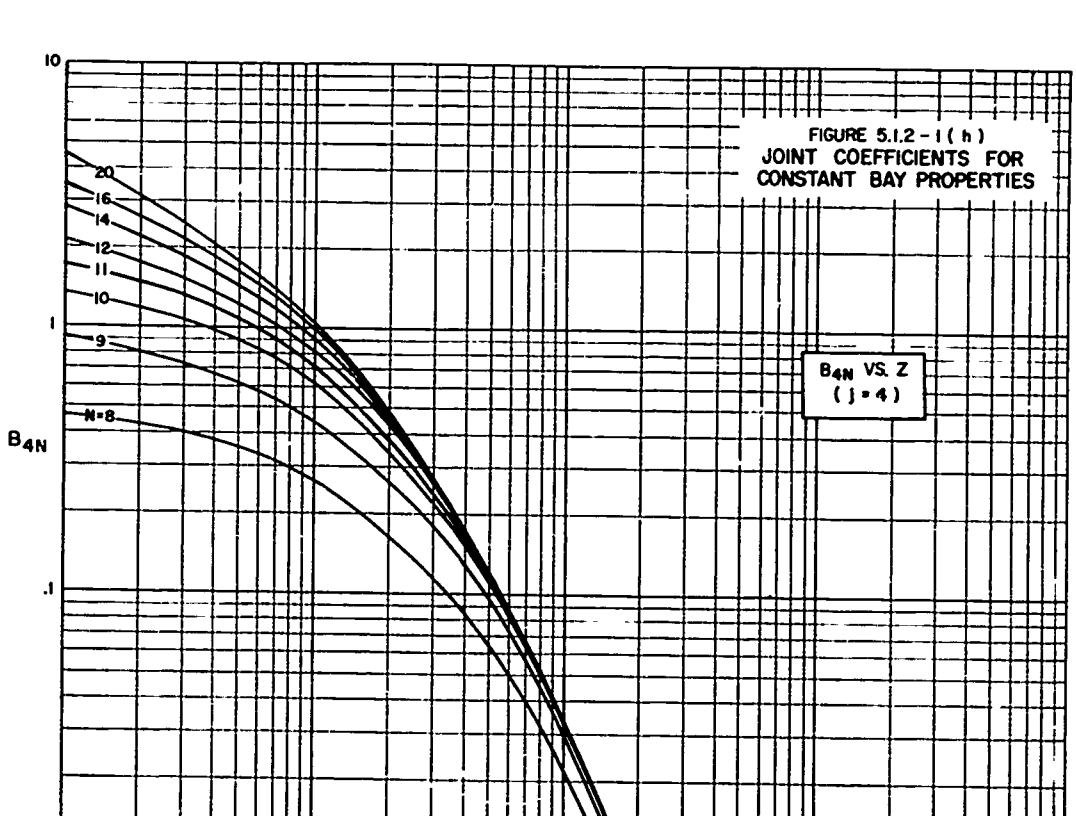
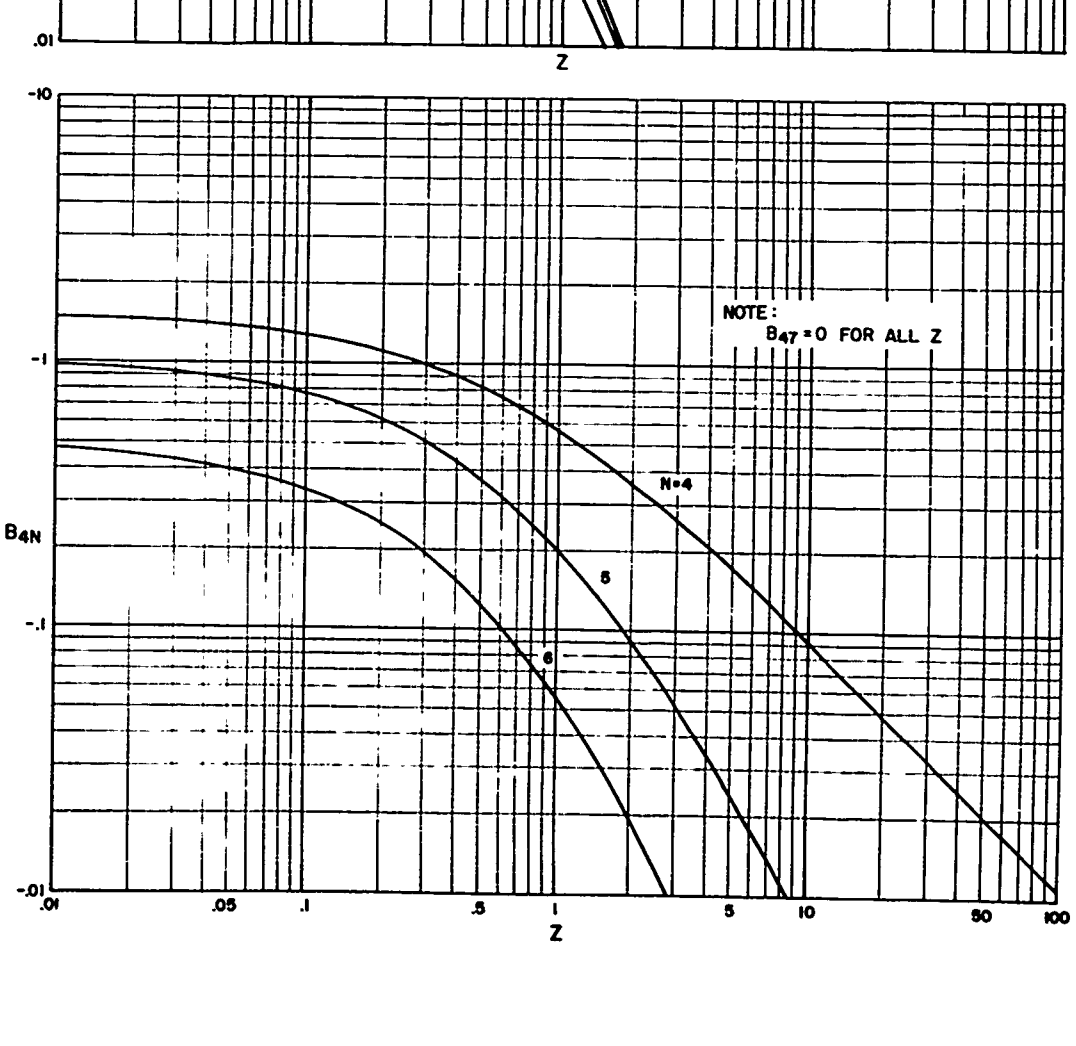


FIGURE 5.1.2-1(h)
JOINT COEFFICIENTS FOR
CONSTANT BAY PROPERTIES



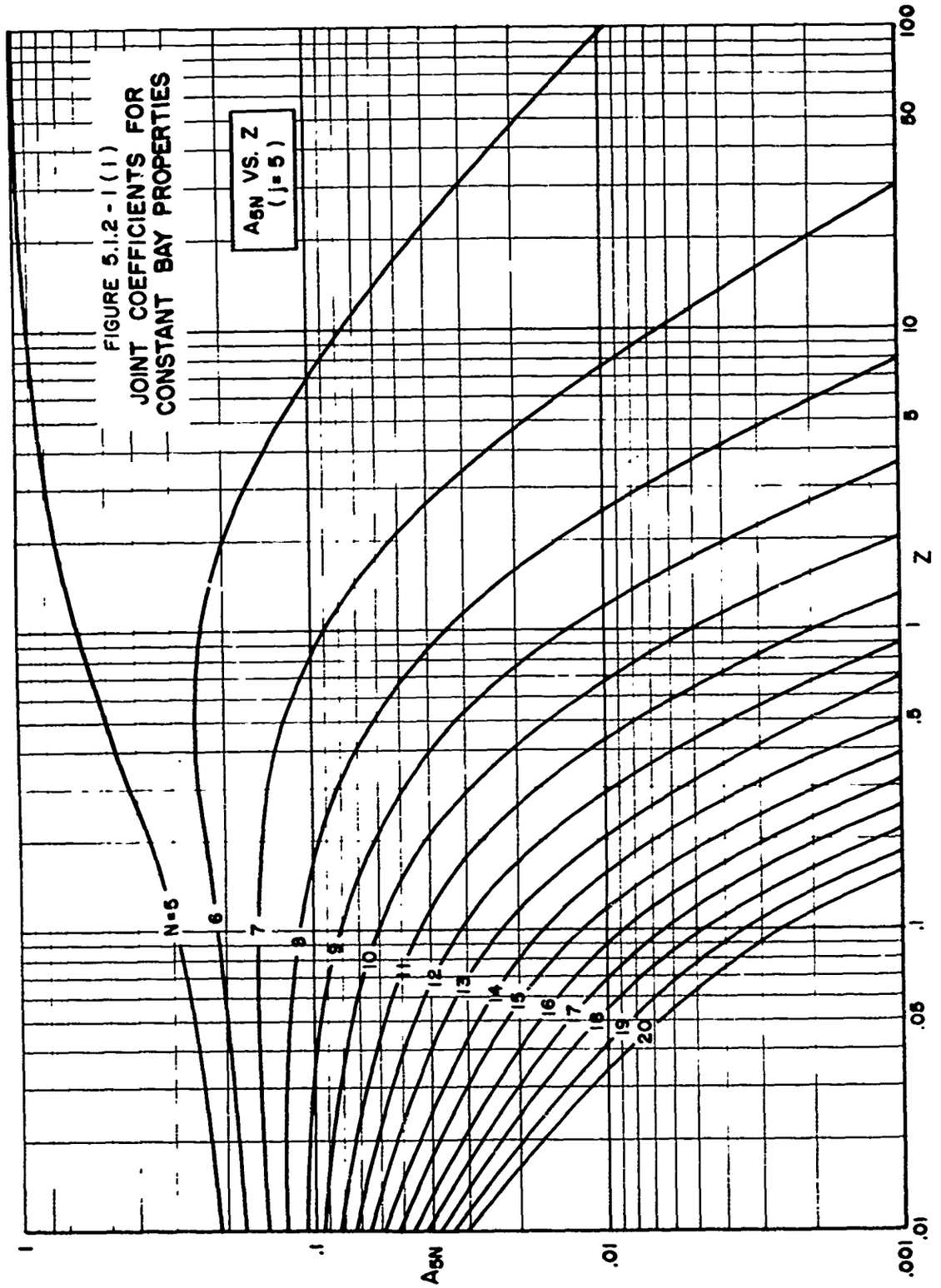
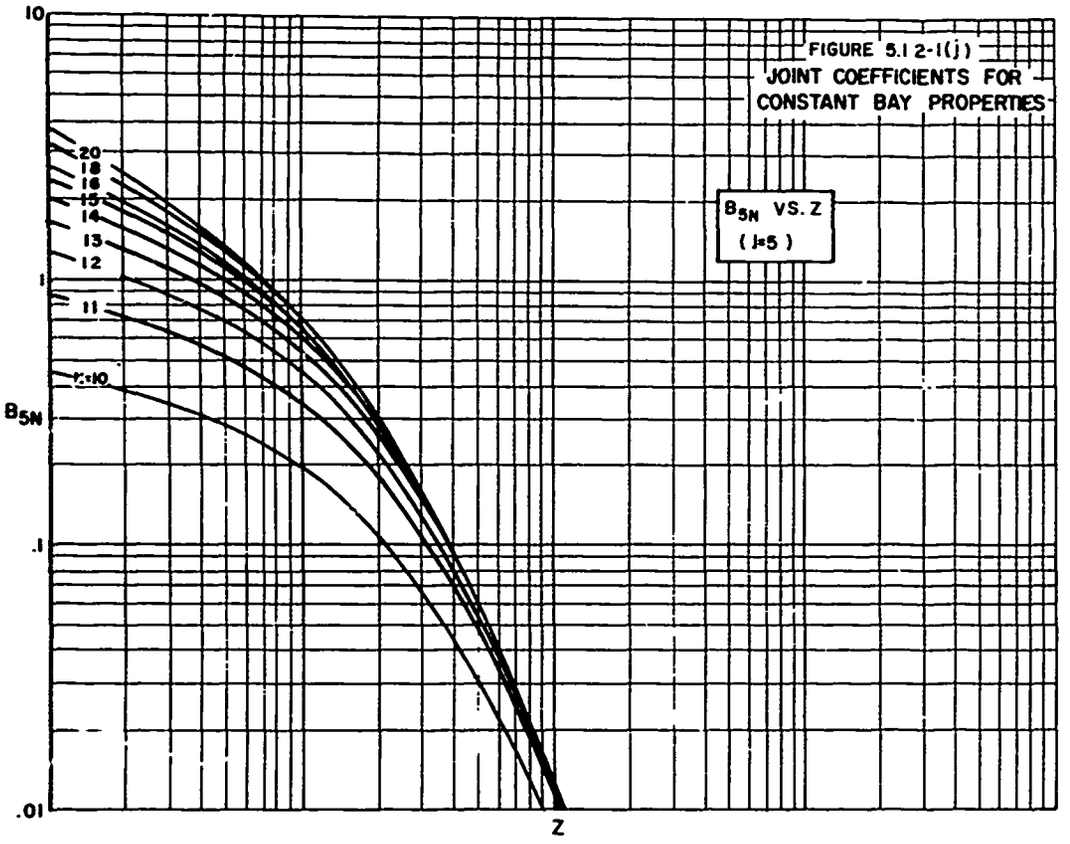
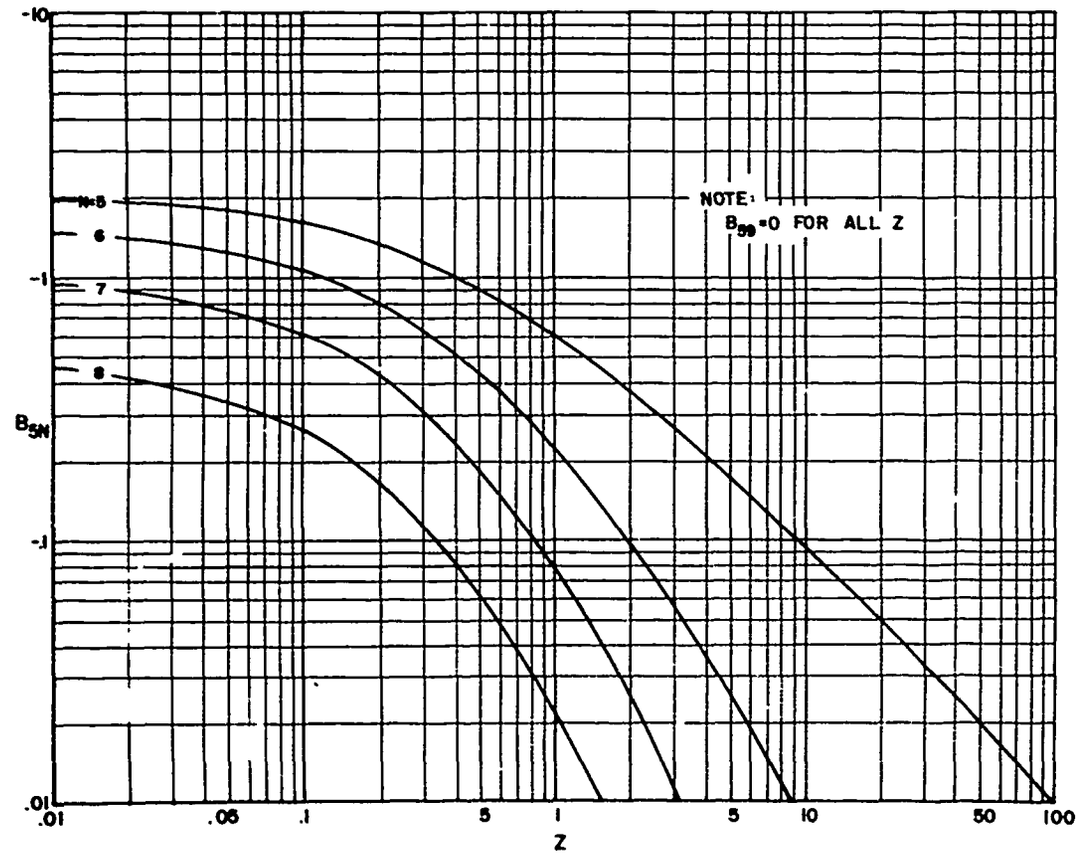

FIGURE 5.1.2-1(1)
JOINT COEFFICIENTS FOR
CONSTANT BAY PROPERTIES
A_{SN} VS. Z
(j=5)
N=5
6
7
8
9
10
11
12
13
14
15
16
17
18
19
20
100
50
10
5
1
.5
.1
.05
.01
.001
Z
1
.1
.01
.001
A_{SN}

FIGURE 5.1 2-1(j)
JOINT COEFFICIENTS FOR
CONSTANT BAY PROPERTIES





5.1.2 (Cont'd)

The solution for the attachment loads in a joint is illustrated by the following problem. A titanium plate and an aluminum plate are bolted together with six attachments as shown in Figure 5.1.2-2(a). Find the attachment loads when the titanium and aluminum plates are subjected to uniform temperature rises of 300°F and 70°F, respectively, and a mechanical load X of 20,000 pounds is applied to the joint.

It is assumed that the bolt hole flexibility has been determined experimentally to be

$$f = .900 \times 10^{-6} \text{ in/lb} \quad \text{(See Sub-section 5.3).}$$

Considering the titanium plate to be the top plate, the plate flexibilities are:

$$\left(\frac{L}{AE}\right)_T = \frac{1}{(1.5)(.125)(15)\times 10^6} = .356 \times 10^{-6} \text{ in/lb,}$$

$$\left(\frac{L}{AE}\right)_B = \frac{1}{(1.5)(.250)(10)\times 10^6} = .267 \times 10^{-6} \text{ in/lb .}$$

Since the temperature rise in each sheet is uniform, the incompatibility due to unrestrained thermal expansion in each bay is given by

$$\begin{aligned} \Delta\phi &= \left[(\alpha\Delta T)_T - (\alpha\Delta T)_B\right] L \\ &= \left[6.5(300) - 12(70)\right] (1) \times 10^{-6} \\ &= 1110 \times 10^{-6} \text{ inch.} \end{aligned}$$

The above quantities are now substituted into Eq. (2) resulting in

$$P_{jN} = \left[A_{jN} + B_{jN} \left(\frac{.356}{.900}\right) \right] (20,000) + B_{jN} \left(\frac{1110}{.900}\right)$$

or

$$P_{jN} = 20,000\, A_{jN} + 9135\, B_{jN} . \qquad (3)$$

The coefficients A_{jN} and B_{jN} are now determined from Figures 5.1.2-1 for

$$Z = \left[\left(\frac{L}{AE}\right)_T + \left(\frac{L}{AE}\right)_B\right]\left(\frac{1}{f}\right) = (.356 + .267)\left(\frac{1}{.900}\right) = .692$$

and N = 6.

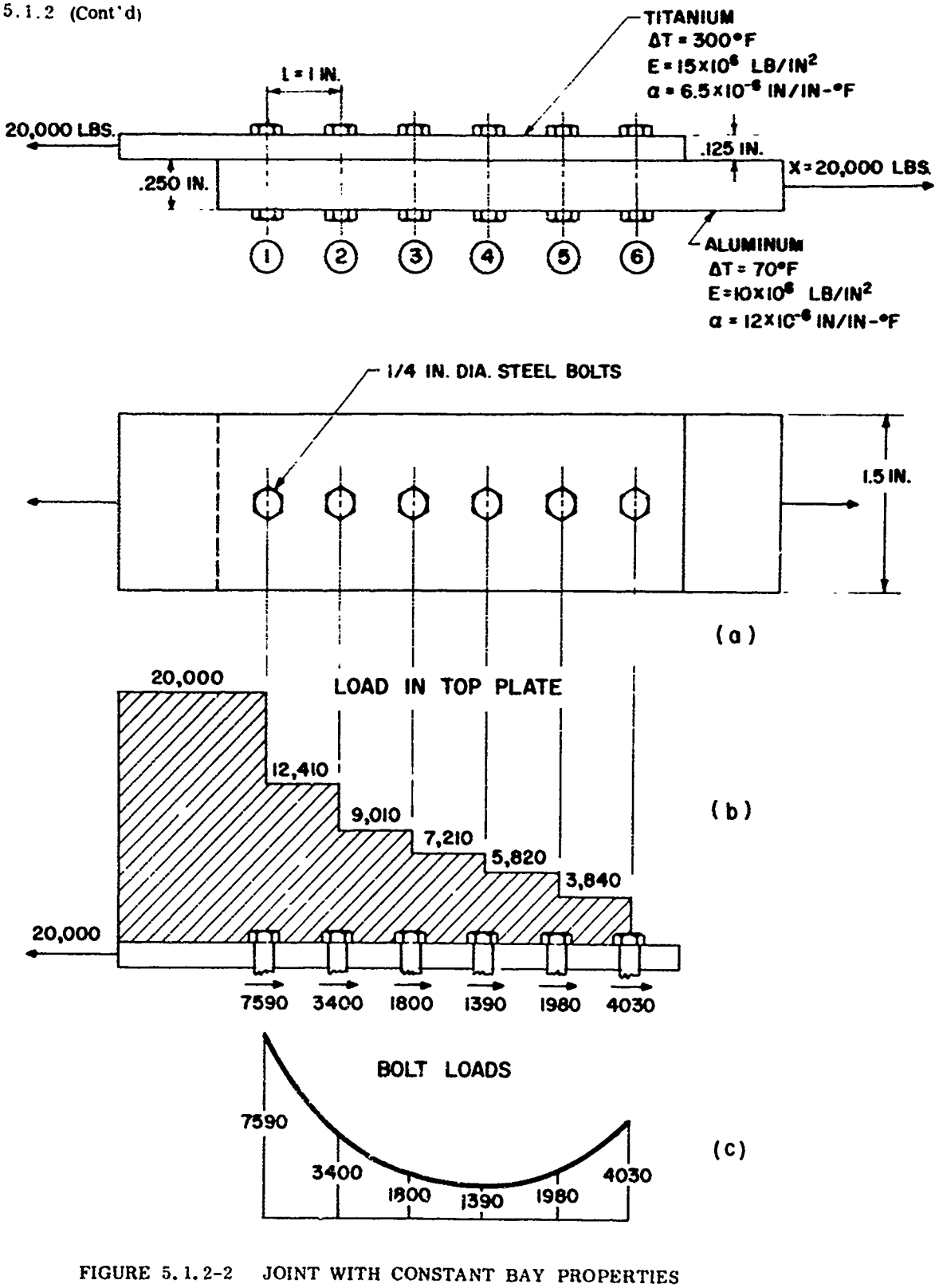


FIGURE 5.1.2-2 JOINT WITH CONSTANT BAY PROPERTIES

5.1.2 (Cont'd)

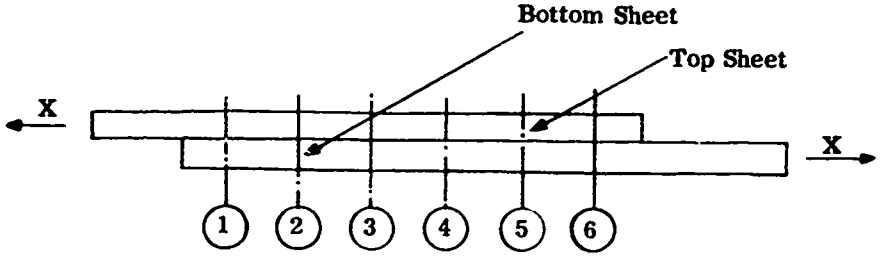
A_{16} = .0140 Figure 5.1.2-1(a)
A_{26} = .0239 -1(c)
A_{36} = .0500 -1(e)
A_{46} = .1090 -1(g)
A_{56} = .2450 -1(i)

B_{16} = .8000 Figure 5.1.2-1(b)
B_{26} = .3200 -1(d)
B_{36} = .0880 -1(f)
B_{46} = −.0860 -1(h)
B_{56} = −.3200 -1(j)

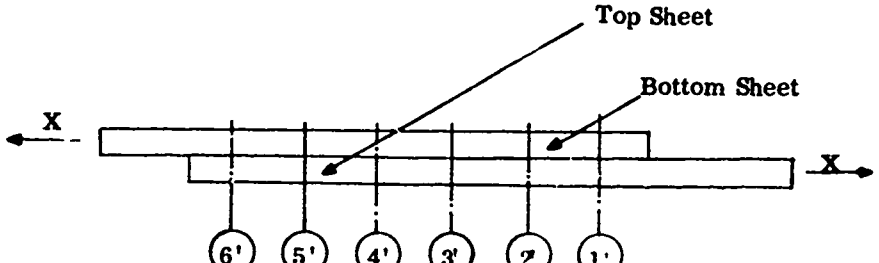
(4)

The curves give values of A_{jN} and B_{jN} up to $j = 5$ and the splice under consideration has 6 attachments. In order to obtain the coefficients for the last attachment, the designation of the top and bottom plates as shown in Figure 5.1.2-3 must be interchanged such that the last attachment ($j = 6$) in the original designation becomes the first attachment ($j = 1$) in the interchanged designation.

Denoting quantities in the interchanged designation by primes, results in



(a) Original Designation



(b) Interchanged Designation

FIGURE 5.1.2-3 ALTERNATE TOP AND BOTTOM SHEET DESIGNATION

5.1.2 (Cont'd)

$f' = f = .900 \times 10^{-6}$ in/lb

$\left(\frac{L}{AE}\right)'_T = \left(\frac{L}{AE}\right)_B = .267 \times 10^{-6}$ in/lb

$\left(\frac{L}{AE}\right)'_B = \left(\frac{L}{AE}\right)_T = .356 \times 10^{-6}$ in/lb

$\Delta\phi' = -\Delta\phi = -1110 \times 10^{-6}$ in

$Z' = Z = .692$

and from Eq. (2),

$$P'_{jN} = \left[A'_{jN} + B'_{jN}\left(\frac{.267}{.900}\right)B'_{jN}\right] (20,000) - B'_{jN}\left(\frac{1110}{.900}\right)$$

or

$$P'_{jN} = 20,000\,A'_{jN} + 4693\,B'_{jN} \qquad (5)$$

As in expressions (4).

$$\left.\begin{aligned} A'_{16} &= A_{16} = .0140 \\ B'_{16} &= B_{16} = .8000 \end{aligned}\right\} \quad (6)$$

From (3) and (4),

$P_{16} = 20,000\ (.0140) + 9135\ (.8000) = 7590$ lbs

$P_{26} = 20,000\ (.0239) + 9135\ (.3200) = 3400$ lbs

$P_{36} = 20,000\ (.0500) + 9135\ (.0880) = 1800$ lbs

$P_{46} = 20,000\ (.1090) + 9135\ (-.0860) = 1390$ lbs

$P_{56} = 20,000\ (.2450) + 9135\ (-.3200) = 1980$ lbs,

and from (5) and (6).

$$P_{66} = P'_{16} = 20,000(.0140) + 4693\ (.8000) = 4030 \text{ lbs}.$$

Equilibrium Check

$$\sum_{j=1}^{N} P_j = 20,190 \text{ lbs} \sim 20,000 \text{ lbs}$$

$$\% \text{ difference} = \frac{190}{20,000} \times (100) = .95\%$$

5.1.2 (Cont'd)

The load in the top plate and the attachment loads are plotted in Figures 5.1.2-2(b) and (c). The results show that the maximum load occurs in the first attachment and that the two end attachments carry more than half of the total applied mechanical load. When the bay properties are constant the maximum load always occurs in an end attachment. However, as discussed in Paragraph 5.1.3, when plastic deformations occur in the vicinity of the bolt holes, the bolts tend to carry equal loads.

5.1.3 Constant Bay Properties - Rigid Sheets

Now the case is considered in which the sheets have negligible axial deformation as compared to the deformations caused by local distortions of the holes and attachments (rigid sheets).

From a practical point of view, this condition is realized when the plates are thick and the attachments have small diameters -- or, when local yielding causes the effective attachment-hole flexibility factor to become large as compared to the axial flexibility of the sheets.

In the limiting case,

$$\left(\frac{L}{AE}\right)_T \longrightarrow 0 \quad \text{and} \left(\frac{L}{AE}\right)_B \longrightarrow 0$$

and the compatibility Eq. (1) of Paragraph 5.1.2 reduces to

$$P_{j+1} = P_j - \frac{\Delta\phi}{f}$$

or, in terms of the first attachment load .

$$P_j = P_1 - (j-1)\frac{\Delta\phi}{f} . \qquad (1)$$

P_1 is obtained by summing Eq. (1) over the total number of attachments:

$$\sum_{j=1}^{N} P_j = X = NP_1 - \frac{\Delta\phi}{f} \sum_{j=1}^{N} (j-1)$$

$$= NP_1 - \frac{N}{2}(N-1)\frac{\Delta\phi}{f}$$

or

$$P_1 = \frac{X}{N} + \frac{(N-1)}{2}\frac{\Delta\phi}{f} . \qquad (2)$$

Substituting (2) in (1) results in

$$\boxed{P_j = \frac{X}{N} + \left(\frac{N+1}{2} - j\right)\frac{\Delta\phi}{f}} \qquad (3)$$

Equation (3) gives the attachment loads for a given thermal and mechanical loading and a known value of attachment-hole flexibility, f .

5.1.3 (Cont'd)

The solution shows that for the case of constant bay properties and infinitely rigid sheets, the mechanical load distributes equally to the attachments while attachment loads due to thermal effects vary symmetrically about the transverse centerline of the joint with magnitudes inversely proportional to the attachment-hole flexibility (Figure 5.1.3.2).

For high loads which cause extensive plastic deformation in the vicinity of the attachment holes, the effective attachment-hole flexibility may become large as compared to the sheet flexibility, in which case the solution of Eq. (3) is approached. If these plastic effects become large enough, the increase in f tends to wipe out the effects of thermal loading with the result that:

$$P_j \sim \frac{X}{N}$$

This indicates that near the failure of ductile materials, the mechanical load tends to distribute equally to the attachments regardless of temperature distribution. The effect of an infinite sheet rigidity for the splice of Figure 5.1.2-2(a) upon attachment loads may be calculated where, as before in Paragraph 5.1.2,

$$X = 20,000 \text{ lbs}$$
$$f = .900 \times 10^{-6} \text{ in/lb}$$
$$\Delta\phi = 1110 \times 10^{-6} \text{ in.}$$
$$N = 6 \ .$$

However,

$$\left(\frac{L}{AE}\right)_T = \left(\frac{L}{AE}\right)_B = 0 \ .$$

Substituting the above in Eq. (3),

$$P_j = \frac{20,000}{6} + \left(\frac{6+1}{2} - j\right) \frac{1110}{.900}$$

or

$$P_j = 3,333 + (3.5 - j)\, 1233 \ .$$

Thus:

$$P_1 = 3,333 + (3.5-1)\ 1,233 = 6,420 \text{ lbs}$$
$$P_2 = 3,333 + (3.5-2)\ 1,233 = 5,180 \text{ lbs}$$
$$P_3 = 3,333 + (3.5-3)\ 1,233 = 3,950 \text{ lbs}$$
$$P_4 = 3,333 + (3.5-4)\ 1,233 = 2,720 \text{ lbs}$$
$$P_5 = 3,333 + (3.5-5)\ 1,233 = 1,480 \text{ lbs}$$
$$P_6 = 3,333 + (3.5-6)\ 1,233 = 250 \text{ lbs}$$

and

$$\sum_{j=1}^{6} P_j = 20,000 \text{ lbs}$$

5.1.3 (Cont'd)

The results are plotted in Figure 5.1.3-1. It is seen that the attachment loads vary linearly with the distance along the splice. A comparison with the flexible sheet results of Figure 5.1.2-2 shows that the attachment loads in the rigid sheet solution drop off constantly as one proceeds from the first to the last attachment, while in the flexible sheet solution the attachment loads are minimum at the center of the splice and build up toward the ends.

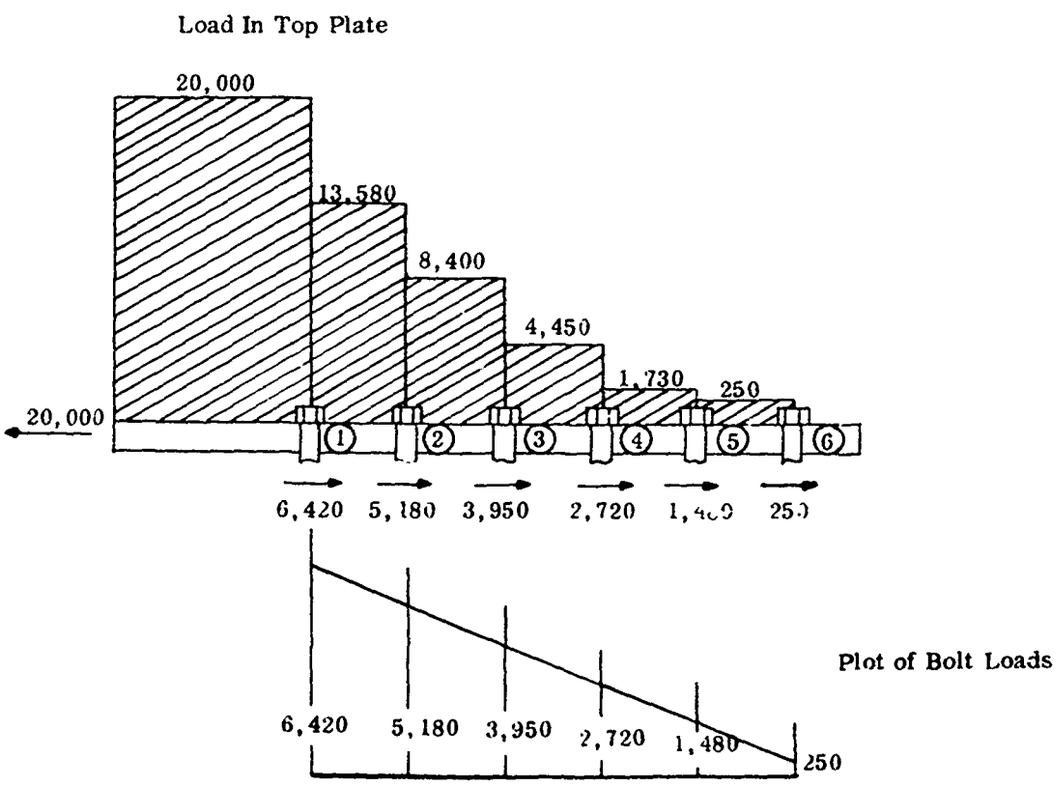
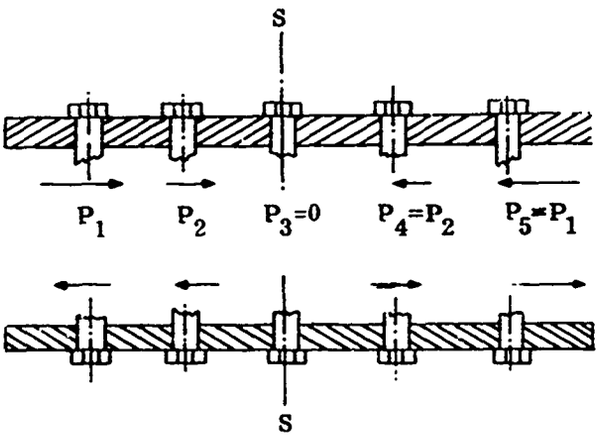


FIGURE 5.1.3-1 RIGID SHEET SOLUTION

5.1.3 (Cont'd)

Qualitatively, the difference in the results is due primarily to the effect of thermal loading (Figure 5.1.3-2) which becomes more severe as the sheet rigidities increase.



The Attachment Loads Are Symmetrical About The Line Of Symmetry S-S and $P_1 > P_2$.

FIGURE 5.1.3-2 ATTACHMENT LOADS DUE TO THERMAL LOADING WHEN THE JOINT HAS CONSTANT BAY PROPERITIES

5.1.4 Constant Bay Properties - Rigid Attachments

The attachments may be considered rigid if the attachment-hole flexibility is negligible when compared to the axial flexibility of the sheets as, for example, when the sheets consist of flexible (soft) materials and the attachments are housed in large diameter rigid bushings. Although this situation seldom occurs in practice, the problem is of interest from a qualitative point of view, since it represents another limiting case of the general one-dimensional problem. In the limiting case, $f \longrightarrow 0$ and the compatibility Eq. (1) of Paragraph 5.1.2 yields

$$P_1 = \frac{\Delta\phi + X\left(\frac{L}{AE}\right)_T}{\left(\frac{L}{AE}\right)_T + \left(\frac{L}{AE}\right)_B} \tag{1}$$

$$P_2 = P_3 = P_4 = \ldots . P_{N-1} = 0 .$$

Thus, from the equilibrium equation,

$$P_N = X - P_1 = \frac{X\left(\frac{L}{AE}\right)_B - \Delta\phi}{\left(\frac{L}{AE}\right)_T + \left(\frac{L}{AE}\right)_B} \tag{2}$$

The above equations show that for infinitely rigid pins and constant bay properties, the two end attachments carry all the thermal and mechanical loads.

When the upper and lower sheets are each heated to different uniform temperatures, then

$$\Delta\phi = \left[(\alpha\Delta T)_T - (\alpha\Delta T)_B\right] L$$

so that

$$P_1 = \frac{X + (AE)_T\left[(\alpha\Delta T)_T - (\alpha\Delta T)_B\right]}{1 + \frac{(AE)_T}{(AE)_B}} \tag{3}$$

$$P_N = X - P_1$$

and the intermediate attachment loads are all zero.

5.1.4 (Cont'd)

The effect of infinitely rigid attachments for the splice of Figure 5.1.2-2(a) upon the attachment loads may be calculated where, as before in Paragraph 5.1.2,

$$X = 20,000 \text{ lbs.}$$

$$\frac{L}{(AE)_T} = .356 \times 10^{-6} \text{ in/lb}$$

$$\frac{L}{(AE)_B} = .267 \times 10^{-6} \text{ in/lb}$$

$$I \cdot \left[(\alpha \Delta T)_T - (\alpha \Delta T)_B \right] = 1110 \times 10^{-6} \text{ inch}$$

but $f = 0$.

Substituting the above quantities in Eq. (3) gives

$$P_1 = \frac{20,000 + \left(\frac{1}{.356}\right)(1110)}{1 + \frac{.267}{.356}} = 13,200 \text{ lbs.}$$

For rigid attachments as stated above,

$$P_2 = P_3 = P_4 = P_5 = 0 \ ,$$

and for equilibrium

$$P_6 = 20,000 - 13,200 = 6,800 \text{ lbs.}$$

5.1.5 The Influence of "Slop" on the Load Distribution

The presence of "slop", due to manufacturing tolerance and differential thermal expansions between the plate holes and attachments, affects load distribution through the basic joint compatibility equation.

The "slop" at each attachment is indicated by the difference in diameters of the plate hole and attachment (Figure 5.1.5-1), as expressed by

$$e = e_{mfg} + e_{temp}; \quad e > 0 \text{ (i.e., e must always be a clearance)},$$

where

e_{mfg} = initial room temperature manufacturing tolerance (clearance or interference. Interference has negative sign.)

and

e_{temp} = thermal slop (clearance or interference due to differential thermal expansion between plate holes and attachments)

$$= \left[(\alpha T)_{sheet} - (\alpha T)_{attach.}\right] D_{hole} \cdot$$

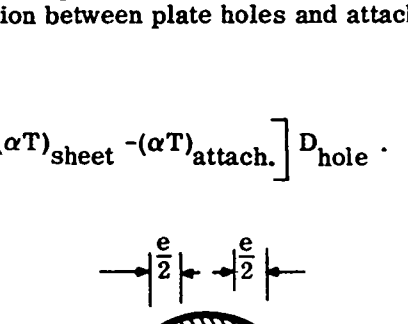


FIGURE 5.1.5-1

FIGURE 5.1.5-1 ATTACHMENT IN AN OVERSIZE HOLE

As discussed in Paragraph 5.1.1, the joint displacements (for compatibility purposes) have been measured from a datum defined by the initial spacing between the centerlines of adjacent attachments. When slop is present, and thermal and mechanical loads are applied to the joint, the attachments are displaced from the centers of the holes until they bear up against sheet material, as shown in Figure 5.1.5-2.

5.1.5 (Cont'd)

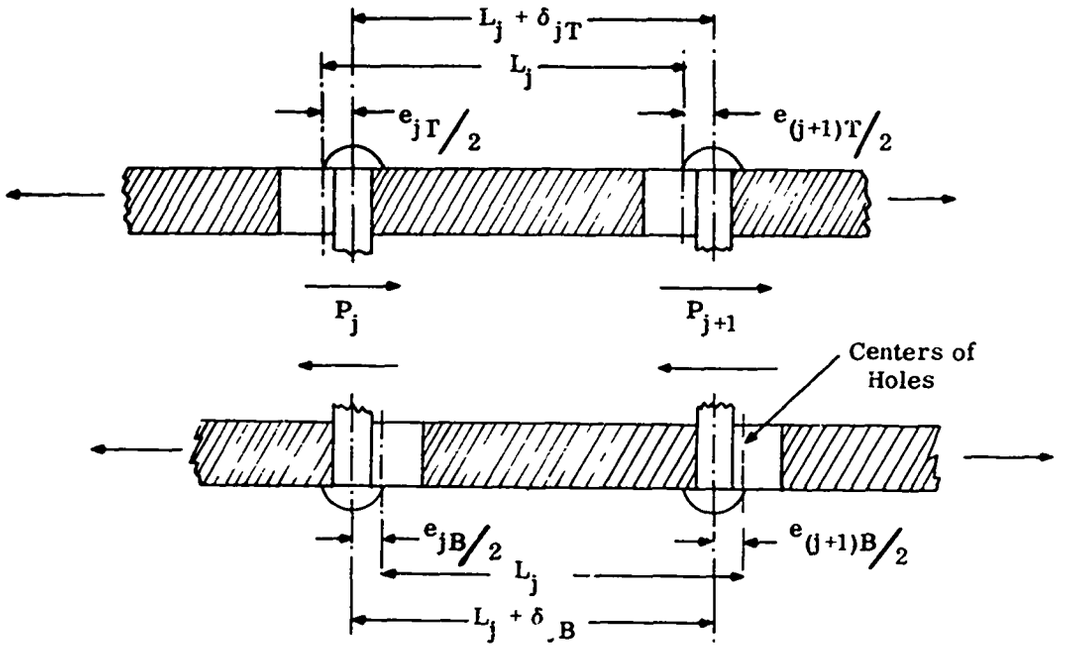


FIGURE 5.1.5-2 ATTACHMENT DISPLACEMENTS DUE TO SLOP - POSITIVE LOADS

The algebraic sign of the slop displacements depends on the direction of the joint loads. For the top sheet, the displacement between adjacent attachments is given by

$$\delta_{jT} = \frac{-e_{jT}}{2} \frac{P_j}{|P_j|} + \frac{e_{(j+1)T}}{2} \frac{P_{j+1}}{|P_{j+1}|}$$

and for the bottom sheet, by

$$\delta_{jB} = \frac{e_{jB}}{2} \frac{P_j}{|P_j|} - \frac{e_{(j+1)B}}{2} \frac{P_{j+1}}{|P_{j+1}|} ,$$

where a positive δ increases the spacing between adjacent attachments and

$\frac{P}{|P|} = +1$ for a positive attachment load,

$\frac{P}{|P|} = -1$ for a negative attachment load.

The incompatibility due to slop is therefore given by

$$\Delta\delta_j = \delta_{jT} - \delta_{jB} = \frac{1}{2}(e_T + e_B)_{j+1} \frac{P_{j+1}}{|P_{j+1}|} - \frac{1}{2}(e_T + e_B)_j \frac{P_j}{|P_j|} \qquad (1)$$

5.1.5 (Cont'd)

Equation (1) is significant in that it brings out the very nature of the slop problem. Consider, for example, that the slop is the same at all attachments. In this case, Eq. (1) reduces to

$$\Delta\delta_j = \frac{1}{2}(e_T + e_B)\left[\frac{P_{j+1}}{|P_{j+1}|} - \frac{P_j}{|P_j|}\right] . \tag{2}$$

As the mechanical loads applied to the joint increase, all the attachment loads tend to act in the same direction (opposite to the externally applied load) or,

$$\frac{P_{j+1}}{|P_{j+1}|} = \frac{P_j}{|P_j|} = \pm 1.$$

The bracketed quantity in Eq. (2) thus becomes zero and therefore

$$\Delta\delta_j = 0 . \tag{3}$$

Since the $\Delta\delta_j$'s determine the influence of slop on the load distribution, Eq. (3) indicates that for high joint loadings the effects of uniform slop are eliminated. To solve for the load distribution with slop, the basic one-dimensional compatibility expression. Eq. (5) of Paragraph 5.1.1, must be modified by the addition of $\Delta\delta_j$. The compatibility equations then become

$$\boxed{\left[\left(\frac{L}{AE}\right)_{jT} + \left(\frac{L}{AE}\right)_{jB}\right]\left[\sum_{i=1}^{j} P_i\right] = (\Delta\phi_j + \Delta\delta_j) - P_j f_j + P_{j+1} f_{(j+1)} + X\left(\frac{L}{AE}\right)_{jT}} \tag{4}$$

The above equation, together with the equilibrium equation

$$\boxed{X = \sum_{j=1}^{N} P_j} ,$$

provides N equations for the N required attachment loads, P_j. The solution of these equations, however, involves more than simply solving a set of simultaneous algebraic equations. The values of $\Delta\delta_j$ on the right side of Eq. (4) are given by (1) from which, in order to determine the $\Delta\delta_j$'s, the sign of the attachment loads (positive or negative) must be determined. But this is not known in advance. This presents one of the major difficulties of the slop problem. The suggested method of attack is as follows:

(1) Assume a set of directions for the attachment loads.

(2) Determine the $\Delta\delta_i$'s from Eq. (1) and solve the simultaneous compatibility and equilibrium equations (Eq. (1) of Paragraph 5.1.1 and Eq. (4) above).

5.1.5 (Cont'd)

(3) If the directions of the attachment loads as obtained from the solution agree with the initially assumed directions, the solution is correct.

(4) If the directions of the attachment loads as obtained from the solution do not agree with the initially assumed directions, the solution is incorrect. The procedure must be repeated with a new set of attachment load directions, preferably the ones obtained from the solution.

The solution is the correct one when the assumed set of attachment load directions yields a solution with the same set of directions.

Obviously, a digital computer program is desirable in solving problems of this sort.

The following example illustrates the method of solution.

Scarfed steel and aluminum plates are bolted together with three attachments as shown in Figure 5.1.5-3. Find the attachment loads when the steel and aluminum plates are subjected to uniform temperature rises of 640°F and 80°F, respectively, and a mechanical load of X = 5000 lbs. is applied to the joint. The manufacturing tolerance is to be taken as $e_{mfg} = .0003$ inch for all holes. It is assumed that the bolt-hole flexibilities have been determined experimentally to be:

$f_1 = 1.300 \times 10^{-6}$ in/lb
$f_2 = 1.200 \times 10^{-6}$ in/lb (Refer to Sub-section 5.3 for a discussion of bolt-hole flexibility)
$f_3 = 1.300 \times 10^{-6}$ in/lb.

The appropriate quantities for substitution in Eq. (4) are first determined. Using average thicknesses for each bay,

$$\left(\frac{L}{AE}\right)_{1T} = \frac{1.25}{(.175)(2)(30) \times 10^6} = .119 \times 10^{-6} \text{ in/lb}$$

$$\left(\frac{L}{AE}\right)_{2T} = \frac{1.25}{(.125)(2)(30) \times 10^6} = .167 \times 10^{-6} \text{ in/lb}$$

$$\left(\frac{L}{AE}\right)_{1B} = \frac{1.25}{(.225)(2)(10) \times 10^6} = .278 \times 10^{-6} \text{ in/lb}$$

$$\left(\frac{L}{AE}\right)_{2B} = \frac{1.25}{(.275)(2)(10) \times 10^6} = .227 \times 10^{-6} \text{ in/lb.}$$

5.1.5 (Cont'd)

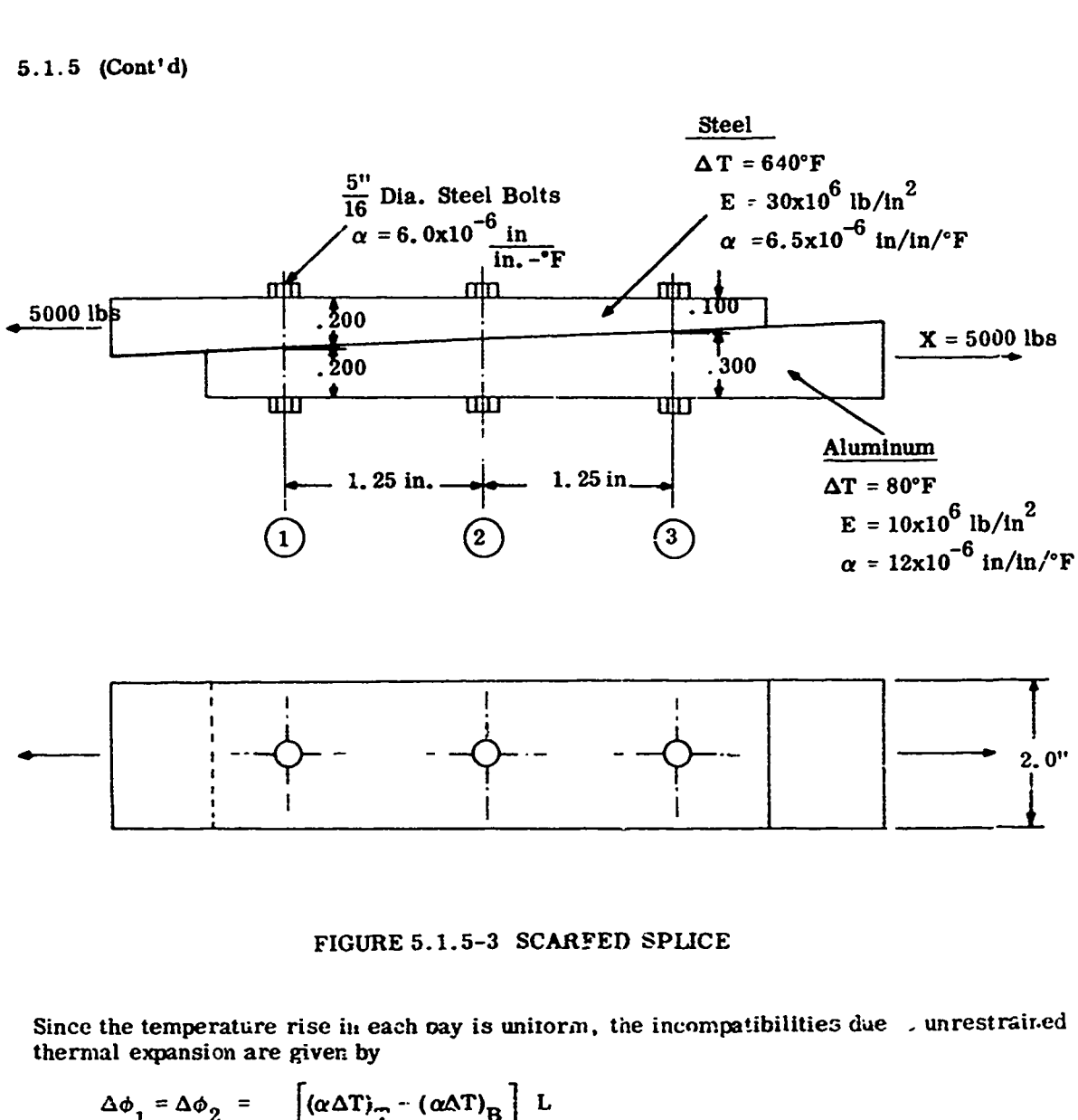


FIGURE 5.1.5-3 SCARFED SPLICE

Since the temperature rise in each bay is uniform, the incompatibilities due to unrestrained thermal expansion are given by

$$\Delta\phi_1 = \Delta\phi_2 = \left[(\alpha\Delta T)_A - (\alpha\Delta T)_B\right] L$$
$$= \left[(6.5)(640) - (12.0)(80)\right] \times 1.25 \times 10^{-6}$$
$$= 4000 \times 10^{-6} \text{ inch}.$$

Assuming the temperature of each bolt to be the same as the surrounding sheet material, the slops due to temperature are given by

$$\left[\delta_{temp}\right]_{top} = \left[(\alpha T)_{top\ sheet} - (\alpha T)_{top\ of\ attach.}\right] D_{hole}$$
$$= \left[(6.5)(640) - (6.9)(640)\right] \times .3125 \times 10^{-6}$$
$$= 100 \times 10^{-6} \text{ inch}.$$

5.1.5 (Cont'd)

$$\left[e_{temp}\right]_{bottom} = \left[(\alpha T)_{bottom\ sheet} - (\alpha T)_{bottom\ of\ attach.}\right] D_{hole}$$
$$= \left[(12.0)(80) - (6.0)(80)\right] \times .3125 \times 10^{-6}$$
$$= 150 \times 10^{-6} \text{ inch.}$$

Since $e_{mfg} = 300 \times 10^{-6}$ in., the total slops are given by

$$e_{1T} = e_{2T} = e_{3T} = \left[e_{mfg} + e_{temp}\right]_{top}$$
$$= \left[300 + 100\right] \times 10^{-6}$$
$$= 400 \times 10^{-6} \text{ inch.}$$

$$e_{1B} = e_{2B} = e_{3B} = \left[e_{mfg} + e_{temp}\right]_{bottom}$$
$$= [300 + 150] \times 10^{-6}$$
$$= 450 \times 10^{-6} \text{ inch.}$$

The incompatibilities due to slop, Eq. (1), are thus

$$\Delta\delta_1 = \frac{1}{2}(400 + 450)\frac{P_2}{|P_2|} - \frac{1}{2}(400 + 450)\frac{P_1}{|P_1|}$$
$$= 425\left(\frac{P_2}{|P_2|} - \frac{P_1}{|P_1|}\right)$$
$$\Delta\delta_2 = 425\left(\frac{P_3}{|P_3|} - \frac{P_2}{|P_2|}\right).$$

Substituting the known quantities in the incompatibility Eq. (4) and collecting terms yields the following expressions:

$$1.697\,P_1 - 1.200\,P_2 = 4595 + 425\left(\frac{P_2}{|P_2|} - \frac{P_1}{|P_1|}\right) \quad \text{(a)}$$

$$.394\,P_1 + 1.594\,P_2 - 1.300\,P_3 = 4835 + 425\left(\frac{P_3}{|P_3|} - \frac{P_2}{|P_2|}\right) \quad \text{(b)}$$

and for equilibrium,

$$P_1 + P_2 + P_3 = 5000. \quad \text{(c)}$$

Expressions (a), (b) and (c) provide 3 simultaneous equations which can be solved for the attachment loads P_1, P_2 and P_3, provided their directions are assumed correctly.

For a first trial, assume that all the attachment loads are positive. In this case the slop terms (2nd terms on the right in (a) and (b)) vanish and the expressions reduce to

$$1.697\,P_1 - 1.200\,P_2 = 4595$$
$$.394\,P_1 + 1.594\,P_2 - 1.300\,P_3 = 4835$$
$$P_1 + P_2 + P_3 = 5000.$$

5.1.5 (Cont'd)

for which the solution is

$$\left.\begin{aligned} P_1 &= +\ 3880 \text{ lbs} \\ P_2 &= +\ 1650 \text{ lbs} \\ P_3 &= -\ \ 530 \text{ lbs} . \end{aligned}\right\} \quad (d)$$

The above solution would be correct if no slop were present. However, since joint slop is present, the solution contradicts the initial assumption that the bolt loads are all positive and it is therefore incorrect. As a second trial, assume that the directions of the attachment loads are as given by the first solution, namely, that the loads in the first two bolts are positive while the load in the last bolt is negative. Expressions (a) and (b) then become

$$1.697\ P_1 - 1.200\ P_2 = 4595$$

$$.394\ P_1 + 1.594\ P_2 - 1.300\ P_3 = 3985 .$$

and as before,

$$P_1 + P_2 + P_3 = 5000 .$$

for which the solution is

$$\left.\begin{aligned} P_1 &= 3730 \text{ lbs} \\ P_2 &= 1440 \text{ lbs} \\ P_3 &= -170 \text{ lbs.} \end{aligned}\right\} \quad (e)$$

This is the correct solution, since the directions of the bolt loads are in agreement with the initial assumption.

Expressions (d) and (e) show that there is not much disagreement between the solutions with and without slop. This was to be expected, since the slop for the joint under consideration is small.

5.2 THE TWO-DIMENSIONAL (BOWING) PROBLEM

When the boundary conditions are such that the joint is allowed to bow out of its own plane, the solution is much more complicated than in the one-dimensional case. Additional factors such as rotational and out-of-plane displacements, beam-column effects, moments at the attachments, etc., enter into the problem. The present state of the art makes an exact analytical solution to the problem impracticable.

The purpose of the analysis presented here is to obtain a first approximation to the solution of the two-dimensional (bowing) problem by modifying the equations of the one-dimensional (uniaxial) solution.

A detailed derivation of the solution is presented in Reference 5-1.

5.2.1 The Joint Equations

Bowing of the joint (Figure 5.2.1-1) occurs due to the combined effects of non-uniform temperature distribution and externally applied mechanical loading.

The solution presented gives the shear loads in the attachments for a known set of applied mechanical and thermal loads where the following simplifying assumptions are made:

(1) The bay properties are constant (sheet thicknesses, attachment size and spacing, stiffnessess, etc., are the same for each bay). The thermal loading is assumed not to vary in the longitudinal direction, but may vary through the thickness.

(2) Vertical out-of-plane deflections and clamping loads are assumed to have a negligible effect on the load distribution (negligible beam column effects).

(3) Moments at the attachments have a negligible effect on, or are included in, the attachment-hole flexibility.

(4) The contact faces of the top and bottom plates of the joint are initially plane; the external axial loading is applied parallel to this plane in the direction of the line of attachments.

(5) As in the one-dimensional case, the joint materials are assumed to deform elastically under load.

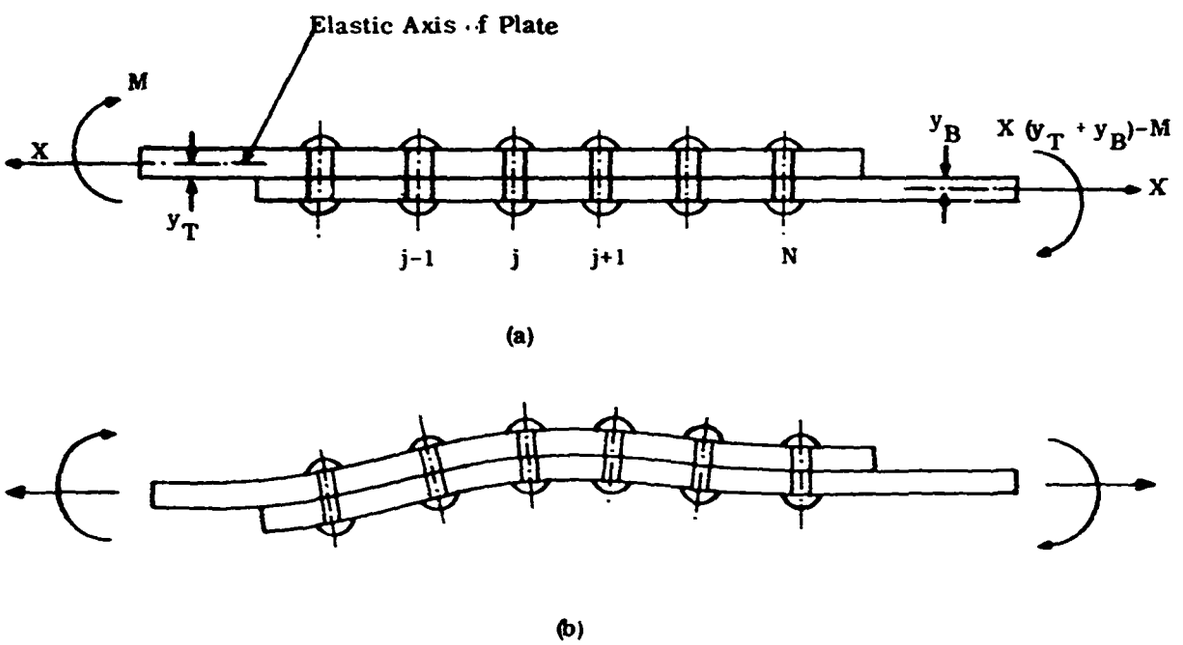


FIGURE 5.2.1-1: (a) JOINT IN UNBOWED CONFIGURATION
(b) BOWING OF JOINT DUE TO COMBINED EFFECTS OF NON-UNIFORM TEMPERATURE DISTRIBUTION AND MECHANICAL LOADING

5.2.1 (Cont'd)

Under the above assumptions the requirement of compatibility at the attachments yields the following compatibility equations:

$$f_A \sum_{i=1}^{j} P_i = \overline{\Delta\phi} - P_{jf} + P_{j+1} f + X f_{AT} \qquad (j = 1, 2, \ldots N-1) , \quad (1)$$

where

$$f_A = \left(\frac{L}{\overline{AE}}\right)_T + \left(\frac{L}{\overline{AE}}\right)_B + \frac{L(y_T + y_B)^2}{(\overline{EI})_T + (\overline{EI})_B} \quad (2)$$

$$\overline{\Delta\phi} = \Delta\phi - L \left[\frac{(\overline{EI})_T w_T + (\overline{EI})_B w_B}{(\overline{EI})_T + (\overline{EI})_B}\right] (y_T + y_B) \quad (3)$$

$$f_{AT} = \left(\frac{L}{\overline{AE}}\right)_T + \frac{ML}{X} \left[\frac{(y_T + y_B)}{(\overline{EI})_T + (\overline{EI})_B}\right] . \quad (4)$$

and w is the curvature due to temperature (Paragraph 4.1.1). If the thermal gradient is linear through the thickness, then w approximately equals $\frac{\alpha\Delta T}{h}$ where $\frac{\Delta T}{h}$ is the linear thermal gradient through the plate thickness (positive for higher temperatures on the upper face of the plate).

Equation (1) together with the equilibrium equation

$$X = \sum_{j=1}^{N} P_j ,$$

provides N simultaneous equations for the determination of the N unknown attachment shears.

A comparison of Eq. (1) with the one-dimensional compatibility equation, Eq. (1) of Paragraph 5.1.2, shows that the two forms are identical. Thus, when the bay properties are constant, the procedure for the two-dimensional solution is exactly the same as for the one-dimensional case if the one-dimensional coefficients

$$\left[\left(\frac{L}{\overline{AE}}\right)_T + \left(\frac{L}{\overline{AE}}\right)_B\right] , \quad [\Delta\phi] , \quad \left[\left(\frac{L}{\overline{AE}}\right)_T\right]$$

are replaced by the expressions on the right side of Eqs. (2), (3) and (4), respectively. Coefficients A_{jN} and B_{jN} can then be obtained, as before, from Figures 5.1.2-1 for determination of the attachment loads (Eq. (2) of Paragraph 5.1.2).

5.3 DETERMINATION OF THE ATTACHMENT-HOLE FLEXIBILITY FACTOR

The flexibility of a given attachment-hole combination must be determined quantitatively in order to make use of the solutions presented. If load deformation curves for the specified splice materials and temperatures are available (Figure 5.3-1), an initially determined slope $K_o = \frac{1}{f_o}$ gives the stiffness (or flexibility) in the elastic, low-load range.

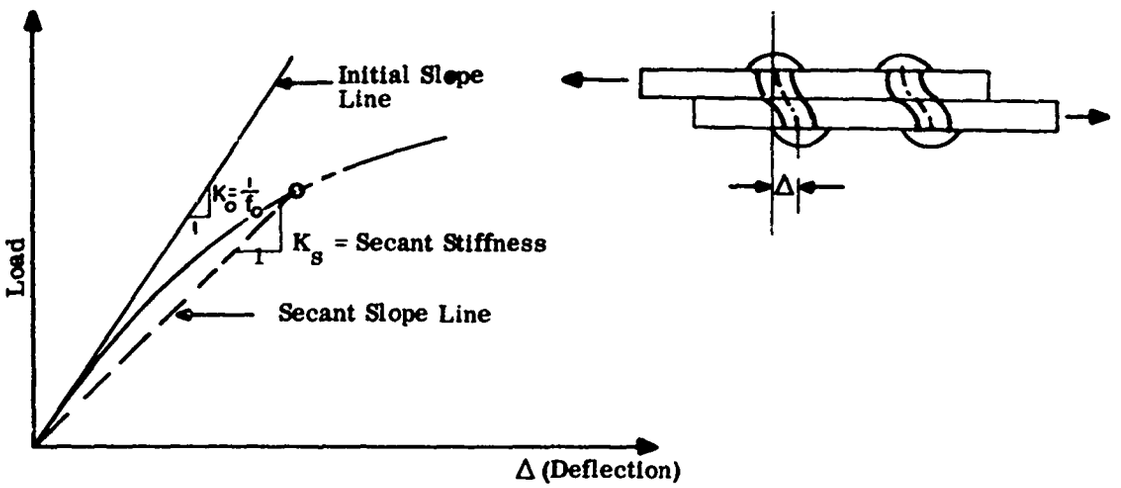


FIGURE 5.3-1 ATTACHMENT-HOLE LOAD VS. DEFLECTION CURVE

This initial slope is larger than the secant slopes encountered at higher load levels; using this initial value would give a conservatively greater stiffness (lower flexibility) than actual for succeedingly higher load ranges. This would result in an overestimate of the maximum attachment load. When load deformation data is available, and the joint analysis shows loads corresponding to secant stiffnesses that are appreciably different from those initially assumed, then the stiffnesses should be corrected and the analysis repeated. Such a procedure should converge rapidly to a valid solution.

If load deformation data is not available, the limit bearing load criteria of Reference 5-2 may be used to obtain an estimate of the attachment-hole flexibility. These criteria result in an overestimate of the attachment-hole flexibility and an underestimate of the maximum attachment load at load levels below yield.

As an example of the way in which the criteria of MIL-HDBK-5 (Reference 5-2) may be used to estimate the attachment-hole flexibility factor, consider the joint(in the illustrative problem)of Figure 5.1.2-2 in which the bolt diameter is 1/4 in.,the upper sheet is .125 in. thick titanium and the lower sheet is .250 in. thick aluminum.

Assuming the aluminum plate to be of clad 2024-T6 material, Table 3.2.3.0(f) of Reference 5-2 gives a bearing yield stress of 78,000 psi. The load at this yield stress is

5.3 (Cont'd)

$P_{alum.} = 78,000\ (.250) \times 1/4 = 4875$ lbs.

If the titanium sheet is taken to be 6AL-4V material, Table 5.2.4.0(b) of Reference 5-2 gives a bearing yield stress of 198,000 psi. The load at this yield stress is

$P_{titan.} = 198,000\ (.125) \times 1/4 = 6200$ lbs.

The average yield stress load is thus

$$P_{avg.} = \frac{6200 + 4875}{2} = 5590 \text{ lbs.}$$

To find the bolt-hole flexibility, the deformation for which the average yield load occurs is taken as being equal to 2% of the hole diameter (Reference 5-3, Paragraph 3.6111). For this deformation

$$f_{avg} = \frac{\Delta}{P_{avg}} = \frac{(.02)(1/4)}{5590} \sim \boxed{.90 \times 10^{-6} \text{ in/lb}}$$

5.4 REFERENCES

5-1 Report RDSR-3, Analysis of Joints, Republic Aviation Corporation (to be issued)

5-2 MIL-HDBK-5, Strength of Metal Aircraft Elements, March 1959

5-3 ANC-5 Bulletin, Strength of Metal Aircraft Elements, March 1955

SECTION 6

THERMO-ELASTIC ANALYSIS OF PLATES

SECTION 6

THERMO-ELASTIC ANALYSIS OF PLATES

TABLE OF CONTENTS

Paragraph	Title	Page
6	Thermo-Elastic Analysis of Plates	6.3
6.1	Theory of Deformation of Plates	6.4
6.1.1	Definition of a Plate	6.4
6 1.2	Assumptions for Linear Plate Theory	6.4
6.1.3	Three Kinds of Plate Problems	6.6
6.1.4	Fundamental Equations of Thermo-Elastic Plate Theory (with illustrative problem)	6.7
6.2	Bending of Plates	6.13
6.2.1	Bending of Rectangular Plates with Linear Gradient Through the Thickness	6.13
6.2.1.1	Unrestrained Rectangular Plates	6.14
6.2.1.2	Clamped Rectangular Plates	6.14
6.2.1.3	Simply Supported Rectangular Plates	6.14
6.2.1.4	Square Plate - One Edge Free	6.17
6.2.2	Bending of Circular Plates with Linear Temperature Gradient Through the Thickness	6.17
6.2.2.1	Unrestrained Solid Circular Plates	6.17
6.2.2.2	Clamped Solid Circular Plates	6.17
6.2.2.3	Simply Supported Solid Circular Plates	6.17
6.2.3	Circular Plates - Temperature Difference as a Function of the Radial Coordinate	6.18
6.2.3.1	Clamped Plates (with illustrative problem)	6.19
6.2.3.2	Simply Supported or Free Plates, $T_D = a_K r^K$	6.25

TABLE OF CONTENTS (Cont'd)

Paragraph	Title	Page
6.24	Approximate Solution of Free Plate with Arbitrary Temperature Variation Through the Thickness Only	6.26
6.3	Slab Problems - Plates	6.29
6.3.1	Thermal Stresses in Rings - Asymmetrical Temperature Distribution	6.31
6.3.2	Thermal Stresses in Solid Circular Plates Due to Asymmetrical Temperature Distribution	6.34
6.3.3	Circular Disk with Concentric Hole Subject to a Power Law Temperature Distribution	6.42
6.3.4	Circular Plate - Central Hot Spot	6.48
6.4	References	6.57

SECTION 6 - THERMO-ELASTIC ANALYSIS OF PLATES

This section is concerned with the determination of thermal stresses in plates. For example, solid and hollow bulkheads are plate-like major components in the semi-monocoque type of construction used in air and space vehicles.

The thermal-mechanical problems related to plates may be divided into bending, slab, instability types. The first two are discussed in this Section 6 while the instability type of problem is treated in Section 9.

The following symbols are used throughout this section:

a, b	Planform dimensions of rectangular plates; radii
h	Thickness of plate
r, Θ	Polar coordinates
u	Radial component of displacement
u, v, w	Middle plane displacement in the x, y, and z directions
x, y, z	Rectangular coordinates
u^*, v^*	Displacements in the x and y directions
D	$\frac{Eh^3}{12\,(1-\nu^2)}$
E	Young's modulus
M_T	$\alpha E \int_{-h/2}^{h/2} Tz\,dz$
M_x, M_y, M_{xy}	Moments per unit of length
N_T	$\alpha E \int_{-h/2}^{h/2} T\,dz$
N_x, N_y, N_{xy}	Forces per unit of length
P	Distributed lateral load
T	Temperature
$T_D, \Delta T$	Temperature difference between the upper and lower faces
α	Coefficient of linear expansion
$\epsilon_{xx}, \epsilon_{yy}, \epsilon_{zz}$; $\epsilon_{xy}; \epsilon_{yz}, \epsilon_{zx}$	Components of strain
ν	Poisson's Ratio
$\sigma_{rr}, \sigma_{r\Theta}, \sigma_{\Theta\Theta}$	Components of stress in polar coordinates
$\sigma_{xx}, \sigma_{yy}, \sigma_{zz}$; $\sigma_{xy}, \sigma_{yz}, \sigma_{zx}$	Components of stress in rectangular coordinates
ϕ	Stress function
∇^2	$\frac{\partial^2}{\partial x^2} + \frac{\partial^2}{\partial y^2}$

$$\nabla^4 \qquad \left(\frac{\partial^2}{\partial x^2} + \frac{\partial^2}{\partial y^2}\right)\left(\frac{\partial^2}{\partial x^2} + \frac{\partial^2}{\partial y^2}\right)$$

6.1 THEORY OF DEFORMATION OF PLATES

6.1.1 Definition of a Plate

A plate is defined as a non-rigid three-dimensional structure in which one dimension, the thickness, is much smaller than the remaining two dimensions. In its simplest form, the theory of plates can be regarded as an extension of beam theory.

6.1.2 Assumptions For Linear Plate Theory

The classical theory of plates is based upon the following assumptions:

(1) The material is assumed to be homogeneous, isotropic, and to obey Hooke's Law.

(2) The constant thickness of the plate is small compared to its other dimensions.

(3) The deflections of the plate are limited in magnitude and are of the order of the plate thickness. It can be shown that this restriction means that the effects of the normal deflections upon stretching of the middle plane of the plate are negligible. Consequently, only negligible stresses are induced in the median plane of the plate when the plate is loaded normally.

(4) Plane sections which before bending are normal to the median plane of the plate remain, under the above conditions, plane and normal to the median plane after bending.

The median plane of the plate is assumed to lie in the xy-plane and the thickness of the plate is h. If the plate is loaded by forces normal to the xy-plane then the element will distort as shown in Figure 6.1.2-1, where u* and w are the displacements in the x and z directions, respectively.

From the assumption that the deflections are small and that no median plane displacements or stresses are induced under deformation, the point O will be displaced normally to the strainless median surface (the upper one) and the plane section AOB will rotate into position A_1OB_1. The angle between the horizontal x-axis and the tangent to the deformed plane at point O is $\frac{\partial w}{\partial x}$.

In accordance with the assumption that plane sections remain plane and normal after bending, the angle of rotation of the cross section A_1OB_1 will also be $\frac{\partial w}{\partial x}$. Then for the small assumed deflections

$$u^* = -z \frac{\partial w}{\partial x} .$$

In a similar manner, the displacement in the y direction for any point a distance z from the median plane is given by

$$v^* = -z \frac{\partial w}{\partial y} .$$

.1.2 (Cont'd)

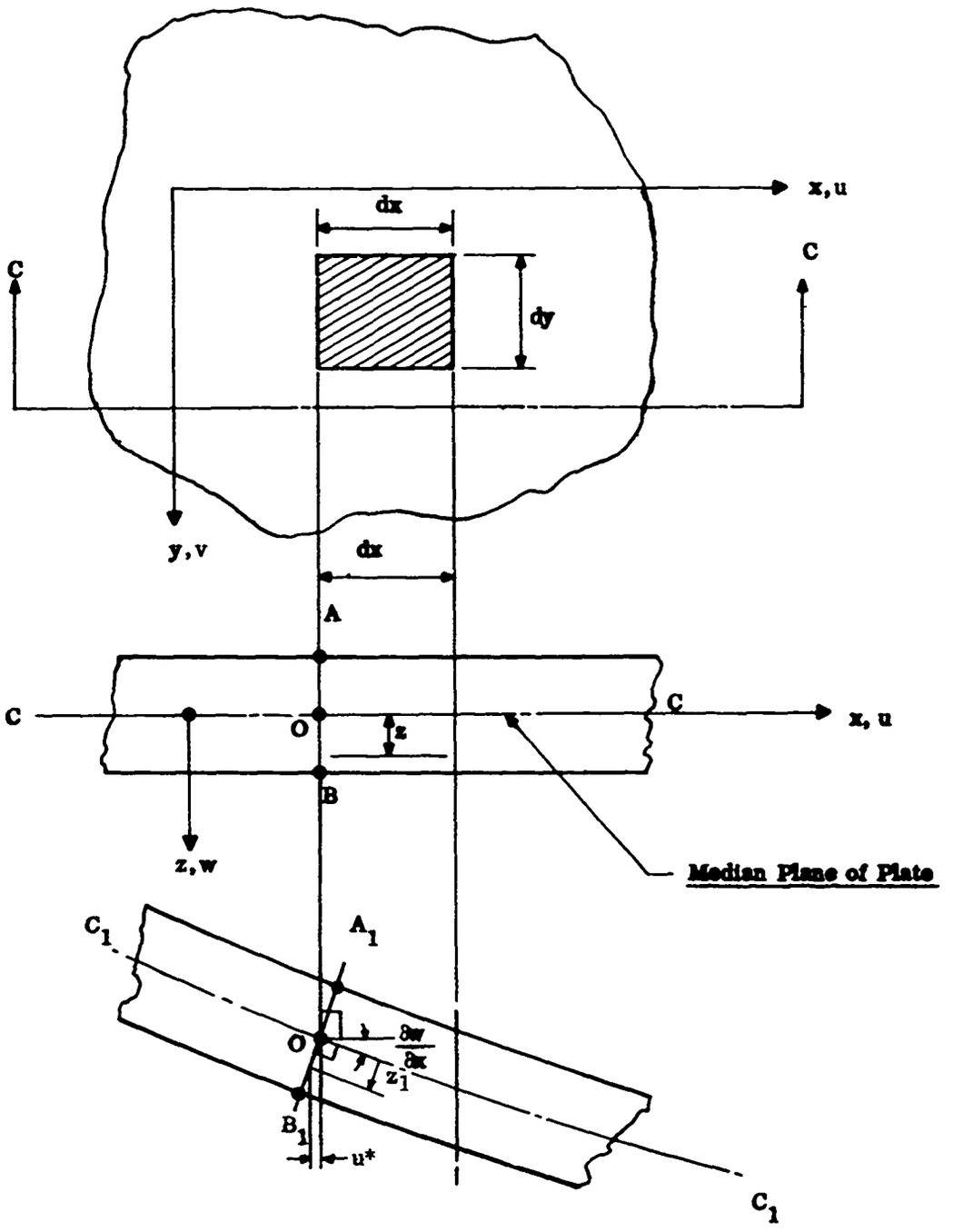


FIGURE 6.1.2-1 CROSS SECTION OF PLATE BEFORE AND AFTER DEFORMATION

6.1.2 (Cont'd)

(5) The normal stresses through the thickness of the plate are negligible because the surface loads are small compared to the bending stresses induced in the plate.

6.1.3 Three Kinds Of Plate Problems

The thermal-mechanical problems to be considered may be divided into

(1) Bending Problems - occur when the temperature varies in the thickness direction and the mechanical loads are normal pressures.

(2) Slab Problems - occur when the plate is loaded by mechanical forces parallel to the middle plane of the plate which are uniform through the thickness and the temperature varies in the planform direction only. This is a plane-stress problem (see Section 2 for definition of plane-stress) and is considered in Sub-section 6.3.

(3) Instability Problems - take place when there is edge restraint to expansion in the direction parallel to the middle plane of the plate (see Section 9).

6.1.4 Fundamental Equations Of Thermo-Elastic Plate Theory

The direct approach to plate problems is to derive the equations of equilibrium of forces and compatibility of displacements. These equations are in the form of partial differential equations which must be solved subject to prescribed boundary conditions.

The differential equations for the thermal-mechanical problem of plates are discussed next, followed by an illustrative example. The xy-plane is assumed to be the middle plane of the plate of constant thickness h and the shape of the boundary is arbitrary. The components of displacement in the x, y, and z directions are denoted by u^*, v^*, w (the symbols u, v, in this section are reserved for middle plane displacements in the x- and y- directions, respectively). Under the assumptions that plane sections remain plane, the displacements u^*, v^*, w are of the form:

$$\begin{aligned} u^*(x,y,z) &= u(x,y) - z\,\frac{\partial w}{\partial x}\quad(x,y) \\ v^*(x,y,z) &= v(x,y) - z\,\frac{\partial w}{\partial y}\quad(x,y) \\ w &= w(x,y)\,. \end{aligned} \tag{1}$$

The strain components in planes parallel to the xy-plane are :

$$\begin{aligned} \epsilon_{xx} &= \frac{\partial u^*}{\partial x} = \frac{\partial u}{\partial x} - z\,\frac{\partial^2 w}{\partial x^2} \\ \epsilon_{yy} &= \frac{\partial v^*}{\partial y} = \frac{\partial v}{\partial y} - z\,\frac{\partial^2 w}{\partial y^2} \\ \epsilon_{xy} &= \frac{\partial u^*}{\partial y} + \frac{\partial v^*}{\partial x} = \frac{\partial u}{\partial y} + \frac{\partial v}{\partial x} - 2z\,\frac{\partial^2 w}{\partial x \partial y}\,. \end{aligned} \tag{2}$$

Note: $\frac{\partial u}{\partial x}$, $\frac{\partial v}{\partial y}$, $\frac{\partial u}{\partial y} + \frac{\partial v}{\partial x}$ are the strain components in the middle plane of the plate and arise as a result of in-plane deformations. The additional terms are due to the bending of the plate.

The corresponding stress components are ($T \equiv$ temperature above room temperature datum):

$$\begin{aligned} \sigma_{xx} &= \frac{E}{1-\nu^2}\left(\epsilon_{xx} + \nu\epsilon_{yy} - (1+\nu)\,\alpha T\right) \\ \sigma_{yy} &= \frac{E}{1-\nu^2}\left(\epsilon_{yy} + \nu\epsilon_{xx} - (1+\nu)\,\alpha T\right) \\ \sigma_{xy} &= \frac{E}{2(1+\nu)}\,\epsilon_{xy}\,, \end{aligned} \tag{3}$$

6.1.4 (Cont'd)

which introduce the following forces and moments per unit of length (Figure 6.1.4-1):

$$N_x = \int_{-h/2}^{h/2} \sigma_{xx}\,dz \qquad M_x = \int_{-h/2}^{h/2} \sigma_{xx}\,z\,dz$$

$$N_y = \int_{-h/2}^{h/2} \sigma_{yy}\,dz \qquad M_y = \int_{-h/2}^{h/2} \sigma_{yy}\,z\,dz \qquad (4)$$

$$N_{xy} = \int_{-h/2}^{h/2} \sigma_{xy}\,dz \qquad M_{yx} = -M_{xy} = \int_{-h/2}^{h/2} \sigma_{xy}\,z\,dz\ .$$

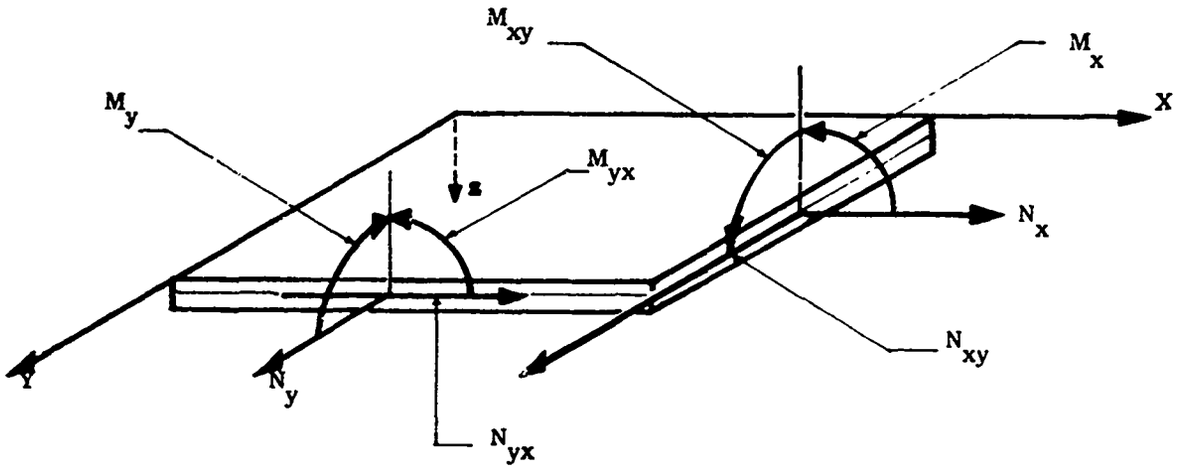


FIGURE 6.1.4-1 POSITIVE DIRECTIONS OF FORCES AND MOMENTS

Substitution of Eqs. (2) and (3) into Eqs. (4) yields

$$N_x = \frac{Eh}{1-\nu^2}\left(\frac{\partial u}{\partial x} + \nu\frac{\partial v}{\partial y}\right) - \frac{N_T}{1-\nu}$$

$$N_y = \frac{Eh}{1-\nu^2}\left(\frac{\partial v}{\partial y} + \nu\frac{\partial u}{\partial x}\right) - \frac{N_T}{1-\nu} \qquad (5)$$

$$N_{xy} = \frac{Eh}{2(1+\nu)}\left(\frac{\partial u}{\partial y} + \frac{\partial v}{\partial x}\right)$$

6.1.4 (Cont'd)

$$M_x = -D\left(\frac{\partial^2 w}{\partial x^2} + \nu \frac{\partial^2 w}{\partial y^2}\right) - \frac{M_T}{1-\nu}$$

$$M_y = -D\left(\frac{\partial^2 w}{\partial y^2} + \nu \frac{\partial^2 w}{\partial x^2}\right) - \frac{M_T}{1-\nu} \qquad \text{(5) cont'd}$$

$$M_{xy} = (1-\nu) D\left(\frac{\partial^2 w}{\partial x \partial y}\right),$$

where the bending rigidity per unit of length of the plate is

$$D \equiv \frac{Eh^3}{12(1-\nu^2)} \qquad (6)$$

and

$$N_T \equiv \alpha E \int_{-h/2}^{h/2} T \, dz$$

$$M_T \equiv \alpha E \int_{-h/2}^{h/2} Tz \, dz \, , \qquad (7)$$

where α and E are assumed to be constant.

The equations of equilibrium in planes parallel to the xy-plane are

$$\frac{\partial N_x}{\partial x} + \frac{\partial N_{xy}}{\partial y} = 0$$

$$\frac{\partial N_{xy}}{\partial x} + \frac{\partial N_y}{\partial y} = 0 \, , \qquad (8)$$

and these equations imply the existence of a stress function $\phi(x,y)$ such that

$$\frac{\partial^2 \phi}{\partial y^2} = N_x$$

$$\frac{\partial^2 \phi}{\partial x^2} = N_y \qquad (9)$$

$$-\frac{\partial^2 \phi}{\partial x \partial y} = N_{xy} \, .$$

6.1.4 (Cont'd)

Integration through the thickness of the compatibility equation for the plane stress problem (Reference 6-1) gives :

$$\nabla^4 \phi = - \nabla^2 N_T ,$$

where

$$\nabla^2 \equiv \frac{\partial^2}{\partial x^2} + \frac{\partial^2}{\partial y^2} \tag{10}$$

$$\nabla^4 \equiv \left(\frac{\partial^2}{\partial x^2} + \frac{\partial^2}{\partial y^2} \right) \left(\frac{\partial^2}{\partial x^2} + \frac{\partial^2}{\partial y^2} \right) .$$

The equation of equilibrium in the z direction (Reference 6-2) is

$$\frac{\partial^2 M_x}{\partial x^2} - \frac{2\partial^2 M_{xy}}{\partial x \partial y} + \frac{\partial^2 M_y}{\partial y^2} = - P - \left(N_x \frac{\partial^2 w}{\partial x^2} + 2N_{xy} \frac{\partial^2 w}{\partial x \partial y} + N_y \frac{\partial^2 w}{\partial y^2} \right), \tag{11}$$

where $P(x,y)$ is the distributed lateral load in the positive z direction; and M_x, M_y, M_{xy} are the conventional bending moments per unit of length. If the quantities M_x, M_y, M_{xy} are expressed in terms of the displacements from Eq. (5), then the equilibrium equation in the z direction becomes:

$$D \nabla^4 w = P + N_x \frac{\partial^2 w}{\partial x^2} + N_y \frac{\partial^2 w}{\partial y^2} + 2N_{xy} \frac{\partial^2 w}{\partial x \partial y} - \frac{1}{1-\nu} \nabla^2 M_T . \tag{12}$$

The solution of a problem requires in general that Eqs. (10) and (12) be solved simultaneously subject to appropriate boundary conditions.

If the plate is supported so that N_x, N_y, N_{xy} are negligible, as would occur if there was no restraint in the median plane of the plate and no applied in-plane forces, then the simpler equation may be used:

$$D \nabla^4 w = P - \frac{1}{1-\nu} \nabla^2 M_T . \tag{13}$$

It is clear that the equation expressed by (13) is equivalent to a "mechanical problem" with normal loading = $P - \frac{1}{1-\nu} \nabla^2 M_T$, so that all the known techniques (Reference 6-1) for non-thermal problems may be used.

6.1.4 (Cont'd)

A solution of the differential equations in the case of a simple plate problem follows.

A clamped circular plate of radius R is subject to a linear gradient through its thickness h where the temperature is T_1 and T_o at the top and bottom faces, respectively ($T_1 > T_o$). Find the deflection and stress assuming that the middle plane of the plate is free to expand.

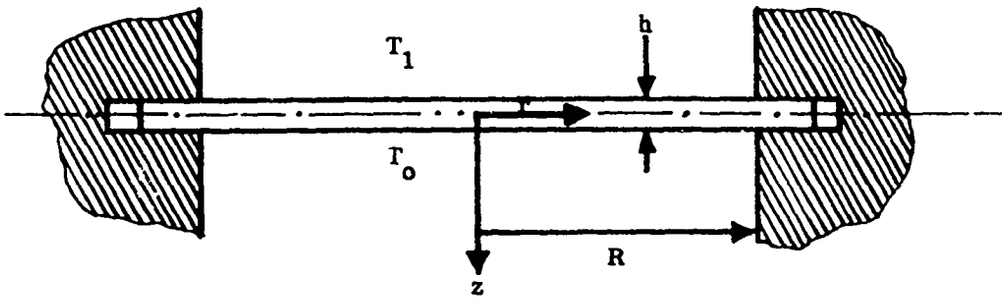


FIGURE 6.1.4-2 CLAMPED CIRCULAR PLATE WITH LINEAR GRADIENT THROUGH THICKNESS

The temperature variation is denoted by

$$T = \frac{T_o + T_1}{2} + (T_o - T_1) \frac{z}{h} .$$

From (13), the differential equation to be solved is

$$D \nabla^4 w = P - \frac{1}{1-\nu} \nabla^2 M_T ,$$

where

$P = 0$, and $\nabla^2 M_T = 0$ as M_T does not depend on x and y.

Therefore

$$\nabla^4 w = 0 , \qquad (14)$$

or in polar coordinates, with r as the radial coordinate:

$$r^4 \frac{d^4w}{dr^4} + 2r^3 \frac{d^3w}{dr^3} - r^2 \frac{d^2w}{dr^2} + r \frac{dw}{dr} = 0 . \qquad (15)$$

6.1.4 (Cont'd)

This is an equi-dimensional differential equation and the solution is readily found in an elementary differential equations text,

$$w = A \log r + B r^2 \log r + Cr^2 + D \ . \tag{16}$$

However, the deflection and bending moment must remain finite as $r \to 0$. This implies that $A = B = 0$. Therefore, w reduces to

$$w = Cr^2 + D \ . \tag{17}$$

The clamped boundary conditions are $w = \frac{dw}{dr} = 0$ when $r = R$. Therefore, substitution of Eq. (17) into the boundary conditions yields $w \equiv 0$, i.e., the normal deflections are identically zero.

From Eqs. (5) or analogous equations in polar coordinates, the radial and transverse moments per unit length are given by

$$M_r = M_\Theta = \frac{-M_T}{1-\nu} \ , \tag{18}$$

where from Eq. (7)

$$M_T = \alpha E \int_{-h/2}^{h/2} \left[\frac{(T_o + T_1)}{2} + (T_o - T_1) \frac{z}{h} \right] z \, dz \ ,$$

or

$$M_T = \frac{\alpha E (T_o - T_1) \ h^2}{12} \ . \tag{19}$$

The components of maximum stress in the radial and transverse directions are

$$\sigma_{rr}\big|_{max} = \sigma_{\Theta\Theta}\big|_{max} = \frac{6}{h^2} \cdot M_r = \frac{6}{h^2} M_O = \frac{\alpha E (T_1 - T_O)}{2(1-\nu)} \tag{20}$$

$$\sigma_{rr}\big|_{max} = \sigma_{\Theta\Theta}\big|_{max} = \frac{\alpha E \Delta T}{2(1-\nu)} \ , \tag{21}$$

where $\Delta T = T_1 - T_o$ = difference in temperature between the upper and lower faces, respectively.

Note that in the simply supported case with boundary conditions $w = M_r = 0$, there result zero stress and paraboloidal deflections (see Paragraph 6.2.2.3). More precise analysis yields spherical deflections.

6.2 BENDING OF PLATES

Bending problems in plates occur when the temperature varies in the thickness direction (and possibly other directions) and the mechanical loads (if they exist) are normal pressures. In the succeeding paragraphs emphasis will be placed upon the linear gradient through the thickness.

6.2.1 Bending of Rectangular Plates With Linear Gradient Through The Thickness

The rectangular plate is shown in Figure 6.2.1-1 and the temperature variation through the thickness is assumed to be linear. Expressions for stresses and deflections corresponding to various support conditions are given in the following paragraphs.

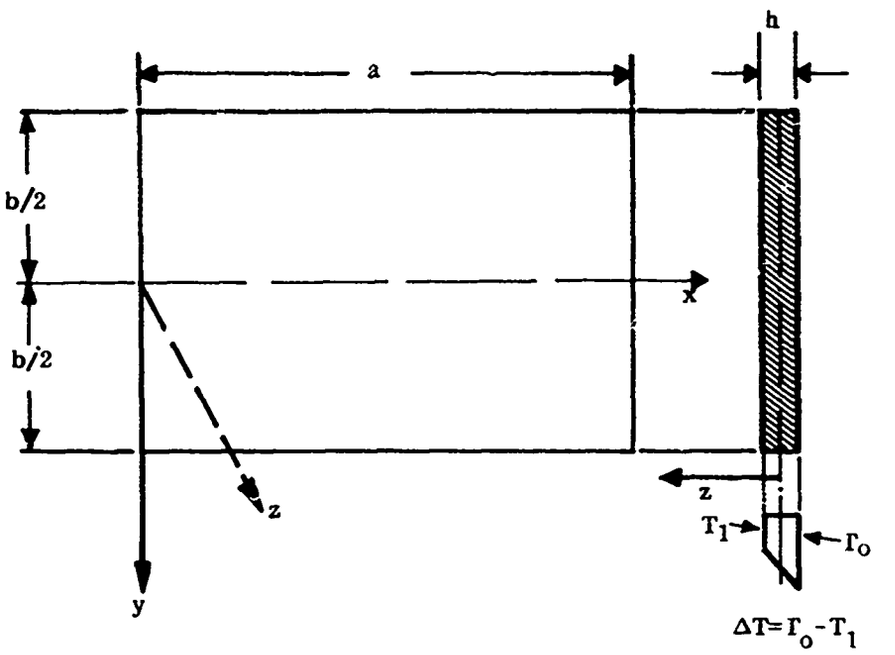


FIGURE 6.2.1-1 PLATE GEOMETRY SHOWING A POSITIVE LINEAR THERMAL GRADIENT THROUGH THE THICKNESS

6.2.1.1 Unrestrained Rectangular Plates

A free rectangular plate subjected to a linear temperature distribution through the thickness and constant temperature over the planform is unstressed. The plate becomes curved and fits a sphere of radius inversely proportional to the difference in surface temperatures and inversely proportional to the thickness.

6.2.1.2 Clamped Rectangular Plates

Maximum Stress:

$$\sigma_{xx} = \sigma_{yy} = \pm \frac{E\alpha\Delta T}{2(1-\nu)} \quad (+ \text{ sign corresponds to face } z = +\frac{h}{2}) \quad (1)$$

where the temperature difference is defined by

$$\Delta T = T(-\frac{h}{2}) - T(\frac{h}{2}) \ .$$

Deflection: The transverse deflection w is identically zero.

6.2.1.3 Simply Supported Rectangular Plates

Deflection (see Figure 6.2.1-1):

$$w = \frac{-\alpha\Delta T(1+\nu)4a^2}{\pi^3 h} \sum_{m=1,3,5\ldots}^{\infty} \frac{\sin(\frac{m\pi x}{a})}{m^3} \left(1 - \frac{\cosh(\frac{m\pi y}{a})}{\cosh\alpha_m}\right), \quad (1a)$$

where

$$\alpha_m = \frac{m\pi b}{2a} \ . \quad (1b)$$

Bending Moments Per Unit of Length:

$$M_x = \frac{4D\alpha\Delta T(1-\nu^2)}{\pi h} \sum_{m=1,3,5\ldots}^{\infty} \frac{\sin(\frac{m\pi x}{a})\cosh(\frac{m\pi y}{a})}{m\cosh\alpha_m} \quad (2a)$$

$$M_y = \frac{\alpha\Delta T(1-\nu^2)D}{h} - \frac{4D\alpha\Delta T(1-\nu^2)}{\pi h} \sum_{m=1,3,5\ldots}^{\infty} \frac{\sin(\frac{m\pi x}{a})\cosh(\frac{m\pi y}{a})}{m\cosh\alpha_m} \ . \quad (2b)$$

The series for w converges very rapidly while the series for the moments converge more slowly. Judgment must be used in choosing a sufficient number of terms for the required accuracy. However, the formulas for the maximum bending moments and stress are expressible in closed form as given below.

6.2.1.3 (Cont'd)

Maximum Bending Moments:
(Reference 6-2)

$$(M_x)_{y=b/2} = (M_y)_{x=o,\ x=a} = \frac{+Eh^2\alpha\Delta T}{12}. \qquad (3a)$$

Maximum Bending Stress:

$$(\sigma_x)_{y=\pm b/2} = (\sigma_y)_{x=o,\ x=a} = \frac{E\alpha\Delta T}{2}. \qquad (3b)$$

Equations (1a), (2a), and (2b) have been evaluated in non-dimensional form for the square plate as shown in Figures 6.2.1.3-1 through -3.

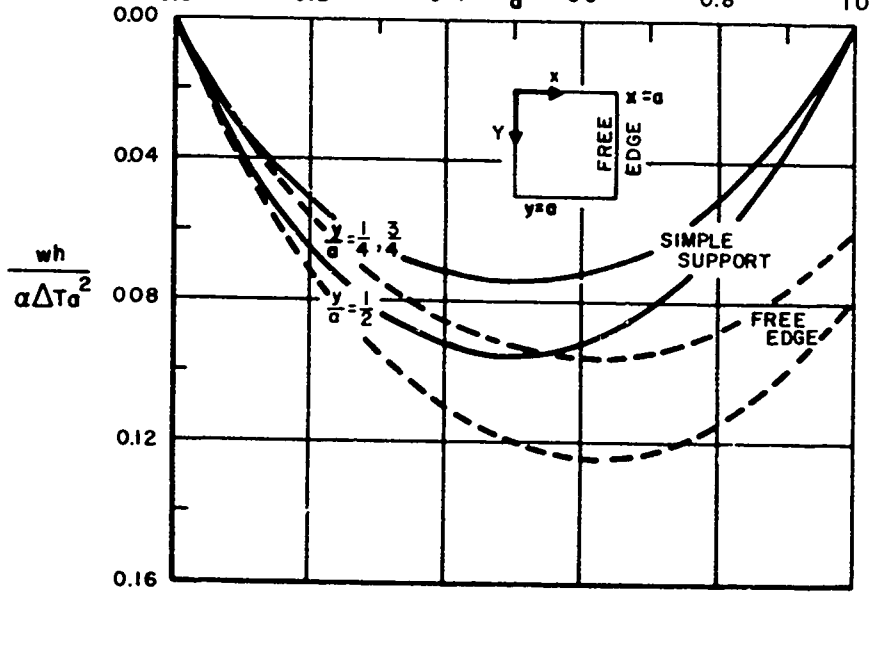


FIGURE 6.2.1.3-1 DEFLECTION (w) VS. POSITION (x) FOR y PARAMETERS

6.2.1.3 (Cont'd)

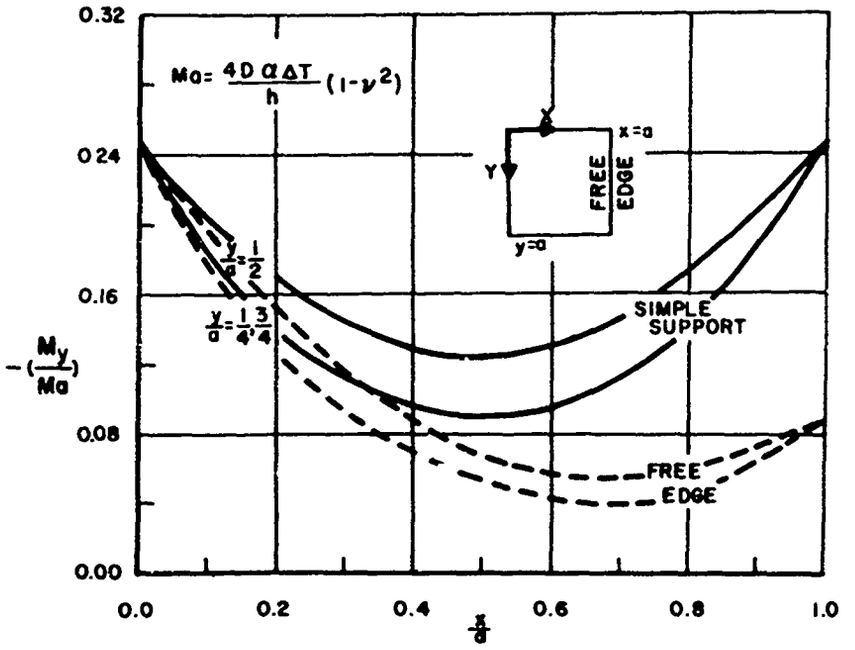


FIGURE 6.2.1.3-2 BENDING MOMENT (M_y) VS. POSITION (x) FOR y PARAMETERS

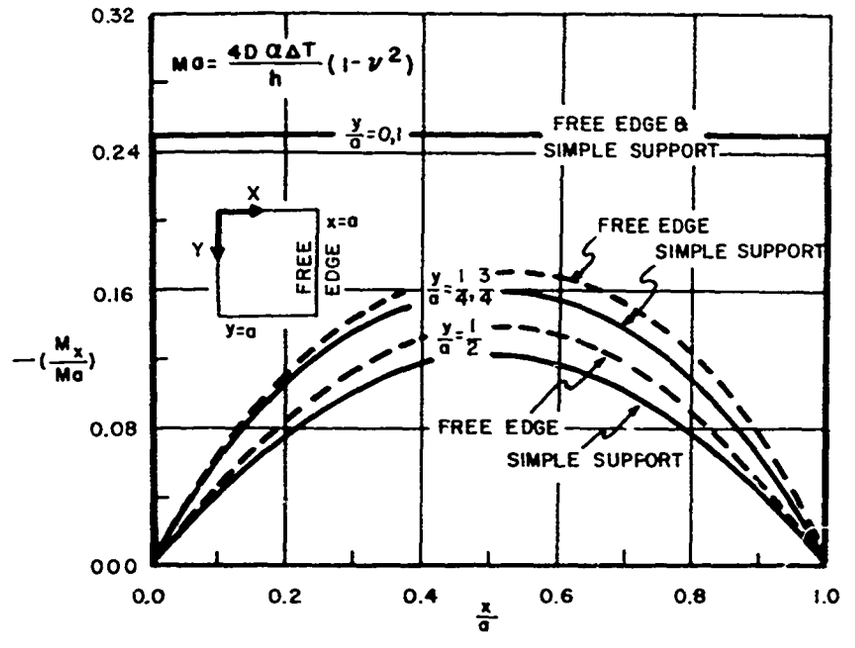


FIGURE 6.2.1.3-3 BENDING MOMENT (M_x) VS. POSITION (x) FOR y PARAMETERS

6.2.1.4 Square Plate -- One Edge Free

Figures 6.2.1.3-1 through -3 demonstrate the deflections and bending moments per unit of length vs. position in non-dimensional form. This shows the effect that freeing an edge has on the deflections and moments (Reference 6-3). The quantity Ma in the denominators of the moment expressions is defined by

$$Ma = \frac{4D\alpha\Delta T}{h}\ (1-\nu^2)\ . \qquad (4)$$

6.2.2 Bending of Circular Plates with Linear Temperature Gradient Through the Thickness

Formulas and curves for the deflection and stresses of circular plates (see Figure 6.2.2-1) subjected to a linear temperature distribution through the thickness are now presented.

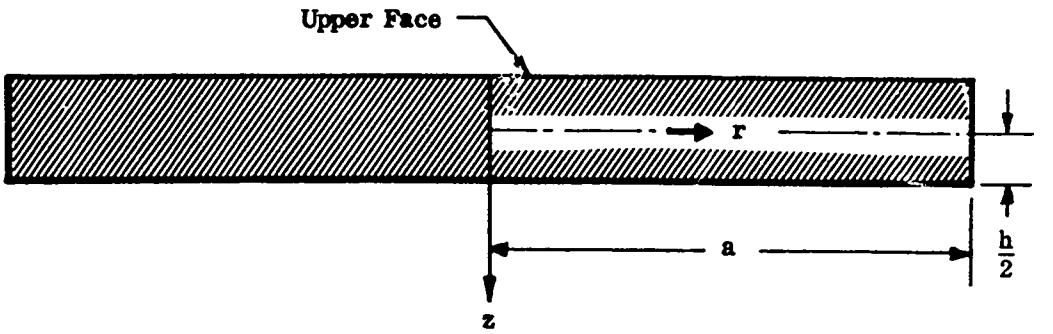


FIGURE 6.2.2.-1 PLATE GEOMETRY

6.2.2.1 Unrestrained Solid Circular Plates

A free circular plate subjected to a linear temperature gradient through the thickness is unstressed. The plate becomes curved and fits a sphere of radius directly proportional to the difference in surface temperatures and inversely proportional to the thickness.

6.2.2.2 Clamped Solid Circular Plates

The maximum stress $\sigma_{rr} = \sigma_{\Theta\Theta} = \pm \frac{E\alpha\Delta T}{2(1-\nu)}$ occurs at the faces where ΔT is the temperature difference between the upper and lower surfaces. The transverse deflection is identically zero.

6.2.2.3 Simply Supported Solid Circular Plates

The plate is unstressed. The deflection w is given by

$$w = \frac{-\alpha\Delta T}{2h}\ (a^2 - r^2)\ ,$$

where a is the radius of the plate.

6.2.3 Circular Plates - Temperature Difference as a Function of the Radial Coordinate

The differential equation for this radially symmetric case is

$$\nabla^4 w = \frac{(1+\nu)\alpha}{h} \nabla^2 T_D \quad , \tag{1}$$

where T_D is the temperature difference between the upper and lower faces. The variation of temperature is assumed to be linear through the thickness, however, the variation with r is arbitrary.

It is assumed that the temperature T is expressible by a convergent power series expansion

$$T = -\frac{z}{h} \sum_{K=0}^{\infty} a_K r^K + C \qquad (a_K, \text{ C are constants})$$

so that the temperature difference T_D is given by

$$T_D = \sum_{K=0}^{\infty} a_K r^K \quad . \tag{2}$$

(Note: Positive z is downward)

The solution of Eq. (1), with the temperature difference representation as shown in Eq. (2), is

$$w = C_1 \frac{r^2}{a^2} + C_2 + \frac{(1+\nu)\alpha}{h} \sum_{K=0}^{\infty} \frac{a_K r^{K+2}}{(K+2)^2} \quad , \tag{3}$$

where C_1, C_2 are arbitrary constants so far and must be determined by the boundary conditions.

6.2.3.1 Clamped Plates

For power series temperature distribution, the solution of Eq. (3) of Paragraph 6.2.3 for a clamped plate of radius a is

$$w = \frac{(1+\nu)\,\alpha}{2h} \sum_{K=0}^{\infty} \frac{a_K}{(K+2)^2} \left[2\, r^{K+2} + K a^{K+2} - r^2 a^{K(K+2)} \right] . \tag{1}$$

The bending moments in the radial and transverse directions are

$$M_r = -\frac{Eh^2\,\alpha}{12(1-\nu)} \left[\sum_{K=0}^{\infty} \frac{a_K a^K}{K+2} \left\{ (K+1+\nu) \left(\frac{r}{a}\right)^K - (1+\nu) \right\} - T_D \right] \tag{2}$$

$$M_\Theta = -\frac{Eh^2\,\alpha}{12(1-\nu)} \left[\sum_{K=0}^{\infty} \frac{a_K a^K}{K+2} \left\{ \left[1 + \nu\,(K+1) \right] \left(\frac{r}{a}\right)^K - (1+\nu) \right\} - T_D \right] . \tag{3}$$

For monomial distribution, the deflections and moments in non-dimensional form when T_D is expressed by the monomial $T_D = a_K r^K$ are

$$\frac{wh}{(1+\nu)a^2\,\alpha T_D(a)} = \frac{1}{(K+2)^2} \left[\left(\frac{r}{a}\right)^{K+2} - \left(\frac{K}{2}+1\right) \left(\frac{r}{a}\right)^2 + \frac{K}{2} \right] \tag{4}$$

$$\frac{M_r}{\frac{Eh^2}{12}\,\alpha\, T_D(a)} = \frac{1}{K+2} \left[\left(\frac{r}{a}\right)^K + \frac{(1+\nu)}{(1-\nu)} \right] \tag{5}$$

$$\frac{M_\Theta}{\frac{Eh^2}{12}\,\alpha\, T_D(a)} = \frac{1}{K+2} \left[(K+1) \left(\frac{r}{a}\right)^K + \frac{(1+\nu)}{(1-\nu)} \right] , \tag{6}$$

where $T_D(a)$ is the temperature difference at r = a. Curves of non-dimensional deflections and moments are presented in Figures 6.2.3.1-1 through -3 for K = 0, 1, 2, ... 5. Superposition may then be used for T_D given by polynomials in r. The determination of the polynomial describing the radial variation of T_D can be obtained in the same manner as shown in Paragraph 4.1.2.3.1.

6.2.3.1 (Cont'd)

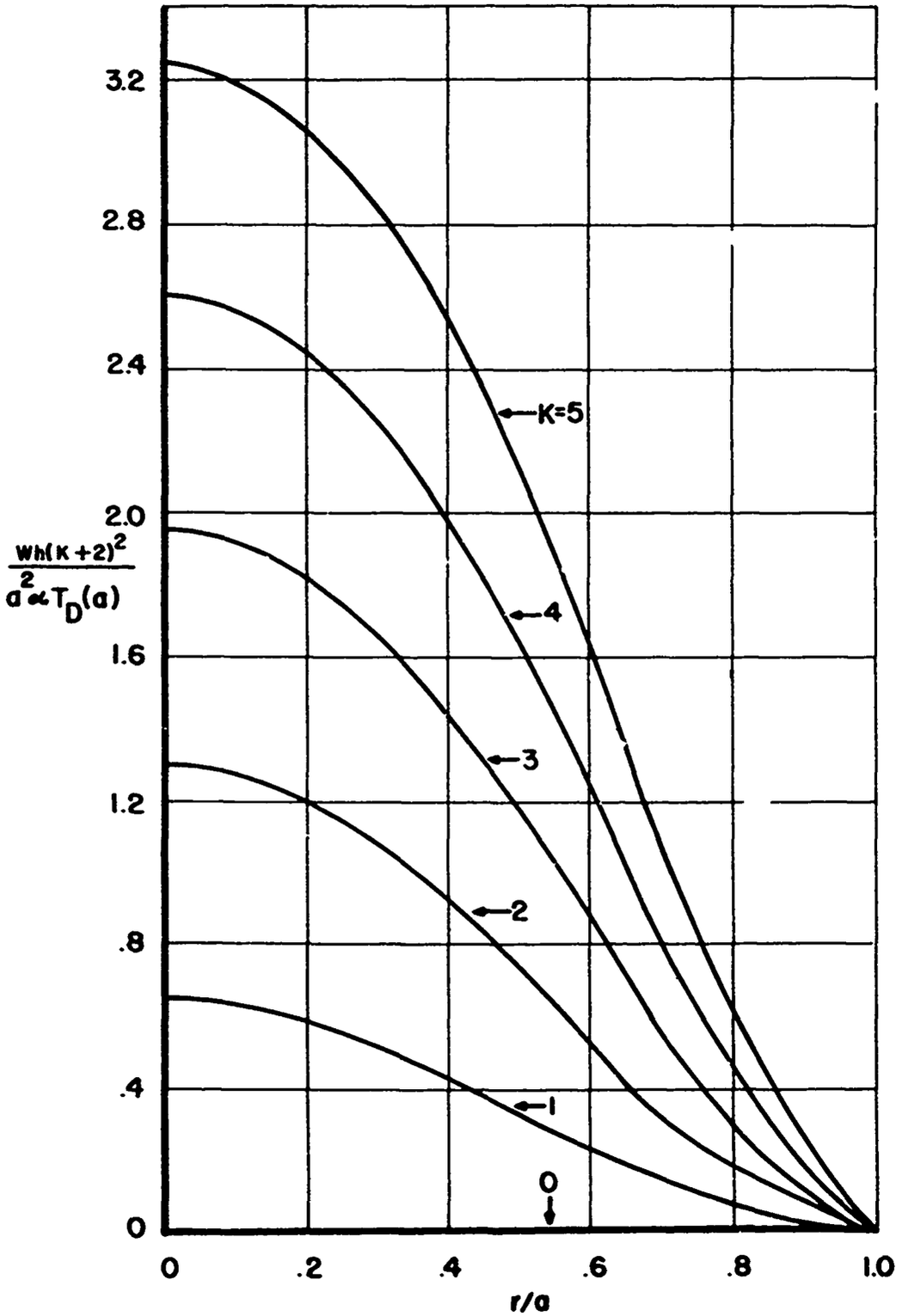


FIGURE 6.2.3.1-1 NON-DIMENSIONAL DEFLECTION

6.2.3.1 (Cont'd)

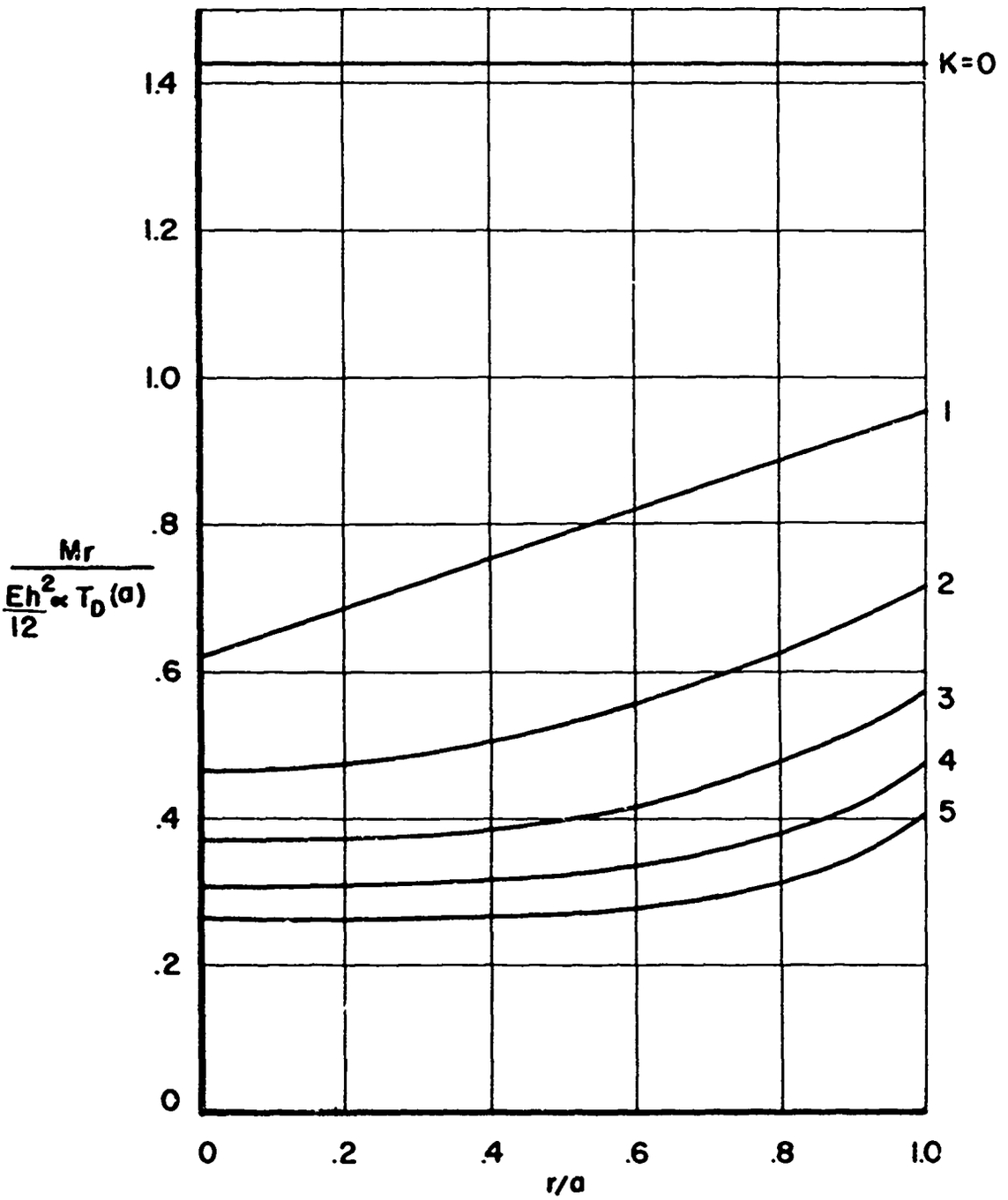


FIGURE 6.2.3.1-2 NON-DIMENSIONAL RADIAL MOMENT

6.2.3.1 (Cont'd)

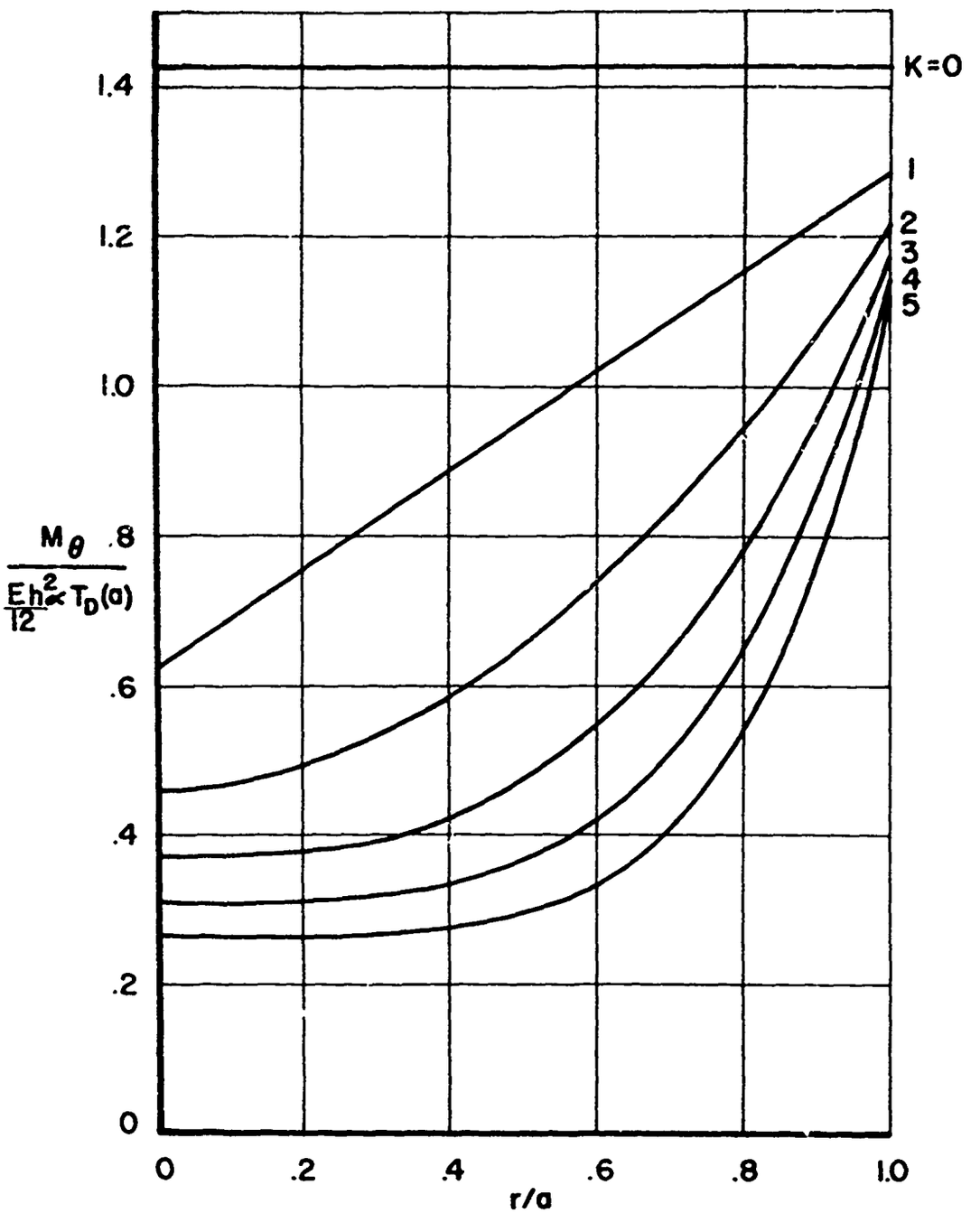


FIGURE 6.2.3.1-3 NON-DIMENSIONAL TANGENTIAL MOMENT

6.2.3.1 (Cont'd)

The following illustrative problem demonstrates the solution for a clamped aluminum plate for which

$a = 10$ inches $\qquad h = 0.20$ inch $\qquad E = 10^7$ psi

$\nu = 0.30 \qquad \alpha = 12 \times 10^{-6}$ in./in./°F

and where the radial variation of temperature difference through the thickness is given by

$$T_D = 200 + r^2/2.$$

Solution of the clamped plate problem involves the determination of the maximum deflections and stress. Thus, if the coefficients of the polynomial expressing the temperature difference distribution are all of the same sign, as above, then the maximum magnitude of deflection occurs at the center of the plate while maximum magnitudes of radial and tangential moments occur at the boundary. Thus, considering the first term of the polynomial,

$$T'_D(r) = T'_D(a) = 200 ,$$

$$K = 0 .$$

From Figure 6.2.3.1-1

$$w' = 0$$

and from Figures 6.2.3.1-2 and 6.2.3.1-3 ,

$$\left.\frac{M'_r}{\frac{Eh^2}{12}\,\alpha\,\Gamma'_D(a)}\right]_{\frac{r}{a}=1} = \left.\frac{M'_\theta}{\frac{Eh^2}{12}\,\alpha\,\Gamma'_D(a)}\right]_{\frac{r}{a}=1} = 1.43 ,$$

$$\frac{Eh^2}{12}\,\alpha\,\Gamma'_D(a) = \frac{10^7 \times 4 \times 10^{-2} \times 12 \times 10^{-6} \times 2 \times 10^2}{12} = 80 .$$

Therefore,

$$M'_r\Big]_{\frac{r}{a}=1} = M'_\theta\Big]_{\frac{r}{a}=1} = 1.43\,(80) = 114.4 \text{ in.lb./in.}$$

For the second term of the polynomial,

$$T''_D(r) = \frac{r^2}{2} \; ; \; \Gamma''_D(a) = \frac{(10)^2}{2} = 50 ,$$

$$K = 2 .$$

From Figure 6.2.3.1-1

$$\left.\frac{w''h\,(K+2)^2}{a^2\,\alpha\Gamma''_D(a)}\right]_{\frac{r}{a}=0} = 1.30,$$

6.2.3.1 (Cont'd)

$$\frac{a^2 \alpha \Gamma''_D(a)}{h(K+2)^2} = \frac{10^2 \times 12 \times 10^{-6} \times 5 \times 10^1}{2 \times 10^{-1} \times 16} = .01875 .$$

Therefore,

$$w''\Big]_{\frac{r}{a}=0} = .01875\ (1.30) = .024 \text{in.}$$

From Figures 6.2.3.1-2 and -3

$$\frac{M''_r}{\frac{Eh^2}{12}\alpha\Gamma''_D(a)}\Bigg]_{\frac{r}{a}=1} = .71 ,$$

$$\frac{M''_\theta}{\frac{Eh^2}{12}\alpha T''_D(a)}\Bigg]_{\frac{r}{a}=1} = 1.21 ,$$

$$\frac{Eh^2}{12}\alpha T''_D(a) = \frac{10^7 \times 4 \times 10^{-2} \times 12 \times 10^{-6} \times 5 \times 10^1}{12} = 20 .$$

Therefore,

$$M''_r\Big]_{\frac{r}{a}=1} = 20(.71) = 14.2 \text{ in.lb./in.} ,$$

$$M''_\theta\Big]_{\frac{r}{a}=1} = 20\ (1.21) = 24.2 \text{ in.lb./in.}$$

By superposition

$$w\Big]_{\frac{r}{a}=0} = w' + w''\Big]_{\frac{r}{a}=0} = 0 + .024 = .024 \text{ in.}$$

$$M_r\Big]_{\frac{r}{a}=1} = M'_r + M''_r\Big]_{\frac{r}{a}=1} = 114.4 + 14.2 = 128.6 \text{ in.lb./in.}$$

$$M_\theta\Big]_{\frac{r}{a}=1} = M'_\theta + M''_\theta\Big]_{\frac{r}{a}=1} = 114.4 + 24.2 = 138.6 \text{ in.lb./in.}$$

6.2.3.1 (Cont'd)

The maximum stress is given by

$$\sigma_{\Theta\Theta}\Big]_{\frac{r}{a}=1} = \frac{6}{h^2}\cdot M_\Theta\Big]_{\frac{r}{a}=1} = \frac{6}{(0.20)^2}(138.6) = 20,790 \text{ psi} .$$

Note: If the polynomial representing the radial variation of the temperature difference consists of mixed signs, the points of maximum moments and deflection occur at the boundary or in the interior where the radial derivatives of the quantities are zero.

6.2.3.2 Simply Supported or Free Plates, $T_D = a_K r^K$

Once the clamped plate problem due to $T_D = a_K r^K$ has been solved then the simply supported or free plates may be solved by using the principle of superposition. It is only necessary to add the solution of the mechanical problem of a circular plate subject to a uniform radial bending moment equal and opposite to

$$M_r\Big|_{\frac{r}{a}=1}$$

(to relieve the moments on the boundary) determined from Eq. (5) of Paragraph 6.2.3.1. A straight forward calculation yields the result that for a simply supported or free plate add the following non-dimensional expression to the solution for a clamped plate:

$$\frac{M_r}{Eh^2\,\alpha T_D(a)/12} = \frac{M_\Theta}{Eh^2\,\alpha T_D(a)/12} = \frac{2}{(K+2)(\nu-1)} \qquad (1)$$

$$\frac{wh}{a^2\,\alpha T_D(a)} = \frac{\left(\frac{r^2}{a^2}-1\right)}{K+2} . \qquad (2)$$

6.2.4 Approximate Solution of Free Plate with Arbitrary Temperature Variation Through the Thickness Only

The problem of the determination of the stresses, strains, and displacements in an unrestrained plate of arbitrary planform (Figure 6.2.4-1) which is subjected to an arbitrary temperature variation in the thickness direction has been solved approximately (Reference 6-1). The procedure used is to solve the problem as a three dimensional elasticity problem using the semi-inverse method of St. Venant. This simply means that the form of the stress distribution is assumed and then the equations of equilibrium, compatibility and boundary conditions are examined in the light of this assumption.

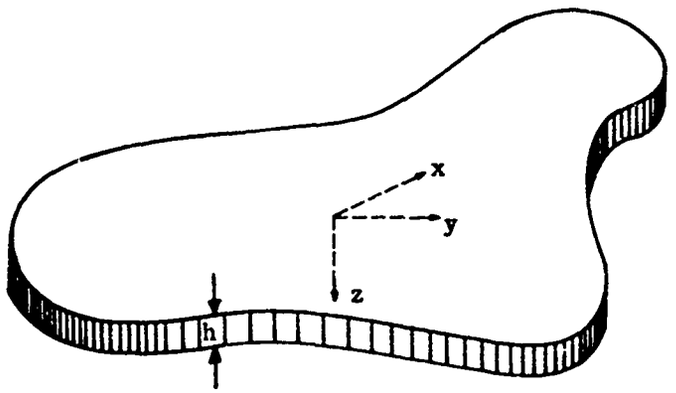


FIGURE 6.2.4-1 PLATE WITH ARBITRARY PLANFORM AND CONSTANT THICKNESS

The temperature of the plate varies in the thickness direction only, that is, $T = \Gamma(z)$. With this assumption, it is further assumed that

$$\sigma_{zz} = \sigma_{zx} = \sigma_{zy} = \sigma_{xy} = 0 \qquad (1)$$

$$\sigma_{xx} = \sigma_{yy} = f(z) \ .$$

It will now be shown that the function $f(z)$ may be determined so that the equations of equilibrium and compatibility are satisfied identically. The boundary conditions of free traction (no restraints) are satisfied on the average.

Substitution of Eqs. (1) into Eqs. (1) of Paragraph 1.2.1 (no body forces) shows that the equilibrium equations are satisfied identically. Furthermore, substitution into the compatibility equations (Section 1) reveals that three of the compatibility equations are satisfied identically, while the other three equations will be satisfied only if

6.2.4 (Cont'd)

$$\frac{d^2}{dz^2}\left(f + \frac{\alpha E T}{1-\nu}\right) = 0 \ , \tag{2}$$

which has the solution

$$f = C_1 + C_2 z - \frac{\alpha E T}{1-\nu} = \sigma_{xx} = \sigma_{yy} \ , \tag{3}$$

where the constants C_1 and C_2 are to be determined from the boundary conditions of zero traction. It is not possible to satisfy the boundary conditions pointwise. However, the constants C_1 and C_2 may be determined so that the resultant force and moment per unit of length produced by σ_{xx} and σ_{yy} are zero over the edge of the plate.

$$\begin{aligned} \int_{-h/2}^{h/2} \sigma_{xx}\, dz &= \int_{-h/2}^{h/2} \sigma_{yy}\, dz = 0 \\ \int_{-h/2}^{h/2} \sigma_{xx} z dz &= \int_{-h/2}^{h/2} \sigma_{yy} z dz = 0 \end{aligned} \tag{4}$$

Substitution of Eq. (3) into Eqs. (4) yields

$$\sigma_{xx} = \sigma_{yy} = \frac{\alpha E}{1-\nu}\left[-T + \frac{1}{h}\int_{-h/2}^{h/2} \Gamma dz + \frac{12z}{h^3}\int_{-h/2}^{h/2} \Gamma z dz\right] \ ,$$

so that finally

$$\sigma_{xx} = \sigma_{yy} = \frac{1}{1-\nu}\left[-\alpha E\Gamma + \frac{N_T}{h} + \frac{12z}{h^3} M_T\right] \ , \tag{5}$$

where N_T and M_T are defined in Eq. (7) of Paragraph 6.1.4. The parallel to the beam equation is apparent.

According to St. Venant's principle, the solution (5) is a very good approximation for traction-free edges at distances from these edges larger than two or three plate thicknesses.

Once the stresses have been determined, the strains are found from the stress-strain relations (Hooke's Law). The displacements are then determined from the strain-displacement relations. The complete solution then appears as follows:

Stress Components:

$$\begin{aligned} \sigma_{xx} = \sigma_{yy} &= \frac{1}{1-\nu}\left[-\alpha E\Gamma + \frac{N_T}{h} + \frac{12z}{h^3} M_T\right] \\ \sigma_{zz} = \sigma_{zx} = \sigma_{zy} = \sigma_{xy} &= 0 \end{aligned} \tag{6}$$

6.2.4 (Cont'd)

Strain Components:

$$\epsilon_{xx} = \epsilon_{yy} = \frac{1}{E}\left[\frac{N_T}{h} + \frac{12z}{h^3} M_T\right]$$

$$\epsilon_{zz} = \frac{-2\nu}{(1-\nu)E}\left[\frac{N_T}{h} + \frac{12z}{h^3} M_T\right] + \left(\frac{1+\nu}{1-\nu}\right) \alpha T \qquad (7)$$

$$\epsilon_{xy} = \epsilon_{yz} = \epsilon_{zx} = 0$$

Displacement Components: (Exclusive of Rigid Body Motion)

$$u = \frac{1}{E}\left[\frac{N_T}{h} + \frac{12z}{h^3} M_T\right] x$$

$$v = \frac{1}{E}\left[\frac{N_T}{h} + \frac{12z}{h^3} M_T\right] y \qquad (8)$$

$$w = -\frac{6}{Eh^3} M_T (x^2 + y^2) + \frac{1}{(1-\nu)E}\left\{(1+\nu)\alpha E \int_0^z T dz - \frac{2\nu z}{h} N_T - \frac{12\nu z^2}{h^3} M_T\right\}$$

6.3 SLAB PROBLEMS - PLATES

Slab problems occur when the plate is loaded by mechanical forces which are parallel to the middle plane of the plate and uniform through the thickness, and the temperature varies in the planform direction only. This is a plane stress problem, i.e., $\sigma_{zx} = \sigma_{zy} = \sigma_{zz} = 0$. The effects of the mechanical loads and temperature may be superposed.

The differential equation for the slab problem is now derived. In the plane stress problem only one equation of compatibility is satisfied, namely

$$\frac{\partial^2 \epsilon_{xx}}{\partial y^2} + \frac{\partial^2 \epsilon_{yy}}{\partial x^2} = \frac{\partial^2 \epsilon_{xy}}{\partial x \, \partial y} . \tag{1}$$

(See Reference 6-4)

If the stress-strain law expressions

$$\epsilon_{xx} = \frac{1}{E} (\sigma_{xx} - \nu \sigma_{yy}) + \alpha T(x,y)$$

$$\epsilon_{yy} = \frac{1}{E} (\sigma_{yy} - \nu \sigma_{xx}) + \alpha T(x,y) \tag{2}$$

$$\epsilon_{xy} = \frac{2(1+\nu)}{E} \sigma_{xy}$$

$$(\sigma_{zz} = \sigma_{zx} = \sigma_{zy} = 0) ,$$

are substituted into Eq. (1) and the stress equilibrium equations

$$\frac{\partial \sigma_{xx}}{\partial x} + \frac{\partial \sigma_{xy}}{\partial y} = 0$$

$$\tag{3}$$

$$\frac{\partial \sigma_{yx}}{\partial x} + \frac{\partial \sigma_{yy}}{\partial y} = 0.$$

there results the equation

$$\nabla^2 (\sigma_{xx} + \sigma_{yy}) + E\alpha\nabla^2 T = 0 , \tag{4}$$

where

$$\nabla^2 = \frac{\partial^2}{\partial x^2} + \frac{\partial^2}{\partial y^2} \quad \text{in rectangular coordinates.}$$

6.3 (Cont'd)

This is the compatibility equation in terms of stresses and temperature only. If a "stress function" $\phi(x,y)$ is introduced such that the components of stress are derivable from ϕ by

$$\sigma_{xx} = \frac{\partial^2 \phi}{\partial y^2}, \quad \sigma_{yy} = \frac{\partial^2 \phi}{\partial x^2}, \quad \sigma_{xy} = -\frac{\partial^2 \phi}{\partial x \partial y}, \tag{5}$$

then the equilibrium Equations (3) are automatically satisfied, and the compatibility equation on ϕ becomes

$$\nabla^4 \phi = -E\alpha\nabla^2 T, \tag{6}$$

where

$$\nabla^4 = \left(\frac{\partial^2}{\partial x^2} + \frac{\partial^2}{\partial y^2}\right)\left(\frac{\partial^2}{\partial x^2} + \frac{\partial^2}{\partial y^2}\right) \text{ in rectangular coordinates.}$$

Since the effects of the mechanical loads and temperature loads may be superposed, it is sufficient in many areas to consider only the thermal problem with the boundaries unrestrained so that the components of stress normal and tangential to the boundary are zero at all points of the boundary (condition of zero traction).

The solution of Eq. (6) for circular plates or rings subject to general asymmetrical temperature distributions has been solved in References 6-5 through 6-8. The results of these investigations are shown in Paragraphs 6.3.1 and 6.3.2.

The particular case of radial symmetry is treated in References 6-9 through 6-11, and the results of these investigations are given in Paragraph 6.3.3.

Theoretical and experimental work has been done for the plane stress solution of rectangular plates subject to planform variation of temperature, for example, References 6-12 and 6-13. However, detailed parametric studies have not been made. The above problem indicates an area which should be explored. No further discussion will be given to the slab problem of rectangular plates in this Manual.

6.3.1 Thermal Stresses in Rings - Asymmetrical Temperature Distribution

The plane stress linear elastic solution of a traction-free circular ring of inner radius a and outer radius b, subjected to a general two-dimensional temperature distribution, was considered in References 6-7 and 6-8. Theory and formulae were developed for the determination of the polar coordinate stress components corresponding to temperatures of the form

$$T = T_o \left(\frac{r}{b}\right)^K \cos n\theta \text{ or } T = T_o \left(\frac{r}{b}\right)^K \sin n\theta,$$

where K and n are restricted to non-negative integers. The purpose of this section is to give a tabular set of quantities for the direct calculations of the stress components corresponding to values of K and n from 0 through 3 for $\frac{a}{b} = 0.2,\ 0.5,\ 0.8$, respectively. This range for the parameters K and n should be adequate for most practical application. A numerical example is given for a particular temperature distribution to demonstrate the application of Table 6.3.1-1.

The stress components corresponding to a temperature distribution of the form

$$T = T_o \left(\frac{r}{b}\right)^K \cos n\theta \quad , \tag{1}$$

may be expressed in the form

$$\frac{\sigma_{rr}}{E\alpha T_o} = B_{K,n} \cos n\theta$$

$$\frac{\sigma_{r\theta}}{E\alpha T_o} = C_{K,n} \sin n\theta \tag{2}$$

$$\frac{\sigma_{\theta\theta}}{E\alpha T_o} = D_{K,n} \cos n\theta \ ,$$

while corresponding to

$$T = T_o \left(\frac{r}{b}\right)^K \sin n\theta \ , \tag{3}$$

the stress components are

$$\frac{\sigma_{rr}}{E\alpha T_o} = B_{K,n} \sin n\theta$$

$$\frac{\sigma_{r\theta}}{E\alpha T_o} = -C_{K,n} \cos n\theta$$

6.3.1 (Cont'd)

$$\frac{\sigma_{\theta\theta}}{E\alpha T_o} = D_{K,n} \sin n\theta \ . \qquad (4)$$

The quantities $B_{K,n}$, $C_{K,n}$, and $D_{K,n}$ are functions of $\frac{a}{b}$, $\frac{r}{b}$, K, n and may be found from Table 6.3.1-1. Use of this table is demonstrated by the following example.

$$T = T_o \left(\frac{r}{b}\right)^2 (1 - \cos\theta) + T_1 = T_o \left(\frac{r}{b}\right)^2 - T_o \left(\frac{r}{b}\right)^2 \cos\theta + T_1$$

$$\frac{a}{b} = 0.5 ,$$

then

$$\frac{\sigma_{rr}}{E\alpha T_o} = B_{2,0} - B_{2,1} \cos\theta$$

$$\frac{\sigma_{r\theta}}{E\alpha T_o} = C_{2,0} - C_{2,1} \sin\theta \qquad (5)$$

$$\frac{\sigma_{\theta\theta}}{E\alpha T_o} = D_{2,0} - D_{2,1} \cos\theta \ .$$

The numerically greatest stress component, for example, is given by

$$\left|\frac{\sigma_{\theta\theta}}{E\alpha T_o}\right|_{max} = \left|\frac{\sigma_{\theta\theta}}{E\alpha T_o}\right|_{r/b = 1,\ \theta = \pi} = \left|-.375 - .1733\right| = 0.55 \ .$$

This corresponds to a compressive stress in the transverse direction at the outer boundary

TABLE 6.3.1-1

THERMAL STRESSES IN RINGS

$\frac{R}{t}$	k	n	$\frac{r}{t}$	$B_{k,n}$	$C_{k,n}$	$B_{k,n}$
0.2	0	0	+1	0	0	0
	1	0	.2	0	0	.1689
			.3	.1210	0	.2680
			.4	.1417	0	.1472
			.5	.1333	0	.05556
			.6	.1136	0	-.04870
			.7	.08814	0	-.09954
			.8	.06062	0	-.1215
			.9	.03072	0	-.02818
			1.0	0	0	-.3112
	2	0	.2	0	0	.1800
			.3	.1246	0	.3036
			.4	.1572	0	.2085
			.5	.1575	0	.1125
			.6	.1322	0	.01778
			.7	.1171	0	-.08709
			.8	.08136	0	-.2064
			.9	.04516	0	-.3352
			1.0	0	0	-.4800
	3	0	.2	0	0	.1085
			.3	.1110	0	.2785
			.4	.1138	0	.2087
			.5	.1022	0	.1153
			.6	.1121	0	.05283
			.7	.1228	0	-.04926
			.8	.09795	0	-.1884
			.9	.05286	0	-.3447
			1.0	0	0	-.5835
	0	1	.2	0	0	-.7350
			.3	-.1548	0	-.4477
			.4	-.1675	0	-.3086
			.5	-.1506	0	-.1870
			.6	-.1267	0	-.08041
			.7	-.09527	0	.02262
			.8	-.06820	0	.1260
			.9	-.03833	0	.2256
			1.0	0	0	.3068
	1	1	+1	0	0	0
	2	1	.2	0	0	.1308
			.3	.01358	.01358	.1177
			.4	.01408	.01408	.2163
			.5	.01808	.01808	.1088
			.6	.01696	.01696	.07361
			.7	.01114	.01114	.08929
			.8	.01170	.01170	-.03088
			.9	.01788	.01788	-.1070
			1.0	0	0	-.1990
	3	1	.2	0	0	.1255
			.3	.01608	.01608	.1372
			.4	.01210	.01210	.1510
			.5	.01058	.01058	.1183
			.6	.01297	.01297	.1216
			.7	.01893	.01893	.09546
			.8	.01770	.01770	-.02555
			.9	.02838	.02838	-.1565
			1.0	0	0	-.3323
	0	2	.2	0	0	1.117
			.3	.008948	.2178	.03603
			.4	-.09150	-.07796	-.1833
			.5	-.1240	-.08772	-.2865
			.6	-.1193	-.08500	-.1955
			.7	-.09717	-.1065	-.1168
			.8	-.06718	-.09373	-.002152
			.9	-.03602	-.05783	.1530
			1.0	0	0	.3800
	1	2	.2	0	0	.3736
			.3	.005126	.0085	.03168
			.4	-.03032	.03998	-.0555
			.5	-.0465	-.09375	-.0854
			.6	-.06480	-.09562	-.08516
			.7	-.03978	-.06118	-.05909
			.8	-.02092	-.03084	-.007200
			.9	-.01536	-.02600	.0639
			1.0	0	0	.1600
	2	2	+1	0	0	0
	3	2	.2	0	0	-.1430
			.3	-.006032	-.06122	-.02839
			.4	.01288	-.08637	.01622
			.5	.02238	-.08188	.04225
			.6	.02536	.01305	.05108
			.7	.02605	.02288	.04818
			.8	.02177	.02538	.01947
			.9	.01123	.01284	-.01756
			1.0	0	0	-.1205
	0	3	.2	0	0	1.433
			.3	-.3061	.3960	.02372
			.4	-.3826	.1478	-.1936
			.5	-.3836	-.03049	-.2589
0.2	0	3	.6	-.3173	-.1488	-.2576
			.7	-.2701	-.1956	-.1878
			.8	-.1820	-.1916	-.03935
			.9	-.06386	-.1388	.1993
			1.0	0	0	.5389
	1	3	.2	0	0	.5965
			.3	-.07806	.1714	.06636
			.4	-.1593	.08596	-.05866
			.5	-.1722	.006686	-.1139
			.6	-.1520	-.05136	-.1361
			.7	-.1166	-.09160	-.1160
			.8	-.07572	-.09938	-.06178
			.9	-.03536	-.07102	.00930
			1.0	0	0	.3156
	2	3	.2	0	0	.1730
			.3	-.02315	.05660	.08825
			.4	-.05098	.03672	-.01080
			.5	-.05869	.008976	-.03619
			.6	-.05486	-.01460	-.05208
			.7	-.04137	-.03194	-.05103
			.8	-.03088	-.03062	-.04048
			.9	-.01478	-.02952	-.01939
			1.0	0	0	.1382
	3	3	+1	0	0	0
			.2	0	0	0
			.3	.02657	0	.1438
			.4	.04218	0	.03540
			.5	.03982	0	-.05745
			.6	.3030	0	-.1325
			1.0	0	0	-.2222
	2	0	.5	0	0	.375
			.6	.04890	0	.2163
			.7	.06845	0	.07355
			.8	.05485	0	-.04985
			.9	.02885	0	-.2179
			1.0	0	0	-.375
	0	1	.5	0	0	-.3778
			.6	-.04379	-.04379	-.2095
			.7	-.05077	-.05077	-.07812
			.8	-.04304	-.04304	.03660
			.9	-.02895	-.02895	.1629
			1.0	0	0	.3846
	1	1	+1	0	0	0
	2	1	.5	0	0	.1433
			.6	.02114	.02114	.1169
			.7	.02720	.02720	.06143
			.8	.02031	.02031	-.000980
			.9	.01086	.01086	-.00805
			1.0	0	0	-.1733
	3	1	.5	0	0	.2250
			.6	.03043	.03043	.1726
			.7	.04304	.04304	.1060
			.8	.03039	.03039	.004409
			.9	.01458	.01458	-.1236
			1.0	0	0	-.3000
	2	2	.5	0	0	.1948
			.6	.006185	.02131	-.01315
			.7	-.005336	.002366	-.04816
			.8	-.01111	-.01323	-.05988
			.9	-.008798	-.01170	-.01187
			1.0	0	0	.1137
	1	2	.5	0	0	.3888
			.6	.003602	.02150	-.006889
			.7	-.008849	.001760	-.03681
			.8	-.008015	-.007015	-.04932
			.9	-.006978	-.008890	-.006715
			1.0	0	0	.06665
	2	2	.5	0	0	0
	3	2	.5	0	0	-.08135
			.6	-.0031166	-.03038	-.00007708
			.7	.0013995	-.02865	.01885
			.8	.005263	-.006068	.03066
			.9	.006928	.008164	-.003135
			1.0	0	0	-.07183
	0	3	.5	0	0	.1661
			.6	-.002887	.06385	-.08970
			.7	-.03822	.007897	-.1369
0.5	0	3	.8	-.07896	-.03897	-.1009
			.9	-.08867	-.08460	.00822
			1.0	0	0	.2384
	1	3	.5	0	0	.2637
			.6	-.001371	.06066	-.01181
			.7	-.02008	.00639	-.08980
			.8	-.03866	-.03843	-.07001
			.9	-.03527	-.03976	.01386
			1.0	0	0	.1669
	2	3	.5	0	0	.1950
			.6	-.0006525	.01867	-.008650
			.7	-.0008643	.003775	-.03808
			.8	-.011136	-.01090	-.03653
			.9	-.007383	-.01422	-.006233
			1.0	0	0	.08225
	3	3	.5-1	0	0	0
0.2	0	0	.8-1	0	0	0
	1	0	.8	0	0	.1037
			.85	.0016379	0	.01922
			.9	.0005533	0	-.001889
			.95	.0010868	0	-.005016
			1.0	0	0	-.09632
	2	0	.8	0	0	.1800
			.85	.0071983	0	.08960
			.9	.0099721	0	0
			.95	.0070992	0	-.08960
			1.0	0	0	-.1800
	3	0	.8	0	0	.2350
			.85	.01054	0	.1286
			.9	.012989	0	.006522
			.95	.0097779	0	-.12801
			1.0	0	0	-.3530
	0	1	.8	0	0	-.1183
			.85	-.0055008	-.0055008	-.05883
			.9	-.0060680	-.0060680	-.0080070
			.95	-.0061359	-.0061359	.05113
			1.0	0	0	.1021
	1	1	.8-1	0	0	0
	2	1	.8	0	0	.08883
			.85	.0019901	.0019901	.04795
			.9	.0056909	.0056909	.0080994
			.95	.0031696	.0031696	-.06058
			1.0	0	0	-.08802
	3	1	.8	0	0	.1545
			.85	.0046712	.0046712	.08724
			.9	.0088863	.0088863	.01399
			.95	.0058132	.0058132	-.07289
			1.0	0	0	-.1668
	0	2	.8	0	0	.01888
			.85	.0008976	.0006952	-.008789
			.9	-.0003211	-.0000908	-.008135
			.95	-.0003678	-.0006683	-.0001657
			1.0	0	0	.01507
	1	2	.8	0	0	.01185
			.85	.0008808	.0006672	-.001722
			.9	-.0000781S	-.0000S536	-.005188
			.95	-.0008687	-.0006675	-.001088
			1.0	0	0	.00837
	2	2	.8-1	0	0	0
	3	2	.8	0	0	-.01579
			.85	-.0008700	-.0006877	.000088
			.9	.0000968	.0000S673	.007614
			.95	.0001388	.0006083	.001762
			1.0	0	0	-.01463
	3	2	.8	0	0	.04019
			.85	.0006753	.002315	-.006695
			.9	-.0005883	-.0003015	-.01708
			.95	-.0009531	-.0.5207	-.003288
			1.0	0	0	.01363
	1	3	.8	0	0	.01134
			.85	.0003807	.001884	-.004558
			.9	-.0006293	-.0002134	-.01182
			.95	-.0007685	-.001767	-.002809
			1.0	0	0	.02763
	2	3	.8	0	0	.01722
			.85	.0002187	.0010136	-.002394
			.9	-.0002368	-.0001068	-.008109
			.95	-.0008319	-.0009965	-.001777
			1.0	0	0	.01574
	3	3	.8-1	0	0	0

6.3.2 Thermal Stresses in Solid Circular Plates Due to Asymmetrical Temperature Distribution

Formulas and curves are presented for the stresses and displacements in an unrestrained solid plate (plane stress solution) corresponding to the temperature

$$T = T_o \left(\frac{r}{b}\right)^K \cos n\Theta \quad (K = 0, 1, 2\ldots,\ n = 0,\ 1,\ 2\ldots).$$

Superposition may then be applied if there are several terms in the temperature expression.

The formulas for the stress components are:

Case I: $K \neq n-2$

$$\begin{aligned}
\sigma_{rr} &= (a\rho^K + \bar{b}\rho^{n-2} + c\rho^n)\, E\alpha T_o \cos n\Theta \\
\sigma_{\Theta\Theta} &= (A\rho^K + B\rho^{n-2} + C\rho^n)\ E\alpha T_o \cos n\Theta \\
\sigma_{r\Theta} &= (\delta\rho^K + \beta\rho^{n-2} + \gamma\rho^n)\ E\alpha T_o \sin n\Theta
\end{aligned} \tag{1}$$

Case II: $K = n-2$

$$\begin{aligned}
\sigma_{rr} &= (a'\rho^{n-2} + b'\rho^{n-2}\ln p + c\rho^n)\ E\alpha T_o \cos n\Theta \\
\sigma_{\Theta\Theta} &= (A'\rho^{n-2} + B'\rho^{n-2}\ln\rho + C\rho^n)\, E\alpha T_o \cos n\Theta \\
\sigma_{r\Theta} &= (\delta'\rho^{n-2} + \beta'\rho^{n-2}\ln\rho + \gamma\rho^n)\, E\alpha T_o \sin n\Theta
\end{aligned} \tag{2}$$

6.3.2 (Cont'd)

where

$$\rho = \frac{r}{b}, \qquad A = \frac{-(K+1)(K+2)}{(K+2)^2 - n^2}$$

$$\delta = \frac{-n\,(K+1)}{(K+2)^2 - n^2}, \qquad \bar{b} = \frac{-n(n-1)(n-K)}{2\left[(K+2)^2 - n^2\right]} = -B = -\beta$$

$$c = \frac{-(n+1)(n-2)}{2(K+2+n)}, \qquad C = \frac{(n+1)(n+2)}{2(K+2+n)}, \qquad \gamma = \frac{(n+1)(n)}{2(K+2+n)}$$

$$a' = \frac{(n+1)(n-2)}{4n}, \qquad A' = \frac{-n^2 - 3n + 2}{4n}, \qquad \delta' = \frac{-(n+1)}{4}$$

$$b' = \frac{n-1}{2} = -B' = -\beta', \qquad a = \frac{n^2 - K - 2}{(K+2)^2 - n^2}.$$

The stresses σ_{rr}, $\sigma_{\theta\theta}$, $\sigma_{r\theta}$ are plotted in Figures 6.3.2-1 through -3 for n = 1, 2, 3 with K as a parameter. The axisymmetric case, n = 0 is shown in Figure 6.3.2-4. From symmetry, the shear component $\sigma_{r\theta}$ equals 0.

The following should be noted:

(1) When K = n, the temperature is a harmonic function (i.e., $\nabla^2 T = 0$) since $r^n \cos n\theta$ is the real part of z^n ($z = x + iy$). Thus the corresponding stress components

$$\sigma_{rr} = \sigma_{r\theta} = \sigma_{\theta\theta} = 0.$$

(2) When $T = T_o \left(\frac{r}{b}\right)^K \sin n\theta$ (n = 1, 2, ...), then in the formulas for the stress components, Eqs. (1) and (2), cos nθ and sin nθ must be replaced by sin nθ and -cos nθ, respectively.

In the following example in which a circular bulkhead of radius b is subjected to a temperature distribution

$$T = T_o \left(\frac{r}{b}\right)^2 (1 - \cos\theta) + T_1$$

$$= T_o \left(\frac{r}{b}\right)^2 - T_o \left(\frac{r}{b}\right)^2 \cos\theta + T_1,$$

where T_o, T_1 are constants, the expressions are desired for the stress components.

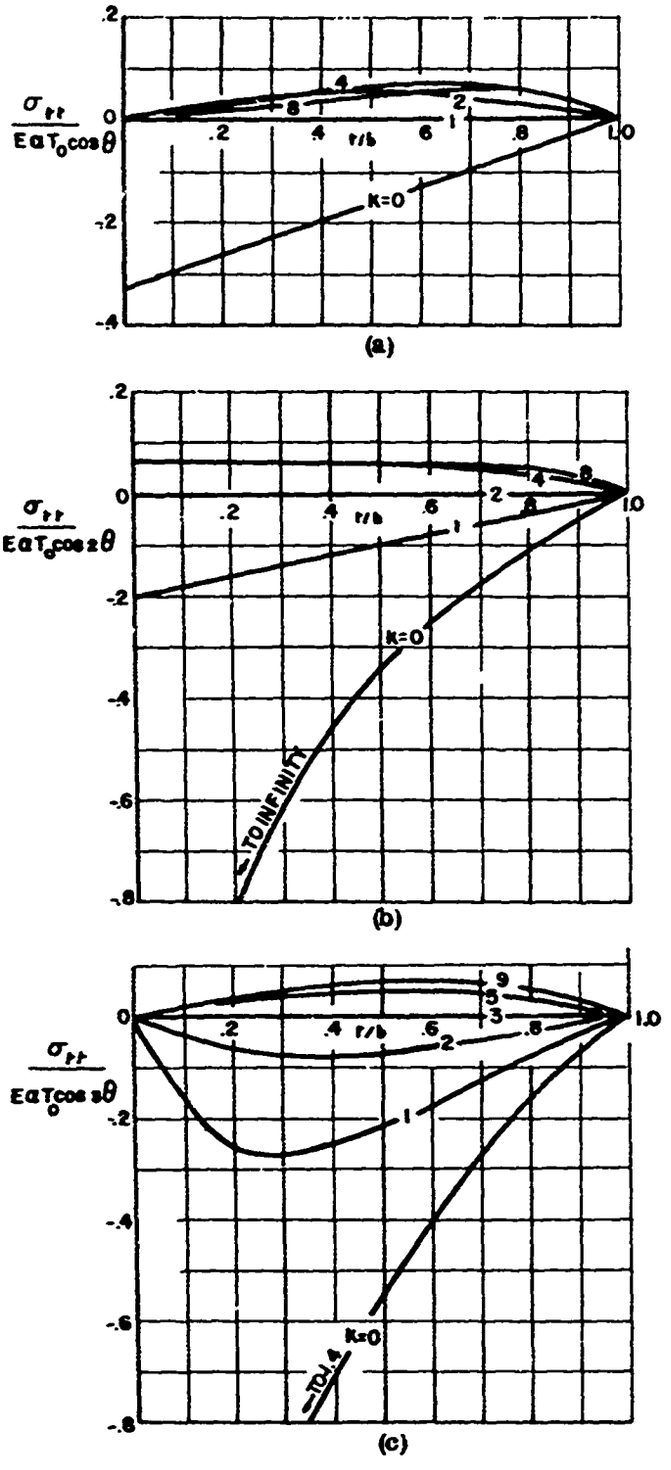


FIGURE 6.3.2-1 RADIAL STRESS DISTRIBUTION IN A DISK WHEN A TEMPERATURE DISTRIBUTION $T = T_0(r/b)^K \cos n\Theta$ (n = 0, 1, 2, 3) IS MAINTAINED

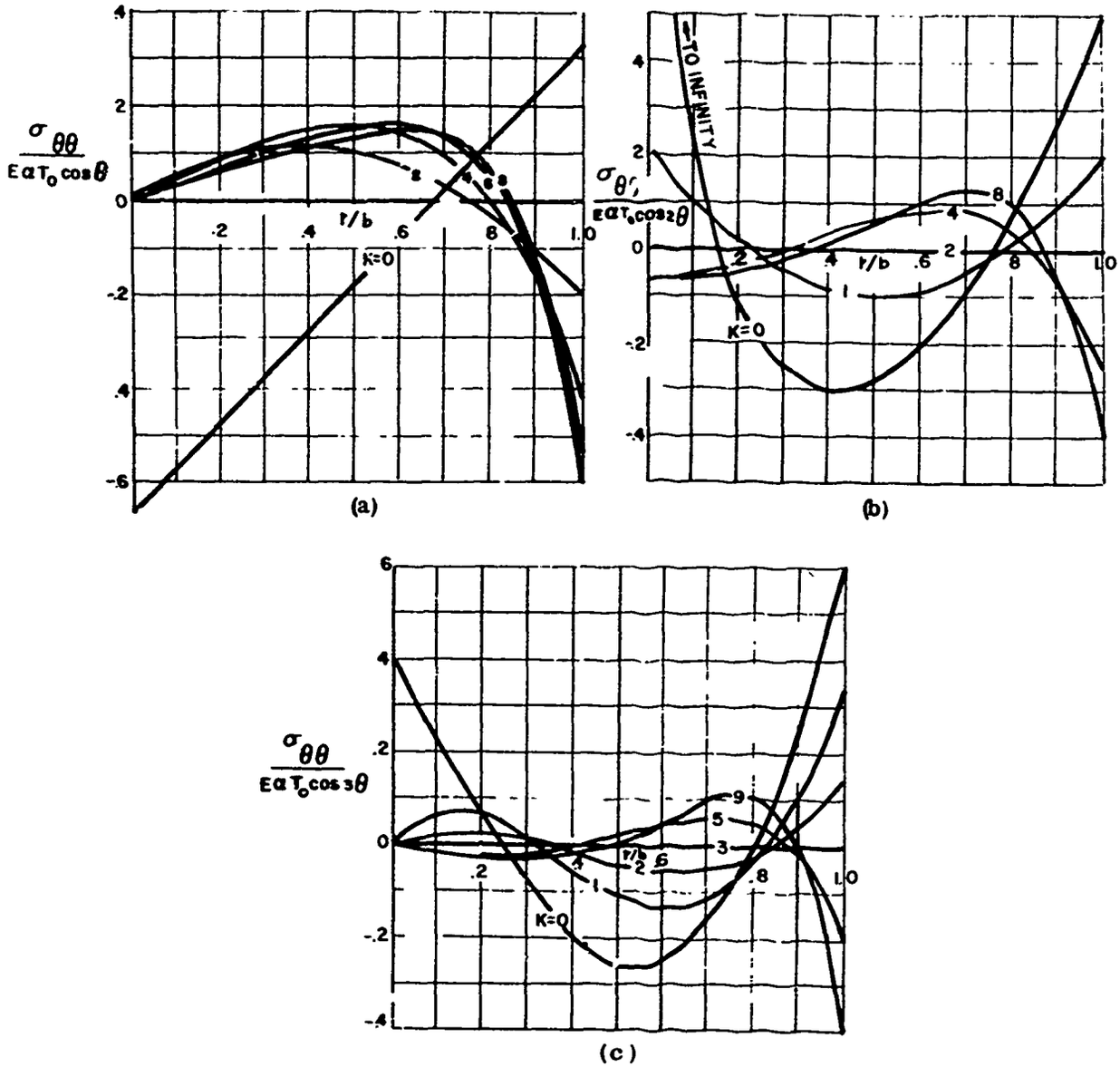
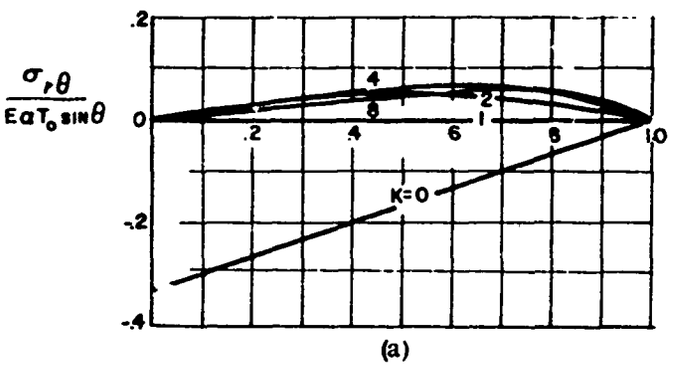
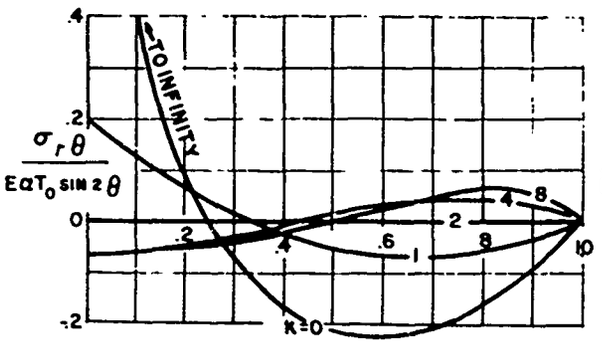


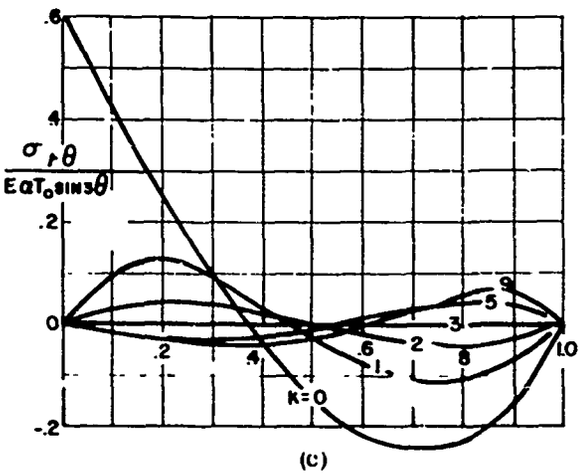
FIGURE 6.3.2-2 HOOP-STRESS DISTRIBUTION IN DISK WHEN TEMPERATURE DISTRIBUTION $T = T_0 (r/b)^K \cos n\Theta$ (n = 0, 1, 2, 3) IS MAINTAINED



(a)



(b)



(c)

FIGURE 6.3.2-3 SHEAR-STRESS DISTRIBUTION IN DISK WHEN TEMPERATURE DISTRIBUTION $T = T_0 (r/b)^K \cos n\Theta$ (n = 1, 2, 3) IS MAINTAINED

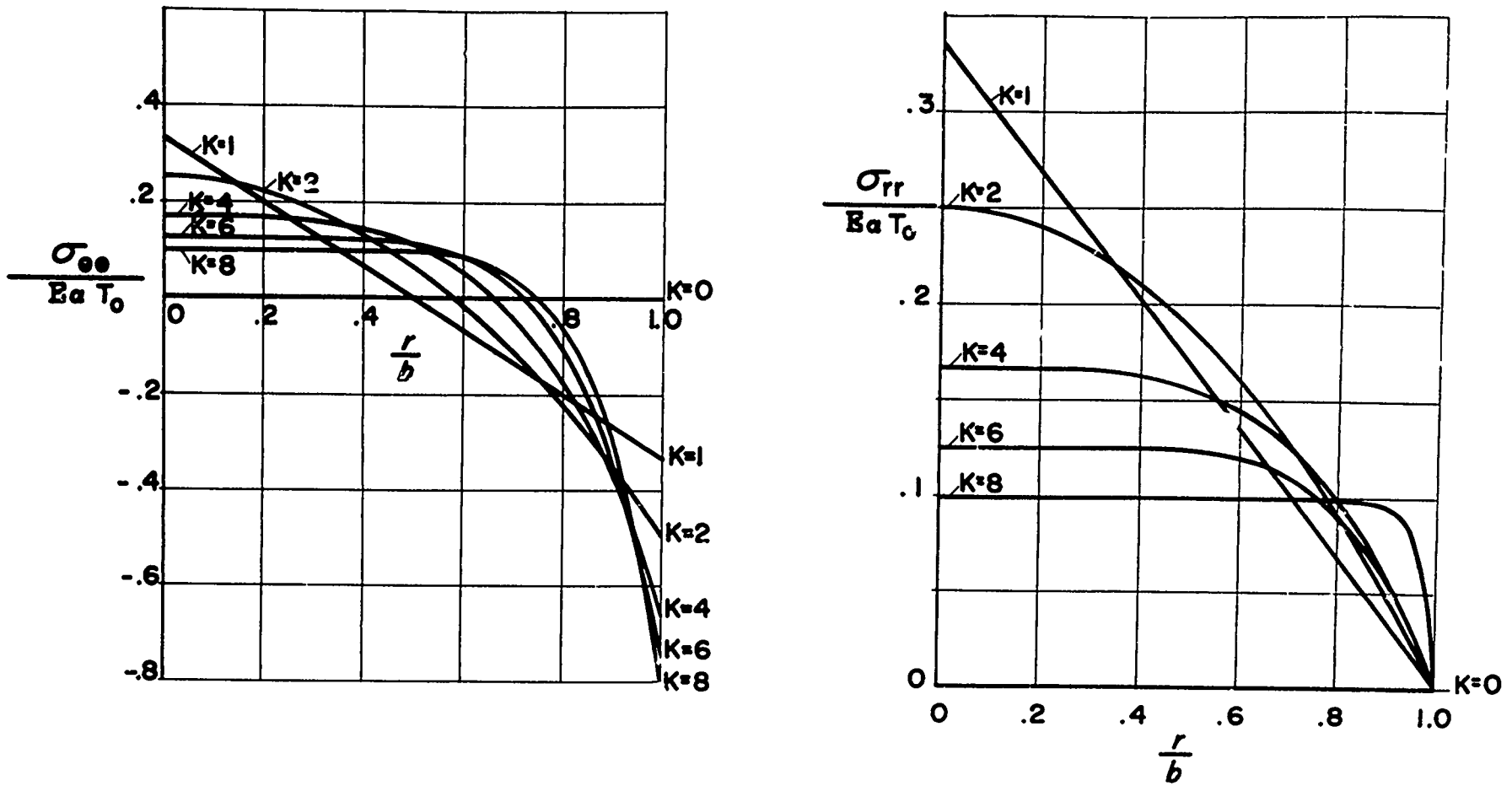


FIGURE 6.3.2-4 RADIAL AND HOOP STRESS DISTRIBUTION FOR THE AXISYMMETRIC TEMPERATURE CASE, $T = T_0 (r/b)^K$

(1) Stress components corresponding to $T_o\left(\frac{r}{b}\right)^2$: (K = 2, n = 0);
Eq. (1) yield the coefficients

$$a = \frac{-4}{16} = -\frac{1}{4}\ , \qquad A = \frac{-(3)(4)}{(4)^2} = -\frac{3}{4}\ , \qquad \delta = 0$$

$$\bar{b} = 0\ , \qquad B = -\bar{b} = 0\ , \qquad \beta = 0$$

$$c = \frac{-(1)(-2)}{2(4)} = \frac{1}{4}\ , \qquad C = \frac{(1)(2)}{2(4)} = \frac{1}{4}\ , \qquad \gamma = 0$$

which in turn yield the desired stress components

$$\frac{\sigma_{rr}}{E\alpha T_o} = \left(-\frac{1}{4}\rho^2 + \frac{1}{4}\right)$$

$$\frac{\sigma_{\theta\theta}}{E\alpha T_o} = \left(-\frac{3}{4}\rho^2 + \frac{1}{4}\right)$$

$$\frac{\sigma_{r\theta}}{E\alpha T_o} = 0\ .$$

(2) Stress components corresponding to $T_o\left(\frac{r}{b}\right)^2 \cos\theta$: (K = 2, n = 1);
Eqs. (1) yield the coefficients

$$a = \frac{-3}{15} = -\frac{1}{5}\ , \qquad A = \frac{-12}{15} = -\frac{4}{5}\ , \qquad \delta = \frac{-3}{15} = -\frac{1}{5}$$

$$\bar{b} = 0\ , \qquad B = 0\ , \qquad \beta = 0$$

$$c = \frac{-(-2)}{2(5)} = \frac{1}{5}\ , \qquad C = \frac{6}{2(5)} = \frac{3}{5}\ , \qquad \gamma = \frac{1}{5}$$

which in turn yield the desired stress components

$$\frac{\sigma_{rr}}{E\alpha T_o} = \left(-\frac{1}{5}\rho^2 + \frac{1}{5}\rho\right)\cos\theta$$

$$\frac{\sigma_{\theta\theta}}{E\alpha T_o} = \left(-\frac{4}{5}\rho^2 + \frac{3}{5}\rho\right)\cos\theta$$

6.3.2 (Cont'd)

$$\frac{\sigma_{r\theta}}{E\alpha T_o} = \left(-\frac{1}{5}\rho^2 + \frac{1}{5}\rho \right) \sin\theta .$$

(3) Stress components corresponding to T_1 are: $\sigma_{rr} = \sigma_{r\theta} = \sigma_{\theta\theta} = 0$.

(4) Total stress components are:

$$\frac{\sigma_{rr}}{E\alpha T_o} = \frac{1}{4}(1 - \rho^2) + \left[\frac{\rho}{5}(\rho - 1)\right] \cos\theta$$

$$\frac{\sigma_{\theta\theta}}{E\alpha T_o} = \frac{1}{4}\left[1 - 3\rho^2\right] + \frac{\rho}{5}\left[4\rho - 3\right] \cos\theta$$

$$\frac{\sigma_{r\theta}}{E\alpha T_o} = \frac{\rho}{5}(\rho - 1) \sin\theta .$$

6.3.3 Circular Disk with Concentric Hole Subject to a Power Law Temperature Distribution

The thermal stresses in thin circular disks of constant thickness with a concentric hole subject to a power law distribution in the radial direction are determined. The following three cases will be considered:

I The disk with a central hole
II The solid disk
III The disk mounted on a shaft

Formulas and curves will be given for the radial displacement and stress components assuming a condition of plane stress (Paragraph 2.1.7). The following symbols are used in this paragraph:

a	Inner radius of plate
b	Outer radius of plate
n	Exponent in temperature distribution
r	Radial coordinate
u	Radial displacement of points on disk
E, ν, α	Modulus of elasticity, Poisson's ratio, and coefficient of linear expansion, respectively
T	Temperature
T*	Mean temperature when referred to the square of the radius = $2\ (r^2 - a^2)^{-1} \int_a^r Trdr = (r^2 - a^2)^{-1} \int_a^r Td(r^2)$
σ_{rr}	Radial component of stress
$\sigma_{\theta\theta}$	Tangential component of stress
Suffix a	Refers to the inner radius of the disk
Suffix b	Refers to the outer radius of the disk .

A circular disk of radius b and constant thickness and with inner concentric hole of radius a is subject to the radial temperature variation

$$T = T_b \left(\frac{r-a}{b-a}\right)^n , \tag{1}$$

where T_b is the temperature at r = b.

The variation of the temperature distribution versus $\frac{r-a}{b-a}$ with n as a parameter is shown in Figure 6.3.3-1.

The expressions for the radial displacement, and the radial and transverse components of stress are:

$$u = Ar + \frac{B}{r} + \left[\frac{\alpha(1+\nu)(r^2 - a^2)\ T^*}{2r}\right] \tag{2}$$

6.3.3 (Cont'd)

$$\sigma_{rr} = \frac{E}{1-\nu^2}\left[A(1+\nu) + \frac{B(\nu-1)}{r^2} - \frac{\alpha}{2r^2}(1-\nu^2)(r^2-a^2)T^*\right] \quad (3)$$

$$\sigma_{\theta\theta} = \frac{E}{1-\nu^2}\left[A(1+\nu) - \frac{B(\nu-1)}{r^2} - (1-\nu^2)\alpha T + (1-\nu^2)\frac{\alpha(r^2-a^2)T^*}{2r^2}\right], \quad (4)$$

where A and B are constants which must be determined from the boundary conditions and

$$T^* = 2\left(r^2-a^2\right)^{-1}\int_a^r Trdr \ . \quad (5)$$

Case I - Unrestrained Disk With Concentric Circular Hole

The boundary conditions $\sigma_{rr} = 0$ at r = a, r = b are imposed.

The expression for the displacement u in non-dimensional form is

$$\frac{2ru}{\alpha a^2 T_b^*} = (1-\nu)\frac{r^2}{a^2} + (1+\nu) + (1+\nu)\left(\frac{r^2}{a^2}-1\right)\frac{T^*}{T_b^*} \ , \quad (6)$$

while the expressions for σ_{rr} and $\sigma_{\theta\theta}$ are:

$$\frac{\sigma_{rr}}{\alpha E T_b} = \left(1-\frac{a^2}{r^2}\right)\left(\frac{T_b^*-T^*}{2T_b}\right) \quad (7)$$

$$\frac{\sigma_{\theta\theta}}{\alpha E T_b} = \frac{1}{2T_b}\left[T_b^*\left(1+\frac{a^2}{r^2}\right) - 2T + \left(1-\frac{a^2}{b^2}\right)T^*\right] \ . \quad (8)$$

Figure 6.3.3-2 shows the radial variation of $\frac{\sigma_{rr}}{\alpha E T_b}$ for a disk with a hole $\left(\frac{a}{b} \doteq 0, 0.4, 0.8\right)$ corresponding to n = 1/3, 1, 3 $\left(\frac{a}{b} \doteq 0$ means a very small hole, not a solid disk$\right)$.

Figure 6.3.3-3 shows the maximum radial components of stress versus n.

From Eqs. (1) and (8),

$$\frac{\sigma_{\theta\theta_a}}{\alpha E T_b} = \frac{T_b^*}{T_b} = \frac{2}{(n+1)(n+2)}\left[\frac{(n+1)b+a}{a+b}\right] \quad (9)$$

$$\frac{\sigma_{\theta\theta_b}}{\alpha E T_b} = \frac{T_b^*}{T_b} - 1 = 2\left[\frac{b(n+1)+a}{(n+1)(n+2)(a+b)} - \frac{1}{2}\right] . \quad (10)$$

Curves showing the variation of $\frac{\sigma_{\Theta\Theta_a}}{\alpha E T_b}$ and $\frac{\sigma_{\Theta\Theta_b}}{\alpha E T_b}$ with a/b and n are given in Figures 6.3.3-4 and 6.3.3-5.

Case II - Solid Disk

The displacement and the stress components for a solid disk (a = 0) are determined by imposing the conditions $u\big]_{r=0} = 0$ and $\sigma_{rr}\big]_{r=b} = 0$.

The radial displacement is

$$u = \frac{\alpha T_b^* \, r}{2} \left[(1 - \nu) + (1 + \nu) \frac{T^*}{T_b^*} \right] . \tag{11}$$

In particular, the radial displacement on the boundary is

$$u\big]_{r=b} = \alpha T_b^* \, b . \tag{12}$$

The equations for σ_{rr} and $\sigma_{\Theta\Theta}$ in non-dimensional form are

$$\frac{\sigma_{rr}}{\alpha E T_b} = \frac{1}{2} \left(\frac{T_b^*}{T_b} - \frac{T^*}{T_b} \right) \tag{13}$$

$$\frac{\sigma_{\Theta\Theta}}{\alpha E T_b} = \frac{1}{2} \left(\frac{T_b^*}{T_b} + \frac{T^*}{T_b} - \frac{2T}{T_b} \right) . \tag{14}$$

When T varies according to the power law (Eq. (1)) with n positive, σ_{rr} falls from its maximum (tensile) value at the center of the disk to zero at the periphery. At the center, $\sigma_{rr} = \sigma_{\Theta\Theta}$ and $\sigma_{\Theta\Theta}$ falls montonically with increasing radius (in an algebraic sense) having its maximum compressive stress at the boundary r = b. From Eqs. (13) and (14),

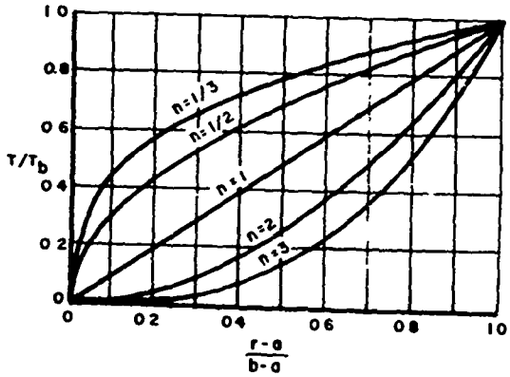
$$\frac{\sigma_{rr_a}}{\alpha E T_b} = \frac{\sigma_{\Theta\Theta_a}}{\alpha E T_b} = \frac{1}{2} \left(\frac{T_b^*}{T_b} - \frac{T_a}{T_b} \right) = \frac{1}{n+2} \tag{15}$$

and

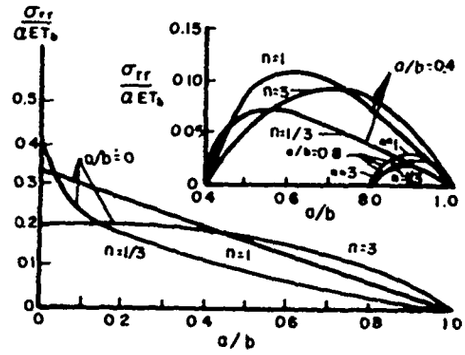
$$\frac{\sigma_{\Theta\Theta_b}}{\alpha E T_b} = - \frac{n}{n+2} . \tag{16}$$

Figure 6.3.3-6 shows the variation of $\frac{\sigma_{rr_a}}{\alpha E T_b}$, $\frac{\sigma_{\Theta\Theta_a}}{\alpha E T_b}$, and $\frac{\sigma_{\Theta\Theta_b}}{\alpha E T_b}$ with n for a solid disk.

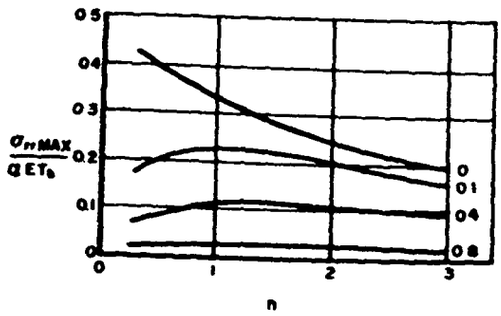
6.3.3 (Cont'd)



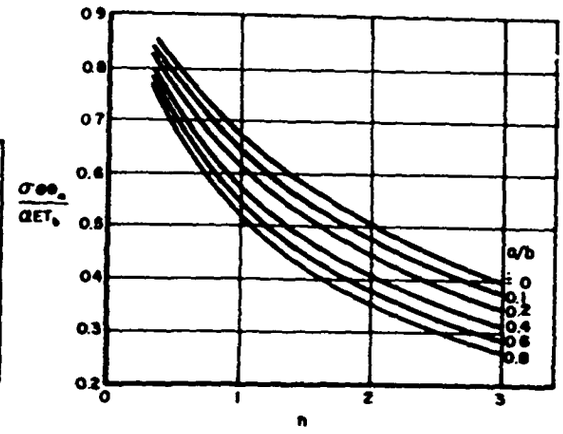
TEMPERATURE PROFILES FOR n = 1/3, 1/2, 1, 2 & 3
FIGURE 6.3.3-1



RADIAL VARIATION OF RADIAL STRESS FOR A DISK WITH A HOLE (a/b = 0, 0.4, 0.8, n = 1/3, 1 & 3)
FIGURE 6.3.3-2

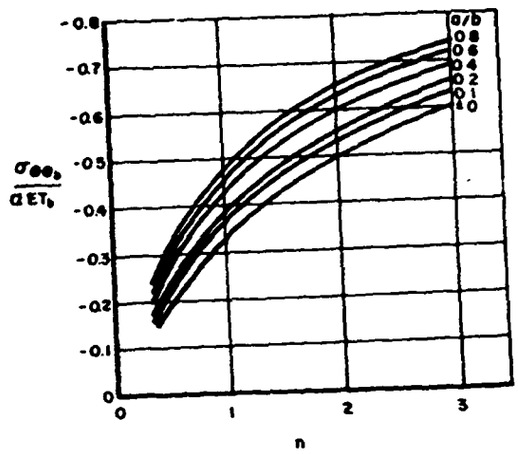


VARIATION OF MAX. RADIAL STRESS WITH n & a/b FOR A DISK WITH A HOLE
FIGURE 6.3.3-3



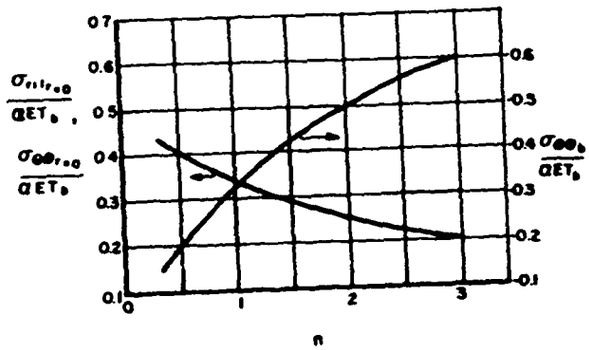
VARIATION OF TANGENTIAL STRESS AT INNER BOUNDARY, WITH n & a/b FOR A DISK WITH A HOLE
FIGURE 6.3.3-4

6.3.3 (Cont'd)



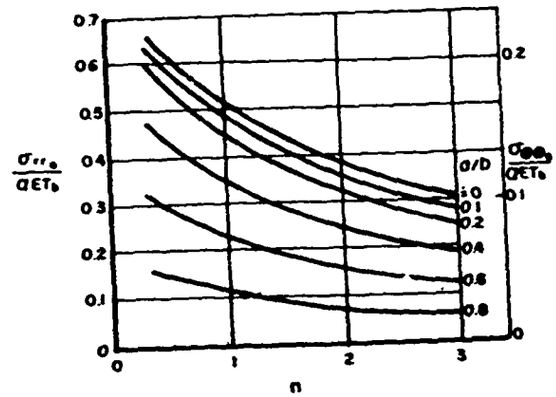
VARIATION OF TANGENTIAL STRESS AT OUTER BOUNDARY WITH n & a/b FOR DISK WITH A HOLE

FIGURE 6.3.3-5



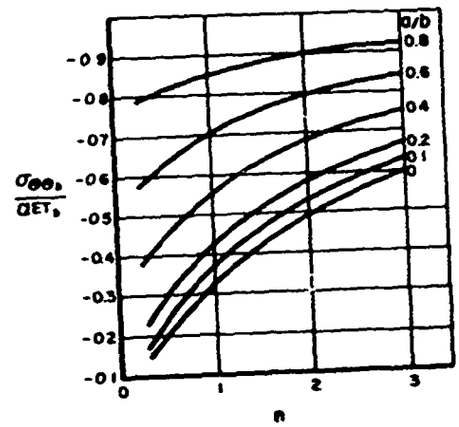
VARIATION OF RADIAL & TANGENTIAL STRESS AT CENTER & BOUNDARY WITH n FOR A SOLID DISK

FIGURE 6.3.3-6



VARIATION OF RADIAL & TANGENTIAL STRESS AT INNER BOUNDARY OF DISK WITH n & a/b FOR A DISK ON A SHAFT

FIGURE 6.3.3-7



VARIATION OF TANGENTIAL STRESS AT OUTER BOUNDARY OF DISK WITH n & a/b FOR A DISK ON A SHAFT

FIGURE 6.3.3-8

6.3.3 (Cont'd)

Case III - Disk With Central Shaft

This case is analyzed as a plane-stress problem, i.e., no account is taken of the stress concentration at the cylindrical interface between the shaft and disk. It is assumed that at the interface no radial movement occurs, i.e., $u\big]_{r=a} = 0$. The other boundary condition is that $\sigma_{rr}\big]_{r=b} = 0$, i.e., the outer boundary is unrestrained.

The following expressions result for σ_{rr} and $\sigma_{\theta\theta}$:

$$\frac{\sigma_{rr}}{\alpha E T_b} = \frac{1}{2}\left[\frac{T_b^*}{T_b}\left(1 - \frac{a^2}{b^2}\right)\frac{\left[\frac{1+\nu}{1-\nu} + \frac{a^2}{r^2}\right]}{\left[\frac{1+\nu}{1-\nu} + \frac{a^2}{b^2}\right]} - \frac{T^*}{T_b}\left(1 - \frac{a^2}{r^2}\right)\right] \tag{17}$$

$$\frac{\sigma_{\theta\theta}}{\alpha E T_b} = \frac{1}{2}\left[\frac{T_b^*}{T_b}\left(1 - \frac{a^2}{b^2}\right)\frac{\left[\frac{1+\nu}{1-\nu} - \frac{a^2}{r^2}\right]}{\left[\frac{1+\nu}{1-\nu} + \frac{a^2}{b^2}\right]} + \frac{T^*}{T_b}\left(1 - \frac{a^2}{r^2}\right) - \frac{2T}{T_b}\right] \tag{18}$$

In particular, the expressions for σ_{rr_a}, $\sigma_{\theta\theta_a}$, and $\sigma_{\theta\theta_b}$ are:

$$\frac{\sigma_{rr_a}}{\alpha E T_b} = \left[\frac{T_b^*}{T_2}\left(1 - \frac{a^2}{b^2}\right)\left(\frac{(1-\nu)^{-1}}{\frac{1+\nu}{1-\nu} + \frac{a^2}{b^2}}\right)\right] \tag{19}$$

$$\frac{\sigma_{\theta\theta_a}}{\alpha E T_b} = \left[\frac{T_b^*}{T_2}\left(1 - \frac{a^2}{b^2}\right)\left(\frac{(\nu/1-\nu)}{\frac{1+\nu}{1-\nu} + \frac{a^2}{b^2}}\right)\right] \tag{20}$$

$$\frac{\sigma_{\theta\theta_b}}{\alpha E T_b} = \left[\frac{T_b^*}{T_2}\left(1 - \frac{a^2}{b^2}\right)\left(\frac{(1+\nu)/(1-\nu)}{(1+\nu)(1-\nu) + \frac{a^2}{b^2}}\right) - 1\right] \tag{21}$$

Curves showing the variation of σ_{rr_a}, $\sigma_{\theta\theta_a}$, and $\sigma_{\theta\theta_b}$ with n and a/b are shown in Figures 6.3.3-7 and 6.3.3-8.

6.3.4 Circular Plate - Central Hot Spot

The stresses in a circular plate due to a concentric hot spot are determined (References 6-10, 6-11). The central hot spot may be another material at constant temperature or a hot fluid passing through the plate. The method of solution is to solve the steady-state heat conduction equation subject to prescribed boundary temperatures. Once this temperature distribution is determined, the equation of equilibrium in the radial direction and the enforcement of single-valuedness of displacements yields the solution.

The following symbols are used in this paragraph:

a	Radius of hot spot (Figure 6.3.4-1)
b	Outer radius of plate
r	Radial polar coordinate
t	Thickness of plate/thickness of hot spot
u	Radial displacement
T	Excess of temperature of hot spot over that relative to the outer edge of plate
σ_{rr}	Radial component of stress
$\sigma_{\theta\theta}$	Transverse or tangential component of stress

The following assumptions are made:

(1) The hot spot is at constant temperature T relative to the outer edge of the plate
(2) The plate is assumed to be insulated so that all heat enters at radius a and leaves at radius b which is at temperature 0.
(3) Plate is assumed to be thin so that plane stress analysis (Section 2) may be used. The outer boundary is assumed to be unrestrained.
(4) $E\alpha$ is constant.

The following design equations pertain to this problem:

(1) Temperature Distribution in Plate:

$$\text{Temperature} = T \frac{\text{Log } (b/r)}{\text{Log } (b/a)} , \tag{1}$$

where $a \leqq r \leqq b$.

(2) Radial Displacement at Junction Line r = a:

$$u\Big]_{r=a} = \alpha T a + \frac{(1-\nu)\,at}{E}\left(\frac{A}{a^2} + B - \frac{E\alpha T}{2}\right) ,$$

where

$$B = \frac{-E\alpha T}{2 \log b/a} \quad \frac{\left[1-(1-\nu)(1-t)\log (b/a)\right]}{\left\{\left[(1+\nu) + (1-\nu)t\right] b^2/a^2 + (1-\nu)(1-t)\right\}} \tag{2a}$$

$$A = -Bb^2 \tag{2b}$$

6.3.4 (Cont'd)

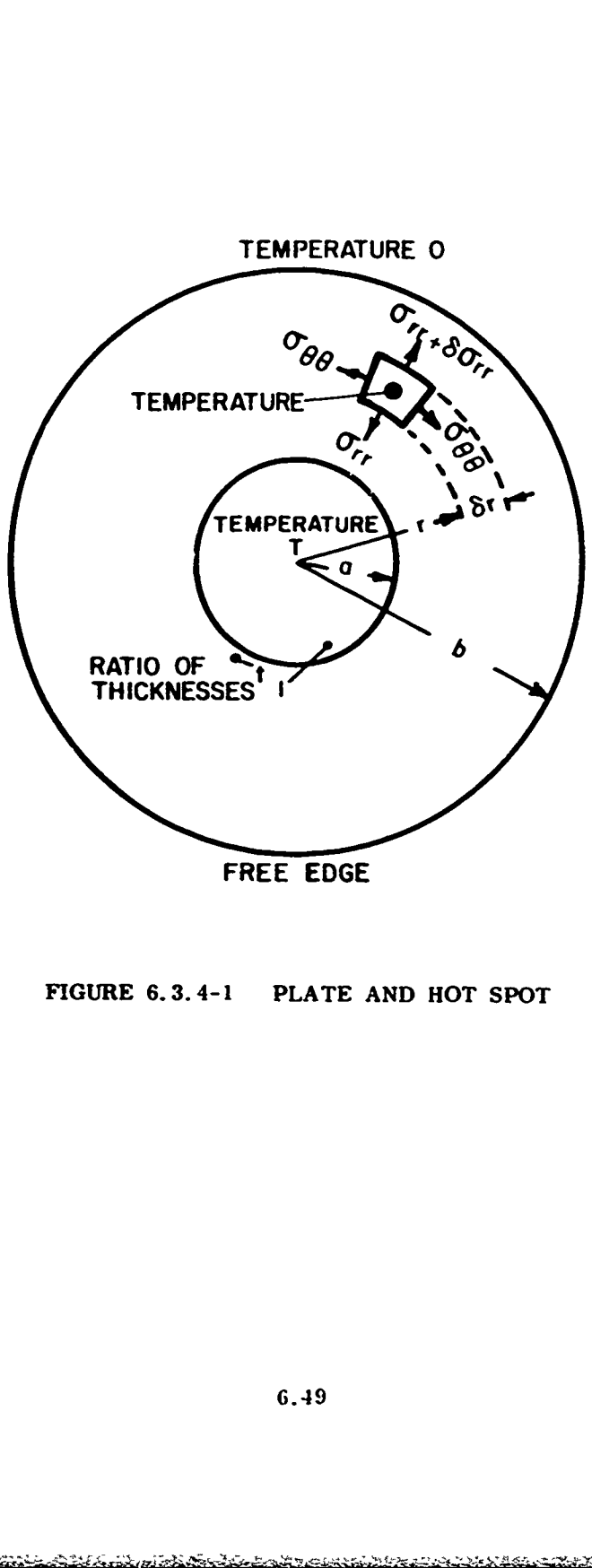


FIGURE 6.3.4-1 PLATE AND HOT SPOT

6.3.4 (Cont'd)

A graph of $\frac{u}{a\alpha T}\Big]_{r=a}$, $\frac{u}{b\alpha T}\Big]_{r=b}$ versus $\frac{b}{a}$, with t as a parameter, is shown in Figures 6.3.4-2a and 6.3.4-2b.

The components of stress in the radial and transverse directions are

$$\sigma_{rr} = \frac{E\alpha T}{2 \text{ Log } b/a}\left\{\frac{[1 - (1-\nu)(1-t) \text{ Log } (b/a)](b^2/r^2 - 1)}{[(1+\nu) + (1-\nu)t]\, b^2/a^2 + (1-\nu)(1-t)} - \text{Log } (b/r)\right\} \quad (3)$$

and

$$\sigma_{\theta\theta} = \frac{E\alpha T}{2 \text{ Log } b/a}\left\{1 - \frac{[1 - (1-\nu)(1-t) \text{ Log } (b/a)](b^2/r^2 + 1)}{[(1+\nu) + (1-\nu)t]\, b^2/a^2 + (1-\nu)(1-t)} - \text{Log } (b/r)\right\} \quad (4)$$

The variation of σ_{rr} and $\sigma_{rr} - \sigma_{\theta\theta}$ with r/a is shown in Figure 6.3.4-3 for $\nu = 0.3$, b/a = 2, 3, ∞ and for t = 0, 0.2, 0.5, 1, 2, 5 and ∞. Values of $\sigma_{\theta\theta}$ may be found by combining the given curves.

Figure 6.3.4-4 shows the variation of $\sigma_{rr} - \sigma_{\theta\theta}$ at r = a and r=b with b/a, with t as a parameter.

The following special cases are considered:

If the extent of the plate is large compared with that of the hot spot (b/a large), then

$$\sigma_{rr} = \frac{-E\alpha T}{2}\left[1 + \frac{(1-\nu)(1-t)\, a^2}{[(1+\nu) + (1-\nu)t]\, r^2}\right] \quad (5)$$

$$\sigma_{\theta\theta} = \frac{-E\alpha T}{2}\left[1 - \frac{(1-\nu)(1-t)\, a^2}{[(1+\nu) + (1-\nu)t]\, r^2}\right] \quad (6)$$

and

$$\sigma_{rr} - \sigma_{\theta\theta} = -E\alpha T\left[\frac{(1-\nu)(1-t)\, a^2}{[(1+\nu) + (1-\nu)t]\, r^2}\right] \quad (7)$$

Note that the majority of the plate is subjected to bi-axial compression of magnitude $\frac{E\alpha T}{2}$. The stress difference has a maximum value obtained by substituting r=a into Eq. (7) which varies with t as shown in Figure 6.3.4-5.

If b/a is near unity, the plate becomes a thin ring, resulting in

$$\sigma_{rr} \longrightarrow 0 \quad \text{and}$$

$$\sigma_{rr} - \sigma_{\theta\theta} \longrightarrow -E\alpha T\left(\frac{r-a}{b-a}\right)$$

6.3.4 (Cont'd)

$$\frac{[U]_{r=a}}{a\alpha T} = 1 - \frac{(1-\nu) + \left[1 + \left(\frac{b^2}{a}\right)\left\{2\ln\left(\frac{b^2}{a}\right) - 1\right\}\right]}{2\ln\left(\frac{b}{a}\right)\left\{(1+\nu)\left(\frac{b}{a}\right)^2 + (1-\nu)\left[\frac{1}{2}\left(\left(\frac{b}{a}\right)^2 - 1\right) + 1\right]\right\}}$$

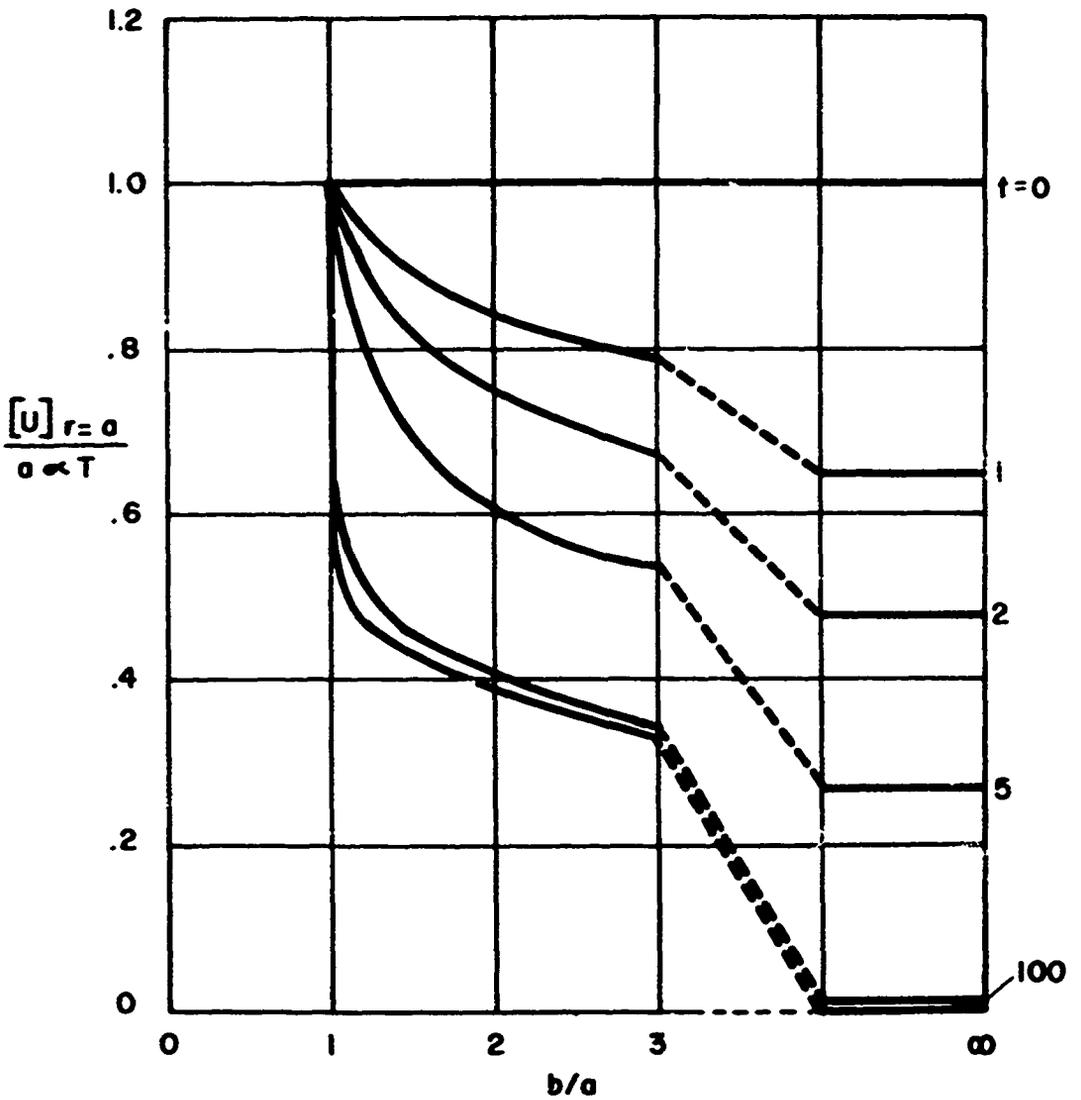


FIGURE 6.3.4-2(a) RADIAL DISPLACEMENT AT BOUNDARY OF HOT SPOT ($\nu = 0.3$)

6.3.4 (Cont'd)

$$\frac{[U]_{r=b}}{b\alpha T} = \frac{1}{2\ln\left(\frac{b}{a}\right)}\left[1 - \frac{2\left\{1-(1-\nu)(1-t)\ln\left(\frac{b}{a}\right)\right\}}{\left[\left\{(1+\nu)+(1-\nu)t\right\}\left(\frac{b}{a}\right)^2+(1-\nu)(1-t)\right]}\right]$$

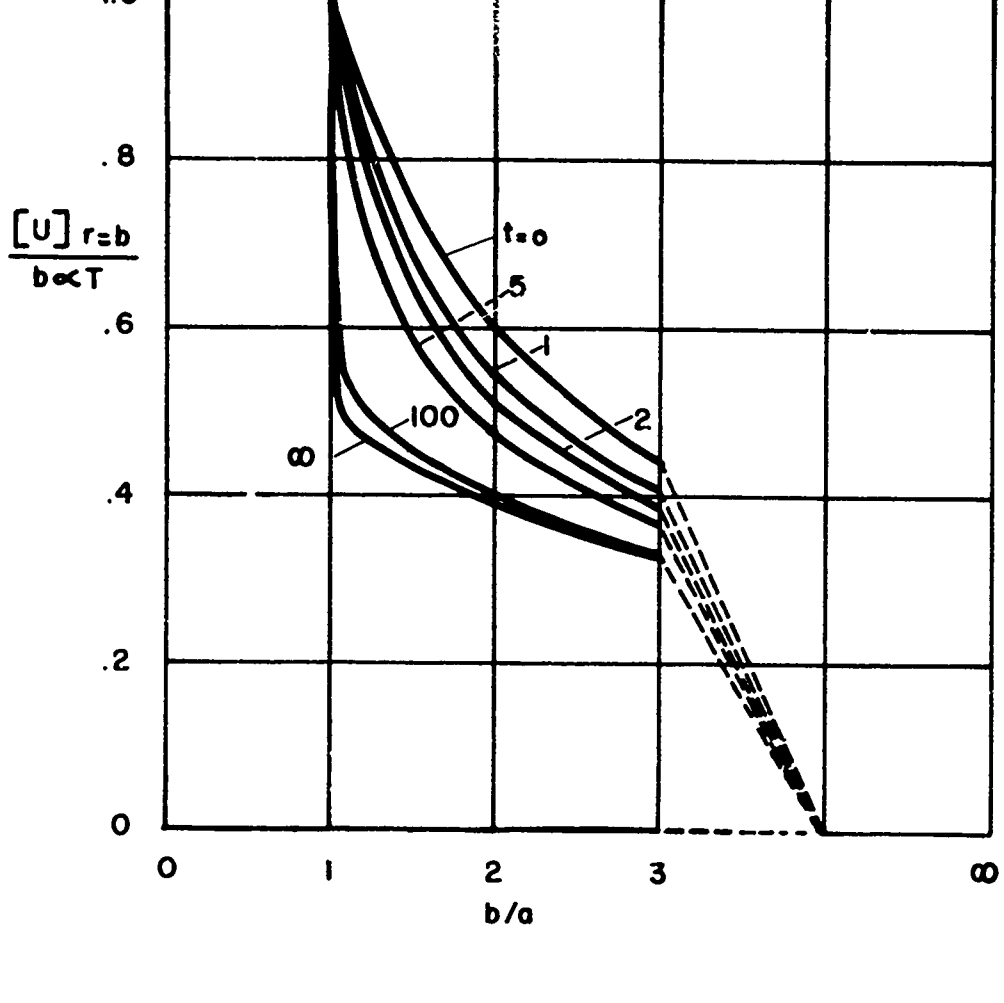


FIGURE 6.3.4-2(b) RADIAL DISPLACEMENT AT OUTER BOUNDARY OF PLATE (ν = 0.3)

6.3.4 (Cont'd)

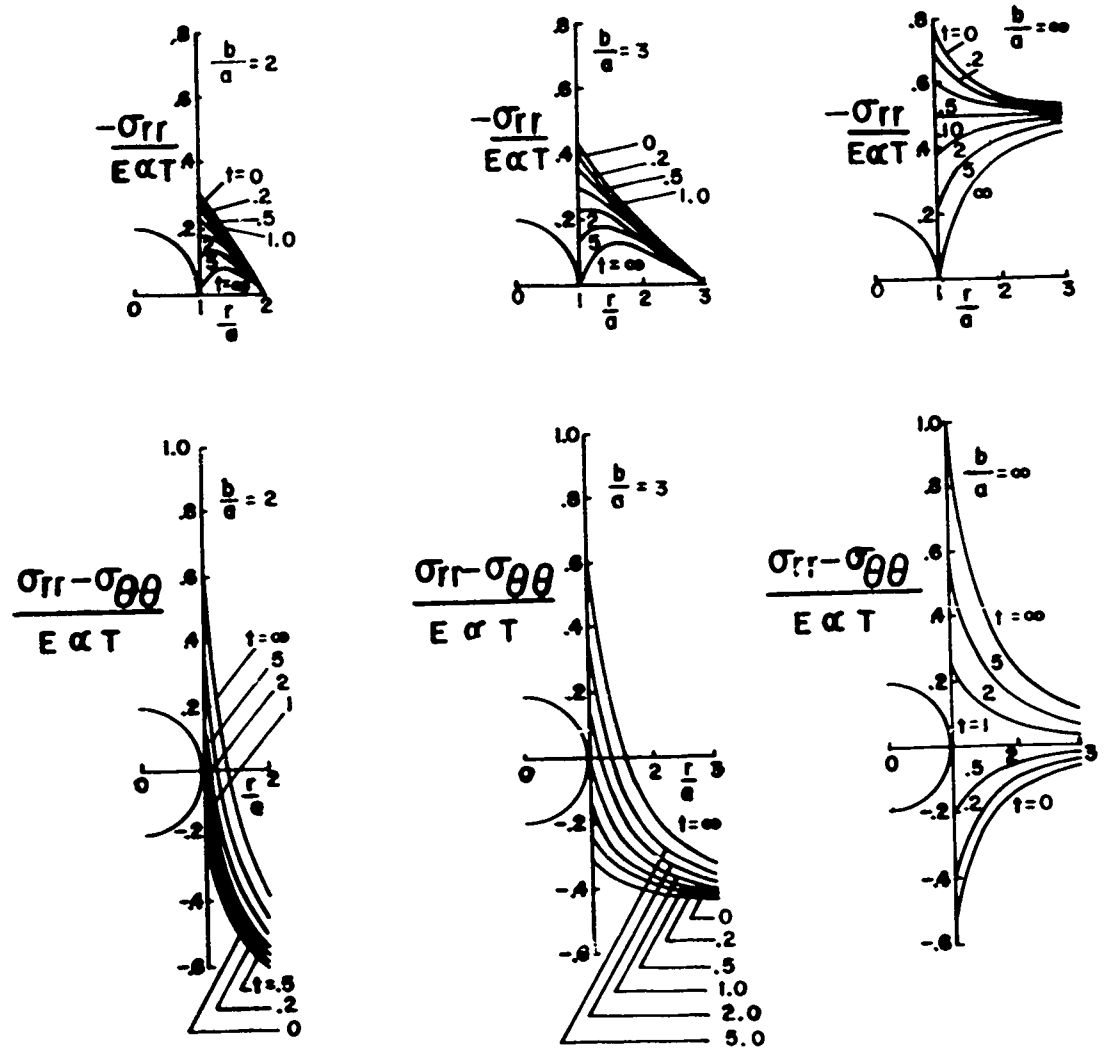


FIGURE 6.3.4-3 STRESSES IN PLATE (ν =0.3)

6.3.4 (Cont'd)

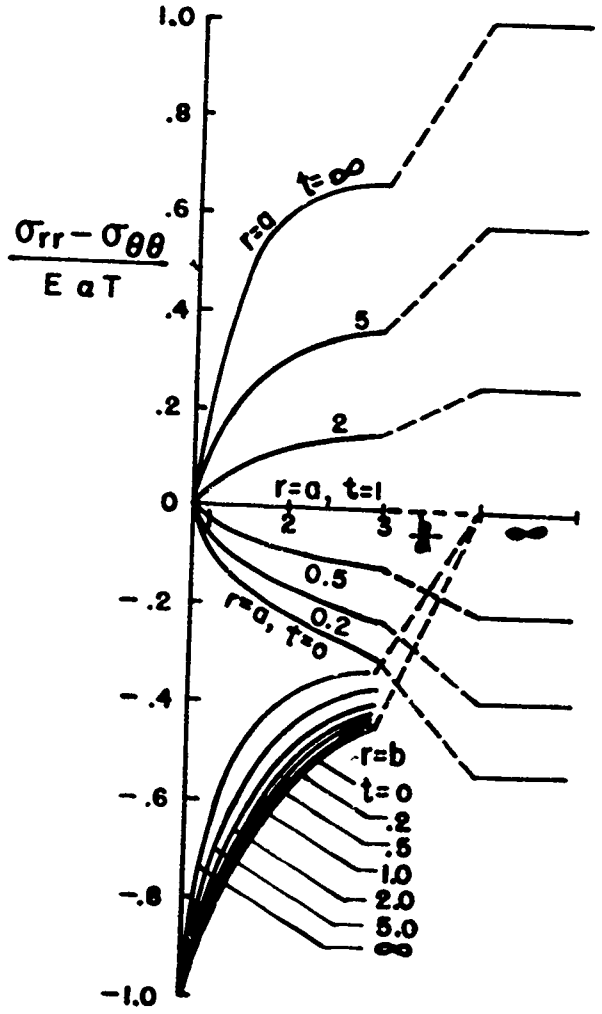


FIGURE 6.3.4-4 VARIATION OF STRESS DIFFERENCE WITH b/a ($\nu = 0.3$)

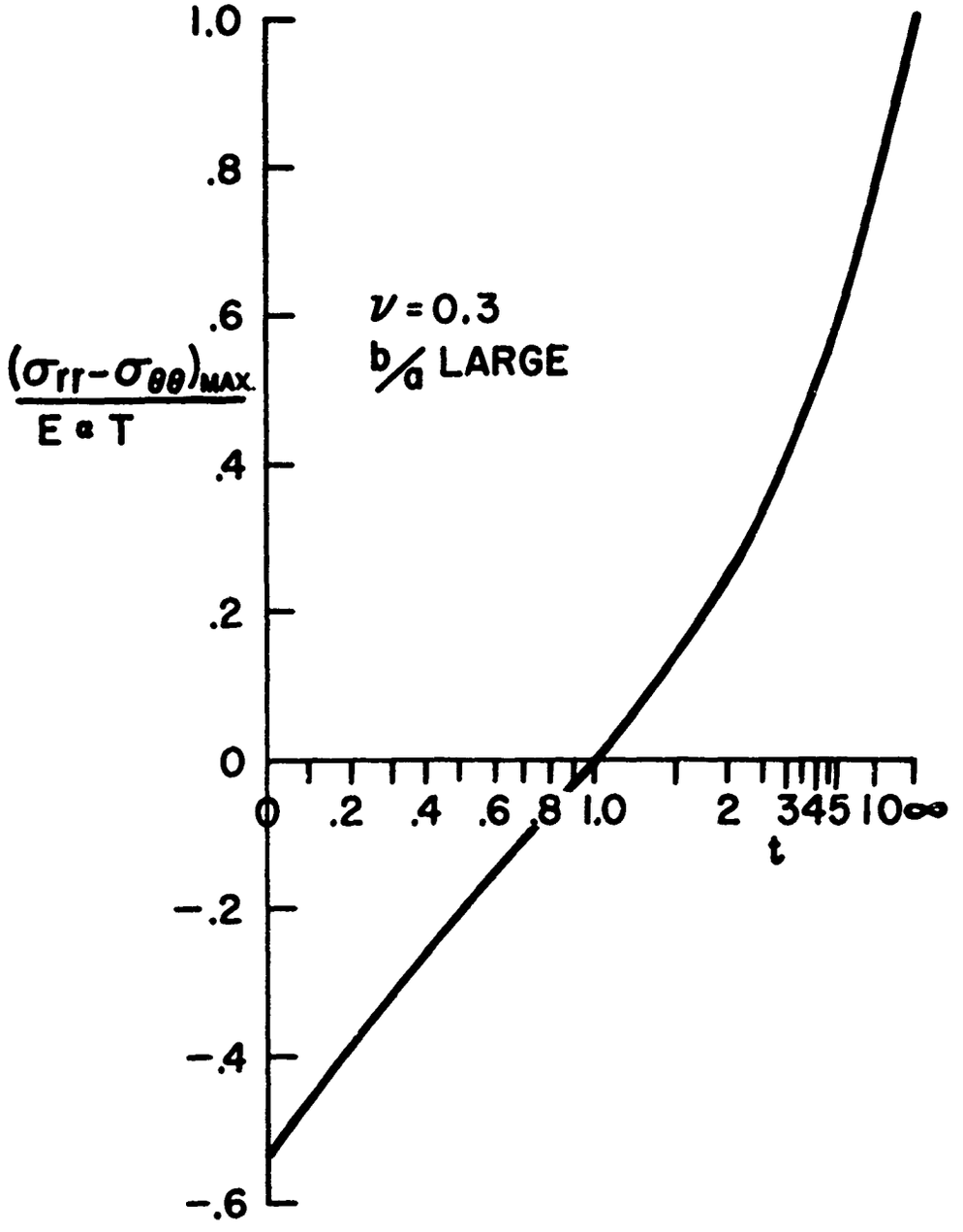


FIGURE 6.3.4-5 VARIATION OF MAXIMUM STRESS DIFFERENCE WITH t FOR b/a LARGE. MAXIMUM OCCURS AT r = a.

6.3.4 (Cont'd)

If t is large, the stresses become

$$\sigma_{rr} = \frac{E\alpha T}{2 \log b/a} \left[\frac{\log (b/a)\,(b^2/r^2 - 1)}{b^2/a^2 - 1} - \log (b/r) \right] \quad (8)$$

and

$$\sigma_{\theta\theta} = \frac{E\alpha T}{2 \log b/a} \left[1 + \frac{\log (b/a)\,(b^2/r^2 + 1)}{(b^2/a^2 - 1)} - \log (b/r) \right]. \quad (9)$$

With the usual conversions from plane stress to plane strain (Section 2), these are the stresses in a pipe containing fluid at temperature T.

For t=1, the plate is of uniform thickness throughout and the stresses are simplified to

$$\sigma_{rr} = \frac{E\alpha T}{2 \log b/a} \left[\frac{a^2}{2b^2} \left(\frac{b^2}{r^2} - 1 \right) - \log (b/r) \right] \quad (10)$$

and

$$\sigma_{\theta\theta} = \frac{E\alpha T}{2 \log b/a} \left[1 - \frac{a^2}{2b^2} \left(\frac{b^2}{r^2} + 1 \right) - \log (b/r) \right]. \quad (11)$$

6.4 REFERENCES

6-1 Boley, B. and Weiner, J., Thermal Stresses for Aircraft Structures, WADC Technical Note 56-102, August 1955.

6-2 Timoshenko, S., Theory of Plates and Shells, First Edition, McGraw-Hill Book Company, Inc., New York, 1940.

6-3 Zaid, M. and Forray M., Bending of Elastically Supported Rectangular Plates, Proceedings of the Society of Civil Engineers, Vol. 84, No. EM 3, July 1958, Proc. Paper 1719.

6-4 Timoshenko, S and Goodier, J. N., Theory of Elasticity, Second Edition, McGraw-Hill Book Company, Inc., New York, 1951.

6-5 Horvay, G., Transient Thermal Stresses in Circular Disks and Cylinders, Transactions of the ASME, January 1954, pp 127-135.

6-6 Forray, M., Thermal Stresses in Plates, Journal of the Aero/Space Sciences, Readers' Forum, Vol. 25, No. 11, pp 716-717, November 1958

6-7 Forray, M., Thermal Stresses in Rings, Journal of the Aero/Space Sciences, Readers' Forum, Vol. 26, No. 5, pp 310-311, May 1959.

6-8 Forray, M., Formulas for the Determination of Thermal Stresses in Rings, Journal of the Aero/Space Sciences, Readers' Forum, Vol. 27, No. 3, 1960, pp 238-240.

6-9 Norburg, J. F., Thermal Stresses in Disks of Constant Thickness, Aircraft Engineering, pp 132-137, May 1957.

6-10 Parkes, E. W., The Stresses in a Plate Due to a Local Hot Spot, Aircraft Engineering, pp 67-69, March 1957

6-11 Forray, M. and Zaid, M., Thermal Stresses in a Solid Circular Bulkhead, Journal of the Aeronautical Sciences, pp 63-64, January 1958.

6-12 Heldenfels, R. R. and Roberts, W. M., Experimental and Theoretical Determination of Thermal Stresses in Flat Plates, NACA TN 2769, August 1952.

6-13 Przemieniecki, J.S., Thermal Stresses in Rectangular Plates, The Aeronautical Quarterly, Volume X, Part 1, pp 65-78, February 1959.

SECTION 7

THERMO-ELASTIC ANALYSIS OF SHELLS

SECTION 7

THERMO-ELASTIC ANALYSIS OF SHELLS

TABLE OF CONTENTS

Paragraph	Title	Page
7	Thermo-Elastic Analysis of Shells	7.2
7.1	Truncated Conical Shells	7.3
7.1.1	Radial Loading Perpendicular to the Cone Axis	7.4
7.1.1.1	The Hoopring Approximation for Radial Loading	7.4
7.1.1.2	Solution for Edge Loading (with illustrative problem)	7.13
7.1.2	Meridional Loading - Membrane Analysis (with illustrative problem)	7.20
7.1.3	Meridional Temperature Variation	7.26
7.2	Approximate Solution for Non-Conical Axisymmetric Shells	7.28
7.3	Cylindrical Shells	7.30
7.3.1	Cylindrical Shells with Axisymmetric Loading and Meridional Temperature Variation	7.30
7.3.1.1	Hoopring Analysis	7.30
7.3.1.2	Solution for Edge Loading (with illustrative problem)	7.32
7.3.2	Cylindrical Shells with Temperature Gradient Through the Thickness	7.37
7.3.2.1	Cylindrical Tube - Steady Heat Flow in Radial Direction	7.37
7.3.2.2	Transient Thermal Stresses in Circular Cylinders	7.45
7.4	References	7.51

SECTION 7 - THERMO-ELASTIC ANALYSIS OF SHELLS

The deformations and stresses in shells which have axisymmetric geometry, loads, and temperature distributions are presented. The case of thermal loading is shown to be equivalent to a pressure loading which is proportional to the local meridional temperature.

Solutions are also given for the case of edge loads and moments on the shell. The deformations at the shell edges are then employed to calculate the forces required to enforce the edge boundary conditions (compatibility). For the most part, the analysis cosiders temperature distributions which are constant through the thickness of thin shells, although special consideration is given to right-circular cylindrical shells having temperature variations through the thickness.

The following symbols are used throughout this section:

a, b	Inner and outer radii, respectively
h	Thickness; Thermal conductivity
ℓ	Attenuation length
r	Radius
r_o	Reference radius
t	Time
w	Normal deflection
x	Distance along meridion
D	Flexural rigidity $= \frac{Eh^3}{12(1-\nu^2)}$
E	Young's modulus
F_k	Edge loading functions
H	Horizontal force per unit of circumferential length
$\mathcal{H}$	Value of H at a shell edge
K	Hoopring stiffness; Incremental stiffness due to restrained ends; Thermal diffusivity
L	Meridional length of a shell section
M	Bending moment per unit of length
$\mathcal{M}$	Value of M at a shell edge
N	Normal force per unit of length
P	Surface traction (force per unit of area)
Q	Meridional shear force, per unit of circumferential length, perpendicular to shell wall
R	Radius of thin-walled cylinder
T	Temperature
ΔT	Temperature rise above reference level
W	Weight
α	Linear coefficient of thermal expansion
δ	Radial (horizontal) deflection

Δ	Vertical extension
ϵ	Strain
η	Value of N_x at a shell edge
Θ	Azimuthal angle
ν	Poisson's ratio
σ	Stress
ϕ	Angle between axis of revolution and the normal to the shell surface

Superscripts

'	Quantities corresponding to a particular solution
o	Quantities corresponding to the meridional loading membrane solution

Subscripts

e	Resulting from edge loadings
h	Horizontal component
i,o	Inner and outer
Θ	Hoop component
x	Meridional component
rr,$\Theta\Theta$,zz	Components in cylindrical coordinates

7.1 TRUNCATED CONICAL SHELLS

An approximate analysis is presented which may be regarded as adequately describing the behavior of truncated conical shells (Figure 7.1-1) subjected to axisymmetric load and temperature distributions (Reference 7-1) when the following conditions apply:

(1) The shell is thin walled ($h \leq .2r$).
(2) The inclination angle ϕ is between 45° and 135° (preferably between 60° and 120°) and the shell is rather short.
(3) Deformations due to thermal and mechanical loading are linear-elastic and the principle of superposition may be employed.

For very flat conical shells (ϕ between 30° and 45°) the analysis gives reliable results when the cone is analyzed in sections that are short ($L < 3\ell$), i.e., where the meridional length L of each section analyzed is less than three times the so-called "attenuation length" of the shell (Paragraph 7.1.1).

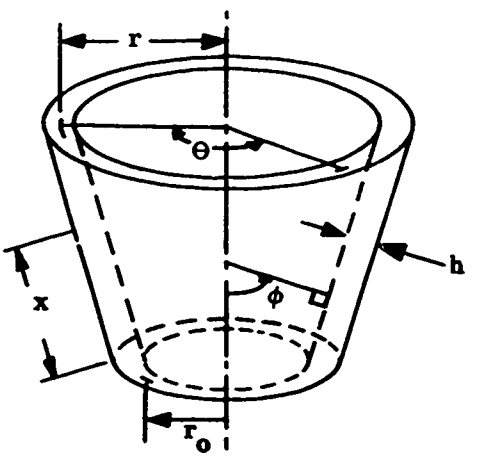


FIGURE 7.1-1 TRUNCATED CONICAL SHELL GEOMETRY

7.1.1 Radial Loading Perpendicular to the Cone Axis

Any general axisymmetric loading can be resolved into radial and meridional components as shown in Figures 7.1.1-1 (a) and (b). A shell analysis for the radial (horizontal) component of the loading, based on the so-called hoopring approximation of shells, is presented. The analysis is valid when the conditions listed in Sub-section 7.1 apply.

A membrane analysis for the meridional loading component is presented in Paragraph 7.1.2. The solution of the conical shell problem for arbitrary axisymmetric loading is obtained by superposing the hoopring solution for the radial component of the loading and the membrane solution for meridional loading component.

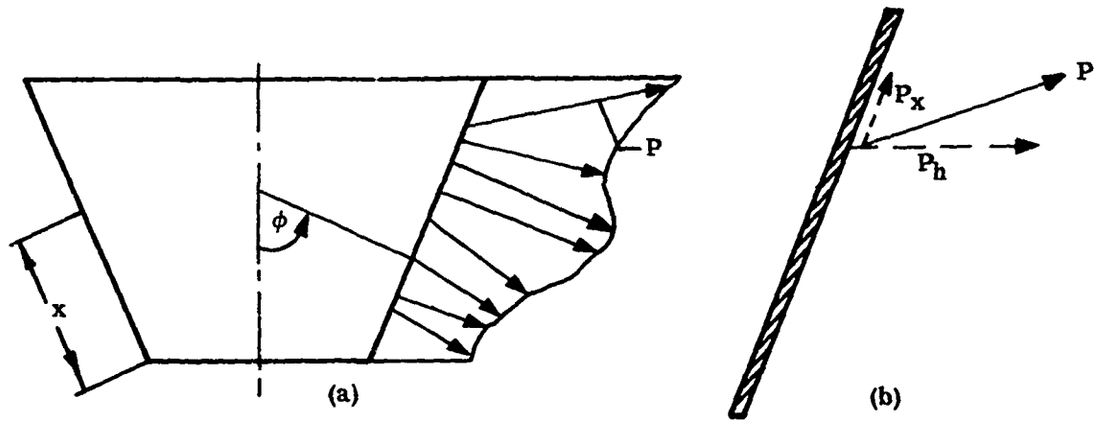


FIGURE 7.1.1-1: (a) CONICAL SHELL WITH AXISYMMETRIC BUT OTHERWISE ARBITRARY LOADING
(b) RADIAL AND MERIDIONAL LOAD COMPONENTS P_h AND P_x, RESPECTIVELY

7.1.1.1 The Hoopring Approximation for Radial Loading

The axisymmetric shell under axisymmetric radial loading is visualized as an assembly of beams in the meridional direction (Figure 7.1.1.1-1(a)), supported by an elastic foundation (hooprings) of stiffness

$$K = \frac{Eh \sin^2 \phi}{r^2} \quad , \quad \frac{lb/in}{in^2} \quad . \tag{1}$$

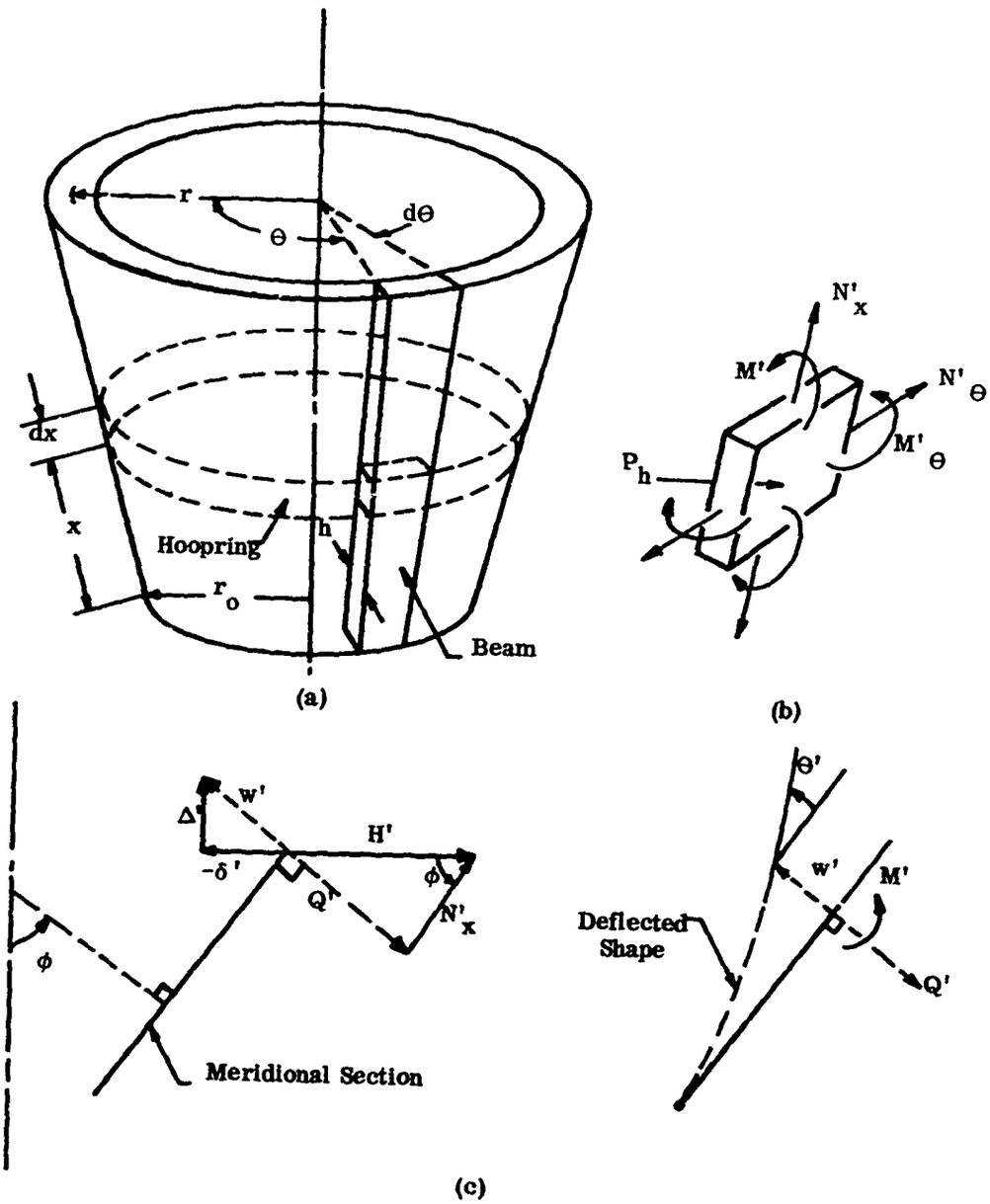


FIGURE 7.1.1.1-1 CONICAL SHELL - HOOPRINGS AND MERIDIONAL BEAM STRIPS

7.1.1.1 (Cont'd)

For this structural model, the differential equation for the radial deflection δ' becomes

$$\frac{r}{r_o}\ \frac{\ell^4}{4}\ \frac{d^2}{dx^2}\left(\frac{r}{r_o}\ \frac{d^2\delta'}{dx^2}\right)+\delta' = \frac{r^2 P_h}{Eh}\ , \tag{2}$$

where P_h is the distributed radial (horizontal) loading $\left(\frac{lb}{in^2}\right)$ and

$$\ell = \frac{\sqrt{r_o h/\sin\phi}}{\sqrt[4]{3\,(1-\nu^2)}}$$

$$= .778\ \sqrt{r_o h/\sin\phi} \quad \text{for } \nu = 0.3\ , \tag{3}$$

where "ℓ" is the so-called "attenuation length" of the shell; it is a measure of the degree to which the effects of self-equilibrating edge loads die out away from the edges.

The internal shell loads, moments and deflections are expressed in terms of δ' as

$$\Theta' = -\frac{d\delta'}{dx} \Big/ \sin\phi$$

$$M' = -D\,\frac{d^2\delta'}{dx^2} \Big/ \sin\phi\ , \quad D = \frac{Eh^3}{12(1-\nu^2)}$$

$$M'_\Theta = \nu\ M$$

$$H' = -\frac{D}{r\sin^2\phi}\ \frac{d}{dx}\left(r\,\frac{d^2\delta'}{dx^2}\right) \tag{4}$$

$$Q' = H'\sin\phi$$

$$N'_x = H'\cos\phi$$

$$N'_\Theta = Eh\delta'/r\ ,$$

and the vertical deflection relative to the base is

$$\Delta' = \int_o^x \left[\frac{(N'_x - \nu N'_\Theta)}{Eh}\ \sin\phi + \Theta'\cos\phi\right] dx\ ,$$

where the positive directions for the above quantities are as shown in Figure 7.1.1.1-1 (b) and (c).

7.1.1.1 (Cont'd)

It is convenient to find a particular solution for Eq. (2) where the loading is expressed as a polynomial.

In general, this particular solution will not satisfy the boundary conditions at the edges of the shell; i.e., the horizontal edge loads, moments or edge deflections and rotations derived from the particular solution do not satisfy prescribed conditions. Additional horizontal edge loads and moments must then be applied to the shell which, when superposed on the edge loads and moments resulting from the particular solution, satisfy the prescribed boundary conditions.

Following this approach, the loading term on the right side of Eq. (2) is expressed by a polynomial, such that

$$\frac{r_o P_h}{Eh} = \sum_{k=0}^{N} C_k \left(\frac{r}{r_o}\right)^k = C_0 + C_1\left(\frac{r}{r_o}\right) + C_2\left(\frac{r}{r_0}\right)^2 + \ldots + C_N\left(\frac{r}{r_o}\right)^N . \qquad (5)$$

A given meridional load distribution can be expressed in this manner by the method of Paragraph 4.1.2.3.1.

A particular solution of Eq. (2) can then be obtained in the form of a polynomial

$$\delta' = \sum_{j=2,4,6,\ldots\ldots}^{k+2} a_j r^j, \text{ if } k \text{ is even}$$

or

$$\delta' = \sum_{j=1,3,5,\ldots\ldots}^{k+2} a_j r^j, \text{ if } k \text{ is odd}, \qquad (6)$$

where

$$\frac{a_{k+2}}{C_k} = \frac{1}{(r_o)^{k+1}}$$

$$\frac{a_j}{C_k} = -(-1)^{\frac{k-j}{2}} (k+2) \left[(k+1)(k)\ldots(j+1)\right]^2 j \Big/ (r_o)^{k+1} (A)^{\frac{k+2-j}{2}} \qquad (7)$$

and $j = k, k-2, k-4, \ldots 4, 2$ if k is even
$j = k, k-2, k-4, \ldots 3, 1$ if k is odd .

The quantity "A" is defined by

$$A = \frac{4r_o^2}{L^4 \cos^4 \phi} \qquad (8)$$

7.1.1.1 (Cont'd)

The particular solutions for δ' are given in non-dimensional form in the following table for monomials $(C_k(r/r_o)^k)$ up to $k = 4$.

TABLE 7.1.1.1-1

Particular Solutions for δ', Corresponding to Monomial Radial Pressure Distributions

k	$\frac{r_o P_h}{Eh}$	$\frac{\delta'_k}{r_o C_k}$
0	C_0	$\left(\frac{r}{r_o}\right)^2$
1	$C_1 \frac{r}{r_o}$	$\left(\frac{r}{r_o}\right)^3 - 3\left(\frac{\ell \cos\phi}{r_o}\right)^4 \frac{r}{r_o}$
2	$C_2\left(\frac{r}{r_o}\right)^2$	$\left(\frac{r}{r_o}\right)^4 - 18\left(\frac{\ell \cos\phi}{r_o}\right)^4 \left(\frac{r}{r_o}\right)^2$
3	$C_3\left(\frac{r}{r_o}\right)^3$	$\left(\frac{r}{r_o}\right)^5 - 60\left(\frac{\ell \cos\phi}{r_o}\right)^4 \left(\frac{r}{r_o}\right)^3 + 180\left(\frac{\ell \cos\phi}{r_o}\right)^8 \frac{r}{r_o}$
4	$C_4\left(\frac{r}{r_o}\right)^4$	$\left(\frac{r}{r_o}\right)^6 - 150\left(\frac{\ell \cos\phi}{r_o}\right)^4 \left(\frac{r}{r_0}\right)^4 + 2700\left(\frac{\ell \cos\phi}{r_o}\right)^8 \left(\frac{r}{r_o}\right)^2$

To illustrate the application of Eq. (7), consider the particular case $k = 2$. Then

$$\frac{a_{k+2}}{C_k} = \frac{a_4}{C_2} = \frac{1}{r_o^3}$$

and

$$\frac{a_2}{C_2} = \frac{-(-1)^0 4 (3^2)(2)}{r_o^3 A} = -\frac{72}{r_o^3 A},$$

so that in non-dimensional form

7.1.1.1 (Cont'd)

$$\frac{\delta'_2}{C_2 r_o} = \left(\frac{r}{r_o}\right)^4 - 18\left(\frac{\ell \cos \phi}{r_o}\right)^4 \left(\frac{r}{r_o}\right)^2$$

The solutions of Table 7.1.1.1-1 are shown graphically in Figures 7.1.1.1-2 (a) and (b).

Once δ' has been determined as above, the internal shell loads, moments, and deflections corresponding to this particular solution can be obtained from Eqs. (4). The results in non-dimensional form are summarized in Table 7.1.1.1-2.

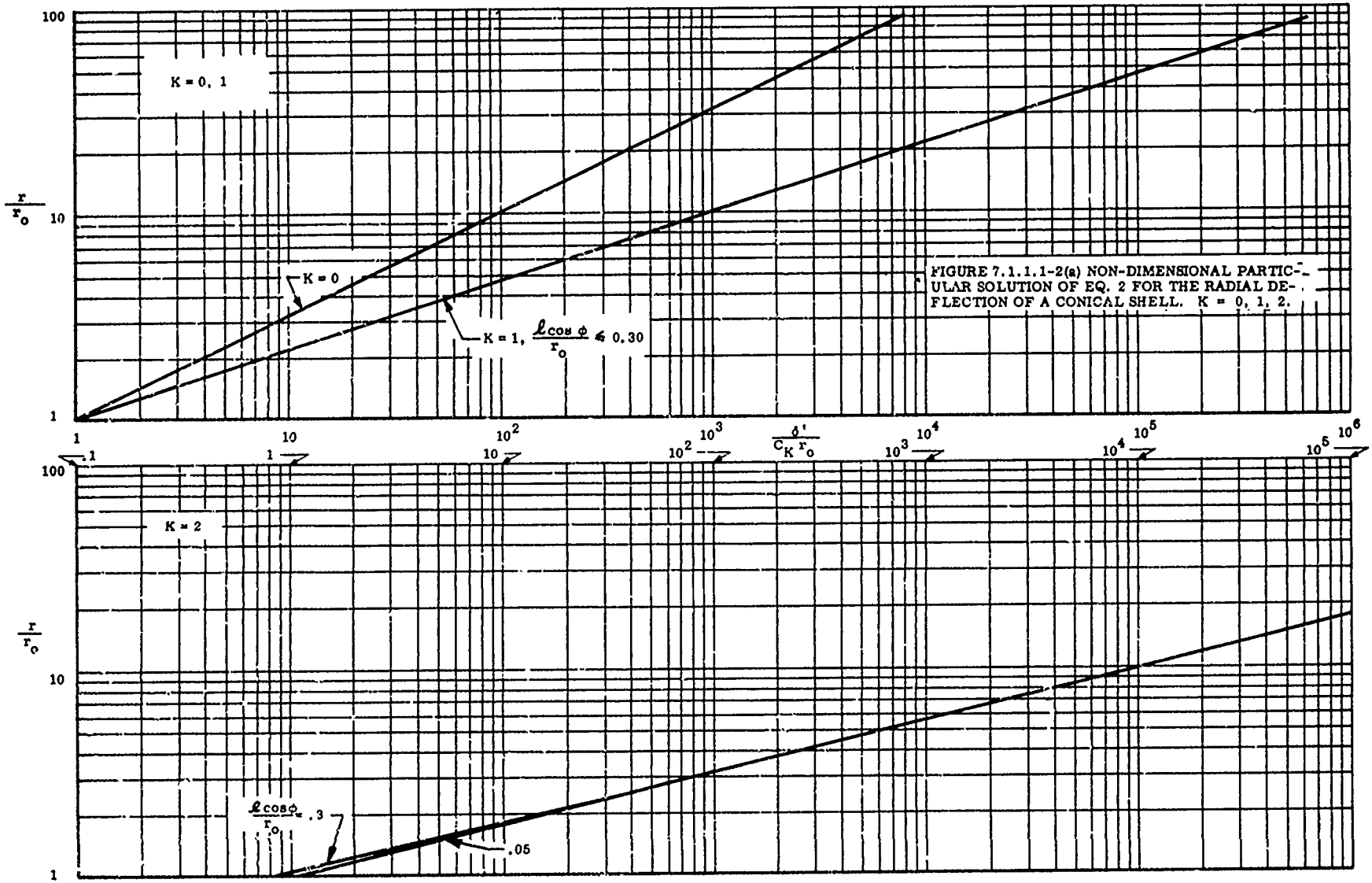


FIGURE 7.1.1.1-2(a) NON-DIMENSIONAL PARTICULAR SOLUTION OF EQ. 2 FOR THE RADIAL DEFLECTION OF A CONICAL SHELL. K = 0, 1, 2.

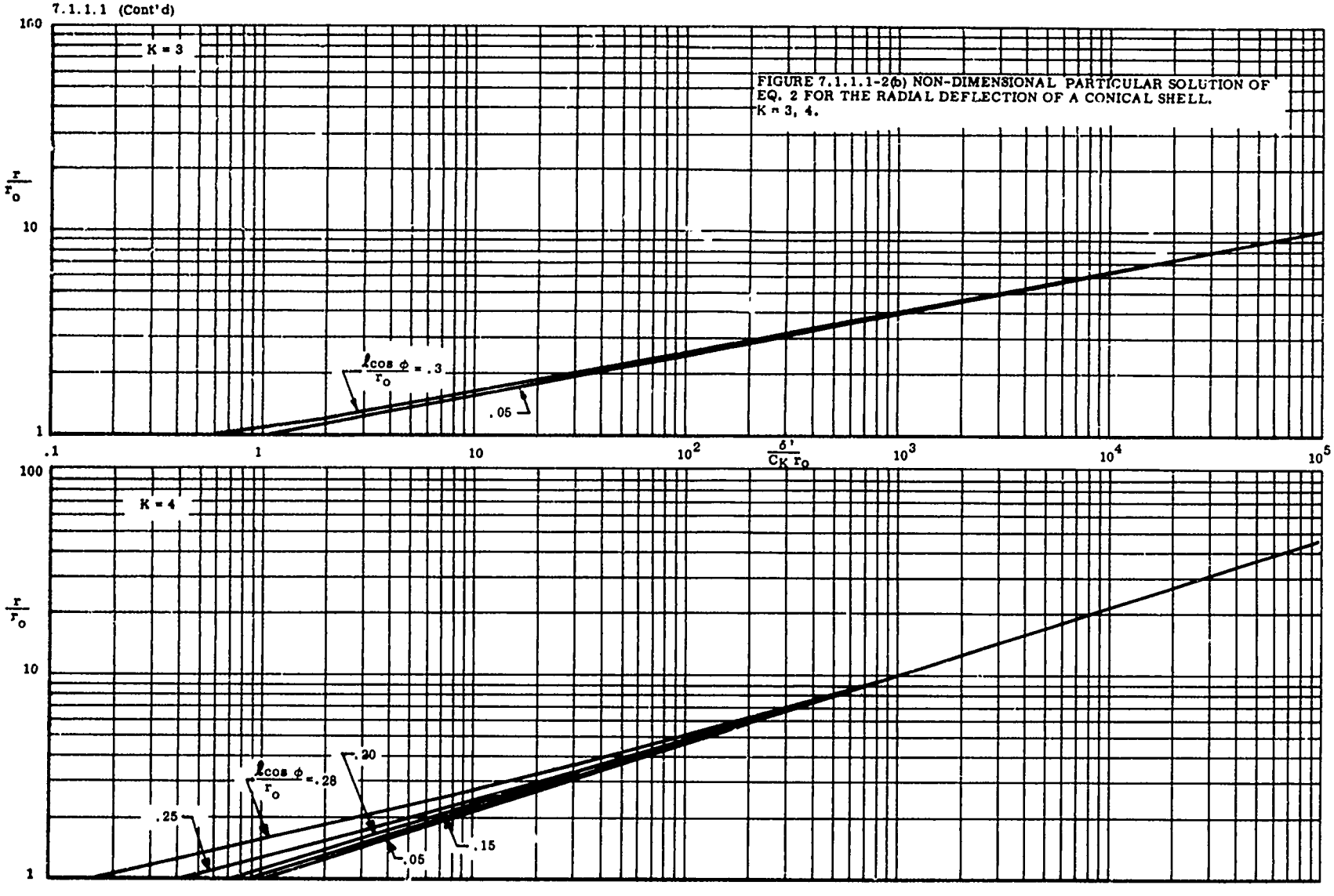


FIGURE 7.1.1.1-2(b) NON-DIMENSIONAL PARTICULAR SOLUTION OF EQ. 2 FOR THE RADIAL DEFLECTION OF A CONICAL SHELL. K = 3, 4.

TABLE 7.1.1.1-2

Internal Shell Loads, Moments and Deflections Corresponding to Particular Solutions for Monomial Radial Pressure Distributions

$A = \left(\frac{\ell \cos\phi}{r_o}\right)^4$	k = 0	k = 1	k = 2	k = 3	k = 4
$\frac{-\Theta' \tan\phi}{C_k}$	$2\frac{r}{r_o}$	$3\left[\left(\frac{r}{r_o}\right)^2 - A\right]$	$4\left[\left(\frac{r}{r_o}\right)^3 - 9A\left(\frac{r}{r_o}\right)\right]$	$5\left[\left(\frac{r}{r_o}\right)^4 - 36A\left(\frac{r}{r_o}\right)^2 + 36A^2\right]$	$6\left[\left(\frac{r}{r_o}\right)^5 - 100A\left(\frac{r}{r_o}\right)^3 + 900A^2\left(\frac{r}{r_o}\right)\right]$
$\frac{-r_o M' \sin\phi}{C_k D \cos^2\phi}$, $\frac{-r_o M'_\Theta \sin\phi}{\nu C_k D \cos^2\phi}$	2	$6\frac{r}{r_o}$	$12\left[\left(\frac{r}{r_o}\right)^2 - 3A\right]$	$20\left[\left(\frac{r}{r_o}\right)^3 - 18A\left(\frac{r}{r_o}\right)\right]$	$30\left[\left(\frac{r}{r_o}\right)^4 - 60A\left(\frac{r}{r_o}\right)^2 + 180A^2\right]$
$\frac{-H' r_o^2 \sin^2\phi}{C_k D \cos^3\phi}$, $\frac{-N'_x r_o^2 \sin^2\phi}{C_k D \cos^4\phi}$, $\frac{-Q' r_o^2 \sin\phi}{C_k D \cos^3\phi}$	$\frac{2}{r/r_o}$	12	$36\left[\frac{r}{r_o} - \frac{A}{r/r_o}\right]$	$80\left[\left(\frac{r}{r_o}\right)^2 - 9A\right]$	$150\left[\left(\frac{r}{r_o}\right)^3 - 36A\left(\frac{r}{r_o}\right) + \frac{36A^2}{r/r_o}\right]$
$\frac{N'_\Theta}{C_k E h}$	r/r_o	$\left(\frac{r}{r_o}\right)^2 - 3A$	$\left(\frac{r}{r_o}\right)^3 - 18A\left(\frac{r}{r_o}\right)$	$\left(\frac{r}{r_o}\right)^4 - 60A\left(\frac{r}{r_o}\right)^2 + 180A^2$	$\left(\frac{r}{r_o}\right)^5 - 150A\left(\frac{r}{r_o}\right)^3 + 2700A^2\left(\frac{r}{r_o}\right)$

NOTE: $\phi \neq 90°$

7.1.1.2 Solution for Edge Loading

When the conical shell is subject only to an end moment and end force as in Figure 7.1.1.2-1, then for a shell of lateral length greater than three times the attenuation length, it is permissible to consider the shell as infinite. Assuming this condition to hold, it is only necessary to satisfy the homogeneous form of Eq. (2) of Paragraph 7.1.1.1 ($P_h = 0$) subject to the boundary conditions

$$M(0) = \mathcal{M} \qquad H(0) = \mathcal{H}$$

$$M(\infty) = 0 \qquad H(\infty) = 0 \ .$$

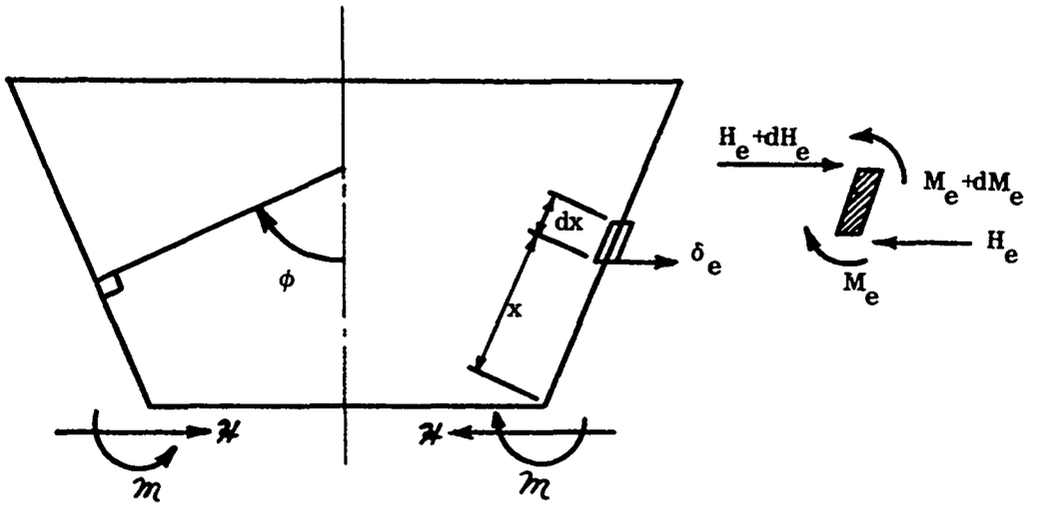


FIGURE 7.1.1.2-1 SELF-EQUILIBRATING LOADS AND MOMENTS $\mathcal{H}$ AND $\mathcal{M}$ AT A CONICAL SHELL EDGE

Recognizing that these are short range edge effects, the variation of r/r_o in the region of significant stresses (i.e., $r/r_o \approx 1$) are ignored. Under these conditions the solution of the edge loading problem may be written as

7.1.1.2 (Cont'd)

$$\delta_e = -\frac{\ell^2 \sin\phi}{2D}\left[\mathcal{M}\, F_3 + \mathcal{H}\ell(\sin\phi)\, F_4\right]$$

$$\Theta_e = -\frac{\ell}{D}\left[\mathcal{M}\, F_4 + \mathcal{H}\ell\,(\sin\phi)\, F_1\right] \qquad (1)$$

$$M_e = \mathcal{M} F_1 + \mathcal{H}\ell\,(\sin\phi)\, F_2$$

$$H_e = -\frac{2\mathcal{M} F_2}{\ell \sin\phi} + \mathcal{H} F_3$$

$$M_{\Theta_e} = \nu\, M_e$$

$$Q_e = H_e \sin\phi$$

$$N_{x_e} = H_e \cos\phi \qquad (2)$$

$$N_{\Theta_e} = \frac{Eh\delta_e}{r}$$

$$\Delta_e = \int_o^x \left[\left(\frac{N_{x_e} - \nu N_{\Theta_e}}{Eh}\right)\sin\phi + \Theta_e \cos\phi\right] dx\,,$$

where the functions F_k are given by

$$F_1 = \sqrt{2}\,(e)^{-x/\ell}\cos\left(\frac{x}{\ell} - \frac{\pi}{4}\right)$$

$$F_2 = (e)^{-x/\ell}\sin\frac{x}{\ell}$$

$$F_3 = -\sqrt{2}\,(e)^{-x/\ell}\sin\left(\frac{x}{\ell} - \frac{\pi}{4}\right) \qquad (3)$$

$$F_4 = (e)^{-x/\ell}\cos\frac{x}{\ell}\,.$$

The above functions are damped sinusoidals which cause the boundary loads to attenuate with distance from the edge as $e^{-x/\ell}$. They are plotted in Figure 7.1.1.2-2 for the range $0 \le \frac{x}{\ell} \le 4.0$.

7.1.1.2 (Cont'd)

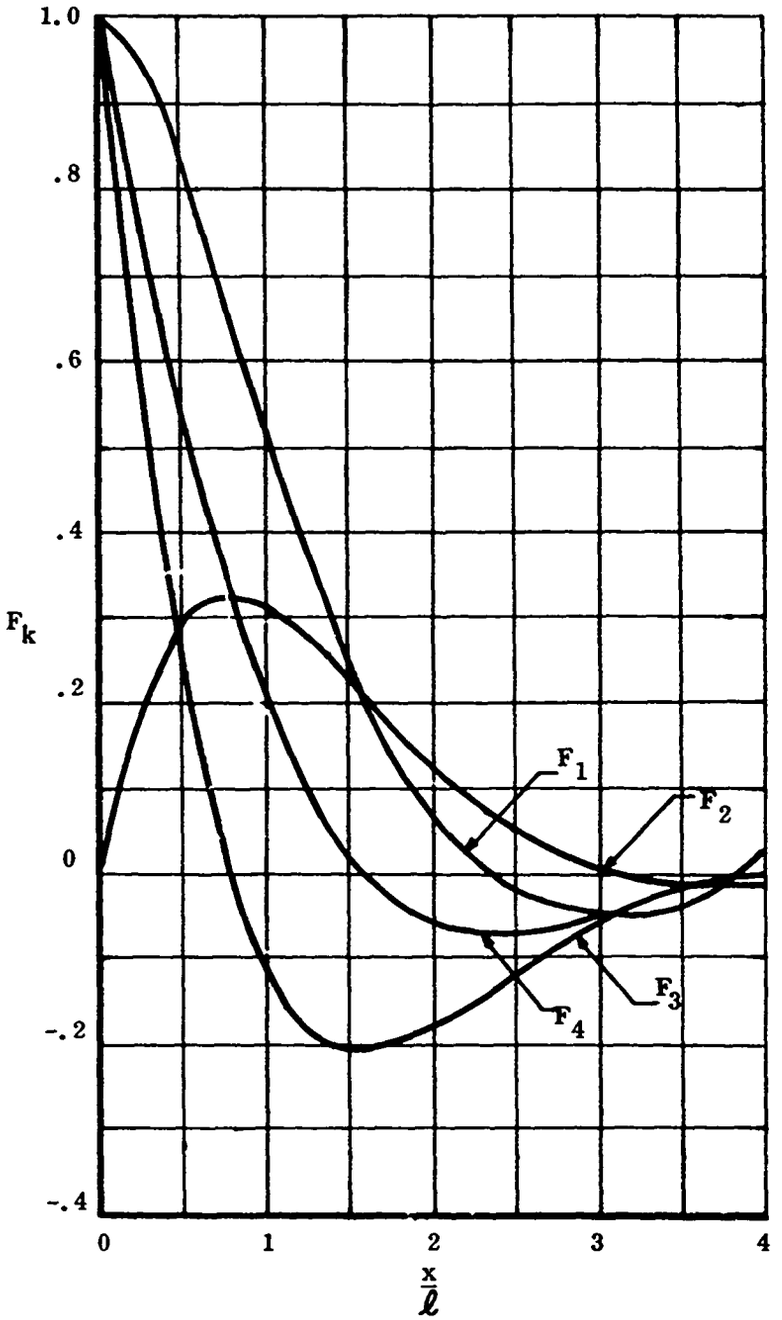


FIGURE 7.1.1.2-2 EDGE LOADING FUNCTIONS

To illustrate the application of the preceding equations, consider the radial (horizontal) loading problem for the conical shell of Figure 7.1.1.2-3.

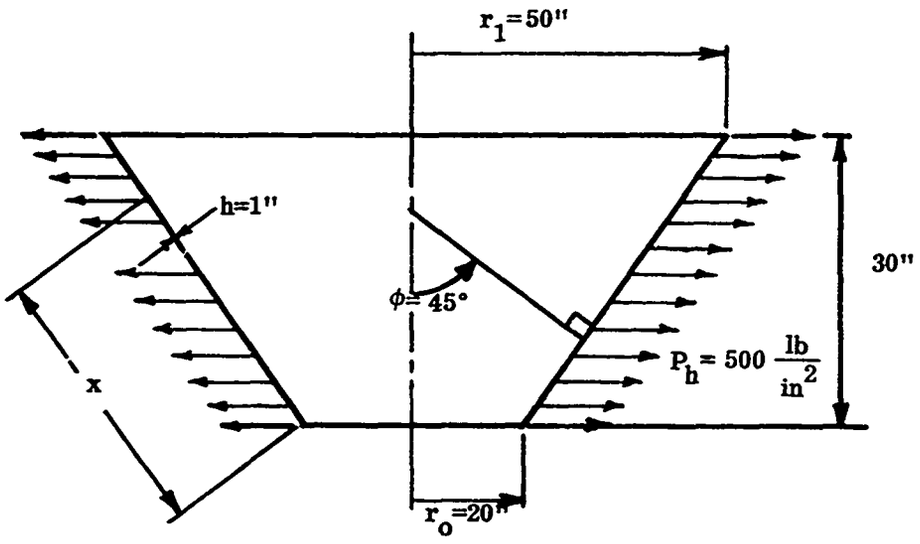


FIGURE 7.1.1.2-3 CONICAL SHELL UNDER UNIFORM RADIAL LOADING

The top and bottom edges of the shell are unrestrained (free), the radial pressure is constant at $P_h = 500 \ \frac{lb}{in^2}$ and

$r_o = 20"$ $\qquad$ $P_h = 500 \ \frac{lb}{in^2}$

$h = 1"$ $\qquad$ $E = 30\,(10)^6$ psi

$\phi = 45°$ $\qquad$ $\nu = 0.30$

$$D = \frac{Eh^3}{12(1-\nu^2)} = \frac{30(10)^6(1)^3}{12\,(1-.3^2)} = 2.75\,(10)^6 \text{ in - lb} .$$

Next, it is necessary to obtain the solution for the stresses and deflections in the vicinity of the bottom of the shell. The first step is to obtain the particular solution.

From Eq. (5), since $k = 0$,

$$\frac{r_o P_h}{Eh} = C_0 ,$$

7.1.1.2 (Cont'd)

so that

$$C_0 = \frac{(20)(500)}{30(10)^6(1)} = 3.33(10)^{-4} .$$

Then from Table 7.1.1.1-1,

$$\frac{\delta'}{r_o C_0} = \left(\frac{r}{r_o}\right)^2$$

or

$$\delta' = \frac{C_0 r^2}{r_o} = \frac{3.33(10)^{-4} r^2}{20} = 16.67\ r^2 (10)^{-6} . \qquad \text{(a)}$$

Also, from Table 7.1.1.1-2, for $k = 0$,

$$\frac{-\Theta' \tan\phi}{C_0} = 2\left(\frac{r}{r_o}\right)$$

$$\frac{-r_o M' \sin\phi}{C_0 D \cos^2\phi} = \left(\frac{-r_o M'_\Theta}{\nu C_0 D}\right)\left(\frac{\sin\phi}{\cos^2\phi}\right) = 2$$

$$\frac{-H' r_o^2 \sin^2\phi}{C_0 D \cos^3\phi} = \frac{-N_x' r_o^2 \sin^2\phi}{C_0 D \cos^4\phi} = \frac{-Q' r_o^2 \sin\phi}{C_0 D \cos^3\phi} = \frac{2}{r/r_o}$$

$$\frac{N'_\Theta}{C_0 E h} = \frac{r}{r_o} .$$

Substituting the known quantities into the above expressions,

$$\Theta' = -33.33\ r\ (10)^{-6} \text{ radians}$$

$$M' = -64.8\ \frac{\text{in-lb}}{\text{in}}$$

$$M'_\Theta = -19.4\ \frac{\text{in-lb}}{\text{in}} \qquad \text{(b)}$$

$$H' = \frac{-64.7}{r}\ \frac{\text{lb}}{\text{in}}$$

$$N_x' = Q' = \frac{-45.7}{r}\ \frac{\text{lb}}{\text{in}}$$

$$N'_\Theta = 500\ r\ \frac{\text{lb}}{\text{in}} .$$

7.1.1.2 (Cont'd)

From the second and fourth expressions of (b), the particular solution yields moments and horizontal loads at the shell edges ($r_o = 20''$, $r_1 = 50''$) as shown in Figure 7.1.1.2-4(a).

To obtain the solution for the shell problem with free edges ($\mathcal{M} = \mathcal{H} = 0$), superpose on the particular solution given by expressions (a) and (b), the solution of the edge loading problem for equal and opposite edge loads and moments (Figure 7.1.1.2-4(b)).

In the edge loading problem, the attenuation length (Eq. (3) of Paragraph 7.1.1.1) for the bottom edge of the shell is

$$\ell = .778\sqrt{\frac{20(1)}{.707}} = 4.15 \text{ in}$$

and

$$\mathcal{M} = 64.8 \ \frac{\text{in-lb}}{\text{in}}$$

$$\mathcal{H} = 3.24 \ \frac{\text{lb}}{\text{in}} \ .$$

(Positive directions are as shown in Figure 7.1.1.2-1)

Thus, from Eqs. (1),

$$\delta_e = \frac{-(4.15)^2(.707)}{2\,(2.75)(10)^6}\left[\,(64.8)\,F_3 + (4.15)\,(.707)\,(3.24)\,F_4\,\right]$$

$$\Theta_e = \frac{-4.15}{2.75(10)6}\left[\,(64.8)\,F_4 + \left(\frac{4.15}{2}\right)(.707)\,(3.24)\,F_1\,\right]$$

$$M_e = 64.8\,F_1 + 3.24\,(4.15)\,(.707)\,F_2$$

$$H_e = \frac{-2(64.8)}{4.15\,(.707)}\,F_2 + 3.24\,F_3$$

or

$$\begin{aligned}
\delta_e &= -(143.5 \times 10^{-6})\,F_3 - (21 \times 10^{-6})\,F_4 \\
\Theta_e &= -(97.8 \times 10^{-6})\,F_4 - (7.15 \times 10^{-6})\,F_1 \\
M_e &= 64.8\,F_1 + 9.5\,F_2 \\
H_e &= -44.2\,F_2 + 3.24\,F_3 \ ,
\end{aligned} \qquad \text{(c)}$$

7.1.1.2 (Cont'd)

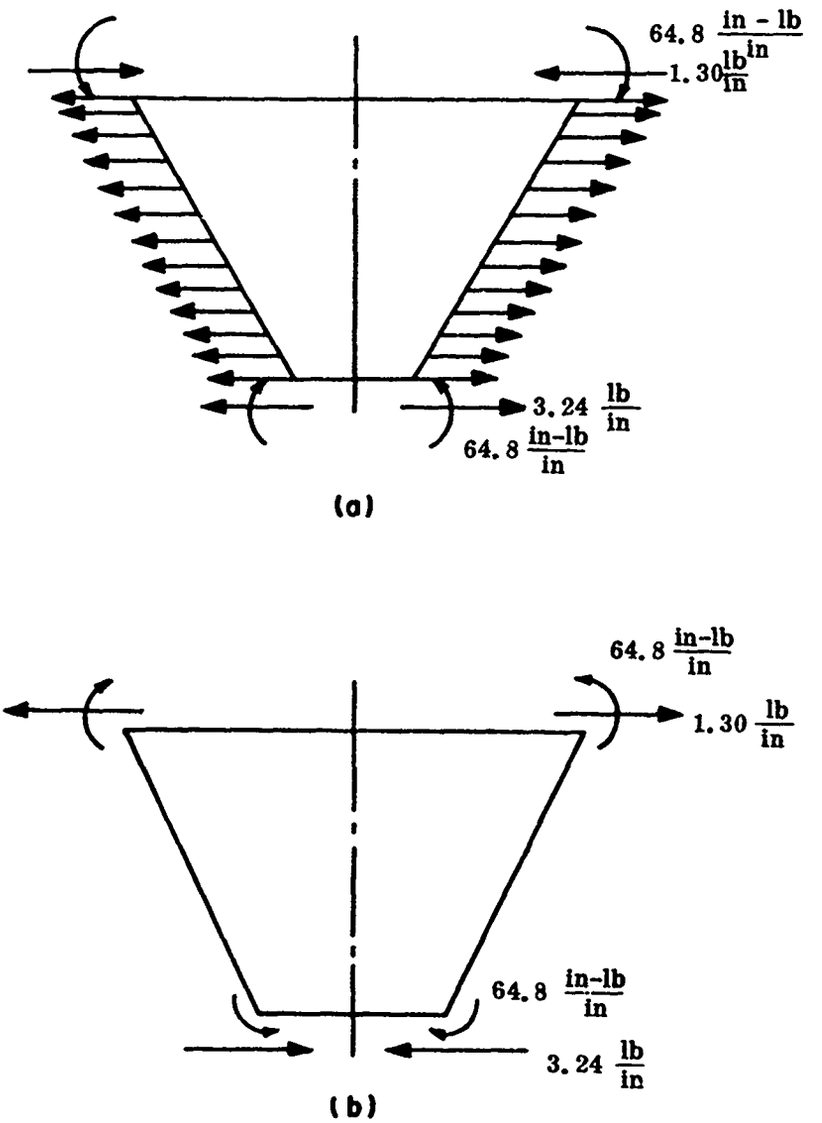


FIGURE 7.1.1.2-4 (a) EDGE FORCES AND MOMENTS CORRESPONDING TO THE PARTICULAR SOLUTION
(b) EDGE LOADING EQUAL IN MAGNITUDE BUT OPPOSITE IN DIRECTION TO THE PARTICULAR SOLUTION EDGE LOADING

7.1.1.2 (Cont'd)

and from Eqs. (2),

$$M_{\Theta_e} = 19.5\ F_1 + 2.85\ F_2$$

$$Q_e = N_{x_e} = 31.2\ F_2 + 2.29\ F_3 \qquad \text{(d)}$$

$$N_{\Theta_e} = -\frac{1}{r}\left(4300\ F_3 + 630\ F_4\right),$$

where F_i ($i = 1, 2, 3, 4$) are functions of x/ℓ.

The final solution for the deflections and stresses in the vicinity of the bottom of the shell is then obtained by adding expressions (a) and (b) to expressions (c) and (d).

The results for the meridional moment $M = M' + M_e$ and the radial load $H = H' + H_e$ (in the vicinity of the base) are plotted in Figure 7.1.1.2-5.

The stresses can be obtained from the equations

$$\sigma_x = \frac{N_x}{h} \pm \frac{6M}{h^2}$$

$$\sigma_\Theta = \frac{N_\Theta}{h} \pm \frac{6M_\Theta}{h^2}.$$

7.1.2 Meridional Loading - Membrane Analysis

An analysis for radial (horizontal) axisymmetric loading components was presented in Paragraph 7.1.1. The present paragraph presents a membrane analysis for the meridional components of the general axisymmetric loading (Figure 7.1.2-1). Having done this, the problem of a general axisymmetric distributed loading can be treated by resolving the loading into radial (horizontal) and meridional components; the effects of radial loading are then evaluated by the hoopring approximation of Paragraph 7.1.1 and the effects of meridional loading are evaluated by the following membrane analysis.

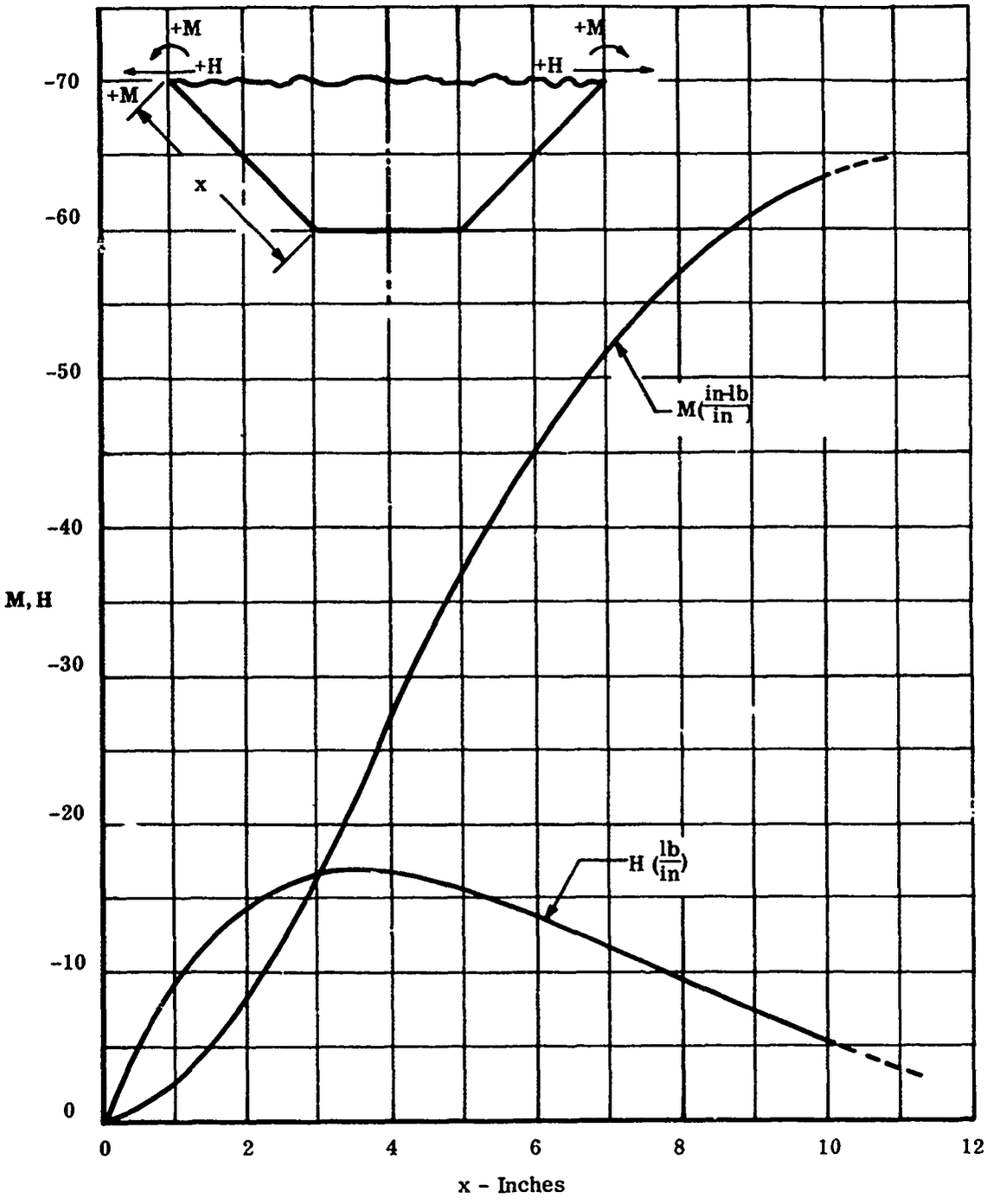


FIGURE 7.1.1.2-5 MERIDIONAL MOMENT AND RADIAL LOAD MEASURED FROM BASE OF THE SHELL SHOWN IN FIGURE 7.1.1.2-4

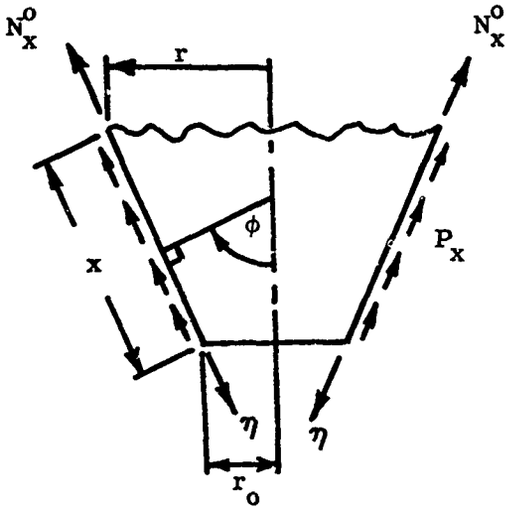


FIGURE 7.1.2-1 MERIDIONAL LOADING ON A CONICAL SHELL

For the membrane analysis, the moments $M^{()}$ and M^o_Θ are considered negligible. The meridional and radial equilibrium and the stress strain relations then give the required internal loads and deflections as

$$
\begin{aligned}
\delta^o &= \frac{\nu}{Eh}\left[\left(\frac{r_o + r}{2}\right)(x)\quad P_x - r_o\,\eta\right] \\
N_x^o &= \frac{r_o}{r}\eta - \frac{1}{r}\int_o^x r\,P_x\,dx \\
\Theta^o &= \frac{N_x^o}{Eh}\left(\frac{\cos\phi}{\sin\phi}\right) - \frac{\nu}{Eh\sin\phi}\left[rP_x + \left(\frac{r + r_o}{2}\right)(x)\quad \frac{dP_x}{dx}\right] \qquad (1) \\
\Delta^o &= \int_o^x \left[\frac{N_x^o}{Eh}\sin\phi + \Theta^o\cos\phi\right]dx \\
N_\Theta^o &= Q^c = M^o = M_\Theta^o = H^o = 0 \quad ,
\end{aligned}
$$

where $r = r_o + x\cos\phi$ and superscript "o" refers to membrane effects.

If the membrane deflections and rotations as given by the above equations do not satisfy prescribed conditions at the edges, then horizontal edge loads and restraining moments must be applied such that the edge boundary conditions are satisfied. The effects of these edge loadings, discussed in Paragraph 7.1.1, are then superposed on the membrane effects to give the required solution.

7.1.2 (Cont'd)

The following illustrative problem demonstrates the computational techniques for solution of a conical shell (Figure 7.1.2-2) supporting a weight W. This solution requires the determination of the stresses at the fixed bottom of the shell (a similar procedure can be employed at the top).

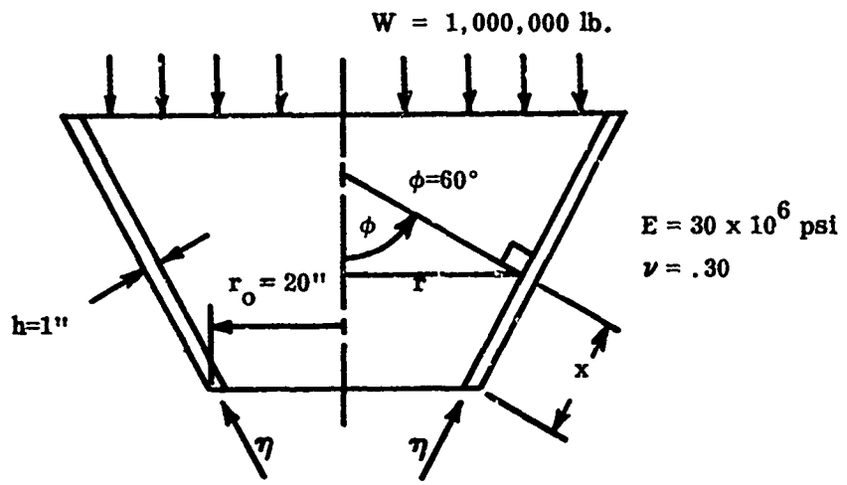


FIGURE 7.1.2-2 CONICAL SHELL UNDER VERTICAL LOADING

Assume first that the bottom of the shell is unrestrained. Then for vertical equilibrium, the statically determinate meridional membrane reaction at the base is

$$\eta = -\frac{W}{2\pi r_o \sin\phi} = -\frac{1,000,000}{2\pi(20)(.866)} = -9200\ \frac{lb}{in}$$

and the significant parameters are

$$D = \frac{Eh^3}{12(1-\nu^2)} = \frac{30(10)^6(.1)^3}{12(.91)} = 2.74(10)^6 \text{ in lb}$$

$$\ell = .778\sqrt{\frac{r_o h}{\sin\phi}} = .778\sqrt{\frac{20 \times 1}{.866}} = 3.74 \text{ in}$$

$$\frac{\ell}{D} = \frac{3.74}{2.74(10)^6} = 1.37(10)^{-6}\ \frac{in}{in\text{-}lb}.$$

7.1.2 (Cont'd)

From the first and third of Eqs. (1), with $P_x = 0$ and $N_x = \eta$, the membrane deflection and slope at the base of the shell are

$$\delta^o = \frac{\nu}{Eh}(-r_o\eta) = \frac{.30\,(20)\,(9200)}{30\,(10)^6\,(1)} = .00184 \text{ in}$$

$$\theta^o = \frac{\eta}{Eh}\frac{\cos\phi}{\sin\phi} = \frac{-9200\,(.500)}{30(10)^6(1)(.866)} = -.000177 \text{ radians.}$$

Since the base of the shell is fixed, an edge radial load, $\mathcal{H}$ and moment $\mathcal{M}$ must be applied such that

$$\delta = \delta^o + \delta_e = 0$$

$$\Theta = \Theta^o + \Theta_e = 0,$$

i.e.,

$$\delta_e = -\delta^o$$

$$\Theta_e = -\Theta^o. \qquad \text{(a)}$$

The values of $\mathcal{H}$ and $\mathcal{M}$ are then obtained by inverting the first two equations from (1) of Paragraph 7.1.1.2. where δ_e and Θ_e are given above by (a) and x = 0. This leads to

$$\mathcal{M} = \frac{2\Theta^o}{(\ell/D)} - \frac{2\delta^o}{(\ell^2/D)\sin\phi}$$

and

$$\mathcal{H}\ell\sin\phi = -\frac{2\Theta^o}{(\ell/D)} + \frac{4\delta^o}{(\ell^2/D)\sin\phi},$$

or

$$\mathcal{M} = \frac{-2(.000177)}{1.37\,(10)^{-6}} - \frac{2(.00184)}{1.37(10)^{-6}(3.74)(.866)} = -1090 \ \frac{\text{in lb}}{\text{in}}$$

and

$$\mathcal{H}\ell\sin\phi = \frac{2\,(.000177)}{1.37(10)^{-6}} + \frac{4(.00184)}{1.37\,(10)^{-6}(3.74)(.866)} = 1920 \text{ lb}$$

$$\mathcal{H} = \frac{1920}{(3.74)(.866)} = 592 \ \frac{\text{lb}}{\text{in}}.$$

7.1.2 (Cont'd)

The final results are now obtained by summing up the effects of membrane action due to η, plus edge load action due to $\mathcal{M}$ and $\mathcal{H}$, or,

$$N_x = N_x^o + N_{x_e}$$

$$N_\Theta = 0 + N_{\Theta_e}$$

$$M = 0 + M_e$$

$$M_\Theta = 0 + \nu M_e .$$

But from Eq. (1),

$$N_x^o = \frac{r_o}{r} \eta$$

and from Eqs. (1) and (2) of Paragraph 7.1.1.2,

$$N_{x_e} = \frac{-2\mathcal{M}F_2}{\ell} \frac{\cos\phi}{\sin\phi} + \mathcal{H} F_3 \cos\phi$$

$$N_{\Theta_e} = \frac{-Eh}{r} \frac{\ell^2}{2D} \sin\phi \left(\mathcal{M} F_3 + \mathcal{H}\ell \sin\phi \; F_4 \right)$$

$$M_e = \mathcal{M} F_1 + \mathcal{H}\ell \sin\phi \; F_2 ,$$

where $F_1, \ldots F_4$ are the known edge loading functions of $\frac{x}{\ell}$ (Eqs. (3) of Paragraph 7.1.1.2). Substituting the known values of η, $\mathcal{M}$, $\mathcal{H}$, ϕ, r_o, D, E, ℓ and h into the above, and making use of the relation $r = r_o + x \cos\phi$, the following is obtained:

$$N_x = \frac{-9200}{1+.5(x/r_o)} + 336 \; F_2 + 296 \; F_3$$

$$N_\Theta = \frac{1}{1+.5(x/r_o)} (3630 \; F_3 - 6400 \; F_4)$$

$$M = -1090 \; F_1 + 1920 \; F_2$$

$$M_\Theta = -330 \; F_1 + 580 \; F_2 .$$

The stresses at the extreme fibers are given by the expressions

$$\sigma_x = \frac{N_x}{h} \pm \frac{6M}{h^2} \quad \text{and} \quad \sigma_\Theta = \frac{N_\Theta}{h} \pm \frac{6M_\Theta}{h^2} .$$

7.1.2 (Cont'd)

In particular, for the edge $x = 0$,

$$F_1 = F_3 = F_4 = 1$$

and

$$F_2 = 0 \ ,$$

so that the stresses at the edge $x = 0$ become

$$\sigma_x\Big|_{x=0} = -9200 + 296 \pm (-6550) = \begin{cases} -15500 \text{ psi outer fiber} \\ -2400 \text{ psi inner fiber} \end{cases}$$

$$\sigma_\theta\Big|_{x=0} = -2770 \pm (-1980) = \begin{cases} -800 \text{ psi inner fiber} \\ -4750 \text{ psi outer fiber} \end{cases} .$$

In the present problem, the maximum stresses in the vicinity of the base occur at the edge $x = 0$ as given above. This is usually the case when the functions F_1 and F_2 are of the opposite sign. However, in problems where the F_1 and F_2 terms appear with the same signs in the moment expression, the location of maximum stress will often be at a small distance from the edge, usually within $\frac{\ell}{2}$.

7.1.3 Meridional Temperature Variation

The purpose of the following is to reduce the problem of a truncated conical shell with a meridional temperature variation (Figure 7.1.3-1(a)) to an equivalent mechanical loading problem, which can then be treated by the methods presented in Paragraph 7.1.1 (Radial Loading).

To this end, consider the shell to be sliced into elemental rings in which free thermal expansions take place (Figure 7.1.3-1(b)). The free thermal strains in the meridional and radial strains are

$$\epsilon_x = \epsilon_\theta = \alpha \Delta T \ . \tag{1}$$

Under these conditions, since ΔT varies with the element, the edges of adjacent rings do not match. To reestabiish radial continuity of the rings, a radial distributed pressure

$$P_h^* = \frac{-Eh}{r} \epsilon_\theta = \frac{-Eh}{r} \alpha \Delta T \tag{2}$$

is applied (Figure 7.1.3-1(c)) which negates the radial thermal expansion of each ring, but causes an axial extension of

$$\begin{aligned} d\Delta^* &= (1+\nu) \epsilon_x \, dx \sin\phi \\ &= (1+\nu) \alpha \Delta T \, dx \sin\phi \\ \Delta^* &= (1+\nu) \sin\phi \int_0^x \alpha \Delta T dx . \end{aligned} \tag{3}$$

7.1.3 (Cont'd)

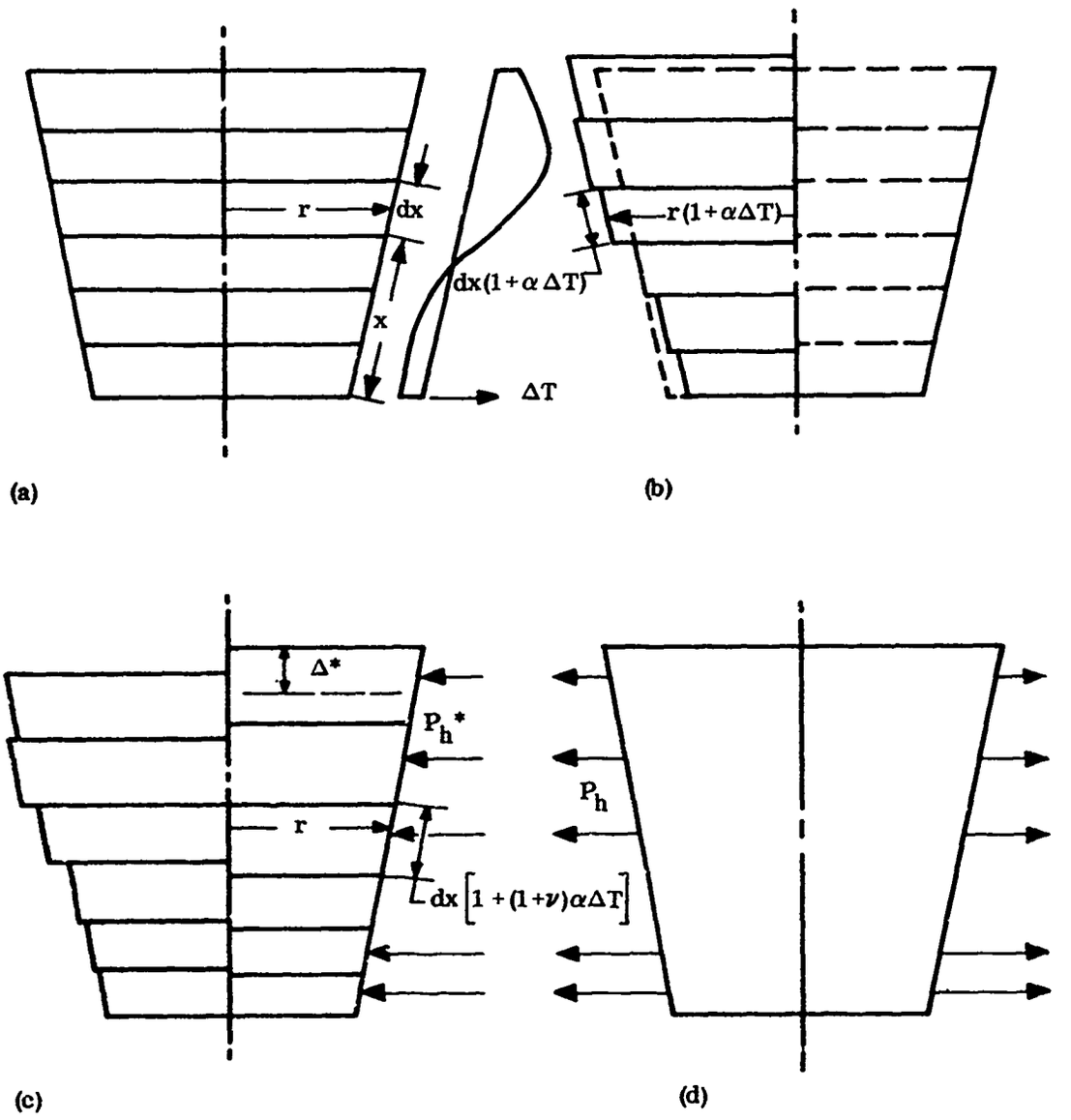


FIGURE 7.1.3-1 REDUCTION OF THERMAL PROBLEM TO EQUIVALENT MECHANICAL LOADING PROBLEM

7.1.3 (Cont'd)

Since the radial pressures P_h^* are really absent, a radial pressure P_h is applied to the rejoined, continuous shell (Figure 7.1.3-1(d)) which negates P_h^*, or

$$P_h + P_h^* = 0$$

so that

$$P_h = - P_h^* \quad . \tag{4}$$

The total stress in the shell is then obtained by superposition of the restoring hoop forces

$$N_\theta^* = P_h^* \, r = - E \, h \, \alpha \, \Delta T \tag{5}$$

produced by P_h^* in rejoining the rings, and the stress distribution which results from the radial, distributed pressure P_h in the continuous shell, where

$$P_h = \frac{Eh}{r} \, \alpha \Delta T \, . \tag{6}$$

The solution of this latter problem was presented in Paragraph 7.1.1.

Thus, in summary, to obtain the solution for the truncated conical shell with a meridional temperature variation $\Delta T(x)$:

(1) Find the hoop force N_θ^* from Eq. (5) and the axial extension Δ^* from Eq. (3). If the shell is free to elongate axially, then this latter quantity is of no interest.

(2) The total solution is obtained by superposing on the above effects the solution of the radial (horizontal) loading problem (Paragraph 7.1.1) for P_h given by Eq. (6).

7.2 APPROXIMATE SOLUTION FOR NON-CONICAL AXISYMMETRIC SHELLS

When an axisymmetric shell with axisymmetric loading is non-conical, the approximate solutions previously stated may still be used. The shell structure can most often be approximated by a series of separate conical shells (Figure 7.2-1(a)) and a spherical cap "O" (the theory of shallow spherical caps is given in Reference 7-2). The individual shell sections can first be analyzed by the hoopring and membrane approximations of Sub-section 7.1. The common edges of adjacent sections are then joined (Figure 7.2-1(b)) by satisfying the equilibrium requirement that

$$\begin{aligned} \mathcal{H}_A &= \mathcal{H}_B \\ m_A &= m_B \end{aligned} \tag{1}$$

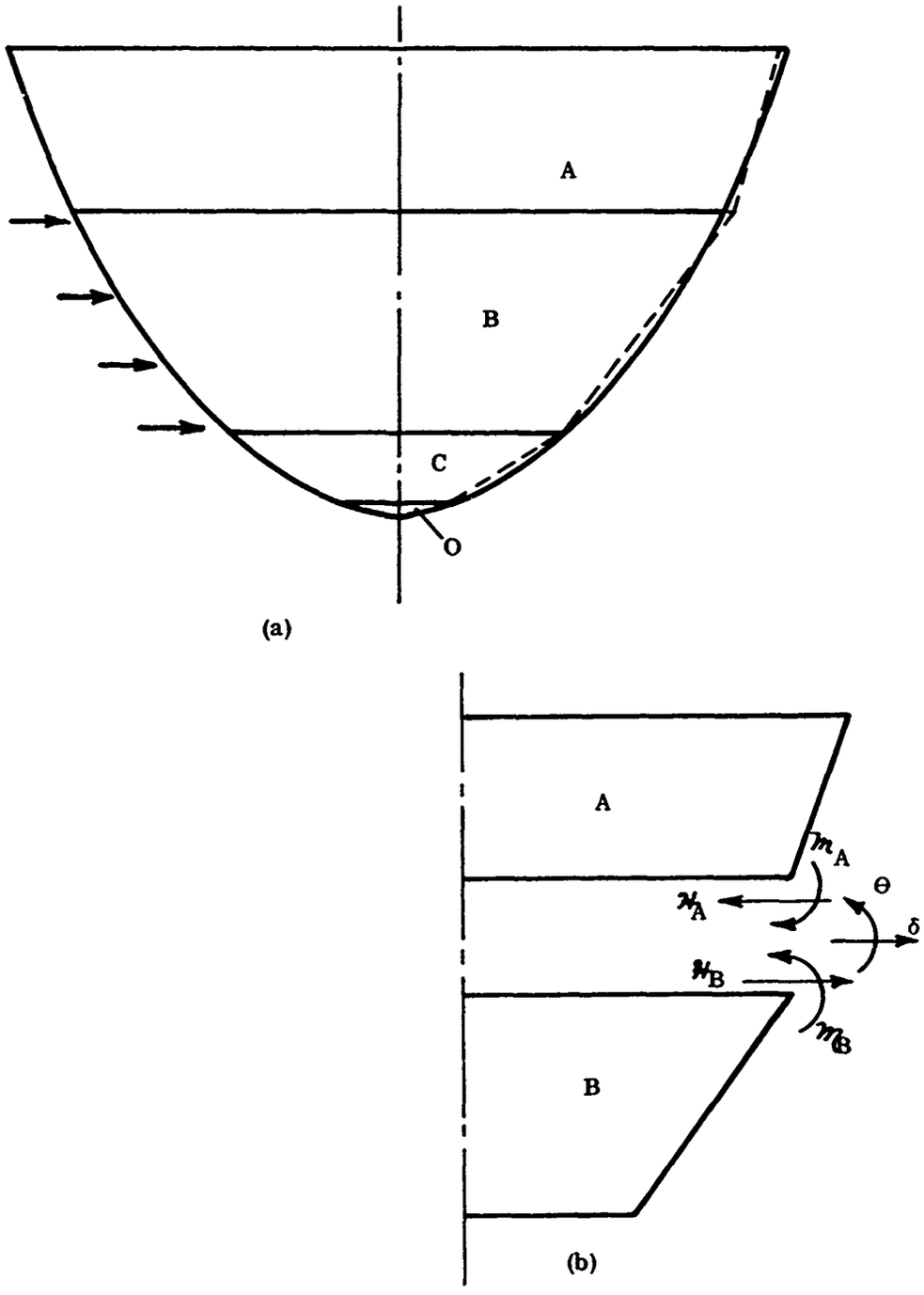


FIGURE 7.2-1 APPROXIMATION OF A NON-CONICAL SHELL BY A SERIES OF CONICAL SECTIONS

7.2 (Cont'd)

and the compatibility conditions

$$\delta_A = \delta_B$$
$$\Theta_A = \Theta_B \,. \tag{2}$$

The solution is thus obtained by superposition.

To prevent interaction of the effects of the edge loads and moments $\mathcal{M}$ and $\mathcal{H}$ which propagate from the upper and lower edges toward the center, the meridional length L of the conical sections should be made larger than three times the "mean" attenuation length ℓ of the section. However, for reliable results in a very flat conical shell section (inclination between 30° and 45°), the meridional length should be made very short ($L < 3\ell$). In this case the interaction between upper and lower edges of the section cannot be ignored in analyzing each element and the more complex analysis of Reference 7-3 must be employed.

7.3 CYLINDRICAL SHELLS

The following paragraphs are concerned with the analysis of cylindrical shells subject to axisymmetric thermal and mechanical loads. A thermal analysis is presented in Paragraph 7.3.1 for the combined problems of normal pressure loading and temperatures which vary in the axial direction only. The analysis is rigorous within the customary approximations of thin shell theory.

Paragraph 7.3.2 discusses the cases of thermal stresses in cylindrical shells due to a variation of temperature through the thickness for both steady state and transient problems.

7.3.1 Cylindrical Shells With Axisymmetric Loading and Meridional Temperature Variation

The preceding analysis becomes much simpler for the special case of a cylindrical shell ($\phi = 90°$; $r = R$ = constant). Within the customary shell theory approximations, the hoopring and edge loading analysis of Paragraph 7.1.1 is rigorous for the thin-walled cylinder.

7.3.1.1 Hoopring Analysis

For the case of the cylinder, Eqs. (2) through (4) of Paragraph 7.1.1.1 become

$$\frac{\ell^4}{4}\,\frac{d^4\delta'}{dx^4} + \delta' = R\left[\frac{R}{Eh}\,P(x) + \alpha\,\Delta T(x)\right], \tag{1}$$

where

$$\ell = \frac{\sqrt{Rh}}{\sqrt[4]{3(1-\nu^2)}}$$
$$= .778\,\sqrt{Rh} \quad (\text{for } \nu = .30).$$

Both normal axisymmetric pressure loading and axisymmetric temperature variation are included on the right side of Eq. (1). The equations for the deflections, internal loads, and moments become

7.3.1.1 (Cont'd)

$$\theta' = -\frac{d\delta'}{dx}$$

$$M' = -D\,\frac{d^2\delta'}{dx^2}$$

$$M'_\theta = \nu M'$$

$$Q' = H' = -D\,\frac{d^3\delta'}{dx^3} \qquad (2)$$

$$N'_\theta = Eh\left[\frac{\delta'}{R} - \alpha\Delta T\right]$$

$$N'_x = 0\ ,$$

and

$$\Delta' = \int_0^x \left[-\frac{\nu N'_\theta}{Eh} + \alpha\Delta T\right] dx\ ,$$

where positive directions for the above quantities are as shown in Figures 7.1.1.1-1 (b) and (c).

As in the case of conical shells, it is convenient to find a particular solution for Eq. (1) where the pressure and thermal loading are expressed by a polynomial.

In general, this particular solution will not satisfy the boundary conditions at the edges of the cylinder. As in the case of the conical shell, additional edge forces and edge moments must be applied to the cylinder which,when superposed on the edge loads and moments resulting from the particular solution, satisfy the prescribed boundary conditions.

Following this approach, the pressure and temperature terms on the right side of Eq. (1) are expressed by a polynomial such that

$$\frac{RP}{Eh} + \alpha\Delta T = \sum_{k=0}^{N} C_k \left(\frac{x}{R}\right)^k$$

$$= C_0 + C_1\,\frac{x}{R} + C_2\left(\frac{x}{R}\right)^2 + \ldots + C_N\left(\frac{x}{R}\right)^N . \qquad (3)$$

A given meridional distribution can be expressed in this manner by the method of Paragraph 4.1.2.3.1

The particular solutions for δ' can then be obtained by substituting Eq. (3) into Eq. (1) and solving the differential equation. The particular solutions for δ' are given in nondimensional form in Table 7.3.1.1-1 for monomials $C_k(x/R)^k$ up to k = 4.

7.3.1.1 (Cont'd)

TABLE 7.3.1.1-1

Particular Solutions for δ', Corresponding to Monomial Pressure Distributions

k	$\frac{RP}{Eh} + \alpha \Delta T$	$\delta'/C_k R$
0	C_0	1
1	C_1 x/R	x/R
2	$C_2 (x/R)^2$	$(x/R)^2$
3	$C_3 (x/R)^3$	$(x/R)^3$
4	$C_4 (x/R)^4$	$(x/R)^4 - 6\left(\frac{\ell}{R}\right)^4$

Once the δ' has been determined as above, the internal loads, moments, slopes and axial deflections corresponding to this particular solution, can be obtained from Eqs. (2).

7.3.1.2 Solution for Edge Loading

When the cylindrical shell is subjected only to an end moment and end load as shown in Figure 7.3.1.2-1 and the longitudinal length of the shell is greater than three times the attenuation length, the edge loading equations (Eqs. (1) and (2) of Paragraph 7.1.1.2) become

$$\begin{aligned} \delta'_e &= -\frac{\ell^2}{2D}\left[\mathcal{M} F_3 + \mathcal{H}\ell F_4 \right] \\ \Theta_e &= \frac{-\ell}{D}\left[\mathcal{M} F_4 + \tfrac{1}{2} \mathcal{H}\ell F_1 \right] \\ M_e &= \mathcal{M} F_1 + \mathcal{H}\ell F_2 \\ H_e &= Q_e = \frac{-2}{\ell} \mathcal{M} F_2 + \mathcal{H} F_3 \end{aligned} \qquad (1)$$

and

$$\begin{aligned} M_{\Theta_e} &= M_e \nu & N_{x_e} &= 0 \\ N_{\Theta_e} &= \frac{Eh\delta_e}{R} & \Delta_e &= \int_0^x \left[-\nu \frac{N_{\Theta_e}}{Eh} \right] dx \end{aligned} \qquad (2)$$

7.3.1.2 (Cont'd)

where the F_k's are those functions of x/ℓ given by Eqs. (3) of Paragraph 7.1.1.2.

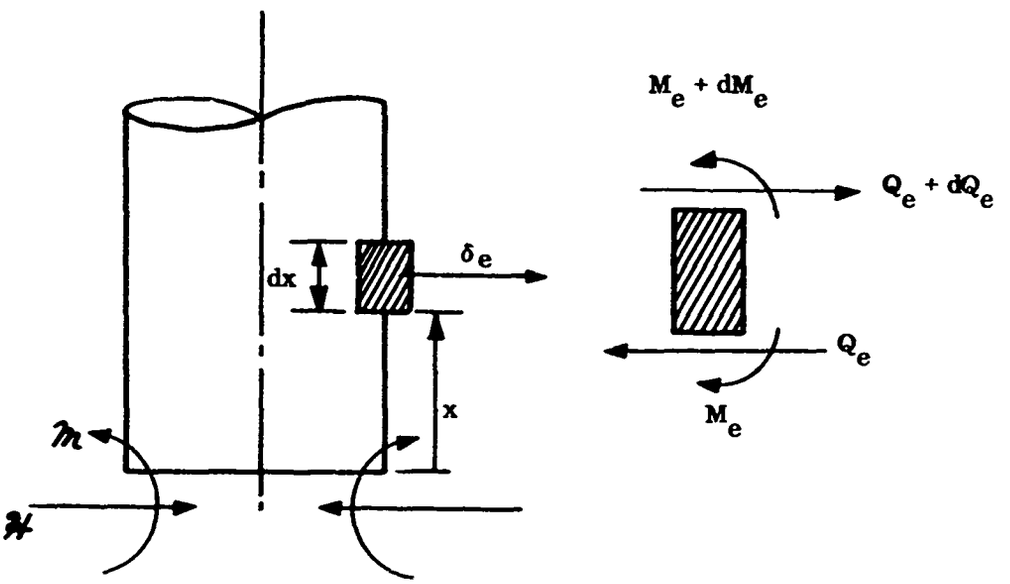


FIGURE 7.3.1.2-1 SELF-EQUILIBRATING LOADS AND MOMENTS $\mathcal{N}$ AND $\mathcal{M}$ AT A CYLINDER EDGE

The following illustrative problem demonstrates the solution for a cylinder subjected to an axisymmetric temperature distribution. The infinitely long cylinder of Figure 7.3.1.2-2 has a radius of R = a and is subjected to a temperature distribution given by

$$\Delta T = T' \text{ when } x < 0$$
$$= 0 \text{ when } x > 0.$$

Find the deflections and stresses due to this thermal loading.

The boundary conditions are

$$\left.\begin{aligned} \delta &= 0 \\ \Theta &= 0 \end{aligned}\right\} \text{at } x = +\infty$$

7.3.1.2 (Cont'd)

and

$$\left.\begin{aligned} \delta &= a\,\alpha T' \\ \Theta &= 0 \end{aligned}\right\} \text{at } x = -\infty .$$

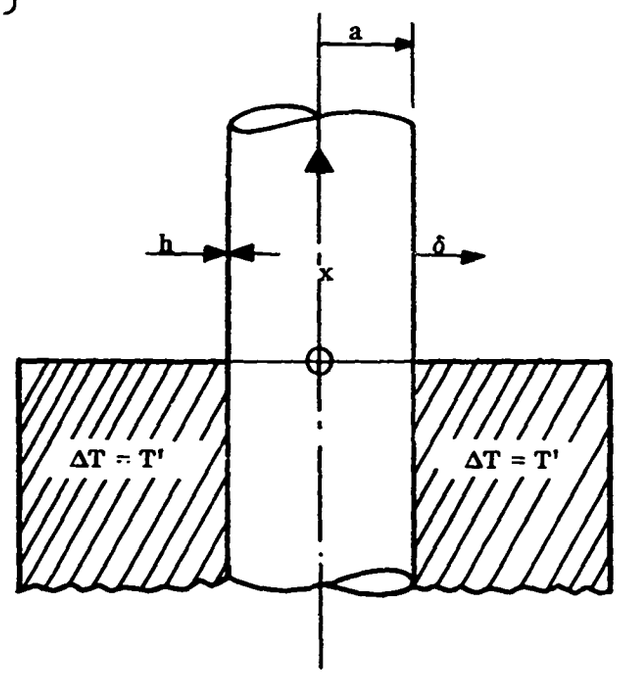


FIGURE 7.3.1.2-2 INFINITELY LONG CYLINDER WITH DISCONTINUOUS AXISYMMETRIC TEMPERATURE DISTRIBUTION

To begin with, the continuous shell is cut into upper and lower portions at $x = 0$. All the stresses and deflections in the upper half are identically zero (no loading or temperature exists in the upper half).

The loading for the lower half is defined by

$P = 0$

$\alpha \Delta T = \alpha T'$.

7.3.1.2 (Cont'd)

Therefore, from Table 7.3.1.1-1, $\alpha T' = C_0$ and the particular solution of Eq. (1) of Paragraph 7.3.1.1 becomes

$$\bar{\delta}' = C_0 R = a\alpha T' \qquad \text{(this is easily seen to be simply the thermal strain times the cylinder radius)}$$

where the upper and lower halves are now denoted by + and −, respectively.

Since $\bar{\delta}'$ is a constant, Eqs. (2) of Paragraph 7.3.1.1 give

$$\bar{\Theta}' = \bar{M}' = \bar{M}'_{\Theta} = \bar{N}'_{\Theta} = \bar{N}'_{x} = 0,$$

or the slope and stresses are identically zero everywhere in the unrestrained lower half of the cylinder. Thus in this case, the particular solution satisfies the boundary conditions identically.

In general, it may be stated that $\alpha \Delta T$ variations which vary linearly with Cartesian coordinates in the form

$$\alpha\Delta T = A + Bx + Cy + Dz$$

cause no stresses if the displacements are unrestrained externally.

Compatibility at the cut edges requires that

$$\overset{+}{\delta}(0) = \overset{-}{\delta}(0)$$
$$\overset{+}{\Theta}(0) = \overset{-}{\Theta}(0) .$$

In other words,

$$\overset{+}{\delta}'(0) + \overset{+}{\delta}_e(0) = \overset{-}{\delta}'(0) + \overset{-}{\delta}_e(0)$$

$$\overset{+}{\Theta}'(0) + \overset{+}{\Theta}_e(0) = \overset{-}{\Theta}'(0) + \overset{-}{\Theta}_e(0)$$

but

$$\overset{+}{\delta}'(0) = 0$$
$$\overset{-}{\delta}'(0) = a\alpha T'$$
$$\overset{+}{\Theta}'(0) = \overset{-}{\Theta}'(0) = 0,$$

therefore

$$\overset{+}{\delta}_e(0) = a\alpha T' + \overset{-}{\delta}_e(0)$$
$$\overset{+}{\Theta}_e(0) = \overset{-}{\Theta}_e(0) .$$

7.3.1.2 (Cont'd)

Edge loads and moments must be applied at the cut (Figure 7.3.1.2-3) to satisfy the above conditions.

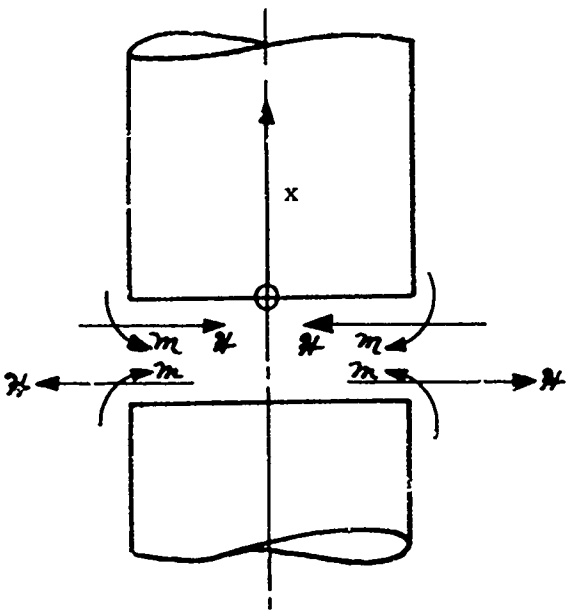


FIGURE 7.3.1.2-3 HORIZONTAL LOADS AND MOMENTS AT CUT EDGES

Expressing the edge deflections and slopes by Eqs. (1) with

$$F_1(0) = F_3(0) = F_4(0) = 1$$

gives

$$-\frac{\ell^2}{2D}\left[\mathcal{M} + \mathcal{H}\ell\right] = a\,\alpha\,T' - \frac{\ell^2}{2D}\left[\mathcal{M} - \mathcal{H}\ell\right]$$

$$-\frac{\ell}{D}\left[\mathcal{M} + \frac{\ell}{2}\mathcal{H}\right] = -\frac{\ell}{D}\left[-\mathcal{M} + \frac{\ell}{2}\mathcal{H}\right].$$

7.3.1.2 (Cont'd)

Solution of the above yields

$$\mathcal{M} = 0$$

$$\mathcal{H} = \frac{-a\alpha T' D}{\ell^3} .$$

The deflection for $x \geq 0$ then becomes

$$\overset{+}{\delta} = \overset{+}{\delta}' + \overset{+}{\delta}_e = 0 + \left(\frac{-a\alpha T' D}{\ell^3} \right) \left(\frac{-\ell^3}{2D} F_4 \right) = \frac{a\alpha T'}{2} F_4 \left(\frac{x}{\ell} \right)$$

and for $x < 0$,

$$\overset{-}{\delta} = \overset{-}{\delta}' + \overset{-}{\delta}_e = a\alpha T' - \frac{a\alpha T'}{2} F_4 \left(\frac{-x}{\ell} \right) = a\alpha T' \left[1 - \frac{1}{2} F_4 \left(\frac{-x}{\ell} \right) \right]$$

The slopes, moments and hoop forces can be obtained in a similar manner from Eqs. (1) and (2). The stresses are then obtained from

$$\sigma_x = \pm \frac{6M}{h^2}$$

$$\sigma_\Theta = \frac{N_\Theta}{h} \pm \frac{6\nu M}{h^2} \qquad \text{(Since } M_\Theta = \nu M\text{)} .$$

The resulting radial deflection δ and stresses σ_x, σ_Θ at extreme fibers are plotted in Figure 7.3.1.2-4.

7.3.2 Cylindrical Shells with Temperature Gradient Through the Thickness

Design nomographs and analysis are presented for the solution of the steady state thermal stress problem. Cylinders with free and completely fixed ends are both considered.

The transient problem for long unrestrained solid and hollow cylinders follows. Tables and curves are given for the determination of the stresses in nondimensional form.

7.3.2.1 Cylindrical Tube - Steady State Heat Flow in Radial Direction

The temperature distribution in the instance of a steady state radial temperature distribution in a cylindrical tube (Figure 7.3.2.1-1(a)) is

$$T = (T_i - T_o) \frac{\log\left(\frac{b}{r}\right)}{\log\left(\frac{b}{a}\right)} + T_o \qquad (1)$$

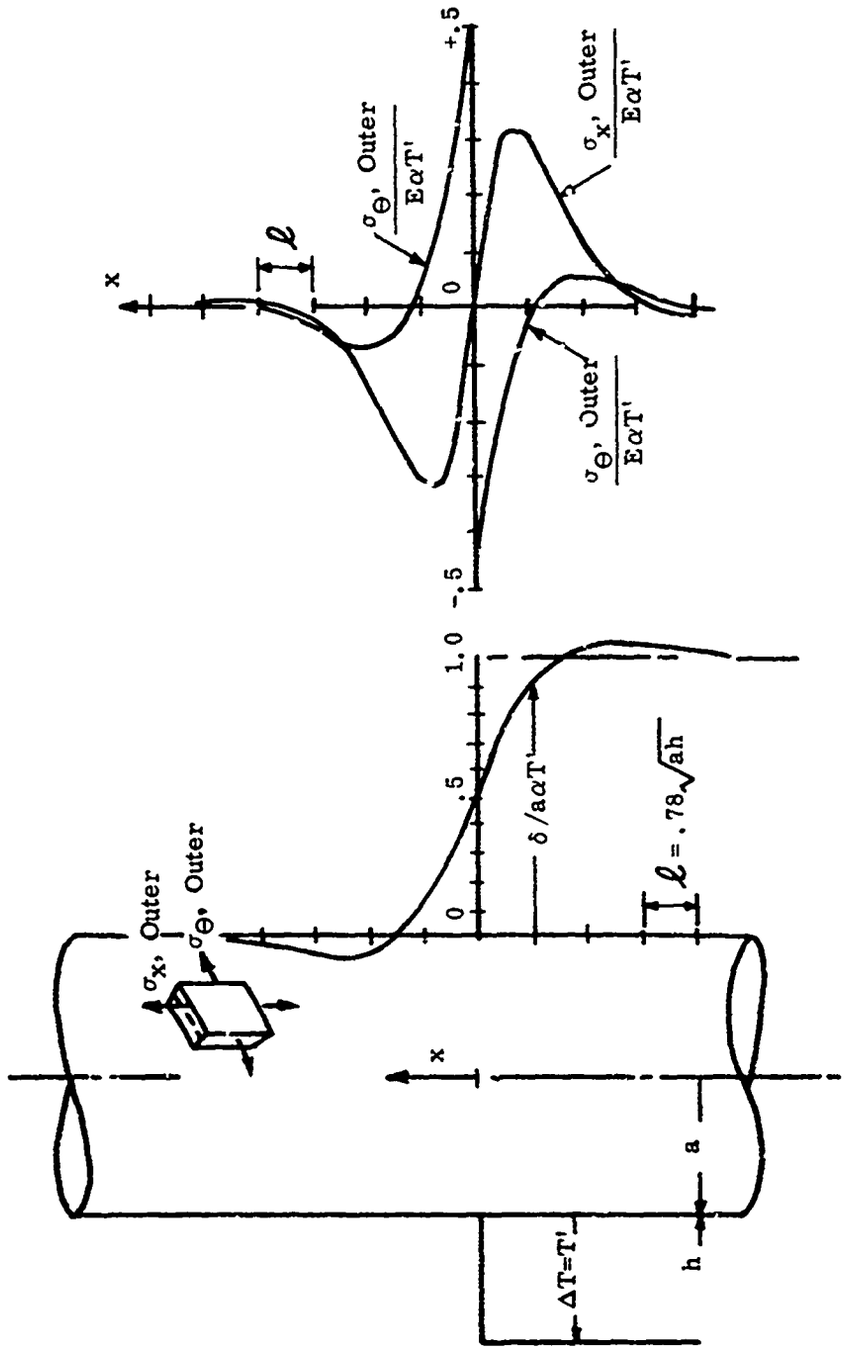


FIGURE 7.3.1.2-4 NONDIMENSIONAL STRESSES AND RADIAL DEFLECTIONS

7.3.2.1 (Cont'd)

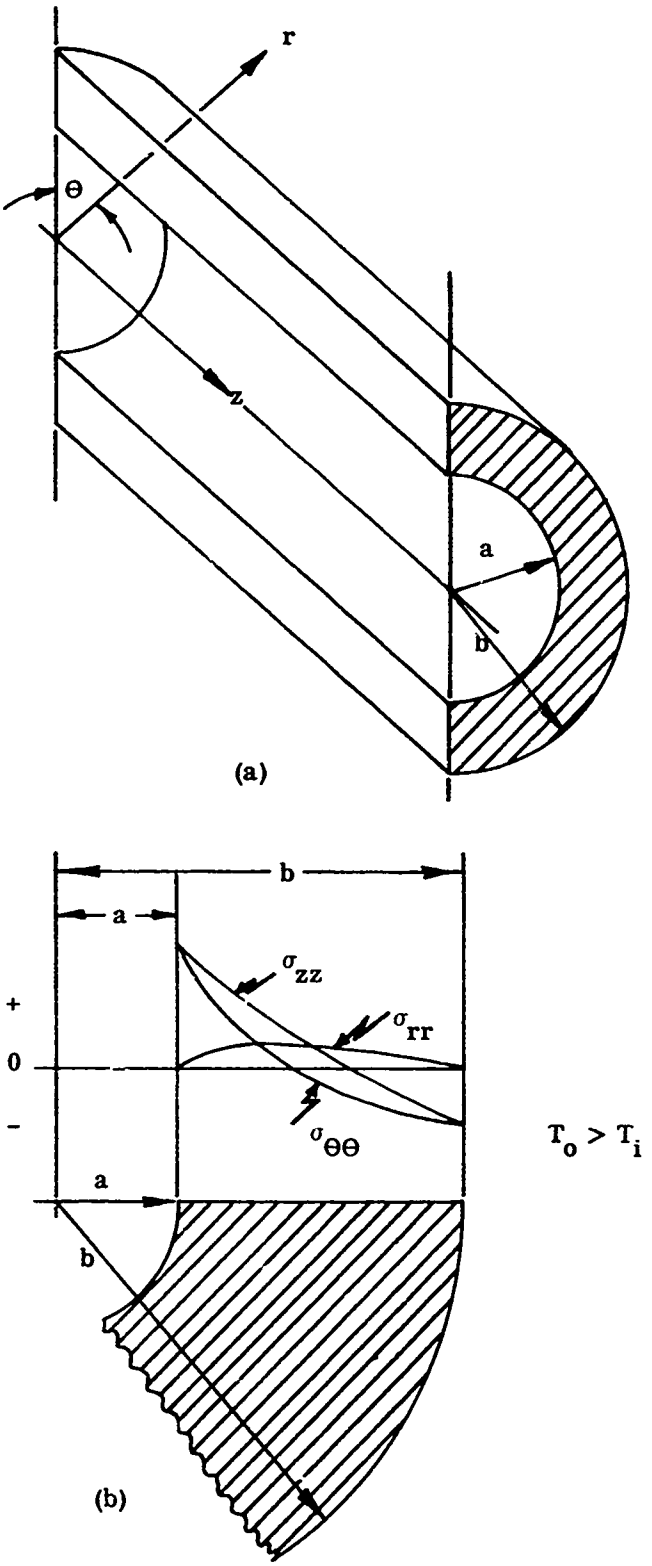


FIGURE 7.3.2.1-1: (a) SHELL GEOMETRY
(b) VARIATION OF STRESSES THROUGH THE CYLINDER THICKNESS

where T_i and T_o are the temperatures in the inside (r=a) and outside (r=b), respectively.

The stress components in the radial, tangential, and longitudinal directions are as follows for the case when the tube is completely unrestrained.

$$\sigma_{rr} = \frac{E\alpha(T_i - T_o)}{2(1-\nu)\log(b/a)} \left[-\log\frac{b}{r} - \frac{a^2}{b^2-a^2} \cdot \left(1 - \frac{b^2}{r^2}\right) \log\frac{b}{a} \right] \quad (2)$$

$$\sigma_{\theta\theta} = \frac{E\alpha(T_i - T_o)}{2(1-\nu)\log(b/a)} \left[1 - \log\frac{b}{r} - \frac{a^2}{b^2-a^2} \cdot \left(1 + \frac{b^2}{r^2}\right) \log\frac{b}{a} \right] \quad (3)$$

$$\sigma_{zz} = \frac{E\alpha(T_i - T_o)}{2(1-\nu)\log(b/a)} \left[1 - 2\log\frac{b}{r} - \frac{2a^2}{b^2-a^2} \log\frac{b}{a} \right] . \quad (4)$$

NOTE: $\sigma_{zz} = \sigma_{rr} + \sigma_{\theta\theta}$; σ_{zz} max. and $\sigma_{\theta\theta}$ max. occurs at r = b.

The results given in Eqs. (2) through (4) are accurate away from the ends of the tube since the boundary conditions of zero traction at the ends are not satisfied pointwise. Instead, the average value of the normal stress is zero.

The character of the stress distribution in a thick-walled tube in steady heat conduction with temperature varying only radially (corresponding to Eqs. (2) through (4)) is shown in Figure 7.3.2.1-1(b).

The following tabulation gives the signs of the stresses for internal heating ($T_i > T_o$):

Stress	Radius	Kind of Stress
Tangential	Inside	Compression
Tangential	Outside	Tension
Longitudinal	Inside	Compression
Longitudinal	Outside	Tension
Radial	All Radii	Compression

For external heating, $T_o > T_i$, the signs of all the stresses are changed.

Figures 7.3.2.1-2 through 5 are alignment charts giving values of the above stress components in terms of the geometry and the physical constants for one degree fahrenheit differential between the outside and inside surfaces. For a temperature difference of T degrees Fahrenheit, results found by the nomograph must be multiplied by T.

7.3.2.1 (Cont'd)

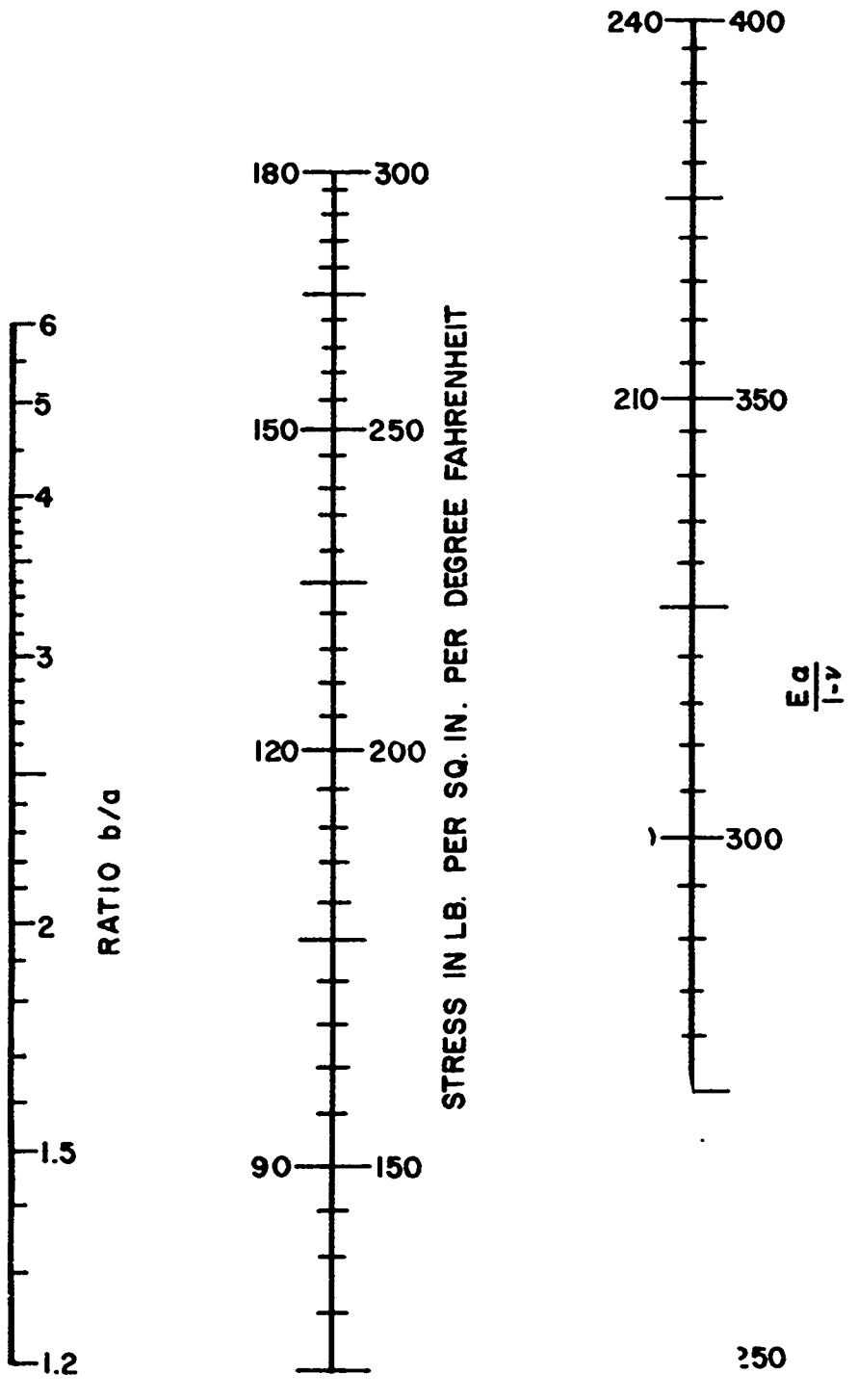


FIGURE 7.3.2.1-2 MAXIMUM TANGENTIAL AND LONGITUDINAL STRESS IN CYLINDER PER °F TEMPERATURE DIFFERENCE BETWEEN THE OUTER AND INNER RADII

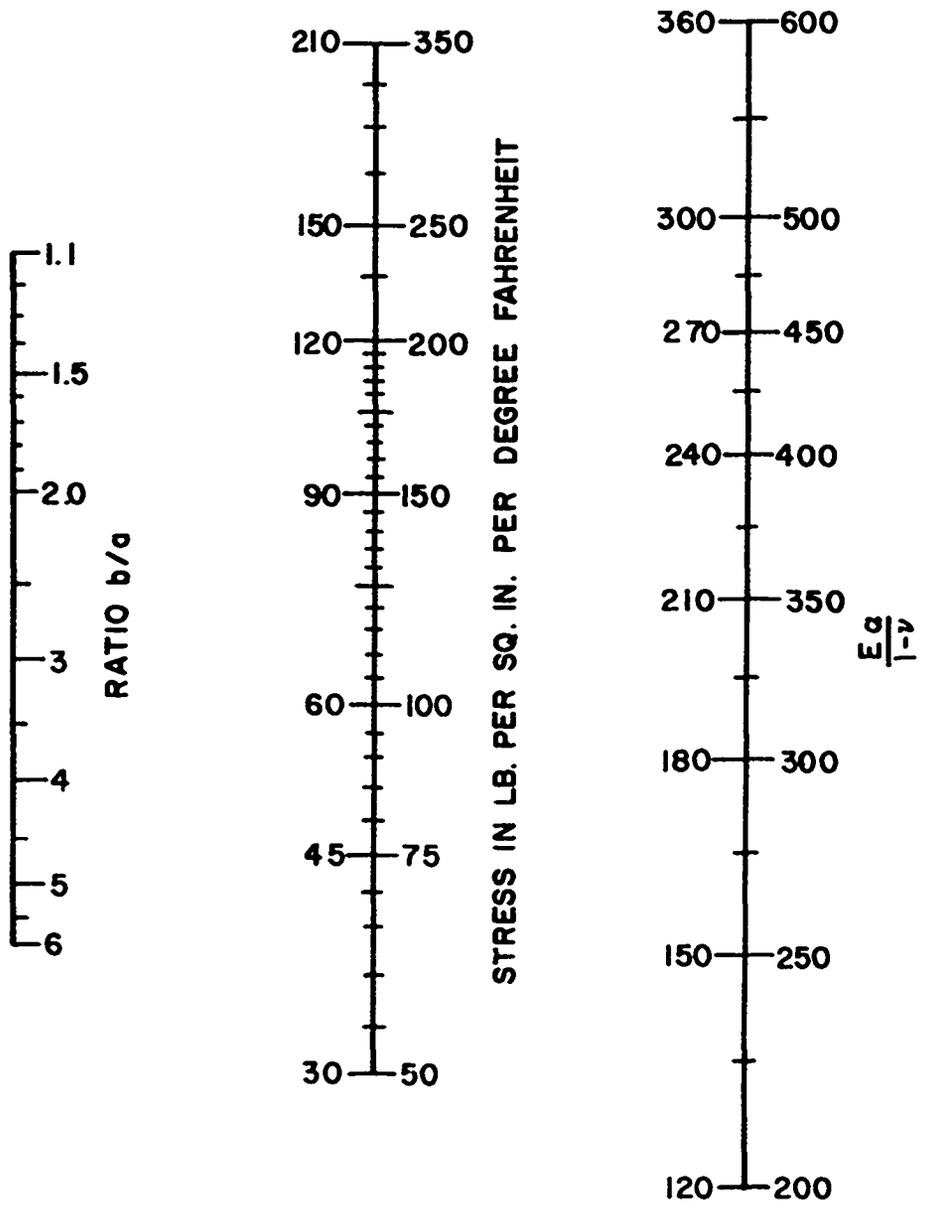


FIGURE 7.3.2.1-3 TANGENTIAL STRESS AT OUTSIDE RADIUS PER °F TEMPERATURE DIFFERENCE BETWEEN THE OUTER AND INNER RADII

7.3.2.1 (Cont'd)

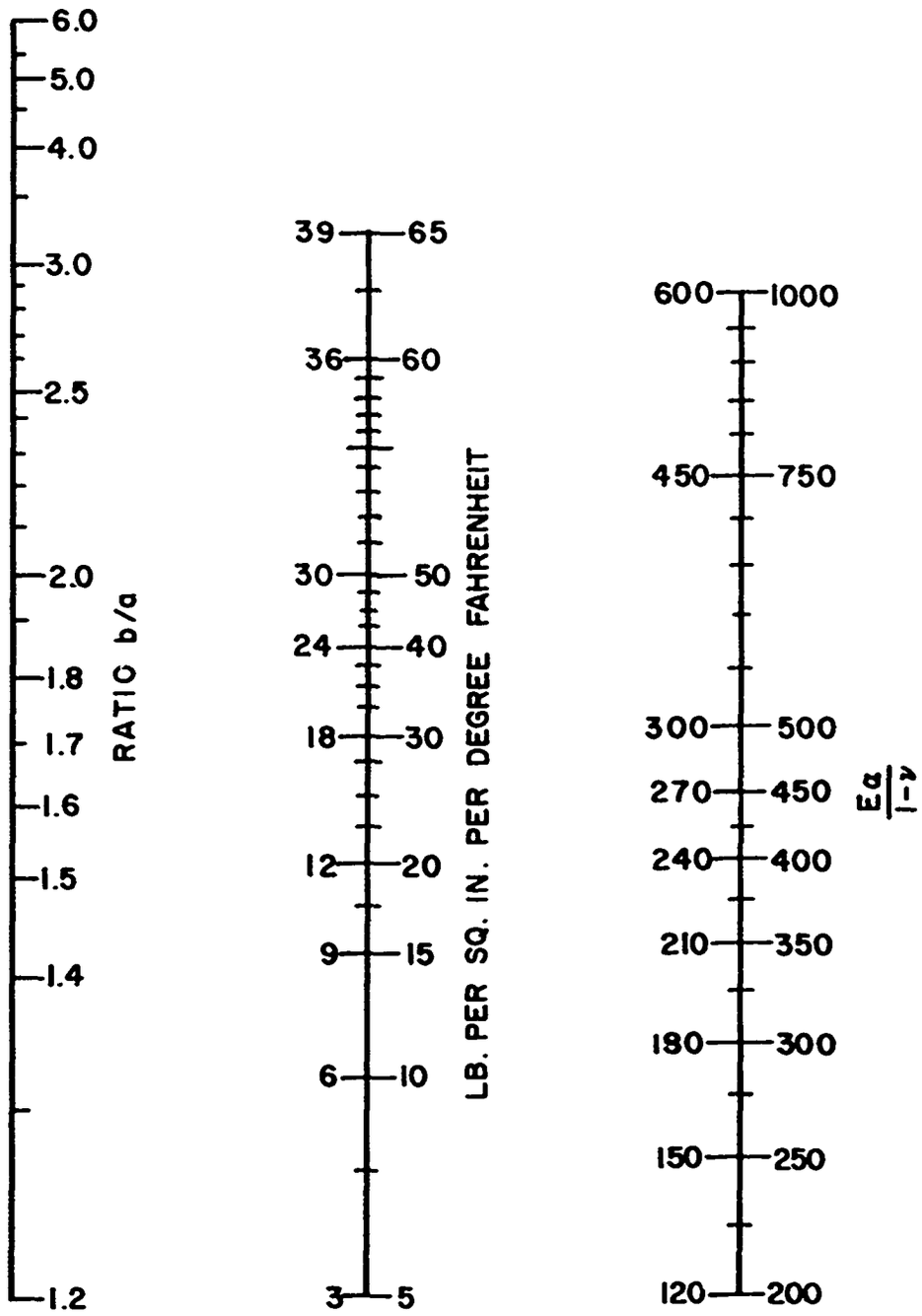


FIGURE 7.3.2.1-4 MAXIMUM RADIAL STRESS PER °F TEMPERATURE DIFFERENCE BETWEEN THE OUTER AND INNER RADII

7.3.2.1 (Cont'd)

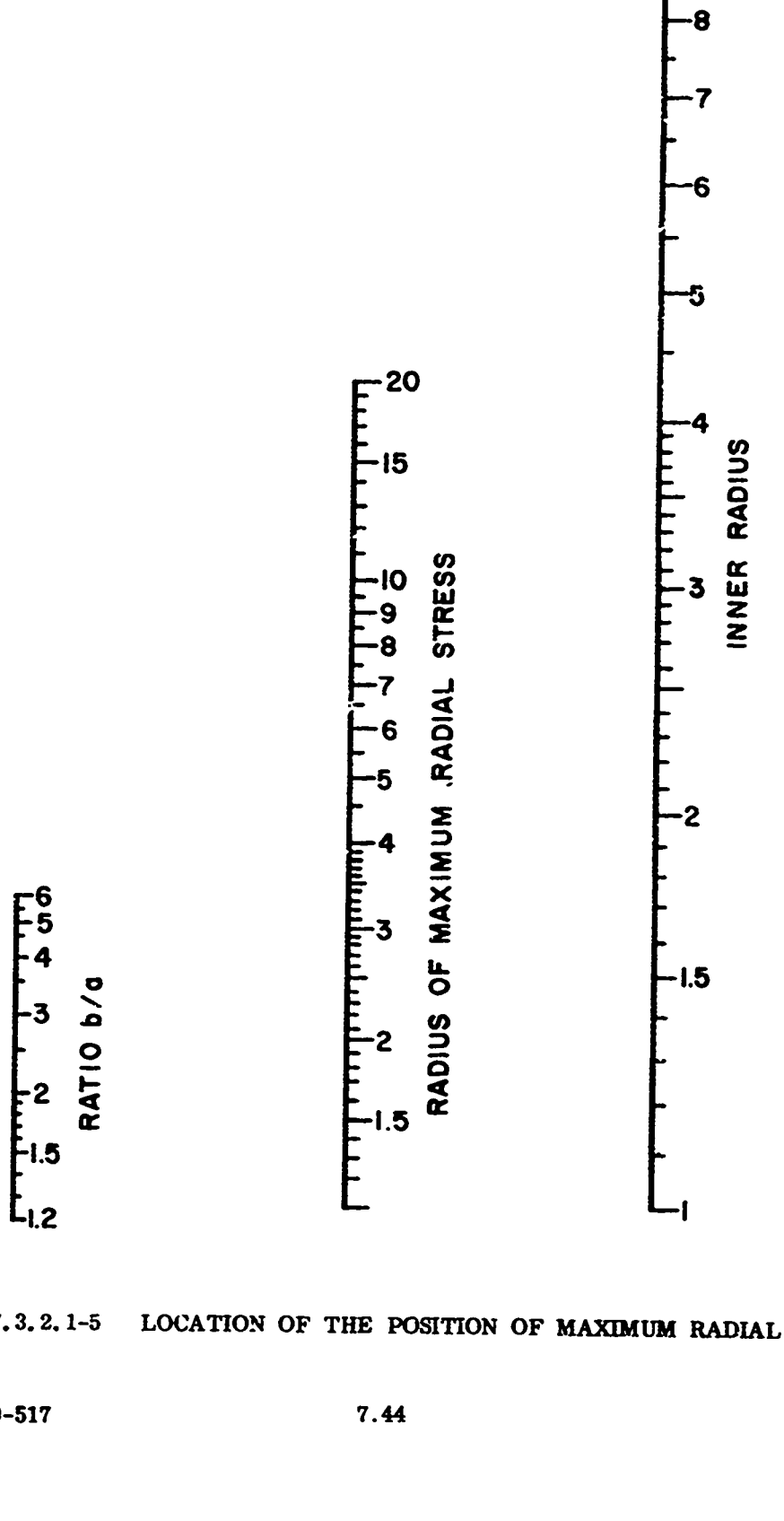


FIGURE 7.3.2.1-5 LOCATION OF THE POSITION OF MAXIMUM RADIAL STRESS

7.3.2.1 (Cont'd)

Stress formulas for unrestrained thin-walled cylindrical tubes are now presented. If the thickness of the wall "b-a" is small in comparison with the inner radius "a" of the cylinder, then $\frac{b}{a} = 1 + \frac{b-a}{a}$ where $\frac{b-a}{a} \ll 1$. Therefore, $\log \frac{b}{a} = \log (1 + \frac{b-a}{a}) \approx \frac{b-a}{a}$

so that for a thin-walled unrestrained cylindrical tube the stress at the boundaries are given approximately by

$$(\sigma_{\theta\theta})_{r=a} = (\sigma_{zz})_{r=a} = \frac{-E\alpha(T_i - T_o)}{2(1-\nu)} \left(1 + \frac{b-a}{3a}\right)$$

$$(\sigma_{\theta\theta})_{r=b} = (\sigma_{zz})_{r=b} = \frac{E\alpha(T_i - T_o)}{2(1-\nu)} \left(1 - \frac{b-a}{3a}\right) , \qquad (5)$$

where σ_{rr} is negligible.

It is now assumed that end displacement is completely prevented. This condition is exemplified by a cylinder with completely restrained ends. The formulas for the radial and tangential stress components are the same as for the unrestrained case. The axial stress is modified by the stress necessary to prevent axial displacements. The additional stress "K" necessary to prevent axial displacements is

$$K = \frac{-E\alpha(T_i - T_o)}{2 \log \frac{b}{a}} \left[1 - \left(\frac{2a^2}{b^2 - a^2}\right) \log \frac{b}{a} \right] - E\alpha T_o \qquad (6)$$

and the total stress is $\sigma_{zz}\big|_{Total} = K + \sigma_{zz}$ where σ_{zz} is given by Eq. (4).

7.3.2.2 Transient Thermal Stresses in Circular Cylinders

This paragraph presents the determination of transient thermal stresses in long unrestrained cylinders subject to temperatures which vary only with the radial coordinate and the time t , and where inertia effects are ignored.

For solid cylinders, the following results are presented:

The radial and tangential stresses for a solid cylinder (Reference 7-4) are

$$\sigma_{rr} = \frac{E\alpha}{1-\nu} \left[\frac{1}{a^2} \int_0^a rTdr - \frac{1}{r^2} \int_o^r rTdr \right] \qquad (1)$$

$$\sigma_{\theta\theta} = \frac{E\alpha}{1-\nu} \left[\frac{1}{a^2} \int_o^a rTdr + \frac{1}{r^2} \int_o^r rTdr - T \right] , \qquad (2)$$

where a is the radius of the cylinder, E is Young's Modulus, ν Poisson's Ratio, α the coefficient of linear expansion of the solid, and T its temperature at radius r.

7.3.2.2 (Cont'd)

Since the resultant of the normal forces over the cross section of the cylinder is zero, then

$$\sigma_{zz} = \sigma_{rr} + \sigma_{\theta\theta}$$

The direct application of Eqs. (1) and (2) would require a knowledge of the temperature distribution. The heat transfer problem from which the temperature distribution is determined will not be considered here.

The temperature distributions and the non-dimensional stresses for the following transient problem are found in Reference 7-5.

Case I: Thermal stress in the cylinder $o \leq r \leq a$ initially at constant temperature T_o whose surface is kept at temperature T_1 for $t > o$.

Tables 7.3.2.2-1 and 7.3.2.2-2 give values of $\frac{-(1-\nu)\sigma_{rr}}{E\alpha(T_o - T_1)}$ and $\frac{(1-\nu)\sigma_{\theta\theta}}{E\alpha(T_o - T_1)}$ as functions of the dimensionless parameters r/a and $\frac{Kt}{a^2}$ where K is the thermal diffusivity of the material and is defined by

$$K = \frac{\text{(thermal conductivity)}}{\text{(mass density)} \quad \text{(specific heat)}}$$

Case II: Thermal stresses in the cylinder $o \leq r \leq a$, initially at uniform temperature T_o, with heat transfer between the cylinder and a medium at temperature T_1 for $t > o$.

It is assumed that the normal gradient of temperature at the surface is directly proportional to the difference between the surface temperature and the medium. This relation is expressed by

$$\left[\frac{\partial T}{\partial r} + h(T - T_1) \right]_{r=a} = 0 \qquad (3)$$

NOTES: (1) $h = 0$ corresponds to no heat transfer (complete insulation), $\left.\frac{\partial T}{\partial r}\right|_{r=o} = 0$

(2) $h = \infty$ corresponds to infinite heat transfer, $T|_{r=a} = T_1$ (Case I)

Therefore, the results will involve three dimensionless parameters which are most conveniently taken as $\frac{Kt}{a^2}$, $\frac{r}{a}$ and ah. In Figures 7.3.2.2-1 and 7.3.2.2-2, respectively, the values of $\frac{-(1-\nu)\sigma_{rr}}{E\alpha(T_o - T_1)}$ and $\frac{(1-\nu)\sigma_{\theta\theta}}{E\alpha(T_o - T_1)}$ as functions of $\frac{Kt}{a^2}$ are shown for $ah = 5$ and values of $\frac{r}{a}$ ranging from 0 to 1.0.

To illustrate the way in which the stresses vary with ah, the variation with $\frac{Kt}{a^2}$ of the surface tangential stress, $\sigma_{\theta\theta}$ for $\frac{r}{a} = 1$, is shown in Figure 7.3.2.2-3 for ah values of 0.2, 0.5, 1, 2, 5, 10, 20, and ∞.

TABLE 7.3.2.2-1

RADIAL STRESSES IN CIRCULAR CYLINDERS

$$-(1-\nu)\sigma_{rr}/E\alpha\,(T_o - T_1)$$

kt/a² \ r/a	0.	0.1	0.2	0.3	0.4	0.5	0.6	0.7	0.75	0.8	0.85	0.9	0.95
0.005	.0773	.0773	.0773	.0773	.0773	.0773	.0772	.0771	.0766	.0749	.0699	.0582	.0357
0.01	.1077	.1077	.1077	.1077	.1077	.1077	.1073	.1049	.1012	.0942	.0820	.0628	.0355
0.015	.1305	.1305	.1305	.1305	.1304	.1300	.1280	.1209	.1135	.1021	.0855	.0630	.0344
0.02	.1493	.1493	.1493	.1492	.1487	.1471	.1424	.1303	.1198	.1053	.0861	.0621	.0332
0.03	.1797	.1796	.1792	.1782	.1757	.1701	.1589	.1385	.1238	.1057	.0841	.0591	.0309
0.04	.2029	.2026	.2012	.1983	.1926	.1824	.1654	.1394	.1225	.1029	.0806	.0558	.0288
0.05	.2196	.2188	.2161	.2108	.2018	.1875	.1663	.1370	.1190	.0988	.0766	.0526	.0269
0.06	.2300	.2287	.2246	.2172	.2053	.1879	.1640	.1328	.1145	.0943	.0726	.0495	.0252
0.07	.2349	.2332	.2280	.2187	.2048	.1853	.1597	.1277	.1094	.0897	.0687	.0466	.0236
0.08	.2353	.2333	.2273	.2168	.2014	.1806	.1542	.1222	.1043	.0851	.0650	.0439	.0222
0.09	.2324	.2302	.2236	.2123	.1960	.1747	.1481	.1166	.0991	.0807	.0614	.0414	.0209
0.1	.2271	.2248	.2178	.2061	.1895	.1679	.1416	.1109	.0940	.0764	.0580	.0390	.0196
0.15	.1850	.1828	.1761	.1652	.1503	.1316	.1095	.0846	.0713	.0576	.0435	.0291	.0146
0.2	.1418	.1400	.1348	.1261	.1144	.0998	.0827	.0637	.0536	.0432	.0326	.0218	.0109
0.3	.0802	.0792	.0762	.0713	.0645	.0562	.0466	.0358	.0301	.0243	.0183	.0122	.0061
0.4	.0450	.0445	.0428	.0400	.0362	.0315	.0261	.0201	.0169	.0136	.0103	.0069	.0034
0.5	.0253	.0249	.0240	.0224	.0203	.0177	.0146	.0113	.0095	.0076	.0058	.0038	.0019
0.6	.0142	.0140	.0134	.0126	.0114	.0099	.0082	.0063	.0053	.0043	.0032	.0022	.0011
0.7	.0079	.0078	.0075	.0071	.0064	.0056	.0046	.0035	.0030	.0024	.0018	.0012	.0006
0.8	.0045	.0044	.0042	.0040	.0036	.0031	.0026	.0020	.0017	.0013	.0010	.0007	.0003
0.9	.0025	.0025	.0024	.0022	.0020	.0018	.0014	.0011	.0009	.0008	.0006	.0004	.0002
1.0	.0014	.0014	.0013	.0012	.0011	.0010	.0008	.0006	.0005	.0004	.0003	.0002	.0001

TABLE 7.3.2.2-2

TANGENTIAL STRESSES IN CIRCULAR CYLINDERS

$(1 - \nu)\, \sigma_{\theta\theta}/E\alpha\, (T_o - T_1)$

kt/a^2 \ r/a	0.	0.1	0.2	0.3	0.4	0.5	0.6	0.7	0.8	0.85	0.9	0.95	1.0
0.005	-.0773	-.0773	-.0773	-.0773	-.0773	-.0773	-.0772	-.0742	-.0286	.0605	.2384	.5146	.8455
0.01	-.1077	-.1077	-.1077	-.1077	-.1077	-.1072	-.1021	-.0700	.0549	.1803	.3534	.5630	.7845
0.015	-.1305	-.1305	-.1305	-.1304	-.1298	-.1255	-.1059	-.0402	.1194	.2447	.3972	.5670	.7390
0.02	-.1493	-.1493	-.1492	-.1486	-.1455	-.1337	-.0971	-.0077	.1628	.2806	.4153	.5589	.7014
0.03	-.1797	-.1794	-.1780	-.1736	-.1610	-.1306	-.0673	.0144	.2114	.3127	.4213	.5323	.6402
0.04	-.2029	-.2018	-.1973	-.1861	-.1621	-.1163	-.0385	.0783	.2328	.3204	.4115	.5027	.5904
0.05	-.2196	-.2171	-.2084	-.1900	-.1562	-.1002	-.0158	.0992	.2404	.3175	.3960	.4736	.5479
0.06	-.2300	-.2261	-.2134	-.1887	-.1476	-.0855	.0010	.1114	.2406	.3092	.3783	.4460	.5106
0.07	-.2349	-.2298	-.2137	-.1843	-.1384	-.0730	.0129	.1179	.2365	.2983	.3599	.4201	.4772
0.08	-.2353	-.2293	-.2108	-.1782	-.1294	-.0629	.0211	.1204	.2298	.2859	.3416	.3957	.4471
0.09	-.2324	-.2258	-.2057	-.1711	-.1209	-.0547	.0266	.1203	.2216	.2730	.3238	.3729	.4195
0.1	-.2271	-.2202	-.1991	-.1636	-.1132	-.0481	.0300	.1184	.2125	.2599	.3065	.3515	.3942
0.15	-.1850	-.1783	-.1586	-.1263	-.0827	-.0292	.0319	.0978	.1654	.1988	.2313	.2624	.2919
0.2	-.1418	-.1365	-.1208	-.0954	-.0614	-.0203	.0259	.0752	.1252	.1498	.1735	.1963	.2179
0.3	-.0802	-.0772	-.0682	-.0537	-.0343	-.0111	.0150	.0426	.0705	.0842	.0974	.1101	.1220
0.4	-.0450	-.0433	-.0383	-.0301	-.0193	-.0062	.0084	.0239	.0396	.0472	.0546	.0617	.0684
0.5	-.0253	-.0243	-.0215	-.0169	-.0108	-.0035	.0047	.0134	.0222	.0265	.0306	.0346	.0384
0.6	-.0142	-.0136	-.0120	-.0095	-.0061	-.0020	.0026	.0075	.0124	.0149	.0172	.0194	.0215
0.7	-.0079	-.0076	-.0068	-.0053	-.0034	-.0011	.0015	.0042	.0070	.0083	.0096	.0109	.0121
0.8	-.0045	-.0043	-.0038	-.0030	-.0019	-.0006	.0008	.0024	.0039	.0047	.0054	.0061	.0068
0.9	-.0025	-.0024	-.0021	-.0017	-.0011	-.0003	.0005	.0013	.0022	.0026	.0030	.0034	.0038
1.0	-.0014	-.0013	-.0012	-.0009	-.0006	-.0002	.0003	.0007	.0012	.0015	.0017	.0019	.0021

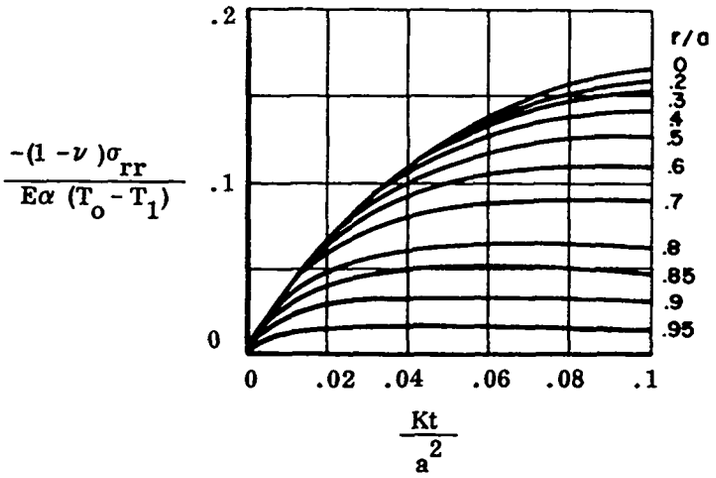


FIGURE 7.3.2.2-1 NONDIMENSIONAL RADIAL STRESS AS FUNCTION OF $\frac{Kt}{a^2}$ FOR THE CASE ah = 5

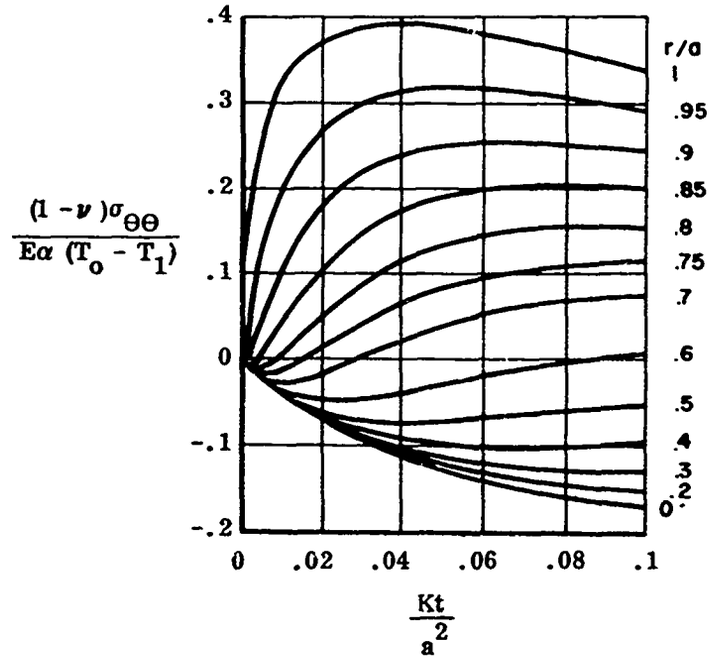


FIGURE 7.3.2.2-2 NONDIMENSIONAL TANGENTIAL STRESS AS FUNCTION OF $\frac{Kt}{a^2}$ FOR THE CASE ah = 5

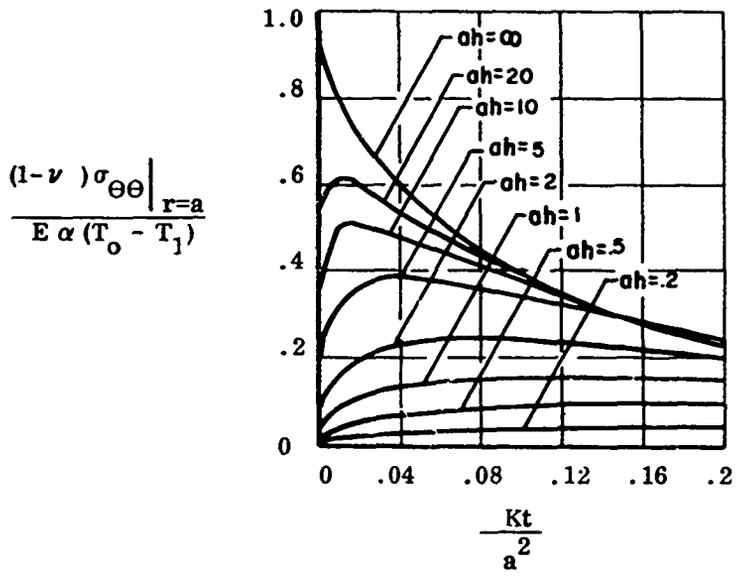


FIGURE 7.3.2.2-3 NONDIMENSIONAL SURFACES TANGENTIAL STRESS AS FUNCTION OF $\frac{Kt}{a^2}$ WITH ah AS A PARAMETER

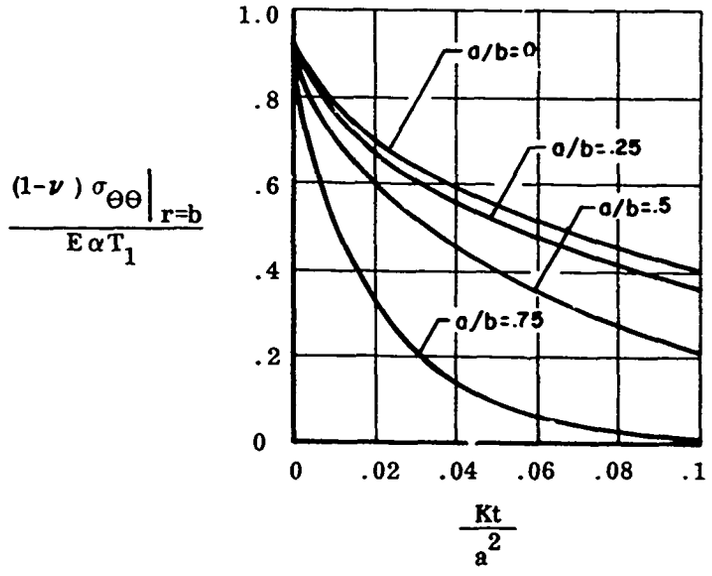


FIGURE 7.3.2.2-4 NONDIMENSIONAL SURFACES TANGENTIAL STRESS FOR A HOLLOW CYLINDER WITH OUTER SURFACES AT TEMPERATURE T_1 AND INNER SURFACE INSULATED

7.3.2.2 (Cont'd)

For hollow cylinders, the solution of the thermal stresses is more complicated than that of solid cylinders because of the additional (inner) boundary. A parametric study becomes very unwieldy. As an example, a particular case of a hollow cylinder will be considered in which the outer surface (r=b) is kept at an elevated temperature T_1 for $t > o$ and there is no loss of heat from the inner surface $\left.\frac{\partial T}{\partial r}\right|_{r=a} = 0$. Figure 7.3.2.2-4 presents the ordinate $\frac{(1-\nu)\sigma_{\theta\theta}\big]_{r=b}}{E\alpha T_1}$ against Kt/a^2 for values 0, 0.25, 0.5, and 0.75 of the ratio a/b. It appears that the values for the solid cylinder are reasonable approximations to those for the hollow cylinder only in the case of fairly thick-walled cylinders.

7.4 REFERENCES

7-1 Horvay, G., Thermal Stress Problems in Nuclear Reactors, Summer Session Course in Stress Analysis at the Massachusetts Institute of Technology, June 17-28, 1957.

7-2 Reissner, E., Stresses and Small Displacements of Shallow Spherical Shells II, Journal Mathematics and Physics, Volume 27, 1948, p 240.

7-3 Horvay, G., Linkous, C. and Born, J. S., Analysis of Short Thin Axisymmetrical Shells Under Axisymmetric Edge Loading, Journal Applied Mechanics, Volume 23, 1956, (a) p 68, (b) p 489.

7-4 Timoshenko, S. and Goodier, J. N., Theory of Elasticity, McGraw-Hill Book Company, Inc., New York.

7-5 Jaeger, J. C., On Thermal Stresses in Circular Cylinders, Philosophic Magazine, Volume 36, 1945, pp 418-428.

SECTION 8

STRUCTURAL ASSEMBLIES

SECTION 8

STRUCTURAL ASSEMBLIES

TABLE OF CONTENTS

Paragraph	Title	Page
8	Structural Assemblies	8.2
8.1	Shells of Revolution with Bulkheads	8.3
8.2	Determination of Interaction Forces and Moments	8.6
8.2.1	Solution for the Interior Bulkhead	8.7
8.2.2	Solution for External Bulkhead	8.8

SECTION 8 - STRUCTURAL ASSEMBLIES

The structural elements analyzed in this Manual are, in almost all cases, integral components of a complete structural assembly. The beams analyzed in Section 4, for example, are usually components of a larger frame or beam-like structure; the purely monocoque shells analyzed in Section 7 are components of a larger semimonocoque stiffened structure.

In all such cases the boundaries or edges of each structural subsystem are subject to the restraint of adjacent structure. Since the over-all structure is an integral assembly, the deflections at the boundaries of adjacent structural components must be compatible with each other. This section considers the mutual interaction of these components, thereby providing the tools necessary for the over-all structural analysis.

The following symbols are used throughout this section:

f	Influence coefficient
h	Thickness
r	Radial coordinate
D	Flexural rigidity = $\frac{Eh^3}{12(1-\nu^2)}$
E	Young's modulus
H	Interaction force per unit of length
M	Interaction moment per unit of length
P	Uniform normal pressure on bulkhead
α	Coefficient of linear thermal expansion
δ	Radial deflection
Θ	Rotation
ϕ	Angle between the normal to shell surface and axis of revolution
ΔT	Elevated temperature with respect to base

Subscripts

1, 2	Shells
B	Bulkhead
H, M	Due to edge interaction loads and moments, respectively.

8.1 SHELLS OF REVOLUTION WITH BULKHEADS

This sub-section considers the interaction of shells of revolution, under axisymmetric loading (mechanical and thermal), with transverse circular bulkheads lying perpendicular to the axis of revolution (Figure 8.1-1(a)).

For general shells of revolution, the analysis is approximate, giving reliable results within the limitations spelled out in Sub-sections 7.1 and 7.2. For cylindrical shells, the analysis is rigorous according to thin shell theory.

In order to determine the interaction stresses at the junction of shell and bulkhead components, the deflections and slopes at the unjoined shell and bulkhead edges are first determined (Figure 8.1-1(b)).

The deflections and slopes δ'_1, δ'_2 and Θ'_1, Θ'_2 at the unjoined shell edges, due to axisymmetric thermal and mechanical loads, can be determined by the methods of Section 7. The bulkhead is considered to be a circular plate (with or without a concentric hole). Its edge slope and deflection, Θ'_B and δ'_B, for radially symmetric transverse load may be determined from a plate bending analysis. Thus, as shown by Timoskenko,* for a uniformly loaded solid circular plate free to rotate at the outer edges (Figure 8.1-2),

$$\Theta'_B = \frac{Pr^3}{8D} \quad , \tag{1}$$

and $\delta'_B \sim 0$.

After the unjoined edge deflections have been determined as above, edge moments and loads are applied (Figure 8.1-1(c)), such that the radial deflections and changes in edge slopes of the shell components and the bulkhead are all equal, and the joint is in equilibrium. These conditions require that

$$\begin{aligned} \delta'_1 + \delta''_1 &= \delta'_B + \delta''_B = \delta'_2 + \delta''_2 \\ \Theta'_1 + \Theta''_1 &= \Theta'_B + \Theta''_B = \Theta'_2 + \Theta''_2 \quad , \end{aligned} \tag{2}$$

and

$$\begin{aligned} M_1 + M_B + M_2 &= 0 \\ H_1 + H_B + H_2 &= 0 \quad , \end{aligned} \tag{3}$$

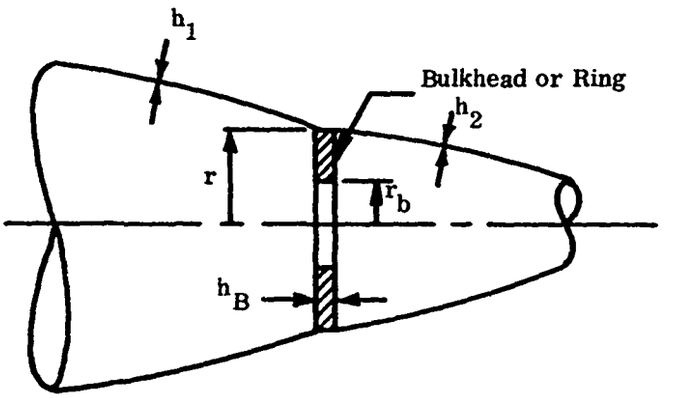
where the double primes refer to the effects of the edge interaction loads (M, H). However, the edge deflections and rotations due to the interaction loads can be written as

$$\begin{aligned} \delta''_1 &= f_{1H} H_1 + f_{1M} M_1 \\ \Theta''_1 &= f'_{1H} H_1 + f'_{1M} M_1 \\ \delta''_2 &= f_{2H} H_2 + f_{2M} M_2 \end{aligned} \tag{4}$$

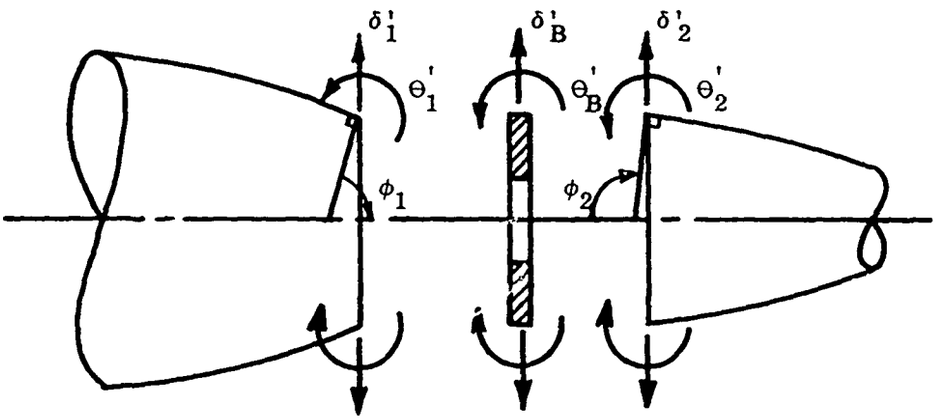
---

* Timoskenko, S., "Theory of Plates and Shells," McGraw-Hill Book Co., Inc.

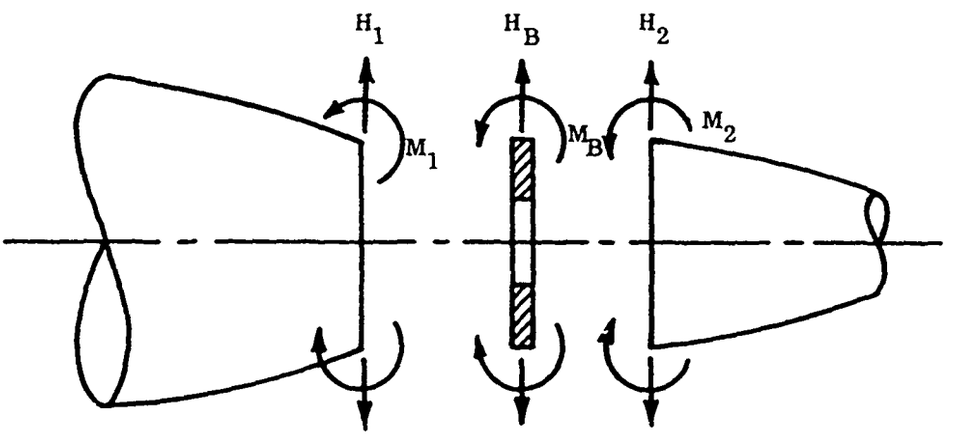
8.1 (Cont'd)



(a) Integral Shells and Bulkhead



(b) Deflections of Unjoined Shell and Bulkhead Edges



(c) Interaction Loads at Joined Shell and Bulkhead Edges

FIGURE 8.1-1 DEFLECTIONS, LOADS AND MOMENTS AT A SHELL AND BULKHEAD JUNCTION

8.1 (Cont'd)

$$\Theta''_2 = f'_{2H}\ H_2 + f'_{2M}\ M_2$$

$$\delta''_B = f_{BH} \cdot H_B \qquad (4)$$

$$\Theta''_B = f'_{BM} \cdot M_B \ , \qquad \text{cont'd}$$

where, from Paragraph 7.1.1, for $\nu = .30$

$$f_{1H} = \frac{2.571}{E} (\sin \phi_1)^{1/2} \left(\frac{r}{h_1}\right)^{3/2}$$

$$f_{1M} = f'_{1H} = 3.305 \frac{r}{Eh_1^2}$$

$$f'_{1M} = \frac{8.496}{Eh_1^3} \sqrt{\frac{rh_1}{\sin \phi_1}} \qquad (5)$$

$$f_{2H} = \frac{2.571}{E} (\sin \phi_2)^{1/2} \left(\frac{r}{h_2}\right)^{3/2}$$

$$f_{2M} = f'_{2H} = - 3.305 \frac{r}{Eh_2^2}$$

$$f'_{2M} = \frac{8.496}{Eh_2^3} \sqrt{\frac{rh_2}{\sin \phi_2}} \ ,$$

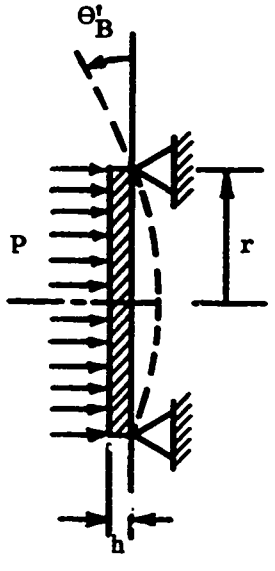


FIGURE 8.1-2 EDGE ROTATION OF SOLID CIRCULAR BULKHEAD DUE TO UNIFORM PRESSURE LOADING

8.1 (Cont'd)

and from Timoshenko* and Figure 8.1-1(a),

$$f_{BH} = \left[\frac{r^2 + r_b^2}{r^2 - r_b^2} - .30\right] \frac{r}{Eh_B}$$

$$f'_{BM} = \left[\frac{r^2 + r_b^2}{r^2 - r_b^2}\right] - .30\Bigg] \frac{12r}{Eh_B^3} \qquad (6)$$

Inserting Eqs. (4) into (2) and (3) and combining equations, results in

$$\begin{aligned}
(f_{1H} + f_{BH})\, H_1 &+ (f_{BH})\, H_2 &+ (f_{1M})\, M_1 &+ 0 &= (\delta'_B - \delta'_1) \\
(f_{BH})\, H_1 &+ (f_{2H} + f_{BH})\, H_2 &+ 0 &+ (f_{2M})\, M_2 &= (\delta'_B - \delta'_2) \\
(f'_{1H})\, H_1 &+ 0 &+ (f'_{1M} + f'_{BM})\, M_1 &+ (f'_{BM})\, M_2 &= (\Theta'_B - \Theta'_1) \\
0 &+ (f'_{2H})\, H_2 &+ (f'_{BM})\, M_1 &+ (f'_{2M} + f'_{BM})\, M_2 &= (\Theta'_B - \Theta'_2)
\end{aligned} \qquad (7)$$

and

$$\begin{aligned}
M_B &= -(M_1 + M_2) \\
H_B &= -(H_1 + H_2) \ .
\end{aligned} \qquad (8)$$

Thus, once the deflections and slopes at the unjoined shell and bulkhead edges (corresponding to the right side of Eqs. (7)) are determined, (7) and (8) provide six algebraic simultaneous equations for the determination of the three interaction forces (H_1, H_2, H_B) and moments (M_1, M_2, M_B).

8.2 DETERMINATION OF INTERACTION FORCES AND MOMENTS

The long cylinder shown in Figure 8.2-1 is heated to a uniform temperature of ΔT, while the bulkheads remain unheated ($\Delta T_B = 0$). Find the restraining forces at the interior and end bulkheads.

---

* Timoshenko, S., "Theory of Plates and Shells," McGraw-Hill Book Co., Inc.

8.2 (Cont'd)

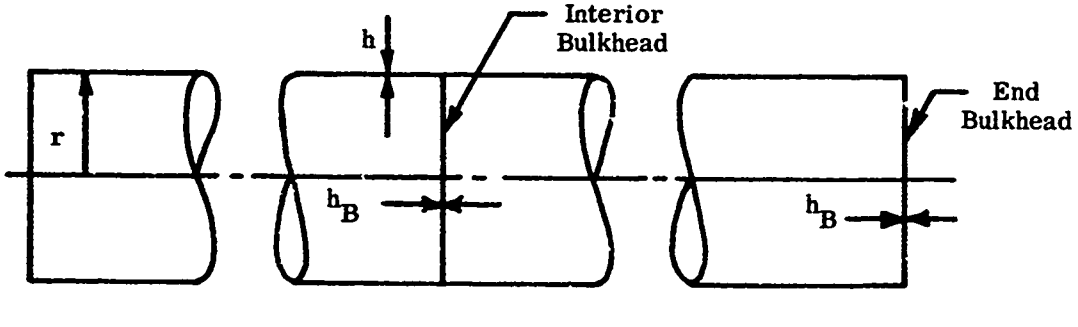


FIGURE 8.2-1 LONG CYLINDER WITH INTERIOR AND END BULKHEADS

8.2.1 Solution for the Interior Bulkhead (Figure 8.2.1-1)

The free expansions due to the uniform temperature elevation are

$$\delta_1' = \delta_2' = r\alpha\Delta T$$

$$\delta_B' = \Theta_1' = \Theta_2' = \Theta_B' = 0 \quad .$$

Also from the symmetry of the problem

$$M_1 = -M_2 = M$$

$$M_B = 0$$

$$H_1 = H_2 = -H_B/2 = H \quad .$$

Substituting the above in Eqs. (7) of Paragraph 8.1 yields the independent equations

$$(f_{1H} + 2f_{BH})\, H + (f_{1M})\, M = -r\alpha\Delta T$$

$$(f'_{1H})\, H + (f'_{1M})\, M = 0$$

Solving the above equations results in

8.2.1 (Cont'd)

$$H = \frac{-r\alpha\Delta T}{\left[f_{1H} + 2f_{BH} - f'_{1H}\frac{f_{1M}}{f'_{1M}}\right]} \quad ,$$

and

$$M = \frac{-f'_{1H}}{f'_{1M}} H \quad ,$$

where the influence coefficients f, f' are determined from Eqs. (5) and (6) of Paragraph 8.1.

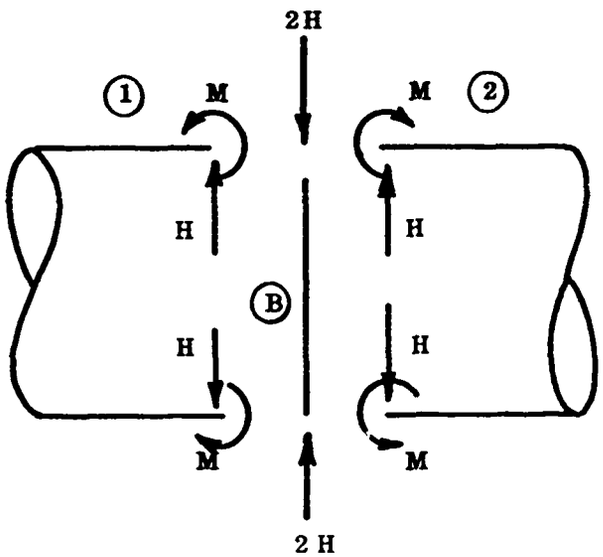


FIGURE 8.2.1-1 INTERIOR BULKHEAD

8.2.2 Solution for the External Bulkhead (Figure 8.2.2-1)

As in the case of the interior bulkhead,

$$\delta'_1 = r\alpha\Delta T$$
$$\delta'_B = \Theta'_1 = \Theta'_B = 0 \quad .$$

Also, for equilibrium of the joint (Eqs. (8) of Paragraph 8.1)

$$M_1 = -M_B = M$$
$$H_1 = -H_B = H \quad .$$

Substituting the above in Eqs. (7) of Paragraph 8.1 yields the independent equations

8.2.2 (Cont'd)

$$(f_{1H} + f_{BH})\ H + (f_{1M})\ M = -r\alpha\Delta T$$

$$(f'_{1H})\ H + (f'_{1M} \div f'_{BM})\ M = 0 \quad ,$$

from which

$$H = \frac{-r\alpha\Delta T}{\left[(f_{1H} + f_{BH}) - \dfrac{f_{1M} f'_{1H}}{(f'_{1M} + f'_{BM})}\right]} \quad ,$$

and

$$M = \frac{-f'_{1H}}{(f'_{1M} + f'_{BM})}\ H \quad .$$

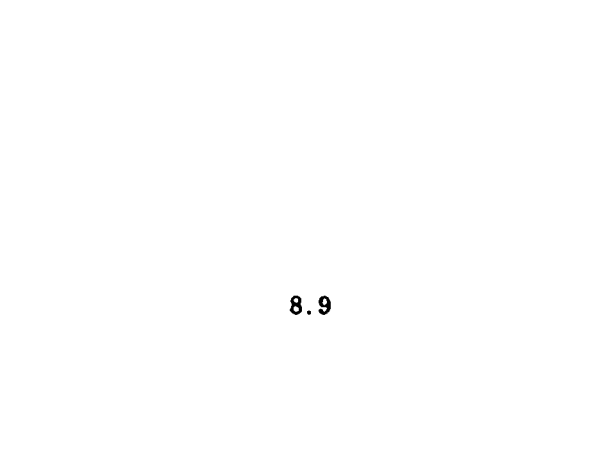


FIGURE 8.2.2-1 EXTERNAL BULKHEAD

SECTION 9

STABILITY OF STRUCTURES

SECTION 9

STABILITY OF STRUCTURES

TABLE OF CONTENTS

Paragraph	Title	Page
9	Stability of Structures	9.2
9.1	Stability Criteria	9.4
9.1.1	Stability by Eigenvectors	9.7
9.1.1.1	Euler Equilibrium Equation	9.7
9.1.1.2	Buckling Load	9.11
9.1.2	Stability by Virtual Work	9.14
9.1.3	Properties of Eigenvectors (Deflection Modes) and Eigenvalues (Critical Loads)	9.15
9.1.4	Approximate Methods of Determining Stability	9.18
9.1.4.1	Single Functions	9.18
9.1.4.1.1	Upper Bound	9.18
9.1.4.1.2	Lower Bound	9.19
9.1.4.2	Multiple Functions	9.22
9.1.5	Shear Energies	9.26
9.1.6	Plasticity and Eccentricity	9.29
9.1.7	Temperature	9.31
9.2	Non-Dimensional Buckling Curves	9.32
9.2.1	Non-Dimensional Stability	9.32
9.3	Curved Plates and Shells	9.48
9.4	References	9.50

SECTION 9 - STABILITY OF STRUCTURES

The solution of the structural problem requires the determination of the displacement due to a given loading. As the magnitude of compressive loading is increased a limiting value is approached at which a small lateral force will produce considerable lateral deflection. This limiting value is called a critical (buckling) load at which the structure becomes metastable. This section is concerned with a discussion of the criteria of stability and the characteristic deformation modes of structures (eigenvectors). Methods to calculate the buckling load from the eigenvectors or to approximate the buckling load by determining upper and lower bounds are presented. The effect of neglecting various flexibilities is discussed and formulations are presented. The effects of eccentricity, plasticity and temperature are discussed qualitatively. Non-dimensional buckling curves and examples which include the effects of uniform temperature and creep are also presented.

The following symbols are used throughout this section:

a_i	Coefficients of eigenvectors defining the lateral deflection
b	Length of half wave of buckle (length of pin-connected column, width of plate)
e	Distance from shear center to line of action of transverse shear V.
f	Deflection pattern or eigenvector; Average thickness of sandwich faces
h	Thickness of plate; Centroidal thickness of sandwich plate
h_c	Thickness of sandwich core
k	Stability constant
l	Length of column
m	Virtual internal moment due to a unit virtual force
q	Lateral load intensity
r	Distance from shear center
t	Thickness of plate; Time
u	Displacement
u_i	Eigenvector
w	Lateral displacement
w_0	Maximum lateral displacement; Initial approximation of lateral displacement
$w_{,j}$	Slope in j direction
$w_{,ij}$	Change of slope (negative of curvature)
x, y, z	Distances along coordinate axes
A	Area; Linear operator
A_V	Effective transverse shear area
C	Constant coefficient
D	Stiffness of isotropic plate
D_{ij}	Stiffness associated with the moment M_{ij}
E_A	Initial (Young's) modulus
E_R	Effective stability modulus
E_S	Secant modulus $= \frac{\epsilon - \alpha T}{\sigma}$
E_T	Tangent modulus $= d\epsilon / d\sigma$

F	Generalized force or buckling load
F_{cr}	Buckling load
F_M	Buckling load considering bending energy only
F_V	Buckling load considering transverse shear energy only
F_Q	Buckling load considering torsional energy only
G_S	Secant shear modulus
G_c	Shear modulus of core
I	Moment of inertia of cross section
K	Non-dimensional stability constant
L	Potential energy
L^*	Complementary energy
M_{ij}	Moment on i^{th} plane in the $\bar{j} \times \bar{z}$ direction
N_{ij}	Load on i^{th} plane and in j^{th} direction
Q	Torque acting on cross section
T	Temperature
δU	Change in strain energy due to a virtual displacement
δU^*	Change in complementary strain energy due to a virtual force
V	Transverse shear load on cross section; Volume
δW	Change in potential energy of external loads due to a virtual displacement
δW^*	Change in potential energy of external displacements due to a virtual force
$A_V G$	Transverse shear stiffness of cross section = $\int E_S dA_V$
$\overline{EI}$	Bending stiffness of cross section = $\int E_S y^2 dA$
$\overline{EA}$	Axial stiffness of cross section = $\int E_S dA$
$\overline{JG}$	Torsional stiffness of cross section = $\int G_S r^2 dA$
α	Coefficient of linear thermal expansion
δ_{ij}	Kronecker delta = 1 if $i = j$ = 0 if $i \neq j$
ϵ	Strain
ϵ_{ij}	Strain component associated with stress component σ_{ij}
ϵ_σ	Strain due to stresses
η	Ratio of bending stiffness
κ	Curvature - rate of change of slope
λ_i	Eigenvalue associated with eigenvector u_i and buckling load F_i
μ	Constant - Lagrangian multiplier
ν	Poisson's ratio
ρ	Radius of gyration of cross section = $\sqrt{\frac{\overline{EI}}{\overline{EA}}}$
σ	Stress
σ_{ij}	Stress on i^{th} plane in j^{th} direction
τ	Shear stress
cr	Subscript denoting critical value

9.1 STABILITY CRITERIA

A structure will deform under given loading and boundary conditions in such a manner as to make the potential energy stationary. As the load is increased, the structure deforms more and more into one of its characteristic buckling patterns. The buckling pattern for which the strain energy is a minimum for given boundary displacements is called the lowest eigenvector of the structure and corresponds to the lowest buckling load (or eigenvalue). More generally, the eigenvectors are those deformation patterns for which the potential energy is stationary with respect to an arbitrary virtual displacement. Consequently, the eigenvectors also satisfy the Euler Equilibrium Equation. This equation is obtained by a calculus of variation procedure which makes the potential energy stationary.

Any initial eccentricities of the structure can be expressed as the sum of eigenvectors. As the load is applied and increased, the magnitudes of the eigenvectors (which define the displacement of the structure) will increase. The percentage increase (of the order of $\frac{1}{1-F/F_i}$) is greatest for the smallest eigenvector (corresponding to the smallest characteristic load $F_i = F_1$) and becomes exceedingly large as $F \rightarrow F_1$. Thus the structure will tend to buckle in the lowest eigenvector mode no matter what initial eccentricities exist. (The eccentricity can even be in the form of a small lateral disturbance to a straight column.)

It is possible to investigate the stability of a structure by examining the change in the potential energy ($\delta L = \delta U - \delta W$), defined in Paragraph 1.7.2.1, due to an arbitrary virtual displacement which satisfies restraining displacement boundary conditions.

Consider an eccentric column (Figure 9.1-1(a)) which is in stable equilibrium under the force and displacement systems F_1, u_1. For an arbitrary virtual displacement δu_i, the reciprocal theorem (Paragraph 1.7.1) yields

$$\delta L = 0 \ . \tag{1a}$$

Further, since the column is in a state of stable equilibrium, then according to the minimum potential energy theorem (Paragraph 1.7.2.3),

$$\delta^2 L > 0 \ . \tag{1b}$$

When the load on the column becomes equal to the so-called buckling load F_{cr} (Figure 9.1-1(b)), the column deflections can vary over a wide range with only small variations of this load. To all intents and purposes, the deflections u_2 are arbitrary and the column is considered to be in a state of metastable equilibrium, for which

$$\delta L = \delta^2 L = 0 \ . \tag{1c}$$

Another form of metastable equilibrium, involving the complementary potential, occurs if a stop is placed under one end of the column (Figure 9.1-1(c). In this case, additional load is absorbed by the stop, and the forces F_3 for a given deflection u_3 are abitrary, with the result that

$$\delta L^* = \delta^2 L^* = 0 \ . \tag{1d}$$

If the column is initially straight (actually, this can never be achieved) and a load F_4, greater

9.1 (Cont'd)

than F_{cr} is applied (Figure 9.1-1(d)), a small lateral displacement δu_4 will cause the column to buckle. The straight column, in this case, is considered to be in a state of unstable equilibrium, for which

$$\begin{aligned} &\delta L = 0 \\ &\delta^2 L < 0 \ . \end{aligned} \tag{1e}$$

The criteria of stability are summarized below,

$$\text{Stable Equilibrium} \quad \begin{cases} \delta L = 0; \ \delta^2 L > 0 & (2) \\ \delta L^* = 0; \ \delta^2 L^* > 0 & (3) \end{cases}$$

Metastable Equilibrium:

(a) Arbitrary Displacement $\quad \delta L = \delta^2 L = 0 \qquad (4)$

(b) Arbitrary Forces $\quad \delta L^* = \delta^2 L^* = 0 \qquad (5)$

Unstable Equilibrium - Deflections $\quad \delta L = 0; \ \delta^2 L < 0 \ , \qquad (6)$

where δL, $\delta^2 L$ are variations due to virtual displacements δu, and δL^*, $\delta^2 L^*$ are variations due to virtual forces (or stresses) δF.

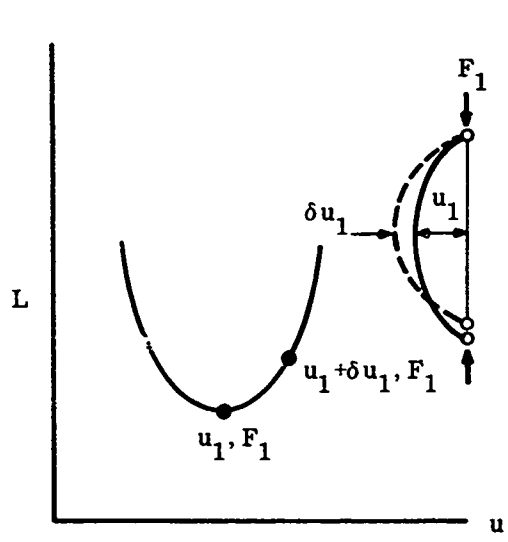
Employing Eq. (4) will result in the solution for the buckling load provided u is the eigenvector. If u is not the eigenvector, then employing Eq. (4) results in a buckling load for a stiffer structure (δU expressed in terms of displacements) which is higher than the buckling load of the actual structure. Employing Eq. (5) results in a displacement for a more flexible structure (δU^* expressed in terms of the forces) which can be utilized to obtain a buckling load lower than that of the actual structure.

The first variation (δL) can be viewed as the difference in potential energy between a system defined by the true forces and displacements and a system defined by the true forces but assumed displacement (which is the true one modified by a virtual displacement). The variation (δL) is zero (and the potential is stationary) when the assumed displacement happens to be the true displacement. The second variation ($\delta^2 L$) can similarly be envisioned as the change in potential for the system of the true loads and the assumed displacements when subjected to a similar virtual displacement. Thus the stability of a structure can be investigated by assuming a deflection pattern and evaluating the change in potential of such a system when subjected to a virtual displacement having the same pattern as the assumed displacement. In such a case, this change in potential energy δL is in effect a second variation upon the true potential energy. Similar arguments can be applied to the complementary potential (L^*).

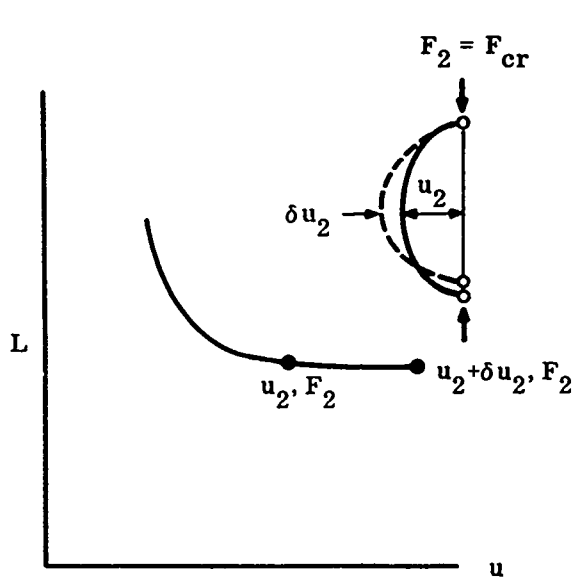
The conditions for metastable equilibrium as defined by Eqs. (4) and (5) can be redefined as

$$\delta U = \delta W \tag{7}$$
$$\delta U^* = \delta W^* \ , \tag{8}$$

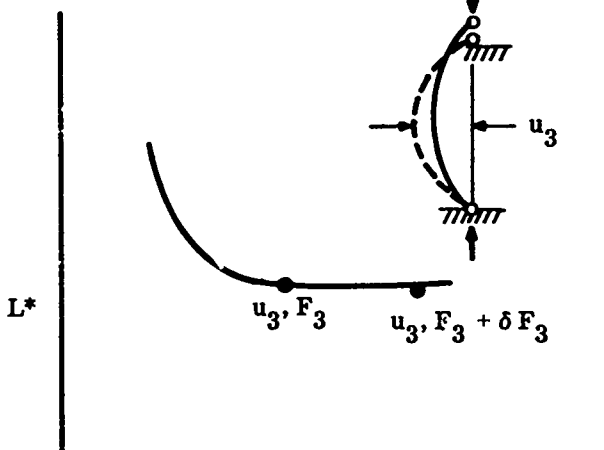
where δU is in terms of the assumed strain pattern and δU^* is in terms of the assumed stress pattern.



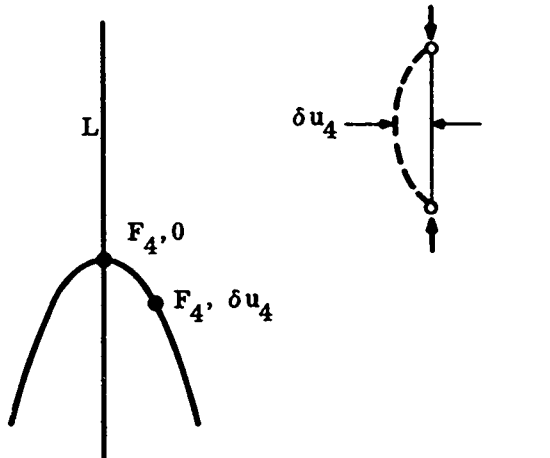
(a) Stable Equilibrium $\begin{Bmatrix} \delta L = 0 \\ \delta^2 L > 0 \end{Bmatrix}$



(b) Metastable Equilibrium-Undefined Displacements $\{\delta L = \delta^2 L = 0\}$



(c) Metastable Equilibrium - Undefined Forces $\{\delta L^* = \delta^2 L^* = 0\}$



(d) Unstable Equilibrium-Straight Column $\begin{Bmatrix} \delta L = 0 \\ \delta^2 L < 0 \end{Bmatrix}$

FIGURE 9.1-1 STABILITY OF COLUMNS

9.1.1 Stability By Eigenvectors

The Euler Equilibrium Equation, which expresses the internal equilibrium of the structure in terms of the displacements, is obtained by determining the condition that the displacements must satisfy in order to make the potential energy stationary. The method of obtaining the Euler Equation is shown in Paragraph 9.1.1.1. The solutions to these equations are the possible deflection modes of the structure and are called eigenvectors.

The solution of the Euler Equilibrium Equation for the eigenvectors "u_i" contains an eigenvalue "λ_i" which is a function of the buckling load. Techniques for obtaining the buckling load are shown in Paragraph 9.1.1.2. The buckling load depends upon the boundary conditions (types of supports, aspect ratio) and the loading conditions. The exact solution for the eigenvalues can only be obtained in a limited number of cases in which the exact solution of the Euler Equilibrium Equation can be obtained. Solutions for rectangular plates with various types of boundary conditions and loadings are shown in Figures 2 and 14 to 26 of Reference 9-1. These solutions as well as solutions for other geometries and loadings can be found throughout the literature; for example References 9-2 and 9-3. This information should be utilized in a manner described in Sub-section 9.2 to determine the buckling stress.

In general the solutions are quite complex, and approximate methods are attempted which place upper and lower bounds upon the buckling load. Properties of the eigenvectors and the eigenvalues are described in Paragraph 9.1.3. Some approximate methods and the effects of these approximations will be discussed in Paragraph 9.1.4 These methods utilize the energy principles discussed previously.

9.1.1.1 Euler Equilibrium Equation

The method for obtaining the equilibrium equation for a rectangular plate, with transverse shear energy neglected, is indicated in the following. The potential is minimized by a function defined by the equilibrium equation. Symbols are defined below and in Figure 9.1.1.1-1.

σ_{ij}	Stress component acting on i^{th} plane (plane perpendicular to i^{th} direction) and acting in j direction
σ_{xx}	Normal stress on x plane acting in x direction
σ_{xy}	Shear stress on x plane acting in y direction
ϵ_{ij}	Strain component associated with stress component σ_{ij}
N_{ij}	Load per unit of length acting on i^{th} plane and in j^{th} direction
N_{xx}	Normal load per unit of length on x plane and in x direction
N_{xy}	Shear load per unit of length on x plane and in y direction
w	Deflection in z direction
q	Lateral load per unit of area in z direction
M_{ij}	Moment per unit of length action on i^{th} plane in the $\bar{j} \times \bar{z}$ direction
M_{xx}	Moment per unit of length acting on x plane and in $\bar{x} \times \bar{z} = -\bar{y}$ direction, causes rotation (bending) about the y axis
M_{xy}	Moment per unit of length acting on x plane and in $\bar{y} \times \bar{z} = \bar{x}$ direction; causes rotation (twist) about the x axis
$w_{,ij}$	Negative of curvature = $\frac{\partial^2 w}{\partial i \, \partial j}$

9.1.1.1 (Cont'd)

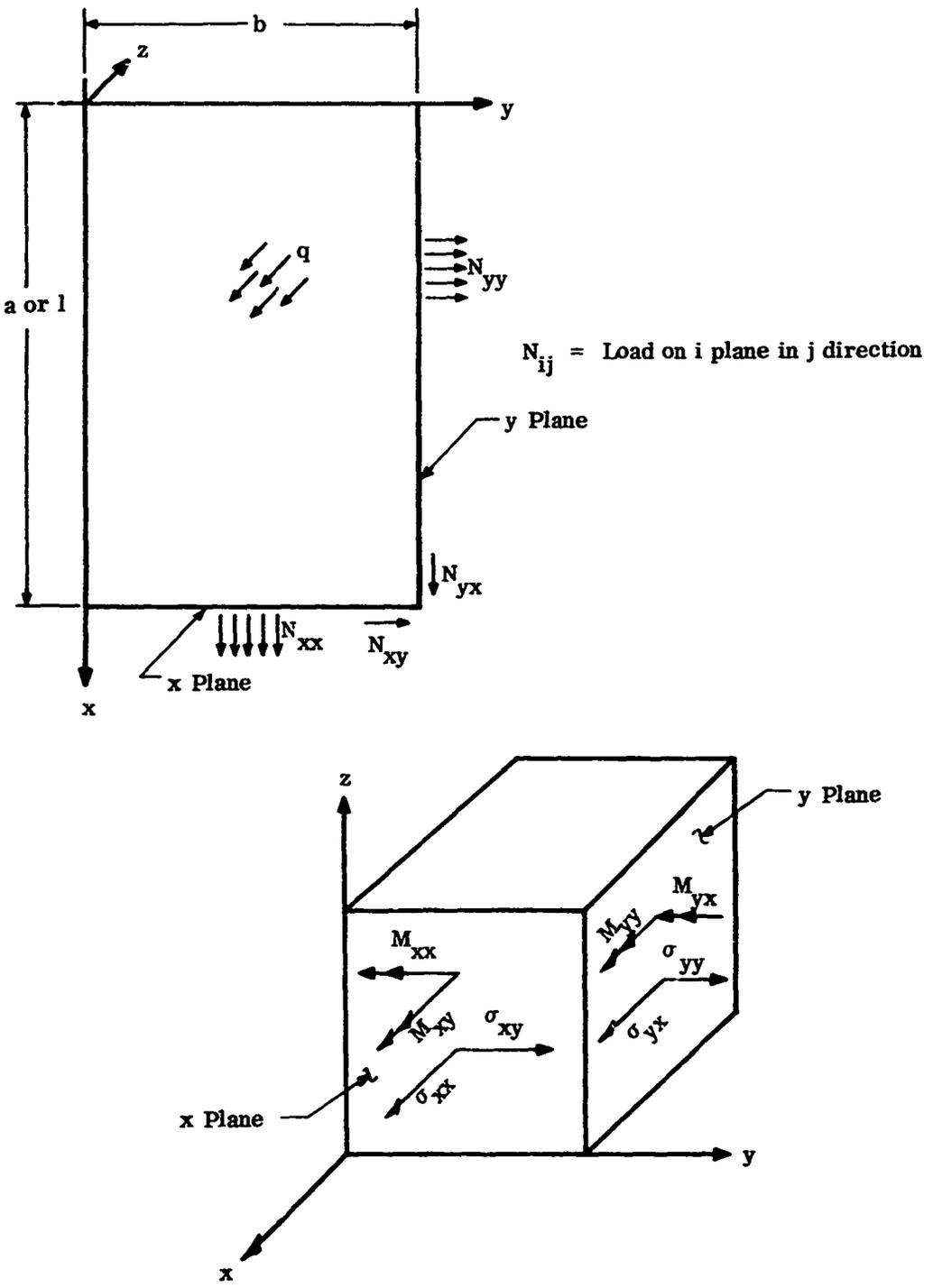


FIGURE 9.1.1.1-1 LOADS ON PLATE

9.1.1.1 (Cont'd)

D_{ij} Stiffness associated with the moment M_{ij} and curvature $w_{,ij}$

$$D_{xx} = \frac{M_{xx}}{w_{,xx} + \nu w_{,yy}}$$

$$D_{yy} = \frac{M_{yy}}{w_{,yy} + \nu w_{,xx}}$$

$$D_{xy} = \frac{M_{xy}}{(1-\nu) w_{,xy}}$$

For isotropic plate

$$D_{xx} = D_{yy} = D_{xy} = D = \int \frac{E_S}{1-\nu^2} z^2 dz$$

ν Poisson's ratio
E_S Secant modulus

The potential is defined for non-linear elastic material in order to obtain a more general equilibrium equation:

$$L = U - W = \int_V \int_0^{\epsilon_{ij}} \sigma_{ij} \, d\epsilon_{ij} \, dV - \sum F_i u_i \tag{1a}$$

$$L = \int \left\{ \int_0^{w_{,ij}} M_{ij} \, d(w_{,ij}) + \frac{1}{2} N_{ij} w_{,i} w_{,j} - q w \right\} dx dy, \tag{1b}$$

or

$$L = \int \left\{ \int_0^{w_{,xx}} D_{xx}(w_{,xx} + \nu w_{,yy}) \, d(w_{,xx}) + 2 \int_0^{w_{,xy}} D_{xy} (1-\nu) w_{,xy} \, dw_{,xy} \right.$$

$$+ \int_0^{w_{,yy}} D_{yy} (w_{,yy} + \nu w_{,xx}) \, d(w_{,yy}) + \frac{1}{2} N_{xx} w_{,x}^2 \tag{1c}$$

$$\left. + N_{xy} w_{,x} w_{,y} + \frac{1}{2} N_{yy} w_{,y}^2 - q w \right\} dx dy.$$

From the calculus of variations, if

$L = \int \phi \, dx dy$ is stationary, then

$$\left[\phi\right]_w = 0 = \frac{\partial \phi}{\partial w} - \frac{\partial}{\partial x}\left(\frac{\partial \phi}{\partial w_{,x}}\right) - \frac{\partial}{\partial y}\left(\frac{\partial \phi}{\partial w_{,y}}\right) + \frac{\partial^2}{\partial x^2}\left(\frac{\partial \phi}{\partial w_{,xx}}\right) + \tag{2}$$

9.1.1.1 (Cont'd)

$$+ \frac{\partial^2}{\partial x \partial y} \left(\frac{\partial \phi}{\partial w_{,xy}} \right) + \frac{\partial^2}{\partial y^2} \left(\frac{\partial \phi}{\partial w_{,yy}} \right) \cdots + (-1)^n \frac{\partial^n}{\partial x^n} \frac{\partial \phi}{\partial w_{,xx\ldots x}} \cdot \qquad (2)$$

Cont'd

Therefore,

$$0 = -q - (N_{xx} w_{,x})_{,x} - (N_{xy} w_{,y})_{,x} - (N_{xy} w_{,x})_{,y} - (N_{yy} w_{,y})_{,y} + \left[D_{xx} (w_{,xx} + \nu w_{,yy}) \right]_{,xx} + \left[2(1-\nu) D_{xy} w_{,xy} \right]_{,xy} + \left[D_{yy} (w_{,yy} + \nu w_{,xx}) \right]_{,yy} \cdot \qquad (3a)$$

Let

I = $-q$ = lateral load

II = $-(N_{xx} w_{,x})_{,x} - (N_{xy} w_{,y})_{,x} - (N_{xy} w_{,y})_{,y} - (N_{yy} w_{,y})_{,y}$

= lateral contribution of in-plane loads when plate deforms (first derivative of shear),

where

IIa = $-N_{xx} w_{,xx} - 2 N_{xy} w_{,xy} - N_{yy} w_{,yy}$

= contribution for non-changing in-plane loads

IIb = $-w_{,x} (N_{xx,x} + N_{xy,y}) - w_{,y} (N_{yy,y} + N_{xy,x})$

= contribution for changing in-plane loads

III = $M_{xx,xx} + 2M_{xy,xy} + M_{yy,yy}$

= effects of lateral contribution of moment (second derivative of moment),

where

IIIa = $D_{xx} w_{,xxxx} + 2D_{xy} w_{,xxyy} + D_{yy} w_{,yy}$

= moment effects for isotropic plate

IIIb = $\nu w_{,xxyy} \left[D_{xx} - 2D_{xy} + D_{yy} \right]$

= effects due to ν (zero for isotropic plate)

IIIc = $\left[2D_{xx,x} w_{,xxx} + D_{xy,y} w_{,xyx} + D_{xy,x} w_{,xyy} + 2D_{yy,y} w_{,yyy} \right]$

= effects of changes in stiffness and curvature

IIId = $\left[D_{xx,x} w_{,yyx} - D_{xy,y} w_{,xyx} - D_{xy,x} w_{,xyy} + D_{yy,y} w_{,xxy} \right] 2\nu$

= effects of ν for changes in stiffness and curvature

9.1.1.1 (Cont'd)

$$\text{IIIe} = \left[D_{xx,xx} w_{,xx} + 2D_{xy,xy} w_{,xy} + D_{yy,yy} w_{,yy} \right]$$

= effects due to change in stiffness

$$\text{IIIf} = \nu \left[D_{xx,xx} w_{,yy} - 2D_{xy,xy} w_{,xy} + D_{yy,yy} w_{,xx} \right]$$

= effects due to ν for changes in stiffness.

Then

$$0 = \text{I} + \text{II} + \text{III} \tag{3b,}$$

$$0 = \text{I} + \text{IIa} + \text{IIb} + \text{IIIa} + \text{IIIb} + \text{IIIc} + \text{IIId} + \text{IIIe} + \text{IIIf}. \tag{3c}$$

The linear elastic isotropic plate with constant loads results in the simple form

$$0 = \text{I} + \text{IIa} + \text{IIIa} \tag{4a}$$

$$0 = -q - N_{xx} w_{,xx} - 2N_{xy} w_{,xy} - N_{yy} w_{,yy} + D\nabla^4 w, \tag{4b}$$

where

$$\nabla^4 w = w_{,xxxx} + 2w_{,xxyy} + w_{,yyyy} ,$$

$$D = \frac{Eh^3}{12(1-\nu^2)}.$$

The problem of a non-linear anisotropic plate results in an exceedingly complex equation with non-linear coefficients and recourse must be made to approximate procedures.

9.1.1.2 Buckling Load

The buckling load of a structure can be found by determining the eigenvalue which permits non-trivial solutions to the Euler Equilibrium Equation. The lowest load which satisfies an eigenvalue is the buckling load of the structure.

The technique is illustrated for a pin-ended column of constant stiffness. More complex illustrations can be found in various texts, including References 9-2, 9-3, and 9-4.

Example: Simply supported column of constant stiffness (neglecting shear energy)

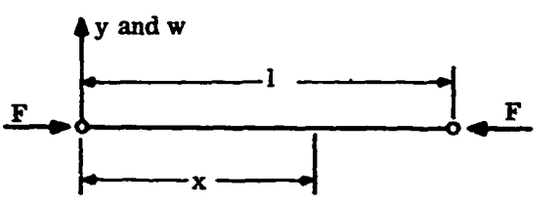


FIGURE 9.1.1.2-1 PIN-ENDED COLUMN

9.1.1.2 (Cont'd)

Equation (4b) of Paragraph 9.1.1.1 is used where D = EI, $-N_{xx} = F$ & $q = N_{xy} = N_{yy} = 0$ and deflection w is independent of y.

The Euler Equilibrium Equation becomes

$$EI \frac{d^4 w}{dx^4} + F \frac{d^2 w}{dx^2} = 0 , \tag{1a}$$

or

$$\frac{d^4 w}{dx^4} + \lambda \frac{d^2 w}{dx^2} = 0. \tag{1b}$$

where

$$\lambda = \frac{F}{EI} \tag{1c}$$

General Solution:

$$w = (C_1 + C_2 x) + C_3 \cos\sqrt{\lambda}\, x + C_4 \sin\sqrt{\lambda}\, x \tag{2}$$

Boundary Conditions (Simple Supports):

$$w(0) = w(l) = 0$$

$$\frac{d^2 w(0)}{dx^2} = \frac{d^2 w(l)}{dx^2} = 0$$

$\therefore C_1 = C_2 = C_3 = 0$ and $\sqrt{\lambda} = n\pi/l$ (n is an integer)

$$\therefore \sqrt{\lambda_n} = \sqrt{\frac{F_n}{EI}} = \frac{n\pi}{l}$$

for a non-trivial solution.

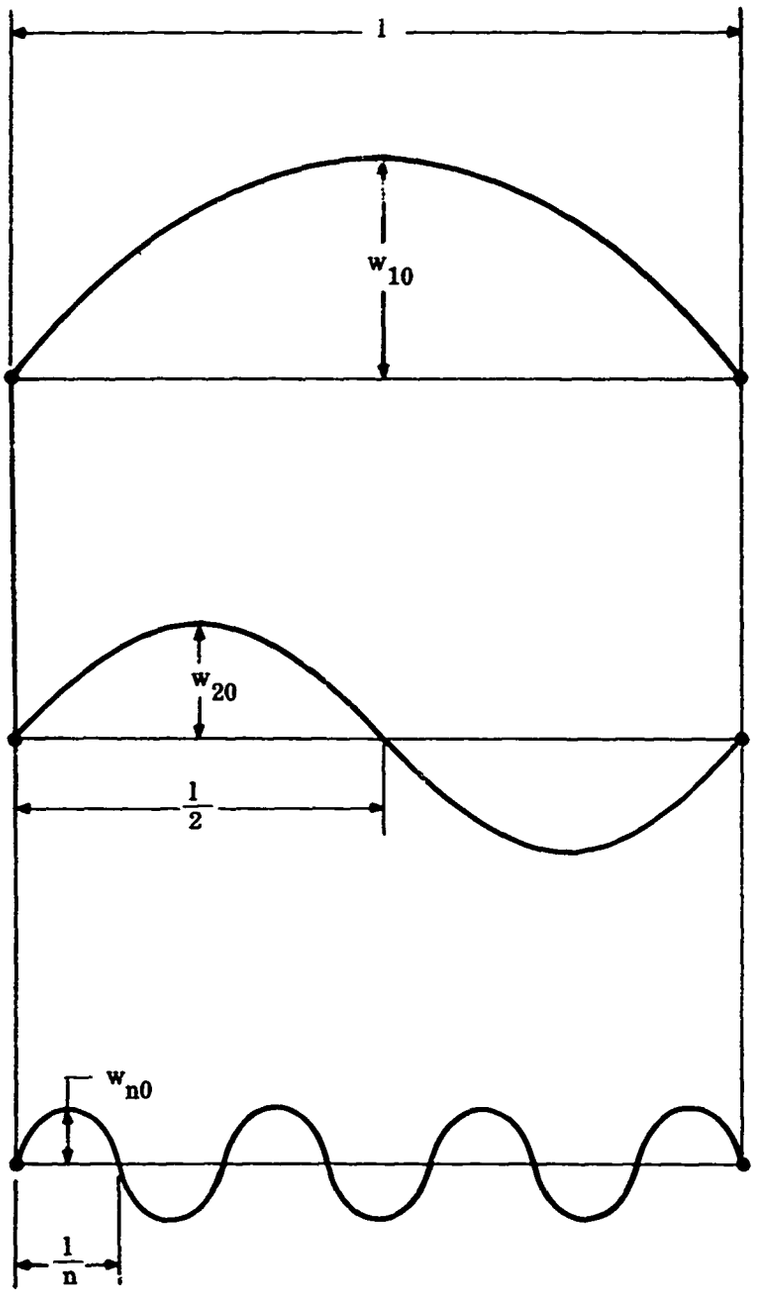
$$\therefore \lambda_n = \frac{F_n}{EI} = \frac{n^2\pi^2}{l^2} \text{ (Eigenvalue)} \tag{3}$$

$$F_n = n^2 \frac{\pi^2 EI}{l^2} \quad \text{(Critical Loads)} \tag{4a}$$

$$F_1 = \frac{\pi^2 EI}{l^2} = \text{Buckling Load} = \text{Lowest Critical Load} \tag{4b}$$

Successive eigenvectors and corresponding critical loads are listed in Figure 9.1.1.2-2. Note that the deflection amplitudes w_{10} --- w_{n0} are undetermined.

9.1.1.2 (Cont'd)



$$w_1 = w_{10} \sin\sqrt{\lambda_1}\, x$$

$$F_1 = \frac{\pi^2 EI}{l^2}$$

$$w_2 = w_{20} \sin\sqrt{\lambda_2}\, x$$

$$F_2 = \frac{4\pi^2 EI}{l^2}$$

$$w_n = w_{n0} \sin\sqrt{\lambda_n}\, x$$

$$F_n = \frac{n^2 \pi^2 EI}{l^2}$$

FIGURE 9.1.1.2-2 EIGENVECTORS AND EIGENVALUES OF COLUMN

9.1.2 Stability by Virtual Work

It has been shown that when the structure buckles, it buckles in the eigenvector shape. For this situation, changes in virtual strain energy (δU) are equal to the changes in virtual work (δW). The principle is again illustrated for this column:

$$\delta U = \int_V \sigma_{ij}\, \delta\, (\epsilon_{ij})\, dV = \int_0^1 -M \delta \kappa \; dx = \int_0^1 EI \; \frac{d^2w}{dx^2} \; \delta \; \frac{d^2w}{dx^2} \; dx \tag{1}$$

$$\delta W = F\, \delta\, u = F\delta \left[1 - \int_0^1 \left(1 - \left(\frac{dw}{dx} \right)^2 \right)^{\frac{1}{2}} dx \right] \tag{2a}$$

$$\delta W = F\, \delta \int_0^1 \frac{1}{2} \left(\frac{dw}{dx} \right)^2 dx = F \int_0^1 \frac{dw}{dx} \; \delta \left(\frac{dw}{dx} \right) dx \; . \tag{2b}$$

$$\therefore \int_0^1 EI \; \frac{d^2w}{dx^2} \; \delta \; \frac{d^2w}{dx^2} \; dx = F \int_0^1 \frac{dw}{dx} \; \delta \; \frac{dw}{dx} \; dx \; . \tag{3a}$$

Let

$$w = w_0 f; \; \delta w = \delta w_0 f$$

where

w_0 = maximum deflection

and

f = eigenvector of the structure.

Then

$$w_0 \delta w_0 \int_0^1 EI \; f_{,xx}^2 \; dx = F\, w_0 \delta w_0 \int_0^1 f_{,x}^2 \; dx \tag{3b}$$

$$\frac{\int EI \; f_{,xx}^2 \; dx}{\int f_{,x}^2 \; dx} = F = \text{buckling load} \; . \tag{3c}$$

Similarly, expressing the moment and change in curvatures for a pin-ended column ($M = -Fw$, $w(0) = w_{,xx}(0) = 0$, $w(1) = w_{,xx}(1) = 0$).

The following is obtained:

$$\int_0^1 EI \left(\frac{-Fw}{EI} \right) \; \delta \; \left(\frac{-Fw}{EI} \right) = F \int_0^1 \frac{dw}{dx} \; \delta \left(\frac{dw}{dx} \right) \; dx$$

$$\therefore \; F = \frac{\int_0^1 f_{,x}^2 \; dx}{\int_0^1 \frac{f^2}{EI} \; dx} \tag{4a}$$

9.1.2 (Cont'd)

and integrating by parts the following alternate expression is obtained:

$$F = -\frac{\int_0^l f\, f_{,xx}\, dx}{\int_0^l \frac{f^2}{EI}\, dx} \quad . \tag{4b}$$

Note that this is true only if f symbolizes the eigenvectors. For a pin-ended column $f_n = \sin \frac{n\pi x}{l}$, which yields the critical loads

$$F_n = \frac{n^2 \pi^2 EI}{l^2} \quad , \quad \text{(Eq. (4a) of Paragraph 9.1.1.2)}$$

The same critical loads would result if an initial eccentricity is assumed.

The eigenvector f (which is obtained by solving the Euler Equilibrium Equation) may be exceedingly difficult to obtain. However, one can use the properties of eigenvalues (Paragraph 9.1.3) or the energy principles to obtain approximate solutions to the buckling load.

9.1.3 Properties of Eigenvectors (Deflection Modes) and Eigenvalues (Critical Loads)

The following properties of eigenvectors and eigenvalues are of use in the determination of the stability of structures by direct or approximate procedures. The properties are illustrated for a one-dimensional problem but can be extended to the two-dimensional case.

(1) An eigenvector is a deformation pattern compatible with the boundary conditions of the structure which makes the potential energy of the structure stationary, i.e., $\left[\delta L\right]_u = 0$.

(2) The eigenvectors of a structure with homogeneous boundary conditions are orthogonal to the curvatures of the eigenvectors. When the eigenvectors are orthonormal (weighing function is unity), then

$$\int u_i\, u_j\, dx = \delta_{ij}$$

(3) Associated with each eigenvector is an eigenvalue which is associated with a buckling load of the structure. The eigenvalues are non-decreasing for the structural problems considered.

(4) Restricting the possible (admissible) classes of functions which can be eigenvectors cannot result in a reduction of the buckling load. This is equivalent to saying that additional restraints at the boundary can only increase the stability of the structure. The less restrained the boundary, the lower the buckling load, which increases as boundary goes from free, to simple supported, and to clamped.

(5) The addition of restrictions within the structure is equivalent to stiffening the boundary conditions (property 4). Thus the addition of another support at the center of a column can increase the stability four-fold.

(6) If two structures have the same cross-sectional stiffness and boundary conditions but the size of one is smaller than the other, then the eigenvalue of the first is never less than the second. Thus, the stability of structures with identical boundary conditions is never less for the smaller structure. A short column is more stable than a long column and a square shear panel is more stable than a rectangular shear panel that has the same boundary conditions and smaller side equal to that of the square.

9.1.3 (Cont'd)

(7) If two structures have the same geometry and boundary conditions but the stiffnesses of one structure is greater at each corresponding point than the other structure, then the buckling load of the first is at least as great as the second. Thus if the bending stiffness of a column varied, the critical load for this column would lie between the critical loads for similar columns with constant bending stiffnesses equal to the largest and smallest value of the bending stiffness of the column in question.

(8) The u_j eigenvector has j-1 nodes in the interior of the structure. The sub-division of a structure into elements bounded by nodes permits analysis of the sub-structure without considering compatibility of deflections.

(9) A continuous (compatible) deflection can be taken as a sum of weighted orthonormal eigenvectors.

$$w = \Sigma a_i u_i \quad \text{where} \quad a_i = \int w u_i \, dx$$

(10) The orthonormality of the eigenvectors simplifies operations upon a function which is expressed in terms of the eigenvectors. Continued operations (iterations) causes the resulting function to be heavily weighted in favor of the extreme eigenvalue. If the extreme eigenvector is not known, then any arbitrary smooth function (it is assumed that the sought after eigenvector is the extreme component of this function) will, upon iteration, approximate the eigenvector. The eigenvalue, or buckling load, can then be found.

Let A be any non-singular operation where

$$A u_i = \lambda_i^{-1} u_i \;\&\; \lambda_i u_i = A^{-1} u_i \tag{1a}$$

(e.g., let $A^{-1} u_i = -\frac{d^2 u_i}{dx^2}$, $A = -\iint u_i \, dxdx$, $\lambda_i = \frac{F_i}{EI}$).

Let $w_0 = \Sigma a_i u_i$, where w_0 = initial approximation of the lateral deflection.

$$\begin{aligned} Aw_0 &= A \Sigma (a_i u_i) = \Sigma a_i (Au_i) = \Sigma (a_i \lambda_i^{-1}) u_i = w_1 \\ A(Aw_0) &= A^2 w_0 = \Sigma a_i \lambda_i^{-1} (Au_i) = \Sigma (a_i \lambda_i^{-2}) u_i = w_2 \\ A^n w_0 &= \Sigma (a_i \lambda_i^{-n}) u_i = w_n \qquad (n = 0, 1, 2 \ldots .) \end{aligned} \tag{1b}$$

$$\frac{w_n}{w_{n+1}} = \frac{\Sigma a_i \lambda_i^{-n} u_i}{\Sigma a_i \lambda_i^{-(n+1)} u_i} = \frac{\lambda_1^{-n} \Sigma a_i u_i + \Sigma a_i u_i (\lambda_i^{-n} - \lambda_1^{-n})}{\lambda_1^{-n-1} \Sigma a_i u_i + \Sigma a_i u_i (\lambda_i^{-n-1} - \lambda^{-n-1})} \tag{1c}$$

For the structural problems considered it is assumed that $\lambda_1 \leq \lambda_i$. Consequently,

$$\lim_{n \to \infty} \frac{w_n}{w_{n+1}} = \lambda_1 . \tag{1d}$$

9.1.3 (Cont'd)

Operating upon an assumed deflection pattern results in a calculated deflection pattern which is closer to the true buckling pattern. If the assumed deflection pattern is the true one, then the operation gives the eigenvector modified by a constant $Au_i = \lambda_i^{-1} u_i$. Thus if w_0 were exactly $a_i u_i$ then

$$\frac{w_0}{w_1} = \lambda_i \, . \tag{1e}$$

The ratio $\frac{w_n}{w_{n+1}}$ will vary along the length of the column (except when w_n is an eigenvector). This ratio will have a maximum and minimum value for different values of x. It is noted in paragraph 16 of Reference 9-2 that

$$\left(\frac{w_n}{w_{n+1}}\right)_{Min} \leq \frac{F_{cr}}{F} \leq \left(\frac{w_n}{w_{n+1}}\right)_{Max} \, . \tag{1f}$$

A lower bound on the buckling load can be found by employing this principle. The technique is to assume an initial eccentricity of the column w_0 and determine the deflection w_1 due to an axial load F ($w_1 = \int_0^x \int_0^x \frac{F w_0}{EI} dxdx$ with applicable boundary conditions) and determine the maximum and minimum ratio of $\frac{w_0}{w_1}$. The ratio at the point of maximum deflection usually results in a lower bound on the buckling load. Closer approximations will result if the process is repeated with the new deflection pattern.

(11) An upper bound can be obtained by a scalar product method as follows since $A^{-1} u_i = \lambda_i u_i$, the following is obtained:

$$\frac{\int (A^{-1} u_i)\,(u_i)\, dx}{\int (u_i)\,(u_i)\, dx} = \frac{\int \lambda_i u_i^2 \, dx}{\int u_i^2 \, dx} = \lambda_i \, . \tag{2a}$$

Similarly,

$$\frac{\int (A^{-1} w)\, w \, dx}{\int (w)\,(w)\, dx} = \frac{\int (\Sigma A^{-1} a_i u_i)\,(\Sigma a_i u_i)\, dx}{\int \Sigma (a_i u_i)\ \Sigma\ (a_i u_i)\, dx}$$

$$= \frac{\int (\Sigma a_i \lambda_i u_i)\,(\Sigma a_i u_i)\, dx}{\int \Sigma\ (a_i u_i)\ \Sigma\ (a_i u_i)\, dx}$$

$$= \frac{\Sigma a_i^2 \lambda_i}{\Sigma a_i^2} = \frac{\lambda_1 \Sigma a_i^2 + \Sigma a_i^2 (\lambda_i - \lambda_1)}{\Sigma a_i^2} \geq \lambda_1 \, , \tag{2b}$$

since $a_i^2 (\lambda_i - \lambda_1) \geq 0$.

$$\therefore \quad \frac{\int (A^{-1} w)\,(w)\, dx}{\int (w)\,(w)\, dx} \geq \lambda_1 \, . \tag{2c}$$

If $A^{-1} w = -\frac{d^2 w}{dx^2} = -w_{,xx}$,

9.1.3 (Cont'd)

then from Eq. (2c)

$$- \frac{\int (w_{,xx})\,(w)\,dx}{\int w^2\,dx} \geq \lambda_1 . \qquad (2d)$$

Assuming any w, and operating upon the assumed function as shown in Eq. (2c), results in a value which is never less than the lowest eigenvalue. The evaluation of the eigenvalue (buckling load) is relatively insensitive to the inaccuracy of the assumed deflection. In both cases (10 and 11), equality results when the assumed value w is the eigenvector $a_1 u_1$ and the difference is small when w is approximately $a_1 u_1$.

9.1.4 Approximate Methods of Determining Stability

The solution to the differential equilibrium equation may be quite difficult to determine directly. Approximate solutions are obtain from energy considerations. The physical arguments parallel the properties of eigenvalues noted in Paragraph 9.1.3. A deflection pattern (w) is chosen, corresponding to the given boundary conditions, and is hoped to be a good approximation to the first eigenvector. This corresponds to applying a virtual displacement to the actual structure. The solutions are presented for the column but the technique can be extended to all structures. The stiffness (EI) is retained inside the integral sign to permit equations to be applied to structures of variable stiffness such as occur when structures are subjected to variations in temperature.

The deflection can be assumed as a single function or a sum of such functions. The assumed deflection can be employed to produce a upper and lower bounds on the stability by appropiate manipulations. A sum of functions with undetermined coefficients provides a means whereby the upper and lower bound solutions may be made to approach each other as closely as desired. The closer the assumed deflection curve is to the true deflection curve, the closer the approximation to the buckling load.

9.1.4.1 Single Functions

Assuming a displacement pattern is equivalent to increasing the stiffness of a structure by adding additional restraints. The buckling force calculated by the Method of Virtual Displacements, where the strain energy is expressed in terms of the assumed deflection, will be greater than the actual buckling force. Employing the Method of Virtual Forces, where the complementary strain energy is expressed in terms of the actual force, would result in an overestimate of the deflection (flexibility) of the structure and a lower bound on the buckling load.

9.1.4.1.1 Upper Bound

Assuming a compatible displacement pattern with the corresponding strain distribution results in a larger estimate of the strain energy when expressed in terms of the displacements. The buckling load in this case will be an upper bound on the actual buckling load.

$$\delta U \geq \delta W$$

Let $w = w_0 f$ where f need not be the eigenvector.

Then

$$\frac{\int EI\, f_{,xx}^2\, dx}{\int f_{,x}^2\, dx} \geq F. \qquad (1)$$

9.1.4.1.1 (Cont'd)

This equation is identical to Eq. (2d) of Paragraph 9.1.3 and becomes Eq. (3c) of Paragraph 9.1.2 when the assumed deflection pattern is the eigenvector.

Similarly it can be concluded for the usual boundary condition where (f) ($f_{,x}$) is identically zero at the boundaries (e.g., simple or clamped) that

$$-\frac{\int f_{,xx} f \, dx}{\int \frac{f^2}{EI} \, dx} = \frac{\int f_{,x}^2 \, dx}{\int \frac{f^2}{EI} \, dx} \geq F . \qquad \text{(2a) and (2b)}$$

The inequality expressed by Eqs. (2a) and (2b) is usually smaller than Eq. (1) and should be employed in obtaining an upper bound. The approximation of the derivatives of the assumed deflection pattern to the derivatives of the eigenvector pattern becomes more inaccurate as the order of the derivatives increases.

It is important that the assumed deflection shape should have no component of deflection modes which correspond to the buckling of the structure with some restraints removed The assumed deflection must satisfy all the boundary conditions (restraints) of the structure. This represents a structure with the same or more restraint than the actual structure and results in an upper bound on the buckling load. Thus, if a column has a center support, then the assumed deflection must similarly have zero deflection at the center of the column.

9.1.4.1.2 Lower Bound

Assuming a force and stress distribution is equivalent to underestimating the stiffnesses and overestimating the displacements of the structure. Employing the Principle of Virtual Force and expressing the complementary strain energy in terms of an assumed stress distribution results in a calculated deflection which is greater than the actual deflection. This inequality can be employed to obtain a lower bound on the buckling load. A closer bound is obtained when the maximum deflection is computed.

The hinged column is analyzed by taking a virtual force at the center of the column and resisting it at the hinged ends.

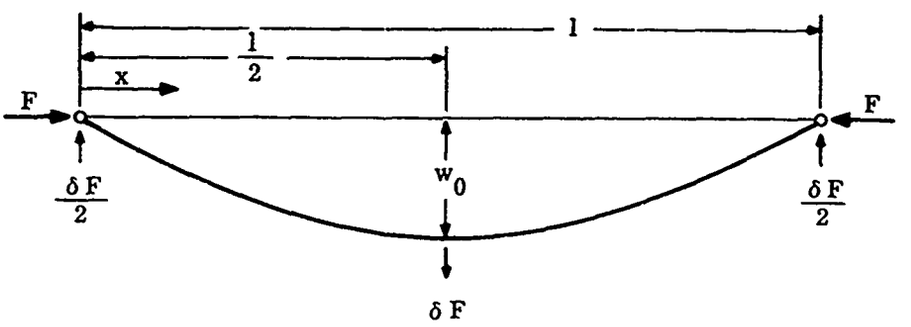


FIGURE 9.1.4.1.2-1 VIRTUAL FORCE ON PIN-ENDED COLUMN

9.1.4.1.2 (Cont'd)

The increased flexibility due to assuming a stress distribution results in an overestimate of the deflection.

$$\therefore \quad \delta U^*(F) \geq \delta W^*$$

$$\int \kappa \delta M \geq w_0 \delta F$$

$$\therefore \int_0^{l/2} \frac{Fw}{EI} \left(x \frac{\delta F}{2} \right) dx + \int_{l/2}^{l} \frac{F_w}{EI} (l - x) \frac{\delta F}{2} \geq w_0 \delta F$$

Since $w = w_0 f$ where w_0 = deflection at the center, the following is obtained:

$$F \geq \frac{2}{\int_0^{l/2} \frac{fx}{EI} dx + \int_{l/2}^{l} \frac{f(l - x)}{EI} dx} \quad . \tag{1}$$

In general

$$F \geq \frac{1}{\int_0^{l} \frac{fm}{EI} dx} \quad , \tag{2}$$

where f is the assumed deflection mode = 1 at point of virtual load and where m is the virtual internal moment on the structure due to virtual unit load.

Equation (1) is the ratio of the deflection at the center before and after the axial load is applied. The resulting deflection pattern is closer to the actual eigenvector than the original assumed value. This deflection pattern can be obtained by integrating the curvature $w_{,xx} = w_0 f_{,xx}$ (i.e., $f_1 = \iint f_{,xx}\, dxdx$ and $f_1(l/2) = 1$) and employing the new deflection mode in Eq. (2b) of Paragraph 9.1.4.1.1 and Eq. (2) of this paragraph, to obtain closer bounds. This can be continued until the difference between the upper and lower bounds is within acceptable limits (the upper bound is usually the closer of the two).

The lower bound technique described above is mathematically similiar to the procedure shown in Paragraph 16 of Reference 9-2.

Example: Pin ended column of constant EI

Let $w = \frac{4w_0}{l^2} x(l-x)$ (zero deflection at ends x = 0, l but with curvature at the ends representing some moment restraint)

$f = \frac{4}{l^2} x(l-x)$

$f_{,x} = (f/l^2)(l-2x)$

$f_{,xx} = -8/l^2$.

9.1.4.1.2 (Cont'd)

Upper Bound:

Using Eq. (2b) of Paragraph 9.1.4.1.1,

$$\frac{\int f_{,x}^{2}\,dx}{\int \frac{f^2}{EI}\,dx} = \frac{(16/l^4)\int_0^l (l-2x)^2\,dx}{(16/l^4)\int_0^l \frac{x^2(l-x)^2\,dx}{EI}} = \frac{l^3\,(1 - 4/2 + 4/3)}{\frac{l^5}{EI}\left(\frac{1}{3} - \frac{2}{4} + \frac{1}{5}\right)} = \frac{10EI}{l^2} > F.$$

Lower Bound:

Using Eq. (2),

$$\frac{2}{\int_0^{l/2} \frac{4}{l^2}\,\frac{x(l-x)x}{EI}\,dx + \int_{l/2}^{l} \frac{4}{l^2}\,\frac{x(l-x)\,(l-x)dx}{EI}} = \frac{2}{\frac{4l^2}{EI}\left(\frac{1}{24} - \frac{1}{64}\right)(2)} = \frac{9.6EI}{l^2} < F.$$

$$\therefore \quad \frac{9.6EI}{l^2} \le F_{cr} \le \frac{10.0\ EI}{l^2}\ .$$

The buckling load $= \dfrac{\pi^2\ EI}{l^2} = \dfrac{9.8697\ EI}{l^2}$

Closer Bounds:

A loading of $Fw_1 = F\dfrac{4x}{l^2}(l-x)w_{10}$, upon integration results in

$$w_2 = \frac{16x}{5l}\left(1 - \frac{2x^2}{l^2} + \frac{x^3}{l^3}\right) w_{20}.$$

Repeating the above operations with the closer approximation results in

$$\frac{9.836\ EI}{l^2} \le F_{cr} \le \frac{9.871\ EI}{l^2}\ .$$

Closer bounds are more probable if the assumed deflection pattern matches the boundary conditions identically. The upper bound procedure is a Rayleigh-Ritz method in which a function with a limited number of undetermined coefficients is assumed. The coefficients can be uniquely determined by satisfying the boundary conditions identically. The function

$$\frac{96}{31}\ w_0\left[\frac{x}{l}\left[1 - \frac{11}{6}\left(\frac{x}{l}\right)^2 + 5/6\left(\frac{x}{l}\right)^3\right]\right]$$

satisfies the requirements of zero deflection and moment at the ends x=0, ! and would result in upper and lower bounds which are quite close

9.1.4.2 Multiple Functions

The closer the assumed deflection pattern is to the true deflection pattern, the closer is the approximation (see example in Paragraph 9.1.4.1.2). It is convenient to take the assumed deflected shape as a sum of functions, with undetermined coefficients, which correspond to known eigenvector solutions of the equilibrium equation for structures which are similar to the actual structure (e.g., slightly different boundary conditions). Since the eigenvectors are orthogonal, the energy is easily calculated as a function of the squares of undetermined coefficients (a_i^2). The coefficients (relative weight) to be assigned to the functions are determined by making the potential stationary with respect to the undetermined coefficients $\left(\frac{\partial L}{\partial a_i} = 0\right)$. If the energy is expressed in terms of the displacements and the functions satisfy boundary conditions which are the same or more restrained than the actual structure, then the resulting solution must be an upper bound. (See Eq. (2a) of Paragraph 9.1.3). An adequate number of terms representing the deflection, each with less restrained boundary conditions would result in a lower bound. If the individual functions do not satisfy the actual boundary conditions, then a constraint (Lagrangian Multiplier) relationship can be imposed among the coefficients (in additional to $\frac{\partial L}{\partial a_i} = 0$) so that the total assumed deflection ($\Sigma a_i u_i$) satisfies the boundary conditions. It is shown in Reference 9-4 that a termwise matching of the higher derivatives (e.g., slope w_x) with an over-all matching of the lower derivatives (e.g., deflection w) results in a more rapid convergence (closer bounds). Some methods of obtaining an upper bound by assuming functions which satisfy boundary conditions of equal or greater restraint are known as the Rayleigh-Ritz and Galerkin Methods. The upper bound is the solution of a structure which is stiffer (more restrained) than the actual structure.

The "Rayleigh-Ritz Method" is an extension of Eqs. (1) and (2) of Paragraph 9.1.4.1 to multiple functions where the coefficients are selected to minimize the potential energy. The "Galerkin Method" is an application of the principle of virtual work. If the lateral displacement is $w = \sum_{i=1}^{n} a_i u_i$, then the stationary property of the potential ($\delta L = 0$) requires that the virtual energy of the virtual lateral displacement $\delta w = u_i \, \delta a_i$ acting over the equivalent lateral load as expressed by the equilibrium equation, Eq. (3) of Paragraph 9.1.1.1, (i.e. $D\nabla^4 w - N\nabla^2 w - q = 0$) must be zero:

$$\int (D\nabla^4 w - N \cdot \nabla^2 w - q) \left[\delta \, (a_i \, u_i) \right] \, dxdy = 0 \qquad (1a)$$

$$\int \left(D\nabla^2 \, (\Sigma \, a_i u_i) - N \cdot \nabla^2 \, (\Sigma \, a_i u_i) - q \right) u_i \, dxdy = 0. \qquad (1b)$$

Equation (1b) is a set of n simultaneous equations which determines the best value of the coefficients of the n functions for obtaining a close upper bound. The Galerkin Method usually results in a closer or more rapidly convergent upper bound.

The Trefftz Method obtains upper and lower bounds by assuming deflection patterns which represent less restraint at the boundaries. Selecting coefficients which make the potential stationary and simultaneously satisfy the given boundary (constraint) conditions results in a computed upper bound upon the buckling of the structure. Ignoring some of the boundary constraint conditions results in a new computed stability which is less than the originally computed one. Care must be taken with the Trefftz Method since a sufficiently large number of functions must be employed before the lower value can be assumed to be a lower bound. The deflection pattern must be fairly accurate or it is possible that the computed buckling load with the less restrained boundary may overestimate the stability. Employing only a few terms may overestimate the internal energy within the boundary to overcompensate for the lower energy in the region of the boundary.

9.1.4.2 (Cont'd)

The computational techniques for multiple functions are illustrated in two very simple examples. These techniques, though powerful, cannot be shown advantageously in the simple problems presented.

Example of Rayleigh-Ritz Method - Column of non-constant stiffness with pin ends:

$EI = \eta D, \quad 0 \leq x < l/2 \quad$ where $\eta \leq 1$
$EI = D, \quad l/2 \leq x \leq l$

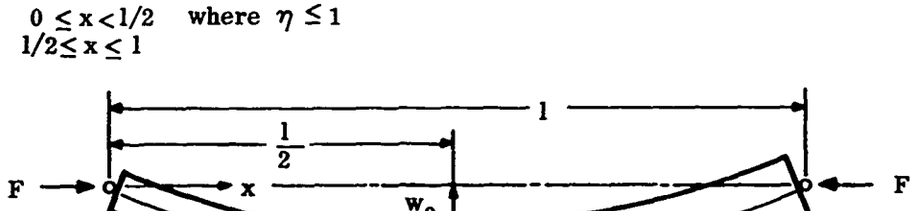


FIGURE 9.1.4.2-1 PIN-ENDED COLUMN WITH VARIABLE STIFFNESS

Assume a deflection $w = \sum_{n=1}^{\infty} a_{2n-1} \sin \frac{(2n-1)\pi x}{l}$.

Then $$\frac{dw}{dx} = w_{,x} = \frac{\pi}{l} \sum_{n=1}^{\infty} (2n-1)\, a_{2n-1} \cos \frac{(2n-1)\pi x}{l}$$

$$\frac{d^2w}{dx^2} = w_{,xx} = -\frac{\pi^2}{l^2} \sum_{n=1}^{\infty} (2n-1)^2 a_{2n-1} \sin \frac{(2n-1)\pi x}{l} .$$

Each term of this deflection pattern satisfies boundary condition

$$w(o) = w(l) = 0$$
$$w_{,xx}(o) = w_{,xx}(l) = 0 ,$$

and is a eigenvector for columns of constant EI. They are orthogonal in the region 0 to 1/2.

For an elastic structure

$$2L = \int \left[EI \left(\frac{d^2w}{dx^2} \right)^2 - F \left(\frac{dw}{dx} \right)^2 \right] dx ,$$

or

$$2L = \int_0^l \eta D \frac{\pi^4}{l^4} (2n-1)^4 a_{2n-1}^2 \sin^2 \frac{(2n-1)\pi x}{l} dx + \int_{1/2}^l D \frac{\pi^4}{l^4} (2n-1)^4 a_{2n-1}^2 \sin^2 \frac{(2n-1)\pi x}{l} dx$$
$$- F \int_0^l \frac{\pi^2}{l^2} (2n-1)^2 a_{2n-1}^2 \cos^2 \frac{(2n-1)\pi x}{l} dx$$

$$2L = \int_0^l D \frac{\pi^4}{l^4} (2n-1)^4 a_{2n-1}^2 \sin^2 \frac{(2n-1)\pi x}{l} dx + \int_0^{l/2} (\eta - 1) D \frac{\pi^4}{l^4} (2n-1)^4 a_{2n-1}^2 \sin^2 \frac{(2n-1)\pi x}{l} dx$$
$$- F \int_0^l \frac{\pi^2}{l^2} (2n-1)^2 a_{2n-1}^2 \cos^2 \frac{(2n-1)\pi x}{l} dx .$$

9.1.4.2 (Cont'd)

Since $$\int_0^l \sin^2 \frac{(2n-1)\pi x}{l}\, dx = \int_0^l \cos^2 \frac{(2n-1)\pi x}{l}\, dx = 1/2$$

$$\int_0^{1/2} \sin^2 \frac{(2n-1)\pi x}{l}\, dx = 1/4 \quad ;$$

$$\therefore\ 2L = \frac{\pi^4}{l^4} D \frac{1}{2} \Sigma (2n-1)^4 a_{2n-1}^2 + \frac{\pi^4}{l^4} (\eta - 1) D \frac{1}{4} \Sigma (2n-1)^4 a_{2n-1}^2$$

$$- \frac{\pi^2}{l^2} F \frac{1}{2} \Sigma (2n-1)^2 a_{2n-1}^2 \quad ,$$

$$2L = \frac{\pi^4}{2l^3} D \frac{1+\eta}{2} \Sigma (2n-1)^4 a_{2n-1}^2 - \frac{\pi^4}{2l} F \Sigma (2n-1)^2 a_{2n-1}^2 \quad ,$$

and $$2 \frac{\partial L}{\partial a_{2n-1}} = \frac{\pi^4}{l^3} D \frac{1+\eta}{2} (2n-1)^4 a_{2n-1} - \frac{\pi^2}{l} F (2n-1)^2 a_{2n-1} = 0 \quad ;$$

$$\therefore\ a_{2n-1} = 0 \quad \text{and} \quad F = (2n-1)^2 \frac{\pi^2}{l^2} k_D \frac{1+\eta}{2} \quad .$$

F min occurs at n = 1.

$$\therefore\ F = \frac{\pi^2}{l^2} D \frac{1+\eta}{2} \quad \text{and} \quad 0 = a_3 = a_5 = a_7 \ldots\ .$$

The calculated critical load is the same as that for a column of constant average stiffness which is an upper bound to the true solution with increasing inaccuracy for smaller values of η . Ignoring the even eigenvectors (for computation simplicity) is justified by the lower internal energy level of the first eigenvector but permits only symmetrical buckling modes. The error is an overestimate of the stability due to the fact that the actual deflection is not fully described by the odd eigenvectors alone (when $\eta \neq 1$.)

Example of the Trefftz Method - Clamped column with constant EI, determination of upper bound:

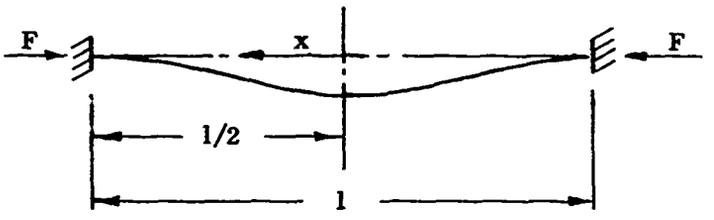


FIGURE 9.1.4.2-2 CLAMPED COLUMN

Let $$w = \Sigma a_i \cos \frac{(2i-1)\pi x}{l} \quad .$$

Then $$w_{,x} = -\Sigma (2i-1) \frac{\pi}{l} a_i \sin \frac{(2i-1)\pi x}{l}$$

9.1.4.2 (Cont'd)

$$w_{,xx} = -\Sigma\,(2i-1)^2\,\frac{\pi^2}{l^2}\,a_i \cos\frac{(2i-1)\pi x}{l}$$

The boundary condition of the displacements are satisfied identically, i.e., $w(l/2) = w(-l/2) = 0$. The requirement of zero slope at the ends can be satisfied for the upper limit as follows:

$$0 = w_{,x}\left(-\frac{l}{2}\right) = w_{,x}\left(\frac{l}{2}\right) = -\Sigma\,(2i-1)\,\frac{\pi}{l}\,a_i \sin\frac{(2i-1)\pi}{2} = \frac{\pi}{l}\,\Sigma(-1)^i\,(2i-1)\,a_i\,.$$

$$\therefore\ \Sigma(-1)^i\,(2i-1)\,a_i = 0$$

is the constraint condition on the coefficients which ensures an upper bound.

Determine the coefficient (a_i) by making the potential stationary but modify the potential by a term which is identically zero and represents the constraint condition on the coefficients. The technique is known as the Lagrangian Multiplier Method. Thus,

$$2L = \int\left[EI\left(\frac{d^2w}{dx^2}\right)^2 - F\left(\frac{dw}{dx}\right)^2\right]dx - \mu\,\Sigma\,(-1)^i\,(2i-1)\,a_i\,,$$

where μ is a Lagrangian Multiplier.

$$2L = EI\,\frac{\pi^4}{l^4}\,\Sigma\,a_i^2\,(2i-1)^4\int\cos^2\frac{(2i-1)\pi x}{l}\,dx$$

$$- F\,\frac{\pi^2}{l^2}\,\Sigma\,a_i^2\,(2i-1)^2\int\sin^2\frac{(2i-1)\pi x}{l}\,dx - \mu\,\Sigma\,(-1)^i\,(2i-1)\,a_i$$

$$0 = 2\,\frac{\partial L}{\partial a_i} = \frac{EI\pi^4}{l^3}(2i-1)^4\,a_i - \frac{F\pi^2}{l}(2i-1)^2\,a_i - \mu\,(-1)^i\,(2i-1)$$

$$\therefore\ a_i = \frac{\mu(-1)^i}{\frac{EI\pi^4}{l^3}(2i-1)^3 - \frac{F\pi^2}{l}(2i-1)}$$

$$0 = \Sigma\,(-1)^i\,(2i-1)\,a_i$$

$$0 = \sum\frac{\mu}{\frac{\pi^2}{l^2}\left[\frac{EI\pi^2}{l^2}(2i-1)^2 - F\right]}$$

$$\frac{\mu}{\frac{\pi^2}{l}\,\frac{EI\pi^2}{l^2}}\sum_{i=1}^{n}\frac{1}{(2i-1)^2 - k} = 0\,,$$

9.1.4.2 (Cont'd)

where

$$k = \frac{F}{\frac{EI\pi^2}{l^2}} = \frac{F}{F_E} = \text{ratio of buckling load to Euler buckling load.}$$

Solving the above equation for n = 2, 3, 4, 5, ... gives approximate value $F = 5\ F_E$, $4.63\ F_E$, $4.45\ F_E$, $4.35\ F_E$, ... which convèrges to $F = 4\ F_E = \frac{4\pi^2 EI}{l^2}$.

More rapid convergence would occur if the slopes $\frac{dw}{dx}$ at $x = \pm l/2$ were satisfied identically by employing an odd sine series and a constraint condition on the deflections $\left(\sum_{i=1}^{n} a_i \sin\frac{(2i-1)\pi x}{l} = 0\right)$. This would result in $\sum_{i=1}^{n} \frac{1}{(2i-1)^2\left[(2i-1)^2 - k\right]} = 0$.

9.1.5 Shear Energies

Ignoring the strain energy due to shear is equivalent to overestimating the stiffness of the structure and results in higher calculated buckling load. Ignoring the axial strain energy does not affect the stability calculations if the axial work of external loads is ignored. These conclusions become obvious upon examination of the potential of the column in which the transverse shear and torsional energies should be considered.

When a column is axially loaded, it deflects laterally due to initial eccentricities. The slope ($w_{,x}$) of the column gives rise to a transverse shear load as shown in Figure 9.1.5-1. The equivalent transverse shear load (V) acts with the equivalent axial force F at the centroid of the effective areas of the cross section. Twisting due to a torsional moment Q will occur if the transverse shear vector, acting in the direction of the lateral deflection, does not pass through the shear center of the cross section. The loads acting upon the cross section can be defined as follows:

$$M = -Fw \tag{1a}$$
$$V = Fw_{,x} \tag{1b}$$
$$Q = eFw_{,x}. \tag{1c}$$

Examining the change in potential due to a virtual displacement,

$$\delta_L = \delta U - \delta W = \delta U_M + \delta U_V + \delta u_Q + \delta U_A - (\delta W_M + \delta W_Q + \delta W_V) - \delta W_A = 0, \tag{2a}$$

where

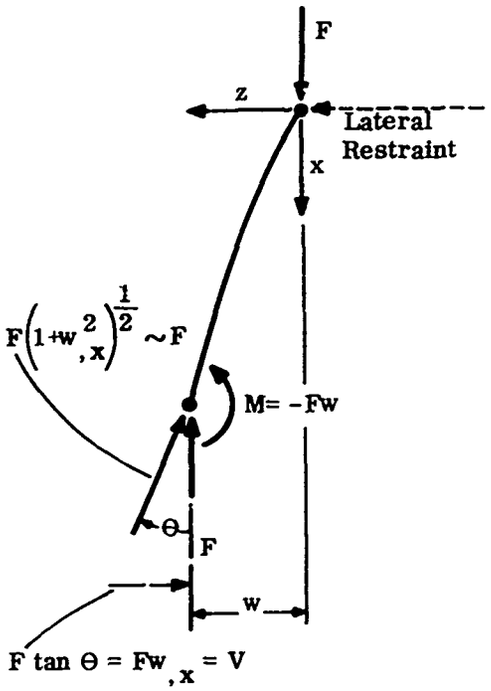
δU_M = change in bending strain energy $= \int M\delta\left(\frac{M}{EI}\right) dx$

δU_Q = change in torsional strain energy $= \int Q\delta\left(\frac{Q}{JG}\right) dx$

δU_V = change in transverse shear strain energy $= \int V\delta\left(\frac{V}{A_V G}\right) dx$

δU_A = change in axial strain energy $= \int F\delta\left(\frac{F}{AE}\right) dx$

9.1.5 (Cont'd)



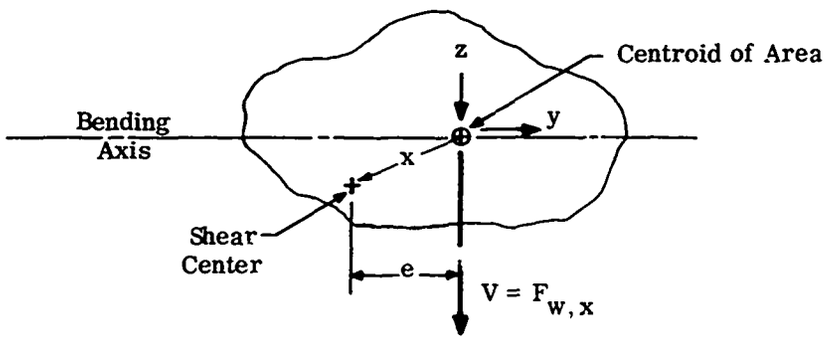


FIGURE 9.1.5-1 SHEAR AND TORSIONAL LOAD ON A PIN-ENDED COLUMN

9.1.5 (Cont'd)

$\delta W_{MQV} = \delta W_M + \delta W_Q + \delta W_V$ = change in potential energy of the external loads (assuming inextensibility) $= F\ \delta\left[\int \frac{1}{2}\left(\frac{dw}{dx}\right)^2 dx\right]$

δW_A = change in potential energy of external loads due to axial deformation of the cross section $= F\ \delta \int \frac{du}{dx}\ dx,$

and

e = distance from shear center to line of action of the transverse shear V

M = moment acting on cross section = -Fw

V = transverse shear load on cross section = $F\ \frac{dw}{dx}$

Q = torque acting on cross section = $e\ F \frac{dw}{dx}$

$\overline{EI}$ = bending stiffness = $\int E_S z^2\ dA$

$\overline{JG}$ = torsional stiffness = $G_S r^2\ dA$

$\overline{A_V G}$ = transverse shear stiffness = G_S times effective shear area

E_S = secant modulus = $\frac{\epsilon - \alpha T}{\sigma}$.

The changes in axial energy are exactly equal since

$$\delta U_A - \delta W_A = \int F\ \delta\left(\frac{F}{AE}\right) dx - F\ \delta \int \frac{du}{dx}\ dx = F\ \delta \int \left(\frac{du}{dx} - \frac{du}{dx}\right) dx = 0. \qquad (2b)$$

Equation (2a) becomes

$$\delta U_M + \delta U_V + \delta U_Q - \delta W_{MQV} = 0. \qquad (2c)$$

Substituting the equivalent expression containing F into Eq. (2c) results in

$$\int \left\{ Fw\delta\left(\frac{Fw}{EI}\right) + Fw_{,x}\ \delta\left(\frac{Fw_{,x}}{A_V G}\right) + e\ Fw_{,x}\ \delta\left(\frac{e\ Fw_{,x}}{JG}\right) - F\ \delta\left(\frac{1}{2}\ w_{,x}^2\right)\right\} dx = 0$$

$$F^2 \int \left\{ \frac{w\ \delta w}{EI} + w_{,x}\ \delta w_{,x}\ \left(\frac{1}{A_V G} + \frac{e^2}{JG}\right)\right\} dx - F \int w_{,x}\ \delta w_{,x}\ dx = 0.$$

$$\therefore\ F_{cr} = \frac{\int f_{,x}^2\ dx}{\int \frac{f^2 dx}{EI} + \int f_{,x}^2 \left(\frac{1}{A_V G} + \frac{e^2}{JG}\right) dx} \qquad (3a)$$

$$F_{cr} = \frac{1}{\frac{\int \frac{f^2}{EI}\ dx}{\int f_{,x}^2\ dx} + \frac{\int f_{,x}^2 \left(\frac{1}{A_V G} + \frac{e^2}{JG}\right) dx}{\int f_{,x}^2\ dx}} \qquad (3b)$$

The bending solution always overestimates the stability of the structure since it assumes infinite shear stiffness $\overline{A_V G}$ and $\overline{JG}$. Comparing stability Eq. (4a) of Paragrah 9.1.2

9.1.5 (Cont'd)

with Eq. (3b) above indicates that the true stability is smaller since $\frac{1}{A_V G} + \frac{e^2}{JG}$ is a non-negative term. If $\frac{1}{A_V G} + \frac{e^2}{JG}$ is constant, and

$$F_M = \frac{\int f_{,x}^2 \, dx}{\int \frac{f^2}{EI} \, dx} = \text{buckling of column with infinite shear stiffness,}$$

then

$$F_{cr} = \frac{1}{\frac{1}{F_M} + \frac{1}{A_V G} + \frac{e^2}{JG}} , \tag{4a}$$

or

$$\frac{1}{F_{cr}} = \frac{1}{F_M} + \frac{1}{A_V G} + \frac{e^2}{JG} = \frac{1}{F_M} + \frac{1}{F_V} + \frac{1}{F_Q} \tag{4b}$$

and

$$F_{cr} = \frac{F_M}{1 + \frac{F_M}{F_V} + \frac{F_M}{F_Q}} . \tag{4c}$$

This is analagous to springs in series where F is the effective stiffness of the three springs and F_M is the stiffness of the bending spring $= \frac{C_M EI}{l^2}$. F_V is the stiffness of the transverse shear spring $= C_V A_V G$. F_Q is the stiffness of the torsion spring $= \frac{C_Q}{e^2} JG$.

$$F = \frac{C_M (EI/l^2)}{1 + \frac{C_M}{C_V}\left(\frac{EI}{A_V G\, l^2}\right) + \frac{C_M}{C_Q}\frac{EI}{JG}\left(\frac{e}{l}\right)^2} \tag{5}$$

If any spring is very flexible as compared to the other springs then the effective stiffness of the springs in series is approximately equal to, but slightly less than, the stiffness of the very flexible spring. Thus when the shear and torsional springs are very stiff, the bending solution presents a good upper bound approximation to the stability of the structure. Similarly, if a structure is relatively weak in shear (e.g., a sandwich construction with a soft core), when the value $A_V G$ represents a good upper bound upon the stability. The torsional effect is usually insignificant for closed sections (large J) or sections symmetrical about the axis perpendicular to the bending axis (e = 0).

9.1.6 Plasticity and Eccentricity

The Euler equation becomes non-linear when the bending stiffness becomes a function of the applied load N and the deflection w and its derivatives. The lateral deflections w increases with load, and the moment acting on the section increases at a much greater rate than the load. Instability occurs when the rate of increase of external moment becomes greater than the structure can generate by an increase in internal moment (bending stiffness times curvature). The load and moment on the cross section tend to reduce the bending stiffness when the stresses exceed the proportional limit. The computed stability of the structure with elastic properties must be an overestimate. The effect of the plasticity of the material can only reduce the stability and can only be approximated (References 9-1 through -6) at the present state of the art.

9.1.6 (Cont'd)

Preliminary investigations (References 9-1 through -8) have indicated that for structures of small initial eccentricities, an upper bound on stability is obtained when the stiffness is computed assuming an effective modulus of the material equal to the secant modulus (E_S) of the mean stress on the cross section. A lower bound is obtained when the effective modulus is the tangent modulus (E_T). When the initial eccentricity is large, however, the stability can be below the tangent modulus load. References 9-5 and -6 consider the case of plates and columns of small initial eccentricities where the bending stiffnesses (D_{xx}, D_{yy}) are assumed to have an effective modulus of E_T and the twisting stiffnesses ($D_{xy} = D_{yx}$) are assumed to have an effective modulus of E_S. The relative weight of the moduli is determined by the boundary conditions and the resulting (assumed) deflection patterns ($w_{,ii}$ and $w_{,ij}$). The solutions are dependent upon an assumption of isotropy of the material defined by an octohedral stress-strain law (Section 3) and a constant Poisson ratio of .5 (which slightly overestimates the stability). The stability criteria obtained in this manner are presented in non-dimensional form in subsection 9.2.

The effect of eccentricity is quite pronounced since it initiates plasticity at an earlier load and causes the bending stiffness to decrease more rapidly. The bending stiffness is reduced by the high stresses and the shifting of the neutral axis. Both these effects reduce the stability of the structure. The eccentricity can cause large deflections of the structure which can change the initial geometry and cause rapid buckling towards a lower buckling mode as exemplified by some shell structures.

The effect of curvature on the stability is qualitatively described below. The quantitative effect of initial conditions upon the stability of the structure remains to be determined. The effect is discussed for a pin-ended column but can be applied to most structural problems.

For a pin-ended column $M = EI \dfrac{d^2w}{dx^2} = EI\, w_{,xx}$ and $M = -Fw$. As the load increases, the change in internal moment $\delta\,(EI\, w_{,xx})$ must equal the change in external moment $\delta\,(Fw)$.

$$\therefore\ EI\,\delta\, w_{,xx} + w_{,xx}\,\delta\,(EI) = F\delta w + w\delta F\,. \tag{1a}$$

When the column buckles, $\delta F = 0$.

$$\therefore\ F_M = EI\,\frac{\delta w_{,xx}}{\delta w} + w_{,xx}\,\frac{\delta\,(EI)}{\delta w}$$

$$= EI\,\frac{\delta w_{,xx}}{\delta w} + w_{,xx}\,\frac{\delta\,(EI)}{\delta w_{,xx}}\,\frac{\delta w_{,xx}}{\delta w}$$

$$F_M = \left(EI + w_{,xx}\,\frac{\delta\, EI}{\delta w_{,xx}} \right) \frac{\delta w_{,xx}}{\delta w} \tag{1b}$$

For EI independent of the loading it can be shown that

$$F_M = \frac{\int EI\, f^2_{,xx}\, dx}{\int f^2_{,x}\, dx} = \frac{EI(x)\,\delta w_{,xx}}{\delta w}\,. \tag{1c}$$

Thus, for an EI which varies with the loading, a comparison of Eqs. (1b) and (1c) leads to

9.1.6 (Cont'd)

$$F_M = \frac{\int \left(EI + w_{,xx} \frac{\delta EI}{\delta w_{,xx}} \right) f_{,xx}^2 \, dx}{\int f_{,x}^2 \, dx}, \qquad (2)$$

where $w = w_0 f$.

Employing D for EI generalizes the results. When the structure is linear elastic $\left(\frac{\delta D}{\delta w_{,xx}} = 0 \right)$, the classical result is obtained. If the structure is not linear elastic, then D must be modified by the factor $\Delta D = w_{,xx} \frac{\delta D}{\delta (w_{,xx})}$ which is always negative. The value of ΔD depends upon the curvature and bending stiffness, which in turn are dependent upon the load level and the eccentricity.

D is reduced as the material is stressed beyond the proportional limit; this reduces the effective modulus and shifts the bending axis. If the eccentricities are small, then the expression in the bracket $(D + \Delta D)$ can be approximated by moduli corresponding to the average stress (e.g., $E_T I$ is a lower bound for a column). If the eccentricity is not small (this may occur due to thermal deflections), then the stability may be below the "Tangent Modulus Stability."

9.1.7 Temperature

The application of heat to a structure reduces the stiffness of the structure, causes deformations, and may cause compatibility forces at the boundaries and internal stresses. These effects in general will reduce the stability of the structure.

For thermal loads it is essential to define the axial stiffness, as well as the rotational and lateral stiffnesses, of the supports since the temperature will try to make the supports move relative to each other and will generate boundary forces to satisfy compatibility at the boundary, these compatibility forces will affect the stability of the structure.

If the axial and rotational stiffnesses of the supports are zero (unrestrained), then the temperature reduces the moduli of the material, changes the initial eccentricity of the structure, and may generate internal stresses to enforce the internal compatibility condition that strains in a cross section be in a plane.

Calculation of the buckling load is quite simple if it is assumed that the structure remains elastic up to the buckling load. In that case the bending stiffness is simply computed at each cross section where the modulus varies (due to temperature) at every point in the cross section (Paragraph 4.1.1 illustrates the computation technique.) The over-all stability is then computed as a structure with a space variable stiffness

$$\left(\text{e.g.,} \quad F_M = \frac{\int (f_{,x})^2 \, dx}{\int \frac{f^2}{EI} \, dx} \right).$$

The result will be lower than for the structure without temperature since the bending stiffness is reduced. The effects of additional eccentricities and internal stresses cannot be evaluated at the present time but the probable effect will be to further reduce the stability. For small eccentricities, the stress-strain curve of the material at temperature can be employed to approximate the effect of plasticity.

9.1.7 (Cont'd)

If the axial and rotational stiffnesses of the supports are not zero, then compatibility forces and deformation will be generated which may limit the usability of the structure. The determination of the compatibility forces and deformation is quite complex. For example, a column might be visualized as an axial and a bending spring in series. Compatibility is satisfied by a combination of axial strains and lateral deflections. The amount of axial strain (and load) depends upon the eccentricity ratio (w_0/ρ) and the slenderness ratio (l/ρ). If these ratios are very small (e.g., $w_0 = 0$ for a straight column), compatibility will be satisfied primarily by axial strains. In this case the buckling temperature of the structure can be calculated by computing the temperature which will cause the equivalent buckling strain as defined in Paragraph 9.2.1, i.e.,

$$T_0 = \frac{\int_0^l T \, dx}{l} = \left(\frac{1}{\alpha}\right)\left(\frac{E_R}{E_S}\right)\left(\frac{KI}{Ab^2}\right) , \qquad (1)$$

where the above parameters are defined in Paragraph 9.2.1. The structure is never perfectly straight and the bending stiffness is usually less than the axial stiffness. The non-straight structure satisfies compatibility at the boundaries by deflecting laterally (e.g., $u = \int \frac{1}{2} w_{,x}^2 \, dx$) whenever the temperature increases. This is accompanied by an increase of load which is much smaller than would occur with a perfectly straight structure. The change in load is a function of the initial eccentricity. The non-straight structure never actually buckles but continues to deflect. Snap buckles are probably due to a change of the deflection pattern from the thermally induced pattern to the buckling (eigenvector) mode.

Depending upon the initial boundary conditions and geometries, there is a temperature corresponding to a given maximum deflection but this is essentially different (and higher) than a buckling temperature corresponding to the temperature which will generate the mechanical buckling load in a perfectly flat structure. The problem is graphically represented in Figure 9.1.7-1 which indicates that the boundary load may never attain the mechanical "stability" load and that excessive deflections which violate the original assumptions or destroy the utility of the structure may occur well before a "stability" load is attained. The general problem is complex and a exposition of analytical techniques that consider compatibility forces, deflections, eccentricities, and plasticity must be deferred.

9.2 Non-Dimensional Buckling Curves

The present state of the art indicates that sufficiently accurate stability predictions can be obtained by utilizing the stress-strain curve of the material at the given temperature with some combination of the secant modulus (representing twisting) and the tangent modulus (representing bending) as indicated in Paragraph 9.1.6. The immense number of structural materials and operating temperatures makes it imperative to employ a non-dimensional stress-strain law and stability criteria. The non-dimensional stress-strain law is presented in Section 3. The non-dimensional stability criteria is developed below and could be extended to include, as a first approximation, the creep buckling of a structure.

9.2.1 Non-Dimensional Stability

The stability equation can always be presented in the following form:

$$N = \frac{KD}{b^2} = \frac{K E_R I}{b^2} , \qquad (1)$$

which defines the condition of stationary potential for adjacant deflection patterns.

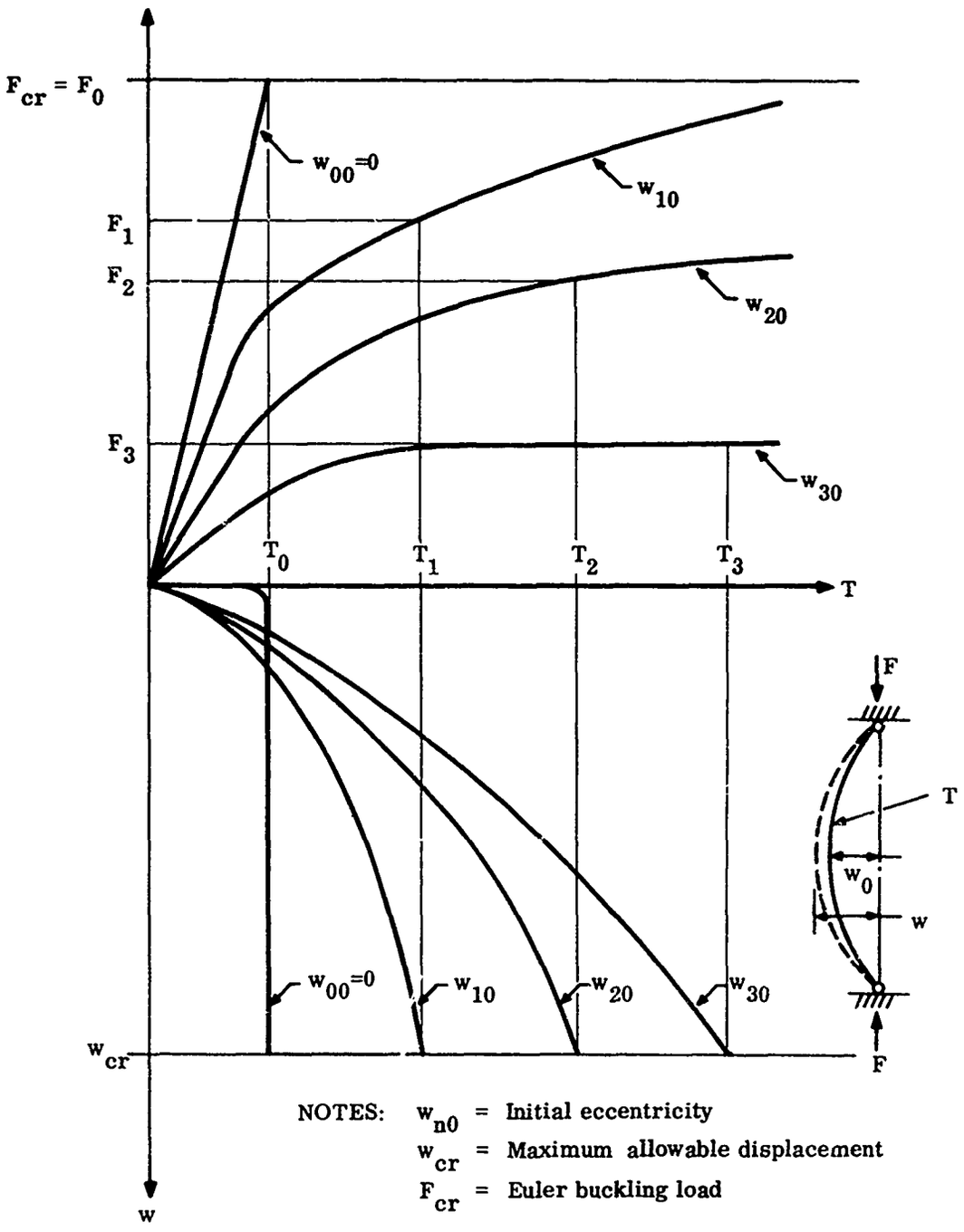


FIGURE 9.1.7-1 DEFLECTION AND LOAD IN A RESTRAINED COLUMN

9.2.1 (Cont'd)

$$\therefore \sigma = \frac{N}{A} = K E_R \frac{I}{Ab^2} \tag{2}$$

$$\frac{\sigma}{E_R} = \frac{\sigma}{E_S} \frac{E_S}{E_R} = \epsilon\left(\frac{E_S}{E_R}\right) = K \frac{I}{Ab^2} \quad , \tag{3}$$

where

N	=	axial load per inch of width
K	=	stability constant defined by linear elastic parameters
I	=	inertia of structure per inch of width
b	=	length of buckle (length of column, width of plate, etc.)
E_R	=	effective stability modulus
E_S	=	secant modulus
E_A	=	Apparent initial modulus
A	=	area per inch of width
D	=	bending stiffness per inch of width.

The function on the right is a function of the non-dimensional K, (which is a function of boundary conditions, type of loading, and the aspect ratio) and the non-dimensional geometry parameter I/Ab^2 (which is equivalent to the slenderness ratio for column and thickness ratio for plates). It is independent of the material. The non-dimensional expression on the left is a function of the stress-strain curve of the material, the magnitude of the stresses and the boundary conditions (and to some degree on the geometry of the cross section). Values of E_S/E_R can be found in References 9-1, 9-3, 9-5 and 9-6 and Table 9.2.1-1.

Since the secant modulus is an upper bound on the stability (with the possible expection for creep at low stresses),

$$\frac{E_S}{E_R} \geq 1$$

$$\epsilon \leq K I/Ab^2 . \tag{4}$$

Thus, the median strain of the cross section is never greater than a number which depends upon boundary conditions, type of loading, aspect ratio, and geometry but not upon the material.

The variation δw can be viewed as a time-induced phenomenon which does not alter the equilibrium equation or the relationship (Eq. (3)) derived from energy considerations. Creep buckling can be investigated by employing a strain relationship which includes time as well as stress and temperature. Instability can be approximated by whatever stimulations of stress, temperature and time applied to the material will cause this critical strain. A strain relationship which includes the effects of temperature and time as well as stress was presented in Section 3 and was employed with Eq. (3) to obtain the curves shown in Figures 9.2.1-1 through -5. These curves should give approximate results even when the structure is subjected to elevated temperatures for extended times.

Figures 9.2.1-1 through -5 are obtained in non-dimensional form

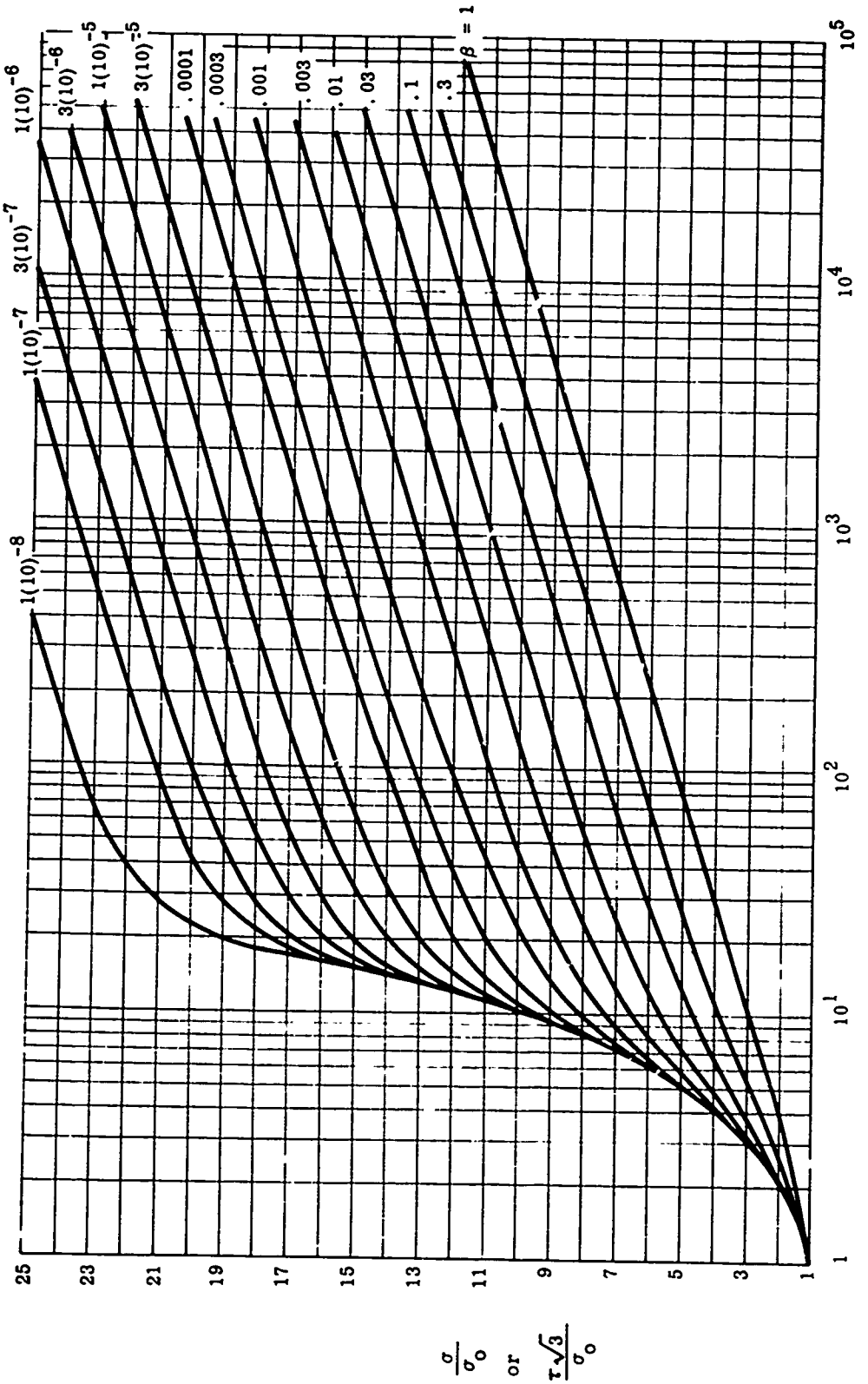


FIGURE 9.2.1-1(a) STABILITY OF SIMPLE FREE FLANGE, SHEAR PANEL, OR SHELLS

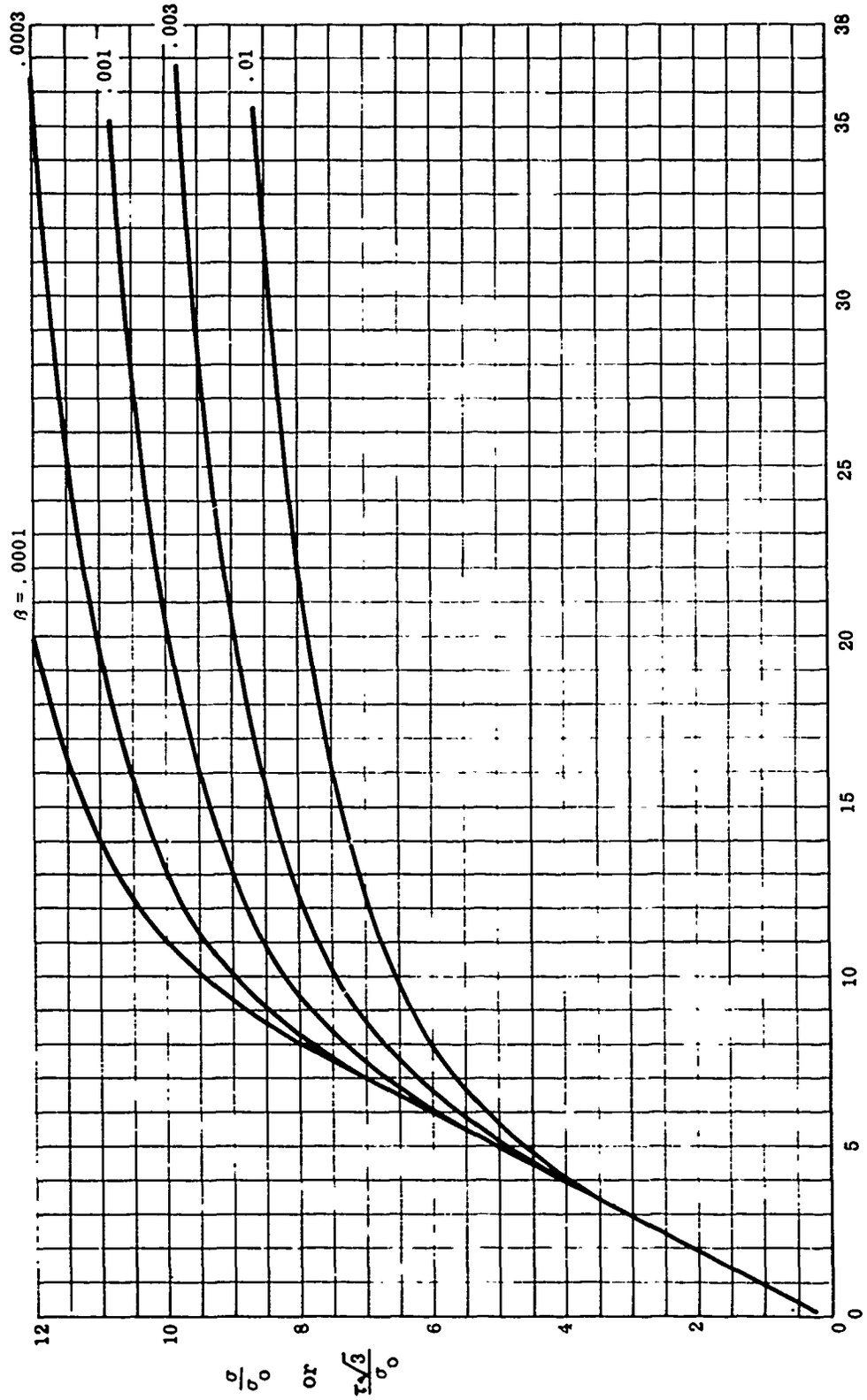


FIGURE 9.2.1-1(b) STABILITY OF SIMPLE FREE FLANGE, SHEAR PANEL, OR SHELLS

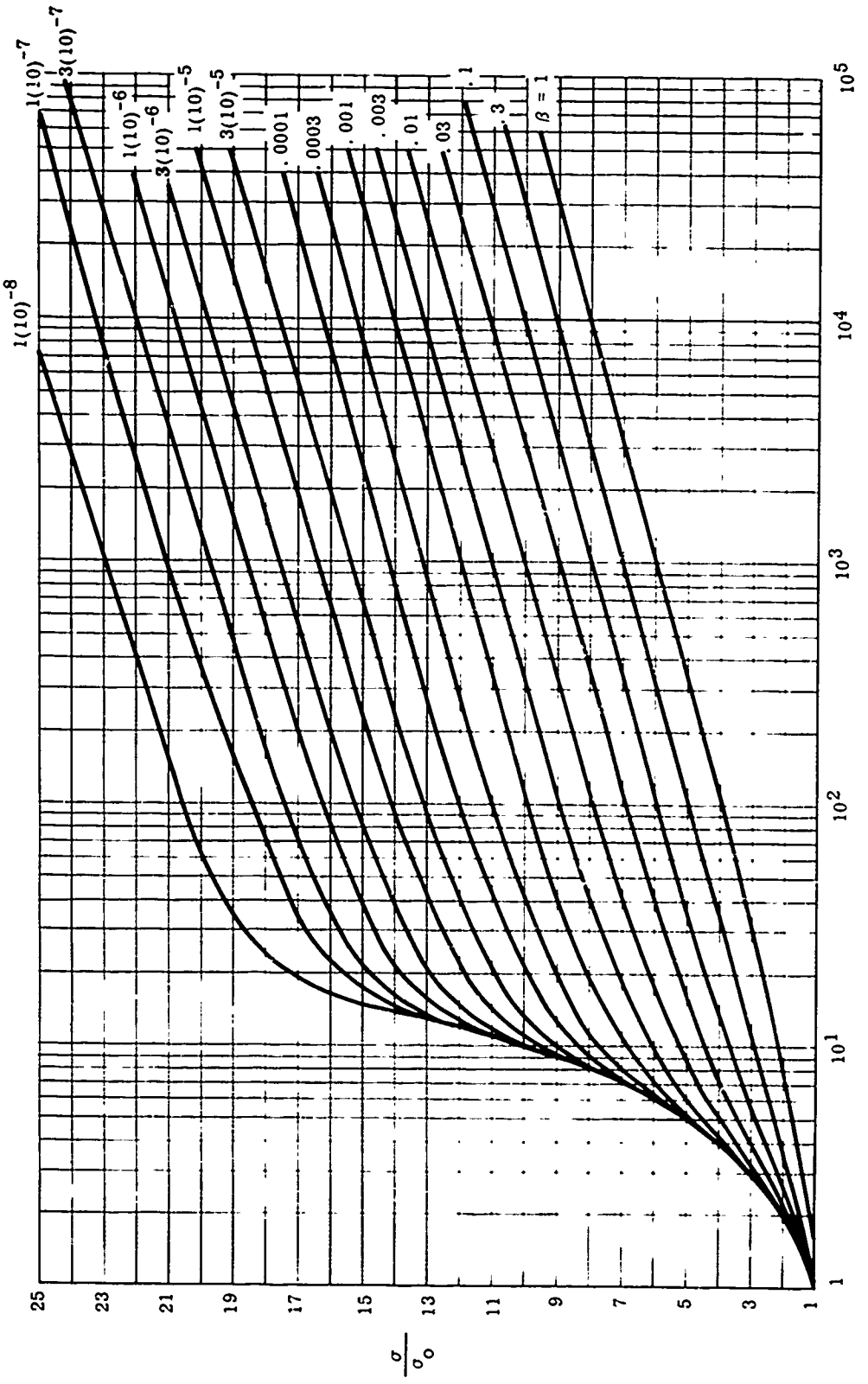


FIGURE 9.2.1-2(a) STABILITY OF COLUMN OR PLATE-COLUMN

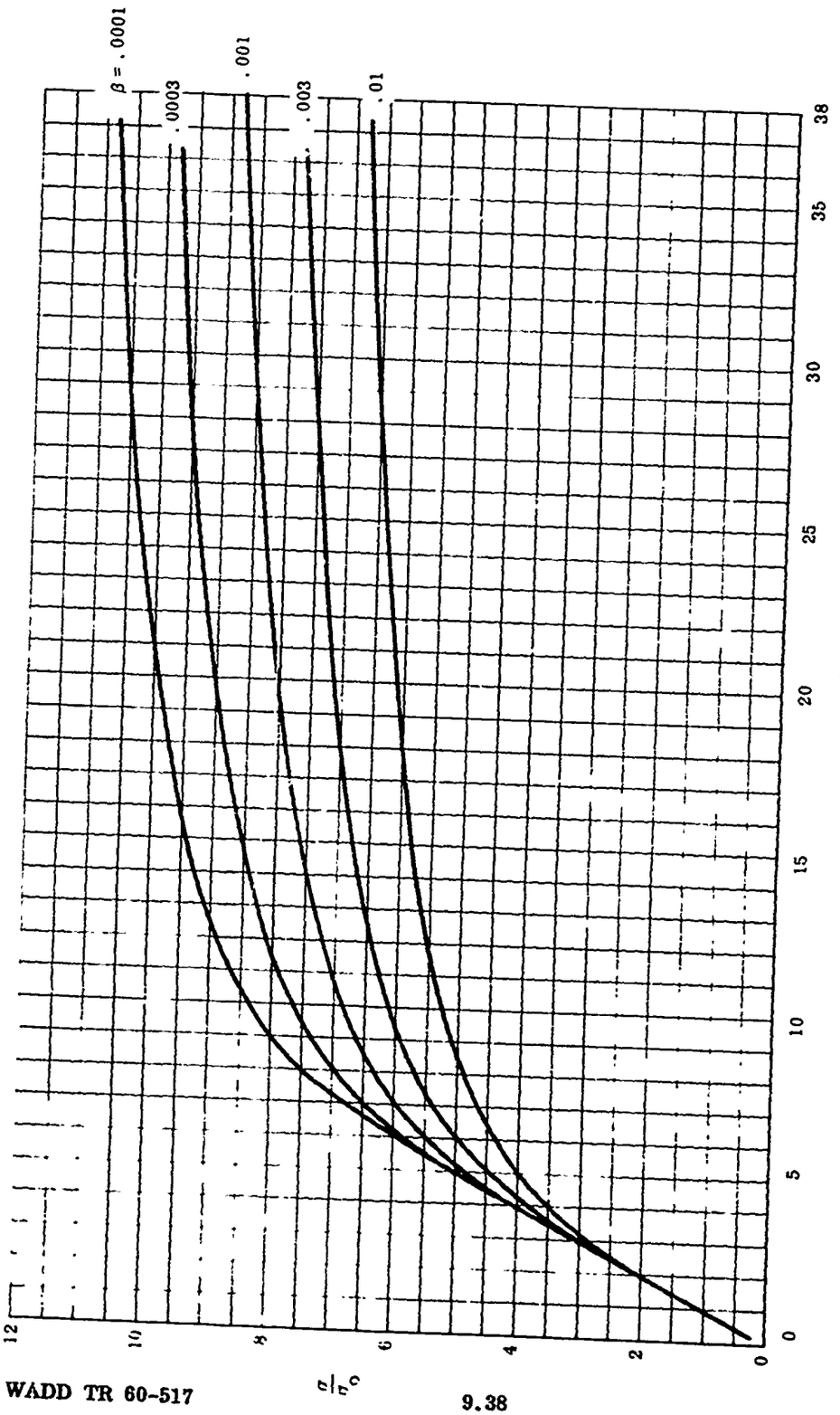


FIGURE 9.2.1-2(b) STABILITY OF COLUMN OR PLATE COLUMN

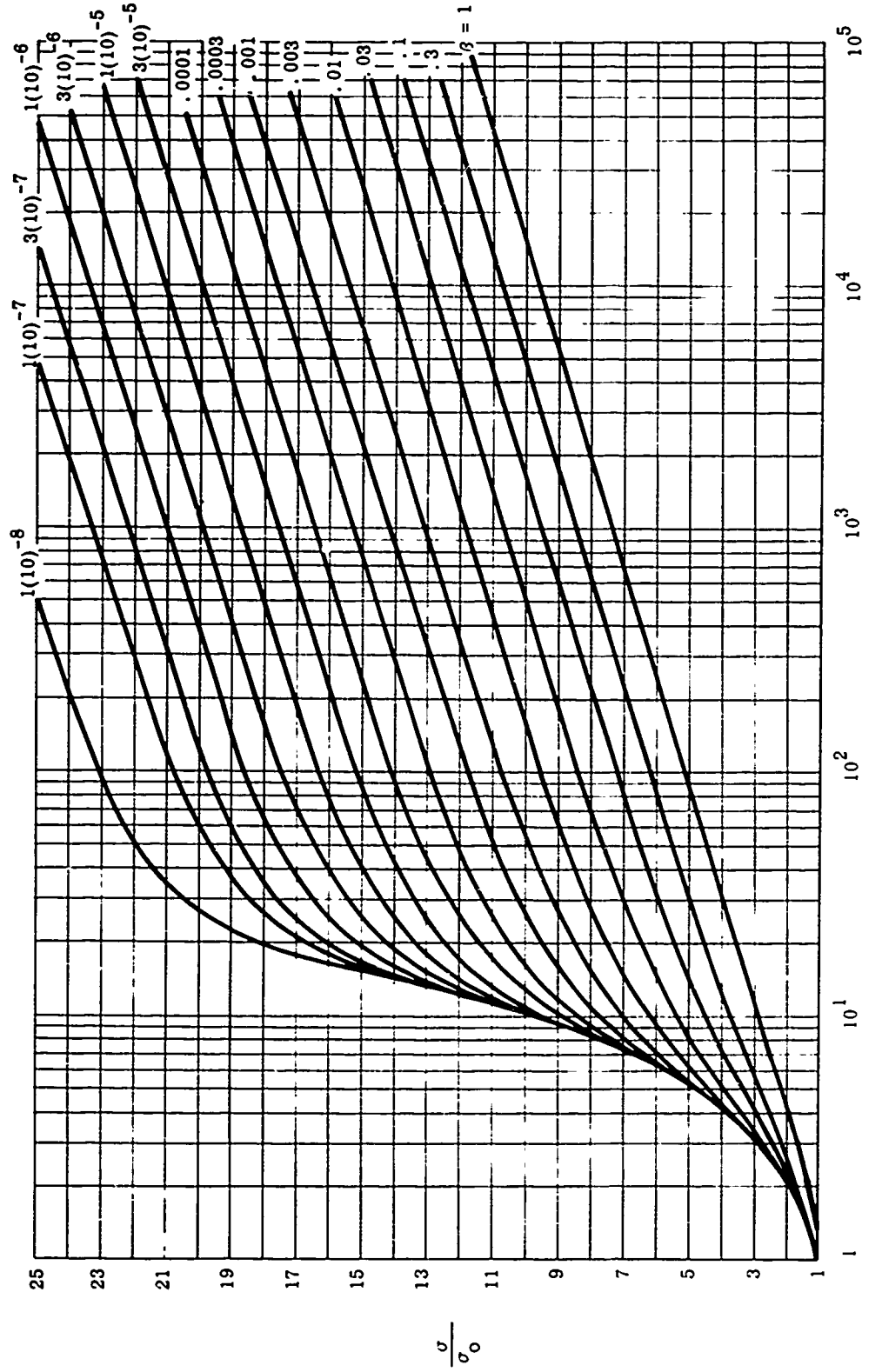


FIGURE 9.2.1-3(a) STABILITY OF SIMPLE-SIMPLE PLATE

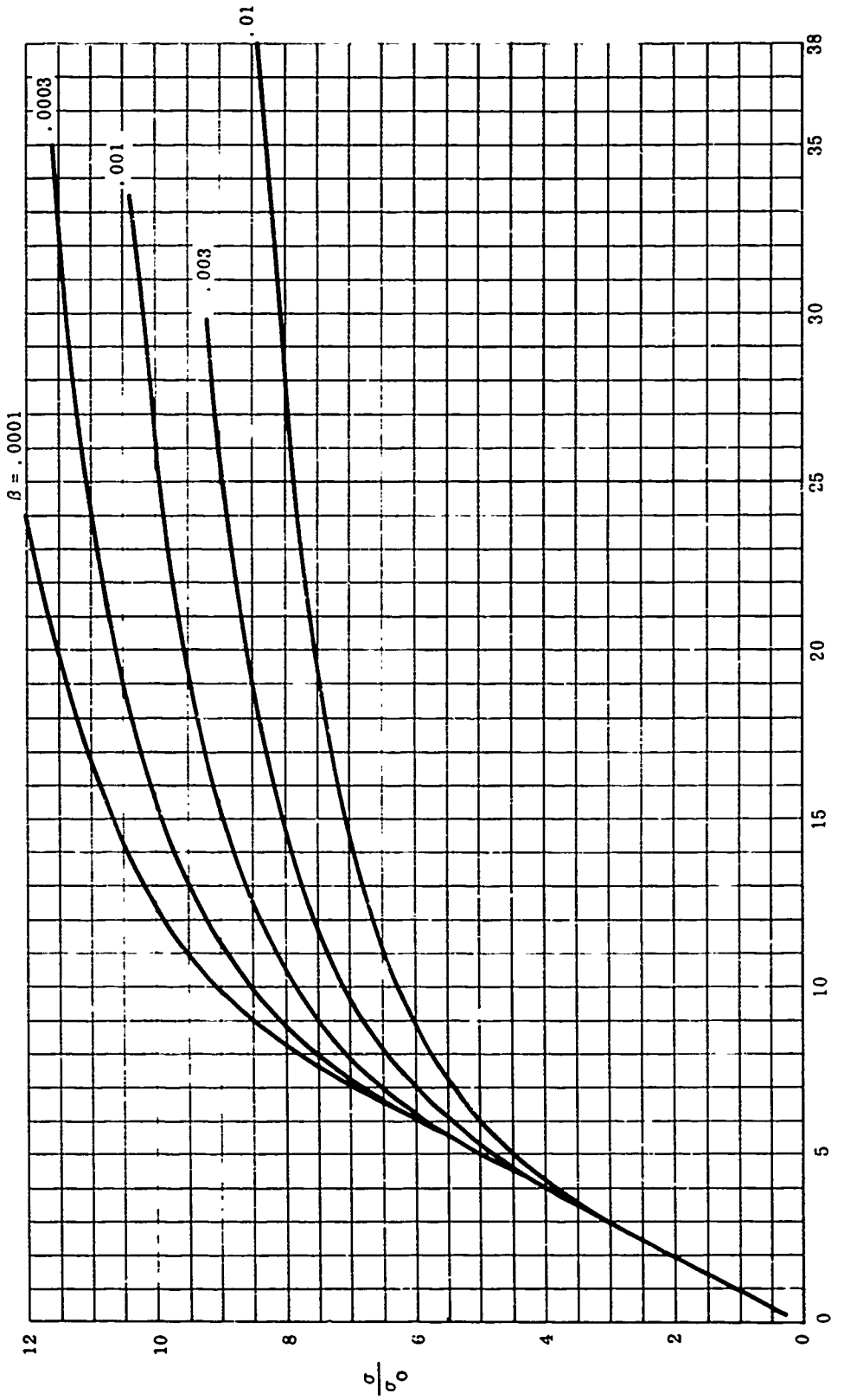


FIGURE 9.2.1-3(b) STABILITY OF SIMPLE-SIMPLE PLATE

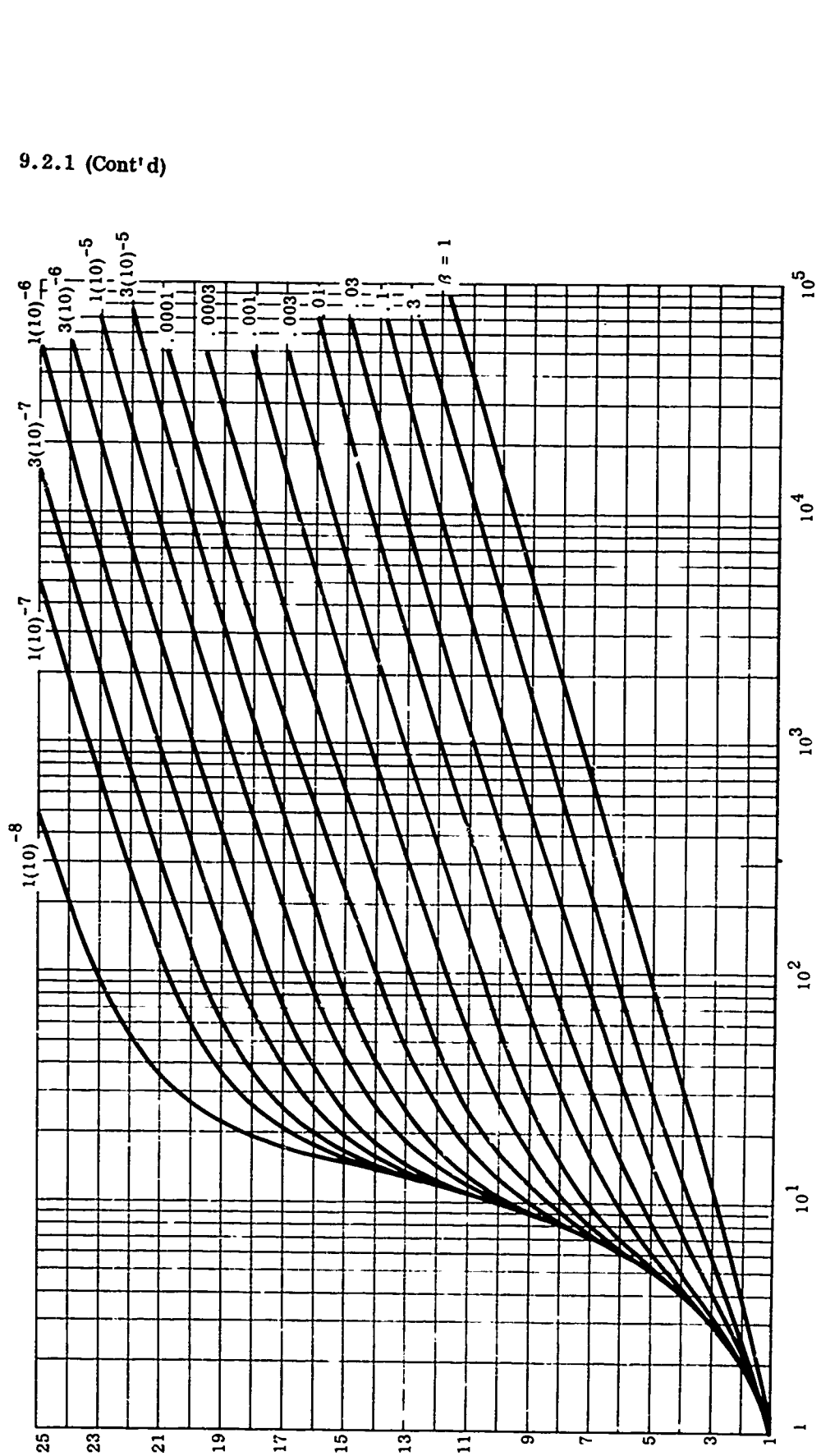


FIGURE 9.2.1-4 STABILITY OF CLAMPED-FREE PLATE

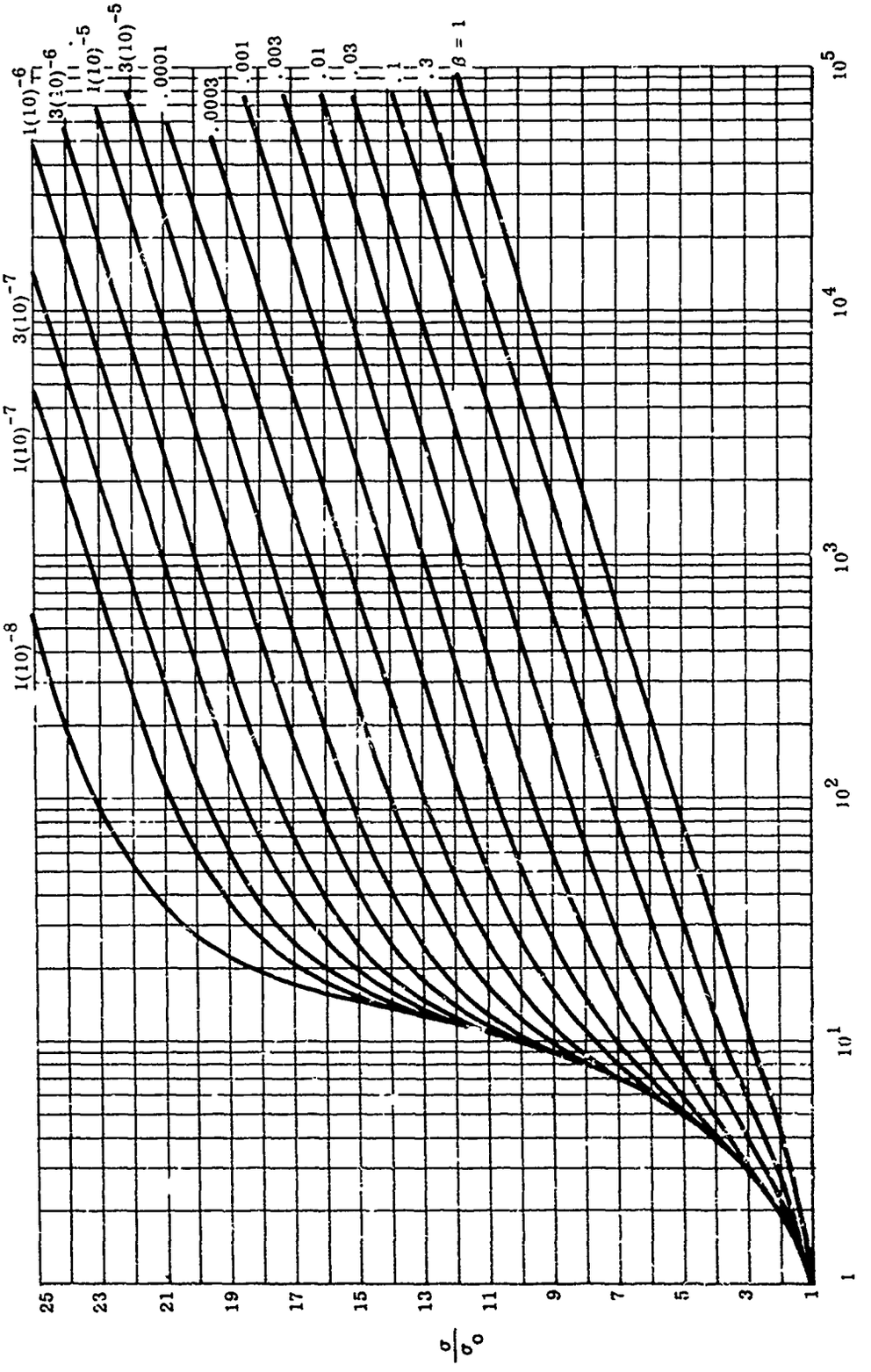


FIGURE 9.2.1-5 STABILITY OF CLAMPED-CLAMPED PLATE

9.2.1 (Cont'd)

from $$\frac{E_A}{E_R}\,\frac{\sigma}{\sigma_0} = \frac{E_A}{\sigma_0}\left(\frac{KI}{Ab^2}\right), \qquad (5)$$

and the non-dimensional stress-strain law,

$$\frac{E_A}{\sigma_0} = (1-\beta)\,\sigma/\sigma_0 + \beta \sinh \sigma/\sigma_0 \text{ (Eq. (2a) of Paragraph 3.2.1),}$$

in the following manner.

(1) The effective modulus E_R depends upon the boundary conditions and type of loading and is expressed as a function of the secant (E_S) and tangent moduli (E_T) as tabulated in Reference 9-5 and Table 9.2.1-1.

(2) The stress-strain law of the material is assumed to be characterized by the three parameters E_A, σ_0, and β; which can be obtained from simple uniaxial short time and long time tests as described in Paragraph 3.2.2. The value of $\left(\frac{E_A}{E_R}\right)\left(\frac{\sigma}{\sigma_0}\right)$ is computed for various values of σ/σ_0 for a given β; this value is $\left(\frac{E_A}{\sigma_0}\right)\left(\frac{KI}{Ab^2}\right)$.

(3) A plot of $\left(\frac{E_A}{E_R}\right)\left(\frac{\sigma}{\sigma_0}\right) = \left(\frac{E_A}{\sigma_0}\right)\left(\frac{KI}{Ab^2}\right)$ versus σ/σ_0 for various β is shown in Figures 9.2.1-1 through -5, The curves are then employed to obtain the stability of a structure as illustrated in the examples shown below. In Figures 9.2.1-1 through -3 two graphs for each effective modulus are presented to improve the accuracy in reading the curves.

(4) The values of the critical strain parameter (KI/Ab^2) is defined below for various types of constructions.

(a) Column $$\left(\frac{KI}{Ab^2}\right)_c = \frac{C_c\,\pi^2\,(\rho/l)^2}{1 + 2(1+\nu)\pi^2 C_c\left[\left(\frac{\rho}{l}\right)^2\frac{A}{A_V} + \left(\frac{e}{l}\right)^2\frac{I}{J}\right]} \qquad (6)$$

where C_c = end fixity of column
ρ = radius of gyration $= \sqrt{I/A}$
l = length of column

(b) Plate or Shell

$$\left(\frac{KI}{Ab^2}\right)_P = \frac{\frac{1}{12}\left(\frac{\pi^2 k}{1-\nu^2}\right)\left(\frac{t}{b}\right)^2}{1 + \left(\frac{\pi^2 k}{6(1-\nu)}\right)\left(\frac{t}{b}\right)^2} \qquad (7)$$

where k = stability constant evaluated in various texts, such as References 9-1, -2, -3, and -8.
t = plate thickness
b = width of plate

9.2.1 (Cont'd)

(c) Sandwich Construction

$$\left(\frac{KI}{Ab^2}\right)_S = \frac{\frac{\pi^2 k}{4(1-\nu^2)}\left(\frac{h}{b}\right)^2}{1+\frac{\pi^2 k}{2(1-\nu)^2}\left(\frac{f E_f}{h_c G_c}\right)\left(\frac{h}{b}\right)^2} \qquad (8)$$

where k = stability constant
h = centroidal distance between faces
f = average thickness of faces
E_f = modulus of faces
h_c = thickness of core
G_c = shear modulus of core

TABLE 9.2.1-1

EFFECTIVE MODULUS OF PLASTIC STRUCTURES
(References 9-5 and 9-6)

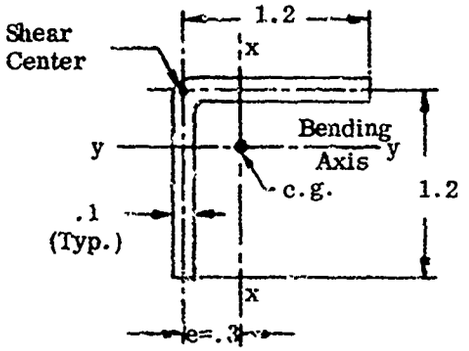
Unloaded Ends	Type	E_R/E_A
Unaxial Load		
Free - Free	Column or Long Plate	E_T/E_A
	Short Plate	$(E_S/E_A)\left[1/4 + 3/4\ (E_T/E_S)\right]$
	Square Plate	$(E_S/E_A)\left[.114 + .886\ (E_T/E_S)\right]$
Simple - Free	Long Flange	E_S/E_A
Clamped - Free	Long Flange	$(E_S/E_A)\left[.428 + .572\sqrt{1/4 + 3/4\ (E_T/E_S)}\right]$
Simple - Simple	Long Panel	$(E_S/E_A)\left[1/2 + 1/2\sqrt{1/4 + 3/4\ (E_T/E_S)}\right]$
Clamped- Clampled	Long Panel	$(E_S/E_A)\left[.352 + .648\sqrt{1/4 + 3/4\ (E_T/E_S)}\right]$
Shear		
Simple - Simple	Shear Panel	E_S/E_A
Clamped - Clamped	Clamped Shear Panel	E_S/E_A

9.2.1 (Cont'd)

The use of the non-dimensional buckling curves is illustrated in the following examples

Example 1 - Column with Shear and Twisting

A sheet stringer whose cross section is shown in Figure 9.2.1-6 is assumed to be hinged at the ends and forced to bend about the y-y axis due to the planar stiffness of the sheet.



$$A = (1.2 + 1.2)\ .1 = .24$$

$$A_V = (1.2)\ .1 = .12$$

$$I = (1.2)(.1)(.3)^2 + (1.2)(.1)(.3)^2 + \frac{1}{12}(1.2)^3(.1)$$

$$= .0108 + .0108 + .0144 = .0360$$

$$J = \frac{1}{3}(1.2 + 1.2)(.1)^3 = .0008$$

$$\rho^2 = I/A = \frac{.036}{.24} = .15$$

$$l = 31.62 \qquad l^2 = 1000$$

$$C_c = 1.0 \qquad \nu = .3$$

FIGURE 9.2.1-6 SHEET STRINGER CROSS SECTION

Static Buckling:

From Eq. 6

$$\frac{KI}{Ab^2} = \frac{\pi^2 \left(\frac{\rho}{l}\right)^2}{1 + 2(1+\nu)\pi^2 \left[\left(\frac{\rho}{l}\right)^2 \frac{A}{A_V} + \left(\frac{e}{l}\right)^2 \frac{I}{J}\right]}$$

$$= \frac{9.87 \left(\frac{.15}{1000}\right)}{1 + 2.6\left[\left(\frac{.15}{1000}\right)\frac{.24}{.12} + \left(\frac{.03}{1000}\right)\frac{.036}{.0003}\right]} = \frac{.0015}{1 + .0078 + .105} = .00135.$$

The above calculations are independent of the material and depend upon the geometry alone. In the above example, the transverse shear has little effect upon the stability parameter but the torsional shear reduces the stability parameter by 10%. This is an exceptional case since the cross section is usually symmetrical (e=0) or closed (large J).

The following material properties can be assumed, if the material is 2024ST81 aluminum alloy at 300°F:

$$E_A = 10^7 \text{ psi}; \quad \nu = .3; \quad \sigma_o = 5\ (10)^3 \text{ psi} \quad \beta = .0001$$

$$\therefore \frac{E_A}{\sigma_o}\left(\frac{KI}{Ab^2}\right) = \frac{(10)^7}{5(10)^3}\ (.00135) = 2.7$$

9.2.1 (Cont'd)

From Figure 9.2.1-2(a) or -2(b)

$$\sigma/\sigma_o = 2.7 .$$

The stress is linear elastic since

$$\frac{\sigma}{\sigma_o} = \frac{E_A}{\sigma_o} \quad \frac{KI}{Ab^2} .$$

The buckling stress σ_{cr} is obtained as

$$\sigma_{cr} = \frac{\sigma}{\sigma_o} \quad \sigma_o = (2.7)\, 5(10)^3 = 13,500 \text{ psi.}$$

Creep Buckling:

Equation (6) is modified to Equation (6a) to account for the smaller shear energy under the creep load. This modification is usually quite small and in view of the inaccuracies of creep buckling the denominator can usually be assumed to be equal to 1.

$$\epsilon = \frac{KI}{Ab^2} = \frac{\pi^2 (\rho/l)^2}{1 + 2(1+\nu)\pi^2 \left[\left(\frac{\rho}{l}\right)^2 \frac{A}{A_V} + \left(\frac{e}{l}\right)^2 \frac{I}{J}\right] F/F_{cr}} \tag{6a}$$

where F = applied creep load
F_{cr} = short time buckling load.

Let $F = 1620$

$$\therefore \quad \sigma = \frac{F}{A} = \frac{1620}{.24} = 6750 \text{ psi}$$

$\epsilon_\sigma = .000675$ (from stress-strain data)

and

$\dot{\epsilon} = .0001$ in/in hr (assumed creep rate)

$$\therefore \quad \epsilon = \frac{.0015}{1 + \left[.0078 + .105\right] \frac{6750}{13500}} = .00143$$

$$t_{cr} = \frac{\epsilon - \epsilon_\sigma}{\dot{\epsilon}} = \frac{.00143 - .000675}{.0001} = 7.55 \text{ hours.}$$

9.2.1 (Cont'd)

Example 2 - Simply Supported Sandwich Panel (Figure 9.2.1-7):

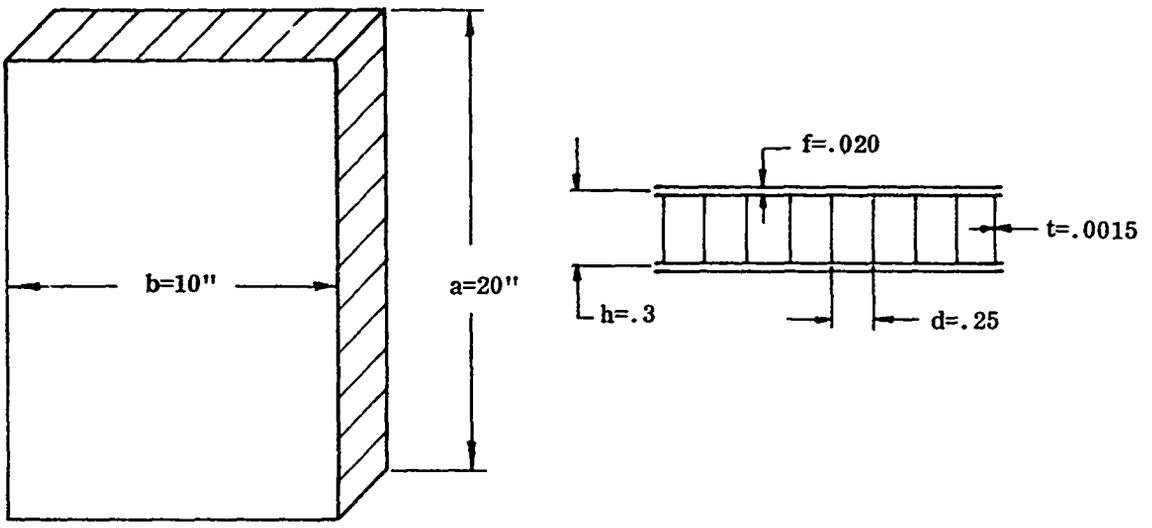


FIGURE 9.2.1-7 SANDWICH PANEL

Assuming 2024ST81 aluminum alloy faces and core at 300°F,

$$E_A = 10^7 \text{ psi}, \quad \nu = .3, \quad \sigma = 5(10)^3, \quad \beta = .0001$$

and $\dfrac{E_f}{G_c} \sim 2(1+\nu)\dfrac{d}{t} = 2(1+.3)\dfrac{.25}{.0015} = 435$ (Reference 9-9).

Compression Loading (k = 4):

From Eq. (8),

$$\frac{KI}{Ab^2} = \frac{\dfrac{\pi^2 k}{4(1-\nu^2)}\left(\dfrac{h}{b}\right)^2}{1+\dfrac{\pi^2 k}{4(1-\nu^2)}\dfrac{2fE_f}{h_c G_c}\left(\dfrac{h}{b}\right)^2} = \frac{\dfrac{\pi^2 4}{4(1-.3^2)}\left(\dfrac{.3}{10}\right)^2}{1+\dfrac{\pi^2 4}{4(1-.3)^2}\dfrac{2(.020)}{.3}435\left(\dfrac{.3}{10}\right)^2}$$

$$= \frac{.0098}{1+.0098(58)} = .64(.0098) = .00626 .$$

The shear deformation of the core causes a 36 percent reduction in the stability strain.

$$\frac{E_A}{\sigma_o}\left(\frac{KI}{Ab^2}\right) = \frac{10^7}{5(10)^3}(.00626) = 12.52 .$$

9.2.1 (Cont'd)

From Figure 9.2.1-3(a) or 3(b).

$$\frac{\sigma}{\sigma_o} = 10.05 \quad \left(\text{Plastic since } \sigma/\sigma_o \neq \frac{E_A}{\sigma_o}\frac{KI}{Ab^2}\right)$$

$$\sigma_{cr} = (\sigma/\sigma_o)\,\sigma_o = (10.05)\,5000 = 50,250 \text{ psi}$$

$$N_{cr} = (2f)\,\sigma_{cr} = (.040)\,50,250 = 2010 \text{ lb/in}.$$

Shear Loading $\left(k_S \sim 5.34 + \frac{4.0}{(a/b)^2} = 6.34\right)$:

From Eq. (8),

$$\frac{K_S I}{Ab^2} = \frac{\frac{\pi^2(6.34)}{4(1-.3^2)}\left(\frac{.3}{10}\right)^2}{1 + \frac{\pi^2(6.34)}{4(1-.3)^2}\,\frac{2(.02)}{.3}\,435\left(\frac{.3}{10}\right)^2}$$

$$= \frac{.0157}{1 + (.0157)(58)} = .00823$$

$$\sqrt{3}\,\frac{E_A}{\sigma_o}\,\frac{K_S I}{Ab^2} = (1.73)\,\frac{(10)^7}{5(10)^3}\,.00823 = 28.5\,.$$

From Figure 9.2.1-1(a) or 1(b),

$$\frac{\tau\sqrt{3}}{\sigma_o} = 12.5 \quad \text{(Plastic)}$$

$$\tau_{cr} = \left(\frac{\tau\sqrt{3}}{\sigma_o}\right)\frac{\sigma_o}{\sqrt{3}} = \frac{12.5\ (5000)}{1.73} = 36,100 \text{ psi}$$

$$N_{xy} = 2f\tau = 2(.020)36100 = 1444 \text{ lb/in}.$$

9.3 CURVED PLATES AND SHELLS

The stability of plates assumes that the lateral loads (q) are resisted by bending in the plate since the boundaries are free to move in the plane of the plate. If the boundaries are restrained or the geometry of the structure is capable of resisting these lateral loads, then membrane type stresses coupled with the curvature of the structure can resist the lateral load. The ability of a structure to provide more than one load path cannot decrease the stability of the structure. The load will be distributed in accordance with the stiffnesses of the load paths so as to minimize the strain energy. The additional load path is analagous to an additional restraint which cannot decrease the stability. The shell therefore is inherently more stable than the flat plate. Unfortunately the energy functions and the equilibrium equations are more complicated because of the interaction of the membrane and bending stiffnesses.

9.3 (Cont'd)

The equilibrium equation for small elastic deflections has been derived by Donnell (cited in Reference 9-8) and can be expressed as

$$D_M \cdot \nabla^8 w + D_A \cdot \nabla^4 w + \nabla^4 (N \cdot \nabla^2 w + q) = 0$$

and can be employed to obtain eigenvalues, where D_M = bending stiffness $\sim \frac{Et^3}{12(1-\nu^2)}$

and D_A = axial stiffness $\sim$ Et.

The assumption of small deflections and a stiff load path by membrane action is not usually met by a curved plate due to significant initial eccentricities and changes in geometry with loading. The curved panel can buckle at a load significantly below that predicted by the membrane-bending model; and may even fail suddenly if the deflection pattern changes under load and the membrane action becomes limited. This can be visualized as equilibrium existing for the initial loadings and small deflection eigenvector modes. As loading is continued, the shell deforms along the original eigenvector but apporach a crest similar to Figure 9.1-1(d) and becomes unstable, deforming to a different eigenvector representing a solution with smaller membrane action. The geometry may be changing simultaneously so that the structure could suddenly deflect to the different eigenvector with a lower eigenvalue. The amount of initial eccentricity can significantly affect the load at which this cross over can occur. Radially outward pressures should forestall this phenomenon to some degree whereas inward pressure should precipitate it at an earlier loading.

The stability of the curved panel and shells will depend upon its bending stiffness D_M, its axial stiffness D_A, the boundary conditions, the initial condition (geometry, eccentricities, etc.), and the material properties. It is recommended that the present analysis of the curved plates be based on semi-empirical stability criteria shown in Reference 9-8 (e.g., C(Et/r) or $\frac{\pi^2 k E}{12(1-\nu^2)} (t/r)^2$). The stability coefficients are based on theoretical cosiderations and modified by the statistics of available experimental data. The stability coefficients should be used in the manner described in Subsection 9.2 except that the correction for shear is not warranted in view of empiricism of the coefficients. The effective modulus is assumed to be E_S (which slightly overestimates the stability) since the twisting and axial stiffnesses should play a more significant role than for flat plates.

The stability of a shell is illustrated in the following:

Example: A cylinder shown in Figure 9.3-1 is loaded with a uniform compression loading along the edges. The edges are simply supported.

From Reference 9-8,

$$\frac{\sigma}{E_S} = C \; t/r$$

since $\frac{r}{t} = \frac{10}{15} = 67 \; \therefore \; C = .42$ (Figure 7 of Reference 9-8).

$$\therefore \; \frac{\sigma}{E_S} = .42 \; \frac{(.15)}{10} = .0063.$$

9.3 (Cont'd)

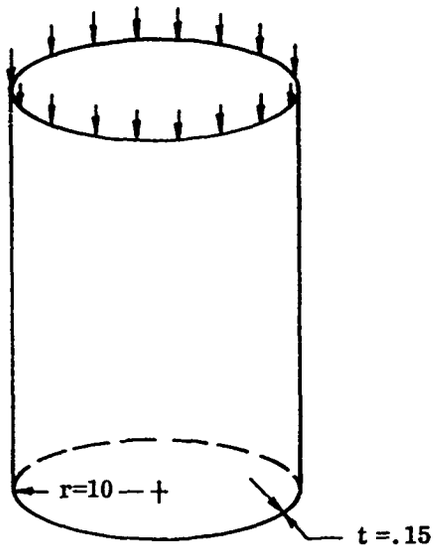


FIGURE 9.3-1 CYLINDER IN COMPRESSION

Assuming 2024ST81 aluminum alloy at 300°F,

$$E_A = 10^7 \text{ psi}, \qquad \sigma_o = 5(10)^3, \qquad \beta = .0001$$

and

$$\frac{E_A}{\sigma_o} C \frac{t}{r} = \frac{10^7}{5(10)^3} (.0063) = 12.6 .$$

From Figure 9.2.1-1(a) or -1(b),

$$\frac{\sigma}{\sigma_o} = 10.6$$

$$\sigma_{cr} = 10.6\ (5000) = 53{,}000 \text{ psi}$$

$$N_{cr} = \sigma t = 53{,}000\ (.15) = 7950 \text{ lb/in}$$

$$F_{cr} = \sigma\Delta = N_{cr}\ (2\pi r) = 500{,}000 \text{ lb.}$$

9.4 REFERENCES

9-1 Gerard, G. and Becker, H., Buckling of Flat Plates, NACA TN 3781, July 1957.

9-2 Timoshenko, S., Theory of Elastic Stability, McGraw-Hill Book Co., Inc., 1936.

9.4 (Cont'd)

9-3 Bleich, F., Buckling Strength of Metal Structures, McGraw-Hill Book Co., Inc., 1952.

9-4 Budiansky, B. and Hu Pai, C., Lagrangian Multiplier Method of Finding Upper and Lower Limits to Critical Stresses of Clamped Plate, NACA Report 848, 1946.

9-5 Stowell, E.Z.. A Unified Theory of Plastic Buckling of Columns and Plates, NACA Report 898, 1948.

9-6 Stowell, E.Z., Critical Shear Stress of an Infinitely Long Plate in the Plastic Region, NACA TN 1681, 1948.

9-7 Gerard, G., A Creep Buckling Hypothesis, Journal of Aeronautical Sciences, Vol. 23, No. 9, September 1956, p. 879.

9-8 Gerard, G., and Becker, H., Buckling of Curved Plates and Shells, NACA TN 3783, August 1957.

9-9 Switzky, H., Design of Stable Structures, Republic Aviation Corporation, Report No. ESAM-30, October 1958.

Aeronautical Systems Division, Dir/Aeromechanics, Flight Dynamics Lab, Wright-Patterson AFB, Ohio. Rpt Nr WADD-TR-60-517, Vol I. THERMO-STRUCTURAL ANALYSIS MANUAL. Final report, Aug. 62, 445p. incl illus., tables, refs.

Unclassified Report

This Manual includes a compilation of methods of solution for thermal stress problems of the types frequently encountered by aircraft designers. Some of the methods represent original work done at Republic Aviation Corporation and others were obtained from the general literature. Where feasible, graphs and formulas are presented from which the user may obtain answers directly. These are presented in non-dimensional form to extend their applicability. In other cases, tables are furnished which describe methods of solution. Liberal use is made of illustrative problems and examples.

(over)

Within the limitations of linear elastic theory, the following problems are treated in detail: (1) Statically determinate beams, (2) Redundant beams and frames, (3) Riveted or bolted joints, (4) Plates (5) Axially symmetric shells. For more complex linear problems, a general method of attack is presented which reduces the thermal stress problem to an equivalent mechanical loading problem. This approach permits utilization of the great variety of analytical methods which have been developed for stress analysis of structures under purely mechanical loads. A brief review of some of these methods is included with pertinent remarks on their applicability to thermal stress problems. In many cases of practical interest, thermal effects introduce nonlinearity by causing large deflections, by affecting the mechanical properties of the material, or by introducing creep. Solutions for these problems are quite limited. However, they are discussed in some detail and a generalized stress-strain-time-temperature relationship is postulated which is applied to buckling of columns and plates.

1. Structures
2. Deformation
3. Temperature
I. AFSC Project 1367 Task 14002
II. Contract AF 33(616)-6066
III. Republic Aviation Corp., Farmingdale, L. I., New York
IV. H. Switzky et al
V. Secondary Rpt No. RAC-679-1A (128A)
VI. Aval fr OTS
VII. In ASTIA collection

Aeronautical Systems Division, Dir/Aeromechanics, Flight Dynamics Lab, Wright-Patterson AFB, Ohio. Rpt Nr WADD-TR-60-517, Vol I. THERMO-STRUCTURAL ANALYSIS MANUAL. Final report, Aug. 62, 445p. incl illus., tables, refs.

Unclassified Report

This Manual includes a compilation of methods of solution for thermal stress problems of the types frequently encountered by aircraft designers. Some of the methods represent original work done at Republic Aviation Corporation and others were obtained from the general literature. Where feasible, graphs and formulas are presented from which the user may obtain answers directly. These are presented in non-dimensional form to extend their applicability. In other cases, tables are furnished which describe methods of solution. Liberal use is made of illustrative problems and examples.

(over)

Within the limitations of linear elastic theory, the following problems are treated in detail: (1) Statically determinate beams, (2) Redundant beams and frames, (3) Riveted or bolted joints, (4) Plates (5) Axially symmetric shells. For more complex linear problems, a general method of attack is presented which reduces the thermal stress problem to an equivalent mechanical loading problem. This approach permits utilization of the great variety of analytical methods which have been developed for stress analysis of structures under purely mechanical loads. A brief review of some of these methods is included with pertinent remarks on their applicability to thermal stress problems. In many cases of practical interest, thermal effects introduce nonlinearity by causing large deflections, by affecting the mechanical properties of the material, or by introducing creep. Solutions for these problems are quite limited. However, they are discussed in some detail and a generalized stress-strain-time-temperatur relationship is postulated which is applied to buckling of columns and plates.

1. Structures
2. Deformation
3. Temperature
I. AFSC Project 1367 Task 14002
II. Contract AF 33(616)-6066
III. Republic Aviation Corp., Farmingdale, L. I., New York
IV. H. Switzky et al
V. Secondary Rpt No. RAC-679-1A (128A)
VI. Aval fr OTS
VII. In ASTIA collection